ICMRS

2020

3RD INTERNATIONAL CONFERENCE ON MATHEMATICAL AND RELATED SCIENCES: CURRENT TRENDS AND DEVELOPMENTS

ONLINE MEETING, TURKEY
NOVEMBER 20-22, 2020

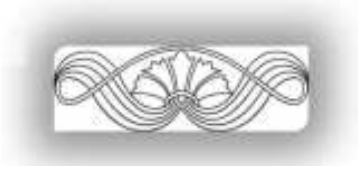

3RD INTERNATIONAL CONFERENCE ON MATHEMATICAL AND RELATED SCIENCES: CURRENT TRENDS AND DEVELOPMENTS

PROCEEDINGS BOOK

ISBN: 978-625-409-146-9

2020

3RD INTERNATIONAL CONFERENCE ON MATHEMATICAL AND RELATED SCIENCES

ICMRS 2020

ONLINE MEETING, TURKEY

NOVEMBER 20-22, 2020

EDITORS

ERHAN SET, PhD

AHMET OCAK AKDEMİR, PhD

ALPER EKİNCİ, PhD

All papers have been peer reviewed.

CHAIR

Prof. Dr. Erhan SET
Ordu University *Turkey*

ORGANIZING COMMITTEE

Assoc. Prof. Dr. Ahmet Ocak AKDEMİR
Ağrı İbrahim Çeçen University *Turkey*

Assoc. Prof. Dr. Alper EKİNCİ
Bandırma Onyedi Eylül University *Turkey*

SECRETARY

PhD Stud. Barış ÇELİK
Ordu University *Turkey*

KEYNOTE SPEAKERS

Prof. Dr. Fikret ALIEV
Institute of Applied Mathematics, Baku State University – Azerbaijan

Prof. Dr. Elvan AKIN
Missouri University of Science and Technology-USA

Prof. Dr. Maria Alessandra RAGUSA
University of Catania – Italy

Prof. Dr. Zlatko PAVIC
University of Slavonski Brod- Croatia

Prof. Dr. Juan Luis Garcia GUIRAO
Technical University of Cartagena, Spain

SCIENTIFIC COMMITTEE

Abdallah BENAISSA, **University of Batna,** Algeria

Ahmet Ocak AKDEMİR, **Ağrı İbrahim Çeçen University,** Turkey

Ali ALLAHVERDI, **Kuwait University,** Kuwait

Ali EMROUZNEJOD, **Aston University,** U.K.

Halit ORHAN, **Atatürk University,** Turkey

Allal GUESSAB, **Université de Pau et des Pays de l'Adour,** France

Alper EKİNCİ, **Bandirma Onyedi Eylul University,** Turkey

Anthony SOFO, **Victoria University,** Australia

Arif RAFIQ, **Hajvery University,** Pakistan

Attila HAZY, **University of Miskolc,** Hungaria

Binod Chandra TRIPATHY, **Institute of Advanced Study in Science and Technology,** India

Borhan ALBISS, **Jordan University of Science and Technology,** Jordan

Burhaneddin İZGİ, **İstanbul Technical University,** Turkey

Ceren Sultan ELMALI, **Erzurum Technical University,** Turkey

Coşkun ÇETİN, **California State University,** USA

Cristescu GABRIELA, **Aurel Vlaicu University of Arad,** Romania

Çetin YILDIZ, **Atatürk University,** Turkey

Djamila SEBA, **University of Boumerdes,** Algeria

Donal O REGAN, **National University of Ireland,** Ireland

Farooq Ahmad GUJAR, **Bahauddin Zakariya University,** Pakistan

Ekrem KADIOĞLU, **Atatürk University, T**urkey

Elman HASANOĞLU, **Işık University,** Turkey

Elman HAZAR, **Iğdır University,** Turkey

Elvan AKIN, **Missouri University of Science and Technology,** USA

Emrah Evren KARA, **Düzce University,** Turkey

Ercan ÇELİK, **Atatürk University,** Turkey

Erdal ÜNLÜYOL, **Ordu University,** Turkey

Erdinç DÜNDAR, **Afyon Kocatepe University,** Turkey

Erhan DENİZ, **Kafkas University,** Turkey

Erhan SET, **Ordu University,** Turkey

Evrim GÜVEN, **Kocaeli University,** Turkey

Feng QI, **Henan Polytechnic University,** China

Ferhan M. ATICI, **Western Kentucky University,** USA

Fikret ALIEV, **Baku State University,** Azerbaijan

Fuad KITTANEH, **University of Jordan Amman,** Jordan

Fuat USTA, **Düzce University,** Turkey

Halima ALHAMDANI, **University of Kirkuk,** Iraq

Kálmán GYORY, **Kossuth Lajos University,** Hungary

Halit ORHAN, **Atatürk University,** Turkey

Hamdullah ŞEVLİ, **Van Yüzüncü Yıl University,** Turkey

Gamar MAMMADOVA, **Baku State University,** Azerbaijan

Hari M. SRIVASTAVA, **University of Victoria,** Canada

Hasan BAL, **Gazi University,** Turkey

Hasan FURKAN, **Kahramanmaraş Sütçü İmam University,** Turkey

Maria Alessandra RAGUSA, **University of Catania,** Italy

Havva KAVURMACI-ÖNALAN, **Yüzüncü Yıl University,** Turkey

Hemen DUTTA, **Gauhati University,** India

H. Özlem GÜNEY, **Dicle University,** Turkey

Gamar H. MAMMADOVA, **Baku State University,** Azerbaijan

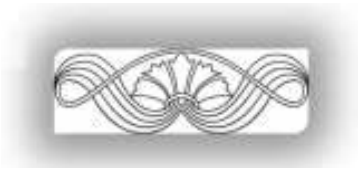

Dear Conference Participants,

Welcome to 3rd International Conference on Mathematical and Related Sciences: Current Trends and Developments.

On behalf of the Organizing Committee, I am very happy to open 3rd International Conference on Mathematical and Related Sciences. I believe that this event, which is the fruit of an intensive and devoted teamwork, will have an invaluable contribution to the scientific world. At the end of busy schedule of nearly one year, we have now achieved to organize this conference .

However, as the COVID-19 pandemic is gaining an ever tighter grip on our daily lives, as in many events, we also are forced to organize our conference as online meeting. This is because of the fact that, we, the organizers, are concerned about your health and we want to do our part to keep everyone safe. The conference is going to be held with zoom platform for participants. All presentations will be virtual presentation. We, organizing committee members, wish you all good health and high spirits. Please keep social distance and try to be realistically optimistic in these challenging coronavirus times.

The aim of the International Conference on Mathematical and Related Sciences is to bring together experts and young researchers from all over the world working in mathematics and applied mathematical sciences to present their researches, exchange new ideas, discuss challenging issues, foster future collaborations and interact with each other. In this sense, we are happy to bring together world mathematicians and exchange information with them.

The main objective of our conference is to discuss recent results in mathematics and applications and their relationship with other disciplines. We expect the participation of many prominent researchers from different countries who will present high quality papers. The conference brings together about over 100 participants from 15 countries (Turkey, Azerbaijan, Indonesia, Pakistan, Georgia, Italy, China, Croatia, Jordan, Saudi Arabia, United Arab Emirates, Uzbekistan, Nigeria, USA, Spain), out

of which 109 are contributing to the meeting with oral online presentations, including five keynote talks.

It is also a purpose of the conference to promote collaborative and networking opportunities among senior scholars and graduate students in order to advance new perspectives. The papers presented in this conference will be considered in the journals listed on the conference websites.

I'd like to express my gratitude to all our authors, members of scientific committee, keynote speakers and contributing reviewers. I believe we will see the best papers of scholars in this event. Special thanks are also due to the organizing committee members, for completing all preparations that are necessary to organize this conference. I express my gratitude to the members of technical committee of the conference for the design and proofreading of the articles.

We wish everyone a fruitful conference and pleasant memories in our online event.

Thank you.

Prof. Dr. Erhan SET

Chair of ICMRS 2020

CONTENTS

Dense Sets in Pythagorean Fuzzy Soft Topological Spaces 1

Analyzing Cerebral Infarction Data to Detect Ischemic Stroke with Ensemble Learning Approach 10

Comparing Some Kernels of Support Vector Machine for Acute Sinusitis Classification 20

Yet Some Other Alternative Asymptotically Isometric Properties Inside Copies of l^1 and Their Implication of Failure of Fixed Point Property 29

The Role of Delay Driven Hopf Bifurcations in A Prey-Predator Type One-Dimensional Mathematical Model of Plankton Interactions 36

f-Lacunary Almost Statistical Convergence and f-Lacunary Almost Summability of Double Sequences of Order α for Fuzzy Numbers 45

Comparison Between Logistic Regression and Support Vector Machine for Hepatitis Classification 55

Some Exact Travelling Wave Solutions of Sixth-Order Ramani Equation and (3+1)-Dimensional Shallow Water Wave Equation (SWWE) 64

Artificial Neural Networks with Gradient-Based Optimizer and Genetic Algorithm to Classify Small Dataset 69

Classification of Small Lung Cancer Data with Artificial Neural Network and Support Vector Machine 77

Fourier Methods for Determination of An Unknown Heat Source Poly(Methyl Methacrylate) (PMMA) with Periodic Boundary Conditions 85

Liver Cancer Classification using Neural Network–Support Vector Machine with several Optimizers 92

Comparison of several Kernel Functions on Neural Network–Support Vector Machine as Classifier for Lung Cancer 99

Generative Adversarial Network for Market Hourly Discrimination 106

Fekete-Szegö Problem for A Subclass of Analytıc Functions Defined By Chebyshev Polynomials 114

Some Inequalities of Grüss Type for a Weighted Fractional Integral Operator 121

On Subclasses of Analytic Functions Defined by q- Derivative and their Some Geometric Properties 129

The Pell-Fibonacci Sequence in Finite Groups 136

The Laplace Transform of Distribution Functions of A Semi-Markovian Random Walk Process with Positive Tendency and Negative Jumps 140
Integral Operators Involving q- Poisson Distribution Series 146
Some Structures on Pythagorean Fuzzy Soft Topological Spaces 154
Mathematical Modeling of the Effect of Laser Scan Speed on Size of Texture Created on Polyvinyl Chloride (PVC) Plate 162
On Copies of c_0 and l^1 and Failure of Fixed Point Property 166
Subordination and Superordination of the Multiplier Transformation for Meromorphic Functions 175
The Hadamard-type Padovan-p Sequences Modulo m 190
Renewed Concept of Neutrosophic Soft Graphs 194
Partial Sums of Generalized Dini Functions 207
The Radii of α-Convexity of The Function $az^2J_v''(z) + bzJ_v'(z) + cJ_v\ (z)$ 216
Comparison of Kernels Function on Twin Support Vector Machines for Lung Cancer Classification 223
Convolutional Neural Networks and Support Vector Machines Applied to CT Scan in Ischemic Stroke Detection 230
Inequalities for Geometrically Convex Functions 238
Some Fractional Integral Inequalities for Geometrically Convex Functions 247
Classification of Hepatocellular Carcinoma (HCC) using An Extended Three-Way C-Means Based on Kernel 254
Differential LG-game of Many Pursuers and One Evader 260
Partial Sums of the Bessel-Struve Kernel Function 267
An Efficient and Robust Ischemic Stroke Detection Using a Combination of Convolutional Neural Network (CNN) and Kernel K-Means Clustering 276
New Exact Solutions for Conformable Time Fractional Equation System Via IBSEFM 284
Some New Fractional Inequalities for Quasi-Convex Functions 291
Some New Bullen Type Inequalities for Different Kinds of Convexity on the Coordinates 299
Generalized Proportional Fractional Integral Operators and Related Inequalities 311
Piece-Homogeneous Elastic Mediums in the Case When the Binder and Inclusions are Weaken by the Cohesion Cracks at A Transverse Shear 318

3rd INTERNATIONAL CONFERENCE
ON MATHEMATICAL AND RELATED SCIENCES:
CURRENT TRENDS AND DEVELOPMENTS
ICMRS 2020

20-22 NOVEMBER, 2020

Dense Sets in Pythagorean Fuzzy Soft Topological Spaces

Adem YOLCU[1] and Taha Yasin ÖZTÜRK[2]

[1,2]*Department of Mathematics, Faculty of Science and Letters, Kafkas University, Kars-TURKEY*

yolcu.adem@gmail.com
taha36100@hotmail.com

Abstract. In this paper, several different types of dense sets such as nowhere dense sets and somewhere dense sets have been investigated in pythagorean fuzzy soft topological spaces and some basic characteristics of these notions have been provided. The interrelationships between the different concepts have been also analyzed in depth.

1. INTRODUCTION

The fuzzy set theory suggested by Zadeh [30] has gained considerable popularity in a variety of areas due to its ability for working with confusion. The Fuzzy Set is defined by a membership function, μ which takes the value from the crisp set to the unit interval $I = [0,1]$. Several studies have been carried out on the use of fuzzy sets [5, 12]. Like the vast majority of imprecise and ambiguous knowledge in the real world, numerous extensions of the fuzzy set have been created by several researchers. The concept of intuitionistic fuzzy sets (IFSs) was introduced by Atanassov [2] as a simplified mathematical paradigm of conventional fuzzy sets. The main benefit of the IFS is that it has the property to cope with the hesitancy that might exist due to imprecise knowledge. This is done by adding a second function, called a non-membership function, ν along with the membership function, μ of the traditional fuzzy set. There are numerous hypotheses in the literature that are used to explore uncertainties and many dynamic structures in architecture, economics, medical sciences, etc. Among these theories, the most common are fuzzy set theory [30], intuitionistic fuzzy set theory , soft set theory [13], rough set theory [16]. One of these theories, soft set theory, emerged in Molodtsov [13], and is distinct from other established theories due to its parametrization tools. Soft set theory is one of the most popular theories of recent years.

No matter how stable the notion of IFSs, there are situations where $\mu + \nu \geq 1$ varies from the condition in IFSs where $\mu + \nu \leq 1$ is the only one. This restriction in IFS is the impetus for the implementation of Pythagorean fuzzy sets (PFSs). Pythagorean fuzzy set (PFS) proposed in Yager [27, 28] is a new method for dealing with vagueness given membership grade μ and non-membership grade ν satisfying condition $\mu^2 + \nu^2 \leq 1$. PFS has a very similar relationship with IFS. To define unclear information more adequately and reliably than IFSs, the notion of PFSs can be used. The principle of PFSs has been thoroughly investigated since its inception [3, 8, 19, 26, 31]. The Pythagorean fuzzy soft set theory was described by Peng et al. [17], and its significant properties were studied. The Pythagorean fuzzy soft matrix and its different potential forms were investigated by Guleria and Bajaj [7]. M. Kirisci [10] defined the current Pythagorean fuzzy soft set form and suggested a decision-making problem solution.

Topological structure of these structures has many uses for decision-making challenges, medical diagnosis, artificial intelligence, pattern recognition, predicting and image processing, etc. Soft topology was introduced by Ahmad and Hussain [1], Cagman et al. [4], Roy and Samanta [24], Shabir and Naz [25]. Osmanoglu and Tokat [15], Coker [6] and Li and Cui [11] introduced intuitionistic fuzzy soft topology (IFS-topology). Mukherjee et al. [9] studied various dense sets on intuitionistic fuzzy soft topological spaces. Riaz et al. [20, 21, 22] introduced N-soft topology and soft rough topology with applications to multi-criteria group decision making (MCGDM). Pythagorean fuzzy topology introduced by Olgun et al [14]. Riaz et al. [23], Yolcu and Ozturk [29] studied Pythagorean fuzzy soft topological spaces.

In this paper, concepts have been presented on pythagorean fuzzy soft topological spaces of different types of dense sets, nowhere dense sets and anywhere dense sets, and some basic characteristics of these concepts are discussed. The interrelationships between the different definitions were also analyzed in depth.

2. PRELIMINARIES

Definition 1. [30] Let X be an universe. A fuzzy set F in X, $F = \{(x, \mu_F(x)) : x \in X\}$, where $\mu_F : X \to 0,1]$ is the membership function of the fuzzy set F; $\mu_F(x) \in 0,1]$ is the membership of $x \in X$ in f. The set of all fuzzy sets over X will be denoted by $FS(X)$.

Definition 2. [2] An intuitionistic fuzzy set F in X is $F = \{(x, \mu_F(x), \nu_F(x)) : x \in X\}$, where $\mu_F : X \to 0,1]$, $\nu_F : X \to 0,1]$ with the condition $0 \leq \mu_F(x) + \nu_F(x) \leq 1, \forall x \in X$. The numbers $\mu_F, \nu_F \in 0,1]$ denote the degree of membership and non-membership of x to F, respectively. The set of all intuitionistic fuzzy sets over X will be denoted by $IFS(X)$.

Definition 3. [13] Let E be a set of parameters and X be the universal set. A pair (F, E) is called a soft set over X, where F is a mapping $F : E \to \mathcal{P}(X)$. In other words, the soft set is a parameterized family of subsets of the set X.

Definition 4. [12] Let E be a set of parameters and X be the universal set. A pair (F, E) is called a fuzzy soft set over X, If $F : E \to FS(X)$ is a mapping from E into set of all fuzzy sets in X, where $FS(X)$ is set of all fuzzy subset of X.

Definition 5. [27] Let X be a universe of discourse. A pythagorean fuzzy set (PFS) in X is given by, $P = \{(x, \mu_P(x), \nu_P(x)) : x \in X\}$ where, $\mu_P : X \to 0,1]$ denotes the degree of membership and $\nu_p : X \to 0,1]$ denotes the degree of nonmembership of the element $x \in X$ to the set P with the condition that $0 \leq (\mu_P(x))^2 + (\nu_P(x))^2 \leq 1$.

Definition 6. [18] Let X be the universal set and E be a set of parameters. The pythagorean fuzzy soft set is defined as the pair (F, E) where, $F : E \to PFS(X)$ and $PFS(X)$ is the set of all Pythagorean fuzzy subsets of X. If $\mu_F^2(x) + \nu_F^2(x) \leq 1$ and $\mu_F(x) + \nu_F(x) \leq 1$, then pythagorean fuzzy soft sets degenerate into intuitionistic fuzzy soft sets.

Definition 7. [18] Let (F, E)two pythagorean fuzzy soft sets over X. The complement of (F, E) is denoted by $(F, E)^c$ and is defined by

$$(F, E)^c = \{(e, (x, \nu_{F(e)}(x), \mu_{F(e)}(x)) : x \in X) : e \in E\}$$

Definition 8. [10]
a) A pythagorean fuzzy soft set (F, E) over the universe X is said to be null pythagorean fuzzy soft set if $\mu_{F(e)}(x) = 0$ and $\nu_{F(e)}(x) = 1; \forall e \in E, \forall x \in X$. It is denoted by $\tilde{0}_{(X,E)}$.
b) A pythagorean fuzzy soft set (F, E) over the universe X is said to be absolute pythagorean fuzzy soft set if $\mu_{F(e)}(x) = 1$ and $\nu_{F(e)}(x) = 0; \forall e \in E, \forall x \in X$. It is denoted by $\tilde{1}_{(X,E)}$.

Definition 9. [10] Let (F, A) and (G, B) be two pythagorean fuzzy soft sets over the universe set X, E be a parameter set and $A, B \subseteq E$.Then,
a) Extended union of (F, A) and (G, B) is denoted by $(F, E) \tilde{\cup}_E (G, B) = (H, C)$ where $C = A \cup B$ and (H, C) defined by;

$$(H, C) = \{(e, (x, \mu_{H(e)}(x), \nu_{H(e)}(x)) : x \in X) : e \in E\}$$

where

$$\mu_{H(e)}(x) = \begin{cases} \mu_{F(e)}(x) & , \text{if } e \in A - B \\ \mu_{G(e)}(x) & , \text{if } e \in B - A \\ \max\{\mu_{F(e)}(x), \mu_{G(e)}(x)\}, & \text{if } e \in A \cap B \end{cases}$$

$$\nu_{H(e)}(x) = \begin{cases} \nu_{F(e)}(x) & , \text{if } e \in A - B \\ \nu_{G(e)}(x) & , \text{if } e \in B - A \\ \min\{\mu_{F(e)}(x), \mu_{G(e)}(x)\}, & \text{if } e \in A \cap B \end{cases}$$

b) Extended intersection of (F, A) and (G, B) is denoted by $(F, E) \tilde{\cap}_E (G, B) = (H, C)$ where $C = A \cup B$ and (H, C) defined by;

$$(H,C) = \{(e,(x,\mu_{H(e)}(x),\nu_{H(e)}(x)):x \in X):e \in E\}$$

where

$$\mu_{H(e)}(x) = \begin{cases} \mu_{F(e)}(x) & ,\text{if } e \in A-B \\ \mu_{G(e)}(x) & ,\text{if } e \in B-A \\ \min\{\mu_{F(e)}(x),\mu_{G(e)}(x)\} & ,\text{if } e \in A \cap B \end{cases}$$

$$\nu_{H(e)}(x) = \begin{cases} \nu_{F(e)}(x) & ,\text{if } e \in A-B \\ \nu_{G(e)}(x) & ,\text{if } e \in B-A \\ \max\{\mu_{F(e)}(x),\mu_{G(e)}(x)\} & ,\text{if } e \in A \cap B \end{cases}$$

Let X be an initial universe and $PFS(X)$ denote the family of pythagorean fuzzy sets over X and $PFSS(X,E)$ be the family of all pythagorean fuzzy soft sets over X with parameters in E.

Definition 10. [29] Let $X \neq \emptyset$ be a universe set and $\tilde{\tau} \subset PFSS(X,E)$ be a collection of pythagorean fuzzy soft sets over X, then τ is said to be on pythagorean fuzzy soft topology on X if

(i) $\tilde{0}_{(X,E)}, \tilde{1}_{(X,E)}$ belong to $\tilde{\tau}$,

(ii) The union of any number of pythagorean fuzzy soft sets in $\tilde{\tau}$ belongs to $\tilde{\tau}$,

(iii) The intersection of any two pythagorean fuzzy soft sets in $\tilde{\tau}$ belongs to $\tilde{\tau}$.

The triple $(X,\tilde{\tau},E)_p$ is called an pythagorean fuzzy soft tpological space over X. Every member of τ is called a pythagorean fuzzy soft open set in X.

Definition 11. [29]

a) Let X be an initial universe set, E be the set of parameters and $\tilde{\tau} = \{\tilde{0}_{(X,E)}, \tilde{1}_{(X,E)}\}$. Then $\tilde{\tau}$ is called a pythagorean fuzzy soft indiscrete topology on X and $(X,\tilde{\tau},E)_p$ is said to be a pythagorean fuzzy soft indiscrete space over X.

b) Let X be an initial universe set, E be the set of parameters and $\tilde{\tau}$ be the collection of all pythagorean fuzzy soft sets which can be defined over X. Then $\tilde{\tau}$ is called a pythagorean fuzzy soft discrete topology on X and $(X,\tilde{\tau},E)_p$ is said to be a pythagorean fuzzy soft discrete space over X.

Definition 12. [29] Let $(X,\tilde{\tau},E)_p$ be a pythagorean fuzzy soft topological space over X. A pythagorean fuzzy soft set (F,E) over X is said to be a pythagorean fuzzy soft closed set in X, if its complement $(F,E)^c$ belongs to $\tilde{\tau}$.

Proposition 1. [29] Let $(X,\tilde{\tau},E)_p$ be a pythagorean fuzzy soft topological space over X. Then, the following properties hold.

(i) $\tilde{0}_{(X,E)}, \tilde{1}_{(X,E)}$ are pythagorean fuzzy soft closed set over X.

(ii) The intersection of any number of pythagorean fuzzy soft closed set is a pythagorean fuzzy soft closed set over X.

(iii) The union of any two pythagorean fuzzy soft closed set is a pythagorean fuzzy soft closed set over X.

Definition 13. [29] Let $(X,\tilde{\tau},E)_p$ be a pythagorean fuzzy soft topological space over X and (F,E) be a pythagorean fuzzy soft sets over X. The pythagorean fuzzy soft closure of (F,E) denoted by $pcl(F,E)$ is the intersection of all pythagorean fuzzy soft closed super sets of (F,E).

Clearly $pcl(F,E)$ is the smallest pythagorean fuzzy soft closed set over X which contain (F,E).

Theorem 1. [29] Let $(X,\tilde{\tau},E)_p$ be a pythagorean fuzzy soft topological space over X and $(F,E) \in PFSS(X,E)$. Then the following propeties hold.

(i) $pcl(\tilde{0}_{(X,E)}) = \tilde{0}_{(X,E)}$ and $pcl(\tilde{1}_{(X,E)}) = \tilde{1}_{(X,E)}$,

(ii) $(F,E) \tilde{\subseteq} pcl(F,E)$,

(iii) (F,E) is a pythagorean fuzzy soft closed set $\Leftrightarrow pcl(F,E) = (F,E)$,

(iv) $pcl(pcl(F,E)) = pcl(F,E)$,

(v) $(F,E) \tilde{\subseteq} (G,E) \Rightarrow pcl(F,E) \tilde{\subseteq} pcl(G,E)$,

(vi) $\mathrm{pcl}\big((\mathsf{F},\mathsf{E})\ \tilde{\cup}_{\mathrm{E}}\ (\mathsf{G},\mathsf{E})\big) = \mathrm{pcl}(\mathsf{F},\mathsf{E})\ \tilde{\cup}_{\mathrm{E}}\ \mathrm{pcl}(\mathsf{G},\mathsf{E})$.

Definition 14. [29] Let $(\mathsf{X},\tilde{\tau},\mathsf{E})_{\mathrm{p}}$ be a pythagorean fuzzy soft topological space over X and $(\mathsf{H},\mathsf{E}) \in \mathrm{PFSS}(\mathsf{X},\mathsf{E})$. The pythagorean fuzzy soft interior of (H,E), denoted by $\mathrm{pint}(\mathsf{H},\mathsf{E})$, is the union of all the pythagorean fuzzy soft open sets contained in (H,E).

Theorem 2. [29] Let $(\mathsf{X},\tilde{\tau},\mathsf{E})_{\mathrm{p}}$ be a pythagorean fuzzy soft topological space over X and $(\mathsf{H},\mathsf{E}) \in \mathrm{PFSS}(\mathsf{X},\mathsf{E})$. Then the following properties hold.
(i) $\mathrm{pint}(\tilde{0}_{(\mathrm{X},\mathrm{E})}) = \tilde{0}_{(\mathrm{X},\mathrm{E})}$ and $\mathrm{pint}(\tilde{1}_{(\mathrm{X},\mathrm{E})}) = \tilde{1}_{(\mathrm{X},\mathrm{E})}$,
(ii) $\mathrm{pint}(\mathsf{H},\mathsf{E}) \tilde{\subseteq} (\mathsf{H},\mathsf{E})$,
(iii) (H,E) is a pythagorean fuzzy soft open set $\Leftrightarrow \mathrm{pint}(\mathsf{H},\mathsf{E}) = (\mathsf{H},\mathsf{E})$,
(iv) $\mathrm{pint}\big(\mathrm{pint}(\mathsf{H},\mathsf{E})\big) = \mathrm{pint}(\mathsf{H},\mathsf{E})$,
(v) $(\mathsf{H},\mathsf{E}) \tilde{\subseteq} (\mathsf{G},\mathsf{E}) \Rightarrow \mathrm{pint}(\mathsf{H},\mathsf{E}) \tilde{\subseteq} \mathrm{pint}(\mathsf{G},\mathsf{E})$,
(vi) $\mathrm{pint}\big((\mathsf{H},\mathsf{E})\ \tilde{\cap}_{\mathrm{E}}\ (\mathsf{G},\mathsf{E})\big) = \mathrm{pint}(\mathsf{H},\mathsf{E})\ \tilde{\cap}_{\mathrm{E}}\ \mathrm{pint}(\mathsf{G},\mathsf{E})$.

Theorem 3. [29] Let $(\mathsf{X},\tilde{\tau},\mathsf{E})_{\mathrm{p}}$ be a pythagorean fuzzy soft topological space over X and $(\mathsf{H},\mathsf{E}) \tilde{\subseteq} \mathrm{PFSS}(\mathsf{X},\mathsf{E})$. Then
(i) $(\mathrm{pcl}(\mathsf{H},\mathsf{E}))^{\mathrm{c}} = \mathrm{pint}((\mathsf{H},\mathsf{E})^{\mathrm{c}})$
(ii) $\mathrm{pint}((\mathsf{H},\mathsf{E}))^{\mathrm{c}} = \mathrm{pcl}((\mathsf{H},\mathsf{E})^{\mathrm{c}})$

3. DENSE SETS ON PYTHAGOREAN FUZZY SOFT TOPOLOGICAL SPACES

Definition 15 *Let $(X,\tilde{\tau},E)_p$ be a pythagorean fuzzy soft topological space over X and $(F,E) \in PFSS(X,E)$. (F,E) is called dense in $(X,\tilde{\tau},E)_p$, if closure of (F,E) is $\tilde{1}_{(X,E)}$, i.e. $pcl(F,E) = \tilde{1}_{(X,E)}$.*

Example 1 *Let $X = \{x_1,x_2\}$, $E = \{e_1,e_2\}$ and*

$$\tilde{\tau} = \{\tilde{0}_{(X,E)}, \tilde{1}_{(X,E)}, (F_1,E), (F_2,E), (F_3,E), (F_4,E)\}$$

where $(G_1,E), (G_2,E), (G_3,E), (G_4,E)$ pythagorean fuzzy soft sets over X, defined as;

$$(F_1,E) = \begin{Bmatrix}(e_1,\{(x_1,0.45,0.12),(x_2,0.52,0.78)\})\\(e_2,\{(x_1,0.21,0.42),(x_2,0.14,0.45)\})\end{Bmatrix}$$
$$(F_2,E) = \begin{Bmatrix}(e_1,\{(x_1,0.76,0.32),(x_2,0.36,0.18)\})\\(e_2,\{(x_1,0.44,0.23),(x_2,0.71,0.67)\})\end{Bmatrix}$$
$$(F_3,E) = \begin{Bmatrix}(e_1,\{(x_1,0.76,0.12),(x_2,0.52,0.18)\})\\(e_2,\{(x_1,0.44,0.23),(x_2,0.71,0.45)\})\end{Bmatrix}$$
$$(F_4,E) = \begin{Bmatrix}(e_1,\{(x_1,0.45,0.32),(x_2,0.36,0.78)\})\\(e_2,\{(x_1,0.21,0.42),(x_2,0.14,0.67)\})\end{Bmatrix}$$

Then $\tilde{\tau}$ defines a pythagorean fuzzy soft topology on X and hence $(X,\tilde{\tau},E)_P$ is a pythagorean fuzzy soft topological space over X. Suppose that any $(G,E) \in PFSS(X,E)$ is defined as following:

$$(G,E) = \begin{Bmatrix}(e_1,\{(x_1,0.67,0.33),(x_2,0.58,0.23)\})\\(e_2,\{(x_1,0.73,0.12),(x_2,0.68,0.72)\})\end{Bmatrix}$$

Then (G,E) is pythagorean fuzzy soft dense set in $(X,\tilde{\tau},E)_P$, since $\tilde{1}_{(X,E)}$ is the only closed set in $(X,\tilde{\tau},E)_p$ containing (G,E) and hence $pcl(G,E) = \tilde{1}_{(X,E)}$.

Proposition 2 *Let $(X,\tilde{\tau},E)_p$ be a pythagorean fuzzy soft topological space over X and $(F,E),(G,E) \in PFSS(X,E)$ and $(F,E) \tilde{\subseteq} (G,E)$. If (F,E) is pythagorean fuzzy soft dense set in $(X,\tilde{\tau},E)_P$ then (G,E) must be dense in $(X,\tilde{\tau},E)_p$.*

Proof. By Theorem 1 if $(F,E) \tilde{\subseteq} (G,E)$, then $pcl(F,E) \tilde{\subseteq} pcl(G,E)$ and from the definition of pythagorean fuzzy soft dense set $pcl(F,E) = \tilde{1}_{(X,E)}$. We have $\tilde{1}_{(X,E)} \tilde{\subseteq} (G,E)$ implies $pcl(G,E) = \tilde{1}_{(X,E)}$. Thus (G,E) is dense set in $(X,\tilde{\tau},E)_p$.

Theorem 4 *A pythagorean fuzzy soft set $(F,E) \in PFSS(X,E)$ is dense set in pythagorean fuzzy soft topological space $(X,\tilde{\tau},E)_p$ if and only if $\tilde{1}_{(X,E)}$ is only closed set in $(X,\tilde{\tau},E)_p$ containing (F,E).*

Proof. Let $\tilde{1}_{(X,E)}$ is the only closed set in $(X,\tilde{\tau},E)_p$ containing (F,E), then from the definition of pythagorean fuzzy soft closure, we have $pcl(F,E) = \tilde{1}_{(X,E)}$ and hence (F,E) is dense in $(X,\tilde{\tau},E)_p$.

Conversely, let $(F,E) \in PFSS(X,E)$ be pythagorean fuzzy soft dense set in $(X,\tilde{\tau},E)_p$. If there exist an another closed set $(G,E) \neq \tilde{1}_{(X,E)}$ containing (F,E) then from the definition of closure, we have $pcl(F,E) = (G,E) \neq \tilde{1}_{(X,E)}$, which contradiction assumption. Thus $\tilde{1}_{(X,E)}$ is the only closed set in $(X,\tilde{\tau},E)_p$ containing (F,E).

Theorem 5 *Let $(X,\tilde{\tau},E)_p$ be a pythagorean fuzzy soft topological space over X and $(F,E),(G,E) \in PFSS(X,E)$. Then their union $(F,E)\ \tilde{\cup}_E\ (G,E)$ is pythagorean fuzzy soft dense in $(X,\tilde{\tau},E)_p$ if and only if one of them is dense in $(X,\tilde{\tau},E)_p$.*

Proof. ($\Rightarrow$) Let $(F,E),(G,E) \in PFSS(X,E)$ and their union $(F,E)\ \tilde{\cup}_E\ (G,E)$ be pythagorean fuzzy soft dense in $(X,\tilde{\tau},E)_p$. If (F,E) and (G,E)not dense in $(X,\tilde{\tau},E)_p$, then $pcl(F,E) \neq \tilde{1}_{(X,E)}$ and $pcl(G,E) \neq \tilde{1}_{(X,E)}$. Therefore $pcl((F,E)\ \tilde{\cup}_E\ (G,E)) = pcl(F,E)\ \tilde{\cup}_E\ pcl(G,E)$. $pcl((F,E)\ \tilde{\cup}_E\ (G,E)) = pcl(F,E)\ \tilde{\cup}_E\ pcl(G,E) \neq \tilde{1}_{(X,E)}$, which contradict our assumption. Thus one of them must be dense in $(X,\tilde{\tau},E)_p$.

($\Leftarrow$) Let $(F,E),(G,E) \in PFSS(X,E)$ and (F,E) be dense in $(X,\tilde{\tau},E)_p$, i.e, $pcl(F,E) = \tilde{1}_{(X,E)}$. Therefore $pcl((F,E)\ \tilde{\cup}_E\ (G,E)) = pcl(F,E)\ \tilde{\cup}_E\ pcl(G,E) = \tilde{1}_{(X,E)}\ \tilde{\cup}_E\ pcl(G,E) = \tilde{1}_{(X,E)}$. Thus $(F,E)\ \tilde{\cup}_E\ (G,E)$ is pythagorean fuzzy dense in $(X,\tilde{\tau},E)_p$.

Corollary 1 *Union of two pythagorean fuzzy soft dense sets in a pythagorean fuzzy soft topological space $(X,\tilde{\tau},E)_p$ is also dense in $(X,\tilde{\tau},E)_p$.*

Corollary 2 *Let $(X,\tilde{\tau},E)_p$ be a pythagorean fuzzy soft topological space over X and $(F,E) \in PFSS(X,E)$. If (F,E) is pythagorean fuzzy soft dense in $(X,\tilde{\tau},E)_p$, then for any $(G,E) \in PFSS(X,E)$, their union $(F,E)\ \tilde{\cup}_E\ (G,E)$ must be pythagorean fuzzy soft dense set in $(X,\tilde{\tau},E)_p$.*

Theorem 6 *Let $(X,\tilde{\tau},E)_p$ be a pythagorean fuzzy soft topological space over X and $(F,E),(G,E) \in PFSS(X,E)$. If $(F,E)\ \tilde{\cap}_E\ (G,E)$ is pythagorean fuzzy soft dense in $(X,\tilde{\tau},E)_p$, then (F,E) and (G,E) must be pythagorean fuzzy soft dense in $(X,\tilde{\tau},E)_p$.*

Proof. Let $(F,E),(G,E) \in PFSS(X,E)$ and their intersection $(F,E)\ \tilde{\cap}_E\ (G,E)$ is pythagorean fuzzy soft dense in $(X,\tilde{\tau},E)_p$. Then $pcl((F,E)\ \tilde{\cap}_E\ (G,E)) = \tilde{1}_{(X,E)}$.

$$\Rightarrow pcl(F,E)\ \tilde{\cap}_E\ pcl(G,E) \tilde{\supseteq} pcl((F,E)\ \tilde{\cap}_E\ (G,E)) = \tilde{1}_{(X,E)}$$
$$\Rightarrow pcl(F,E)\ \tilde{\cap}_E\ pcl(G,E) \tilde{\supseteq} \tilde{1}_{(X,E)}$$
$$\Rightarrow pcl(F,E) \tilde{\supseteq} \tilde{1}_{(X,E)} \text{and} pcl(G,E) \tilde{\supseteq} \tilde{1}_{(X,E)}$$
$$\Rightarrow pcl(F,E) = \tilde{1}_{(X,E)} \text{and} pcl(G,E) = \tilde{1}_{(X,E)}.$$

Remark 1 *The converse of the above theorem may not be true.*

Example 2 *Consider Example 1. Then pythagorean fuzzy soft sets*

$$(H_1,E) = \begin{Bmatrix} (e_1,\{(x_1,0.31,0.75),(x_2,0.12,0.25)\}) \\ (e_2,\{(x_1,0.42,0.16),(x_2,0.68,0.36)\}) \end{Bmatrix}$$

$$(H_2, E) = \begin{Bmatrix}(e_1, \{(x_1, 0.45, 0.82), (x_2, 0.35, 0.71)\}) \\ (e_2, \{(x_1, 0.51, 0.38), (x_2, 0.86, 0.68)\})\end{Bmatrix}$$

are pythagorean fuzzy soft dense in $(X, \tilde{\tau}, E)_p$, but their intersection

$$(H_1, E)\ \tilde{\cap}_E\ (H_2, E) = \begin{Bmatrix}(e_1, \{(x_1, 0.31, 0.82), (x_2, 0.12, 0.71)\}) \\ (e_2, \{(x_1, 0.42, 0.38), (x_2, 0.68, 0.68)\})\end{Bmatrix}$$

is not pythagorean fuzzy soft dense in $(X, \tilde{\tau}, E)_p$, since $pcl((H_1, E)\ \tilde{\cap}_E\ (H_2, E)) = (F_2, E)^c \neq \tilde{1}_{(X,E)}$.

4. NOWHERE DENSE SETS IN PYTHAGOREAN FUZZY SOFT TOPOLOGICAL SPACES

Definition 16 *Let $(X, \tilde{\tau}, E)_p$ be a pythagorean fuzzy soft topological space over X and $(F, E) \in PFSS(X, E)$. (F, E) is called nowhere dense set in $(X, \tilde{\tau}, E)_p$, if closure of $(pcl(F, E))^c$ is $\tilde{1}_{(X,E)}$, i.e. $pcl((pcl(F, E))^c) = \tilde{1}_{(X,E)}$.*

Example 3 *Consider Example 1. Then pythagorean fuzzy soft set*

$$(H, E) = \begin{Bmatrix}(e_1, \{(x_1, 0.12, 0.73), (x_2, 0.14, 0.82)\}) \\ (e_2, \{(x_1, 0.11, 0.91), (x_2, 0, 1)\})\end{Bmatrix}$$

is nowhere dense set in $(X, \tilde{\tau}, E)_p$.

Proposition 3 *Let $(X, \tilde{\tau}, E)_p$ be a pythagorean fuzzy soft topological space over X and $(F, E), (G, E) \in PFSS(X, E)$ such that $(G, E) \tilde{\subseteq} (F, E)$. If (F, E) is nowhere dense set in $(X, \tilde{\tau}, E)_p$ then (G, E) must be nowhere dense in $(X, \tilde{\tau}, E)_p$.*

Proof. Let $(G, E) \tilde{\subseteq} (F, E)$.

$$\Rightarrow pcl(G, E) \tilde{\subseteq} pcl(F, E)$$
$$\Rightarrow (pcl(G, E))^c \tilde{\supseteq} (pcl(F, E))^c$$
$$\Rightarrow pcl((pcl(G, E))^c) \tilde{\supseteq} pcl((pcl(F, E))^c)$$

and since (F, E) is nowhere dense in $(X, \tilde{\tau}, E)_p$, we have $pcl((pcl(F, E))^c) = \tilde{1}_{(X,E)}$. Therefore $pcl((pcl(G, E))^c) \tilde{\supseteq} pcl((pcl(F, E))^c) = \tilde{1}_{(X,E)}$, this implies $pcl((pcl(G, E))^c) \tilde{\supseteq} \tilde{1}_{(X,E)}$ and hence $pcl((pcl(G, E))^c) = \tilde{1}_{(X,E)}$. Thus (G, E) is nowhere dense in $(X, \tilde{\tau}, E)_p$.

Theorem 7 *Let $(X, \tilde{\tau}, E)_p$ be a pythagorean fuzzy soft topological space over X and $(F, E) \in PFSS(X, E)$. (F, E) is nowhere dense in $(X, \tilde{\tau}, E)_p$ if and only if $pint(pcl(F, E)) = \tilde{0}_{(X,E)}$.*

Proof. Let $(F, E) \in PFSS(X, E)$ be pythagorean fuzzy soft nowhere dense set in $(X, \tilde{\tau}, E)_p$. Then

$$pcl((pcl(G, E))^c) = \tilde{1}_{(X,E)}$$
$$\Rightarrow \left(pint(pcl(F, E))\right)^c = \tilde{1}_{(X,E)}, \text{(byTheorem3)}$$
$$\Rightarrow pint(pcl(F, E)) = \tilde{0}_{(X,E)}. \text{(Takingcomplement)}$$

Conversely, Let $pint(pcl(F, E)) = \tilde{0}_{(X,E)}$.

$$\Rightarrow \left(pint(pcl(F, E))\right)^c = \tilde{1}_{(X,E)} \text{(Takingcomplement)}$$
$$\Rightarrow pcl((pcl(G, E))^c) = \tilde{1}_{(X,E)} \text{(byTheorem3)}$$

Thus (F, E) is pythagorean fuzzy nowhere dense set in $(X, \tilde{\tau}, E)_p$.

Theorem 8 *Let $(X, \tilde{\tau}, E)_p$ be a pythagorean fuzzy soft topological space over X and $(F, E) \in PFSS(X, E)$. (F, E) is nowhere dense set in $(X, \tilde{\tau}, E)_p$ if and only if $pcl\big(pint((F, E)^c)\big) = \tilde{1}_{(X,E)}$.*

Proof. Straightforward.

Theorem 9 *Let* $(X,\tilde{\tau},E)_p$ *be a pythagorean fuzzy soft topological space over* X *and* $(F,E)\in PFSS(X,E)$. (F,E) *is nowhere dense set in* $(X,\tilde{\tau},E)_p$ *if and only if* $pint\big((pint((F,E)^c))^c\big)=\tilde{0}_{(X,E)}$.

Proof. Straightforward.

5. SOMEWHERE DENSE SETS IN PYTHAGOREAN FUZZY SOFT TOPOLOGICAL SPACES

Definition 17 *Let* $(X,\tilde{\tau},E)_p$ *be a pythagorean fuzzy soft topological space over* X *and* $(F,E)\in PFSS(X,E)$. (F,E) *is called somewhere dense set in* $(X,\tilde{\tau},E)_p$, *if*(F,E) *is not nowhere dense set, i.e.* $pcl((pcl(F,E))^c)\neq\tilde{1}_{(X,E)}$.

Example 4 *Consider Example 1. Then pythagorean fuzzy soft set*

$$(H,E)=\begin{Bmatrix}(e_1,\{(x_1,0.76,0.12),(x_2,0.52,0.18)\})\\(e_2,\{(x_1,0.44,0.23),(x_2,0.71,0.45)\})\end{Bmatrix}$$

is somewhere dense set in $(X,\tilde{\tau},E)_p$.

Theorem 10 *Every non-empty pythagorean fuzzy soft open set in pythagorean fuzzy soft topological space* $(X,\tilde{\tau},E)_p$ *is somewhere dense in* $(X,\tilde{\tau},E)_p$.

Proof. Let $(F,E)\in PFSS(X,E)$ be non-empty pythagorean fuzzy soft open set inpythagorean fuzzy soft topological space $(X,\tilde{\tau},E)_p$ and $pint(F,E)=(F,E)$. By Theorem 2, we have $(F,E)\tilde{\subseteq}pcl(F,E)$

$\Rightarrow pint(F,E)\tilde{\subseteq}pint(pcl(F,E))$
$\Rightarrow (F,E)\tilde{\subseteq}pint(pcl(F,E))$
$\Rightarrow \tilde{0}_{(X,E)}\neq(F,E)\tilde{\subseteq}pint(pcl(F,E))$
$\Rightarrow pint(pcl(F,E))\neq\tilde{0}_{(X,E)}$
$\Rightarrow \big(pint(pcl(F,E))\big)^c\neq\big(\tilde{0}_{(X,E)}\big)^c$
$\Rightarrow \big(pint(pcl(F,E))\big)^c\neq\tilde{1}_{(X,E)}$
$\Rightarrow pcl((pcl(F,E))^c)\neq\tilde{1}_{(X,E)}$(ByTheorem3).

Thus (F,E) is somewhere dense in $(X,\tilde{\tau},E)_p$.

Theorem 11 *Let* $(X,\tilde{\tau},E)_p$ *be a pythagorean fuzzy soft topological space over* X *and* $(F,E)\in PFSS(X,E)$. (F,E) *is somewhere dense set in* $(X,\tilde{\tau},E)_p$ *if and only if there exist a non-empty pythagorean fuzzy soft open set* $(G,E)\in\tilde{\tau}$ *such that* $(G,E)\tilde{\subseteq}pcl(F,E)$.

Proof. Let $(X,\tilde{\tau},E)_p$ be a pythagorean fuzzy soft topological space over X and $(F,E)\in PFSS(X,E)$. (F,E) is somewhere dense set in $(X,\tilde{\tau},E)_p$, then we have $pcl((pcl(F,E))^c)\neq\tilde{1}_{(X,E)}$.

$\Rightarrow \big(pint(pcl(F,E))\big)^c\neq\tilde{1}_{(X,E)}$(ByTheorem3)
$\Rightarrow pint(pcl(F,E))\neq\tilde{0}_{(X,E)}$(takingcomplement)

Here $pint(pcl(F,E))$ is a pythagorean fuzzy soft open subset of $pcl(F,E)$. Taking $(G,E)=pint(pcl(F,E))$, we have for $(F,E)\in PFSS(X,E)$ is somewhere dense set in $(X,\tilde{\tau},E)_p$, there exist a non-empty pythagorean fuzzy soft open set $(G,E)\in\tilde{\tau}$ such that $(G,E)\tilde{\subseteq}pcl(F,E)$.

Conversely, let for $(F,E)\in PFSS(X,E)$, there exist a non-empty pythagorean fuzzy soft open set $(G,E)\in\tilde{\tau}$ such that $(G,E)\tilde{\subseteq}pcl(F,E)$. This implies $(pcl(F,E))^c\tilde{\subseteq}(G,E)^c$

$\Rightarrow pcl((pcl(F,E))^c)\tilde{\subseteq}pcl((G,E)^c)$
$\Rightarrow pcl((pcl(F,E))^c)\tilde{\subseteq}(G,E)^c$

Also $(G,E) \neq \tilde{0}_{(X,E)} \Rightarrow (G,E)^c \neq \tilde{1}_{(X,E)}$. Thus we have $pcl((pcl(F,E))^c) \neq \tilde{1}_{(X,E)}$ and hence (F,E) is pythagorean fuzzy soft somewhere dense set in $(X,\tilde{\tau},E)_p$.

6. CONCLUSION

In this paper, definitions of different types of dense sets, nowhere dense sets and anywhere dense sets of pythagorean fuzzy soft topological spaces have been presented and some of the basic properties of these concepts have been discussed. The interrelationships between the different notions were also studied in detail. Finally, we have to say that this paper is only the beginning of a new structure and that we have just learned a few theories, it would be important to carry out further theoretical studies in order to develop a general system for functional applications.

REFERENCES

1. B. Ahmad and S. Hussain, On some structures of soft topology, Mathematical Sciences vol.6 no.64 (2012), pp. 1–7.
2. K. Atanassov, Intuitionistic fuzzy sets, Fuzzy Sets and Systems, vol. 20 (1986), pp. 87-96.
3. T. M. Athira, S. J. John and H. Garg, Entropy and distance measures of Pythagorean fuzzy soft sets and their applications, Journal of Intelligent & Fuzzy Systems vol. 37 (2019) pp. 4071–4084, Doi:10.3233/JIFS-190217
4. N. Cagman, S. Karatas and S. Enginoglu, Soft topology, Computers and Mathematics with Applications vol. 62 (2011), pp. 351–358.
5. C. Chang, Fuzzy topological spaces, J. Math. Anal. Appl., vol. 24 (1968), pp.182–190.
6. D. Coker, An introduction of intuitionistic fuzzy topological spaces, Fuzzy Sets and Systems, vol. 88 (1997), pp. 81-89.
7. A. Guleria, R. K. Bajaj, On pythagorean fuzzy soft matrices, operations and their applications in decision making and medical diagnosis, Soft Computing, vol. 23 (2019), pp. 1889–7900, Doi:10.1007/s00500-018-3419-z.
8. A. Hussain, M. I. Ali and T. Mahmood, Pythagorean fuzzy soft rough sets and their applications in decision-making, Journal of Taibah University for Science, vol. 14 no. 1 (2020) , pp. 101-113, doi: 10.1080/16583655.2019.1708541
9. A. Mukherjee, A.K. Das, A. Saha, Theory of dense sets in intuitionistic fuzzy soft topological spaces, Bullettin of Kerala Mathematics Assıciation, vol. 12 no.1 (2015), pp.87-95.
10. M. Kirisci, New type pythagorean fuzzy soft set and decision-making application, arXiv preprint arXiv:1904.04064, (2019).
11. Z. Li and R. Cui, On the topological structure of intuitionistic fuzzy soft sets, Annals of Fuzzy Mathematics and Informatics vol. 5 no.1 (2013), pp. 229–239.
12. P. K. Maji, R. Biswas, A. R. Roy, Fuzzy soft sets, Journal of Fuzzy Mathematics vol. 9 no. 3 (2001), pp. 589–602.
13. D. Molodtsov, Soft set theory-first results, Comput. Math. Appl., vol. 37(4-5) (1999), pp. 19–31.
14. M. Olgun, M. Unver, S. Yardımcı, Complex and Intelligent Systems, (2019).
15. I. Osmanoglu, D. Tokat, On intuitionistic fuzzy soft Topology, Gen. Math. Notes, vol. 19 no. 2 (2013), 59–70.
16. Z. Pawlak, Rough sets, Int. J. Comput. Sci., vol. 11 (1982), pp. 341–356.
17. X. Peng, Y. Yang, Some results for pythagorean fuzzy sets, International Journal of Intelligent Systems vol. 30 no.11 (2015), pp. 1133–1160.
18. X. Peng, Y. Yang, J. Song, Y. Jiang, Pythagoren fuzzy soft set and its application, Computer Engineering vol. 41 no.7 (2015), pp. 224–229.
19. X. Peng, New operations for interval-valued pythagorean fuzzy set, Scientia Iranica E, vol. 26 no.2 (2019), pp. 1049–1076.
20. M. Riaz, N. Cagman, I. Zareef and M. Aslam, N-soft topology and its applications to multi-criteria group decision making, Journal of Intelligent & Fuzzy Systems vol. 36 no.6 (2019), pp.6521–6536.

21. M. Riaz, F. Smarandache,A. Firdous and A. Fakhar,On soft rough topology with multi-attribute group decision making, Mathematics vol. 7 no.67 (2019), pp.1–18.
22. M. Riaz, B. Davvaz, A. Firdous and A. Fakhar, Novel concepts of soft rough set topology with applications, Journal of Intelligent & Fuzzy Systems vol.36 no.4 (2019), pp. 3579–3590.
23. M. Riaz, K. Naeem, M. Aslam, D. Afzal, F. Ahmahdi and S.S. Jamal Multi-criteria Group Decision Making with Pythagorean Fuzzy Soft Topology. Journal of Intelligent and Fuzzy Systems, (2020) pp. 1–18, Doi:10.3233/JIFS-190854.
24. S.Roy and T.K. Samanta,Anote on a soft topological space, Punjab University Journal of Mathematics vol. 46 no.1 (2014), pp.19–24.
25. M. Shabir, M. Naz, On soft topological spaces, Comput. Math. Appl., vol.61 (2011), pp.1786-1799.
26. G. Shahzadi and M. Akram, Hypergraphs based on pythagorean fuzzy soft model, Math. Comput. Appl., (2019), doi:10.3390/mca24040100
27. R.R. Yager, Pythagorean fuzzy subsets, Proc. Joint IFSA World Congress NAFIPS Annual Meet., 1, Edmonton, Canada, pp. 57-61 (2013).
28. R.R. Yager and A.M. Abbasov, Pythagorean membership grades, complex numbers, and decision making, Int. J. Intell. Syst., vol.28 no.5, (2014). pp.436-452
29. A. Yolcu and T.Y. Ozturk, Some New Results on Pythagorean Fuzzy Soft Topological Spaces, TWMS J. App. Eng. Math. Accepted.
30. L. A. Zadeh, Fuzzy Sets, Information and Control, vol. 8 (1965), pp. 338-353.
31. S. Zeng, J. Chen and X. Li, A Hybrid Method for Pythagorean Fuzzy Multiple-Criteria Decision Making, International Journal of Information Technology and Decision Making, Vol. 15, No. 2 (2016) pp. 403–422, Doi: 10.1142/S0219622016500012.

Analyzing Cerebral Infarction Data to Detect Ischemic Stroke with Ensemble Learning Approach

Faisa MAULIDINA[1], Afifah Rofi LAELI[1] and Zuherman RUSTAM[1]

[1]*Department of Mathematics, University of Indonesia, Depok 16424, Indonesia*

faisa.maulidina@ui.ac.id
afifahrl@sci.ui.ac.id
rustam@ui.ac.id

Abstract. Stroke is the second deadliest disease in the world that occurs when blood supply to the brain is disrupted or reduced due to blockage or rupture of a blood vessel. There are two types of stroke, namely hemorrhagic and ischemic stroke. Ischemic stroke is the most common type in Indonesia and accounts for about 52.9% of all stroke cases. Infarction often occurs in ischemic stroke because of insufficient supply of oxygen and nutrients to the brain. This is due to the disruption of blood flow to the brain. The detection of cerebral infarction assists the health sector in diagnosing ischemic stroke. The data used in this study were obtained from the Department of Radiology, Dr. Cipto Mangunkusumo Hospital, Jakarta, Indonesia which consisted of 206 samples and 7 features. The features of the data were obtained from descriptions of brain imaging CT Scans. To analyze cerebral infarction data, two ensemble learning methods were compared. They include Random Forest (RF) and Extreme Gradient Boosting (XGBoost). In terms of accuracy performance, the average accuracy of Random Forest was slightly higher than the average accuracy of XGBoost. However, the highest average accuracy produced by both methods was 95.2% on 90% of training data. In terms of running time computation performance, XGBoost was 10 times faster than RF. Using 90% of training data, XGBoost and RF required 2 and 21.7 seconds of running time computation, respectively. Thus, in analyzing cerebral infarction data, Random Forest produced higher accuracy performance, while XGBoost was faster in running time computation performance.

1. INTRODUCTION

Stroke is a disease that occurs when blood supply to the brain is disrupted or reduced due to blockage or rupture of the blood vessel [1]. Therefore, the brain is unable to receive oxygen and nutrients due to this circulatory disorder [2]. This leads to damage or death of the affected brain cells [2]. The part of the body which is controlled by the damaged brain area may no longer function properly. Stroke is a medical emergency because brain cells can die in a matter of minutes [3]. Prompt treatment is therefore needed to minimize the possibility of complications [3].

Based on data from WHO Global Health Estimates (GHE) in 2016, stroke is the second deadliest disease in the world after ischemic heart disease [4]. This has accounted for about 5.7 million deaths or 10.2% of total deaths [4]. Indonesia's Sample Registration System (SRS) from 2014-2016 consistently reported stroke as the first leading cause of death, responsible for 21.1%, 20.4%, and 19.9% death for all age groups, respectively each year [5]-[6]. According to Indonesia Basic Health Research (*Riskesdas*) 2018, the prevalence of stroke based on diagnosis in population aged more than 15 years is 10.9 per mil, with the highest prevalence occurring in East Kalimantan (14.7 per mil) [7].

There are two types of stroke based on pathological background, namely haemorrhagic and ischemic stroke [8]. Haemorrhagic stroke occurs when a blood vessel ruptures, causing a stop in brain function [8]. The most common cause of this type of stroke is hypertension or aneurysm rupture. Ischemic stroke is caused by a blockage or blood clot in the large arteries that supply blood to the brain due to embolism or atherosclerosis [8]. Of the two types of strokes, ischemic stroke (infarction) is the most common type in Indonesia. This accounts for about 52.9% of all stroke cases [9].

Infarction often occurs in ischemic stroke. This is due to insufficient supply of oxygen and nutrients to an area of the brain caused by disruption in blood flow [10]. Thrombotic cerebral infarction occurs when blood clot forms inside the arteries that supply blood to the brain [8]. Embolic cerebral infarction occurs when blood clot forms inside the

heart or aorta and is then transported to the brain [8]. Lastly, lacunar cerebral infarction occurs when blood clot forms in small penetrating arteries due to local disease of these vessels (for example chronic hypertension) [8].

The detection of cerebral infarction has assisted in the diagnosis of ischemic stroke. This is carried out by a Computed Tomography (CT) Scan. However, the description obtained from a CT Scan alone is not enough to detect cerebral infarction. Therefore, machine learning is used to classify cerebral infarction with the description obtained from a CT Scan as its features. To obtain a better result, two ensemble learning classifiers were compared in this study. They include Random Forest and Extreme Gradient Boosting (XGBoost). Ensemble learning combines several base models to produce a more accurate output [11]. The base models for both classifiers used were Decision Trees.

Several methods have been carried out by previous researchers to classify cerebral infarction data. They include Support Vector Machine (SVM) with hybrid preprocessing method [9], SVM using polynomial and Gaussian kernel [12], SVM with artificial bee colony and particle swarm optimization feature selection [13], Multiple Support Vector Machine (MSVM) with information gain feature selection [14], and Naïve Bayes [15]. Furthermore, Random Forest has also been used to classify breast cancer [16], ovarian cancer [17], prostate cancer [18], thalassemia [19], etc. Meanwhile XGBoost has been used to classify pathways that detect different conditions in gene expression data [20], to classify symptom severity [21], and to detect intrusion in networks [22].

2. MATERIAL AND METHODS

The comparison of two ensemble learning methods, namely Random Forest and XGBoost were proposed as classifiers for the cerebral infarction data. This section explains the research method used in this study. It includes information about cerebral infarction data, ensemble learning, Random Forest classifier, XGBoost classifier and model performance used to compare both classifiers.

A. Dataset

In this study, cerebral infarction data was used to detect ischemic stroke in patients. This was carried out by the Department of Radiology, Dr. Cipto Mangunkusumo Hospital, Jakarta, Indonesia in 2018 with 206 samples and 7 features. The 206 samples consisted of 103 samples each from patients having cerebral infarction and individuals without cerebral infarction. The features of the data were obtained from descriptions of brain imaging CT Scans.

Fig. 1 Brain imaging CT Scans from individuals without infarction (left) and individuals with infarction (right) [12]

Information of cerebral infarction data features:

- Area : Size of infarction area (in cm^2)
- Min : Minimum value of infarction
- Max : Maximum value of infarction
- Average : Average value of infarction
- SD : Standard error value of infarction

- Sum : Total amount value of infarction
- Length : Length of infarction (in cm)

B. Ensemble Learning

Ensemble learning is one of the supervised learning methods in machine learning. This method combines several base models to improve the performance of the base model to be used [11]. It was developed initially to reduce variance in automatic decision-making system. Subsequently, it was upgraded continuously until it could successfully overcome various machine learning problems, such as missing features, error correction, imbalance data, feature selection, etc [23]. Furthermore, for several years, it has been proven that ensemble learning is very effective and has numerous purposes in real world applications, especially in handling large volume of data.

There are two main approaches in ensemble learning, namely averaging and boosting [24]. In averaging or bagging method, several base models are built independently, the final prediction is obtained from the average value of each base model's prediction or voting for regression and classification problems, respectively [24]. Meanwhile in boosting method, several base models are built sequentially, where the building of one base model depends on the performance of the previous model [24]. Random Forest and XGBoost are examples of each approach, respectively. The base model used for both approaches was Decision Tree.

C. Random Forest

Random forest is an ensemble learning method that uses Decision Tree as its base model. It was first developed by Tin Kam Ho in 1995 [25]. Decision Tree is a white box machine learning model. This implies that the knowledge extracted by this model is in form of rules that can be easily explained with Boolean logic [24]. In Decision Tree, a node represents the test for a particular feature, a branch represents result of the previous test, a leaf node represents a class target or score and a path from the root to leaf node states the rules.

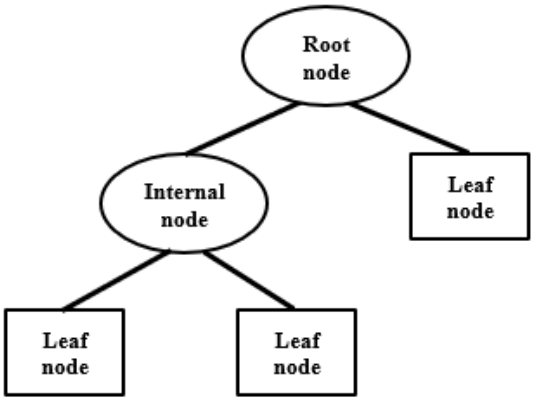

Fig. 2 Illustration of Decision Tree

Random forest uses the bagging approach of ensemble learning. This implies that target prediction in this model was obtained by combining the prediction results from several randomized decision trees which were built independently [24]. Each randomized decision tree was built from each bootstrap. Bootstrap is a set of samples from training data which are drawn randomly with replacement. The feature selected as a node in the decision tree is the best from the randomly selected features. As a classifier, Random Forest gives the final prediction based on the highest vote, i.e. the class which appears often as the predicted target of each randomized decision tree [24]. Despite being known to reduce variance and relatively robust against outliers and noise, Random Forest takes longer time computation especially in large number of trees.

Random Forest Algorithm
Input: A training set $D=\{(x_i, y_i)\}_{i=1:n}$, P features, and M number of trees.

Process:
For m = 1 to M:
1. Draw a bootstrap sample D_m from training data D
2. Grow a decision tree model $h_m(x)$ from bootstrap sample D_m by repeating the steps bellow until the stopping criteria are fulfilled.
   i. Select randomly, small subset of P consisting of p features
   ii. Select the best feature as node of the decision tree using Gini impurity function
   iii. Split the node into two internal nodes
   iv. Recursively repeat step ii and iii until it reaches leaf nodes

Output: $F(x)=\frac{1}{M}\sum_{m=1}^{M}h_m(x)$

Fig. 3 Random Forest Algorithm [24]

D. Extreme Gradient Boosting (XGBoost)

Gradient boosting is a boosting-based ensemble learning method in machine learning. This method combines several weak base learners incrementally, to form a stronger learner with higher accuracy [26]. XGBoost is an upgraded method from bagging approach that handles bias and deals with large volume of data with high computational speed [27]. Decision Tree of a fixed size, especially CART (Classification and Regression Tree), was used as weak learners in XGBoost classifier.

Given $\{(x_i, y_i)\}_{i=1:n}$ as n samples of training data, XGBoost sequentially adds tree learners from previous ensemble residual values. For m number of iterations or boosting rounds, $m>0, m\in \mathrm{N}$ the ensemble at m-th iteration is written as:

$$F_m(x)=\hat{y}^m=\sum_{i=0}^{m}h_i(x) \tag{2.1}$$

where $h_m(x)$ learns from the previous ensemble model F_{m-1} that minimize loss function L. The initialization ensemble $F_0(x)$ was obtained from the original dataset. The optimization problem in XGBoost was solved by minimizing the objective function L^t, that is:

$$\min L^{(m)}=\min\sum_{i=1}^{n}l(y_i,\hat{y}^{m-1}+h_m(x_i))+\alpha(h_m) \tag{2.2}$$

$$\alpha(h_m)=\gamma T+\frac{\lambda\|w\|^2}{2} \tag{2.3}$$

where l is a loss function, $\hat{y}^{m-1}$ is the label predicted in last iteration, h_m is the decision tree output, T is number of tree nodes, w is weight value, γ is regularization parameter and λ is minimum loss parameter.

XGBoost Algorithm
Input: A training set $D = \{(x_i, y_i)\}_{i=1:n}$, loss function L, M number of trees.
Process:

1. Model initialization: $F_0(x) = \min \sum_{i=1}^{n} L(y_i, \alpha)$
2. For m = 1 to M:

   Calculate ensemble model $F_m(x) = \hat{y}^m = \sum_{i=0}^{m} h_i(x)$ that minimizes loss function L in previous (m-1)-th iteration

$$\min L^{(m)} = \min \sum_{i=1}^{n} l(y_i, \hat{y}^{m-1} + h_m(x_i)) + \alpha(h_m)$$

$$\alpha(h_m) = \gamma T + \frac{\lambda \|w\|^2}{2}$$

Output: $F_m(x)$

Fig. 4 XGBoost Algorithm [24]

E. Model Performance

In this study, two ensemble learning methods in machine learning were compared, namely Random Forest and XGBoost. To evaluate which method produces the best performance, the measure of accuracy value obtained from confusion matrix and running time computation of each algorithm were calculated. The better method produced a higher accuracy value and faster running time compared to the other method.

Table 1. Confusion Matrix

Class		Prediction	
		Infarction	Normal
Actual	Infarction	True Positive (TP)	False Negative (FN)
	Normal	False Positive (FP)	True Negative (TN)

Based on the confusion matrix, the measure of accuracy value was:

$$\text{Accuracy} = \frac{TP + TN}{TP + FN + FP + TN} \tag{2.4}$$

3. RESULTS AND ANALYSIS

The implementation of Random Forest and XGBoost to classify the cerebral infarction data was carried out using Python3 programming language. Each classifier fits the training data with a proportion ranging from 10% to 90%, which was divided using holdout validation. Holdout validation randomly divides a dataset into training and testing data thus it is very dependent on the data used. To overcome this problem, the simulations were done 5 times for each proportion of training data.

Random Forest and XGBoost have several parameters. However, both methods have one parameter in common, namely n_estimators, which represents number of trees to be built. In this study, this parameter was optimized using Grid Search hyperparameter optimization method with the list of value assigned to be optimized is {10, 50, 100, 500, 1000} on each classifier used.

A. Random Forest Classifier Results Analysis

The tests were performed on cerebral infarction data using Random Forest classifier. The accuracy and running time results performance for each proportion of training data are shown in Table 2 and Table 3, respectively.

Table 2. Accuracy of Random Forest Classifier

Training Data (%)	Running Time (s)					Average Running Time (s)
	1	2	3	4	5	
10	19.8	19.8	20.0	20.4	20.0	**20.0**
20	20.2	20.4	20.7	20.3	20.4	20.4
30	20.4	20.3	20.4	20.3	20.4	20.4
40	20.8	20.5	22.0	21.0	20.8	21.0
50	20.7	20.8	21.1	20.9	20.7	20.8
60	21.5	20.7	20.8	20.9	20.8	20.9
70	22.3	21.1	22.4	21.0	21.8	21.7
80	21.5	21.6	21.5	21.3	21.4	21.5
90	21.6	21.5	21.5	22.1	21.9	**21.7**

From Table 2, the accuracy results of each simulation using Random Forest were different for the same proportion of training data. This is likely because Random Forest builds tree independently and holdout validation randomly divides data into train and test sets. Thus, every simulation on each proportion of training data produced different accuracy.

The lowest accuracy obtained using Random Forest classifier was 81.7% with 10% training data on fourth simulation, while the highest accuracy obtained was 100% with 90% training data on fifth simulation. The average accuracy values of the five simulations at each training data show that the highest average accuracy that Random Forest can obtain was 95.2% on 90% training data, while the lowest average accuracy was 87% on 10% of training data.

Table 3. Running Time of Random Forest Classifier

Training Data (%)	Accuracy (%)					Average Accuracy (%)
	1	2	3	4	5	
10	88.2	90.9	89.8	**81.7**	84.4	**87.0**
20	90.9	90.3	90.9	90.9	91.5	90.9
30	90.3	88.3	90.3	88.3	89.7	89.4
40	91.1	90.3	90.3	90.3	90.3	90.5
50	90.3	91.3	87.4	90.3	89.3	89.7
60	89.2	88.0	88.0	86.7	86.7	87.7
70	91.9	91.9	90.3	91.9	90.3	91.3
80	88.1	92.9	92.9	90.5	97.6	92.4
90	90.5	95.2	95.2	95.2	**100**	**95.2**

From Table 3, the running times computation of Random Forest varied from 19.5 to 22.5 seconds for every simulation of each proportion of training data used. The fastest average running time was 20 seconds on 10% training data, while the lowest running time was 21.7 seconds on 90% training data.

B. XGBoost Classifier Results Analysis

The tests were performed on cerebral infarction data using XGBoost classifier. The accuracy and running time results performance for each proportion of training data are shown in Table 4 and Table 5, respectively.

Table 4. Accuracy of XGBoost Classifier

Training Data (%)	Running Time (s)					Average Running Time (s)
	1	2	3	4	5	
10	0.8	0.8	0.8	0.8	0.8	**0.8**
20	1.0	0.9	0.9	1.0	0.9	0.9
30	1.1	1.1	1.1	1.1	1.1	1.1
40	1.3	1.3	1.2	1.2	1.2	1.2
50	1.4	1.4	1.4	1.4	1.4	1.4
60	1.5	1.5	1.5	1.5	1.5	1.5
70	1.7	1.7	1.7	1.7	1.7	1.7
80	1.9	1.8	1.8	1.8	1.8	1.8
90	2.0	2.0	2.0	2.0	2.0	**2.0**

From Table 4, the accuracy results of each simulation using XGBoost were the same for every proportion of training data. This is likely because XGBoost builds tree sequentially, it learns from previous model and improve the performance on next model. Thus, although holdout validation randomly divides the data, every simulation on each proportion of training data produced the same accuracy. This shows that XGBoost classifier produced more stable accuracy compared to Random Forest classifier.

The lowest accuracy obtained using XGBoost classifier was 85.5% with 60% training data on every simulation, while the highest accuracy obtained was 95.2% with 90% training data on every simulation. The average accuracy values of the five simulations at each training data were the same as every accuracy value on every simulation.

Table 5. Running Time of XGBoost Classifier

Training Data (%)	Accuracy (%)					Average Accuracy (%)
	1	2	3	4	5	
10	88.2	88.2	88.2	88.2	88.2	88.2
20	89.7	89.7	89.7	89.7	89.7	89.7
30	89.7	89.7	89.7	89.7	89.7	89.7
40	89.5	89.5	89.5	89.5	89.5	89.5
50	87.4	87.4	87.4	87.4	87.4	87.4
60	**85.5**	**85.5**	**85.5**	**85.5**	**85.5**	**85.5**
70	88.7	88.7	88.7	88.7	88.7	88.7
80	90.5	90.5	90.5	90.5	90.5	90.5
90	**95.2**	**95.2**	**95.2**	**95.2**	**95.2**	**95.2**

From Table 5, increasing the training data proportion, produced a higher running time computation with XGBoost classifier program. The running times computation varied from 0.8 to 2 seconds for every simulation of each proportion of training data used. The fastest average running time was 0.8 seconds with 10% training data, while the lowest running time was 2 seconds with 90% training data.

C. Performance Comparison of Random Forest and XGBoost

To analyze the comparison of accuracy and running time computation for Random Forest and XGBoost, two graphs were provided for each performance as shown in Fig. 5 and Fig. 6.

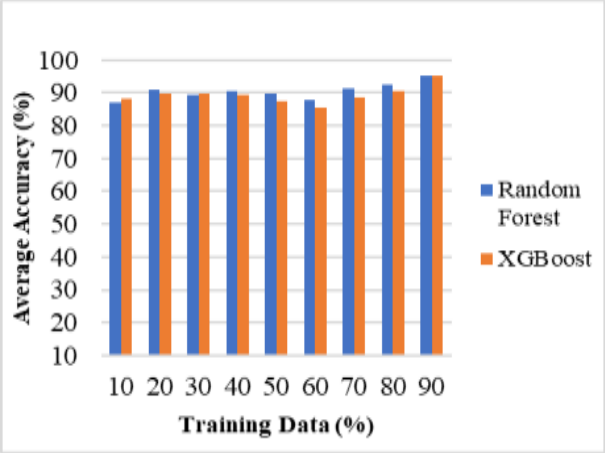

Fig. 5 Accuracy comparison of Random Forest and XGBoost classifiers

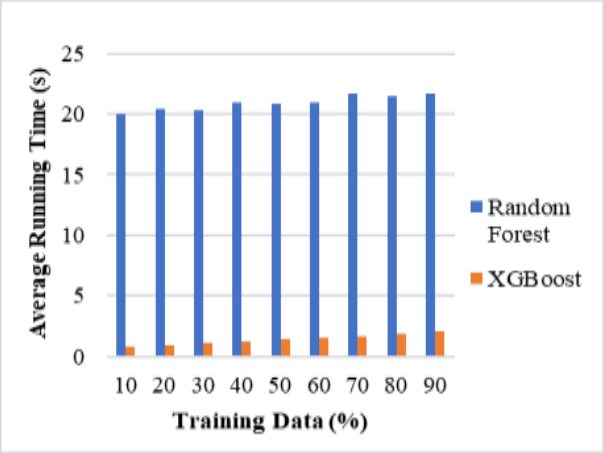

Fig. 6 Running time comparison of Random Forest and XGBoost classifiers

Fig. 5 shows that was no significant difference between the average accuracy of Random Forest and XGBoost classifiers. The graph of the average accuracy for each training data tends to have similar changes on both methods. However, the average accuracy of Random Forest was slightly higher than the average accuracy of XGBoost. The highest average accuracy value produced was same for both methods, which was 95.2% on 90% training data. The lowest average accuracy value produced by XGBoost was 85.5% on 60% training data. This value is 1.5% lower than the lowest accuracy value of the Random Forest classifier, which was 87% on 10% training data.

From Fig. 6, it is seen that the average running time computation of XGBoost method tends to increase with the proportion of training data, while that of Random Forest method was not very stable as the proportion of training data increased. There was a significant difference between the average running time of Random Forest and XGBoost classifiers. For each proportion of training data used, the average running time of XGBoost had a time ranged from 0 to 2 seconds. This was far different from the running time of Random Forest which ranged from 20 to 22 seconds. Therefore, XGBoost classifier is better than Random Forest classifier in terms of running time computation.

4. CONCLUSION

The classification of cerebral infarction as one of the causes of ischemic stroke assists the health sector in making its diagnoses. The images from brain CT Scans of patients with infarction and individuals without infarction provided some descriptions that were used as features for the dataset. To find the model that has the best performance in classifying cerebral infarction data, two ensemble learning methods were compared as classifiers, namely Random Forest and XGBoost.

From several experiments and analyzes that have been carried out, Random Forest and XGBoost produced average accuracy values that were not very different. However, the average accuracy of Random Forest was slightly higher than the average accuracy of XGBoost. Both methods produced an accuracy value of 95.2% with 90% training data as their highest average accuracy. Meanwhile, for running time computation performance, XGBoost was a lot faster than Random Forest. XGBoost and Random Forest required an average running time of 2 and 21.7 seconds respectively, with 90% of training data. Random Forest was 10 times longer than XGBoost. Thus, in analyzing cerebral infarction data, Random Forest produced higher accuracy performance, while XGBoost was faster in running time computation performance.

ACKNOWLEDGEMENT

This research is supported financially by The Indonesian Ministry of Research, Technology, with a KEMENRISTEK/BRIM 2021 research grant scheme.

REFERENCES

1. M. O. Owolabi *et al*, The burden of stroke in Africa: a glance at the present and a glimpse into the future, Cardiovasc. J. Afr., vol. 26(2 H3Africa Suppl), pp. S27-S38, 2015.
2. C. Rink and S. Khanna, Significance of brain tissue oxygenation and the arachidonic acid cascade in stroke, Antioxidants & Redox Signaling, vol. 14, no. 10, pp. 1889-1903, 2011.
3. J. Emberson *et al*, Effect of treatment delay, age, and stroke severity on the effects of intravenous thrombolysis with alteplase for acute ischaemic stroke: a meta-analysis of individual patient data from randomised trials, The Lancet, vol. 384(9958), pp. 1929-1935, 2014.
4. World Health Organization (WHO), Global Health Estimates 2016: Deaths by Cause, Age, Sex, by Country and by Region 2000-2016, World Health Organization, Geneva, 2018.
5. National Institute for Health Research and Development (NIHRD), Indonesia Sample Registration System – Deaths 2014, Ministry of Health Republic of Indonesia, Jakarta, 2015.
6. Y. Usman *et al*, Indonesia's sample registration system in 2018: A work in progress, JPSS, vol. 27, pp. 39-52, 2019.
7. National Institute for Health Research and Development (NIHRD), National Report on Basic Health Research (*Riskesdas*) 2018, Ministry of Health Republic of Indonesia, Jakarta, 2019.
8. T. Truelsen, S. Begg and C. Mathers, The global burden of cerebrovascular disease, World Health Organization, Geneva, 2000.
9. Z. Rustam *et al*, Hybrid preprocessing method for Support Vector Machine for classification of imbalanced cerebral infarction datasets, International Journal on Advanced Science, Engineering and Information Technology, vol. 9, no. 2, pp. 685-691, 2019.
10. L. Zhao *et al*, Strategic infarct location for post-stroke cognitive impairment: a multivariate lesion-symptom mapping study, Journal of Cerebral Blood Flow & Metabolism, vol. 38(8), pp. 1299-1311, 2018.
11. G. Seni and J. F. Elder, Ensemble methods in data mining: improving accuracy through combining predictions, Synthesis Lectures on Data Mining and Knowledge Discovery, vol. 2, pp. 1-126, 2010.
12. A. R. Bagasta *et al*, Comparison of cubic SVM with gaussian SVM: classification of infarction for detecting ischemic stroke, IOP Conf. Series: Materials Science and Engineering, vol. 546(5), article no. 052016, 2019.
13. Z. Rustam *et al*, Analyzing cerebral infarction using support vector machine with artificial bee colony and particle swarm optimization feature selection, J. Phys.: Conf. Series, vol. 1490(1), article no. 012031, 2020.
14. Z. Rustam, A. Arfiani and J. Pandelaki, Cerebral infarction classification using multiple support vector machine with information gain feature selection, Bulletin of Electrical Engineering and Informatics, vol. 9, no. 4, pp. 1578-1584, 2020.
15. S. G. Fitri *et al*, Naïve bayes classifier models for cerebral infarction classification, J. Phys.: Conf. Series, vol. 1490(1), article no. 012019, 2020.
16. C. Aroef, Y. Rivan and Z. Rustam, Comparing random forest and support vector machines for breast cancer classification, Telkomnika, vol. 18(2), pp. 815-821, 2020.
17. A. Arfiani and Z. Rustam, Ovarian cancer data classification using bagging and random forest, AIP Conf. Proc., vol. 2168(1), article no. 020046, 2019.
18. M. Huljanah *et al*, Feature selection using Random Forest classifier for predicting prostate cancer, IOP Conf. Series: Materials Science and Engineering, vol. 546(5), article no. 052031, 2019.
19. F. R. Aszhari *et al*, Classification of thalassemia data using random forest algorithm, J. Phys.: Conf. Series, vol. 1490(1), article no. 012050, 2020.
20. G. N. Dimitrakopoulos, Pathway analysis using XGBoost classification in biomedical data, Proceedings of the 10th Hellenic Conference on Artificial Intelligence, article no. 46, pp. 1-6, 2018.
21. Y. Liu *et al*, Symptom severity classification with gradient tree boosting, Journal of Biomedical Informatics, vol. 75, pp. S105-S111, 2017.
22. S. Bhattacharya *et al*, A novel PCA-firefly based XGBoost classification model for intrusion detection in networks using GPU, Electronics, vol. 9(2), pp. 219, 2020.
23. C. Zhang and Y. Ma, Ensemble Machine Learning: Methods and Applications, Springer Science & Business Media, New York, 2012.
24. C. H. Bishop, Pattern Recognition and Machine Learning, Springer, New York, 2006.

25. T. K. Ho, Random decision forests (PDF), Proceedings of the 3rd International Conference on Document Analysis and Recognition, vol. 1, pp. 278-282, 1995.
26. J. H. Friedman, Greedy function approximation: a gradient boosting machine, Annals of Statistics, vol. 29, no. 5, pp. 1189-1232, 2001.
27. T. Chen and C. Guestrin, XGBoost: a scalable tree boosting system, Proceedings of the 22nd ACM SIGKDD International Conference on Knowledge Discovery and Data Mining, pp. 785-794, 2016.

Comparing Some Kernels of Support Vector Machine for Acute Sinusitis Classification

Alva Andhika SA'ID, Fildzah ZHAFARINA, Zuherman RUSTAM

Department of Mathematics, Faculty of Mathematics and Science, University of Indonesia, Depok-INDONESIA

alva@sci.ui.ac.id
fildzah.zhafarina@sci.ui.ac.id
rustam@ui.ac.id

Abstract. Sinusitis is an inflammatory condition of the paranasal sinuses, which according to its onset is further classified into acute, sub – acute, chronic, and recurrent. Antibiotics are usually prescribed to treat patients with acute sinusitis. However, due to concerns and guidelines regarding the use of antibiotics, it is essential to determine an accurate diagnosis on acute sinusitis. Therefore, adequate diagnosis is needed to prevent acute sinusitis become worse and obtain the best treatment. This research studied the use of an improved machine learning process for the appropriate diagnosis of acute sinusitis. The purpose was to compare some kernel functions with Support Vector Machines classifier for proper diagnosis. To measure the most accurate kernel function, the Support Vector Machines classifier with linear, polynomial, and Gaussian radial basis functions were applied as the commonly used kernels. The main advantage of this method is determining the best kernel function to support the healthcare sector in diagnosing acute sinusitis with Support Vector Machines. The idea is proven in four criteria, namely accuracy, precision, recall, and F1 score. The highest average of accuracy and F1 score were the criterion used to determine the best kernel function classification. The result showed that linear kernel function is the best for acute sinusitis classification with 99.37% average of accuracy, followed by a polynomial and Gaussian radial basis. In addition, all three kernels reached 100% accuracy, with different precision, recall, and F1 score of the training data and future studies need to be carried out to improve machines learning classification for medical diagnosis with kernel function contribution.

1. INTRODUCTION

Sinusitis is an inflammation of the paranasal sinuses or swelling of the tissues lining the sinuses [1]. Blockage of the sinuses due to fluid, promote growth of germs that could manifest as headaches and yellowish nasal secretions.

Sinusitis is classified based on its onset period, which comprises of acute, sub-acute, chronic, and recurrent [2]. Acute sinusitis usually starts with symptoms lasting less than 4 weeks, such as common cold, while sub-acute sinusitis lasts up to 12 weeks. Worse, chronic sinusitis lasts for more than 12 weeks, while recurrent sinusitis occurs several times a year, lasting from 7 – 10 days or more with a complete resolution between the onset [2]. Acute sinusitis is a common diagnosis that is found on patients, with approximately 30 million visits and $11 billion spending on treatment. Antibiotics are usually prescribed to treat patients with acute sinusitis. However, due to concerns and guidelines regarding the use of antibiotics, it is essential to determine an accurate diagnosis on acute sinusitis, hence this project aims to improve the diagnosis of acute sinusitis.

Therefore, an appropriate diagnosis is needed to identify acute sinusitis patients, thereby ensuring their benefit from the administration of antimicrobial agent [1]. According to several studies, clinicians face difficulty in determining the symptoms and signs of viral URI because they are tightly related to bacterial processes [1]. These are the following three clinical identifications for patients with acute bacterial sinusitis: 1) period of onset lasts at least 10 days without sign of substantial improvement., 2) onset with high fever more than 39°C and purulent nasal discharge, and 3) onset with worsening symptoms indicated by the fever, headache, or increase in nasal discharge [1]. The methods used in this diagnosis consist of nasal endoscopy, Computed Tomography (CT) scan, nasal and sinus cultures, and Magnetic Resonance Imaging (MRI), which provide a detailed description of the condition.

This process is driven by machine learning algorithms as a branch in computer science that is gaining development of handling diseases within the healthcare sector [3]. It is classified based on supervised learning for labelled data such as classification, regression, and unsupervised learning for clustering data. Many studies have been carried out on the use of machine learning to classify medical diagnoses such as sinusitis with data image [4], schizophrenia [5], and breast cancer [6].

One popular algorithm in machine learning is Support Vector Machine (SVM) [7], which was developed by V. Vapnik in 1995 as a supervised statistical learning technique. SVM is used for classification and regression. Studies carried out by [6] and [8] stated that the support vector machine is good for classification. Therefore, this research uses the SVM classifier to categorize acute sinusitis to obtain an optimal result and help medical diagnosis perform better.

Previous studies on the classification of sinusitis using other methods include the Fuzzy Support Vector Machine [9], Kernel Spherical K- Means [10], Imaging Features [4, 11, 12], and Kernel Perceptron [13]. Furthermore, the Support Vector Machine method was used for Classification of Cancer Data [14], Schizophrenia [5], Face Recognition [15], Policyholders Satisfactorily in Automobile Insurance [16], Brain Tumor MRIs [17], Intrusion Detection System [8] and Dementia Prediction [18]. Despite the numerous works carried out on the same subject, this research was proposed to investigated the different classification results between Linear, Polynomial, and Gaussian radial basis function kernels on support vector machine used for classifying acute sinusitis for supporting the development of machine learning in medical treatment. Therefore, this study compared the result of these three kernels and selected the best one to classify acute sinusitis.

2. RESEARCH METHODS

I. Data

Data were obtained from the CT scan of patients suffer acute sinusitis from the Department of Radiology Dr. RSUPN Cipto Mangkunsumo (RSCM), Central Jakarta. The dataset consists of four features including Gender, Age, Hounsfield Unit for acute sinusitis, and Air Cavity. Hounsfield unit described how much the absorption of x-rays was on the body's tissues, when the tissues were denser, the higher result obtained for the Hounsfield unit. Air cavity is a cavity containing air, such a cavity occurring in the body or bones. Gender consists of binary classification, with 1 and 2 used to represent male and female, respectively. This dataset consists of 200 observations with 102 and 98 labelled acute and non-acute sinusitis, as shown in Table 1.

Table 1. Samples of Sinusitis Dataset

Gender	Age	Hounsfield Unit	Air Cavity	Diagnosis
1	15	29	-522	1
2	58	20	-720	1
1	45	93	-663	0
2	20	47	-889	1
1	15	28	-467	1
1	18	54	-496	0
2	58	107	-852	0
1	31	83	-550	0
1	45	16	-988	1

II. Support Vector Machine

Support Vector Machine (SVM) tries to determine an optimized hyper-plane in a kernel space where training data are linearly separable. The SVM classifier aims to determine a classification criterion capable of separating data accurately [19]. The binary class classification criterion can be a line with linear separable data or non-linear separable data by maximizing the margin between each class.

III. Characteristic of Support Vector Machine

Given the dataset $\{x_i, y_i\}_{i=1}^{n}$ where n denotes the number of data, $x_i \in R^D$ is a feature vector from data sample-i. D denotes dimension of data, and y_i denotes class label of data sample-i. According to Figure 1, the separating line known as hyperplane for training data, $x_i, (i = 1, 2, 3, \ldots, n)$, is defined as:

$$w^T \cdot x + b = 0 \tag{1.1}$$

Figure 1. SVM solves the classification problem by performing a hyperplane, which maximizes the data's margin [19]

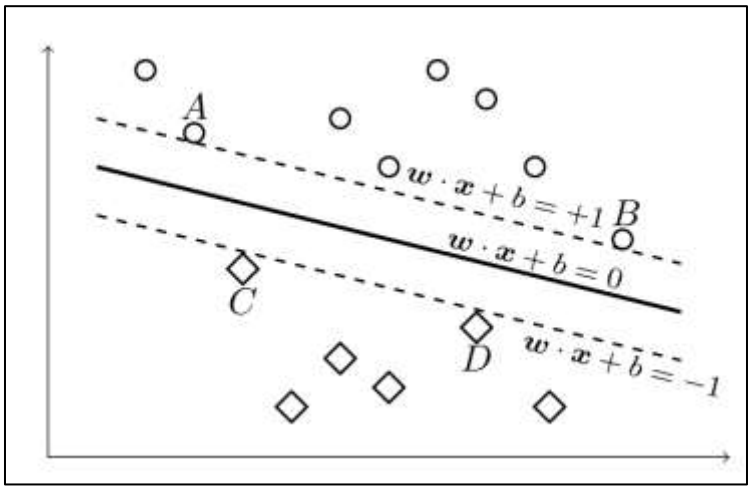

where the general objective is to find w and b. The hyperplane needs to possess minimum error in separating the data and a maximal distance from the closest sample of each class. In these substances, sample of each class is in the left ($y = -1$) or the right ($y = 1$) sides of the hyperplane [19]. Figure 1 shows that the two margins used to control separate data as follows:

$$w^T \cdot x + b = \begin{cases} \geq 1 , y_i = 1 \\ \leq -1, y_i = -1 \end{cases} \tag{1.2}$$

The best hyperplane is obtained by maximized the distance between the margins:

$$d(w, b; x) = \frac{|(w^T \cdot x + b - 1) - (w^T \cdot x + b + 1)|}{||w||} = \frac{2}{||w||} \tag{1.3}$$

The general problem to determine the optimal hyperplane for linear separable data is defined as follows:

$$Min_{w,b} = \frac{1}{2} ||w||^2 \tag{1.4}$$

$$s.t.\ y_i(w^T \cdot x + b) \geq 1,\ i = 1, \ldots, n \tag{1.5}$$

For non-linearly separable data, there is slack variable, $\xi_i \geq 0$ where $i = 1, 2, \ldots, n$ [20], which was the distance between error labelled data and the margin that needs to minimized. Hence, the optimization function in Eq. (4) for a non-linearly separable data changes to a new function as follows:

$$Min_{w,b} = \frac{1}{2} ||w||^2 + C\sum_{i=1}^{n} \xi i \ , C>0 \quad (1.6)$$

$$s.t. \ y_i(w^T \cdot x + b) \geq 1 - \xi i \ , \ i = 1, 2, \ldots, n \quad (1.7)$$

The C in Eq. (6) is known as the regularization parameter [21]. According to a research carried out by [18], when the value of C is high, the training data is accurately categorized by hyperplane and focuses on error minimization. Similarly, when C is a low value, the optimizer looks for higher-margin separating hyperplane while misclassifying the more data points to maximize the emphasized margin.

Eq. (6) and (7), are used to solve the optimization problem for margin constraints, using Lagrange multipliers (α ($\alpha i \geq 0$), β ($\beta i \geq 0$)) [19]. The unconstrained form is obtained as follows:

$$L(w, b, \xi, \alpha, \beta) = \frac{1}{2} ||w||^2 + C\sum_{i=1}^{n} \xi_i - \sum_{i=1}^{n} \alpha_i\{y_i(w^T \cdot x_i + b) - 1 + \xi_i)\} - \sum_{i=1}^{n} \beta_i \xi_i \quad (1.8)$$

The optimal solution of Eq. (8) is obtained by satisfying Karush-Kuhn-Tucker condition:

$$\frac{\partial L}{\partial w} = 0 \rightarrow w = \sum_{i=1}^{n} \alpha_i y_i x_i \quad (1.9)$$

$$\frac{\partial L}{\partial b} = 0 \rightarrow \sum_{i=1}^{n} \alpha_i y_i = 0 \quad (1.10)$$

$$\frac{\partial L}{\partial \xi} = 0 \rightarrow \alpha i + \beta i = C \quad (1.11)$$

Substituting Eq. (9) – (11) into Eq. (8), the following dual problem for a non-linear separable SVM is formulated as follows:

$$L(\alpha) = \sum_{i=1}^{n} \alpha_i - \frac{1}{2}\sum_{i=1}^{n} \alpha_i \alpha_j y_i y_j x_i^T x_j \quad (1.12)$$

$$s.t. \begin{cases} 0 \leq \alpha i \leq C \\ \sum_{i=1}^{n} \alpha_i y_i = 0 \end{cases} \quad (1.13)$$

The above equations and its constraints are used by SVM to obtain the optimal classification solution.

IV. Kernel Function

Kernel methods are useful for the successful application of SVM. These are used to map data from the original feature space to the kernel without knowing the mapping function φ, which maps data into the feature space, explicitly [20]. Kernel function is defined as follows:

$$K(x_i, x_j) = <\varphi(x_i), \varphi(x_j)> \quad (1.14)$$

Kernel function is used to defined the hyperplane as follows:

$$g(x) = w^T \cdot \varphi(x) + b \quad (1.15)$$

For Eq. (9) is defined as follows:

$$w = \sum_{i=1}^{n} \alpha_i y_i \varphi(x_i) \quad (1.16)$$

By substituting Eq. (16) into (15), the optimal decision function is obtained by a suitable kernel. The general equation for the hyperplane is specified as follows:

$$g(x) = \sum_{i=1}^{n} y_i \alpha_i K(x_i, x_j) + b \quad (1.17)$$

Support Vector Machines is efficiently used to solve non-linear problems by selecting a proper kernel function [19]. There are some kernel functions on support vector machine problem. However, this study uses the linear, polynomial, and Gaussian radial basis function, as the commonly used kernels for SVM [22], to optimize classification of acute sinusitis. All three kernels have the same parameter, C, as regularization parameter.

- Linear Kernel defined as [23]:

$$K(x_i, x_j) = \langle x_i x_j \rangle \quad (1.18)$$

- Polynomial defined as:

$$K(x_i, x_j) = (\langle x_i x_j \rangle + 1)^r, \; r \geq 2, \; r \in N \quad (1.19)$$

  where r denotes the degree of the polynomial kernel. High r increases data transformation complexity and overfitting, while low r creates an underfitting model.

- Gaussian radial basis function kernel defined as:

$$K(x_i, x_j) = exp\left(-\gamma \|x_i - x_j\|^2\right), \; \gamma > 0 \quad (1.20)$$

  The research carried out by [24], shows that the γ controls the width of the radial basis function kernel. Intuitively, a small γ value defines a gaussian radial basis function with large variance, while a large γ value defines a small variance.

V. Parameter Optimization

Several parameters were optimized by using the grid search method, which was widely used due to its simplicity [23]. Grid search optimizes the SVM parameters C and γ using cross-validation (CV) technique as a performance metric [17]. This study used 10-folds cross-validation with the following optimized parameters:

- Regularization parameter C = 10
- For gaussian radial basis function kernel, $\gamma = 0.1$
- For polynomial kernel, $r = 3$

VI. Model Performance Evaluation

The research carried out by [25], stated that the commonly-accepted performance evaluation is based on accuracy. Then this study used a performance evaluation by measuring accuracy, precision, recall, and F1 score, where TN, TP, FN, FP denote True Negative, True Positive, False Negative, and False Positive, respectively, [26]:

- TP is the number of correct acute sinusitis predictions;
- TN is the number of correct non-acute sinusitis predictions;
- FP is the number of incorrect acute sinusitis predictions;
- FN is the number of incorrect non-acute sinusitis predictions;

The following formulas are used [27]:

$$accuracy = \frac{T_P + T_N}{T_P + T_N + F_P + F_N} \; x\,100\% \tag{1.21}$$

$$precision = \frac{T_P}{T_P + F_P} \; x\,100\% \tag{1.22}$$

$$recall = \frac{T_P}{T_P + F_N} \; x\,100\% \tag{1.23}$$

$$F1\ score = \frac{2\,x\,precision\,x\,recall}{precision + recall} \tag{1.24}$$

3. RESEARCH METHODS

This study used Python 3.6 for support vector machines and kernels.

I. Classification SVM Results Using Linear Function Kernel

The performance evaluation result using linear function kernel with regularization parameter C = 10, is shown in Table 2:

Table 2. The accuracy, precision, recall, and f-1 score of SVM with linear kernel.

SVM with linear function kernel				
Data Training	Accuracy	Precision	Recall	F1 score
10%	98.33%	98.00%	99.00%	98.00%
20%	98.13%	100.00%	96.00%	98.00%
30%	97.86%	100.00%	96.00%	98.00%
40%	100%	100.00%	100.00%	100.00%
50%	100%	100.00%	100.00%	100.00%
60%	100%	100.00%	100.00%	100.00%
70%	100%	100.00%	100.00%	100.00%
80%	100%	100.00%	100.00%	100.00%
90%	100%	100.00%	100.00%	100.00%
Average	99.37%	99.78%	99.00%	99.33%

According to Table 2, SVM classification with linear kernel function peaked at the highest and lowest data training accuracy of 40% - 90% and 30% at 100% and 97.86%, respectively.

II. Classification SVM Results Using Polynomial Function Kernel

The polynomial kernel has the hyperparameter C and r (degree). This study used C and r values of 10 and 3 to prevent complexity and overfitting. The results SVM with polynomial kernel function are shown in Table 3:

Table 3. The accuracy, precision, recall, and f-1 score of SVM with polynomial kernel degree 3.

SVM with Polynomial Kernel Function Degree 3				
Data Training	Accuracy	Precision	Recall	F1 score
10.00%	91.67%	87.00%	98.00%	92.00%
20.00%	96.88%	98.00%	96.00%	97.00%
30.00%	95.71%	99.00%	93.00%	96.00%
40.00%	99.17%	98.00%	100.00%	99.00%
50.00%	98.00%	96.00%	100.00%	98.00%
60.00%	98.75%	98.00%	100.00%	99.00%
70.00%	98.33%	97.00%	100.00%	98.00%
80.00%	97.50%	95.00%	100.00%	98.00%
90.00%	100.00%	100.00%	100.00%	100.00%
Average	97.33%	96.44%	98.56%	97.44%

According to Table 3, SVM classification with linear kernel function peaked at the highest and lowest data training accuracy of 90% and 10% at 100% and 97.86%.

III. Classification SVM Results Using Gaussian Radial Basis Function Kernel

The performance evaluation result using the Gaussian radial basis function kernel with regularization parameter C = 10 and γ = 0.1, as shown in Table 4.

Table 4. The accuracy, precision, recall, and f-1 score of SVM with gaussian radial basis function

SVM with gaussian radial basis function kernel				
Data Training	Accuracy	Precision	Recall	F1 score
10%	97.78%	97.00%	99.00%	98.00%
20%	98.13%	98.00%	99.00%	98.00%
30%	98.57%	97.00%	100.00%	99.00%
40%	99.17%	98.00%	100.00%	99.00%
50%	99.00%	98.00%	100.00%	99.00%
60%	98.75%	98.00%	100.00%	99.00%
70%	100.00%	100.00%	100.00%	100.00%
80%	100.00%	100.00%	100.00%	100.00%
90%	100.00%	100.00%	100.00%	100.00%
Average	99.04%	98.44%	99.78%	99.11%

According to Table 4, SVM classification with linear kernel function peaked at the highest and lowest data training accuracy of 70%-90% and 10% at 100% and 97.78%, respectively.

IV. Comparison Result

The average accuracy of each kernel measured in 3.1, 3.2, and 3.3 are compared in Tables 5 and 6.

Table 5. Comparison accuracy and precision between linear, polynomial, and gaussian radial basis function kernel.

	accuracy			precision		
	Linear Kernel	Polyno-mial Kernel	Gauss-ian Kernel	Linear Kernel	Polyno-mial Kernel	Gauss-ian Kernel
Average	99.37%	97.33%	99.04%	99.78%	96.44%	98.44%

Table 6. Comparison recall and F1 score between linear, polynomial, and gaussian radial basis function kernel

	recall			F1 score		
	Linear Kernel	Polynomial Kernel	Gaussian Kernel	Linear Kernel	Polynomial Kernel	Gaussian Kernel
Average	99.00%	98.56%	99.78%	99.33%	97.44%	99.11%

According to Table 5, the linear kernel has the highest average accuracy at 99.37%, while polynomial has the lowest at 97.33%. The research carried out by [26] stated that a high value of F1 score indicates an increase in classification performance. In Table 6, the linear kernel has the highest classification performance for classifying acute sinusitis with 99.33% F1 score, with the lowest found in polynomial at 97.44. Therefore, the linear kernel is the best for the SVM classifier for acute sinusitis because it consists of high accuracy and F1 score.

4. CONCLUSION

In conclusion, the main goal of this study was carried out to determine the best kernel function with support vector machine for classifying acute sinusitis. After comparing Linear, polynomial, and Gaussian radial basis functions, the research showed that the linear kernel is best for classifying acute sinusitis with an average of accuracy of 99.37% and highest classification performance 99.33% average of F1 score. Further studies need to be carried out using the same experimental setup for the development of machine learning in medical diagnosis and classifying other diseases. Furthermore, this study believes the methods are suitable to classifying other disease.

ACKNOWLEDGMENT

This research is supported financially by The Indonesian Ministry of Research and Technology, with a KEMENRISTEK/BRIM 2021 research grant scheme.

REFERENCES

1. G. P. DeMuri and E. R. Wald, "Sinusitis," Bennett JE, Dolin R, Blaser MJ, editors. Mandell, Douglas, and Bennett's Principles and Practice of Infectious Diseases. 9th ed. Philadelphia: Elsevier., pp. 844-854, 2020.
2. P. Dhingra and S. Dhingra, Diseases of ear, nose, and throat & head and neck surgery 7th ed., India: Elsevier, 2018.
3. V. B. Kolachalama and G. P. S., "Machine learning and medical education," natural partner journals Digital Medicine, pp. 1-54, 2018.
4. V. Velayudhan, Z. A. Chaudhry, S. W. R. K., R. Shinder and R. D., "Imaging of Intracranial and Orbital Complications of Sinusitis and Atypical Sinus Infection: What the Radiologist Needs to Know," Current Problems in Diagnostic Radiology, 2017.
5. T. V. Rampisela and Z. Rustam, "Classification of Schizophrenia Data Using Support Vector Machine (SVM)," J. Phys. Conf. Series 1108 012044., 2018.

6. C. Aroef, Y. Rivan and Z. Rustam, "Comparing random forest and support vector machines for breast cancer classification," TELKOMNIKA Telecommunication, Computing, Electronics and Control, vol. 18, pp. 815-821, 2020.
7. V. Vapnik, The Natural of Statistical Learning Theory, New York: Springer, 1995.
8. Z. Rustam and D. Zahras, "Comparison between Support Vector Machine and Fuzzy C Means as Classifier for Intrusion Detection System," J. Phys. Conf. Series 1028 012227, 2018.
9. Z. Rustam, N. Angie, J. Pandelaki and R. E. Yunus, " Acute sinusitis classification using support and fuzzy support vector machines," J. Phys. Conf. Series 1490 (2020) 012029, 2019.
10. Arfiani, Z. Rustam, J. Pandelaki and A. Siahaan, "Kernel Spherical K-Means and Support Vector Machine for Acute Sinusitis Classification," IOP Conference Series: Materials Science and Engineering 546 052011, 2019.
11. K. J. T. Lakhan, " Sinus Headaches Sinusitis Versus Migraine," Physician Assist. Clin. 3, pp. 181-192, 2018.
12. C. O. d. Lima, K. L. Devita, L. R. B. Vasconcelos, M. d. Prado and C. N. Campos, "Correlation between Endodontic Infection and Periodontal Desease and Their Association with Chronic Sinusitis: A Clinical-tomographic Study," American Association of Endodontist, 2017.
13. Z. Rustam, S. Hartini, and J. Pandelaki, "Kernel perceptron algorithm for sinusitis classification" J. Phys. Conf. Series 1490 012025, 2020.
14. T. Nadira and Z. Rustam, ". “Classification of Cancer Data using Support Vector Machines with Features Selection Method Based on Global Artificial Bee Colony”.," AIP Conference Proceedings: 3rd International Sympossium on Current Progress in Mathematics and Sciences (ISCPMS) vol. 2023, 2017.
15. Z. Rustam and R. Faradina, "Face Recognition to Identify Look-Alike Faces using Support Vector Machine," J. Phys. Conf. Series 1108 012071, 2018.
16. Z. Rustam and N. P. N. A. Ariantari, "Support Vector Machines for Classifying Policyholders Satisfactorily in Automobile Insurance," J. Phys. Conf. Series 1028 012005., 2018.
17. M. K. Abd-Ellah, *et al*., "Classification of Brain Tumor MRIs Using a Kernel Support Vector Machine," Li H., Nykänen P., Suomi R., Wickramasinghe N., Widén G., Zhan M. (eds) Building Sustainable Health Ecosystems. WIS 2016. Communications in Computer and Information Science, vol. 636, 2016.
18. G. Battinenia, N. Chintalapudi, and F. Amenta, "Machine learning in medicine: Performance calculation of dementia prediction by support vector machines (SVM)," Informatics in Medicine Unlocked: Elsevier, 2019.
19. X.-S. Yang, “Support Vector Machine,” *Introduction to Algorithms for Data Mining and Machine Learning*, Elsevier, 2019, pp. 129-132.
20. C. M. Bishop, Patter Recognition and Machine Learning, vol. 8, New York: Springer, 2006, pp. 163-177.
21. C. Chang, C. Lin and T. T, "LIBSVM: A Library for Support Vector Machines," ACM Trans. Intell. Syst. Technol., 2008.
22. A. Karatzoglou, D. Meyer and K. Hornik, Support vector machines in R. J. Stat. Softw. 2005, 15, 1–28.
23. Z. Liu and H. Xu, "Kernel Parameter Selection for Support Vector Machine Classification," J. Alg. Comp. Technol., vol. 8, pp. 163-177, 2013.
24. J. Alvarsson, et al., "Benchmarking Study of Parameter Variation When Using Signature Fingerprints Together with Support Vector Machines," J. Chem. Inf. Mod. 54(11), 2014.
25. M. Sokolova, N. Japkowicz, and S. Szpakowicz, "Beyond Accuracy, F-score and ROC: A Family of Discriminant Measures for Performance Evaluation," in Conference Paper in Advances in Artificial Intelligence DBLP, 2006.
26. A. Tharwat, "Classification assessment methods," Applied Computing and Informatics: ScienceDirect, 2018.
27. S. Visa, B. Ramsay, A. Ralescu and E. VanDerKnaap, "Confusion Matrix-Based Feature Selection," in Proceedings of the 22nd Midwest Artificial Intelligence and Cognitive Science Conference 2011. p. 120-127, 2011.

Yet Some Other Alternative Asymptotically Isometric Properties Inside Copies of ℓ^1 and Their Implication of Failure of Fixed Point Property

Veysel NEZİR[1], Nizami MUSTAFA[2], Aysun GÜVEN[3]

[1,2,3]*Department of Mathematics, Faculty of Science and Letters, Kafkas University, Kars-TURKEY*

veyselnezir@yahoo.com
nizamimustafa@gmail.com
aysun.guven.tr@gmail.com

Abstract. James' Distortion theorems played a vital role to investigate Banach spaces containing nice copies of c_0 or ℓ^1 and their failure of the fixed point property for nonexpansive mappings. His tools leaded researchers to see that every classical nonreflexive Banach space contains an isomorphic copy of either c_0 or ℓ^1. There have been many researches done using these tools developed by James and followed by Dowling, Lennard and Turett mainly to see if a Banach space can be renormed to have the fixed point property for nonexpansive mappings when there is failure. Recently, in a study in preparation, the first and the third authors obtained alternative asymptotically isometric properties implying failure of the fixed point property inside copies of c_0 or ℓ^1. In this study, we provide more alternative asymptotically isometric properties in copies of ℓ^1. Analogously, we introduce a new property equivalent for a Banach space to contain asymptotically isometric copy of ℓ^1. That is, we show that a Banach space contains an asymptotically isometric copy of ℓ^1 if and only if it has the property we introduce.

1. INTRODUCTION AND PRELIMINARIES

A Banach space is called to have the fixed point property for non-expansive mappings [fpp(n.e.)] if any non-expansive self-mappings defined on any non-empty closed, bounded and convex subset of the Banach space has a fixed point. It has been seen that most classical Banach spaces fail the fixed point property and especially there is a fact that if a Banach space is a non-reflexive Banach lattice then it fails the fixed point property if it contains either an isomorphic copy of c_0 or ℓ^1, Banach space of scalar sequences converging to 0, or an isomorphic copy of ℓ^1, Banach space of absolutely summable scalar sequences [5].

James [4] developed a tool which leaded researchers to understand if a Banach space contains an isomorphic copy of c_0 or ℓ^1. Strengthening James' Distortion theorems, Dowling et al. [2] obtained new tools to test if a Banach space contains an asymptotically isometric copy of ℓ^1 which implies the failure of the fixed point property for nonexpansive mappings.

The notions of asymptotically isometric copies of the classical Banach spaces c_0 and ℓ^1 have applications in metric fixed point theory because they arise naturally in many places. For example, every non-reflexive subspace of $(L_1[0,1], \|.\|_1)$, every infinite dimensional subspace of $(\ell^1, \|.\|_1)$, and every equivalent renorming of ℓ^∞ contains an asymptotically isometric copy ℓ^1 and so all of these spaces fail the fixed point property [1, 3]. The concept of containing an asymptotically isometric copy ℓ^1 also arises in the isometric theory of Banach spaces in an intriguing way: a Banach space X contains an asymptotically isometric copy ℓ^1 if and only if X^* contains an isometric copy of $(L_1[0,1], \|.\|_1)$ [3].

The first author and the third author recently introduced new properties for a Banach space to check if it fails the fixed point property. They proved that a Banach space contains an asymptotically isometric copy of ℓ^1 if and only if it has one of the properties they introduced. So they obtained equivalent properties.

In this study, we provide more alternative asymptotically isometric properties. Analogously, we show that if a Banach space satisfies the property we introduce then it fails to have the fixed point property for nonexpansive mappings; moreover, we show that a Banach space contains an asymptotically isometric copy of ℓ^1 if and only if it has the property we introduce.

Now we provide some preliminaries before giving our main results. First of all, the following is a well-known definition.

Definition 1. Let K be a non-empty closed, bounded, convex subset of a Banach space $(X, \|\cdot\|)$. Let $T: K \to K$ be a mapping. We say T is nonexpansive if $\| T(x) - T(y) \| \leq \| x - y \|$ for all $x, y \in K$. Also, we say that K has the fixed point property for nonexpansive mappings [fpp(n.e.)] if for all nonexpansive mappings $T: K \to K$, there exists $z \in K$ with $T(z) = z$.

As usual, $(c_0, \|\cdot\|_\infty)$ is given by $c_0 := \left\{x = (x_n)_{n\in N} : \text{each } x_n \in \mathbb{R} \text{ and } \lim_{n\to\infty} x_n = 0\right\}$. Further, $\| x \|_\infty := \sup_{n\in N} |x_n|$, for all $x = (x_n)_{n\in N} \in c_0$. Also, c_{00} is the space of sequences with finetely many nonzero terms. Furthermore, $(\ell^1, \|\cdot\|_1)$ is the vector space of all absolutely summable scalar sequences such that $\| x \|_1 := \sum_{n=1}^{\infty} |x_n|$ for all $x = (x_n)_{n\in N} \in \ell^1$.

Definition 2. [2] A Banach space $(X, \|\cdot\|)$ is said to contain an asymptotically isometric copy of ℓ^1 if there exist a sequence $(x_n)_n$ in X and a null sequence $(\varepsilon_n)_n$ in $(0,1)$ so that

$$\sum_{n=1}^{\infty} (1 - \varepsilon_n)|a_n| \leq \left\| \sum_{n=1}^{\infty} a_n x_n \right\| \leq \sum_{n=1}^{\infty} |a_n| ,$$

for all $(a_n)_n \in \ell^1$.

Theorem 1. [2] A Banach space $(X, \|\cdot\|)$ contains an asymptotically isometric copy of ℓ^1 if and only if there is a sequence $(x_n)_n$ in X and there are scalars $0 < k \leq K < \infty$ such that

1. for all $(a_n)_n \in \ell^1$,

$$k \sum_{n=1}^{\infty} |a_n| \leq \left\| \sum_{n=1}^{\infty} a_n x_n \right\| \leq K \sum_{n=1}^{\infty} |a_n|$$

and

2. $\lim_{n\to\infty} \| x_n \| = k$.

Then, the following theorem is given as one of their results in [2].

Theorem 2. If a Banach space $(X, \|\cdot\|)$ contains an asymptotically isometric copy of ℓ^1, then X fails fpp(n.e.).

2. MAIN RESULTS

In this section, define a new property that implies the failure of the fixed point property for nonexpansive mappings. That is, we show that if a Banach space has the property we introduce then it fails to have the fixed point property for nonexpansive mappings. We find an alternative way of detecting our property. Then, we show that a Banach space contains an asymptotically isometric copy of ℓ^1 if and only if it has the property we introduce.

Definition 3. *We will say a Banach space $(X, \|\cdot\|)$ has property N-AAIP-ℓ^1 (which stands for new alternative asymptotically isometric property for spaces in a copy of ℓ^1) if there exist a sequence $(x_n)_n$ in X and a null sequence $(\varepsilon_n)_n$ in $(0,1)$ so that*

$$\sqrt{\left[\sum_{n=1}^{\infty}(1-\varepsilon_n)\left|\sum_{j=n}^{\infty}a_j\right|\right]^2+\left[\sum_{n=1}^{\infty}\frac{(1-\varepsilon_n)}{2^n}\frac{\left|\sum_{j=n}^{\infty}a_j\right|}{1+\left|\sum_{j=n}^{\infty}a_j\right|}\right]^2}\leq\left\|\sum_{n=1}^{\infty}a_nx_n\right\|$$
$$\leq\sqrt{\left[\sum_{n=1}^{\infty}\left|\sum_{j=n}^{\infty}a_j\right|\right]^2+\left[\sum_{n=1}^{\infty}\frac{1}{2^n}\frac{\left|\sum_{j=n}^{\infty}a_j\right|}{1+\left|\sum_{j=n}^{\infty}a_j\right|}\right]^2},$$

for all $(a_n)_n \in \ell^1$.

Theorem 3. *A Banach space $(X, \|\cdot\|)$ has property N-AAIP-ℓ^1 if and only if there is a sequence $(x_n)_n$ in X and there are scalars $0 < k < K < \infty$ such that*

1. *for all $(a_n)_n \in \ell^1$,*

$$k\sqrt{\left[\sum_{n=1}^{\infty}|a_n|\right]^2+\left[\sum_{n=1}^{\infty}\frac{1}{2^n}\frac{|a_n|}{1+|a_n|}\right]^2}\leq\left\|\sum_{n=1}^{\infty}a_nx_n\right\|\leq K\sqrt{\left[\sum_{n=1}^{\infty}|a_n|\right]^2+\left[\sum_{n=1}^{\infty}\frac{1}{2^n}\frac{|a_n|}{1+|a_n|}\right]^2} \quad (1)$$

and

2. $\lim_{n\to\infty}\|x_n\| = k.$ (2)

Proof. Assume that a Banach space $(X, \|\cdot\|)$ has property N-AAIP-ℓ^1. Then, there exist a sequence $(x_n)_n$ in X and a null sequence $(\varepsilon_n)_n$ in $(0,1)$ so that

$$\sqrt{\left[\sum_{n=1}^{\infty}(1-\varepsilon_n)\left|\sum_{j=n}^{\infty}a_j\right|\right]^2+\left[\sum_{n=1}^{\infty}\frac{(1-\varepsilon_n)}{2^n}\frac{\left|\sum_{j=n}^{\infty}a_j\right|}{1+\left|\sum_{j=n}^{\infty}a_j\right|}\right]^2}\left\|\sum_{n=1}^{\infty}a_nx_n\right\|$$
$$\leq\sqrt{\left[\sum_{n=1}^{\infty}\left|\sum_{j=n}^{\infty}a_j\right|\right]^2+\left[\sum_{n=1}^{\infty}\frac{1}{2^n}\frac{\left|\sum_{j=n}^{\infty}a_j\right|}{1+\left|\sum_{j=n}^{\infty}a_j\right|}\right]^2},$$

for all $(a_n)_n \in \ell^1$.

Now for each $n \in \mathbb{N}$, define $y_n := x_n - x_{n-1}$ with $x_0 = 0$. So there exist a null sequence $(\varepsilon_n)_n$ in $(0,1)$ so that for all $(a_n)_n \in \ell^1$

$$\sqrt{\left[\sum_{n=1}^{\infty}(1-\varepsilon_n)|a_n|\right]^2+\left[\sum_{n=1}^{\infty}(1-\varepsilon_n)\frac{1}{2^n}\frac{|a_n|}{1+|a_n|}\right]^2}\le\left\|\sum_{n=1}^{\infty}a_ny_n\right\|\le\sqrt{\left[\sum_{n=1}^{\infty}|a_n|\right]^2+\left[\sum_{n=1}^{\infty}\frac{1}{2^n}\frac{|a_n|}{1+|a_n|}\right]^2}\ .$$

We may suppose $(\varepsilon_n)_{n\in\mathbb{N}}$ to be a decreasing sequence.

Let $z_n=(1-\varepsilon_n)^{-1}y_n$ for each $n\in\mathbb{N}$. Then, for all $(t_n)_n\in\ell^1$,

$$\sqrt{\left[\sum_{n=1}^{\infty}|a_n|\right]^2+\left[\sum_{n=1}^{\infty}\frac{1}{2^n}\frac{|a_n|}{1+|a_n|}\right]^2}\le\left\|\sum_{n=1}^{\infty}a_n(1-\varepsilon_n)^{-1}y_n\right\|$$

$$\le\sqrt{\left[\sum_{n=1}^{\infty}(1-\varepsilon_n)^{-1}|a_n|\right]^2+\left[\sum_{n=1}^{\infty}\frac{(1-\varepsilon_n)^{-1}}{2^n}\frac{|a_n|}{1+|a_n|}\right]^2}\ .$$

Let $K=\frac{1}{1-\varepsilon_1}$. Then we obtain the condition (2) for the sequence $(z_n)_n$. Next, taking $(a_n)_n$ as the unit basis $(e_n)_n$ of c_0 in the , we get $\lim_{n\to\infty}\|y_n\|=1$ and so $\lim_{n\to\infty}\|z_n\|=1$ which means condition (2) holds as well.

Conversely, assume that there exist a sequence $(x_n)_n$ in X and $k,K\in(0,\infty)$ with $k\le K$ so that for all $(a_n)_n\in\ell^1$,

$$k\sqrt{\left[\sum_{n=1}^{\infty}|a_n|\right]^2+\left[\sum_{n=1}^{\infty}\frac{1}{2^n}\frac{|a_n|}{1+|a_n|}\right]^2}\le\left\|\sum_{n=1}^{\infty}a_nx_n\right\|\le K\sqrt{\left[\sum_{n=1}^{\infty}|a_n|\right]^2+\left[\sum_{n=1}^{\infty}\frac{1}{2^n}\frac{|a_n|}{1+|a_n|}\right]^2}$$

and $\lim_{n\to\infty}\|x_n\|=k$.

Equivalently we can get that there exist a sequence $(x_n)_n$ in X and $k\in(0,1]$ so that for all $(a_n)_n\in\ell^1$,

$$\sqrt{\left[\sum_{n=1}^{\infty}|a_n|\right]^2+\left[\sum_{n=1}^{\infty}\frac{1}{2^n}\frac{|a_n|}{1+|a_n|}\right]^2}\le\left\|\sum_{n=1}^{\infty}a_nx_n\right\|\le K\sqrt{\left[\sum_{n=1}^{\infty}|a_n|\right]^2+\left[\sum_{n=1}^{\infty}\frac{1}{2^n}\frac{|a_n|}{1+|a_n|}\right]^2}$$

and $\lim_{n\to\infty}\|x_n\|=1$.

Let $(\varepsilon_n)_n$ be a null sequence in $(0,1)$. Since $\lim_{n\to\infty}\|x_n\|=1$, and $\|x_n\|\ge1$ for all $n\in\mathbb{N}$, by passing to subsequences, if necessary, we can assume that $1\le\|x_n\|\le1+\varepsilon_n$ for all $n\in\mathbb{N}$. Define $y_n=\frac{x_n}{1+\varepsilon_n}$ for all $n\in\mathbb{N}$. Then, since $\|y_n\|\le1$, we have for all $(a_n)_n\in\ell^1$,

$$\left\|\sum_{n=1}^{\infty}a_ny_n\right\|\le\sum_{n=1}^{\infty}|a_n|\le\sqrt{\left[\sum_{n=1}^{\infty}|a_n|\right]^2+\left[\sum_{n=1}^{\infty}\frac{1}{2^n}\frac{|a_n|}{1+|a_n|}\right]^2}.$$

Moreover, by the left hand side inequality of (1), we have

$$\left\|\sum_{n=1}^{\infty}a_ny_n\right\|=\left\|\sum_{n=1}^{\infty}a_n\frac{x_n}{(1+\varepsilon_n)}\right\|$$

$$\ge\sqrt{\left[\sum_{n=1}^{\infty}\frac{|a_n|}{1+\varepsilon_n}\right]^2+\left[\sum_{n=1}^{\infty}\frac{1}{(1+\varepsilon_n)2^n}\frac{|a_n|}{1+|a_n|}\right]^2}$$

$$\geq \sqrt{\left[\sum_{n=1}^{\infty}(1-\varepsilon_n)|a_n|\right]^2+\left[\sum_{n=1}^{\infty}\frac{(1-\varepsilon_n)}{2^n}\frac{|a_n|}{1+|a_n|}\right]^2}$$

Hence, we obtain that there exist a sequence sequence $(y_n)_n$ in X and a null sequence $(\varepsilon_n)_n$ in $(0,1)$ so that for all $(a_n)_n \in \ell^1$,

$$\sqrt{\left[\sum_{n=1}^{\infty}(1-\varepsilon_n)|a_n|\right]^2+\left[\sum_{n=1}^{\infty}\frac{(1-\varepsilon_n)}{2^n}\frac{|a_n|}{1+|a_n|}\right]^2} \leq \left\|\sum_{n=1}^{\infty}a_n y_n\right\| \leq \sqrt{\left[\sum_{n=1}^{\infty}|a_n|\right]^2+\left[\sum_{n=1}^{\infty}\frac{1}{2^n}\frac{|a_n|}{1+|a_n|}\right]^2}.$$

Now for each $n \in \mathbb{N}$, define $z_n := \sum_{j=1}^{n} y_j$. Then, there exist a null sequence $(\varepsilon_n)_n$ in $(0,1)$ so that for all $(a_n)_n \in \ell^1$,

$$\sqrt{\left[\sum_{n=1}^{\infty}(1-\varepsilon_n)\left|\sum_{j=n}^{\infty}a_j\right|\right]^2+\left[\sum_{n=1}^{\infty}\frac{(1-\varepsilon_n)}{2^n}\frac{\left|\sum_{j=n}^{\infty}a_j\right|}{1+\left|\sum_{j=n}^{\infty}a_j\right|}\right]^2} \leq \left\|\sum_{n=1}^{\infty}a_n z_n\right\|$$
$$\leq \sqrt{\left[\sum_{n=1}^{\infty}\left|\sum_{j=n}^{\infty}a_j\right|\right]^2+\left[\sum_{n=1}^{\infty}\frac{1}{2^n}\frac{\left|\sum_{j=n}^{\infty}a_j\right|}{1+\left|\sum_{j=n}^{\infty}a_j\right|}\right]^2}.$$

So we are done.

Theorem 4. *If a Banach space $(X, \|\cdot\|)$ has property N-AAIP-ℓ^1, then X fails fpp(n.e.).*

Proof. Assume that a Banach space $(X, \|\cdot\|)$ has property N-AAIP-ℓ^1. Then, there exist a sequence $(x_n)_n$ in X and a null sequence $(\varepsilon_n)_n$ in $(0,1)$ so that

$$\sqrt{\left[\sum_{n=1}^{\infty}(1-\varepsilon_n)\left|\sum_{j=n}^{\infty}a_j\right|\right]^2+\left[\sum_{n=1}^{\infty}\frac{(1-\varepsilon_n)}{2^n}\frac{\left|\sum_{j=n}^{\infty}a_j\right|}{1+\left|\sum_{j=n}^{\infty}a_j\right|}\right]^2} \leq \left\|\sum_{n=1}^{\infty}a_n x_n\right\|$$
$$\leq \sqrt{\left[\sum_{n=1}^{\infty}\left|\sum_{j=n}^{\infty}a_j\right|\right]^2+\left[\sum_{n=1}^{\infty}\frac{1}{2^n}\frac{\left|\sum_{j=n}^{\infty}a_j\right|}{1+\left|\sum_{j=n}^{\infty}a_j\right|}\right]^2},$$

for all $(a_n)_n \in \ell^1$.

Now for each $n \in \mathbb{N}$, define $y_n := x_n - x_{n-1}$ with $x_0 = 0$. So there exist a null sequence $(\varepsilon_n)_n$ in $(0,1)$ so that for all $(a_n)_n \in \ell^1$,

$$\sqrt{\left[\sum_{n=1}^{\infty}(1-\varepsilon_n)|a_n|\right]^2+\left[\sum_{n=1}^{\infty}\frac{(1-\varepsilon_n)}{2^n}\frac{|a_n|}{1+|a_n|}\right]^2} \leq \left\|\sum_{n=1}^{\infty}a_n y_n\right\| \leq \sqrt{\left[\sum_{n=1}^{\infty}|a_n|\right]^2+\left[\sum_{n=1}^{\infty}\frac{1}{2^n}\frac{|a_n|}{1+|a_n|}\right]^2}.$$

Let $(\gamma_n)_n$ be a strictly decreasing sequence in $(1,\infty)$ with $\lim_{n\to\infty}\gamma_n = 1$. By passing to subsequences if necessary we can assume that $\gamma_{n+1} < (1-\varepsilon_n)\gamma_n$.

Define $z_n = \gamma_n y_n$, for all $n \in \mathbb{N}$, and let $C = \{\sum_{n=1}^{\infty} t_n z_n : t_n \geq 0 \text{ and } \sum_{n=1}^{\infty} t_n = 1\}$ which is a closed bounded convex subset of X.

Now, consider the mapping $T: C \to C$ given by $T(\sum_{n=1}^{\infty} t_n z_n) = z_1 + \sum_{n=1}^{\infty} t_n z_{n+1}$, where $1 \geq t_n \geq 0$ for all $n \in \mathbb{N}$. It is clear that T has no fixed points in C.

We will now show that T is nonexpansive (in fact, T is contractive).

Write $u = \sum_{n=1}^{\infty} t_n z_n$ and $w = \sum_{n=1}^{\infty} s_n z_n$ as two arbitrary elements of C with $u \neq w$.

Then,

$$\begin{aligned}
\| Tu - Tw \| &= \left\| \sum_{n=1}^{\infty} (t_n - s_n) z_{n+1} \right\| \\
&= \left\| \sum_{n=1}^{\infty} (t_n - s_n) \gamma_{t+1} y_{n+1} \right\| \\
&\leq \sqrt{\left[\sum_{n=1}^{\infty} \frac{1}{2^n} \frac{|t_n - s_n|}{1 + |t_n - s_n|} \gamma_{n+1} \right]^2 + \left[\sum_{n=1}^{\infty} |t_n - s_n| \gamma_{n+1} \right]^2} \\
&< \sqrt{\left[\sum_{n=1}^{\infty} \frac{1}{2^n} \frac{|t_n - s_n|}{1 + |t_n - s_n|} \gamma_n (1 - \varepsilon_n) \right]^2 + \left[\sum_{n=1}^{\infty} |t_n - s_n| \gamma_n (1 - \varepsilon_n) \right]^2} \\
&\leq \left\| \sum_{n=1}^{\infty} (t_n - s_n) \gamma_n y_n \right\| \\
&= \| u - w \|.
\end{aligned}$$

This completes the proof.

Theorem 5. *A Banach space $(X, \|\cdot\|)$ contains an asymptotically isometric copy of ℓ^1 if and only if X has property N-AAIP-ℓ^1.*

Proof. Assume that a Banach space X contains an asymptotically isometric copy of ℓ^1. Then, by Theorem 1, there exist a sequence $(x_n)_n$ in X with $\lim_n \| x_n \| = 1$ and $1 \leq K$ such that for all $(a_n)_n \in \ell^1$,

$$\sum_{n=1}^{\infty} |a_n| \leq \left\| \sum_{n=1}^{\infty} a_n x_n \right\| \leq K \sum_{n=1}^{\infty} |a_n| .$$

Then, letting $y_n = \left(1 + \frac{1}{2^n}\right) x_n$ for each $n \in \mathbb{N}$ and $S = \frac{3K}{2}$, we have

$$\begin{aligned}
\sqrt{\left[\sum_{n=1}^{\infty} (1 - \varepsilon_n) |a_n| \right]^2 + \left[\sum_{n=1}^{\infty} \frac{(1 - \varepsilon_n)}{2^n} \frac{|a_n|}{1 + |a_n|} \right]^2} &\leq \sum_{n=1}^{\infty} |a_n| + \sum_{n=1}^{\infty} \frac{|a_n|}{2^n} \\
&\leq \left\| \sum_{n=1}^{\infty} a_n y_n \right\| \\
&\leq K \left(\sum_{n=1}^{\infty} |a_n| + \sum_{n=1}^{\infty} \frac{|a_n|}{2^n} \right)
\end{aligned}$$

$$\leq S \sum_{n=1}^{\infty} |a_n|$$

$$\leq S \sqrt{\left[\sum_{n=1}^{\infty} |a_n|\right]^2 + \left[\sum_{n=1}^{\infty} \frac{1}{2^n} \frac{|a_n|}{1+|a_n|}\right]^2}$$

and $\lim_n \| y_n \| = 1$.

Hence, by Theorem 3, X has property N-AAIP-ℓ^1.

Conversely assume that X has property N-AAIP-ℓ^1. Then, using Theorem 3, equivalently we can get that there exist a sequence $(x_n)_n$ in X and $k \in (0,1]$ so that for all $(a_n)_n \in \ell^1$,

$$\sqrt{\left[\sum_{n=1}^{\infty} |a_n|\right]^2 + \left[\sum_{n=1}^{\infty} \frac{1}{2^n} \frac{|a_n|}{1+|a_n|}\right]^2} \leq \left\| \sum_{n=1}^{\infty} a_n x_n \right\| \leq K \sqrt{\left[\sum_{n=1}^{\infty} |a_n|\right]^2 + \left[\sum_{n=1}^{\infty} \frac{1}{2^n} \frac{|a_n|}{1+|a_n|}\right]^2}$$

and $\lim_{n\to\infty} \| x_n \| = 1$.

Thus,

$$\sum_{n=1}^{\infty} |a_n| \leq \left\| \sum_{n=1}^{\infty} t_n x_n \right\| \leq \frac{3K}{2} \sum_{n=1}^{\infty} |a_n| \ .$$

Hence, we are done by Theorem 1.

REFERENCES

1. P.N. Dowling, C.J. Lennard, Every nonreflexive subspace of $L_1[0,1]$ fails the fixed point property, Proc. Amer. Math. Soc., 1997, 125: 443–446.
2. P.N. Dowling, C.J. Lennard, B. Turett, Reflexivity and the fixed-point property for nonexpansive maps, J. Math. Anal. Appl., 1996, 200(3): 653–662.
3. P.N. Dowling, C.J. Lennard, B. Turett, Renormings of l^1 and c_0 and fixed point properties, in: Handbook of Metric Fixed Point Theory, Springer, Netherlands, 2001, pp. 269–297.
4. R.C. James, Uniformly non-square Banach spaces. Ann. of Math. (2), 1964, 542–550.
5. J. Lindenstrauss, L. Tzafriri, Classical Banach spaces I: sequence spaces, ergebnisse der mathematik und ihrer grenzgebiete, Vol. 92, Springer-Verlag, New York, 1977.

The Role of Delay Driven Hopf Bifurcations in A Prey-Predator Type One-Dimensional Mathematical Model of Plankton Interactions

Aytül GÖKÇE

Department of Mathematics, Faculty of Science and Arts, Ordu University, Ordu, Turkey

aytul.gokce1@gmail.com

Abstract. Most of the preliminary results on prey-predator interactions focus on the direct and immediate relationship between prey and predator species, usually described by the system of ordinary differential equations. However, the existence of time delay, often degenerating the system dynamics, has been proven in many experimental studies. One main objective of this paper is to mathematically analyse the dynamical system of plankton species interacting with dissolved oxygen and discuss how a constant time delay in predator gestation affects their interactions. The local stability and delay induced Hopf bifurcation analysis around the positive equilibria of the system of delay differential equations is also examined. Various numerical simulations including time simulations, phase portraits and numerical bifurcation analysis are performed to support the theoretical results presented in this paper. In this context, the other main objective of this paper is to analyse the dynamics of oxygen concentration as a function of two main parameters of the system via numerical continuation. The findings of this paper show that, compared to non-delayed case, delay form of the model support multiple Hopf bifurcations and the continuation of periodic orbits emanating from Hopf points demonstrate various dynamics such as transcritical bifurcation, Neimark-Sacker bifurcation, period doubling bifurcation and saddle node bifurcation.

1. INTRODUCTION

Marine ecosystem has very complex dynamics with many non-linearly interacting species from micro-scale to macro-scale, and thus numerous mathematical work has been performed and is still required to approximate its complex dynamics. In order to develop mathematically attainable models, most of the research in theoretical ecology have been conducted on simple and instantaneous spatial and temporal models of prey-predator interactions and their potential outcomes; zoo-plankton and phytoplankton interactions in particular [1, 2, 3, 4, 5]. In real world, time delay occurs in most of the biological systems and leads natural oscillation in the concentration or density of the species [6, 7, 8]. In fact, the most obvious case is that the reproduction rate of predator after predation is not immediate and occurs after some time delay[9, 10]. There is a great interest in theoretical ecology community to analyse biological systems in the presence of delay and many models have been created to explain their dynamics.

Studying numerical bifurcation and different properties of the system stability in the ecological system is constantly extending with a new knowledge. Dynamics of plankton interactions in particular has attracted a great attention. Moreover, since 2010, research community has attempted to examine the role of oxygen interacting with plankton species [11, 12, 13, 14, 15]. In this paper a three component model of plankton-oxygen dynamics based on the paper by Dhar *et al.* [11] is taken into consideration. Then we extend this paper in several directions; firstly, non-dimensionalisation of the system is performed to remove the physical quantities and dimensions. After introducing new dimensionless variables and parameters, equilibria of the system is determined. Incorporating gestation delay in the animal form of the plankton (zoo-plankton) we analyse the changes in the dynamics of the original model. Analytical and numerical findings of this paper show that system is stable under critical threshold and unstable above critical threshold, for which instability occurs at a Hopf bifurcation. In the last part of the paper we present the results for one-parameter numerical bifurcation analysis, where oxygen concentration is plotted with respect to two main parameters (i) phytoplankton growth rate with respect to oxygen and (ii) constant intake rate of the oxygen. Constructing an orbit with a small amplitude close to the Hopf bifurcations, the continuation of periodic orbits emanating from Hopf points demonstrates very complex behaviours.

2. MATHEMATICAL MODEL

The model considered in this paper is based on the system given in [11] :

$$\frac{dp}{dt} = \frac{rp}{\kappa + c_0 - c} - \delta_1 p - \frac{\beta pz}{p+a}, \tag{2.1}$$

$$\frac{dc}{dt} = \eta(c_0 - c) - \alpha_1 p - \alpha_2 z, \tag{2.2}$$

$$\frac{dz}{dt} = \frac{\beta_1 pz}{p+a} - \delta_2 z. \tag{2.3}$$

Here p and z stand for the density of phytoplankton and zoo-plankton respectively and c represents the concentration of oxygen. c_0 demonstrates the constant intake of oxygen. r/κ is related to the growth rate of phytoplankton. δ_1 and δ_2 are the natural death rates of phytoplankton and zoo-plankton respectively. α_1 and α_2 represent the consumption of oxygen by per capita planktons. Zoo-plankton feed on phytoplankton thus interactions between the two taxa of plankton occurs with Holling- type II functional response. Lastly β_1 stands for the conversion rate from phytoplankton into zoo-plankton. For further information we refer the reader to [11].

a. Non-dimensionalisation and equilibria analysis:

In order to determine the relative importance of terms in the mathematical model (2) and reduce the number of parameters, all variables are scaled with representative dimensional quantities. Introducing the following dimensionless variables:

$$t = \frac{\bar{t}}{\mu}, \quad z = \frac{\mu(\kappa + c_0)}{\alpha_2}\bar{z}, \quad c = (\kappa + c_0)\bar{c}, \quad p = a\bar{p},$$

and substituting in the system (2) with the new dimensionless parameters:

$$\bar{r} = \frac{r}{\mu(\kappa + c_0)}, \quad \bar{\delta}_{1,2} = \frac{\delta_{1,2}}{\mu}, \quad \bar{\beta} = \frac{\beta(\kappa + c_0)}{\alpha_2 a}, \quad \bar{\alpha_1} = \frac{\alpha_1 a}{\mu(\kappa + c_0)},$$

$$\bar{\eta_1} = \frac{\eta c_0}{\mu(\kappa + c_0)}, \quad \bar{\beta_1} = \frac{\beta_1}{\mu}, \quad \bar{\delta_2} = \frac{\delta_2}{\mu}, \quad \bar{\eta_2} = \frac{\eta}{\mu}$$

Thus the model (2) can be rewritten in a dimensionless form as

$$\frac{dp}{dt} = \frac{rp}{1-c} - \delta_1 p - \frac{\beta pz}{p+1} \equiv f^{(1)}(p,c,z), \tag{2.4}$$

$$\frac{dc}{dt} = \eta_1 - \eta_2 c - \alpha_1 p - z, \equiv f^{(2)}(p,c,z), \tag{2.5}$$

$$\frac{dz}{dt} = \frac{\beta_1 pz}{p+1} - \delta_2 z \equiv f^{(3)}(p,c,z). \tag{2.6}$$

Equilibria of the model: The temporal model (2.1) in the absence of delay has three possible steady states: (i) plankton free steady state $S_1 = (0, \frac{\eta_1}{\eta_2}, 0)$, (ii) zoo-plankton free steady state $S_2 = \left(1 - \frac{r}{\delta_1}, \frac{\eta_1\delta_1 - \eta_2(\delta_1 - r)}{\delta_1\alpha_1}, 0\right)$ and (iii) coexistence state $S_3 = (p^*, c^*, z^*)$ where

$$p^* = \frac{\delta_2}{\beta_1 - \delta_2}, \quad c^* = \frac{1}{\eta_2}\left(\eta_1 - \frac{\alpha_1\delta_2}{\beta_1 - \delta_2} - z^*\right), \quad z^* = \frac{\beta_1}{\beta(\beta_1 - \delta_2)}\left(\frac{r}{1 - c^*} - \delta_1\right).$$

Here p^* exists only when $\beta_1 > \delta_2$. The stability of plankton free steady state (S_1) and zoo-plankton free steady state (S_2) can be determined in a similar spirit as described in [11].

The stability of the positive coexistent equilibrium $S_3 = (p^*, c^*, z^*)$ is determined using linearisation with transformations: $p = p^* + \tilde{p}(t), \quad c = c^* + \tilde{c}(t), \quad z = z^* + \tilde{z}(t),$ where $\tilde{\cdot}$ represent perturbations around the equilibrium points. Then the linearised model is rewritten as

$$\frac{d\varphi}{dt} = \mathsf{A}_0\varphi(t) + \mathsf{A}_\tau\varphi(t - \tau), \tag{2.7}$$

where A_0 and A_τ stand for the characteristic matrices incorporated with constant time delay in zoo-plankton gestation and given as

$$\mathsf{A} = \begin{bmatrix} f_p^{(1)} & f_c^{(1)} & f_z^{(1)} \\ f_p^{(2)} & f_c^{(2)} & f_z^{(2)} \\ f_p^{(3)} & f_c^{(3)} & f_z^{(3)} \end{bmatrix}_{S^*} \quad and \quad \mathsf{A}_\tau = \begin{bmatrix} 0 & 0 & 0 \\ 0 & 0 & 0 \\ f_{p_\tau}^{(3)} & 0 & 0 \end{bmatrix}_{S^*}$$

where

$$\begin{aligned} f_p^{(1)}\big|_{S^*} &= \frac{r}{1 - c^*} - \delta_1 - \frac{\beta z^*}{(p^* + 1)^2} = \frac{\beta z^* p^*}{(p^* + 1)^2}, \quad f_c^{(1)}\big|_{S^*} = \frac{r p^*}{(1 - c^*)^2}, \quad f_z^{(1)}\big|_{S^*} = \frac{-\beta p^*}{p^* + 1}, \\ f_p^{(2)}\big|_{S^*} &= -\alpha_1, \quad f_c^{(2)}\big|_{S^*} = -\eta_2, \quad f_z^{(2)}\big|_{S^*} = -1, \quad f_p^{(3)}\big|_{S^*} = 0, \quad f_c^{(3)}\big|_{S^*} = 0, \\ f_z^{(3)}\big|_{S^*} &= -\delta_2 + \frac{\beta_1 p^*}{p^* + 1} \quad and \quad f_{p_\tau}^{(1)}\big|_{S^*} = \frac{\beta_1 z^*}{(p^* + 1)^2}. \end{aligned} \tag{2.8}$$

The characteristic matrix corresponding to equation (2.7) is then given by

$$\Delta(\lambda) = \lambda I_3 - \mathsf{A}_0 - \mathsf{A}_\tau e^{-\lambda\tau}, \tag{2.9}$$

and the associated characteristic equation is $Det(\Delta(\lambda)) = 0$. This leads to stability of the coexistent state where infinite number of solutions can be obtained. However, the finite number of solutions with $\Re(\lambda) > k$, $k \in \mathsf{R}$ is found. Characteristic equation results in third order equation of

$$\lambda^3 + \mathsf{K}_1\lambda^2 + \mathsf{K}_2\lambda + \left(\mathsf{K}_3^{(1)} + \mathsf{K}_3^{(2)}\lambda\right)e^{-\lambda\tau} + \mathsf{K}_4 = 0, \tag{2.10}$$

where

$$\begin{aligned} \mathrm{K}_1 &= -\left(f_p^{(1)} + f_c^{(2)} + f_z^{(3)}\right), \quad \mathrm{K}_2 = f_p^{(1)} f_c^{(2)} + f_p^{(1)} f_z^{(3)} + f_c^{(2)} f_z^{(3)} - f_p^{(2)} f_c^{(1)}, \\ \mathrm{K}_3^{(1)} &= -\left(f_c^{(1)} f_z^{(2)} - f_z^{(1)} f_c^{(2)}\right) f_{p_d}^{(3)}, \quad \mathrm{K}_3^{(2)} = -f_z^{(1)} f_{p_d}^{(3)}, \quad \mathrm{K}_4 = \left(f_c^{(1)} f_p^{(2)} - f_p^{(1)} f_c^{(2)}\right) f_z^{(3)}. \end{aligned} \tag{2.11}$$

In order to prove the existence of the Hopf bifurcation, a critical time delay must occur such that $\lambda = \pm i\omega$, ($\omega > 0$) and all other eigenvalues have negative real parts. Furthermore, $Re\left(\frac{d\lambda}{d\tau}\right) \neq 0$ should satisfied. Let $i\omega_c$ be a root of equation (2.10), thus we obtain a pair of equations:

$$Im: \mathrm{K}_3^{(2)} \omega_c \cos(\omega_c \tau) - \mathrm{K}_3^{(1)} \sin(\omega_c \tau) = \omega_c^3 - \mathrm{K}_2 \omega_c, \tag{2.12}$$

$$Re: \mathrm{K}_3^{(1)} \cos(\omega_c \tau) - \mathrm{K}_3^{(2)} \omega_c \sin(\omega_c \tau) = \mathrm{K}_1 \omega_c^2 - \mathrm{K}_4. \tag{2.13}$$

Using equations (2.12)-(2.13) we have

$$\left(\mathrm{K}_3^{(2)}\right)^2 + \left(\mathrm{K}_3^{(1)}\right)^2 = \left(\omega_c^3 - \mathrm{K}_2 \omega_c\right)^2 + \left(\mathrm{K}_1 \omega_c^2 - \mathrm{K}_4\right)^2 \tag{2.14}$$

leading to

$$\nu^3 + d_1 \nu^2 + d_2 \nu + d_3 = 0, \ \nu = \omega_c^2, \tag{2.15}$$

where

$$d_1 = \mathrm{K}_1^2 - 2\mathrm{K}_2, \quad d_2 = \mathrm{K}_2^2 - 2\mathrm{K}_1 \mathrm{K}_4 - \left(\mathrm{K}_3^{(2)}\right)^2, \quad d_3 = \mathrm{K}_4^2 - \left(\mathrm{K}_3^{(1)}\right)^2. \tag{2.16}$$

Equation (2.15) has at least one positive root. Solving equations (2.12)-(2.13) with respect to τ , one can obtain

$$\tau_{c_j} = \frac{1}{\omega_c} \cos^{-1} F(\omega_c) + \frac{2\pi j}{\omega_c}, \tag{2.17}$$

where

$$F(a) = \frac{\mathrm{K}_3^{(2)} a^2 (a^2 - \mathrm{K}_2) + \mathrm{K}_3^{(1)} (\mathrm{K}_1 a^2 - \mathrm{K}_4)}{\left(\omega_c \mathrm{K}_3^{(1)}\right)^2 + \left(\omega_c \mathrm{K}_3^{(2)}\right)^2}. \tag{2.18}$$

Differentiation of equation (2.10) with respect to τ and substituting in (2.12) and (2.13) gives

$$Re\left(\frac{d\lambda^{-1}}{d\tau}\right)\Bigg|_{\lambda = i\omega_c, \tau = \tau_c} = \frac{3\omega_c^3 + \left(2\mathrm{K}_1 + \mathrm{K}_4^2 - 4\mathrm{K}_2\right)\omega_c^2 + d_2}{\left(\omega_c \mathrm{K}_3^{(1)}\right)^2 + \left(\omega_c \mathrm{K}_3^{(2)}\right)^2} > 0.$$

3. NUMERICAL RESULTS

In this section, numerical findings of the three component model presented in (2.1) is presented. A particular attention will be paid on the existence of Hopf bifurcation around the positive steady state $S_3 = (p^*, c^*, z^*)$ in the presence and absence of constant time delay in zoo-plankton gestation. The sign of the Hopf point is the existence of a pair of purely imaginary eigenvalues. Apart from the eigenvalues corresponding to Hopf point, all other eigenvalues are found with a negative real part. In this section, parameters are fixed to $\eta_1 = 3.2$, $\delta_1 = 0.07$, $\beta = 2.1$, $\eta_2 = 2.9$, $\alpha_1 = 0.24$, $\beta_1 = 0.9$, $\delta_2 = 0.28$. In the absence of delay τ , parameter r which is related to the growth rate of phytoplankton with respect to oxygen can be chosen as a control

parameter. At $r = 0.056$, a Hopf bifurcation occur and a limit cycle appears around the positive equilibria. In Figure 1, time simulations of all three species are shown for different values of r parameter. When the growth rate of phytoplankton is zero ($r = 0$) as seen in Fig 1(a), only oxygen presents in the system and plankton species extinct. The model present damping oscillations when $r = 0.01$ as all components converge to positive steady state in Fig 1(b). Stable dynamics in Fig 1(c) for $r = 0.045$ becomes unstable when $r = 0.09$ in Fig 1(d), where higher amplitude oscillations are observed away from the Hopf bifurcation.

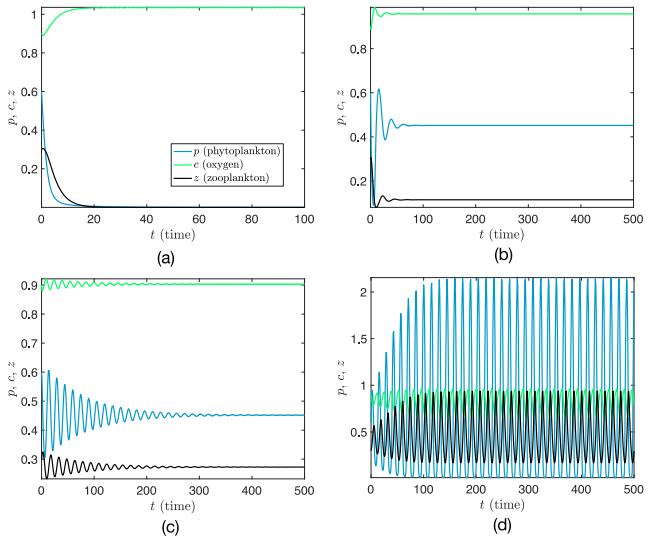

Figure 1: Time evolutions of three component system with the effect of various r values in the absence of delay, (a)*r = 0, (b)r = 0.01, (c)r = 0.045, (d)r = 0.09* with initial conditions $p_0 = 0.6$, $c_0 = 0.9$, $z_0 = 0.3$.

An alternative way to show system dynamics is given in Figure 2, where corresponding phase trajectories are shown. Here (p_0, c_0, z_0) stands for initial condition for each species and presented by red dot. When system is stable, see Fig. 2 (b,c), trajectories approaches to positive steady state (black point), and that is unstable as trajectory gets away from this equilibrium, see Fig. 2 (d).

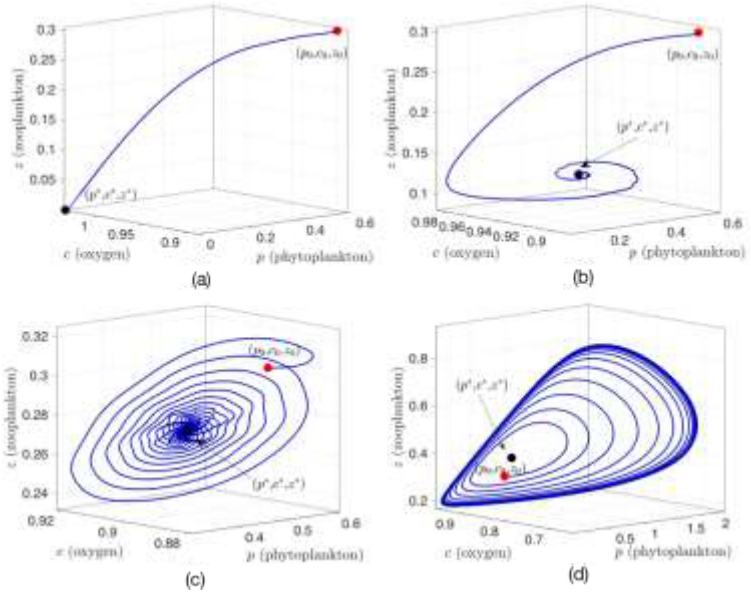

Figure 2: Corresponding phase portraits for *(a)r = 0, (b)r = 0.01, (c)r = 0.045, (d)r = 0.09* in the absence of delay.

The role of delay in the population densities are demonstrated in Figures 3 and 4. For this purpose, the growth rate of phytoplankton with respect to oxygen is fixed to be $r = 0.01$ in the rest of the paper. Taking this stable state as a reference point as seen in Fig 1(b) and Fig 2 (b), one can examine the role of gestation delay in the system. In Figure 2 and 4, one can discuss the existence and stability of Hopf bifurcation induced by various delay rates (τ). Using parameters described at the beginning of section 3, critical delay values is found as $\tau = 2.0075$ (see equation (2.17)), for which Hopf bifurcation occurs. The plots given in 2 (a,c) present stable dynamics of oxygen, phytoplankton and zoo-plankton based on time when delay parameter is under critical threshold, i.e. $\tau = 1.7$. In Fig. 2 (b,d) limit cycle appears with Hopf bifurcations.

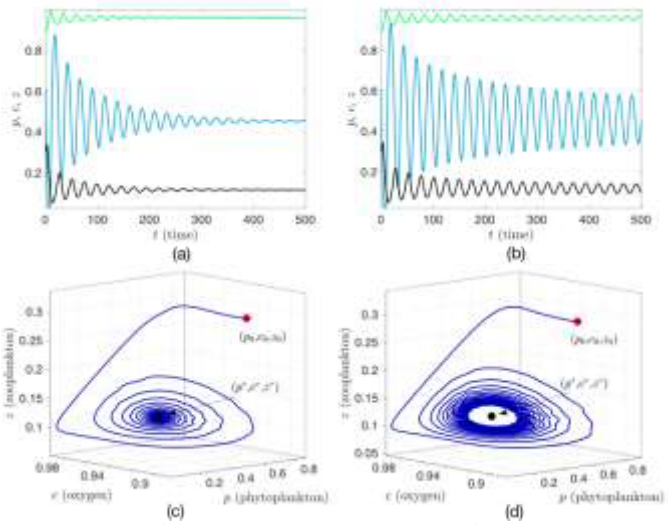

Figure 3: Time evolution and trajectories of the corresponding phase portraits of three component system with delay values *(a,c)* $\tau = 1.7$, *(b,d)* $\tau = 2.0075$

Further away from the bifurcation point, periodic oscillations with high amplitude can be observed and size of the corresponding limit cycle increases as seen in Fig. 4 (a,c). However, excessive delay in the system may result in negative effect on the population, leading to extinction of phytoplankton and zoo-plankton, see Fig. 4 (b,d) where $\tau = 6$.

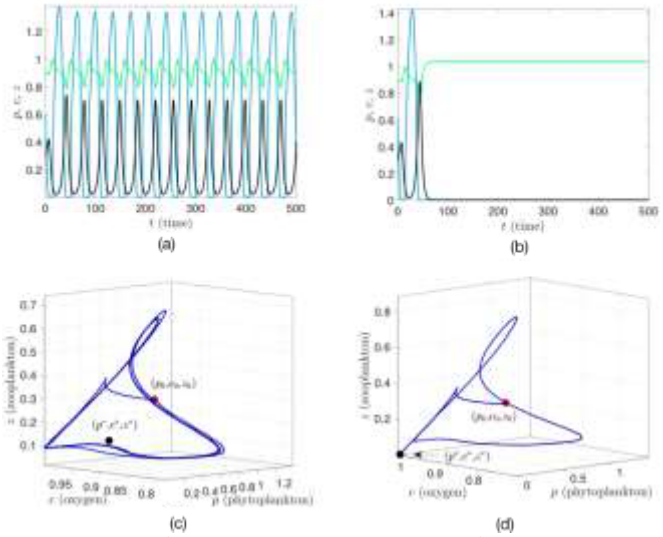

Figure 4: Time evolution and trajectories of the corresponding phase portraits of three component system with delay *values (a,c)* $\tau = 5.5$, *(b,d)* $\tau = 6$

In Figure 5, the curves with the real part of the eigenvalue are plotted as a function of parameter r in the absence (left) and presence (right) of time delay. Here when the curves cross the zero line, instability with a Hopf bifurcation is observed. Compared to non-delayed case (left), Hopf bifurcation is observed for smaller values of r (right).

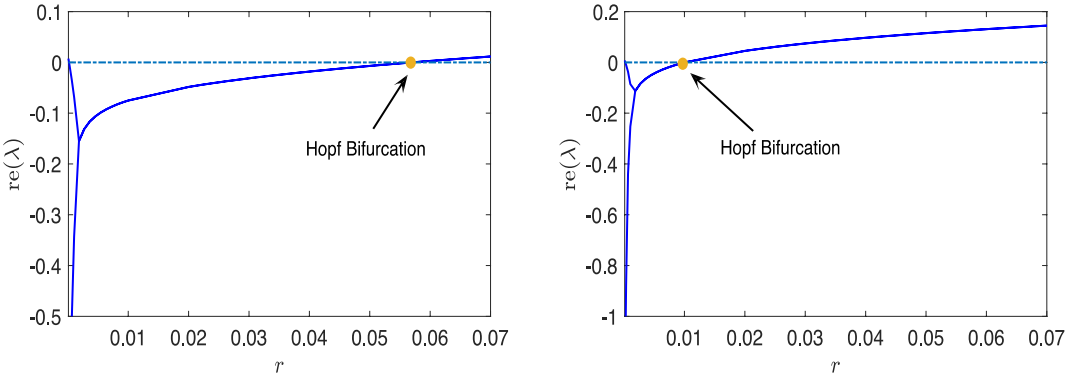

Figure 5: Real part of the eigenvalue is plotted as a function of phytoplankton growth rate r. Hopf bifurcations are detected crossing the zero axes for no delay (left) and with delay (right).

4. NUMERICAL BIFURCATION ANALYSIS

In Figures 6 and 7, the effect of time delay in the system is determined through numerical bifurcation analysis. Here the dynamics of oxygen is examined under the variation of parameters r (phytoplankton growth rate related to oxygen) and η_1 (intake of dissolved oxygen). Similar procedure can be done to explore the dynamics of plankton species, however we are only interested in the role of dissolved oxygen in the water. For the case where delay is absent in the system, the stability of c with respect to parameter r is presented in Fig. 6 (a), where one saddle-node and one Hopf bifurcation are detected. Here n_λ represents the number of eigenvalues with positive real part. In the presence of delay, in Fig. 6 (b), the only change is observed in the stability of coexisting state, where Hopf bifurcation and corresponding limit cycle surrounding unstable positive steady state are seen for smaller r values.

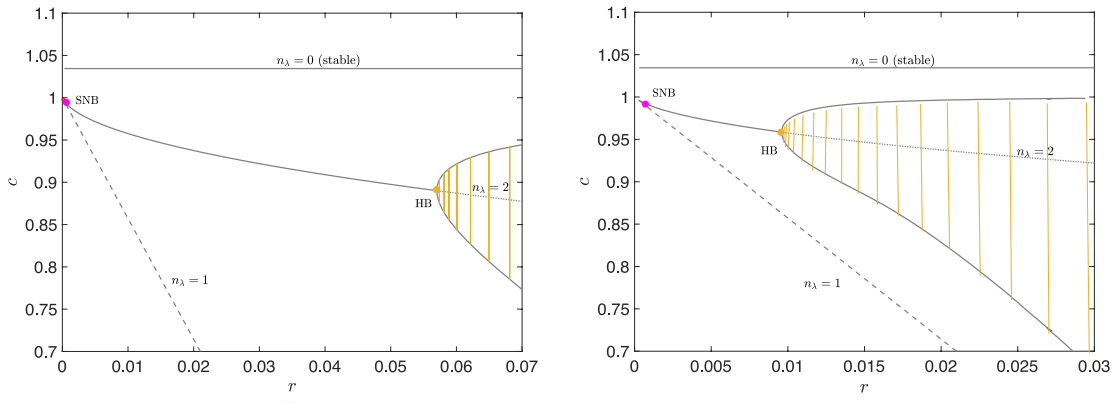

Figure 6: Numerical continuation of c with respect to the parameter r in the absence of delay, and with delay value 2.0075. Here n_λ stands for the number of eigenvalues with positive real parts, thus dashed and dotted lines are unstable and straight line is stable.

In Figure 7, the stability of c around the steady state is visualised as a function of η_1 in the absence and presence of constant time delay, see Figs. 7 (a,b) and 7 (c,d). Compared to Fig. 6, much complex dynamics can

be observed for η_1. Here, two transcritical bifurcations are independent of delay and can be observed in both cases. In fact, delay rate has a main impact on the existence and stability of Hopf bifurcations. When delay is absent, there is a single Hopf bifurcation, where stable branch looses its stability, see Fig 7 (a). Gray lines in 7 (b) represent the copies of branches given in 7 (a) and here unstable branches emanating from Hopf bifurcation with $n_\lambda = 1$ is obtained. When delay is incorporated in the model, three extra Hopf bifurcations appear. A zoomed-in view of the gray square plotted in Fig. 7 (c) is presented in 7 (d), where stable and unstable branches arising from these Hopf points may exhibit various bifurcation dynamics, including saddle node bifurcation, Neimark-Sacker bifurcation and period doubling bifurcation. The number of eigenvalues with positive real parts are associated with various colors. Insets in 7 (d) present zoomed-i view around two bifurcation points, where changes occur in a very small region.

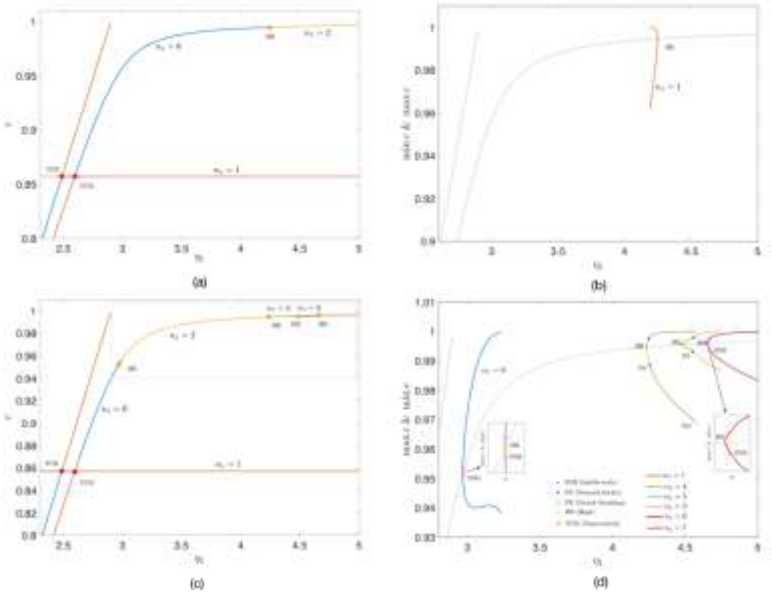

Figure 7: Bifurcations for of c with respect to the parameter η_1 in the absence of delay, and with delay value 2.0075.

5. DISCUSSION

In this paper, we have demonstrated that constant time delay in the population dynamics has a great impact on the stability of the positive steady state for a three component system and this delay may give us the opportunity to analyse the properties of Hopf bifurcations obtained with zoo-plankton gestation. When delay parameter crosses a critical value, stability switches from stable to unstable and Hopf bifurcation occurs. In particular, taking η_1 as a control parameter, multiple Hopf bifurcations can be seen, and the branches emanating from Hopf points display many complex behaviours including transcritical bifurcation, Neimark-Sacker bifurcation, period doubling bifurcation and saddle node bifurcation.

Time simulations and phase trajectories are computed using Matlab 2017 and single parameter continuation and stability analyses in the presence of constant time delay are performed using DDE-BIFTOOL [16, 17]. The most obvious result of this study would be that the model with time delay is realised as biologically more realistic form. Introducing time delay in predator gestation has lead particularly interesting dynamics where fluctuations can be seen for moderate values of time delay. Furthermore, if plankton communities are exposed to large delay, e.g. $\tau = 6$, plankton taxa suffer and extinct, thus only dissolved oxygen exist in the water.

One possible extension of this paper would be the analytical derivation of the stability of Hopf bifurcations near the positive steady state and the direction of the periodic orbits arising from the Hopf points using center manifold theorem [18]. Another natural extension would be to use of brownian motion to explore the stochastic effects in the system [19].

REFERENCES

1. K. Chakraborty and K. Das, "Modeling and analysis of a two-zooplankton one-phytoplankton system in the presence of toxicity," *Applied Mathematical Modelling*, vol. 39, no. 3-4, pp. 1241–1265, 2015.
2. M. Rehim and M. Imran, "Dynamical analysis of a delay model of phytoplankton–zooplankton interaction," *Applied Mathematical Modelling*, vol. 36, no. 2, pp. 638–647, 2012.
3. M. Kretzschmar, R. Nisbet, and E. McCauley, "A predator-prey model for zooplankton grazing on competing algal populations," *Theoretical population biology*, vol. 44, no. 1, pp. 32–66, 1993.
4. Y. Li, H. Liu, R. Yang, and L. Tang, "Dynamics in a diffusive phytoplankton–zooplankton system with time delay and harvesting," *Advances in Difference Equations*, vol. 2019, no. 1, p. 79, 2019.
5. S. Ruan, "Persistence and coexistence in zooplankton-phytoplankton-nutrient models with instantaneous nutrient recycling," *Journal of Mathematical Biology*, vol. 31, no. 6, pp. 633–654, 1993.
6. N. MacDonald and N. MacDonald, *Biological delay systems: linear stability theory*. Cambridge University Press, 2008.
7. R. May, A. R. McLean, *et al.*, *Theoretical ecology: principles and applications*. Oxford University Press on Demand, 2007.
8. J. Zhao and J. Wei, "Dynamics in a diffusive plankton system with delay and toxic substances effect," *Nonlinear Analysis: Real World Applications*, vol. 22, pp. 66–83, 2015.
9. B. Dubey and A. Kumar, "Dynamics of prey–predator model with stage structure in prey including maturation and gestation delays," *Nonlinear Dynamics*, vol. 96, no. 4, pp. 2653–2679, 2019.
10. Z. Zhang, R. K. Upadhyay, R. Agrawal, and J. Datta, "The gestation delay: a factor causing complex dynamics in gause-type competition models," *Complexity*, vol. 2018, 2018.
11. J. Dhar and R. S. Baghel, "Role of dissolved oxygen on the plankton dynamics in spatio-temporal domain," *Modeling Earth Systems and Environment*, vol. 2, no. 1, p. 6, 2016.
12. A. Misra and P. Tiwari, "A model for the effect of density of human population on the depletion of dissolved oxygen in a water body," *Environment, Development and Sustainability*, vol. 17, no. 3, pp. 623–640, 2015.
13. J. Shukla, A. Misra, and P. Chandra, "Mathematical modeling and analysis of the depletion of dissolved oxygen in eutrophied water bodies affected by organic pollutants," *Nonlinear Analysis: Real World Applications*, vol. 9, no. 5, pp. 1851–1865, 2008.
14. A. Gökçe, S. Yazar, and Y. Sekerci, "Delay induced nonlinear dynamics of oxygen-plankton interactions," *Chaos, Solitons & Fractals*, vol. 141, p. 110327, 2020.
15. S. Khare, S. Kumar, and C. Singh, "Modelling effect of the depleting dissolved oxygen on the existence of interacting planktonic population," *Elixir Appl Math*, vol. 55, pp. 12739–12742, 2013.
16. K. Engelborghs, T. Luzyanina, and D. Roose, "Numerical bifurcation analysis of delay differential equations using dde-biftool," *ACM Transactions on Mathematical Software (TOMS)*, vol. 28, no. 1, pp. 1–21, 2002.
17. K. Engelborghs, T. Luzyanina, and G. Samaey, "Dde-biftool: a matlab package for bifurcation analysis of delay differential equations," *TW Report*, vol. 305, pp. 1–36, 2000.
18. B. D. Hassard, B. Hassard, N. D. Kazarinoff, Y.-H. Wan, and Y. W. Wan, *Theory and applications of Hopf bifurcation*, vol. 41. CUP Archive, 1981.
19. C. Ji, D. Jiang, and X. Li, "Qualitative analysis of a stochastic ratio-dependent predator–prey system," *Journal of Computational and Applied Mathematics*, vol. 235, no. 5, pp. 1326–1341, 2011.

$f-$ Lacunary Almost Statistical Convergence and $f-$ Lacunary Almost Summability of Double Sequences of Order α for Fuzzy Numbers

Damla BARLAK[1] and Birgül TORGUT[2]

[1]*Department of Statistics , Faculty of Science, Dicle University, Diyarbakır, TURKEY*
[2]*Department of Mathematics, Faculty of Science, Fırat University, Elazığ, TURKEY*

damla.barlak@dicle.edu.tr
bsatorgut@gmail.com

Abstract. In this study we introduce the concept of $f-$ lacunary almost statistical convergence and $f-$ lacunary almost summability of double sequences of order α for fuzzy numbers. We give some inclusion relations between these concepts.

Key words and phrases: Fuzzy numbers**,** Modulus function, $f-$ Lacunary almost statistical convergence, $f-$ Lacunary almost summability.

1. INTRODUCTION

The fuzzy set concept and some theories related to this concept are given by Zadeh [44]. Bounded and convergent sequences of fuzzy numbers were defined and some of their properties were examined by Matloka [16]. Later Nanda [17] reached the knowledge that the set of bounded and convergent sequences of fuzzy numbers form a complete metric space. Subsequently, Nuray and Savaş [19] reached some results by defining the fuzzy numbers as statistically convergent and statistically Cauchy sequences.. Also, fuzzy sequences have been studied by many authors; Altinok et al. ([4],[5]), Altin et al. [6], Burgin [7], Hanéel et al. [9], Fang and Hung [11], Kumar et al. ([12], [13], [14]),Wang and Xi [45], Aytar and Pehlivan [3], Mursaleen and Başarır [18], Tripathy and Baruah [20], Tripathy and Dutta[21] and others.

A fuzzy real number X is a fuzzy set on R, i.e. a mapping $X:\mathsf{R}\to L(=[0,1])$ associating each real number t with its grade of membership. The $\beta-$ level set of a fuzzy real number X, for $0\le\beta\le 1$ denoted by $[X]^{\beta}$ is defined by $[X]^{\beta}=\{t\in\mathsf{R}:X(t)\ge\beta\}$. A fuzzy real number X is called convex if $X(t)\ge X(s)\wedge X(r)=\min(X(s),X(r))$, where $s<t<r$. If there exist $t_0\in\mathsf{R}$ such that $X(t_0)=1$ then the fuzzy real number X is called normal. A fuzzy real number X said to be upper semi-continuous if for each $\varepsilon>0$, $X^{-1}([0,a+\varepsilon))$, for all $a\in L$ is open in the usual topology of R. The set of all upper semi-continuous, normal, convex fuzzy numbers is denoted by $L(\mathsf{R})$. Every real number r can be expressed as a fuzzy real number $\bar{r}$ as follows:

$$\bar{r}(t)=\begin{cases}1 & \text{if } t=r,\\ 0 & \text{otherwise.}\end{cases}$$

The notion of a modulus was given by Nakano [22]. Maddox [15] used a modulus function to construct some sequence spaces. Afterwards, different sequence spaces defined by modulus have been studied by Altın and Et [2], Et et al.[8], Işık [23], Gaur and Mursaleen [24], Nuray and Savaş [25] , Pehlivan and Fisher [26], Şengül [27], Şengül et al.[28] and many others.

A modulus f is a function from $[0,\infty)$ to $[0,\infty)$ such that

$i)$ $f(x)=0$ if and only if $x=0$,

$ii)$ $f(x+y)\le f(x)+f(y)$ for $x,y\ge 0$,

iii) f is increasing,

iv) f is continuous from the right at 0.

It follows that f must be continuous everywhere on $[0,\infty)$. A modulus function may be unbounded or bounded.

Aizpuru et al. [1] defined $f-$ density of a subset $E \subset \mathbb{N}$ for any unbounded modulus f by

$$d^f(E) = \lim_{n\to\infty} \frac{f(|\{k \le n : k \in E\}|)}{f(n)}, \text{ if the limit exists}$$

and defined $f-$ statistical convergence for any unbounded modulus f by

$$d^f(\{k \in \mathbb{N} : |x_k - l| \ge \varepsilon\}) = 0$$

i.e.

$$\lim_{n\to\infty} \frac{1}{f(n)} f(\{k \le n : |x_k - l| \ge \varepsilon\}) = 0$$

and we write it is as $S^f - \lim x_k = l$ or $x_k \to l(S^f)$. Every $f-$ statistically convergent sequence is statistically convergent, but a statistically convergent sequence does not need to be

$f-$ statistically convergent for every unbounded modulus f.

The concept of almost convergence in single sequences was studied by Lorentz [29], and this work was given by Moricz and Rhoades [30], for double sequences.

A fuzzy real valued double sequence $X = (X_{nk})$ is a double infinite array of fuzzy real numbers, i.e. $X_{nk} \in L(\mathbb{R})$, for all $n,k \in \mathbb{N}$.

Let E be the set of all closed bounded intervals $X = [X^L, X^R]$. Let $d(X,Y) = \max(|X^L - Y^L|, |X^R - Y^R|)$. Then (E,d) is a complete metric space.

Let $\bar{d} : L(\mathbb{R}) \times L(\mathbb{R}) \to \mathbb{R}$ be defined by

$$\bar{d}(X,Y) = \sup_{0\le\alpha\le 1} d([X]^\beta, [Y]^\beta), X, Y \in L(\mathbb{R}).$$

Then $\bar{d}$ defines a metric on $L(\mathbb{R})$.

Fuzzy sequence concept has been studied by Tripathy and Baruah [31], Tripathy and Borgohain ([32],[33]), Tripathy and Das [34], Tripathy and Dutta ([35], [36], [37]), Tripathy and Sarma ([39], [40]) and many others.

In [41], Bronwich was the first to work on double sequences with real or complex terms. Regular convergence of real or complex double sequences has been defined by Hardy. [10]. Some works on double sequences on crisp set are due to Tripathy and Sarma [42] and others. Different types of spaces of fuzzy real-valued binary sequences have also been studied by the authors of Tripathy and Dutta ([35], [36]), Tripathy and Sarma [40] .

A double sequence $\theta_{r,s} = \{(k_r, l_s)\}$ is called double lacunary if there exist two increasing sequences of integers $\{k_r\}$ and $\{l_s\}$ such that

$$k_0 = 0, h_r = k_r - k_{r-1} \to \infty \text{ as } r \to \infty$$

$$\text{and } l_0 = 0, \hat{h}_s = l_s - l_{s-1} \to \infty \text{ as } s \to \infty.$$

Troughout we denote $k_{r,s} = k_r l_s$, $h_{r,s} = h_r \hat{h}_s$ for all $r,s \in \mathbb{N} \cup \{0\}; q_r = \frac{k_r}{k_{r-1}}, \hat{q}_s = \frac{l_s}{l_{s-1}}$, $q_{r,s} = q_r \hat{q}_s$. Interval determined by $\theta_{r,s}$ are denoted by $I_{r,s} = \{(k,l): k_{r-1} \le k \le k_r$ and $l_{s-1} \le l \le l_s\}$. Also $\hat{h}_{r,s} = k_r l_s - k_{r-1} l_{s-1}$. $\theta = \hat{\theta}_{r,s}$ is determined by $\hat{I}_{r,s} = \{(k,l): k_{r-1} < k \le k_r$ or $l_{s-1} < l \le l_s\} \setminus (I^1 \cup I^2)$, where $I^1 = \{(k,l): k_{r-1} < k \le k_r$ and $l_s < l < \infty\}$, $I^2 = \{(k,l): l_{s-1} < l \le l_s$ and $k_r < k < \infty\}$.

Denote

$$B_{\alpha,\beta}^{m,n} = \{(i,j): \alpha < i \le \alpha + m \text{ or } \beta < j \le \beta + n\} \setminus (I_B^1 \cup I_B^2),$$

where $I_B^1 = \{(i,j): \beta < j \le \beta + n$ and $\alpha + m < i < \infty\}$, $I_B^2 = \{(i,j): \alpha < i \le \alpha + m$ and $\beta + n < j < \infty\}$,

$$B_{\alpha,\beta}^{x,y} = \{(i,j): \alpha + xh_r < i \le \alpha + (x+1)h_r \text{ or } \beta + y\hat{h}_s \le \beta + (y+1)\hat{h}_s\}(I_A^1 \cup I_A^2),$$

where $I_A^1 = \{(i,j): \alpha + xh_r < i \le \alpha + (x+1)h_r$ and $\beta + (y+1)\hat{h}_s < j < \infty\}$, $I_A^2 = \{(i,j): \beta + y\hat{h}_s < j \le \beta + (y+1)\hat{h}_s$ and $\alpha + (x+1)h_r < i < \infty\}$.

In [43] , Tripathy and Sen introduced the concept of lacunary almost convergence in the sense that sequence $\langle X_{nk} \rangle$ of fuzzy real valued is called lacunary almost convergent to the fuzzy real number X_0, if for every $\varepsilon > 0$

$$P - \lim_{r,s \to \infty} \frac{1}{\hat{h}_{rs}} \left| \{(n,k) \in \hat{I}_{r,s} : \bar{d}(X_{n+r,k+s}, X_0)\} \right| = 0, \text{uniformly in } r,s \ge 0,$$

where the vertical bars denote the cardinality of the enclosed set.

2. MAIN RESULTS

In the section, we will be introduce the concepts of $f-$ lacunary almost statistical convergence of order α of double sequences for fuzzy numbers and $f-$ lacunary summability of order α of double sequences for fuzzy numbers where f is an unbounded modulus give some results related to these concepts.

Definition 2.1 Let f be unbounded modulus, $\theta'' = \{(k_r, l_s)\}$ be a double lacunary sequence and α be a real number such that $0 < \alpha \le 1$. We say that the fuzzy real valued double sequence $X = \langle X_{nk} \rangle$ is $f-$ lacunary statistically convergent of order α for fuzzy numbers, if there is a fuzzy real number X_0 such that

$$\lim_{r,s \to \infty} \frac{1}{[f(h_{rs})]^\alpha} f\left(\left| \{(n,k) \in I_{r,s} : \bar{d}\left(X_{n+r,k+s}, X_0\right)\} \right| \right) = 0, \text{uniformly in } r,s \ge 0$$

This space will be denoted by $\hat{S}_\theta^{f,\alpha}$. In this case, we write $\hat{S}_\theta^{f,\alpha} - \lim X_{nk} = X_0$. In the special case $\theta'' = \{(2^r, 2^s)\}$, we shall write $\hat{S}^{f,\alpha}$ instead of $\hat{S}_\theta^{f,\alpha}$.

Definition 2.2. Let f be unbounded modulus, $\theta'' = \{(k_r, l_s)\}$ be a double lacunary sequence, $p = (p_k)$ be a sequence of strictly positive real numbers and α be a real number such that $0 < \alpha \le 1$. We say that the fuzzy real

valued double sequence $X=\langle X_{nk}\rangle$ is $\hat{w}^{\alpha}_{\theta}{}_{,,f}(p)$ - almost summable to X_0 (a fuzzy number), if there is a fuzzy real number X_0 such that

$$\frac{1}{[f(h_{rs})]^{\alpha}}\sum_{(n,k)\in I_{r,s}}\left[\bar{d}\left(X_{n+r,k+s},X_0\right)\right]^{p_k}=0,\text{uniformly in } r,s\geq 0$$

This space will be denoted by $\hat{w}^{\alpha}_{\theta}{}_{,,f}(p)$. In this case, we write $\hat{w}^{\alpha}_{\theta}{}_{,,f}(p)-\lim X_{nk}=X_0$. The set of strongly $\hat{w}^{\alpha}_{\theta}{}_{,,f}(p)-$ almost summable sequences will be denoted by $\hat{w}^{\alpha}_{\theta}{}_{,,f}(p)$. If we take $p_k=p$ for all $k\in\mathbb{N}$, we write $\hat{w}^{\alpha}_{\theta}{}_{,,f}[p]$ instead of $\hat{w}^{\alpha}_{\theta}{}_{,,f}(p)$.

Definition 2.3. Let f be unbounded modulus, $\theta''=\{(k_r,l_s)\}$ be a double lacunary sequence, $p=(p_k)$ be a sequence of strictly positive real numbers and α be a real number such that $0<\alpha\leq 1$. We say that the fuzzy real valued double sequence $X=\langle X_{nk}\rangle$ is $\hat{w}^{\alpha}[\theta'',f,p]$ - almost summable to X_0 (a fuzzy number), if there is a fuzzy number X_0 such that

$$\lim_{r,s\to\infty}\frac{1}{[h_{rs}]^{\alpha}}\sum_{(n,k)\in I_{r,s}}\left[f(\bar{d}\left(X_{n+r,k+s},X_0\right))\right]^{p_k}=0,\text{uniformly in } r,s\geq 0$$

in this case we write $\hat{w}^{\alpha}[\theta'',f,p]-\lim X_{n,k}=X_{0.}$ The set of all strongly almost summable sequences will be denoted by $\hat{w}^{\alpha}[\theta'',f,p]$. If we take $p_k=1$ for all $k\in\mathbb{N}$, we write $\hat{w}^{\alpha}[\theta'',f]$ instead of $\hat{w}^{\alpha}[\theta'',f,p]$.

Definition 2.4. Let f be unbounded modulus, $\theta''=\{(k_r,l_s)\}$ be a double lacunary sequence, $p=(p_k)$ be a sequence of strictly positive real numbers and α be a positive real number. We say that the fuzzy real valued double sequence $X=\langle X_{nk}\rangle$ is $\hat{w}^{f,\alpha}_{\theta}{}_{,,}(p)$ - almost summable to X_0 (a fuzzy number), if there is a fuzzy number X_0 such that

$$\lim_{r,s\to\infty}\frac{1}{[f(h_{rs})]^{\alpha}}\sum_{(n,k)\in I_{r,s}}\left[f(\bar{d}\left(X_{n+r,k+s},X_0\right))\right]^{p_k}=0,\text{uniformly in } r,s\geq 0.$$

Then we write $\hat{w}^{f,\alpha}_{\theta}{}_{,,}(p)-\lim X_{n,k}=X_{0.}$

In order not to indicate in each of the following theorems, we will assume that the sequence $p=(p_k)$ is bounded and $0<h=\inf_k p_k\leq p_k\leq\sup_k p_k=H<\infty$.

Maddox [15] proved the existence of an infinite modulus f with inequality $f(xy)\geq cf(x)f(y)$, for all $x\geq 0,\ y\geq 0$, where c is a positive constant.

Teorem 2.1. Let f be an unbounded modulus function and α be a positive real number. If $\lim_{u\to\infty}\frac{[f(u)]^{\alpha}}{u^{\alpha}}>0$, then $\hat{w}^{\alpha}[\theta'',f]\subset\hat{S}^{f,\alpha}_{\theta}{}_{,,}$.

Proof. Let $X \in \hat{w}^{\alpha}[\theta^{''}, f]$ and $\lim_{u\to\infty}\frac{[f(u)]^{\alpha}}{u^{\alpha}} > 0.$ For $\varepsilon > 0,$ we have

$$\frac{1}{[h_{rs}]^{\alpha}}\sum_{(n,k)\in I_{r,s}} f(\bar{d}(X_{n+r,k+s}, X_0)) \geq \frac{1}{[h_{rs}]^{\alpha}}\left(\sum_{(n,k)\in I_{r,s}} \bar{d}(X_{n+r,k+s}, X_0)\right)$$

$$\geq \frac{1}{[h_{rs}]^{\alpha}}\left(\sum_{\substack{(n,k)\in I_{r,s} \\ \bar{d}(X_{n+r,k+s}, X_0)\geq\varepsilon}} \bar{d}(X_{n+r,k+s}, X_0)\right)$$

$$\geq \frac{1}{[h_{rs}]^{\alpha}} f\left(\left|\{(n,k)\in I_{rs} : \bar{d}(X_{n+r,k+s}, X_0)) \geq \varepsilon\}\right|\varepsilon\right)$$

$$\geq \frac{c}{[h_{rs}]^{\alpha}} f\left(\left|\{(n,k)\in I_{rs} : \bar{d}(X_{n+r,k+s}, X_0)) \geq \varepsilon\}\right|\right) f(\varepsilon)$$

$$= \frac{c}{[h_{rs}]^{\alpha}} \frac{f\left(\left|\{(n,k)\in I_{rs} : \bar{d}(X_{n+r,k+s}, X_0)) \geq \varepsilon\}\right|\right)}{[f(h_{rs})]^{\alpha}} [f(h_{rs})]^{\alpha} f(\varepsilon).$$

Therefore, $\hat{w}^{\alpha}[\theta^{''}, f] - \lim X_{n,k} = X_0$ implies $\hat{S}_{\theta}^{f;\alpha}{}_{''} - \lim X_{n,k} = X_0.$

Teorem 2.2. Let α_1, α_2 be two real numbers such that $0 < \alpha_1 \leq \alpha_2 \leq 1,$ f be an unbounded modulus function and let $\theta^{''} = \{(k_r, l_s)\}$ be a double lacunary sequence. The sequence $p = (p_k)$ is bounded and $0 < h = \inf_k p_k \leq p_k \leq \sup_k p_k = H < \infty.$ Then we have $\hat{w}_{\theta}^{\alpha_1}{}_{''}(p) \subset \hat{S}_{\theta}^{f,\alpha_2}{}_{''}.$

Proof. Let $X = \langle X_{nk}\rangle \in \hat{w}_{\theta}^{\alpha_1}{}_{''}(p)$ and $\varepsilon > 0$ be given and $\sum_1, \sum_2$ denote the sums over $(n,k)\in I_{r,s}$, $\bar{d}(X_{n,k}, X_0) \geq \varepsilon$ and $(n,k)\in I_{r,s}$, $\bar{d}(X_{n,k}, X_0) < \varepsilon$ respectively. Since

$f(h_{rs})^{\alpha_1} \leq f(h_{rs})^{\alpha_2}$ for each r and s, we may write

$$\frac{1}{[f(h_{r,s})]^{\alpha_1}}\sum_{(n,k)\in I_{r,s}} \left[f(\bar{d}(X_{n+r,k+s}, X_0))\right]^{p_k}$$

$$= \frac{1}{[f(h_{r,s})]^{\alpha_1}}\left[\sum_1 \left[f(\bar{d}(X_{n+r,k+s}, X_0))\right]^{p_k} + \sum_2 \left[f(\bar{d}(X_{n+r,k+s}, X_0))\right]^{p_k}\right]$$

$$\geq \frac{1}{[f(h_{r,s})]^{\alpha_2}}\left[\sum_1 \left[f(\bar{d}(X_{n+r,k+s}, X_0))\right]^{p_k} + \sum_2 \left[f(\bar{d}(X_{n+r,k+s}, X_0))\right]^{p_k}\right]$$

$$\geq \frac{1}{[f(h_{r,s})]^{\alpha_2}}\left[\sum_1 [f(\varepsilon)]^{p_k}\right]$$

$$\geq \frac{1}{H.[f(h_{r,s})]^{\alpha_2}}\left[f\left(\sum_1 [\varepsilon]^{p_k}\right)\right]$$

$$\geq \frac{1}{H.[f(h_{r,s})]^{\alpha_2}}\left[f\left(\sum_1 \min([\varepsilon]^h,[\varepsilon]^H)\right)\right]$$

$$\geq \frac{1}{H.[f(h_{r,s})]^{\alpha_2}} f\left(\left|\{(n,k)\in I_{rs}: \bar{d}\left(X_{n+r,k+s},X_0\right)\geq\varepsilon\}\right|\left[\min([\varepsilon]^h,[\varepsilon]^H)\right]\right)$$

$$\geq \frac{c}{H.[f(h_{r,s})]^{\alpha_2}} f\left(\left|\{(n,k)\in I_{rs}: \bar{d}\left(X_{n+r,k+s},X_0\right)\geq\varepsilon\}\right|\right) f\left(\left[\min([\varepsilon]^h,[\varepsilon]^H)\right]\right)$$

Hence $X \in \hat{S}_{\theta}^{f,\alpha_2}$.

Teorem 2.3. Let f be an unbounded modulus, $\theta'' = \{(k_r,l_s)\}$ be a double lacunary sequence and α be a fixed number such that $0<\alpha\leq 1$. If $\lim\inf_r q_r > 1$, $\lim\inf_s q_s > 1$ and $\lim_{u\to\infty}\frac{[f(u)]^\alpha}{u^\alpha} > 0$, then $\hat{S}^{''f,\alpha} \subset \hat{S}_{\theta}^{f,\alpha}$.

Proof. Suppose first that $\lim\inf_r q_r > 1$ and $\lim\inf_s q_s > 1$; then there exist $a,b>0$ such that $q_r \geq 1+a$ and $q_s \geq 1+b$ for sufficiently large r and s, which implies that

$$\frac{h_r}{n_r} \geq \frac{a}{1+a} \Rightarrow \left(\frac{h_r}{n_r}\right)^\alpha \geq \left(\frac{\alpha}{1+\alpha}\right)^\alpha$$

and

$$\frac{\bar{h}_s}{k_s} \geq \frac{b}{1+b} \Rightarrow \left(\frac{\bar{h}_s}{k_s}\right)^\alpha \geq \left(\frac{b}{1+b}\right)^\alpha.$$

If $\hat{S}^{''f,\alpha} - \lim X_{n,k} = X_0$, then for every $\varepsilon>0$ and for sufficiently large r and s, we have

$$\frac{1}{[f(n_r k_s)]^\alpha} f\left(\left|\{n\leq n_r, k\leq k_s : \bar{d}\left(X_{n+r,k+s},X_0\right)\geq\varepsilon\}\right|\right)$$

$$\geq \frac{1}{[f(n_r k_s)]^\alpha} f\left(\left|\{(n,k)\in I_{r,s}: \bar{d}\left(X_{n+r,k+s},X_0\right)\geq\varepsilon\}\right|\right)$$

$$= \frac{[f(h_{r,s})]^\alpha}{[f(n_r k_s)]^\alpha}\frac{1}{[f(h_{r,s})]^\alpha} f\left(\left|\{(n,k)\in I_{r,s}: \bar{d}\left(X_{n+r,k+s},X_0\right)\geq\varepsilon\}\right|\right)$$

$$= \frac{[f(h_{r,s})]^\alpha}{[h_{r,s}]^\alpha}\frac{n_r^\alpha}{[f(n_r k_s)]^\alpha}\frac{[h_{r,s}]^\alpha}{n_r^\alpha} f\left(\left|\{(n,k)\in I_{r,s}: \bar{d}\left(X_{n+r,k+s},X_0\right)\geq\varepsilon\}\right|\right)$$

$$= \frac{[f(h_{r,s})]^{\alpha}}{[h_{r,s}]^{\alpha}} \frac{n_r^{\alpha} k_s^{\alpha}}{[f(n_r k_s)]^{\alpha}} \frac{[h_{r,s}]^{\alpha}}{n_r^{\alpha} k_s^{\alpha}} \frac{f\left(\left|\{(n,k) \in I_{r,s} : \bar{d}\left(X_{n+r,k+s}, X_0\right)) \geq \varepsilon\}\right|\right)}{[f(h_{r,s})]^{\alpha}}$$

$$\geq \frac{[f(h_{r,s})]^{\alpha}}{[h_{r,s}]^{\alpha}} \frac{(n_r k_s)^{\alpha}}{[f(n_r k_s)]^{\alpha}} \left(\frac{a}{1+a}\right)^{\alpha} \left(\frac{b}{1+b}\right)^{\alpha} \frac{f\left(\left|\{(n,k) \in I_{r,s} : \bar{d}\left(X_{n+r,k+s}, X_0\right)) \geq \varepsilon\}\right|\right)}{[f(h_{r,s})]^{\alpha}},$$

so the proof is complete.

Teorem 2.4. Let f be an unbounded modulus, $\theta = (k_r)$ and $\theta' = (l_s)$ be two lacunary sequences, $\theta'' = \{(k_r, l_s)\}$ be a double lacunary sequence and $0 < \alpha \leq 1$. If $\hat{S}^{\alpha}_{f,\theta} - \lim X_n = X_0$ and $\hat{S}^{\alpha}_{f,\theta'} - \lim X_k = X_0$, then $\hat{S}^{\alpha}_{f,\theta''} - \lim X_{n,k} = X_0$.

Proof. Suppose $\hat{S}^{\alpha}_{f,\theta} - \lim X_n = X_0$ and $\hat{S}^{\alpha}_{f,\theta'} - \lim X_k = X_0$. Then for $\varepsilon > 0$ we can write

$$\lim_r \frac{1}{[f(h_r)]^{\alpha}} \left|\{n \in I_r : \bar{d}\left(X_{n+r}, X_0\right)\right| = 0$$

and

$$\lim_s \frac{1}{[f(\bar{h}_s)]^{\alpha}} \left|\{k \in I_s : \bar{d}\left(X_{k+s}, X_0\right)\right| = 0$$

so we have

$$\frac{1}{[f(h_{r,s})]^{\alpha}} \left|\{(n,k) \in I_{r,s} : \bar{d}\left(X_{n+r,k+s}, X_0\right) \geq \varepsilon\right|$$

$$\leq \frac{1}{[cf(h_r) f(\bar{h}_s)]^{\alpha}} \left|\{(n,k) \in I_{r,s} : \bar{d}\left(X_{n+r,k+s}, X_0\right) \geq \varepsilon\}\right|$$

$$\leq \frac{1}{c^{\alpha}\left[f(h_r)\right]^{\alpha}\left[f(\bar{h}_s)\right]^{\alpha}} \left|\{(n,k) \in I_{r,s} : \bar{d}\left(X_{n+r,k+s}, X_0\right) \geq \varepsilon\}\right|$$

$$\leq \left[\frac{1}{[f(h_r)]^{\alpha}} \left|\{n \in I_r : \bar{d}\left(X_{n+r}, X_0\right) \geq \varepsilon\}\right|\right]\left[\frac{1}{[f(\bar{h}_s)]^{\alpha}} \left|\{k \in I_s : \bar{d}\left(X_{k+s}, X_0\right) \geq \varepsilon\}\right|\right].$$

Hence $\hat{S}^{\alpha}_{f,\theta''} - \lim X_{n,k} = X_0$.

Teorem 2.5. Let f be an unbounded modulus. If $\lim p_k > 0$, then $\hat{w}^{f,\alpha}_{\theta''}(p) - \lim X_{n,k} = X_0$ uniquely.

Proof. Let $\lim p_k = t > 0$. Assume that $\hat{w}^{f,\alpha}_{\theta''}(p) - \lim X_{n,k} = X_0$ and $\hat{w}^{f,\alpha}_{\theta''}(p) - \lim X_{n,k} = X_0'$. Then

$$\lim_{r,s\to\infty}\frac{1}{[f(h_{rs})]^{\alpha}}\sum_{(n,k)\in I_{r,s}}\left[f\left(\bar{d}\left(X_{n+r,k+s},X_0\right)\right)\right]^{p_k}=0,\text{uniformly in } r,s\geq 0,$$

and

$$\lim_{r,s\to\infty}\frac{1}{[f(h_{rs})]^{\alpha}}\sum_{(n,k)\in I_{r,s}}\left[f\left(\bar{d}\left(X_{n+r,k+s},X_0^{'}\right)\right)\right]^{p_k}=0,\text{uniformly in } r,s\geq 0.$$

By definition of f, we have

$$\frac{1}{[f(h_{rs})]^{\alpha}}\sum_{(n,k)\in I_{r,s}}\left[f\left(\bar{d}\left(X_0,X_0^{'}\right)\right)\right]^{p_k}$$

$$\leq\frac{D}{[f(h_{rs})]^{\alpha}}\left(\sum_{(n,k)\in I_{r,s}}\left[f\left(\bar{d}\left(X_{n+r,k+s},X_0\right)\right)\right]^{p_k}+\sum_{(n,k)\in I_{r,s}}\left[f\left(\bar{d}\left(X_{n+r,k+s},X_0^{'}\right)\right)\right]^{p_k}\right)$$

$$=\frac{D}{[f(h_{rs})]^{\alpha}}\sum_{(n,k)\in I_{r,s}}\left[f\left(\bar{d}\left(X_{n+r,k+s},X_0\right)\right)\right]^{p_k}+\frac{D}{[f(h_{rs})]^{\alpha}}\sum_{(n,k)\in I_{r,s}}\left[f\left(\bar{d}\left(X_{n+r,k+s},X_0^{'}\right)\right)\right]^{p_k}$$

where $\sup_k p_k = H$ and $D=\max(1,2^{H-1})$. Hence

$$\lim_{r,s\to\infty}\frac{1}{[f(h_{rs})]^{\alpha}}\sum_{(n,k)\in I_{r,s}}\left[f\left(\bar{d}\left(X_0,X_0^{'}\right)\right)\right]^{p_k}=0.$$

Since $\lim p_k = t$ we have $\bar{d}\left(X_0,X_0^{'}\right)=0$. Thus the limit is unique.

REFERENCES

1. A. Aizpuru, M.C. Listan-Garcia and F. Rambla-Barreno, Density by moduli and statistical convergence. Quaest. Math. **37**(4), (2014), 525-530.
2. Y. Altin and M. Et, Generalized difference sequence spaces defined by a modulus function in a locally convex space. Soochow J. Math. **31**(2) (2005), 233-243.
3. S. Aytar and S. Pehlivan, Statistically convergence of sequences of fuzzy numbers and sequences of $\alpha-$cuts, International J General Systems (2007), 1-7.
4. H. Altinok, On $\lambda-$statistical convergence of order β of sequences of fuzzy numbers, Internat J Uncertain Fuziness Knowledge-Based Systems **20**(2) (2012), 303-314.
5. H. Altinok, R. Çolak and M. Et, $\lambda-$difference sequences of fuzzy numbers, Fuzzy Sets and Systems **160**(21) (2009), 3128-3139.
6. Y. Altin, M. Et and M. Başarır, On some generalized difference sequences of fuzzy numbers, Kuwait J Sci Eng **34**(1A) (2007), 1-14.
7. M. Burgin, Theory of fuzzy limits, Fuzzy Sets Syst **115** (2000), 433-443.
8. M. Et, Y. Altin and H. Altinok, On some generalized difference sequence spaces defined by a modulus function. Filomat **17** (2003), 23-33.
9. J. Hanéel, L. Misik, L and J Toth, Cluster points of sequences of fuzzy real numbers, Soft Computing **14**(4) (2010), 399-404.
10. G. H. Hardy, On the convergence of certain multiple series, Proc. Camb. Phil. Soc. **19**(1917), 86-95.
11. J.X. Fang and H. Hung, On the level convergence of a sequence of fuzzy numbers, Fuzzy Sets Syst **147** (2004), 417-435.
12. P. Kumar, V. Kumar and S.S. Bhatia, Lacunary statistical limit and cluster points of generalized difference sequences of fuzzy numbers, Adv Fuzzy Syst, Art. **ID 459370**, (2012), 6.

13. P. Kumar, S.S. Bhatia and V. Kumar, On lacunary statistical cluster points of sequences of fuzzy numbers, Iran J Fuzzy Syst. (in press).
14. V. Kumar and M. Mursaleen, On $(\lambda,\mu)-$statistical convergence of double sequences on intuitionistic fuzzy normed spaces, Filomat **25**(2) (2011), 109-120.
15. I. J. Maddox, Sequence spaces defined by a modulus. Math. Proc. Cambridge Philos. Soc. **100** (1986), no. 1, 161–166.
16. M. Matloka, Sequences of fuzzy numbers, BUSEFAL **28** (1986), 28-37.
17. S. Nanda, On sequences of fuzzy numbers, Fuzzy Sets Syst **33** (1989), 123-126.
18. M. Mursaleen and M. Başarır, On some new sequences spaces of fuzzy numbers, Indian J Pure Appl Math **34**(9) (2003), 1351-1357.
19. F. Nuray and E. Savaş, Statistical convergence of sequences of fuzzy real numbers, Math Slovaca **45**(3) (1995), 269-273.
20. B.C. Tripathy and A. Baruah, New type of difference sequence spaces of fuzzy real numbers, Math Modelling and Analysis **14**(3) (2009), 391-397.
21. B.C. Tripathy and A.J. Dutta, Bounded variation double sequence space of fuzzy numbers, Comput and Math Appl **59**(2) (2010), 1031-1037.
22. H. Nakano, Modulared sequence spaces. Proc. Japan Acad. **27** (1951), 508-512.
23. M. Işık, Generalized vector-valued sequence spaces defined by modulus functions. J. Inequal. Appl. 2010 Art. **ID 457892** (2010), 7 pp.
24. A. K. Gaur and M. Mursaleen, Difference sequence spaces defined by a sequence of moduli. Demonstratio Math. **31**(2) (1998), 275-278.
25. F. Nuray and E. Savaş, Some new sequence spaces defined by a modulus function. Indian J. Pure Appl. Math. **24**(11) (1993), 657-663.
26. S. Pehlivan and B. Fisher, Some sequence spaces defined by a modulus. Math. Slovaca **45**(3) (1995), 275-280.
27. H. Şengül, Some Cesaro-type summability spaces defined by a modulus function of order (α,β). Commun. Fac. Sci. Univ. Ank.Ser. A1 Math. Stat. **66**(2) (2017). 80-90.
28. H. Şengül; M. Et, ; Y. Altin. f -lacunary statistical convergence and strong f -lacunary summability of order α of double sequences. Facta Univ. Ser. Math. Inform. 35 (2020), no. 2, 495–506.
29. G.G. Lorentz, A contribution to the theory of divergent sequences, Acta Math. 80 (1948) 167–190.
30. F. Moricz, B.E. Rhoades, Almost convergence of double sequences and strong regularity of summability matrices. Math. Proc. Camb. Soc. **104**, 283-294 (1988).
31. B. C. Tripathy and A. Baruah, Lacunary statistically convergent and lacunary strongly convergent generalized difference sequences of fuzzy real numbers, Kyungpook Math. J. **50**(4), (2010), 565-574.
32. B. C. Tripathy and S. Borgogain, Some classes of difference sequence spaces of fuzzy real numbers defined by a Orlicz function, Advances Fuzzy Syst. 2011, Article ID216414, 6pages.
33. B. C. Tripathy and S. Borgogain, On a class of n-normed sequences related to the l_p – space, Bol. Soc. Paran. Mat. **31**(1) (2013), 167-173.
34. B. C. Tripathy and P. C. Das, On convergence of series of fuzzy real numbers, Kuwait J Sci Eng **39**(1A) (2012), 57-70.
35. B. C. Tripathy and A. J. Dutta, On fuzzy real-valued double sequence spaces, Math. Computer Modell. **46**(9-14) (2007), 1294-1299.
36. B. C. Tripathy and A. J. Dutta, On fuzzy real-valued double sequence spaces, Math. Computer Modell. **46** (2007), 1294-1299.
37. B. C. Tripathy and A. J. Dutta, On I-acceleration convergence of sequences of fuzzy real numbers, Math. Modell. Analysis **17**(4) (2012), 549-557.
38. B. C. Tripathy and A. J. Dutta, Lacunary bounded variation sequence of fuzzy real numbers, Jour. Intell. Fuzzy Syst. **24**(1) (2013), 185-189.
39. B. C. Tripathy and B. Sarma, Sequence spaces of fuzzy real numbers defined by a Orlicz functions, Math. Slovaca **58**(5) (2008), 621-628.
40. B. C. Tripathy and B. Sarma, Double sequence spaces of fuzzy real numbers defined by a Orlicz function, Acta Math. Scientia **31**(B1) (2011), 134-140.

41. T. J. Ia. Bromwich, An Inroduction to the Theory of Infinite Series, New York, MacMillan and Co Ltd., 1965.
42. B. C. Tripathy and B. Sarma, Vector valued double sequence spaces defined by a Orlicz function, Math. Slovaca **59**(6) (2009), 757-776.
43. B.C. Tripathy and Sen, On lacunary strongly almost convergent double sequences of fuzzy numbers, An. Univ. Craiova Ser. Mat. Inform. **42**(2), (2015), 254-259.986), 161-166.
44. L.A. Zadeh, Fuzzy sets, Inform and Control **8** (1965), 338-353.
45. G. Wang and X. Xi, Convergence of sequences on the fuzzy real line, Fuzzy Sets and Systems **127**(3) (2002), 323-331.

Comparison Between Logistic Regression and Support Vector Machine for Hepatitis Classification

Faisa MAULIDINA, Afifah Rofi LAELI, Zuherman RUSTAM

Department of Mathematics, University of Indonesia, Depok 16424, Indonesia

faisa.maulidina@ui.ac.id
afifahrl@sci.ui.ac.id
rustam@ui.ac.id

Abstract. Hepatitis refers to an inflammatory condition of the liver, with symptoms including fatigue, flu-like symptoms, dark urine, yellowing of the eyes and skin. The most common type of hepatitis in the world are Hepatitis B and C. Early diagnosis should be carried out on individuals that infected by this virus. Furthermore, they should be properly treated to curb the risks that may occur. Machine learning has been useful in helping doctors improve their medical decisions regarding diagnosis of Hepatitis. Some researchers have used several machine learning methods to diagnose Hepatitis. In this study, Logistic Regression and Support Vector Machine were compared to discover which method is best for diagnosing Hepatitis dataset from Tangerang District General Hospital. This dataset consists of 29 Hepatitis B patients and 84 Hepatitis C patients. The target type of this dataset is Hepatitis B or Hepatitis C. In this research, both methods were used and compared because they have some advantages. Logistic Regression provides great training efficiency and easy implementation. The predicted parameters gave a conclusion about the importance of the features. Meanwhile, Support Vector Machine performs well when there is a clear margin of separation between classes and it also has a relatively efficient memory. Based on this experiment, Logistic Regression yielded 96.04% accuracy using 90% of data training, while Support Vector Machine yielded 94.96% accuracy using 70% of data training. Therefore, it can be concluded that Logistic Regression is a better method for classifying Hepatitis dataset.

1. INTRODUCTION

Hepatitis refers to an inflammatory condition of the liver which occurs when an individual becomes infected by the Hepatitis virus, but it can also be caused by using drugs, excessive consumption of alcohol and autoimmune diseases. When this happens to an individual, the symptoms include fatigue, flu-like symptoms, dark urine, yellowing of the eyes and skin.

The most common Hepatitis virus in the world are Hepatitis B and C [1-3], which commonly transmitted through contact with body fluids such as blood, vaginal secretions or semen.

Hepatitis B and C viruses are the main causes of liver disease [4]. The prevalence of hepatitis C virus (HCV) infection reached at 40% among kidney transplant patients [5]. Majority of liver disease due to kidney transplantation is caused by hepatitis C virus infection.

According to The World Health Organization (WHO), approximately 257 million are living with hepatitis B, and 71 million are living with hepatitis C worldwide [6]. One million deaths each year is caused by this viral infection. It is the seventh most common cause of death worldwide and is a significant public health problem in South East Asia.

Early diagnosis should be carried out on individuals that infected by this virus. Furthermore, they should be properly treated to curb the risks that may occur. Hepatitis is usually diagnosed by using blood tests which is associated with various risk factors [7-14]. Although there have been very good results from using this method, the progress made in diagnosing this disease is still unclear. Therefore, many studies have been carried out to aid the diagnosis of hepatitis by some researchers such as data mining. The discovery of data mining has been able to help doctors improve their medical decisions [15].

Data mining is a semi-automatic process that uses mathematical techniques, artificial intelligence, and machine learning to access useful knowledge and information kept in a huge database (Turban, 2005).

Machine learning is one area of computer science that is useful in predicting various outcomes depending on the data used [16]. Such algorithms have a significant contribution to medical decision making [17-18]. In this research, two methods were proposed and compared for the prediction of Hepatitis. They include Logistic Regression and Support Vector Machine (SVM). The dataset that used in this study was obtained from Tangerang District General Hospital.

Logistic sigmoid function was used in Logistic Regression to transform its output and return a probability value. This value was mapped to two or more classes. Conversely, Support Vector Machine uses kernel trick to find the optimal boundary between the possible outputs.

SVM and Logistic Regression have been used to classify many diseases. Z. Rustam and Rampisela T.V used SVM to classify Schizophrenia data and obtained an accuracy of 90.1% [19]. Nadira and Z. Rustam also used SVM and feature selection to classify cancer. An accuracy of 96.4286% was obtained on breast cancer dataset, and 99.9999% on lung cancer dataset [20]. C. Aroef, R. P. Yuda, Z. Rustam, and J. Pandelaki used Multinomial Logistic Regression and SVM in Osteoarthritis Classification. An accuracy of 85% and 71% was obtained using SVM and Multinomial Logistic Regression respectively [21].

Hepatitis has also been predicted using several methods. G. Kurniawan and Z. Rustam used K-Means Clustering in predicting hepatitis disease and obtained an accuracy of 84.85% [22]. Karthikeyan Thirunavu and Dr. P. Thangaraju obtained an accuracy of 84% using Naive Bayes, and 83% using Random Forest, J48 and Multilayer Perceptron [23].

Therefore, in this study, Logistic Regression and Support Vector Machine methods will be compared by using hepatitis dataset that obtained from Tangerang District General Hospital.

2. MATERIAL & METHODS

2.1 Dataset

The dataset was obtained from Tangerang District General Hospital. It consisted of 113 instances with four features and two classes, with 29 Hepatitis B patients and 84 Hepatitis C patients. The target type of this dataset is Hepatitis B or Hepatitis C. Table 1 shows the features.

Table 1. The features in hepatitis dataset

Feature Name	Description
Gender	Male or Female
SGOT	Aspartate Amino transferase
SGPT	Alkaline Amino transferase
Anti-HCV	Anti Hepatitis C Virus
Hepatitis B or Hepatitis C	Class

a. Logistic Regression

Logistic Regression (LR) is a type of regression used in binary classification. It is also a predictive analysis. To build a binary classification model, it uses the maximum log-likehood principle. The attribute may be ordinal, nominal, ratio scale or interval, but the output is only a binary value.

The main function of Linear Regression method is finding a linear decision boundary that separates the attribute space when the probability of the outcome is 0.5, i.e:

$$p(y=1|x)=p(y=0|x) \tag{2.2.1}$$

To match the logarithmic form of the odds ratio, the model used the linear regression optimization algorithm such as:

$$\log\frac{p(y=1|x)}{p(y=0|x)}=\log\frac{p(y=1|x)}{1-p(y=1|x)}=\beta^T x \tag{2.2.2}$$

where β^T is the transpose of the coefficient vector. The logit function is a log of the odds ratio that links the linear model's output to the outcome. By using sigmoid (logistic) function, Equation (2.2.2) was reformulated to find the probability of the outcome:

$$p(y=1|x)=\frac{e^{\beta^T x}}{1+e^{\beta^T x}} \tag{2.2.3}$$

Linear function with the coefficient vector β was used to describe the hyperplane decision. Furthermore, the LR algorithm determined the optimal d-dimensional vector $\beta=[\beta_0,\beta_1,\ldots\beta_d]$ that fits the training observations:

$$\begin{aligned}&\text{logistic function}\quad \phi(z)=\frac{1}{1+e^{-z}}\\ &\text{Where}\quad z=\beta_0+\beta_1x_1+\ldots+\beta_dx_d\\ &y=1, z>0\\ &y=0, otherwise\end{aligned} \tag{2.2.4}$$

By using all of the data points $x \in R^d$, the decision boundary was determined by:

$$\beta_0+\beta_1x_1+\ldots+\beta_dx_d=0 \tag{2.2.5}$$

If $\beta^T x$ is positive, LR classifier will assign x to class (1), otherwise it will be assigned to the other class (0). The rule of LR classification is:

$$y=1_{p(x,\beta)>0.5} \tag{2.2.6}$$

By maximizing the Log-likelihood function with an iterative numerical algorithm, the values of βs can be calculated (Hosmer and Lemeshow, 2000).

b. Support Vector Machine

The SVM concept is useful to discover the best hyperplane that acts as a separator between two classes in the input space. Figure 1 (a) draws several patterns which are members of two classes: positive (+1) and negative (–1). Patterns that are joined in the positive class are represented by circles, while the negative class are represented by squares. The varieties of the dividing lines are shown in Figure 1 (a).

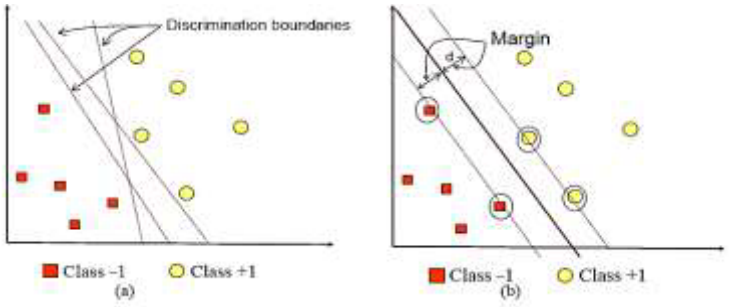

Figure 8. Finding the best hyperplane with Support Vector Machine

Measuring the hyperplane margin and finding the maximum point was carried out to obtain the best hyperplane separator between the two classes. The distance between the hyperplane and the closest data from each class determined the margin. A hyperplane is said to be optimum if it is located in the middle of the two classes. Figure 1 (b) shows the best hyperplane located in the middle of the two classes. Support vectors were the points represented by squares and circles inside the black circle. The concept of Support Vector Machine (SVM) is finding a hyperplane that separates data sets into two classes. The existing data was denoted by $\vec{x}_i \in R^d$, while its label was denoted by $y_i \in \{-1, +1\}$ for i = 1, 2, ...,l, where i is the amount of data. Assuming that class -1 and +1 can be separated by a hyperplane without dimensions, which is determined by:

$$\vec{w}.\vec{x} + b = 0 \tag{2.3.1}$$

A pattern X_i that belongs to class -1 is defined by:

$$\vec{w}.\vec{x} + b \leq 1 \tag{2.3.2}$$

while pattern X_i which belongs to class +1 is defined by:

$$\vec{w}.\vec{x} + b \geq 1 \tag{2.3.3}$$

By maximizing the value of the distance between the hyperplane and its closest point, the maximum margin was determined as $\frac{1}{\|\vec{w}\|}$. From finding the minimum point of equation (2.3.4) and noting the constraints of equation (2.3.5), a Quadratic Programming (QP) problem was formulated.

(2.3.4)

$$\min \tau(w) = \frac{1}{2}\|w\|^2$$

$$y_i(\vec{x}_i.\vec{w} + b) = \frac{1}{2}\|w\|^2 \quad (2.3.5)$$

This problem can be solved by several computational techniques, such as Lagrange Multiplier as shown in equation (2.3.6):

$$L(\vec{w}, b, \alpha) = \frac{1}{2}\|w\|^2 - \sum_{i=1}^{l} \alpha_i (y_i((\vec{x}.\vec{w} + b) - 1)) \quad (2.3.6)$$

α_i is a Lagrange multiplier, whose value is either zero or positive ($\alpha_i \geq 0$). By minimizing L with respect to w and b, and maximizing L with respect to α_i, the optimal value of equation (2.3.6) can be calculated. Equation (2.3.6) can also be modified as the maximization of problems that only contain α_i by considering the optimal point gradient L = 0, as shown in equation (2.3.7).

Maximize:

$$\sum_{i=1}^{l} \alpha_i - \frac{1}{2}\sum_{i,j=1}^{l} \alpha_i \alpha_j y_i y_j \vec{x}_i \vec{x}_j \quad (2.3.7)$$

Subject to:

$$\alpha_i \geq 0 (i = 1, 2, \ldots l) \sum_{i=1}^{l} \alpha_i y_i = 0 \quad (2.3.8)$$

From this calculation α_i were mostly obtained. This positive correlated data with α_i is called support vector [24].

c. Statistical Measures

To measure the accuracy, precision, recall, and f1-score, the data was classified using Logistic Regression and Support Vector Machine. The dataset was initially divided into training and testing. Furthermore, the model was tested and calculations were carried out on several measurements whose description are shown in Table 2 and 3.

Table 2. Confusion matrix

Actual vs Predicted	Positive	Negative
Positive	TP	FN
Negative	FP	TN

Table 3. Terminology of statistical measurement

Actual vs Predicted	Formula

Accuracy (A)	$A = \frac{TP + TN}{TP + TN + FP + FN}$
Precision (P)	$P = \frac{TP}{TP + FP}$
Recall (R)	$R = \frac{TP}{TP + FN}$
f1 score (f1)	$f1 = 2 \times \frac{P \times R}{P + R}$

3. RESULTS & ANALYSIS

The hepatitis dataset contained 113 instances, four features with one class. This study compared both Logistic Regression and Support Vector Machine to ascertain which method has the best performance.

This type of testing was a training test. The dataset were classified using the two methods. By using 10%-90% of the training data, accuracy, precision, recall, and f1 score from both methods are shown Table 4 and 5

Table 4. The accuracy, precision, recall, and f1 score with logistic regression

Data Training	Accuracy	Precision	Recall	f1 score
10%	83.33%	66.66%	66.66%	77.74%
20%	90.47%	88.88%	83.33%	87.74%
30%	90.85%	91.66%	72.22%	85.76%
40%	91.11%	86.66%	83.33%	88.95%
50%	92.98%	93.33%	80.00%	90.19%
60%	95.51%	100.00%	82.22%	93.66%
70%	94.96%	100.00%	80.15%	92.79%
80%	93.40%	95.23%	78.57%	90.84%
90%	96.04%	100.00%	84.72%	94.53%

From the results of Table 3, it was discovered that the highest accuracy by using Logistic Regression was 96.04%, which was obtained when using 90% of data training. The lowest accuracy was 83.33% by using 10% of data training. It also can bee seen that the highest precision was reached at 60%, 70%, and 90% of data training, which is 100%, while the lowest precision was 66.66% when using 10% of data training. For the recall, the highest value was 84.72% when using 90% of the data training, while the lowest recall was 66.66% when using 10% off data training. Lastly, the highest f1 score was 94.53% when using 90% of the data training, while the lowest f1 score was 77.74% when using 10% of data training.

Table 5. The accuracy, precision, recall, and f1 score with support vector machine

Data Training	Accuracy	Precision	Recall	f1 score
10%	63.88%	50.00%	66.66%	58.73%
20%	72.02%	30.00%	88.88%	86.49%
30%	69.54%	64.28%	72.22%	83.46%
40%	88.88%	91.66%	83.33%	66.74%
50%	78.84%	100.00%	55.00%	75.11%
60%	92.61%	82.14%	100.00%	80.26%
70%	94.96%	95.23%	45.23%	84.16%
80%	86.65%	93.33%	64.28%	82.57%
90%	92.00%	100.00%	66.66%	80.55%

From the results in Table 4, the highest accuracy when using Support Vecror Machine was 94.96%, by using 70% of data training. The lowest accuracy was 63.88%, by using 10% of data training. For the precision, the highest value was 100% when using 50% and 90% of data training, while the lowest precision was obtained when using 20% of data training, which is 30%. It also can be seen that the highest recall was obtained when using 60% of data training, which is 100%, while the lowest recall was 45.23% when using 70% of data training. Lastly, for the f1 score, the highest value was reached when using 20% of data training, which is 86.49%, while the lowest f1 score was 58.73% when using 10% of data training. From the both Table, we can see that the better method was Logistic Regression, because the highest accuracy was reached when using this method, which is 96.04%. While the highest accuracy when using SVM was lower than the Logistic Regression's accuracy, which is 94.96%.

Comparisons were made to discover a better method between Logistic Regression and Support Vector Machine (SVM). The highest accuracy obtained was 96.04%, and the highest f1 score was 94.53% by using Logistic Regression. It can be concluded that Logistic Regression was the better method compared to Support Vector Machine.

4. CONCLUSION

In this study, Logistic Regression (LR) and Support Vector Machine (SVM) were used to classify the model and also to determine the best performance of the methods based on accuracy. The performance indicators for this dataset in evaluating the model were accuracy, precision, recall, and f1 score.

Logistic Regression had the best accuracy compared to SVM. It yielded an accuracy of 96.04% using 90% of data training, and 94.53% of f1-score. Conversely, SVM yielded an accuracy of 94.96%, and 86.49% of f1-score at its best. In other words, Logistic Regression was the better method compared to Support Vector Machine.

Although Logistic Regression has shown a good performance in classifying hepatitis, it also has its advantages and disadvantages. Logistic Regression is one of the simplest machine learning algorithms. It provides great training efficiency and easy implementation. The predicted parameters gave a conclusion about the importance of the features. Therefore, it is used to discover the relationship between the features.

Logistic Regression is used in predicting probabilistic outcomes based on independent features. This may lead to an over-fit model on the training set on high dimensional datasets. Therefore, the model will not be able to predict accuracy value on the testing set. This condition happens when the dataset has a lot of features.

SVM performs well when there is a clear margin of separation between classes and it also has a relatively efficient memory. Conversely, its test phase is very slow and maybe difficult to perform. (Burges, 1996; Osuna and Girosi, 1998). When the dataset becomes noisy, i.e target classes are overlapping, SVM also does not perform well.

For upcoming studies, Logistic Regression method is recommended for classifying any other disease. It is expected that results from these methods are better than those from other methods and will benefit the medical field.

ACKNOWLEDGEMENT

This research is supported financially by The Indonesian Ministry of Research and Technology, with a KEMENRISTEK/BRIM 2021 research grant scheme.

REFERENCES

1. Ryder, S.D. and I.J. Beckingham, ABC of diseases of liver, pancreas, and biliary system: Chronic viral hepatitis, BMJ (Clinical research ed.), vol. 322 (7280), pp. 219-221, 2001.
2. F. Franc *et al.*, Hepatitis B: Epidemiology and prevention in developing countries, World J. Hepatol., vol. 4, pp. 74-80, 2012.
3. C. W. Shepard, L. Finelli and M. J. Alter, Global epidemiology of hepatitis C virus infection, Lancet Infect. Dis., vol. 5, no. 9, pp. 558–567, 2005.
4. Baseke, Joy et al., Prevalence of hepatitis B and C and relationship to liver damage in HIV infected patients attending Joint Clinical Research Centre Clinic (JCRC), Kampala, Uganda, Afr. Health Sci., vol. 15 (2), pp. 322-327, 2015.
5. N. Latt, N. Alachkar and A. Gurakar, Hepatitis C virus and its renal manifestations: A review and update, Gastroenterol Hepatol. (NY), vol. 8 (7), pp. 434-445, 2012.
6. M. Jefferies, B. Rauff, H. Rashid, T. Lam and S. Rafiq, Update on global epidemiology of viral hepatitis and preventive strategies, World J. Clin. Cases, vol. 6, (13), pp. 589-599, 2018.
7. C. Fernández-Carrillo *et al.*, Treatment of hepatitis C virus infection in patients with cirrhosis and predictive value of model for end-stage liver disease: Analysis of data from the Hepa-C registry, Hepatology (Baltimore, Md.), vol. 65 (6), pp. 1810-1822, 2017.
8. S. Rashid, A. Ahmed, I. Al Barazanchi, A. Mhana and H. Rasheed, Lung cancer classification using data mining and supervised learning algorithms on multi-dimensional data set, Period. Eng. Nat. Sci., vol. 7, no. 2, pp. 438–447, 2019.
9. B. Lykiardopoulos *et al.*, Development of Serum Marker Models to Increase Diagnostic Accuracy of Advanced Fibrosis in Nonalcoholic Fatty Liver Disease: The New LINKI Algorithm Compared with Established Algorithms, PloS one, vol. 11 (12), pp. e0167776, 2016.
10. S. Liu, T. Kawamoto, O. Morita, K. Yoshinari and H. Honda, Discriminating between adaptive and carcinogenic liver hypertrophy in rat studies using logistic ridge regression analysis of toxicogenomic data: The mode of action and predictive models, Toxicol. Appl. Pharmacol., vol. 318, pp. 79-87, 2017.
11. H. R. Bdulshaheed, Z. T. Yaseen and I. I. Al-barazanchi, New approach for Big Data Analysis using Clustering Algorithms in Information, Jour Adv Res. Dyn. Control Syst., vol. 2, no. 4, pp. 1194–1197, 2019.
12. H. Ma, C. Xu, Z. Shen, C. Yu and Y. Li, Application of Machine Learning Techniques for Clinical Predictive Modeling: A Cross-Sectional Study on Nonalcoholic Fatty Liver Disease in China, Biomed Res. Int., 2018.
13. H. Hagström *et al.*, Fibrosis stage but not NASH predicts mortality and time to development of severe liver disease in biopsy-proven NAFLD, J. Hepatol., vol. 67 (6), 2017.
14. M. Pons, *et al.*, Basal values and changes of liver stiffness predict the risk of disease progression in compensated advanced chronic liver disease, Dig. Liver Dis., vol. 48 (10), 2016.
15. A.M. Elsayad, A.M. Nassef and M. Al-Dhaifallah, Diagnosis of Hepatitis Disease with Logistic Regression and Artificial Neural Networks, J. Comput. Sci., vol. 16 (3), pp. 364-377, 2020.
16. Y. Xie *et al.*, Evaluation of a logistic regression model for predicting liver necroinflammation in hepatitis B e antigen-negative chronic hepatitis B patients with normal and minimally increased alanine aminotransferase levels, J. Viral Hepat., vol. 26, (S1), pp. 42-49, 2019.
17. M.A. Konerman *et al.*, Assessing risk of fibrosis progression and liver-related clinical outcomes among patients with both early stage and advanced chronic hepatitis C, PloS One, vol. 12 (11), pp. e0187344-e0187344, 2017.

18. S. Petta *et al.*, Metabolic syndrome and severity of fibrosis in nonalcoholic fatty liver disease: An age-dependent risk profiling study, Liver Int., vol. 37 (9), pp. 1389-1396, 2017.
19. T. V. Rampisela and Z. Rustam, Classification of Schizophrenia Data Using Support Vector Machine (SVM), J. Phys. Conf. Ser., vol. 1108 (1), pp. 012044, 2018.
20. T. Nadira and Z. Rustam, Classification of cancer data using support vector machines with features selection method based on global artificial bee colony, Proceedings of the 3rd International Symposium on Current Progress in Mathematics and Sciences (AIP Conference Proceedings, vol. 2023), 2017.
21. C. Aroef, R. Yuda, Z. Rustam and J. Pandelaki, Multinomial Logistic Regression and Support Vector Machine for Osteoarthritis Classification, J. Phys. Conf. Ser., 2019.
22. G. Kurniawan and Z. Rustam, Enhancement of hepatitis virus outcome predictions with application of K-means clustering, Proceedings of the 4th International Symposium on Current Progress in Mathematics and Sciences, ISCPMS 2018 (AIP Conference Proceedings, vol. 2168), 2019.
23. T. Karthikeyan and P. Thangaraju, Analysis of Classification Algorithms Applied to Hepatitis Patients, International Journal of Computer Applications, vol. 62, pp. 25-30, 2013.
24. N. Christianini and J. Shawe-Taylor, An Introduction to Support Vector Machines and Other Kernel-based Learning Methods, Cambridge: Cambridge University Press, 2000.

Some Exact Travelling Wave Solutions of Sixth-Order Ramani Equation and (3+1)-Dimensional Shallow Water Wave Equation (SWWE)

İbrahim Enam İNAN

Firat University, Faculty of Education, Elazig, Turkey

einan@firat.edu.tr

Abstract. In this paper, we implemented an Generalized $\left(\frac{G'}{G}\right)$ – expansion method for some exact solutions of Sixth-order Ramani equation and (3+1)-dimensional shallow water wave equation. By using this scheme, we found several exact travelling wave solutions of the sixth-order Ramani equation and (3+1)-dimensional shallow water wave equation. These solutions are both exponential function solutions and rational function solutions. In addition, graphs of some solutions and numerical explanations of these graphs were given. Recently, this method has been studied for obtaining exact travelling wave solutions of nonlinear partial differential equations.

Keywords. Sixth-order Ramani equation, (3+1)-dimensional shallow water wave equation, Generalized $\left(\frac{G'}{G}\right)$ – expansion method, Exact travelling wave solutions.

1. INTRODUCTION

Nonlinear partial differential equations have an important place in many areas of the scientific World. Some of these areas are applied mathematics, optical fibers, physics, cosmology and fluid dynamics. Many analytical methods have been developed to solve nonlinear partial differential equations. [1-11]. Apart from these methods, there are many methods in which these equations are solved using an auxiliary equation. Using these methods, partial differential equations are transformed into ordinary differential equations. These nonlinear partial differential equations are solved with the help of ordinary differential equations. Some of these methods given in [12-28]. We used the generalized $\left(\frac{G'}{G}\right)$ – expansion method for find the exact travelling wave solutions solutions of Sixth-order Ramani equation and (3+1)-dimensional SWWE in this study. This method is presented by H. L. Lü, X. Q. Liu, L. Niu [25].

2. ANALYSIS OF METHOD

Let us consider the general form of a nonlinear partial differential equation with two variables;

$$Q(u, u_t, u_x, u_{xx}, \dots) = 0, \tag{1}$$

If $v(x,t) = v(\xi), \xi = x + \omega t$ conversion is applied to the above equation, we get

$$Q'(u', u'', u''', \dots) = 0. \tag{2}$$

We are looking for a solution in the form below

$$u = A_0 + \sum_{i=1}^{m} A_i \left(\frac{f'}{f}\right)^i, \ A_m \neq 0, \tag{3}$$

where $f = f(\xi)$ provides the following ordinary differential equation,

$$f' = h_0 + h_1 f + h_2 f^2 + h_3 f^3, \tag{4}$$

where h_0, h_1, h_2, h_3 are constants. Also m is a positive integer. m can be determined by balancing the highest order derivative with the highest nonlinear terms in to (2). Substituting (3) and (4) into Eq.(5) yields a set of algebraic equations for $h_0, h_1, h_2, h_3, A_0, A_1, \dots, A_m$ and ω because all coefficients of f^m have to vanish. From here $h_0, h_1, h_2, h_3, A_0, A_1, \dots, A_m$ and ω can be determined.

3. EXAMPLES

Example 3.1
We consider the Sixth-order Ramani equation [20],

$$v_{xxxxxx} + 15v_x v_{xxxx} + 15v_{xx} v_{xxx} + 45v_x^2 v_{xx} - 5v_{xxxt} - 15v_x v_{xt} - 15v_t v_{xx} - 5v_{tt} = 0, \quad (5)$$

If $v(x,t) = v(\xi), \xi = x + \omega t$ conversion is applied to the above equation, we get

$$v^{(6)} + 15v'v^{(4)} + 15v''v''' + 45(v')^2 v'' - 5\omega v^{(4)} - 30\omega v'v'' - 5\omega^2 v'' = 0, \quad (6)$$

When balancing $v^{(6)}$ with $v''v'''$ then gives *m=1*. The solution is as follows,

$$v = A_0 + A_1\left(\frac{f'}{f}\right), \quad (7)$$

Substituted (7) into (6), the obtained following linear algebraic equation system for $h_0, h_1, h_2, h_3, A_0, A_1$ and ω;

$720A_1h_0^7 - 540A_1^2h_0^7 + 90A_1^3h_0^7 = 0,$
$2520A_1h_0^6h_1 - 1890A_1^2h_0^6h_1 + 315A_1^3h_0^6h_1 = 0,$
$-10\omega^2A_1h_0h_1h_2 - 10\omega A_1h_0h_1^3h_2 + 2A_1h_0h_1^5h_2 - 80\omega A_1h_0^2h_1h_2^2 + 104A_1h_0^2h_1^3h_2^2 - 90A_1^3h_0^2h_1^3h_2^2 + 272A_1h_0^3h_1h_2^3 - 180A_1^3h_0^3h_1h_2^3 - 15\omega^2A_1h_0^2h_3 - 135\omega A_1h_0^2h_1^2h_3 + 90\omega A_1^2h_0^2h_1^2h_3 + 123A_1h_0^2h_1^4h_3 - 180A_1^2h_0^2h_1^4h_3 - 200\omega A_1h_0^3h_2h_3 + 60\omega A_1^2h_0^3h_2h_3 + 1520A_1h_0^3h_1^2h_2h_3 - 1560A_1^2h_0^3h_1^2h_2h_3 - 540A_1^3h_0^3h_1^2h_2h_3 + 868A_1h_0^4h_2^2h_3 - 600A_1^2h_0^4h_2^2h_3 - 315A_1^3h_0^4h_2^2h_3 + 1296A_1h_0^4h_1h_3^2 - 1620A_1^2h_0^4h_1h_3^2 - 405A_1^3h_0^4h_1h_3^2 = 0,$
$-120\omega A_1h_0^5 + 60\omega A_1^2h_0^5 + 3360A_1h_0^5h_1^2 - 2490A_1^2h_0^5h_1^2 + 405A_1^3h_0^5h_1^2 + 1680A_1h_0^6h_2 - 1020A_1^2h_0^6h_2 + 90A_1^3h_0^6h_2 = 0,$
$-300\omega A_1h_0^4h_1 + 150\omega A_1^2h_0^4h_1 + 2100A_1h_0^4h_1^3 - 1500A_1^2h_0^4h_1^3 + 225A_1^3h_0^4h_1^3 + 4200A_1h_0^5h_1h_2 - 2280A_1^2h_0^5h_1h_2 + 90A_1^3h_0^5h_1h_2 + 1260A_1h_0^6h_3 - 540A_1^2h_0^6h_3 - 45A_1^3h_0^6h_3 = 0,$
$-10\omega^2A_1h_0^3 - 250\omega A_1h_0^3h_1^2 + 120\omega A_1^2h_0^3h_1^2 + 602A_1h_0^3h_1^4 - 390A_1^2h_0^3h_1^4 + 45A_1^3h_0^3h_1^4 - 200\omega A_1h_0^4h_2 + 60\omega A_1^2h_0^4h_2 + 3584A_1h_0^4h_1^2h_2 - 1470A_1^2h_0^4h_1^2h_2 - 135A_1^3h_0^4h_1^2h_2 + 1232A_1h_0^5h_2^2 - 300A_1^2h_0^5h_2^2 - 90A_1^3h_0^5h_2^2 + 3024A_1h_0^5h_1h_3 - 810A_1^2h_0^5h_1h_3 - 270A_1^3h_0^5h_1h_3 = 0,$
$-15\omega^2A_1h_0^2h_1 - 75\omega A_1h_0^2h_1^3 + 30\omega A_1^2h_0^2h_1^3 + 63A_1h_0^2h_1^5 - 30A_1^2h_0^2h_1^5 - 300\omega A_1h_0^3h_1h_2 + 60\omega A_1^2h_0^3h_1h_2 + 1176A_1h_0^3h_1^3h_2 - 120A_1^2h_0^3h_1^3h_2 - 180A_1^3h_0^3h_1^3h_2 + 1848A_1h_0^4h_1h_2^2 + 150A_1^2h_0^4h_1h_2^2 - 315A_1^3h_0^4h_1h_2^2 - 150\omega A_1h_0^4h_3 + 30\omega A_1^2h_0^4h_3 + 2436A_1h_0^4h_1^2h_3 + 60A_1^2h_0^4h_1^2h_3 - 405A_1^3h_0^4h_1^2h_3 + 1680A_1h_0^5h_2h_3 + 180A_1^2h_0^5h_2h_3 - 270A_1^3h_0^5h_2h_3 = 0, \cdots$

from the solution of this system are obtained the following situations and solutions;

i) $h_0 \neq 0, h_1 \neq 0, h_2 = 0, h_3 = 0,\ \omega = \frac{h_1^2}{10}\left(-5 - 3\sqrt{5}\right),\ A_0 = A_0,\ A_1 = 2$

$$v(x,t) = A_0 + 2\left(\frac{Ce^{xh_1}h_1^2}{-e^{\frac{1}{10}(5+3\sqrt{5})th_1^3}h_0 + Ce^{xh_1}h_1}\right) \quad (8)$$

ii) $h_0 = 0, h_1 \neq 0, h_2 = 0, h_3 \neq 0,\ \omega = \frac{2h_1^2}{5}\left(-5 + 3\sqrt{5}\right),\ A_0 = A_0,\ A_1 = -4$

$$v(x,t) = A_0 - 4\left(\frac{Ch_1^2}{Ch_1 - e^{2h_1\left(x + \left(-2 + \frac{6}{\sqrt{5}}\right)th_1^2\right)}h_3}\right) \quad (9)$$

iii) $h_0 = 0, h_1 \neq 0, h_2 \neq 0, h_3 = 0,\ \omega = \frac{h_1^2}{10}\left(-5 - 3\sqrt{5}\right),\ A_0 = A_0,\ A_1 = -2$

$$v(x,t) = A_0 - 2\left(\frac{Ch_1^2}{Ch_1 - e^{h_1\left(x - \frac{1}{10}(5+3\sqrt{5})th_1^2\right)}h_2}\right) \quad (10)$$

Example 3.2 We consider the (3+1)- dimensional SWWE [21],

$$v_{xzt} + v_{xxxyz} - 2v_{xx}v_{yz} - 2v_y v_{xxz} - 4v_x v_{xyz} - 4v_{xz}v_{xy} = 0, \quad (11)$$

If $v(x,y,z,t) = v(\xi), \xi = (x + \alpha y + \beta z + \omega t)$ conversion is applied to the above equation, we get

$$\omega v''' + \alpha v^{(5)} - 6\alpha (v'')^2 - 6\alpha v' v''' = 0, \tag{12}$$

when balancing $(v'')^2$, $v'v'''$ with $v^{(5)}$ then gives $m = 1$. The solution is as follows:

$$v = A_0 + A_1 \left(\frac{f'}{f}\right), \tag{13}$$

Substituted (13) into (12), the obtained following linear algebraic equation system for $h_0, h_1, h_2, h_3, A_0, A_1, \alpha$ and ω;

$-120\alpha A_1 h_0^6 - 60\alpha A_1^2 h_0^6 = 0,$
$-360\alpha A_1 h_0^5 h_1 - 180\alpha A_1^2 h_0^5 h_1 = 0,$
$-6\omega A_1 h_0^4 - 390\alpha A_1 h_0^4 h_1^2 - 192\alpha A_1^2 h_0^4 h_1^2 - 240\alpha A_1 h_0^5 h_2 - 96\alpha A_1^2 h_0^5 h_2 = 0,$
$-12\omega A_1 h_0^3 h_1 - 180\alpha A_1 h_0^3 h_1^3 - 84\alpha A_1^2 h_0^3 h_1^3 - 480\alpha A_1 h_0^4 h_1 h_2 - 180\alpha A_1^2 h_0^4 h_1 h_2 - 180\alpha A_1 h_0^5 h_3 -$
$72\alpha A_1^2 h_0^5 h_3 = 0,$
$-7\omega A_1 h_0^2 h_1^2 - 31\alpha A_1 h_0^2 h_1^4 - 12\alpha A_1^2 h_0^2 h_1^4 - 8\omega A_1 h_0^3 h_2 - 292\alpha A_1 h_0^3 h_1^2 h_2 - 96\alpha A_1^2 h_0^3 h_1^2 h_2 - 136\alpha A_1 h_0^4 h_2^2 -$
$36\alpha A_1^2 h_0^4 h_2^2 - 342\alpha A_1 h_0^4 h_1 h_3 - 144\alpha A_1^2 h_0^4 h_1 h_3 = 0,$
$-\omega A_1 h_0 h_1^3 - \alpha A_1 h_0 h_1^5 - 8\omega A_1 h_0^2 h_1 h_2 - 52\alpha A_1 h_0^2 h_1^3 h_2 - 12\alpha A_1^2 h_0^2 h_1^3 - 136\alpha A_1 h_0^3 h_1 h_2^2 - 24\alpha A_1^2 h_0^3 h_1 h_2^2 -$
$6\omega A_1 h_0^3 h_3 - 192\alpha A_1 h_0^3 h_1^2 h_3 - 84\alpha A_1^2 h_0^3 h_1^2 h_3 - 180\alpha A_1 h_0^4 h_2 h_3 - 48\alpha A_1^2 h_0^4 h_2 h_3 = 0,$
$\omega A_1 h_1^3 h_2 + \alpha A_1 h_1^5 h_2 + 8\omega A_1 h_0 h_1 h_2^2 + 52\alpha A_1 h_0 h_1^3 h_2^2 - 12\alpha A_1^2 h_0 h_1^3 h_2^2 + 136\alpha A_1 h_0^2 h_1 h_2^3 - 24\alpha A_1^2 h_0^2 h_1 h_2^3 +$
$13\omega A_1 h_0 h_1^2 h_3 + 61\alpha A_1 h_0 h_1^4 h_3 + 12\alpha A_1^2 h_0 h_1^4 h_3 + 18\omega A_1 h_0^2 h_2 h_3 + 744\alpha A_1 h_0^2 h_1^2 h_2 h_3 + 36\alpha A_1^2 h_0^2 h_1^2 h_2 h_3 +$
$416\alpha A_1 h_0^3 h_2^2 h_3 + 612\alpha A_1 h_0^3 h_1 h_3^2 + 36\alpha A_1^2 h_0^3 h_1 h_3^2 = 0, \cdots$

from the solution of this system are obtained the following situations and solutions;

i) $h_0 \neq 0, h_1 \neq 0, h_2 = 0, h_3 = 0,\ \omega = -\alpha h_1^2,\ A_0 = A_0,\ A_1 = -2$

$$v(x,y,z,t) = A_0 - 2\left(\frac{Ce^{h_1\left(x+\alpha y+\beta z-\alpha h_1^2 t\right)}h_1^2}{-h_0+Ce^{h_1(x+\alpha y+\beta z-\alpha h_1^2 t)}h_1}\right) \tag{14}$$

ii) $h_0 = 0, h_1 \neq 0, h_2 = 0, h_3 \neq 0,\ \omega = -4\alpha h_1^2,\ A_0 = A_0,\ A_1 = 4$

$$v(x,y,z,t) = A_0 + 4\left(\frac{Ch_1^2}{Ch_1-e^{2h_1(x+\alpha y+\beta z-4\alpha h_1^2 t)}h_3}\right) \tag{15}$$

iii) $h_0 = 0, h_1 \neq 0, h_2 \neq 0, h_3 = 0,\ \omega = -\alpha h_1^2,\ A_0 = A_0,\ A_1 = 2$

$$v(x,y,z,t) = A_0 + 2\left(\frac{Ch_1^2}{Ch_1-e^{h_1(x+\alpha y+\beta z-\alpha h_1^2 t)}h_2}\right) \tag{16}$$

4. GRAPHS AND NUMERICAL EXPLANATIONS OF SOME SOLUTIONS

The shapes of Eq.(8) are represented in "Figure 1 and Figure 2" within the interval $-20 \leq x \leq 20, -5 \leq t \leq 5$. The shapes of Eqs.(14) are represented in "Figure 3 and Figure 4" respectively, within the interval $-20 \leq x \leq 20, -5 \leq t \leq 5$.

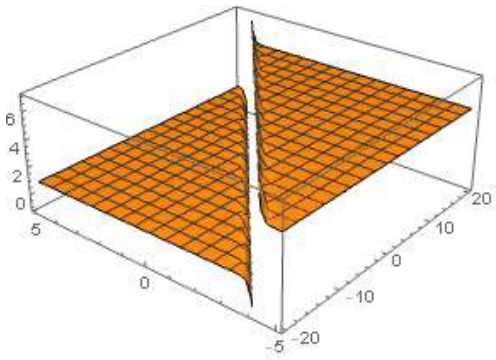

Figure 1. The 3Dimensional surfaces of Eq. (8) for $A_0 = 1, h_1 = 2, h_0 = 1, C = 3$.

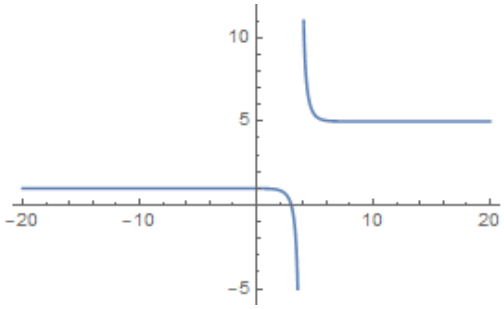

Figure 2. The 2Dimensional surfaces of Eq. (8) for $A_0 = 1, h_1 = 2, h_0 = 1, C = 3, t = 1$.

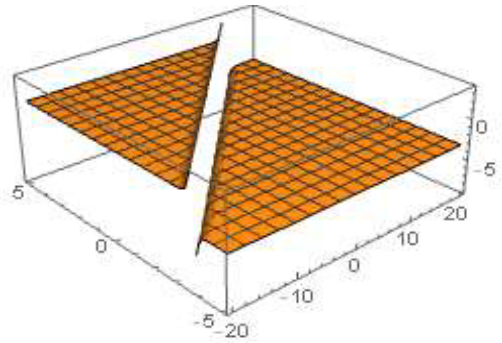

Figure 3. The 3Dimensional surfaces of Eq. (14) for $A_0 = 1, h_1 = 2, h_0 = 1, C = 3, \alpha = 1, \beta = 2, y = 1, z = 2$.

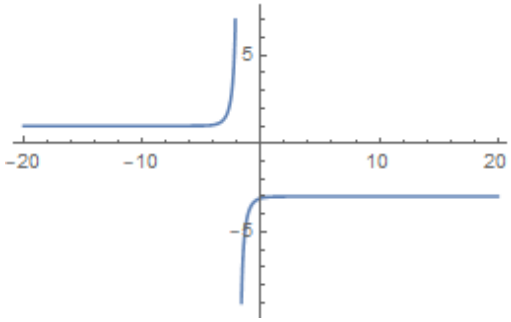

Figure 4. The 2Dimensional surfaces of Eq. (14) for $A_0 = 1, h_1 = 2, h_0 = 1, C = 3, \alpha = 1, \beta = 2, y = 1, z = 2, t = 1$.

5. CONCLUSION

We used the generalized $\left(\frac{G'}{G}\right)$ – expansion method to find the exact travelling wave solutions of Sixth-order Ramani equation and (3+1)-dimensional SWWE. The solutions found as a result of the application of the method are exponential and rational solutions. The accuracy of these solutions was seen by using Mathematica 11.2 computer program. In addition, graphs of some solutions and numerical explanations of these graphs were given. Many nonlinear partial differential equations and system of equations can be solved using this method.

REFERENCES

1. Debtnath, Nonlinear Partial Differential Equations for Scientist and Engineers, Birkhauser, Boston, MA, 1997.
2. A.M. Wazwaz, Partial Differential Equations: Methods and Applications, Balkema, Rotterdam, 2002.
3. Y. Shang, Backlund transformation, Lax pairs and explicit exact solutions for the shallow water waves equation, Appl. Math. Comput. 187, 1286-1297, 2007.
4. T.L. Bock, M.D. Kruskal, A two-parameter Miura transformation of the Benjamin-Ono equation, Phys. Lett. A 74, 173-176, 1979.
5. V.B. Matveev, M.A. Salle, Darboux Transformations and Solitons, Springer, Berlin, 1991.
6. A.M. Abourabia, M.M. El Horbaty, On solitary wave solutions for the two-dimensional nonlinear modified Kortweg-de Vries-Burger equation, Chaos Solitons Fractals 29, 354-364, 2006.
7. W. Malfliet, Solitary wave solutions of nonlinear wave equations, Am. J. Phys. 60, 650-654, 1992.
8. Y. Chuntao, A simple transformation for nonlinear waves, Phys. Lett. A 224, 77-84, 1996.
9. F. Cariello, M. Tabor, Painleve expansions for nonintegrable evolution equations, Physica D 39, 77-94, 1989.
10. E. Fan, Two new application of the homogeneous balance method, Phys. Lett. A 265, 353-357, 2000.
11. P.A. Clarkson, New similarity solutions for the modified boussinesq equation, J. Phys. A: Math. Gen. 22, 2355-2367, 1989.
12. W. Malfliet, Solitary wave solutions of nonlinear wave equations, Am. J. Phys. 60, 650-654, 1992.
13. E. Fan, Extended tanh-function method and its applications to nonlinear equations, Phys. Lett. A 277, 212-218, 2000.
14. S. A. Elwakil, S.K. El-labany, M.A. Zahran, R. Sabry, Modified extended tanh-function method for solving nonlinear partial differential equations, Phys. Lett. A 299, 179-188, 2002.
15. H. Chen, H. Zhang, New multiple soliton solutions to the general Burgers-Fisher equation and the Kuramoto-Sivashinsky equation, Chaos Soliton Fract 19, 71-76, 2004.
16. Z. Fu, S. Liu, Q. Zhao, New Jacobi elliptic function expansion and new periodic solutions of nonlinear wave equations, Phys. Lett. A 290, 72-76, 2001.
17. S. Shen, Z. Pan, A note on the Jacobi elliptic function expansion method, Phys. Let. A 308, 143-148, 2003.
18. H. T. Chen, Z. Hong-Qing, New double periodic and multiple soliton solutions of the generalized (2+1)-dimensional Boussines equation, Chaos Soliton Fract 20, 765-769, 2004.
19. Y. Chen, Q. Wang, B. Li, Jacobi elliptic function rational expansion method with symbolic computation to construct new doubly periodic solutions of nonlinear evolution equations, Z. Naturforsch. A 59, 529-536, 2004.
20. A.M. Wazwaz, H. Triki, Multiple soliton solutions for the sixth-order Ramani equation and a coupled Ramani equation, Applied Mathematics and Computation, 216, 332–336, 2010.
21. A.M. Wazwaz, Multiple soliton- solutions and multiple-singular soliton solutions for two higher-dimensional shallow water wave equations, Applied Mathematics and Computation, 211, 495–501, 2009.
22. Y. Chen, Z. Yan, The Weierstrass elliptic function expansion method and its applications in nonlinear wave equations, Chaos Soliton Fract 29, 948-964, 2006.
23. M. Wang, X. Li, J. Zhang, The $\left(\frac{G'}{G}\right)$-expansion method and travelling wave solutions of nonlinear evolutions equations in mathematical physics, Phys. Lett. A 372, 417-423, 2008.
24. S. Guo, Y. Zhou, The extended $\left(\frac{G'}{G}\right)$-expansion method and its applications to the Whitham-Broer-Kaup-like equations and coupled Hirota-Satsuma KdV equations, Appl.Math.Comput. 215, 3214-3221, 2010.
25. H. L. Lü, X. Q. Liu, L. Niu, A generalized $\left(\frac{G'}{G}\right)$-expansion method and its applications to nonlinear evolution equations, Appl. Math. Comput. 215, 3811-3816, 2010.
26. L. Li, E. Li, M. Wang, The $\left(\frac{G'}{G}, \frac{1}{G}\right)$-expansion method and its application to travelling wave solutions of the Zakharov equations, Appl. Math-A J. Chin. U 25, 454-462, 2010.
27. J. Manafian, Optical soliton solutions for Schrödinger type nonlinear evolution equations by the tan $\left(\frac{\emptyset(\varphi)}{2}\right)$– expansion Method, Optik 127, 4222-4245, 2016.
28. J. H. He, X. H. Wu, Exp-function method for nonlinear wave equations, Chaos Solitons Fractals, 30, 700-708,2006.

Artificial Neural Networks with Gradient-Based Optimizer and Genetic Algorithm to Classify Small Dataset

Ilsya WIRASATI[1] and Zuherman RUSTAM[1]

[1]*Department of Mathematics, Faculty of Mathematics and Natural Science, University of Indonesia, Depok-INDONESIA*

ilsya.wirasati@ui.ac.id
rustam@ui.ac.id

Abstract. The Artificial Neural Network (ANN) is a mathematical predictive model that combines numerous processing units and becomes adaptive nonlinear information processing systems. This Network has certain properties including adaptability and the ability to generalize and learn from examples. Because of that, ANN has been applied in many fields such as classification, pattern recognition, time-series prediction, and others. Previous studies have shown that ANN is beneficial to classify the small dataset. Furthermore, a good ANN should be able to minimize errors by using an optimizer algorithm. Therefore, this study discussed Genetic Algorithm (GA) and several gradient-based optimizers including Stochastic Gradient Descent (SGD), RMSprop, Adadelta, AdaGrad, Adamax, and Adam. Subsequently, a comparison was made to determine the small dataset classifier. Meanwhile, the study used the dataset of patients suffering from thalassemia, (genetic blood disorder) in Harapan Kita Children and Women's Hospital, Indonesia. The results showed that ANN with Adam optimizer is the best choice overall with 89.99% in comparison to the gradient-based algorithm. However, Adam compared to GA, GA has higher accuracy than Adam with 93.33%.

1. INTRODUCTION

Nowadays, machine learning methods are widely used in scientific areas, especially with the rise of Neural Networks (NNs) [1]. Starting from the study of computational learning theory, machine learning (ML) has developed into many methods, which find patterns through historical learning and data training trends to make predictions [2]. Furthermore, the data scientists, analysts, researchers, and engineers use these analytical models to obtain reliable results and make valid decisions. Recently, there is a high demand for research to understand how a specific model operates and the reasons behind its decision [1]. Therefore, researchers are increasingly using ML to optimize and produce reliable results.

In machine learning methods, data act as the fuel. In some cases, however, its collection is very expensive and time-consuming [3]. In health sciences, for example, big datasets are seldom unattainable [4] and this problem requires an urgent solution. Fortunately, with a correct learning algorithm, ANN is a beneficial method for classifying small datasets [5]. Although ANN with a large dataset is still the best choice, nonetheless, the Artificial Neural Network with a small dataset and a good pre-training is a reasonable alternative to make predictions [6].

The Artificial Neural Network (ANN) is a mathematical predictive model that combines numerous processing units and becomes adaptive nonlinear information processing systems [7]-[8]. This tool was introduced by McCulloch and Pitts as a powerful model in 1943 [7]. It is inspired by the human brain with great characteristics such as real-time learning, self-organizing, and self-adapting [8]. Also, it has three basic layers made up of logical units or perceptron. The first is the input layer which receives the data. Followed by the hidden, which consists of one or more layers. The last is the output layer that receives the hidden layer(s) and creates the decision [5]. Furthermore, the complexity of the ANN model is based on the number of hidden layers added [9]. It should be noted that there is a positive relationship between complexity and computation time [10].

These networks have an attractive feature such as their high ability of mapping nonlinear systems, which enable them to learn the underlying behaviors from the known data [11]. Also, ANNs have several advantages over statistical methods, such as being able to recognize linear patterns rapidly and the nonlinear with threshold impacts, categorical, stepwise linear, or even contingency effects [5]. Therefore, ANN is a powerful tool for solving various problems including disease diagnosis [12]-[13], pattern recognition [14]-[15], image processing [16], ecological

modelling [17], etc. This tool has shown good results in each field including previous research about neural network with small dataset such as Shuo Feng [6] predict material defect with a small data set, also, Nasser [18] analyses the parboiling process of rice as well as Rosa [10] on sales prediction, etc.

In order to obtain a better result with high accuracy, the optimization algorithm, which have several choices such as gradient-based, gradient-free, and the evolutionary, should be adopted [19]. However, the most popular and common way of optimizing the neural networks is through gradient-based algorithms or gradient descent [20]. Even though the objective function is non-convex, the gradient descent finds a global minimum in training neural networks [21]. In addition, there are evolutionary algorithms (EAs) as an optimizer for ANN and the most popular is the genetic algorithm (GA) that has been utilized to optimize the connectivity weight of ANN and proven to be useful and efficient [7]. GA applies Darwin's theory of evolution, namely "survival of the fittest". It is expected that GA can produce optimal solutions by going through three operations include selection, crossing, and mutation. [22].

In this research, data were collected from 98 thalassemia sufferers from Harapan Kita Children and Women's Hospital, Indonesia. Thalassemia is a genetic disease caused by an abnormal form of hemoglobin. Furthermore, the research aimed to determine the best optimizers in the neural network for classifying small dataset.

2. METHODS

This research used Artificial Neural Networks to classify the small dataset. Also, various optimization algorithms including Stochastic Gradient Descent, AdaGrad, Adadelta, RMSprop, ADAM, AdaMax, and Genetic Algorithm were applied.

Artificial Neural Networks

The Artificial neural network is a machine learning technique that imitates the neuron system of the brain to simulate human learning mechanisms. It uses connected neurons arranged into a layered structure, such as the input, hidden, and output [23]. This method has computational units called neurons that are connected by weights. The weights have the same function as the synapses in the brain, which are the connection points with other neurons. The weight (**wi**) is represented as the strength of the signal on a connection. The stronger networks tend to activate signals with activation functions such as sigmoid, tansig, softmax, and ReLU [24]. Furthermore, the rectified linear unit (ReLU) was applied because of its simplicity [23].

A successful model fits both the known and unknown data. Therefore, the construction of a neural network requires training known datasets to identify a set of suitable weights and enhance output predictability for the unknown data [25]. Besides, a good ANN is expected to easily minimize loss function.

Yang (2019), reported that the artificial neuron is characterized by n inputs and an output y. This is activated on instances where the signal strength ($\boldsymbol{w_i}$) attains a certain threshold, written as follows:

$$y = f(x) \;;\quad x = \boldsymbol{w_i}.\boldsymbol{u_i} = \sum_{i=1}^{n} w_i u_i \tag{2.1}$$

Where $\boldsymbol{u_i} = [u1, u2, \ldots, u_n]$ contains n input with corresponding weight $\boldsymbol{w_i} = [w1, w2 \ldots, w_n]$. Variable x is known as the observational value, being a part of the training data. Also, the purpose of single-layer neural network is to recognize a function required to calculate the predicted value of y, both in the training and new data. Furthermore, y is obtained by calculating $f(x)$ or the activation function. Fig. 1 shows an illustration of a simple neural network.

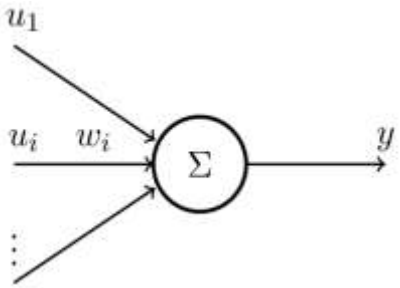

Figure. 1 A Simple Neural Network [23]

The illustration of neural networks is shown in Fig.2. The bold line represent a scheme from the input to output in ANN architecture.

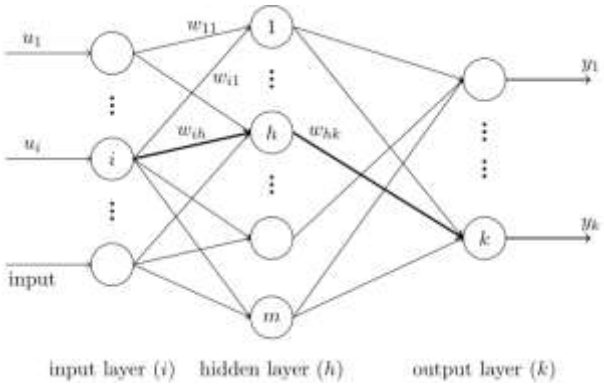

Figure.2 Illustration of Artificial Neural Network [23]

Stochastic Gradient Descent

The gradient-based optimizers are commonly used in previous research about ANN [26]. One of them is stochastic gradient descent (SGD) which has some advantages including its fast convergence and good generalization properties. Consequently, SGD became the standard optimization for neural networks [27]. Furthermore, to obtain good accuracy, the neural networks need an optimizer to minimize the loss function or error. The loss function formula is written as follow:

$$E(w) = \frac{1}{n}\sum_{i=1}^{n} f_i(\boldsymbol{u_i}, \boldsymbol{w}) = \frac{1}{n}\sum_{i=1}^{n}[x_i(\boldsymbol{u_i}, \boldsymbol{w}) - y_i]^2 \quad (2.2)$$

wheres $\boldsymbol{y_i}$ are predicted values based on data testing and $x_i(\boldsymbol{u_i})$ are from the trained neural networks with u_i as inputs. The multilayer connections require an iterative calculation. Therefore, in the case of large-scale problem, the incidence computation intractability is probably reported. This problem is solved by using SGD to approximate the true gradient through this iterative formula:

$$\boldsymbol{w}^{t+1} = \boldsymbol{w}^t - \eta_t \nabla E_i \quad (2.3)$$

The learning rate at iteration t is defined by η_t, and is estimated to vary with iterations. Furthermore, the stochastic gradient is calculated by randomly selecting sample i. This approach tends to significantly reduce computation costs [26].

AdaGrad

This optimizer uses an adaptive learning rate with diagonal matrix $G_k = [g_{ii}] \in \mathbb{R}^{nxn}$. The i-th diagonal element is the sum of the gradient concerning x_i $(i = 1,2,..., n)$ up to k iteration. In AdaGrad, the learning rate is replaced with

$$\eta \leftarrow \frac{\eta}{\sqrt{G_k+\epsilon}} \tag{2.4}$$

In this formula, avoiding division by zero is a must, so there is $\epsilon > 0$. The iterative formula is then written as:

$$x^{(k+1)} = x^k - \frac{\eta}{\sqrt{G_k+\epsilon}} \nabla f(x^k) \tag{2.5}$$

AdaDelta

Adadelta is an improvement from AdaGrad which calculate G_k using

$$g_k = \nabla f(\boldsymbol{x}^{(k)}) \tag{2.6}$$

In this optimizer, the running average of squared gradients at iteration k is used. Then, the update simply becomes

$$E_k(g_k^2) = \gamma E_k(g_{k-1}^2) + (1-\gamma)\, g_k^2 \tag{2.7}$$

The parameter increment is given by

$$\nabla \boldsymbol{x}_k = -\frac{\eta}{RMS\,[g_k]} g_k \tag{2.8}$$

where the root mean squared (RMS) error is represented by $RMS\,[g_k] = \sqrt{\mathrm{E}\,[g_k^2] + \epsilon}$. Therefore, in AdaDelta, the iterative formula is written as:

$$x^{(k+1)} = x^k - \frac{\sqrt{\mathrm{E}\,[(\nabla x_{k-1})^2] + \epsilon}}{RMS\,[g_k]}\, g_k \tag{2.9}$$

RMSprop

Geofrey Hinton introduced another optimizer namely RMSprop, which uses a running average of its recent gradient magnitude with exponential decay. Therefore, the iterative formula becomes

$$x^{(k+1)} = x^k - \frac{\eta}{\sqrt{E_k(g_k^2) + \epsilon}}\, g_k \tag{2.10}$$

ADAM

Kingma and Ba, in 2014, developed Adam, a very popular optimizer with two main steps. These include the first moment defined by m_1 and the second as m_2 at each iteration k, which corresponds to the mean and the uncentered variance. The two main steps are written as follows:

$$\begin{cases} m_1^{(k)} = \alpha m_1^{(k-1)} + (1-\alpha) g_k \\ m_2^{(k)} = \beta m_1^{(k-1)} + (1-\beta) g_k^2 \end{cases} \tag{2.11}$$

wheres α, β are parameters. Then, the iterative formula is written as:

$$x^{(k+1)} = x^k - \frac{\eta}{\sqrt{\bar{m}_2^{(k)} + \epsilon}}\, \bar{m}_1^{(k)} \tag{2.12}$$

$$\bar{m}_1^{(k)} = \frac{m_1^{(k)}}{1-\alpha^k} \quad , \quad \bar{m}_2^{(k)} = \frac{m_2^{(k)}}{1-\beta^k} \tag{2.13}$$

Adamax

This optimizer is variant of Adam. In the Adam update rule, $m_2^{(k)}$ factor scales the gradient to be inversely proportional to the ℓ_2 norm of the past (via the $m_2^{(k-1)}$term) and current gradient $|g_k|^2$

$$m_2^{(k)} = \beta m_1^{(k-1)} + (1-\beta)|g_k|^2 \quad (2.14)$$

To generalize this update to the ℓ_p norm. The norms for large p values generally become numerically unstable. However, Adamax uses ℓ_∞ that has stable behavior.

$$m_2^{(k)} = \beta^\infty m_1^{(k-1)} + (1-\beta^\infty)|g_k|^\infty \quad (2.15)$$

Genetic Algorithm

The Genetic algorithm (GA) is inspired by the evolution and principles of natural selection. This optimization algorithm is one of popular evolutionary algorithm. It requires three things, which are chromosomes, genetic operators, and selection. First, the chromosomes are represented by coding an objective function in the form of bits arrays or character strings. The genetic operators as the second thing required are used for manipulating the strings. The third is the selection according to their fitness in order to determine a problem's solution. Furthermore, GA can be defined as a probabilistic method with genetic operators such as the principle of selection and mutation [28].

There are two types of genetic operators, which include crossover and mutation [29]. The crossover operation is essential to exchange the two parent's chromosomes information received in the selection process. The two parents will produce one new solution or offspring. While the task of the mutation operation is to randomly change new solutions structures to increase its diversity. Furthermore, during iterations of this algorithm, only the high-quality solution survives and participates in the next generation's crossovers [30]. The process of GA is represented in Figure 3 [31].

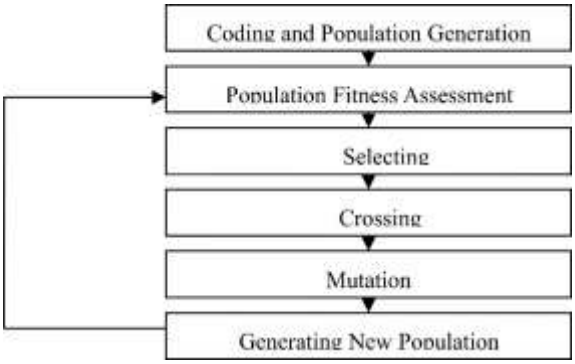

Figure. 3 Genetic Algorithm Process

The first step is coding, in this case, all the related variables are listed as chromosome in the forms of string. Then, a population of chromosomes is created and each indicates one solution. Secondly, the quality is evaluated by a designed fitness function. Thirdly, some are selected where the good individuals reproduce better than the bad and the genetic operations are then applied. Furthermore, to produce a child, this method applies cross to the parents with the proportion of the population (probability Pc). Then, a certain proportion (probability Pm) is applied for a mutation operator. After undergoing all steps, a new population is formed, which will reiterate the same process and stop when a user-defined criterion is reached [29].

Confusion Matrix

A confusion matrix was applied to measure the accuracy of various neural network optimizers. This matrix, which has four combinations of actual and predicted values is shown in Table 1,

TABLE 1. Confusion Matrix

Actual Value	Predicted Value	
	Positive	Negative
Positive	T_p	F_p
Negative	F_N	T_N

$$accuracy = \frac{T_P + T_N}{T_P + T_N + F_P + F_N} \tag{2.16}$$

RESULTS

The thalassemia data from Harapan Kita Children and Women's Hospital, Indonesia was used. This dataset consists of 98 patients with 42 non-thalassemia and 56 thalassemias sufferers. The dataset has 10 features, such as Hemoglobin, Leukocyte Count, Haematocrit, Eosinophils, Basophils, Segment Neutrophils, Rod Neutrophils, Monocytes, Lymphocytes, and Platelet Counts. Furthermore, the artificial neural networks with several optimizers were applied to classify the dataset. The authors used 50 epoch and 70% data training. Table 2 shows ANN accuracy with several optimizers.

TABLE 2. The Accuracy of ANN with Various Optimizers

Optimizers	Accuracy of data testing	Accuracy of data training
SGD	53.33%	58.82%
RMSprop	86.66%	95.58%
Adadelta	53.33%	61.76%
AdaGrad	83.33%	91.17%
Adamax	76.66%	91.17%
Adam	89.99%	95.58%
Genetic Algorithms	93.33%	92.64%

Table 2 shows that Adam has the highest accuracy when compared to other gradient-based optimizers with 89.99% and 95.58% on data testing and training, respectively. Followed by RMSprop with 86.66% on data testing and is the same as Adam on data training. However, SGD and Adadelta were recorded to have the lowest accuracy on data testing with 53.33%. Therefore, Adam is the best choice in all gradient-based optimizer. When accuracy is compared on data testing, Adam is found to be lower than the genetic algorithm (GA) which has 93.33%. This implies that GA's capability for classifying unknown data is better than Adam. Therefore, GA is recommended to classify thalassemia with a small number of data.

CONCLUSION

The Artificial Neural Networks (ANNs) have been applied in many fields to obtain reliable results and make valid decisions in research. This powerful tool has several advantages, such as the ability to learn from examples and generalize, as well as adaptability. Furthermore, previous research have proven that ANN is beneficial to classify the

small dataset. To obtain a better result, ANN with an optimizer algorithm should be adopted because it minimizes errors. This research used several optimization algorithms and compared them to determine the best in classifying a small dataset.

Table 2 showed that Adam optimizer is the best choice, compared to others with 89.99% accuracy on data testing. However, the accuracy of the Genetic Algorithm is higher than Adam, which reached 93.33% on data testing. Therefore, ANN with GA is the best method to classify thalassemia with small data.

ACKNOWLEDGMENT

This research was financially supported by the Indonesian Ministry of Research and Technology, with a KEMENRISTEK/BRIM 2021 research grant scheme. Furthermore, the authors want to thanks to Harapan Kita Children and Women's Hospital, Indonesia, for providing thalassemia dataset.

REFERENCES

1. R. Roscher, B. Bohn, M. F. Duarte and J. Garcke, Explainable Machine Learning for Scientific Insights and Discoveries, IEEE Access, vol. 8, pp. 42200-42216, 2020.
2. S. Angra and S. A. Angra, Machine learning and its applications: A review, International Conference on Big Data Analytics and Computational Intelligence (ICBDAC), pp. 57-60, 2017.
3. Y. Chen, H. Chang, J. Meng and D. Zhang, Ensemble Neural Networks (ENN): A gradient-free stochastic method., Neural Networks, vol. 110, pp. 170-185, 2019.
4. A. Pasini, Artificial neural networks for small dataset analysis, Journal of thoracic disease, vol. 7, no. 5, p. 953, 2015.
5. L. Bertolaccini, P. Solli, A. Pardolesi and A. Pasini, An overview of the use of artificial neural networks in lung cancer research, Journal of Thoracic Disease, vol. 9, no. 4, p. 924, 2017.
6. S. Feng, H. Zhou and H. Dong, Using deep neural network with small dataset to predict material defects, Materials & Design, vol. 162, pp. 300-310, 2019.
7. T. Yanga, An enhanced artificial neural network with a shuffled complex evolutionary global optimization with principal component analysis, Information Sciences, vol. 418, pp. 302-316, 2017.
8. S. Ding, H. Li, C. Su, J. Yu and F. Jin, Evolutionary artificial neural networks: a review, Artificial Intelligence Review, vol. 39, no. 3, pp. 215-260, 2013.
9. K. Pasupa and W. Sunhem, A comparison between shallow and deep architecture classifiers on small dataset, 8th International Conference on Information Technology and Electrical Engineering (ICITEE), vol. 8, pp. 1-6, 2016.
10. R. M. C. Croda, D. E. G. Romero and S. O. C. Morales, Sales prediction through neural networks for a small dataset, IJIMAI, vol. 5, no. 4, pp. 35-41, 2019.
11. I. N. d. Silva, Artificial neural networks: a practical course, Sao Carlos: Springer, 2018.
12. W. Wiharto, H. Kusnanto and H. Herianto, Hybrid system of tiered multivariate analysis and artificial neural network for coronary heart disease diagnosis, International Journal of Electrical and Computer Engineering, vol. 7, no. 2, p. 1023, 2017.
13. A. Caliskan and a. et, Diagnosis of the parkinson disease by using deep neural network classifier, Istanbul University-Journal of Electrical & Electronics Engineering, vol. 2, no. 3311-3318, p. 17, 2017.
14. D. M. D'Addona, A. M. M. S. Ullah and M. D, Tool-wear prediction and pattern-recognition using artificial neural network and DNA-based computing, Journal of Intelligent Manufacturing, vol. 28, pp. 1285-1301, 2017.
15. O. I. Abiodun, Comprehensive review of artificial neural network applications to pattern recognition, IEEE Access, vol. 7, pp. 158820-158846, 2019.
16. J. C. Puno and a. et, Determination of soil nutrients and pH level using image processing and artificial neural network, 2017IEEE 9th International Conference on Humanoid, Nanotechnology, Information Technology, Communication and Control, Environment and Management (HNICEM), vol. 9, pp. 1-6, 2017.

17. J. O. Odigie and J. O. Olomukoro., Ecological modelling using artificial neural network for macroinvertebrate prediction in a tropical rainforest river, Int. J. Environment and Waste Management, vol. 26, no. 3, p. 325, 2020.
18. N. Behroozi-Khazaei and A. Nasirahmadi, A neural network based model to analyze rice parboiling process with small dataset, Journal of Food Science and Technology, vol. 8, no. 2562-2569, p. 54, 2017.
19. X.-S. Yang, Optimization Algorithms, Introduction to Algorithms for Data Mining and Machine Learning, United Kingdom, Academic Press, p. 55., 2019.
20. S. Ruder, An overview of gradient descent optimization algorithms, arXiv preprint arXiv:1609.04747, 2016.
21. S. S. Du, J. D. Lee, H. Li, L. Wang and X. Zhai, Gradient descent finds global minima of deep neural networks, International Conference on Machine Learning, pp. 1675-1685, 2019.
22. T. Li, G. Shao, W. Zuo and S. Huang, Genetic algorithm for building optimization: State-of-the-art survey, Proceedings of the 9th international conference on machine learning and computing, pp. 205-210, 2017.
23. X.-S. Yang, Neural networks and deep learning, Introduction to Algorithms for Data Mining and Machine Learning, London, Elsevier Inc, 2019, p. 149.
24. Y. Chen, H. Chang, J. Meng and D. Zhang, Ensemble Neural Networks (ENN): A gradient-free stochastic method, Neural Networks, vol. 110, pp. 170-185, 2019.
25. R. M. Sadek, Parkinson's Disease Prediction Using Artificial Neural Network," International Journal of Academic Health and Medical Research (IJAHMR), vol. 3, no. 1, pp. 1-8, 2019.
26. X.-S. Yang, Optimization algorithms, Introduction to Algorithms for Data Mining and Machine Learning, London, Elsevier Inc, 2019, p. 53.
27. K. A. Sankararaman, S. De, Z. Xu, W. R. Huang and T. Goldstein, The Impact of Neural Network Overparameterization on Gradient Confusion and Stochastic Gradient Descent, arXiv preprint arXiv:1904.06963, 2019.
28. M. A. J. Idrissi and e. al, Genetic algorithm for neural network architecture optimization, 2016 3rd International Conference on Logistics Operations Management (GOL), vol. 3, pp. 1-4, 2016.
29. F. H.-F. Leung and e. al, Tuning of the structure and parameters of a neural network using an improved genetic algorithm, IEEE Transactions on Neural networks, vol. 14, no. 1, pp. 79-88, 2003.
30. N. Nezamoddin and A. Gholami, Integrated Genetic Algorithm and Artificial Neural Network, 2019 IEEE International Conference on Computational Science and Engineering (CSE) and IEEE International Conference on Embedded and Ubiquitous Computing (EUC), pp. 260-262, 2019.
31. H. Jing, X. Xu and J. Wang, Research on Genetic Neural Network Algorithm and Its Application, 2018 International Conference on Virtual Reality and Intelligent Systems (ICVRIS), pp. 223-226, 2018.

Classification of Small Lung Cancer Data with Artificial Neural Network and Support Vector Machine

Ilsya WIRASATI[1] and Zuherman RUSTAM[1]

[1]*Department of Mathematics, Faculty of Mathematics and Natural Science,*
University of Indonesia, Depok-INDONESIA

ilsya.wirasati@ui.ac.id
rustam@ui.ac.id

Abstract. Lung cancer is the second most common form of cancer and the most frequent cause of related deaths worldwide. As part of the respiratory system, the lungs are the main organs for breathing. Early detection of lung cancer is required for the provision of further care and to improve survival rate. Therefore, it is essential to adopt more advanced technology. Nowadays, machine learning is an advanced technology used to carry out the classification task by learning historical data and finding the pattern. In previous papers, numerous machine learning methods have been proposed to help medical staff easily classify lung cancer. The two methods used in this study were Artificial Neural Network (ANN) and Support Vector Machine (SVM). The idea of ANN is using connected neurons arranged into a layered structure to learn from data training and make a prediction in data testing. Meanwhile, SVM idea is mapping the input space to a higher dimensional space. In classification task, to separate data into classes SVM constructed a hyperplane. The authors made a comparison between ANN and SVM to classify Lung Cancer from CT (computed tomography) scan images presented with a small number of datasets. The data used was obtained from Cipto Mangunkusumo Hospital, Jakarta, Indonesia. Based on experiments carried out, the results showed that Lung Cancer small data classification using Artificial Neural Network and Support Vector Machine had 96% and 90% accuracy, respectively.

1. INTRODUCTION

Lung cancer is the second most common form of cancer known to affect both men and women [1]. This is a deadly disease, which accounts for about 1.8 million death cases according to the World Health Organization (WHO) press release in 2018 [2]. The lungs as part of the respiratory system are the main organs for breathing, comprising of bronchi and bronchioles as large and small airways, respectively. The incidence of cancers in this location is mostly initiated by the growth of abnormal cells lining the bronchi in an uncontrolled manner, which further invades the surrounding tissues and organs directly. In addition, two types have been identified, including non-small cell lung cancer (NSCLC) often managed by a combination of surgery and adjuvant therapy and small cell lung cancer (SCLC) known to be treated non-surgically [3].

The several risk factors documented include tobacco use, indoor and outdoor air pollution, hereditary susceptibility, radon, relative harmful occupational and radiation exposure and unbalanced diet [4]. Specifically, tobacco is identified to have the most significant influence, which responsible for about 85% of deaths [1]. However, people with no history of smoking have also been diagnosed with lung cancer.

The process of detection is carried out through several ways including imaging tests (X-Ray or CT scan), sputum cytology and lung tissue biopsy. Furthermore, most doctors tend to prefer CT scans because of the ability to distinguish the position of the nodule and identify some basic cancer characteristics, either as malign or benign. Unfortunately, detection is very difficult compared to other diseases [5], because of the small nodule size measuring less than 3cm in diameter [6]. Meanwhile, very few patients are diagnosed in the early stages (16%) due to the absence of signs and symptoms [7]. However, it is important to obtain a confirmation promptly for patients to commence the right treatment. This approach is known to improve survival rate.

Therefore, numerous machine learning methods have been proposed to help medical staff easily classify lung cancer. This is achieved through knowledge of patterns, based on the similarity of some data attributes and characteristics [8, 9]. In addition, as the disease data is obtained from CT Scans, image pre-processing techniques

play an important role in nodule detection and segmentation, alongside feature extraction. This is carried out prior to the application of classification techniques.

From previous studies, several have been used to classify lung cancers such as Convolutional Neural Network (CNN) and Kernel K-means [10], Naive Bayes [1] and Fuzzy C-Means [11]. Although, some studies on lung cancer have been carried out with machine learning models, its performance in dealing with small data has not been discussed. Therefore, Artificial Neural Network (ANN) and Support Vector Machine (SVM) were used in this study to classify small dataset which was different from that of previous studied.

ANN has attractive characteristics such as the ability to quickly recognize linear and nonlinear patterns with threshold, categorical and gradual linear contingency effects [12]. In addition, its tools are assumed to be useful in dealing with small datasets, following a correct learning algorithm [13]. This is also beneficial because larger data require longer calculation time [14]. Meanwhile, Support Vector Machines are one of the most popular machine learning method, because of its good capability to classify data [15]. The ANN and SVM were applied to classify lung cancer with small data. The aim of this study was to determine whether ANN or SVM method was the best approach by comparing the accuracy of both methods.

2. METHODS

This study used two different methods, namely ANN and SVM to classify lung cancer data from Cipto Mangunkusumo Hospital, Jakarta, Indonesia. Subsequently, the confusion matrix was applied to calculate the accuracy of both methods. In addition, the accuracies obtained were compared results and discussion sections.

Artificial Neural Networks

The main idea of ANN was using connected neurons arranged into a layered structure to learn from data training and make a prediction in data testing[16]. The layered structure contained three types of layer, which include the input, hidden and output layers. This method employs humans mechanism of learning through nervous system[17]. In the nervous system, there are neurons connected through synapsis (see Figure. 1). Meanwhile in ANN, neuron represents the computational unit and the function of synapsis is same as weight vector. Figure1 illustrates biological and artificial neural network.

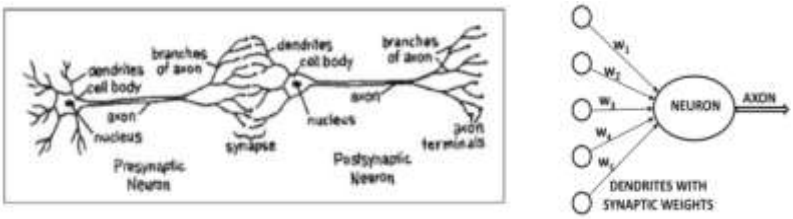

Figure.1 Biological Neural Network and Artificial Neural Network [17]

In addition, the process of learning was dependent on variable weight (**wi**), which represented the strength of neuron connection to each other. The stronger connection tends to activate signals to another neuron by using activation function. There are several choices of activation function, which include sigmoid, tansig and rectified linear unit (ReLU) [13]. The Artificial neural network comprises of the estimation of suitable network system weights. Therefore, it requires training in known data to identify a set of suitable weight and predict output precisely for unknown data [18].

Where n is the number of inputs represented by $\boldsymbol{u_i} = [u1, u2, \ldots, u_n]$, with corresponding weight $\boldsymbol{w_i} = [w1, w2 \ldots, w_n]$. Variable y is the output and the value x is known as observational, being a part of the training data which was written as follows:

$$y = f(x) \;;\quad x = \boldsymbol{w_i}.\boldsymbol{u_i} = \sum_{i=1}^{n} w_i u_i \tag{2.1}$$

Furthermore, $f(x)$ was the activation functions. One of popular activation function was the rectified linear unit (ReLU), because of its simplicity [16]. The illustration of ANN in general is shown in Figure.2

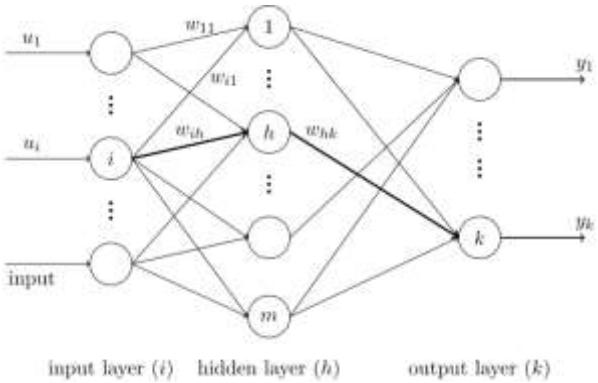

Figure.2 Illustration of Artificial Neural Network [16]

This method was expected to easily minimize error and produce a good accuracy in data classification. The error represented the differences between real and predicted output. Therefore, to minimize error, ANN adopted optimization algorithm. Gradient-based algorithms are well-known to be used as neural network optimizers. There are several examples, which include stochastic gradient descent (SGD), RMSprop and Adam.

Support Vector Machines

In 1963, Vapnik and Lerner introduced Support Vector Machines (SVM) as one of machine learning methods [19], [20]. It is applied in several tasks including classification and regression [21]. The idea of this method was mapping from input to a higher dimensional space. In classification task, to separate data into classes SVM constructed a hyperplane [22]. The optimal hyperplane was obtained by maximizing the margin of classification edges [23].

For the illustration, $\{x_i, y_i\}_i^N$ is the dataset with N number of samples. The Feature of vector was represented by $\boldsymbol{x_i} \epsilon R^D$ and y_i is class label for x_i. To discover the optimal hyperplane, the main formula of support vector machines was written as follows:

$$f(x) = w \cdot x + b \tag{2.2}$$

where **w** (weight) was the orthogonal vector to the hyperplane, which determines its orientation, **x** was the training sample and b (bias) represented the distance from the origin to the hyperplane [24]. The goal was to maximize the margin. Furthermore, SVM constructed the two planes called H1 and H2 as follows:

$$H_1 \longrightarrow \boldsymbol{w}^T \boldsymbol{x}_i + b = +1 \quad for\ \boldsymbol{y}_i = +1 \tag{2.3}$$

$$H_2 \longrightarrow \boldsymbol{w}^T \boldsymbol{x}_i + b = -1 \quad for\ \boldsymbol{y}_i = -1 \tag{2.4}$$

The area for the negative class was $\boldsymbol{w}^T \boldsymbol{x}_i + b \leq -1$ while that of the positive class was $\boldsymbol{w}^T \boldsymbol{x}_i + b \geq +1$. Figure.1 illustrates the hyperplane in Support Vector Machines.

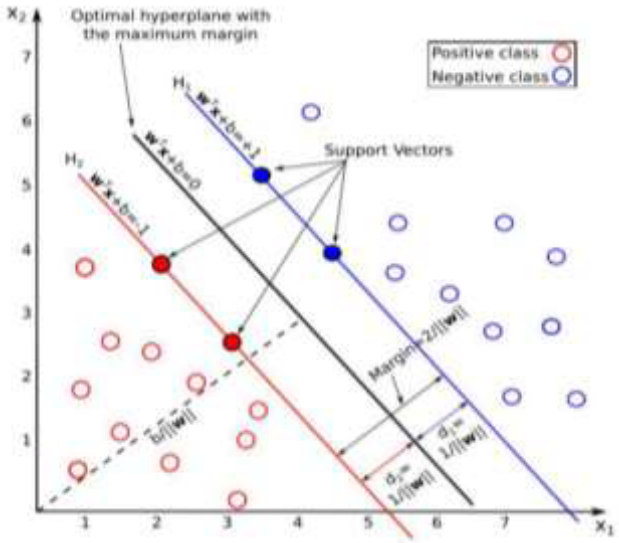

Figure 1. Illustration of Support Vector Machine [20]

The problem of SVM optimization is written as follow:

$$\text{Minimize} \quad \frac{1}{2}\|w\|^2 \tag{2.5}$$

$$\text{s.t.} \quad y_i\,(\boldsymbol{w}^T \cdot x_i + b) \geq 1, \forall i = 1, \ldots, N \tag{2.6}$$

after solving the problem above, formula of $\boldsymbol{w}$ and b became:

$$\boldsymbol{w} = \sum_{i=1}^{N} a_i y_i \boldsymbol{x_i} \tag{2.7}$$

$$b = \frac{1}{N_s}\sum_{i \epsilon S}(y_i - \sum_{m \epsilon S} a_m y_m \boldsymbol{x}_m) \tag{2.8}$$

and the decision formulas of SVM were written as follows

$$f(x) = sign(\boldsymbol{w} \cdot \boldsymbol{x} + b) \tag{2.9}$$

However, in many cases the separation of classes may not be carried out precisely using a linear boundary (See Figure.1). Those cases were called non-linear separable data. Therefore, to approach a non-linear decision boundary, SVM enlarged the original feature space to high dimensional space, which made computations intractable. Furthermore, for this issue, the 'kernel trick' was applied using a kernel function to produce better accuracy results [25]. Figure 2 shows the illustration of non-linear separable data.

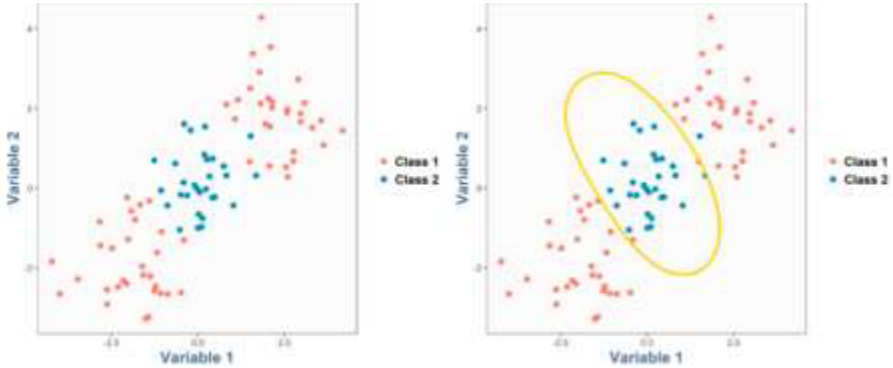

Figure 2. Non-Linear Separable Data [26]

The performance of SVM closely relied on the kernel function that used the method [27]. Specifically, a kernel function was the essential component needed to make the SVM method get higher accuracy [28]. In addition, it was

used for complex real-world applications by mapping the data into a higher-dimensional space [29]. The kernel function is generally written as follow:

$$\kappa(x_i, x_j) = < \varphi(x_i), \varphi(x_j) > \quad (2.10)$$

the problem of SVM optimization became:

$$\text{Minimize} \quad \frac{1}{2}\|w\|^2 + C \sum_{i=1}^{N} \epsilon_i \quad (2.11)$$

$$\text{s.t} \quad y_i (\boldsymbol{w}^T \cdot \varphi(\boldsymbol{x_i}) + b) - 1 + \epsilon_i \geq 0, \quad \forall i = 1, \dots, N \quad (2.12)$$

by solving the problem above, the formula of $\boldsymbol{w}$ and $b$were as follow:

$$\boldsymbol{w}^* = \sum_{i=1}^{N} a_i y_i \varphi(\boldsymbol{x_i}) \quad (2.13)$$

$$b^* = \frac{1}{N_s} \sum_{i \epsilon S} (y_i - \sum_{m \epsilon S} a_m y_m \varphi(\boldsymbol{x_m})) \quad (2.14)$$

And the decision formulas of SVM were as follow:

$$f(x) = sign(\boldsymbol{w}^* \cdot \varphi(\boldsymbol{x_i}) + b^*) \quad (2.15)$$

where ϵ_i was an error that should be minimized and C was the penalty which determined the trade-off between the minimization of error and the maximization of the classification margin.

Confusion Matrix

In this study, the confusion matrix was applied to measure the performance of ANN and SVM. This is a well-known performance measurement for machine learning classification problem, where output may be two or more classes. It requires four variables, which include TP (True Positive), TN (True Negative), FP (False Positive) and FN (False Negative). A detailed confusion matrix is shown in Table 1.

TABLE 1. Confusion Matrix

Actual Value	Predicted Value	
	Positive	Negative
Positive	T_p	F_p
Negative	F_N	T_N

$$accuracy = \frac{T_P + T_N}{T_P + T_N + F_P + F_N} \quad (2.16)$$

$$precision = \frac{T_P}{T_P + F_P} \quad (2.17)$$

$$recall = \frac{T_P}{T_P + F_N} \quad (2.18)$$

$$F1\ Score = \frac{2\ x\ precision\ x\ recall}{precision + recall} \quad (2.19)$$

3. RESULTS

In this study, lung cancer CT scan, which consisted of 98 data was obtained from Cipto Mangunkusumo Hospital, Jakarta, Indonesia. There are 7 features in CT scan data, which include area, minimum value, maximum value, sum

value, average, standard error (SD) and length. Furthermore, the artificial neural network was applied in the classification with 2 hidden layers. The optimizer used was Adam and number of epochs was 50. From the number of the experiment obtained, the parameters produced the best accuracy. This study used 70% of training data. In addition, for Support Vector Machine, the polynomial kernel with degree = 5 was used. The choice of that parameter was based on the experiment carried out. The results obtained are shown in table 2 and 3.

TABLE 2. Accuracy and F1 Score of ANN and SVM

Methods	Accuracy	F1 Score
ANN	96%	96%
SVM	S90%	93%

TABLE 3. Recall and Precision of ANN and SVM

Methods	Recall	Precision
ANN	100%	93%
SVM	100%	86%

Table.2 shows the accuracy and F1 Score of ANN and SVM. It is seen that ANN has 96% accuracy and 96% F1 Score, while SVM only reached 90% accuracy and 93% F1 Score. Therefore, ANN was better than SVM in classifying lung cancer with small data. Furthermore, in Table3 recall was higher than precision in all methods. This indicates that a lower number of malignant nodule samples were incorrectly classified as benign (false negative), compared to the number of benign lung nodule inaccurately categorized as malignant (false positive). Furthermore, both ANN and SVM had 100% in recall matrix however, ANN was higher than SVM in precision metrics.

4. CONCLUSION

The early detection of lung cancer is necessary because of its relation with patients' treatment. Therefore, a quicker diagnosis increases the tendency to obtain the appropriate treatment and consequently improves life expectancy. However, an advanced technology was required to enhance the ease of classification from the CT scan of nodules in lungs. Numerous machine learning methods has previously been used and developments were needed to resolve existing limitations, including the challenges of small datasets.

Therefore, Artificial Neural Network (ANN) and Support Vector Machines (SVM) were used in this study. The results showed that ANN was better than SVM in classifying lung cancer with small data since ANN accuracy reached 96% while SVM reached 90%. In addition, for other metrics such as precision and F1 Score, ANN was higher than SVM. However, in recall, both had same percent which was 100%.

For future studies, it is recommended to use other optimizers and kernel in ANN and SVM respectively to identify the best-fit for lung cancer classification with small data. Furthermore, prospective studies are encouraged to develop or modify this method, in order to produce the best accuracy with possible application in other disease conditions.

ACKNOWLDGEMENT

This research was financially supported by the Indonesian Ministry of Research and Technology, with a KEMENRISTEK/BRIM 2021 research grant scheme. Furthermore, the authors want to thanks to Cipto Mangunkusumo, Jakarta, Indonesia, for providing the lung cancer dataset.

REFERENCES

1. K. R. Pradeep & N. C. Naveen, Lung Cancer Survivability Prediction based on Performance Using Classification Techniques of Support Vector Machines, C4.5 and Naive Bayes Algorithms for Healthcare Analytics, Procedia Computer Science, vol. 132, pp. 412-420, 2018.
2. Latest global cancer data: Cancer burden, World Health Organization, 12 September 2018. [Online]. Available: https://www.who.int/cancer/PRGlobocanFinal.pdf.
3. M. Zheng, Classification and Pathology of Lung Cancer, Surgical Oncology Clinics of North America, vol. 25, no. 3, pp. 447-468, 2016.
4. Y. Mao, D. Yang, J. He & M. J. Krasna, Epidemiology of Lung Cancer, Surgical Oncology Clinics of North America, vol. 25, no. 3, pp. 439-445, 2016.
5. M. A. Khan, Lungs cancer classification from CT images: An integrated design of contrast based classical features fusion and selection, Pattern Recognition Letters, vol. 129, pp. 77-85, 2020.
6. X. Yutonga, Z. Jianpenga, X. Yonga, M. Fulham & Z. Yanning, Fusing texture, shape and deep model-learned information at decision level for automated classification of lung nodules on chest CT, Information Fusion, vol. 42, pp. 102-110, 2018.
7. K. Lakshmanaprabu, Optimal deep learning model for classification of lung cancer on CT images, Future Generation Computer Systems, vol. 92, pp. 374-382, 2019.
8. T. V. Rampisela & Z. Rustam, Classification of Schizophrenia data using Support Vector Machine (SVM), Journal of Physics: Conference Series, vol. 1108, no. 1, 2018.
9. A. W. Lestari & Z. Rustam, Normed kernel function-based fuzzy possibilistic C-means (NKFPCM) algorithm for high-dimensional breast cancer database classification with feature selection is based on Laplacian Score, AIP Conference Proceedings, vol. 1862, no. 1, 2017.
10. Z. Rustam, S. Hartini, R. Y. Pratama, R. E. Yunus & R. Hidayat, Analysis of architecture combining Convolutional Neural Network (CNN) and kernel K-means clustering for lung cancer diagnosis, International Journal on Advanced Science, Engineering and Information Technology, vol. 10, no. 3, pp. 1200-1206, 2020.
11. K. Jalal Deen, R. Ganesan & A. Merline, Fuzzy-C-means clustering based segmentation and CNN-classification for accurate segmentation of lung nodules, Asian Pacific Journal of Cancer Prevention: APJCP, vol. 18, no. 7, p. 1869, 2017.
12. L. Bertolaccini, P. Solli, A. Pardolesi & A. Pasini, An overview of the use of artificial neural networks in lung cancer research, Journal of thoracic disease, vol. 9, no. 4, pp. 924-931, 2017.
13. Y. Chen, H. Chang, J. Meng & D. Zhang, Ensemble Neural Networks (ENN): A gradient-free stochastic method, Neural Networks, vol. 110, pp. 170-185, 2019.
14. Z. Rustam & T. Nadira, Classification of cancer data using support vector machines with features selection method based on global artificial bee colony, AIP Conference Proceedings, vol. 2023, no. 1, p. 020205, 2018.
15. Z. Rustam & N. P. A. A. Ariantari, Support Vector Machines for Classifying Policyholders Satisfactorily in Automobile Insurance, Journal of Physics: Conference Series, vol. 1028, no. 1, 2018.
16. X.-S. Yang, Neural networks and deep learning, Introduction to Algorithms for Data Mining and Machine Learning, London, Elsevier Inc, 2019, p. 149.
17. C. C. Aggarwal, Neural Networks and Deep Learning, Neural Networks and Deep Learning, Switzerland, Springer, p. 1, 2018.
18. R. M. Sadek, Parkinson's Disease Prediction Using Artificial Neural Network, International Journal of Academic Health and Medical Research (IJAHMR), vol. 3, no. 1, pp. 1-8, 2019.
19. M. Ay, D. Stenger, M. Schwenzer, D. Abel & T. Bergs, Kernel Selection for Support Vector Machines for System Identification of a CNC Machining Center, IFAC-Papers OnLine, vol. 59, no. 29, pp. 192-198, 2019.
20. A. Tharwat, Parameter investigation of support vector machine classifier with kernel functions, Knowledge and Information Systems, vol. 61, pp. 1269-1302, 2019.
21. X. Zhang, J. Xiao & F. Gu, Applying support vector machine to electronic health records for cancer classification, 2019 Spring Simulation Conference (SpringSim), pp. 1-9, 2019.
22. Z. Rustam & D. Zahras, Comparison between support vector machine and fuzzy c-means as classifier for intrusion detection system, Journal of Physics: Conference Series, vol. 1028, no. 1, 2018.
23. M. Vatankhah, V. Asadpour & R. Fazel-Rezai, Perceptual pain classification using ANFIS adapted RBF kernel support vector machine for therapeutic usage, Applied Soft Computing, vol. 13, no. 5, pp. 2537-2546, 2013.

24. J. Abukhait, A. M. Mansour & M. Obeidat, Classification based on gaussian-kernel support vector machine with adaptive fuzzy inference system, Margin, vol. 7, no. 8, p. 9, 2018.
25. A. R. Bagasta, Z. Rustam, J. Pandelaki & W. A. Nugroho, Comparison of Cubic SVM with Gaussian SVM: Classification of Infarction for detecting Ischemic Stroke, IOP Conference Series: Materials Science and Engineering, vol. 546, no. 5, 2019.
26. A. Apsemidis, S. Psarakis & J. M. Moguerza, A review of machine learning kernel methods in statistical process monitoring, Computers & Industrial Engineering, vol. 142, p. 106376, 2020.
27. D. Zhao, Whale optimized mixed kernel function of support vector machine for colorectal cancer diagnosis, Journal of biomedical informatics, vol. 92, p. 103124, 2019.
28. Z. Liu & H. Xu, Kernel parameter selection for support vector machine classification, Journal of Algorithms & Computational Technology, vol. 8, no. 2, pp. 163-177, 2014.
29. S. Hartini & Z. Rustam, Hierarchical Clustering Algorithm Based on Density Peaks using Kernel Function for Thalassemia Classification, Journal of Physics: Conference Series, vol. 1417, no. 1, 2019.

Fourier Methods for Determination of An Unknown Heat Source Poly(Methyl Methacrylate) (PMMA) with Periodic Boundary Conditions

İrem BAĞLAN[1], Timur CANEL[2]

[1]*Department of Mathematics, Faculty of Science and Arts,*
Kocaeli University, Kocaeli-TURKEY
[2]*Department of Physics, Faculty of Science and Arts,*
Kocaeli University, Kocaeli-TURKEY

isakinc@kocaeli.edu.tr
tcanel@ kocaeli.edu.tr

Abstract. In this paper, we consider a coefficient problem of an inverse problem of a quasilinear parabolic equation with periodic boundary and integral over determination conditions. We prove the existence, uniqueness and continuously dependence upon the data of the solution by iteration method.

1. INTRODUCTION

The inverse problem of determining unknown coefficient in a quasi-linear parabolic equation has generated an increasing amount of interest from engineers and scientist. Nevertheless the inverse coefficient problems with periodic boundary and integral overdetermination conditions are not investigated by many researchers [1]-[5].This kind of conditions arise from many important applications in heat transfer, life sciences, etc. The inverse problem of unknown coefficients in a quasi-linear parabolic equations with periodic boundary conditions was studied by Kanca and Baglan [5]-[6].

Consider the equation

$$u_t = u_{xx} + l(t)f(x,t,u),(x,t) \in D \tag{1.1}$$

with the initial condition

$$u(x,0) = \varphi(x), x \in [0,\pi] \tag{1.2}$$

the periodic boundary condition

$$\begin{aligned} &u(0,t) = u(\pi,t) \\ &u_x(0,t) = u_x(\pi,t), t \in [0,T] \end{aligned} \tag{1.3}$$

and the overdetermination data

$$g(t) = u(\pi,t), t \in [0,T] \tag{1.4}$$

for a quasilinear parabolic equation with the nonlinear source term f=f(x,t,u).

Here D:={0<x<π, 0<t<T}.The functions $\varphi(x)$ and f(x,t,u) are given functions on [0,π] and D×(-∞,∞), respectively.

The problem of finding the pair {l(t), u(x,t)} in (1.1)-(1.4) will be called an inverse problem.

Definition 1. The pair {l(t),u(x,t)} from the class C[0,T]×(C^{2,1}(D)∩C^{1,0}(D)) for which conditions (1)-(4) are satisfied is called the classical solution of the inverse problem (1)-(4).

The paper organized as follows:

In Section 2, the existence and uniqueness of the solution of the inverse problem (1.1)-(1.4) is proved by using the Fourier method and iteration method. In Section 3, the continuous dependence upon the data of the inverse problem is shown. In Section 4, the numerical procedure for the solution of the inverse problem is given.

2. EXISTENCE AND UNIQUENESS OF THE SOLUTION OF THE INVERSE PROBLEM

The main result on the existence and the uniqueness of the solution of the inverse problem (1.1)-(1.4) is presented as follows:

We have the following assumptions on the data of the problem (1)-(4).

(A1) $g(t) \in C^1[0,T], l(t) \in C[0,T]$.

(A2) $\varphi(x) \in C^3[0,\pi],$

$\varphi(0) = \varphi(\pi),$

$\varphi'(0) = \varphi'(\pi),$

$\varphi''(0) = \varphi''(\pi).$

(A3) Let the function f(x,t,u) is continuous with respect to all arguments in D×(-∞,∞) and satisfies the following condition

(1) $\left|\frac{\partial^{(n)} f(x,t,u)}{\partial x^n} - \frac{\partial^{(n)} f(x,t,\tilde{u})}{\partial x^n}\right| \le b(x,t)|u-\tilde{u}|, n = 0,1,2,$

where $b(x,t) \in L_2(D), b(x,t) \ge 0$,

(2) $f(x,t,u) \in C^3[0,\pi], t \in [0,T]$

$f(x,t,u)|_{x=0} = f(x,t,u)|_{x=\pi}$

$f_x(x,t,u)|_{x=0} = f_x(x,t,u)|_{x=\pi}$

$f_{xx}(x,t,u)|_{x=0} = f_{xx}(x,t,u)|_{x=\pi}$

(3) $\int_0^\pi f(x,t,u)dx \ne 0, t \in [0,T]$.

By applying the standard procedure of the Fourier method, we obtain the following representation for the solution of (1.1)-(1.4) .

$$u(x,t)=\frac{u_0(t)}{2}+\sum_{k=1}^{\infty}[u_{ck}(t)\cos 2kt+u_{sk}(t)\sin 2kt]$$

$$u_0(t)=\varphi_0+\int_0^t\int_0^\pi l(\tau)f(\xi,\tau,\frac{u_0(\tau)}{2}+\sum_{k=1}^{\infty}[u_{ck}(t)\cos 2kt+u_{sk}(t)\sin 2kt])d\xi d\tau$$

$$u_{ck}(t)=\varphi_{ck}e^{-(2k)^2t}+\int_0^t\int_0^\pi l(\tau)f(\xi,\tau,\frac{u_0(\tau)}{2}+\sum_{k=1}^{\infty}[u_{ck}(t)\cos 2kt+u_{sk}(t)\sin 2kt])e^{-(2k)^2(t-\tau)}\cos 2k\xi d\xi d\tau$$

$$u_{sk}(t)=\varphi_{sk}e^{-(2k)^2t}+\int_0^t\int_0^\pi l(\tau)f(\xi,\tau,\frac{u_0(\tau)}{2}+\sum_{k=1}^{\infty}[u_{ck}(t)\cos 2kt+u_{sk}(t)\sin 2kt])e^{-(2k)^2(t-\tau)}\sin 2k\xi d\xi d\tau$$

$$\begin{aligned}u(x,t)&=\varphi_0+\int_0^t l(\tau)f_0(\tau,u)d\tau\\&+\sum_{k=1}^{\infty}\cos 2kx\left[\varphi_{ck}e^{-(2k)^2t}+\int_0^t l(\tau)f_{ck}(\tau,u)e^{-(2k)^2(t-\tau)}d\tau\right]\\&+\sum_{k=1}^{\infty}\sin 2kx\left[\varphi_{sk}e^{-(2k)^2t}+\int_0^t l(\tau)f_{sk}(\tau,u)e^{-(2k)^2(t-\tau)}d\tau\right]\end{aligned}\qquad(2.1)$$

where $\varphi_0=\frac{2}{\pi}\int_0^\pi\varphi(\xi)d\xi,\ \varphi_{ck}=\frac{2}{\pi}\int_0^\pi\varphi(\xi)\cos 2k\xi d\xi,\ \varphi_{sk}=\frac{2}{\pi}\int_0^\pi\varphi(\xi)\sin 2k\xi d\xi.$

Under the condition (A1)-(A3), differentiating (1.4), we obtain

$$g'(t)=u_t(\pi,t),t\in[0,T]\qquad(2.2)$$

(2.1) and (2.2) yield

$$l(t)=\frac{g'(t)+\sum_{k=1}^{\infty}(4k^2)\left(\varphi_{ck}e^{-(2k)^2t}+\int_0^t l(\tau)f_{ck}(\tau,u)e^{-(2k)^2(t-\tau)}d\tau\right)}{f_0(t)+\sum_{k=1}^{\infty}f_{ck}(t)}\qquad(2.3)$$

Definition 2. *Denote the set*

$\{u(t)\}=\{u_0(t),u_{ck}(t),u_{sk}(t),k=1,...,n\}$, *of continuous on [0,T] functions satisfying the condition*

$$\max_{0\le t\le T}\frac{|u_0(t)|}{2}+\sum_{k=1}^{\infty}[\max_{0\le t\le T}|u_{ck}(t)|\cos 2kt+\max_{0\le t\le T}|u_{sk}(t)|\sin 2kt]<\infty$$

$$\|u(t)\|=\max_{0\le t\le T}\frac{|u_0(t)|}{2}+\sum_{k=1}^{\infty}[\max_{0\le t\le T}|u_{ck}(t)|\cos 2kt+\max_{0\le t\le T}|u_{sk}(t)|\sin 2kt]$$

It can be shown that B are the Banach spaces.

Theorem 1 *Let the assumptions (A1)-(A3) be satisfied. Then the inverse problem (1.1)-(1.4) has a unique solution for small T.*

Proof. An iteration for (2.1) is defined as follows:

$$u_0^{(N+1)}(t)=u_0^{(0)}(t)+\int_0^t\int_0^\pi l^{(N)}(\tau)f(\xi,\tau,u^{(N)}(\xi,\tau))d\xi d\tau$$

$$u_{ck}^{(N+1)}(t)=u_{ck}^{(0)}(t)+\int_0^t\int_0^\pi l^{(N)}(\tau)f(\xi,\tau,u^{(N)}(\xi,\tau))e^{-(2k)^2(t-\tau)}\cos 2k\xi d\xi d\tau$$

$$u_{sk}^{(N+1)}(t)=u_{sk}^{(0)}(t)+\int_0^t\int_0^\pi l^{(N)}(\tau)f(\xi,\tau,u^{(N)}(\xi,\tau))e^{-(2k)^2(t-\tau)}\sin 2k\xi d\xi d\tau$$

Applying Cauchy inequality, Hölder inequality, Bessel inequality, Lipschitz condition and taking maximum of both side,

$$\|u^{(1)}(t)\|=\max_{0\le t\le T}\frac{|u_0^{(0)}(t)|}{2}+\sum_{k=1}^{\infty}[\max_{0\le t\le T}|u_{ck}^{(0)}(t)|\cos 2kt+\max_{0\le t\le T}|u_{sk}^{(0)}(t)|\sin 2kt]$$

$$\le\frac{|\varphi_0|}{2}+\sum_{k=1}^{\infty}|\varphi_{ck}|+|\varphi_{sk}|$$

$$+\left(\frac{\sqrt{T}}{\sqrt{\pi}}+\frac{\sqrt{2\pi}}{2\sqrt{3}}\right)\|b(x,t)\|_{L_2(D)}\|u^{(0)}(t)\|_B\|l^{(0)}(t)\|_{C[0,T]}$$

$$+\left(\frac{\sqrt{T}}{\sqrt{\pi}}+\frac{\sqrt{2\pi}}{2\sqrt{3}}\right)\|f(x,t,0)\|_{L_2(D)}\|l^{(0)}(t)\|_{C[0,T]}.$$

From the conditions of the theorem $u^{(1)}(t)\in B$

Same estimations for N,

$$\left\|u^{(N+1)}(t)\right\| = \max_{0\le t\le T}\frac{\left|u_0{}^{(N)}(t)\right|}{2} + \sum_{k=1}^{\infty}\left[\max_{0\le t\le T}\left|u_{ck}{}^{(N)}(t)\right|\cos 2kt + \max_{0\le t\le T}\left|u_{sk}{}^{(N)}(t)\right|\sin 2kt\right]$$

$$\le \frac{\left|\varphi_0\right|}{2} + \sum_{k=1}^{\infty}\left|\varphi_{ck}\right| + \left|\varphi_{sk}\right|$$

$$+\left(\frac{\sqrt{T}}{\sqrt{\pi}} + \frac{\sqrt{2\pi}}{2\sqrt{3}}\right)\left\|b(x,t)\right\|_{L_2(D)}\left\|u^{(N)}(t)\right\|_B\left\|l^{(N)}(t)\right\|_{C[0,T]}$$

$$+\left(\frac{\sqrt{T}}{\sqrt{\pi}} + \frac{\sqrt{2\pi}}{2\sqrt{3}}\right)\left\|f(x,t,0)\right\|_{L_2(D)}\left\|l^{(N)}(t)\right\|_{C[0,T]}.$$

Since $u^{(N)}(t)\in B$ and from the conditions of the theorem, we have $u^{(N+1)}(t)\in B$

$\{u(t)\} = \{u_0(t), u_{ck}(t), u_{sk}(t), k = 1,..., n\} \in B$.

Same estimations for N,

$$\left\|l^{(N)}(t)\right\| \le \frac{\left|g'(t)\right| + 4\sum_{k=1}^{\infty}\left\|\varphi''_{ck}\right\| + \frac{8}{\pi}\left\|b(x,t)\right\|_{L_2(D)}\left\|u^{(N)}(t)\right\|_B\left\|l^{(N)}(t)\right\|_{C[0,T]} + \frac{8}{\pi}\left\|l^{(N)}(t)\right\|_{C[0,T]}M}{M}$$

Since $u^{(N)}(t)\in B$, $l^{(N)}(t)\in C[0,T]$ respectively.(as N→∞)

$$\left\|u^{(1)}(t) - u^{(0)}(t)\right\|$$

$$\le \left(\frac{\sqrt{T}}{\sqrt{\pi}} + \frac{\sqrt{2\pi}}{2\sqrt{3}}\right)\left\|b(x,t)\right\|_{L_2(D)}\left\|u^{(0)}(t)\right\|_B\left\|l^{(0)}(t)\right\|_{C[0,T]}$$

$$+\left(\frac{\sqrt{T}}{\sqrt{\pi}} + \frac{\sqrt{2\pi}}{2\sqrt{3}}\right)\left\|f(x,t,0)\right\|_{L_2(D)}\left\|l^{(0)}(t)\right\|_{C[0,T]}.$$

$$A = \left(\frac{\sqrt{T}}{\sqrt{\pi}} + \frac{\sqrt{2\pi}}{2\sqrt{3}}\right)\left\|b(x,t)\right\|_{L_2(D)}\left(\left\|u^{(0)}(t)\right\|_B\left\|l^{(0)}(t)\right\|_{C[0,T]} + M\right)$$

Applying Cauchy inequality, Hölder Inequality, Lipschitzs condition and Bessel inequality to the last equation and taking maximum of both side of the last inequality, we obtain:

$$\left\|l^{(N+1)}(t) - l^{(N)}(t)\right\| \le \frac{8}{\pi}\left\|b(x,t)\right\|_{L_2(D)}\left\|u^{(N+1)}(t)\right\|_B\left\|l^{(N+1)}(t)\right\|_{C[0,T]}$$

$$\left\|u^{(N+1)}(t)-u^{(N)}(t)\right\|$$
$$\leq \frac{A}{\sqrt{N!}}\left\{\left(\frac{\sqrt{T}}{\sqrt{\pi}}+\frac{\sqrt{2\pi}}{2\sqrt{3}}\right)\left(1+\frac{8}{\pi}\right)\right\}^{N}\left\|b(x,t)\right\|_{L_2(D)}$$
$$\left\|l^{(1)}(t)\right\|_{C[0,T]}\left\|l^{(2)}(t)\right\|_{C[0,T]}...\left\|l^{(N)}(t)\right\|_{C[0,T]}.$$

It is easy to see that $u^{(N+1)}(t)\to u^{(N)}(t)$, N→∞, then $l^{(N+1)}(t)-l^{(N)}(t)$, N→∞.

Now let us show that there exists u and l such that $\lim_{N\to\infty} u^{(N+1)}(t)\to u(t), \lim_{N\to\infty} l^{(N+1)}(t)\to l(t).$

$$\left\|u(t)-u^{(N+1)}(t)\right\|$$
$$\leq 2\left[\frac{A}{\sqrt{N!}}\left\{\left(\frac{\sqrt{T}}{\sqrt{\pi}}+\frac{\sqrt{2\pi}}{2\sqrt{3}}\right)\left(1+\frac{8}{\pi}\right)\right\}^{N+1}\left\|b(x,t)\right\|_{L_2(D)}\left\|l(t)\right\|_{C[0,T]}\right.$$
$$\left.\left\|l^{(1)}(t)\right\|_{C[0,T]}\left\|l^{(2)}(t)\right\|_{C[0,T]}...\left\|l^{(N)}(t)\right\|_{C[0,T]}\right]^2$$
$$x\exp\left(2\left\{\left(\frac{\sqrt{T}}{\sqrt{\pi}}+\frac{\sqrt{2\pi}}{2\sqrt{3}}\right)\left(1+\frac{8}{\pi}\right)\right\}^{2}\left\|b(x,t)\right\|^2_{L_2(D)}\left\|l(t)\right\|^2_{C[0,T]}\right)$$

$u^{(N+1)}(t)\to u(t)$, N→∞ then $l^{(N+1)}(t)-l(t)$, N→∞.

For the uniqueness, we assume that the problem (1.1)-(1.4) has two solution pair (l,u), (k,v). Applying Cauchy inequality, Hölder Inequality, Lipschitzs condition and Bessel inequality to |u(t)-v(t)| and |l(t)-k(t)|, we obtain:

$$\left\|u-v\right\|_B \leq \left\{\left(\frac{\sqrt{T}}{\sqrt{\pi}}+\frac{\sqrt{2\pi}}{2\sqrt{3}}\right)\left(1+\frac{8}{\pi}\right)\right\}\left\|b(x,t)\right\|_{L_2(D)}\left\|l(t)\right\|_{C[0,T]}\left\|u-v\right\|_B.$$

applying Gronwall's inequality to last equation we have

u(t)=v(t). Hence l(t)=k(t).

The theorem is proved.

REFERENCES

1. A. Ergün and R. Amirov, Direct and Inverse problems for diffusion operator with discontinuıty points,Journal of Applied and Engineering Mathematics, vol. 9, no. 1, pp. 9–21, Jan. 2019.
2. A. Ergün, Integral Representation for Solution of Discontinuous Diffusion Operator with Jump Conditions, Cumhuriyet Science Journal, vol. 39, no. 4, pp. 842–863, Jul. 2018.
3. E. Set, A.O. Akdemir, B. Çelik, On Generalization of Fejér Type Inequalities via fractional integral operator, 2018, Filomat, Vol 32: Issue 16.

4. A.O. Akdemir, E. Set and A. Ekinci, On new conformable fractional integral inequalities for product of diferent kinds of convexity, TWMS Journal of Applied and Engineering Mathematics,2019, Vol 9, Issue 1,142-150.
5. F. Kanca, I. Baglan, An inverse coefficient problem for a quasilinear parabolic equation with nonlocal boundary conditions, Boundary Value Problems, V.213,2013.
6. F. Kanca, Baglan I., An inverse problem for a quasilinear parabolic equation with nonlocal boundary and overdetermination conditions, Journal of inequalities and applications, V.76,2014.

Liver Cancer Classification using Neural Network–Support Vector Machine with several Optimizers

Jane Eva AURELIA[1] and Zuherman RUSTAM[1]

[1]*Department of Mathematics, Faculty of Mathematics and Natural Sciences, University of Indonesia*

janeevaaurelia@gmail.com

Abstract. The liver is one of the organs with several essential functions in the body and cancer associated with this organ has been reported not to be due to the malignancy from organs which spread to different organs in the body. Different types of cancer have been classified based on the growth location or metastasis but no symptoms have been observed to indicate liver cancer but different methods of machine learning methods such as the Neural Network (NN) have been designed and developed for easy identification. This method is popular and has a wide range of applications due to its high accuracy value based on a network of small processing units modeled on the human nervous system. A Support Vector Machine (SVM) with several kernel functions is also commonly used in classifying diseases and has been discovered to be highly accurate in classifying algorithms for both linear and non-linear data. For the purpose of this research, a database of Liver Cancer sufferers consisting of 122 data which are 71 significant and 52 minor data was retrieved from Dr. Cipto Mangunkusumo Hospital, Indonesia, and the performance and accuracy of combining NN–SVM as a classifier for the liver cancer dataset were compared with several other optimizers. The findings showed that the Neural Network–Support Vector Machine with Adam Optimizer is the best model to classify Liver Cancer with 97.98% accuracy. Therefore, this method is expected to provide higher accuracy in future studies while a more extensive database is suggested to provide better results for predicting and classifying different diseases.

1. INTRODUCTION

I. Liver Cancer

The liver is one of the organs with several essential functions in the body including the production of bile which helps in digesting nutrients like fat as well as others such as controlling blood clotting and cleaning of the blood from toxins or harmful substances such as alcohol or drugs [1]. Meanwhile, liver cancer has been reported not to be due to the malignancy from organs which spread to different others in the body [2] but happens when cells in the liver mutate to form tumors. It is one of the five types of cancer observed to be causing most deaths and reported by the World Health Organization to be responsible for more than 700,000 out of 9 million deaths from cancer [5].

The disease is classified based on the location of the growth or metastasis into primary and secondary liver cancer [3] with the primary type found to be starting in the liver and has the potential to be fatal while the secondary type starts in other parts of the body and later transmit and sprout to the liver. Moreover, Hepatocellular Carcinoma is one of the most prevalent types of liver cancer which expands from the primary liver cells known as the hepatocytes.

Hepatocellular Carcinoma (HCC) accounts for the occurrence of approximately 75% of primary liver cancers and also serves as the pavement for hepatitis and cirrhosis displaced by scar tissue [4]. Meanwhile, secondary liver cancer is generally named according to the organ the cancer cells initially developed as observed in metastatic colon cancer which originates from the colon and transmits to the liver. The secondary type is observed to be more general than the primary and apart from the transmission associated with the colon, other sources include breast, pancreas, lung, ovary, stomach, and skin or melanoma [5].

Previous studies have shown several methods used in classifying liver cancer and some of them include Random Forest [6], Hybrid–Feature Analysis [7], and Deep Learning [8]. It is important to point out that classification is a learning process used in data labeling. The model applied in this study was, therefore, designed to utilize a collection of training, test, and studying of old class categories to determine the formation of new classes but several data sets

such as stock and diseases were used. Furthermore, a combined machine learning method known as the Neural Network–Support Vector Machine was proposed to classify data and predict the class of liver cancer patients.

II. Methodology

A Neural Network–Support Vector Machine was used in this study to classify the liver cancer dataset after which several algorithm optimizers such as Adam, AdaGrad, and Stochastic Gradient Descent (SGD) were adopted and explained further in the following subsections.

a. *Neural Network*

Neural Network (NN) is a network of small processing units modeled on the human nervous system [9]. It is also an adaptive system with the ability to replace its arrangement to break problems based on external and internal evidence flowing past the network. This network is often called an adaptive network because of its adaptive nature.

NN is simply a non-linear exhibition tool for statistical data which is passable to model complex relationships among input and output in order to discover schemes in data. A theorem known as the "Universal Estimation Theorem" [10] showed that the NN with at least a hidden layer and a non-linear activation function has the ability to model any Boreal measured process from the first dimension to another. The architecture of the network is, therefore, illustrated in Figure 1 [11].

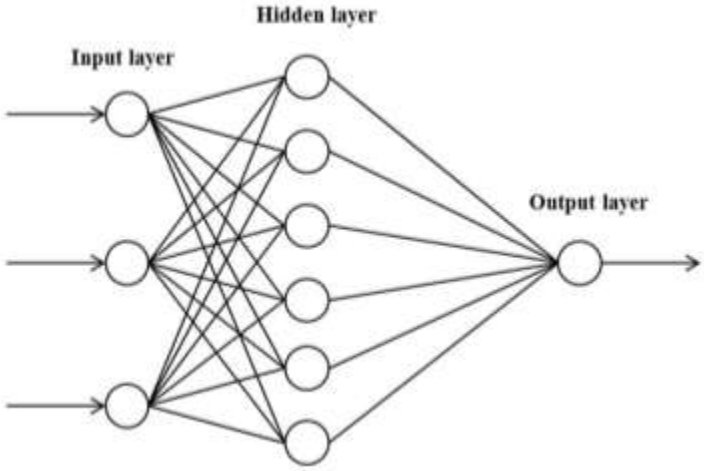

Figure 1 – Illustration of Neural Network Architecture [11].

As stated in the previous section, some of the optimizers usually used include Gradient Descent which is the default, RMSprop, SGD, Adam, Adadelta, Adamax, Adagrad, and Nadam. The ones used in this research are discussed as follows [12]:

a. Adam

Adam is an optimization algorithm designed based on former training data to iteratively reform the weights. It is an adaptive learning rate method which calculates the individual learning rate for different parameters. This optimizer has also been found to be different from classical stochastic gradient descent [13] estimated foremost and secondary moments.

Adam is a prevalent algorithm in the deep learning field due to its ability to quickly produce good outcomes [13] and show the convergence meets the theoretical analysis expectations. It has been discovered to be using the IMDB sentiment analysis dataset, logistic regression algorithm to MNIST digit recognition, and Multilayer Perceptron algorithm on the MNIST dataset.

b. AdaGrad

An improvement was required to provide a different update speed for each dimension of the parameter vector based on specific indicators apart from momentum and this was achieved through the Adaptive Sub-gradient Descent (AdaGrad) method [14].

It is useful to provide the information on the level of changes in the value of an element in the gradient vector which serves as the gradient scale factor while the division operation is observed to be a per element operation between 2 vectors. A decrease in the value at a particular dimension usually leads to an increment in the update speed in the dimension and this further ensures a balance of each dimension of the gradient vector's contribution, thereby, making the optimization path more stable [14]. The limitation attached with AdaGrad is that the value has the potential to be very large at a particular time and this slows down the optimization process. Therefore, a small modification is made through the addition of constants to adjust the magnitudes in order to correct this problem.

c. Stochastic Gradient Descent (SGD)

The gradient is the value of a line's inclination while comparing the abscissa and ordinate components [15] or the slope value of a function such as the rate of change in the parameter relative to the others. It has also been discovered that more gradient makes the slope steeper. Therefore, Gradient Descent is described as an iteration used to find the optimal value of a parameter by applying calculus to determine the minimum value and update the weight in Neural Network by minimizing the loss function in the backpropagation phase [15]. Several recent studies in deep learning are making use of gradient-based optimizers and this makes them more popular and familiar.

Stochastic Gradient Descent (SGD) has become the standard optimization routine for Neural Networks due to its fast convergence and good generalization properties [16] as well as the ability to minimize error function in optimization problems. Moreover, it also reduced computations costs drastically by a factor due to the random selection nature of sample I which makes it very diverse at iteration [16].

b. *Support Vector Machine*

Support Vector Machine (SVM) is a classification algorithm for linear and non-linear data [17]. It uses non–linear mapping to transform initial training data into higher dimensions and also has the ability to predict both classification and regression [18]. At first, it has a linear principle but is now developed to work on non-linear problems [19] in order to incorporate the kernel concept into a high dimensional space and a separator which is often called a hyperplane is determined [20]. An illustration of an SVM architecture is, therefore, presented in the following Figure 2 [21].

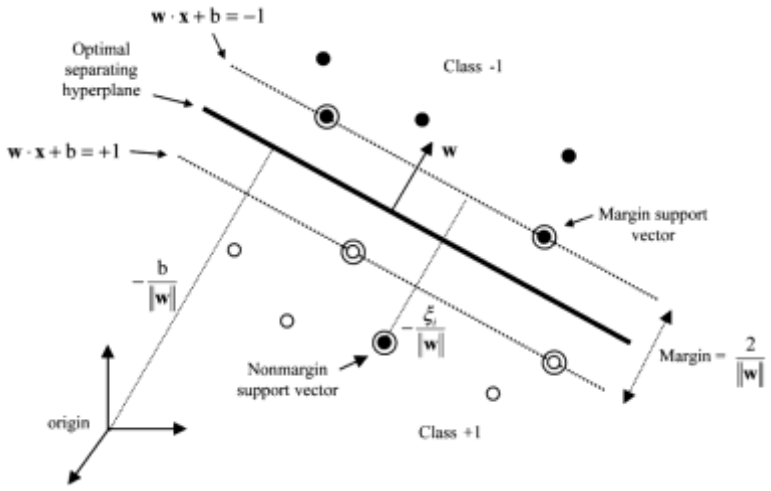

Figure 2 – Illustration of Support Vector Machine Architecture [21].

Hyperplane has the ability to maximize the distance or margin between data classes [22]. It is also possible to establish the optimal hyperplane among the classes by measuring the margin and later inference the maximum point. Meanwhile, the attempt to discover the optimum hyperplane as a class separator is the core objective of the SVM method [23].

Therefore, the main formula of SVM is

$$f(x) = w \cdot x + b \tag{1}$$

Equation (1) is for maximizing the margin using parameters w (weight) and b (biased) which leads to the further definition in equation (2) after which the general and smaller possible errors were produced.

$$\frac{|f(x)|}{||w||} \tag{2}$$

$$\max_{w,b.} \frac{|f(x)|}{||w||} \tag{3}$$

The margin of equation (3) was developed as shown in the following equation

$$\min \frac{1}{2}||w||^2 \tag{4}$$

$$s.t\ y_i(w \cdot x_i + b) \geq 1 \qquad i = 1,2, \dots, N \tag{5}$$

Equation (4) was later constructed as the main optimization of SVM and written as

$$\min(\frac{1}{2}||w||^2 + C\sum_{i=1}^{N} \xi_i) \tag{6}$$

$$s.t\ y_i(w \cdot x_i + b) \geq 1 - \xi_i \ \ i = 1,2, \dots, N \tag{7}$$

$$\xi_i \geq 0 \qquad i = 1,2, \dots, N \tag{8}$$

In equation (6), ξ_i and $C > 0$ are the parameters to minimize error classification and maximize the hyperplane using the smaller margin value.

The kernel function used for the Support Vector Machines (SVM) in this study is a Linear Kernel and it resolves the linear dimension problems and algorithms expression in the inner product between two vectors [24]. This linear kernel function and its parameter are presented as follows [24]:

$$K(x_i, x_j) = [\![x_i]\!]^T x_j \tag{9}$$

c. *Confusion Matrix*

The confusion matrix presented in Table 1 was used to calculate the accuracy [25].

Table 1. Confusion Matrix.

Actual	Prediction	
	Positive	Negative
Positive	T_p	F_P
Negative	F_N	T_N

The accuracy formula which was also used is shown in the following equation [25]:

$$accuracy = \frac{T_p + T_N}{T_P + T_N + F_P + F_N} \tag{10}$$

T_p: Number of samples having liver cancer and classified correctly.

F_P: Number of healthy individuals incorrectly classified with liver cancer.

F_N: Number of samples with liver cancer incorrectly classified as healthy.

T_N: Number of healthy individuals correctly spotted.

2. MAIN RESULTS

I. Data

The database of Liver Cancer patients in Dr. Cipto Mangunkusumo Hospital, Indonesia was obtained with 122 data comprising of 71 significant and 52 minor data. The class of people with liver cancer is the major and labeled '1' while those without liver cancer were minor and the class was labeled '0' as indicated in the dataset of Table 2.

Table 2. The Samples of Liver Cancer Dataset.

Area	Min	Max	Average	SD	Sum	Length	Target
474.93	35	124	70.67	13.49	62898	77.26	1
268.42	38	255	134.29	53.22	67011	58.15	1
314.84	40	227	118.14	37.83	68996	62.9	1
379.11	21	75	52.24	8.43	36258	69.08	0
595.06	22	113	60.75	14.22	52182	86.5	1
530.15	20	101	53.26	12.46	41436	82.09	0
532.99	26	106	54.98	10.4	43104	81.87	1
584.62	16	132	49.73	14.62	41772	85.72	1

Seven features were used in this study which are area, min, max, average, SD, sum, and length, and defined as shown in Table 3.

Table 3. The Features of Liver Cancer Dataset

No	Features of Dataset	Definition
1.	Area	The extent or measurement of an object or surface.
2.	Min	The least or smallest amount or quantity possible, attainable, or required.
3.	Max	The greatest or highest amount possible or attained.
4.	Average	A number expressing the central or typical value in a set of data.
5.	SD	A quantity calculated to indicate the extent of deviation for a group as a whole.
6.	SUM	The total amount from the addition of two or more numbers, amounts, or items.
7.	Length	The measurement or extent of something.

II. Results

This study made use of 10% to 90% as a classification method for the testing data while 100 epochs and 32 batches were used for the Neural Network–Support Vector Machine and the kernel function applied was Linear Kernel. Meanwhile, the results of the comparison made for each optimizer are shown in Table 4.

Table 4. The Accuracy of Each Method.

Testing Data	Accuracy of NN–SVM		
	Adam Optimizer	AdaGrad Optimizer	SGD Optimizer
10%	0.96153	0.99923	0.93846
20%	0.99000	0.98000	0.99000
30%	0.99162	0.96756	0.96756
40%	0.96102	0.99306	0.94061
50%	0.99016	0.96655	0.97377
60%	0.96810	0.96756	0.95405
70%	0.96813	0.98465	0.93488
80%	0.96122	0.96122	0.97142
90%	0.97272	0.99909	0.95454
Average	0.97383	0.97988	0.95836

The Neural Network–Support Vector Machine was compared with some optimizers for Liver Cancer classification and found to be correct and adequate in predicting data. The results further showed its combination with AdaGrad Optimizer had the best accuracy value with an average of 97.98% on the test data while its use with Adam Optimizer produced an average of 97.38% while SGD Optimizer had 95.83%. Therefore, the best optimizer for the Liver Cancer classification was found to be the Neural Network–Support Vector Machine with AdaGrad Optimizer.

CONCLUSION

The presence of the disease was predicted by diagnosing with a machine learning method in order to help medical staff classify the ailments. This is necessary because early detection of disease is essential based on the fact that it allows the patient to receive the immediate and right treatment, thereby, causing an increase in survival rate and reduction in the health risk. This research focuses on liver cancer which is a common health problem and was conducted using 122 data collected and 7 features observed. The method used as a classifier was the combination of Neural Network–Support Vector Machine with several optimizers such as Adam, AdaGrad, SGD optimizer, and experimental results showed the methods were able to predict the data correctly and adequately. The findings further showed the combination of Neural Network–Support Vector Machine with Adam Optimizer was the best model to classify the Liver Cancer dataset as shown in Table 4 with an average of 97.98% accuracy. Therefore, this method is expected to produce higher accuracy and be applicable in a more massive database to predict and classify different diseases in future studies.

ACKNOWLEDGMENT

This research was financially supported by The Indonesian Ministry of Research and Technology through the KEMENRISTEK/BRIM 2021 research grant scheme.

REFERENCES

1. R. Khairi, Z. Rustam, & S. Utama, 2019. Possibilistic C-Means (PCM) Algorithm for the Hepatocellular Carcinoma (HCC) Classification. *IOP Conference Series: Materials Science and Engineering.* Vol. 546, Issue 5. https://doi.org/10.1088/1757-899X/546/5/052038.
2. B. Losic, A. J. Craig, & C. Villacorta-Martin. (2020). Intratumoral heterogeneity and clonal evolution in liver cancer. *Nat Commun*. Vol. 11, pp. 291. https://doi.org/10.1038/s41467-019-14050-z.
3. M. Fujita. (2020). Classification of primary liver cancer with immunosuppression mechanisms and correlation with genomic alterations. *E BioMedicine*. Vol. 53, pp. 102659. https://doi.org/10.1016/j.ebiom.2020.102659.
4. Medium. [Internet]. [Accessed on 2020]. Available at https://medium.com/@magnusmediindia/know-all-about-liver-cancer-caa53777e99d.
5. WHO. [Internet]. [Accessed on 2020]. Available at https://www.who.int/hepatitis/news-events/world-cancer-day/en/#:~:text=WHO%20estimates%20that%20788%20000,primary%20liver%20cancer%20every%20year.&text=More%20than%20half%20of%20these,to%20chronic%20hepatitis%20C%20infection.
6. L. Guo, Z. Wang, & Y. Du. (2020). Random-forest algorithm based biomarkers in predicting prognosis in patients with hepatocellular carcinoma. *Cancer Cell Int*. Vol. 20, pp. 251. https://doi.org/10.1186/s12935-020-01274-z.
7. S. Naeem, A. Ali, S. Qadri, W. K. Mashwani, N. Tairan, H. Shah, M. Fayaz, F. Jamal, C. Chesneau, C, & S. Anam. (2020). Machine-Learning Based Hybrid-Feature Analysis for Liver Cancer Classification Using Fused (MR and CT) Images. *Appl. Sci*. Vol. 10, pp. 3134. https://doi.org/10.3390/app10093134.

8. M. Chen, B. Zhang, & W. Topatana. (2020). Classification and mutation prediction based on histopathology H&E images in liver cancer using deep learning. *npj Precis. Onc*. Vol. 4, No. 14. https://doi.org/10.1038/s41698-020-0120-3.
9. C. Anitescu, E. Atroshchenko, N. Alajlan, & T. Rabczuk. (2019). Artificial Neural Network Methods for The Solution of Second Order Boundary Value Problems. *Computers, Materials and Continua*. Vol. 59, No. 1, pp. 345-359.
10. A. M. Barhoom, A. J. Khalil, B. S. Abu-Nasser, M. M. Musleh, & S. S. A. Naser. (2019). Predicting Titanic Survivors using Artificial Neural Network. *International Journal of Academic Engineering Research (IJAER)*. Vol. 3, No. 9, pp. 8-12.
11. J. Chenhao, J. Shinae, S. Xiaorong, L. Jingcheng, & C. Richard. (2016). Damage detection of a highway bridge under severe temperature changes using extended Kalman filter trained neural network. *Journal of Civil Structural Health Monitoring*. Vol. 6, pp. 545-560. 10.1007/s13349-016-0173-8.
12. I. M. Nasser, M. Al-Shawwa, & S. S. Abu-Naser. (2019). Artificial Neural Network for Diagnose Autism Spectrum Disorder. *International Journal of Academic Information Systems Research (IJAISR)*. Vol. 3, No. 2, pp. 27-32.
13. I. M. Nasser, & S. S. Abu-Naser. (2019). Lung Cancer Detection using Artificial Neural Network. *International Journal of Engineering and Information Systems (IJEAIS)*. Vol. 3, No. 3, pp. 17-23.
14. B. Horvath, A. Muguruza, & M. Tomas. (2020). Deep learning volatility: a deep neural network perspective on pricing and calibration in (rough) volatility models. *Quantitative Finance*. https://doi.org/10.1080/14697688.2020.1817974.
15. X. Li, J. Tang, & Q. Zhang. (2020). Power-efficient neural network with artificial dendrites. *Nat. Nanotechnol*. Vol. 15, pp. 776–782. https://doi.org/10.1038/s41565-020-0722-5.
16. M. Hibat-Allah, M. Ganahl, L. E. Hayward, R. G. Melko, & J. Carrasquilla. (2020). Recurrent neural network wave functions. *Phys. Rev. Research*. Vol. 2, pp. 023358.
17. Z. Rustam, & N. P. A. A. Ariantari. (2018). Support Vector Machines for Classifying Policyholders Satisfactorily in Automobile Insurance. *J. Phys.: Conf. Ser*. Vol. 1028, pp. 012005.
18. Z. Rustam, & F. Yaurita. (2018). Insolvency Prediction in Insurance Companies using Support Vector Machines and Fuzzy Kernel C-Means. *J. Phys.: Conf. Ser*. Vol. 1028, pp. 012118.
19. J. Dou, A. P. Yunus, & D. T. Bui. (2020). Improved landslide assessment using support vector machine with bagging, boosting, and stacking ensemble machine learning framework in a mountainous watershed, Japan. *Landslides*. Vol. 17, pp. 641–658. https://doi.org/10.1007/s10346-019-01286-5.
20. Z. Rustam, & D. Zahras. (2018). Comparison between Support Vector Machine and Fuzzy C-Means as Classifier for Intrusion Detection System. *J. Phys.: Conf. Ser*. Vol. 1028, pp. 012227.
21. M. Farid, & B. Lorenzo. (2004). Classification of Hyperspectral Remote Sensing Images with Support Vector Machines. *Geoscience and Remote Sensing, IEEE Transactions*. Vol. 42, pp. 1778-1790. 10.1109/TGRS.2004.831865.
22. Z. Rustam, & R. Faradina. (2018). Face Recognition to Identify Look-Alike Faces using Support Vector Machine. *Journal of Physics: Conference Series*. Vol. 1108, Issue 1, pp. 012071.
23. T. Nadira, & Z. Rustam. (2018). Classification of cancer data using support vector machines with features selection method based on global artificial bee colony. *AIP Conference Proceedings*. Vol. 2023, pp. 020205.
24. Z. Rustam, & A. S. Talita. (2017). Fuzzy Kernel k-Medoids algorithm for anomaly detection problems. *AIP Conference Proceedings*. Vol. 1862, pp. 030154.
25. Z. Rustam, D. A. Utami, R. Hidayat, J. Pandelaki, & W. A. Nugroho. (2019). Hybrid Preprocessing Method for Support Vector Machine for Classification of Imbalanced Cerebral Infarction Datasets. *International Journal on Advanced Science Engineering Information Technology*. Vol. 9, No. 2.

Comparison of several Kernel Functions on Neural Network–Support Vector Machine as Classifier for Lung Cancer

Jane Eva AURELIA[1] and Zuherman RUSTAM[1]

[1]*Department of Mathematics, Faculty of Mathematics and Natural Sciences, University of Indonesia*

janeevaaurelia@gmail.com

Abstract. Lung cancer is one of the three most common types of cancer in Indonesia and is observed to be delineated by unbridled cell accretion in the lung tissue. The disease has been associated with several causes ranging from diets high in fat, pollution, and genetics with the indicators observed not to be perceptible at the early stages but easily detected with different machine learning methods such as the Neural Network (NN). This method is popular and has a wide range of applications due to its high accuracy. Moreover, the architecture and computation processes are inspired by knowledge of nerve cells in the brain. A Support Vector Machine (SVM) with several kernel functions is commonly used in the classification of diseases due to its high accuracy value as observed in more maturity in producing exact mathematical concepts in comparison with other classification techniques. The data used in this study were the Lung Cancer sufferers' database retrieved from Dr. Cipto Mangunkusumo Hospital, Indonesia, and consisted of 138 data which are 69 primary and 69 minor data. The combination of NN–SVM with several kernel functions as a classifier for the lung cancer dataset was compared and the results showed the Neural Network–Support Vector Machine with Gaussian RBF Kernel is the best model to classify Lung Cancer with an average accuracy of 97.94%. This method is, however, expected to be developed in future studies to produce higher accuracy and apply a more massive database to provide better results to predict and classify different diseases.

1. INTRODUCTION

III. Lung Cancer

Lung cancer is a condition delineated by unbridled cell accretion in the lung tissue [1] and has been observed to be one of the three most common types of cancer in Indonesia. Several factors have been associated with the cause of lung cancer and these include diets high in fat, pollution, and genetics. However, the highly prevalent causative factor was reported to be smoking which was found to be at 80-90%, especially for sufferers at a young age [1]. This is associated with the aggressiveness of this disease for younger people as observed in the spread of the cell growth more rapidly to the bones, brain, glands, kidneys, and liver. Moreover, observations have also shown that people living with lung cancer at a young age only has the ability to survive for four months after being diagnosed.

A specimen of 10 to 15% non-smokers was suspected to have lung cancer and this was found to be due to a coalition of genetic elements, asbestos, gas radon, and air [2]. These cell growths have the ability to disperse outside the lungs by resolving metastasis to imminent tissues or other parts of the body when they are not treated. Moreover, the type of cancers which start from the lungs and known as primary lung cancers include carcinomas which originate from the epithelial cells. Some other significant types include SCLC or Small Cell Lung Cancer and NSCLC or Non–Small Cell Lung Cancer [3] while the most generic indicators of the disease include coughing, short breath, and weight loss.

It is possible to detect lung cancer through CT scan and Chest X–rays while the diagnosis is confirmed using biopsy which is usually conducted via bronchoscopy procedure or guided CT. Meanwhile, the long-term treatment and outcomes depend on the type of cancer, the patient's overall health, stage as well as the general condition, and the treatment usually includes surgery, radiotherapy, and chemotherapy. NSCLC is usually medicated surgically while SCLC generally responds better to chemotherapy and radiotherapy [3]. It has, however, been reported that 15% of the population identified with this cancer generally achieved a five-year life hopefulness after diagnosis [4]. Lung

cancer has been discovered to be the global leading cause of deaths related to cancer in men and women with 1.38 million deaths annually up to 2008 [5].

It is important to note that classification is a learning process used in data labeling and lung cancer has been classified in previous studies using several methods such as Artificial Neural Network [6], K–Nearest Neighbor [7], and Deep Learning [8]. The model is usually built to train, test, and study old class categories in order to determine the formation of new classes. Furthermore, a combined method of machine learning model was proposed known as the Neural Network–Support Vector Machine to classify data required to predict the class of lung cancer patients.

IV. Methodology

A Neural Network–Support Vector Machine was used in this study to classify the lung cancer dataset while another optimization algorithm like Neural Network–Support Vector Machine combined with several kernel functions such as Linear, Polynomial, and Gaussian Radial Basis Function (RBF) kernel was also adopted and compared with the designed model. The classification methods adopted are, therefore, explained in the following sub-sections.

d. *Neural Network*

Artificial Neural Network or Neural Network is a computation system where architecture and computation are inspired by knowledge of nerve cells in the brain [9]. It is a model which mimics biological neural networks' workings with each neuron in the human brain interconnected and the stream is explained. The input with weight is received by each of the neurons after which a dot operation is conducted and weighted sum and bias added. Moreover, the neural network has the ability to produce a consistent response to the input sequence through the learning process [10]. Meanwhile, there is a possibility for the input path of a neuron to contain raw data or data from previously processed neurons while the output can be the final product or the input material for the next neutron. The results of this operation are usually used as a parameter for the activation function which serves as the output of the neuron [10]. The Neural Network architecture is, however, illustrated in the following Figure 1 [11].

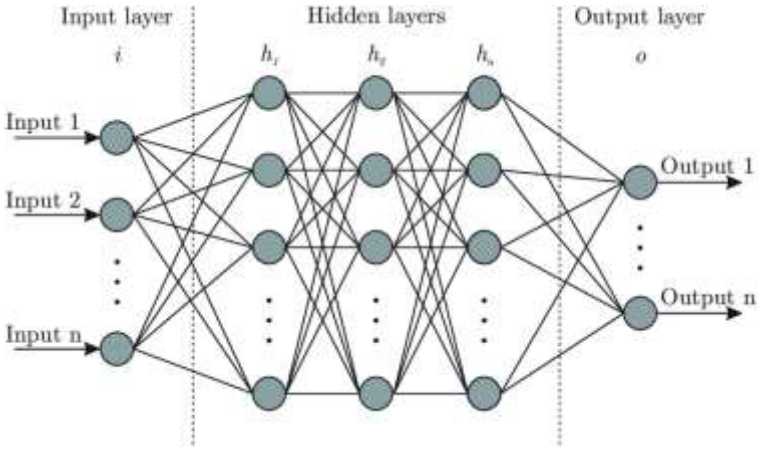

Figure 1 – Illustration of Neural Network Architecture [11].

The architecture presented in Figure 1 is commonly referred to as the Multilayer Perceptron (MLP) or Fully-Connected Layer with the first having three neurons on the Input Layer and two nodes on the Output Layer. The neuron network generally consists of a collection of neuron groups arranged in layers as follows [12]:

1) The Input Layer function is a network link to the data source which only passes this data on to the next layer without performing any operation it.
2) The Hidden Layer is a network with the ability to have more than one hidden layer or even none and the lowest hidden layer receives input from the input layer in the cases of multiple hidden layers.
3) The Output Layer is the working principle on this layer which has the same active principle as observed in the hidden layer and the output is already considered from the output process.

Meanwhile, the Weight and Activation Function specifications are as follows [13]:

1) The Weight in each neuron of the MLP was interconnected as indicated by an arrow. This means weight associated with each connection and the values were later observed to be different. It is important to note that the bias is the hidden layers and an additional input for the output layers.

2) The Activation Function was used to determine the activeness of the neuron based on the input weighted sum. There are, however, two general types of activation functions which are the Linear and Non–Linear.

For example, there is a neural network $f_\theta: X \to Y$, where θ is a parameter set later based on the data being studied and consists of weights and bias [14].

A supervised learning condition, f_θ, which teaches from the data pairs (x, y) and defines the loss function $l: Y \times Y \to R$ was also assumed. Meanwhile, one form of the loss function for $Y \subseteq R$ is the least-square error

$$L(f_\theta(x), y) = (f_\theta(x) - y)^2 \quad (1)$$

$L(\theta) := L(f_\theta(x), y)$ was written to simplify the notation of equation (1) and the optimization in deep learning has been reported to have the aim of narrowing the loss function $\min_\theta L(\theta)$ [14].

Therefore, the gradient of the loss function concerning θ was defined with the notation $\nabla_\theta L(\theta)$.

e. *Support Vector Machine*

Support Vector Machine (SVM) is a supervised learning method which is usually used for classification and regression [15]. It is observed to have a more mature and explicit mathematical concept in classification modeling compared to other techniques and also has the ability to solve both linear and non-linear classification and regression problems. Furthermore, SVM is used to determine the best hyperplane by maximizing the distance between classes [16] and this concept has been discovered to be a function applicable to the separation of classes [16]. The SVM architecture is, however, illustrated in Figure 2 [17].

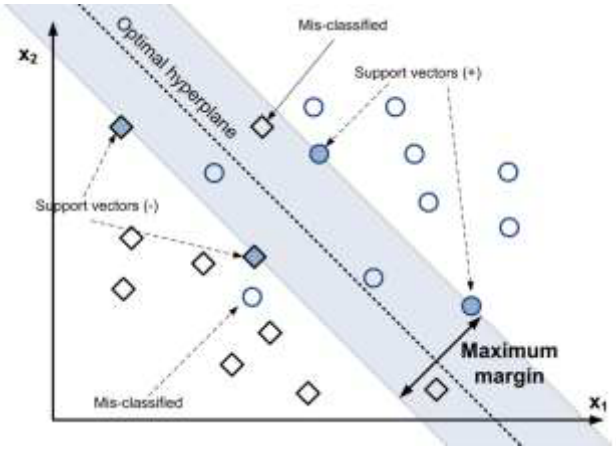

Figure 2 – Illustration of Support Vector Machine Architecture [17].

The position of the SVM is between the two classes and this means the distance between the hyperplane and data objects is different from the adjacent class marked with an empty and positive round [18]. Moreover, the outer data object close to the hyperplane in the SVM is named a support vector which is the most inconvenient class to categorize due to its practical overlap with other classes. Therefore, only the support vector was considered to have passed through SVM's most prime hyperplane due to its serious nature [19].

The main purpose of SVM was to determine the best hyperplane as shown in the following relationship.

$$w \cdot x + b = 0 \quad (2)$$

The optimization problem of SVM was further summarized as

$$min\ \frac{1}{2}||w||^2 \quad (3)$$

$$s.t\ y_i(\boldsymbol{w}^T \cdot x_i + b) \geq 1, \forall i = 1, \dots, N \tag{4}$$

The objective of equation (3) was to determine $\boldsymbol{w} \in R^n$ and $b \in R^n$ which is subject to equation (4) after which the formulas of $\boldsymbol{w}$ (weights) and b (bias) were obtained as follows after the previous problem has been solved.

$$\boldsymbol{w} = \sum_{i=1}^{N} a_i y_i x_i \tag{5}$$

$$b = \frac{1}{N_s} \sum_{i \in S} (y_i - \sum_{m \in S} a_m y_m x_m) \tag{6}$$

$$f(x) = w \cdot x + b \tag{7}$$

The decision function in equation (7) was, however, to maximize the margins.

In general, the data problem cannot be separated linearly in the input space while the SVM soft margin was unable to determine the separator in the hyperplane and this means it was unable to provide great accuracy and effective generalization [20]. Therefore, a kernel is needed to modify the data into a higher-dimensional space called the kernel space which is useful for the linear separation of data [21]. It is important to note that these kernel functions are generally Linear, Polynomial, and Gaussian Radial Basis Function (RBF) [22] with some of them illustrated in the following Figure 3 [23].

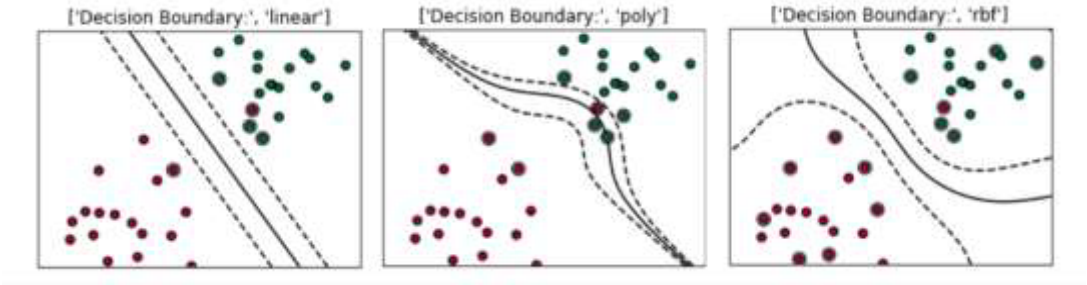

Figure 3 – Illustration of Several Kernel Functions [23].

A kernel function was, therefore, used in the Support Vector Machines (SVM) to be compared in this study and this is due to its ability to resolve linear dimension problems and algorithms expression in the inner product between two vectors [24]. Several kernel functions are, however, listed with their parameters in Table 1 [24].

Table 1. Kernel Function.

Name	Kernel Function
Linear	$K(x_i, x_j) = [\![x_i]\!]^T x_j$
Polynomial	$K(x_i, x_j) = [\![(t + [\![x_i]\!]^T x_j)]\!]^d$
Gaussian Radial Basis Function (RBF)	$K(x_i, x_j) = \exp(-\|x_i - x_j\|^2 / \sigma^2)$

f. *Confusion Matrix*

A confusion matrix was used to calculate the accuracy using the parameters presented in Table 2 and the formula written in Equation 8 [25].

Table 2. Confusion Matrix.

Actual	Prediction	
	Positive	Negative
Positive	T_p	F_P

Negative	F_N	T_N

$$accuracy = \frac{T_p+T_N}{T_P+T_N+F_P+F_N} \quad (8)$$

T_p: Number of samples having lung cancer and classified correctly.

F_P: Number of healthy individuals incorrectly classified to have lung cancer.

F_N: Number of samples with lung cancer incorrectly classified as healthy.

T_N: Number of healthy individuals correctly spotted.

2. MAIN RESULTS

III. Data

The Lung Cancer sufferers' database used in this study was collected from Dr. Cipto Mangunkusumo Hospital, Indonesia, and was found to have 38 data consisting of 69 primary and 69 minor data. The classes indicating the presence of lung cancer were classified as major and labeled '1' while those without lung cancer were noted as minor and labeled '0' as indicated in the lung cancer dataset of Table 3.

Table 3. The Samples of Lung Cancer Dataset.

Area	Min	Max	Average	SD	Sum	Length	Target
106.53	-926	-773	-863	29.5	-156324	36.6	0
76.07	-924	-755	-850	29.02	-121557	31.01	0
109.76	-42	88	28.45	24.68	5576	37.17	1
135.93	-917	-683	-875	41.11	-284527	41.34	0
97.55	-12	65	32.59	14.05	7562	35.01	1
103.04	-14	66	36.39	15.22	9025	35.98	1
106.07	-869	604	-762	40.48	-162501	36.51	0
129.01	-858	-418	-746	75.5	-194800	40.27	0

Seven features were used in this research and they include area, min, max, average, SD, sum, and length with their respective definitions presented in the following Table 4.

Table 4. The Features of Lung Cancer Dataset.

No	Features of Dataset	Definition
1.	Area	The extent or measurement of an object or surface.
2.	Min	The least or smallest amount or quantity possible, attainable, or required.
3.	Max	A maximum amount of setting reach or cause to reach the limit of capacity or ability.
4.	Average	A number expressing the central or constituting the result obtained.
5.	SD	A quantity calculated to indicate the extent of deviation for a group as a whole.
6.	SUM	The total result from adding two or more numbers, items, or amounts.
7.	Length	The measurement of the extent of a particular thing.

IV. Results

This research used 10% to 90% as the classification method to test the data while 1000 epochs and 32 batches were used for the combination of the Neural Network with Adam Optimizer. Meanwhile, several kernel functions combined with the Neural Network–Support Vector Machine are compared in Table 5.

Table 5. The Accuracy of Each Method.

Testing Data	Accuracy of NN–SVM		
	Linear Kernel	Polynomial Kernel	Gaussian RBF Kernel
10%	0.92857	0.92857	1.0
20%	0.96428	0.96428	0.92857
30%	0.95238	1.0	0.95238
40%	1.0	0.98214	0.98214
50%	1.0	0.97826	1.0
60%	0.98795	0.98192	0.98795
70%	0.97938	1.0	0.98969
80%	0.99099	0.95490	0.98198
90%	0.98400	0.98400	0.99200
Average	0.97639	0.97489	0.97941

The Neural Network–Support Vector Machine compared with some kernels for Lung Cancer classification was found to have the ability to predict data correctly and adequately and each method is shown in the table to have the highest accuracy of 100% on several test data. For the Neural Network–Support Vector Machine with Linear Kernel, the highest accuracy of 100% was on 40% to 50%, the combination with Polynomial Kernel was on 30% and 70% while Gaussian RBF Kernel was on 10% and 50%. Moreover, NN–SVM with Gaussian RBF Kernel was also found to have the best accuracy value with an average of 97.94% on the test data. Therefore, the best method for Lung Cancer classification is the Neural Network–Support Vector Machine with Gaussian RBF Kernel.

CONCLUSION

The early detection of diseases using machine learning is important in treating patients to extend their life span, reduce the risk, and help medical staff in classifying the disease. This study was focused on lung cancer which is a common health problem in Indonesia and the world and the research was conducted using 138 data and 7 features as well as the combination of Neural Network–Support Vector Machine with several kernel functions such as Linear, Polynomial, and Gaussian RBF kernel as a classifier. The experimental results showed the methods used were able to predict the data correctly and adequately but the Neural Network–Support Vector Machine with Gaussian RBF Kernel was found to be the best model for the Lung Cancer dataset classification with an average of 97.94% accuracy as shown in Table 5. This method is, however, expected to be further developed in future research to provide higher accuracy and use a more massive database to have better results in predicting and classifying different diseases.

ACKNOWLEDGMENT

This research was financially supported by The Indonesian Ministry of Research and Technology under the KEMENRISTEK/BRIM 2021 research grant scheme.

REFERENCES

1. Z. Rustam, S. Hartini, R. Y. Pratama, R. E. Yunus, & R. Hidayat. (2020). Analysis of architecture combining Convolutional Neural Network (CNN) and kernel K-means clustering for lung cancer diagnosis. *International Journal on Advanced Science, Engineering and Information Technology*. Vol. 10, No. 3, pp. 1200-1206. https://doi.org/10.18517/ijaseit.10.3.12113.
2. A. Khanmohammadi, A. Aghaie, E. Vahedi, A. Qazvini, M. Ghanei, A. Afkhami, A. Hajian, & H. Bagheri. (2020). Electrochemical biosensors for the detection of lung cancer biomarkers: A review. *Talanta*. Vol. 206, pp. 120251. https://doi.org/10.1016/j.talanta.2019.120251.
3. I. Bonavita, X. Rafael-Palou, M. Ceresa, G. Piella, V. Ribasa, & M. A. G. Ballester. (2020). Integration of convolutional neural networks for pulmonary nodule malignancy assessment in a lung cancer classification pipeline. *Computer Methods and Programs in Biomedicine*. Vol. 185, pp. 105172. https://doi.org/10.1016/j.cmpb.2019.105172

4. Medium. [Internet]. [Accessed on 2020]. Available at https://medium.com/good-advice-publishing/worth-the-fight-taking-on-lung-cancer-701cc9fe8940.
5. WHO. [Internet]. [Accessed on 2020]. Available at https://www.who.int/tobacco/healthwarningsdatabase /tobacco_large_canada_lung_07_en/en/.
6. I. M. Nasser, & S. S. Abu-Naser. (2019). Lung Cancer Detection Using Artificial Neural Network. *International Journal of Engineering and Information Systems (IJEAIS)*. Vol. 3, No. 3, pp. 17-23. https://ssrn.com/abstract=3369062.
7. C. Wang, Y. Long, & W. Li. (2020). Exploratory study on classification of lung cancer subtypes through a combined K-nearest neighbor classifier in breathomics. *Sci Rep*. Vol. 10, pp. 5880. https://doi.org/10.1038/s41598-020-62803-4.
8. M. Kriegsmann. (2020). Deep Learning for the Classification of Small-Cell and Non-Small-Cell Lung Cancer. *Cancers*. Vol. 12, No. 6, pp. 1604.
9. C. Anitescu, E. Atroshchenko, N. Alajlan, & T. Rabczuk. (2019). Artificial Neural Network Methods for The Solution of Second Order Boundary Value Problems. *Computers, Materials and Continua*. Vol. 59, No. 1, pp. 345-359.
10. A. M. Barhoom, A. J. Khalil, B. S. Abu-Nasser, M. M. Musleh, & S. S. A. Naser. (2019). Predicting Titanic Survivors using Artificial Neural Network. *International Journal of Academic Engineering Research (IJAER)*. Vol. 3, No. 9, pp. 8-12.
11. B. Facundo, G. Juan, & F. Víctor. (2017). Prediction of wind pressure coefficients on building surfaces using Artificial Neural Networks. *Energy and Buildings*. Vol. 158, No. 10, pp. 1016. j.enbuild.2017.11.045.
12. I. M. Nasser, M. Al-Shawwa, & S. S. Abu-Naser. (2019). Artificial Neural Network for Diagnose Autism Spectrum Disorder. *International Journal of Academic Information Systems Research (IJAISR)*. Vol. 3, No. 2, pp. 27-32.
13. I. M. Nasser, & S. S. Abu-Naser. (2019). Lung Cancer Detection using Artificial Neural Network. *International Journal of Engineering and Information Systems (IJEAIS)*. Vol. 3, No. 3, pp. 17-23.
14. M. Hibat-Allah, M. Ganahl, L. E. Hayward, R. G. Melko, & J. Carrasquilla. (2020). Recurrent neural network wave functions. *Phys. Rev. Research*. Vol. 2, pp. 023358.
15. Z. Rustam, & N. P. A. A. Ariantari. (2018). Support Vector Machines for Classifying Policyholders Satisfactorily in Automobile Insurance. *J. Phys.: Conf. Ser.* Vol. 1028, pp. 012005.
16. Z. Rustam, & F. Yaurita. (2018). Insolvency Prediction in Insurance Companies using Support Vector Machines and Fuzzy Kernel C-Means. *J. Phys.: Conf. Ser.* Vol. 1028, pp. 012118.
17. N. D. Huy, K. Innocent, D. Louis-A, & H. Cao-Duc. (2017). A Novel Approach for Early Detection of Impending Voltage Collapse Events Based on the Support Vector Machine. *International Transactions on Electrical Energy Systems*. Vol. 10, pp. 1002. etep.2375.
18. Z. Rustam, & D. Zahras. (2018). Comparison between Support Vector Machine and Fuzzy C-Means as Classifier for Intrusion Detection System. *J. Phys.: Conf. Ser.* Vol. 1028, pp. 012227.
19. Z. Rustam, & R. Faradina. (2018). Face Recognition to Identify Look-Alike Faces using Support Vector Machine. *Journal of Physics: Conference Series.* Vol. 1108, Issue 1, pp. 012071.
20. Z. Rustam, & A. A. Ruvita. (2018). Application Support Vector Machine on Face Recognition for Gender Classification. *Journal of Physics: Conference Serie.* Vol. 1108, Issue 1, pp. 012067.
21. T. V. Rampisela, & Z. Rustam. (2018). Classification of Schizophrenia Data Using Support Vector Machine (SVM). *Journal of Physics: Conference Series*. Vol. 1108, Issue 1, pp. 012044.
22. T. Nadira, & Z. Rustam. (2018). Classification of cancer data using support vector machines with features selection method based on global artificial bee colony. *AIP Conference Proceedings.* Vol. 2023, pp. 020205.
23. Towards Data Science. [Internet]. [Accessed on 2020]. Available at https://towardsdatascience.com/support-vector-machine-simply-explained-fee28eba5496.
24. Z. Rustam, & A. S. Talita. (2017). Fuzzy Kernel k-Medoids algorithm for anomaly detection problems. *AIP Conference Proceedings*. Vol. 1862, pp. 030154.
25. Z. Rustam, D. A. Utami, R. Hidayat, J. Pandelaki, & W. A. Nugroho. (2019). Hybrid Preprocessing Method for Support Vector Machine for Classification of Imbalanced Cerebral Infarction Datasets. *International Journal on Advanced Science Engineering Information Technology*. Vol. 9, No. 2.

Generative Adversarial Network for Market Hourly Discrimination

Luca GRILLI[1] and Domenico SANTORO[2]

[1]*Department of Economics, Management and Territory, Università degli Studi di Foggia, Foggia-ITALIA*
[2]*Department of Economics and Finance, Università degli Studi di Bari, Bari-ITALIA*

luca.grilli@unifg.it

Abstract. In this paper, we consider 2 types of instruments traded on the markets, stocks and cryptocurrencies. In particular, stocks are traded in a market subject to opening hours, while cryptocurrencies are traded in a 24-hour market. What we want to demonstrate through the use of a particular type of generative neural network (GAN) is that the instruments of the non-timetable market have a different amount of information, and are therefore more suitable for forecasting. In particular, through the use of real data we will also show that there are stocks following same rules as cryptocurrencies.

1. INTRODUCTION

The time series analysis has always attracted the attention of the academic world, in particular by focusing on predicting the future values of these series. Financial time series are optimal candidates for such an analysis. These series base their assumptions on the *random walk hypothesis*, a concept introduced by Bachelier [1] in 1900 and since then remained a central pivot in the theory of time series. Based on the random walk theory, Kendall [2] assumed that the movement of stock prices was random while Cootner [3] defined how the movement of stock prices could not be explained in detail but was better approximated by the Brownian motion. Traditionally the best practice was to focus on logarithmic returns, bringing the advantage of linking statistical analysis with financial theory. It was Taylor [4] who proposed an alternative model to the *random walk*, developing a price trend model: he gave much empirical evidence that the price trend model was useful in analyzing prices on futures markets. From an econometric point of view, Box et al. [5] introduced power transformations to statistical models, also applying them to time series; in particular, they suggested to use a power transformation in order to obtain an adequate *Autoregressive Moving Average* model (ARMA). On this basis, Hamilton [6] gave a formal (mathematically) definition of this model. Several evolutions followed this pattern, like that *Autoregressive Integrate Moving Average* (ARIMA) and *Seasonal Autoregressive Integrated Moving Average* (SARIMA).

Recently, thanks to the development of *artificial neural networks* (ANNs) and their ability to non-linear modeling [7], there has been a strong interest in the application of these methods to time series prediction. Foster et al. [8] were among the first to compare the use of neural networks as function approximators with the use of the same networks to optimally combine the classically used regression methods, highlighting how the use of networks to combine forecasting techniques have led to performance improvements.

The development of the financial time series forecasting has intensified mainly thanks to the new techniques [9] of *Machine Learning* (ML) and *Deep Learning* (DL). As for ML techniques, Kovalerchuk et al. [10] have used models such as *Evolutionary Computations* (ECs) and *Genetic Programming* (GCs); Li et al. [11] have developed a model for forecasting the stock price via ANN; Mittermayer et al. [12] compared different text mining techniques for extracting market response to improve prediction and Mitra et al. [13] have focused their attention on studying the news for predicting anomalous returns in trading strategies. As for the DL techniques, especially in the last 10 years, increasingly complex architectures are being used such as Liu et al. [14] who use a CNN + LSTM for strategic analysis in financial markets, Zhang et al. [15] who use an SFM to predict stock prices by extracting different types of patterns, Long et al. [16] who propose a Multi-Filters Neural Network for feature extraction on financial time series and extreme market prediction or Wan et al [17] who use a variant of LSTM to forecast correlated time series. However, many other types of more complex networks can be readjusted to time series to make predictions, such as GAN networks used for speech synthesis [18], for the denoising of images [19] or, as shown by Xu et al. [20], to predict leakage of pipeline in petrochemical system. Again, other types of combinations

of architectures are represented by DCNN *(Deep Convolutional Neural Network)* and CRF *(Conditional Random Field)* networks, as proposed by Papandreou et al. [21] for high-resolution segmentation and a DRDL *(Deep Relative Distance Learning)* network as proposed by Liu et al. [22] to calculate the distance between vehicles through graphical analysis by translating them into a Euclidean space.

In this paper, we want to forecast problem-related to financial market hours. Many of the stock markets are subject to certain opening and closing times. In these types of markets when news spreads or events occur outside closing hours, price reactions will only appear after the new opening of the market. The cryptocurrency market (and currencies in general), however, is not subject to closing times: it is open 24 hours a day. In this type of market the "opening" price of the new day and the "closing" price of the previous day are recorded in a midnight interval every day, creating continuity in the historical price series; for this reason the recorded prices are the sum of the events relating to 24 hours and therefore containing more information useful for forecasting. Our goal is to verify through an appropriate neural network how this difference of *"information in prices"* can lead to imbalances in the forecast, in particular linked to the discriminative and the predictive power of the prices themselves. Some studies, such as that of Tang [23] and Gorr [24] have shown that neural networks are capable of modeling seasonality and other factors such as trend and cyclicity autonomously, therefore the different *"quantity of information"* contained in the various types of prices would seem to be the only cause that leads to forecast imbalances.

2. GAN AND TIMEGAN

One of the main problems in time series forecasting is the choice of the optimal variables to be taken into consideration so that the neural network is able to capture their links and dynamics over time. There are many types of neural network architectures that can be used, however to overcome this problem we consider the generative adversarial network (GAN) introduced in 2014 by Goodfellow et al. [25]. The GAN model consists of 2 networks: a generative network *G* that produces new data based on a certain distribution p_g and a discriminative network *D* that evaluates them, producing the probability that $x \sim p_{data}$ where p_{data} is the distribution of training data. The networks objective is to encourage *D* to find the binary classifier that provides the best possible discrimination between real and generated data and simultaneously to encourage *G* to fit the true data distribution. *D* and *G* play the following two-player minimax game [48] with value function $V(G, D)$:

$$\min_G \max_D V(D,G) = \mathsf{E}_{x\sim p_{data}(x)}[\log D(x)] + \mathsf{E}_{z\sim p_z(z)}[\log(1 - D(G(z)))] \qquad (1)$$

In particular, Yoon et al. [26] propose a new model, the *Time-series Generative Adversarial Networks* (TimeGAN) for generating realistic time-series data in various domains. Considers both unsupervised adversarial loss and stepwise supervised loss and it uses original data as supervision. According to the authors, this type of GAN is made up of 4 networks [26]: embedding function, recovery function, sequence generator, and sequence discriminator. The autoencoding components are trained jointly with the adversarial components such that TimeGAN simultaneously learns to encode features, generate representations, and it iterates across time. Usually, GAN networks are used (regarding financial time series) for the generation and therefore the replacement of any missing values (NaN), while in this case their main objective is to recreate a time series based on the features used as input.

In this model, the generator is exposed to 2 types of inputs during training: the synthetic embeddings in order to generate the next synthetic vector and the sequences of embeddings of actual data to generate the next latent vector. In the first case, the gradient is computed on the unsupervised loss, while in the second, the gradient is computed on the supervised loss.

3. METHODOLOGY

To highlight generated results, Yoon et al. [26] have introduced a graphical measure for visualization, the t-SNE [27] (so as to visualize how much the generated distribution looks like the original one) and 2 scores (by optimizing a 2-layer LSTM):

- *Discriminative score*, it measures the error of a standardized classifier (RNN) in distinguishing between the real sequence and the one generated on the test set;

- *Predictive score*, represents the MAE *(Mean Absolute Error)* and measures the ability of synthetic data to predict next-step temporal vectors over each input sequence.

In addition, the t-SNE algorithm also returns the Kullback-Leibler Divergence (KL Divergence), which is a measure of the difference between two probability distributions which indicates the information lost when using a distribution (in this case the synthetic one) to approximate it an- other (the original one).

What we want to demonstrate by using this network is that instruments listed on a market subject to time constraints have a lower discriminative and predictive capacity than instruments present in markets not subject to the same constraints. Financial instruments subject to timetables during the continuous trading phase are representative of the information present in those hours, while what occurs after closing cannot be captured by the price and will be recorded at least the following day during the opening auction, which will lead to the price going up or down. On the other hand, for instruments not subject to schedules, this problem does not arise since any type of event that may have an effect on the price (whether it takes place day or night) will be recorded with an increase or a decrease in the price itself. The exchanges give the possibility to carry out negotiations outside the closing hours *(Trading in Pre Market and After Hours)* as in the case of Borsa Italiana in which the Pre Auction phase is possible from 8:00 to 9:00 a.m. while After Hours trading is possible from 17:50 to 20:30 and NASDAQ where the Pre Market trading is possible from 4:00 to 9:30 a.m. (ET) while After Hours trading is possible from 4:00 to 8:00 p.m. (ET), but certain time slots (which could be key) remain uncovered. In this way, the *"amount of information"* contained in each price is therefore an essential element for time series forecasting. The generative adversarial network is used, in this case, to generate synthetic data on the basis of those used as input (in such a way that the network itself understand the links that exist between the data). This network has been optimal to identify which are the best variables (features) to use in order to make forecasting by observing the improvements/worsening of the predictive score and by replacing the different features in the data sets. This network can therefore be understood as a tool to validate financial instruments and variables on which to subsequently make predictions through any tool, so as to obtain the best result. In particular, since many of the tools used to make predictions originate in econometrics, this type of network can be used to "screen" financial instruments in such a way as to improve the accuracy of classical econometric tools.

The empirical analysis was carried out on 2 types of instruments, stocks and cryptocurrencies. Specifically these are

- Stocks (Source: finance.yahoo.com):
  1. AAPL (Apple Inc.), listed on NASDAQ;
  2. GOOG (Alphabet Inc., Google), listed on NASDAQ;
  3. AMZN (Amazon.com), listed on NASDAQ;
  4. TSLA (Tesla Inc.), listed on NASDAQ.
- Cryptocurrencies (all related to USD, Source: investing.com):
  1. BTC (Bitcoin Index);
  2. ETH (Ethereum Index);
  3. BCH (Bitcoin Cash Index).

Prices are considered with a daily time frame, from 20/12/2017 to 31/12/2019. To test the discriminative and predictive ability of prices, the different datasets were divided into 2 types, the first with 5 features such as Open, High, Low, Close (Last in the case of cryptocurrencies) and Volume (generally indicated with the acronym OHLCV) while the second with only 2 features such as Open and Close/Last (indicated with the acronym OC). As for the hyperparameters for setting the TimeGAN, the sequence length of time series data ($seq - len$) has been set to 24 to represent approximately one month, the module used (the cell) is *LSTM*, the iterations were set to 30000 with a batch size of 128. The number of layer (num_layer) was set to 3 for all datasets while the number of neurons (hidden_dim) is 20 for OHLCV dataset and 8 for OC. Training and Test were carried out through Google Colab.

4 NUMERICAL ANALYSIS

In this section, we will compare first from the graphical point of view and then through the scores the capabilities of the different time series in terms of a difference in the amount of information. This comparison is made especially by comparing the OHLCV datasets with the OC datasets for the different instruments, so as to be able to test the basic idea. The graphical analysis will be carried out by comparing the t-SNE plots, while the one based on the score will be carried out by comparing the KL divergence, the discriminative score and the predictive score. The graphical

analysis is based on the t-SNE algorithm, in order to represent a higher dimensional space in a two-dimensional scatter plot and to realize the adhesion between the generated and synthetic data. The first t-SNE analysis concerns the OHLCV dataset, as shown in figure 1.

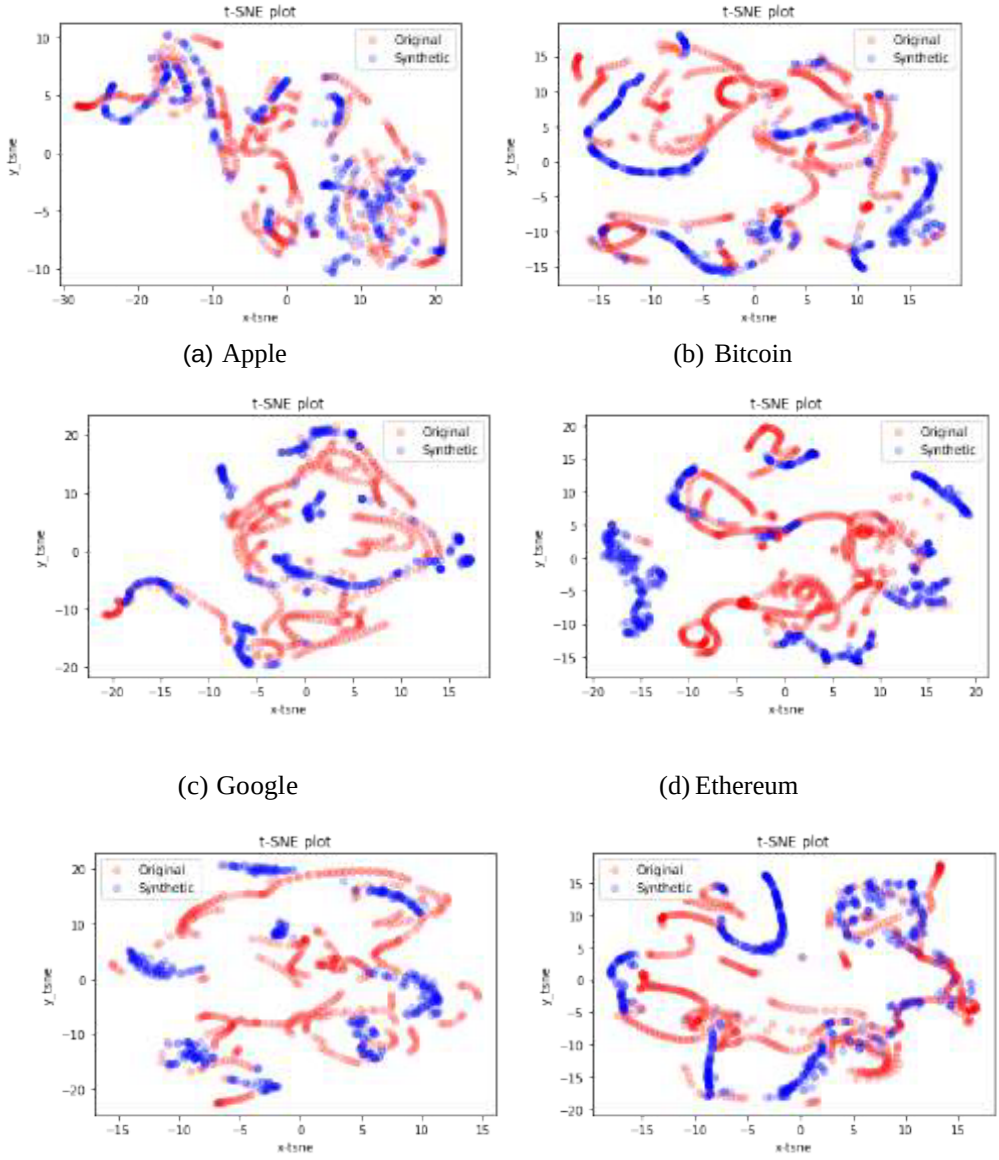

(a) Apple (b) Bitcoin

(c) Google (d) Ethereum

(e) Amazon (f) Bitcoin Cash

Figure 1: t-SNE analysis of synthetic data (blue) and original data (red) dataset OHLCV

From this analysis it is possible to highlight the potential of TimeGAN in the generation of data and in particular in the cases represented in the Figures 5(b) and 5(f) (both cryptocurrencies) there is a very precise adherence of the synthetic data to the original real data. Obviously, in this type of data set there is the presence of greater features that combined together allow the network to improve the forecast. From the graphical analysis it is possible to see how in the case of cryptocurrencies 5(b), (d), (f), the synthetic data extend over a greater surface than the original ones compared to the stocks (in which case they are much more concentrated). The second t-SNE analysis is based precisely on the OC dataset, as shown in Figure 2.

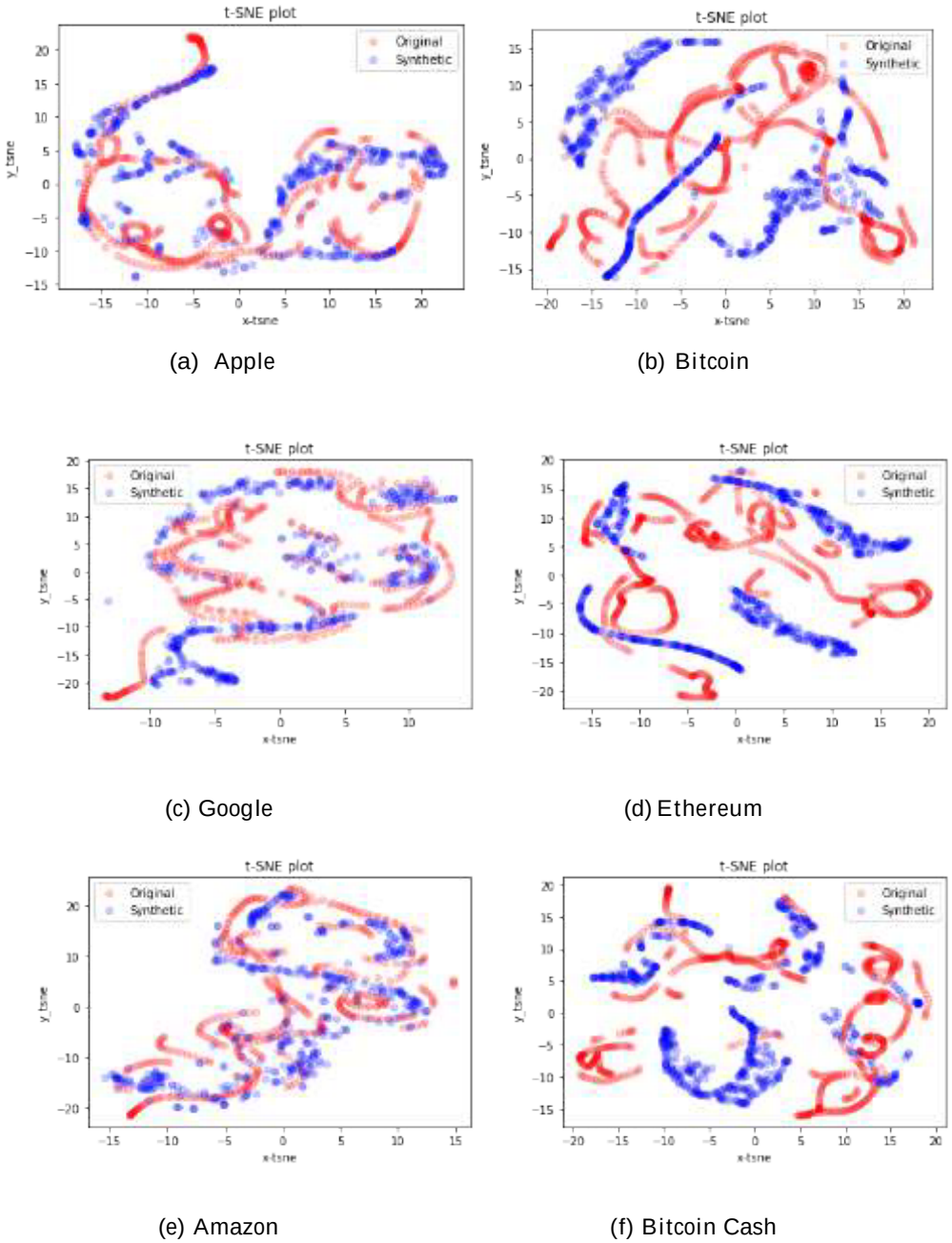

(a) Apple (b) Bitcoin

(c) Google (d) Ethereum

(e) Amazon (f) Bitcoin Cash

Figure 2: t-SNE analysis of synthetic data (blue) and original data (red) dataset OC

In this case, at first glance, it could seem like the synthetic data deviate from the real data, however with a more careful analysis it is possible to notice how in 6(a), 6(c) and 6(f) (all cryptocurrencies) the synthetic data overlap the original data or imitate (albeit to a limited extent) their distribution, while in the stocks' case the distribution of the synthetic data is dispersive and not entirely consistent with the distribution of the original data. The hypothesis we want to discuss is that the prices of cryptocurrencies have a greater amount of information within them and have a greater discriminative and predictive power. This hypothesis has been supported from the graphic point of view, but to leave no doubt we introduce the result of the analysis based on the scores (Ds indicates the discriminative score while Ps the predictive score) and on the KL divergence (D_{KL}), as shown in table 1.

	OHLCV			OC		
	D_{KL}	D_S	P_S	D_{KL}	D_S	P_S
AAPL	54.3214	0.1133	0.1084	53.6518	0.0347	0.0354
GOOG	53.9618	0.1449	0.0722	55.6298	0.0378	0.0431
AMZN	52.2606	0.0755	0.1079	54.9458	0.0316	0.0254
BTC	54.7267	0.0868	0.0672	55.6924	0.0674	0.0109
BCH	53.6472	0.0569	0.0273	53.5539	0.0528	0.0136
ETH	52.9701	0.2458	0.0443	52.0232	0.0382	0.0129

Table 1: Score of both dataset (lower the better)

From the analysis of the values it is possible to notice how, especially in the case of the OC data set, the cryptocurrency scores are the lowest and therefore the most significant. We can also assume that in the markets subject to opening/closing time, especially close to the closing minutes, investors are struck by "euphoria" by being trapped in a bottleneck and going to generate a price that may not be representative of the real trend. On the other hand, situations of this type may not exist in 24/7 markets thanks to the absence of timetables.

5 OUTLIERS

A particular situation occurred when analyzing the stocks of Tesla Inc. (TSLA) listed on NASDAQ. Despite being listed in a market subject to timetables, this analysis, both graphically and through the scores through TimeGAN, resulted in having a price type "loaded" with information, so much so that it achieved almost better results than cryptocurrencies. In particular:

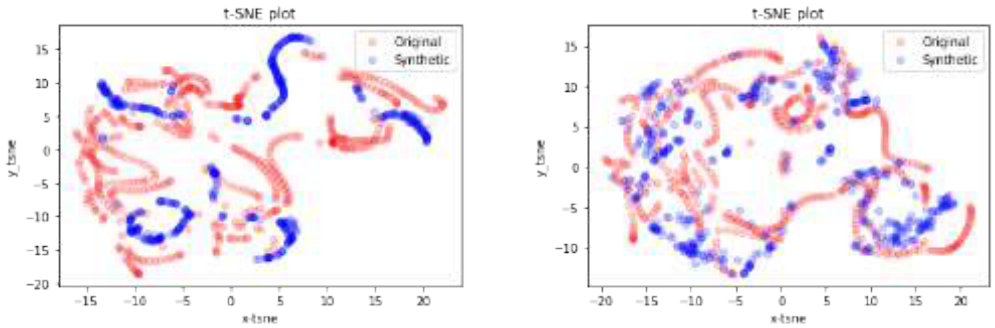

(a) OHLCV data set (b) OC data set

Figure 3: t-SNE analysis of TSLA stock on the different types of datasets

Especially in the second data set, the synthetic data reproduce the distribution of the original data very well. The analysis of the scores is shown in Table 2.

	OHLCV			OC		
	D_{KL}	D_S	P_S	D_{KL}	D_S	P_S
TSLA	54.3992	0.2163	0.1071	55.6569	0.0082	0.0182

Table 2: Score of TSLA in both dataset

In this case, especially in the OC data set, it is noted that the price range has a very low discriminative and predictive score, even higher than that of cryptocurrencies. Thanks to this *"outlier"* we can deduce that there are some financial instruments listed on stock exchanges subject to timetables which despite the limitation are in any case "completely absorbent" of the information concerning the company. This situation could be linked, for example, to the hypothesis that negative events never occurred outside the opening hours of the stock exchange or (in a less realistic but still possible hypothesis) to the hypothesis that in the time range considered no external situations occurred that could influence the price. In these cases, the use of this type of GAN can be a *"form of control"* on prices, especially when these are to be used for forecasting. There may be hidden elements that affect the price, however we can assume that a financial instrument whose price has a "large amount of information" could improve its prediction power compared to a financial instrument with less information.

6 CONCLUSIONS

In this paper, we have shown how TimeGAN is able to highlight which securities have a time series of prices *"loaded with information"*. The prices of cryptocurrencies have shown to have a much higher discriminatory and predictive power than stocks especially in the dataset made up only of the opening and closing prices. Furthermore, in the complete dataset (OHLCV), the prices with high discriminative power, combined with the other features, have made it possible to greatly improve the adherence of the synthetic data to the original ones. From this analysis it emerged that some stocks have the same discriminative and predictive power as cryptocurrencies; for this reason (especially since the time series forecasting is carried out mainly on stocks) it seems appropriate to screen, through this neural network, which are the optimal titles which combined with the different features improve the forecast. The next step is to look for, if any, a relationship between this type of stocks so as to limit the critical issues deriving from markets subject to timetables.

REFERENCES

1. L. Bachelier, Theorie de la speculatione, Ph.D. Thesis (1900).
2. M. G. Kendall, The analysis of economic time series. part i: Prices, Journal of the Royal Statistical Society (1953) 11–34.
3. P. H. Cootner, The Random Character of Stock Market Prices, MIT Press, 1964.
4. S. J. Taylor, Conjectured models for trends in financial prices, tests and forecast, Journal of the Royal Statistical Society Series A (1980).
5. G. E. P. Box, G. M. Jenkins, Time series analysis forecasting and control, San Francisco: Holden-Day (1976).
6. J. D. Hamilton, Time series analysis, Princeton University Press (1994).
7. G. P. Zhang, Time series forecasting using a hybrid arima and neural network model, Neurocomputing 50 (2003) 159–175.
8. W. R. Foster, F. Collopy, L. H. Ungar, Neural network forecasting of short, noisy time series, Computers and Chemical Engineering (1992) 293–297.
9. O. B.Sezer, M. U. Gudelek, A. M. Ozbayoglu, Financial time series forecasting with deep learning: A systematic literature review: 2005-2019, arXiv:1191.13288 (2019).
10. B. Kovalerchuk, E. Vityaev, Data mining in finance: Advances in relational and hybrid methods, Kluwer Academic Publishers (2000).
11. Y. Li, W. Ma, Applications of artificial neural networks in financial economics: A survey, 2010 International Symposium on Computational Intelligence and Design (2010) 211–214.
12. M. Mittelmayer, G. F. Knolmayer, Text mining systems for market response to news: A survey (2006).
13. L. Mitra, G. Mitra, Applications of news analytics in finance: A review, The Handbook of News Analytics in Finance (2012) 1–39.

14. S. Liu, C. Zhang, J. Ma, Cnn-lstm neural network model for quantitative strategy analysis in stock markets, Neural Information Processing (2017) 198–206.
15. L. Zhang, C. Aggarwal, G. J. Qi, Stock price prediction via discovering multifrequency trading patterns, Proceedings of the 23rd ACM SIGKDD International Conference on Knowledge Discovery and Data Mining (2017) 2141–2149.
16. W. Long, Z. Lu, L. Cui, Deep learning-based feature engineering for stock price movement prediction, Knowledge- Based Systems (2018) 163–173.
17. H. Wan, S. Guo, K. Yin, X. Liang, Y. Lin, Cts-lstm: Lstm-based neural networks for correlated time series predic- tion, Knowledge-Based Systems (2019).
18. T. Kaneko, H. Kameoka, N. Hojo, Y. Ijima, K. Hiramatsu, K. Kashino, Generative adversarial network-based postfilter for statistical parametric speech synthesis, IEEE International Conference on Acoustic, Speech and Signal Processing (2017) 4910–4914.
19. Y. Sun, L. Ximing, P. Cong, L. Li, Z. Zhao, Digital radiography image denoising using a generative adversarial network, Journal of X-Ray Science and Technology (2018) 1–12.
20. P. Xu, R. Du, Z. Zhang, Predicting pipeline leakage in petrochemical system through gan and lstm, Knowledge- Based Systems (2019) 50–61.
21. G. Papandreou, L.-C. Chen, K. . Murphy, A. L. Yiulle, Weakly-and semi-supervised learning of a deep convolu- tional network for semantic image segmentation, IEEE International Conference on Computer Vision (2015).
22. H. Liu, Y. Tian, Y. Wang, L. Pang, T. Huang, Deep relative distance learning: Tell the difference between similar vehicles, IEEE International Conference on Computer Vision (2016).
23. Z. Tang, C. Almeida, P. A. Fishwick, Time series forecasting using neural networks vs. box-jenkins methodology, Simulation (1991) 303–310.
24. W. L. Gorr, Research prospective on neural network forecasting, International Journal of Forecasting (1994) 1–4.
25. I. Goodfellow, J. Pouget-Abadie, M. Mirza, B. Xu, D. Warde-Farley, S. Ozair, A. Courville, Y. Bengio, Generative adversarial nets, Advances in Neural Information Processing System (2014).
26. J. Yoon, D. Jarrett, M. van der Schaar, Time-series generative adversarial networks, Advances in Neural Information Processing Systems 32 (NIPS 2019) (2019).
27. L. van der Maaten, G. Hinton, Visualizing data using t-sne, Journal of machine learning research (2008) 2579–2605.

Fekete-Szegö Problem for A Subclass of Analytıc Functions Defined By Chebyshev Polynomials

Murat ÇAĞLAR[1], Erhan DENİZ[1] and Sercan KAZIMOĞLU[1]

[1]*Department of Mathematics, Faculty of Science and Letters, Kafkas University, Kars-TURKEY*

mcaglar25@gmail.com
edeniz36@gmail.com
srcnkzmglu@gmail.com

Abstract. In this paper, we obtain initial coefficients $|a_2|$ and $|a_3|$ for a certain subclass of analytic functions by means of Chebyshev polynomials expansions in $\mathcal{D}$. Then, we solve Fekete-Szegö inequality $|a_3 - \mu a_2^2|$ for functions in this subclass.

Keywords: Analytic and univalent functions, subordination, coefficient inequalites, Chebyshev polynomial, Fekete-Szegö problem.

1. INTRODUCTION

Let $\mathcal{A}$ be the class of the functions of the form:

$$f(z) = z + \sum_{n=2}^{\infty} a_n z^n \tag{1.1}$$

which are analytic in the open unit disc $\mathcal{D} = \{z \in \mathbb{C}: |z| < 1\}$ and satisfying the conditions

$$f(0) = 0 \quad \text{and} \quad f'(0) = 1.$$

Also, let $\mathcal{S}$ be the subclass of $\mathcal{A}$ consisting of the form (1.1) which are univalent in $\mathcal{D}$.
Let f and g be analytic functions in $\mathcal{D}$. We define that the function f is subordinate to g in $\mathcal{D}$ and denoted by

$$f(z) \prec g(z) \quad (z \in \mathcal{D}),$$

if there exists a Schwarz function ω, which is analytic in $\mathcal{D}$ with $\omega(0) = 0$ and $|\omega(z)| < 1$ $(z \in \mathcal{D})$ such that

$$f(z) = g(\omega(z)) \quad (z \in \mathcal{D}).$$

If g is a univalent function in $\mathcal{D}$, then

$$f(z) \prec g(z) \Leftrightarrow f(0) = g(0) \quad \text{and} \quad f(\mathcal{D}) \subset g(\mathcal{D}).$$

The classical Fekete-Szegö inequality [8], presented by means of Loewner's method, for the coefficients of $f \in \mathcal{S}$ is that

$$|a_3 - \mu a_2^2| \leq 1 + 2exp\left(\frac{-2\mu}{1-\mu}\right) \; for \; 0 \leq \mu < 1.$$

As $\mu \to 1^-$, we have the elementary inequality $|a_3 - a_2{}^2| \leq 1$. Moreover, the coefficient functional

$$F_\mu(f) = a_3 - \mu a_2^2$$

on the normalized analytic functions f in the unit disk $\mathcal{D}$ plays an important role in geometric function theory. The problem of maximizing the absolute value of the functional $F_\mu(f)$ is called the Fekete-Szegö problem. In the literature, there exists a large number of results about inequalities for $F_\mu(f)$ corresponding to various subclasses of $\mathcal{S}$ (see [9]).

Chebyshev polynomials play a considerable role in numerical analysis. There are four kinds of Chebyshev polynomials. The first and second kinds of Chebyshev polynomials are defined by

$$T_n(t) = \cos n\varphi \quad \text{and} \quad U_n(t) = \frac{\sin(n+1)\varphi}{\sin\varphi} \quad (-1 < t < 1)$$

where n denotes the polynomial degree and $t = \cos\varphi$. For a brief history of Chebyshev polynomials of the first kind $T_n(t)$, the second kind $U_n(t)$ and their applications one can refer ([1]-[7], [10]-[13]).

Now, we define a subclass of analytic functions in $\mathcal{D}$ with the following subordination condition:

Definition 1. *A function $f \in \mathcal{A}$ given by (1.1) is said to be in the class $M(\gamma, \beta, t, \delta)$ for $\gamma \geq 1, \delta \geq 0,\ \beta \in \mathbb{C}/\{0\}$ and $t \in \left(\frac{1}{2}, 1\right]$ if the following subordination hold:*

$$1 + \frac{1}{\beta}\left((1-\gamma)\frac{f(z)}{z} + \gamma f'(z) + \delta z f''(z) - 1\right) \prec H(z,t) = \frac{1}{1-2tz+z^2} \quad (z \in \mathcal{D}). \qquad (1.2)$$

We consider that if $t = \cos\varphi \left(\frac{-\pi}{3} < \varphi < \frac{\pi}{3}\right)$, then

$$H(z,t) = \frac{1}{1 - 2\cos\varphi z + z^2} = 1 + \sum_{n=1}^{\infty} \frac{\sin(n+1)\varphi}{\sin\varphi} z^n \quad (z \in \mathcal{D}).$$

Thus

$$H(z,t) = 1 + 2\cos\varphi z + (3\cos^2\varphi - \sin^2\varphi)z^2 + \cdots \quad (z \in \mathcal{D}).$$

So, we write the Chebyshev polynomials of the second kind as following:

$$H(z,t) = 1 + U_1(t)z + U_2(t)z^2 + \cdots \quad (-1 < t < 1, z \in \mathcal{D})$$

where

$$U_{n-1}(t) = \frac{\sin(n \arccos t)}{\sqrt{1-t^2}} \quad (n \in \mathbb{N})$$

and we have

$$U_n(t) = 2tU_{n-1}(t) - U_{n-2}(t),$$

$$U_1(t) = 2t,\ U_2(t) = 4t^2 - 1,\ U_3(t) = 8t^3 - 4t,\ U_4(t) = 16t^4 - 12t^2 + 1, \cdots. \quad (1.3)$$

The Chebyshev polynomials $T_n(t)$, $t \in [-1,1]$ of the first kind have the generating function of the form

$$\sum_{n=0}^{\infty} T_n(t) z^n = \frac{1 - tz}{1 - 2tz + z^2} \quad (z \in \mathcal{D}).$$

There is the following connection by the Chebyshev polynomials of the first kind $T_n(t)$ and the second kind $U_n(t)$:

$$\frac{dT_n(t)}{dt} = nU_{n-1}(t), \quad T_n(t) = U_n(t) - tU_{n-1}(t), \quad 2T_n(t) = U_n(t) - U_{n-2}(t).$$

In this paper, we obtain initial coefficients $|a_2|$ and $|a_3|$ for subclass $M(\gamma, \beta, t, \delta)$ by means of Chebyshev polynomials expansions of analytic functions in $\mathcal{D}$. Then, we solve Fekete-Szegö problem for functions in this subclass.

2. COEFFICIENT BOUNDS FOR THE FUNCTION CLASS $M(\gamma, \beta, t, \delta)$

We begin with the following result involving initial coefficient bounds for the function class $M(\gamma, \beta, t, \delta)$.

Theorem 1. *Let the function $f(z)$ given by (1.1) be in the class $M(\gamma, \beta, t, \delta)$. Then*

$$|a_2| \leq \frac{2t|\beta|}{1 + \gamma + 2\delta} \tag{2.1}$$

and

$$|a_3| \leq \frac{(4t^2 + 2t - 1)|\beta|}{1 + 2\gamma + 6\delta}. \tag{2.2}$$

Proof. Let $f \in M(\gamma, \beta, t, \delta)$. From (1.2), we have

$$1 + \frac{1}{\beta}\left((1-\gamma)\frac{f(z)}{z} + \gamma f'(z) + \delta z f''(z) - 1\right) = 1 + U_1(t)p(z) + U_2(t)p^2(z) + \cdots \tag{2.3}$$

for some analytic functions

$$p(z) = c_1 z + c_2 z^2 + c_3 z^3 + \cdots \quad (z \in \mathcal{D}), \tag{2.4}$$

such that $p(0) = 0$, $|p(z)| < 1$ $(z \in \mathcal{D})$. Then, for all $j \in \mathbb{N}$,

$$|c_j| \leq 1 \tag{2.5}$$

and for all $\mu \in \mathbb{R}$

$$|c_2 - \mu c_1^2| \leq \max\{1, |\mu|\}. \tag{2.6}$$

It follows from (2.3) that

$$1 + \frac{1}{\beta}\left((1-\gamma)\frac{f(z)}{z} + \gamma f'(z) + \delta z f''(z) - 1\right) = 1 + U_1(t)c_1 z + [U_1(t)c_2 + U_2(t)c_1^2]z^2 + \cdots. \tag{2.7}$$

It follows from (2.7) that

$$\frac{(1 + \gamma + 2\delta)a_2}{\beta} = U_1(t)c_1, \tag{2.8}$$

and

$$\frac{(1 + 2\gamma + 6\delta)a_3}{\beta} = U_1(t)c_2 + U_2(t)c_1^2. \tag{2.9}$$

From (1.3), (2.8) and (2.5), we have

$$|a_2| \leq \frac{2t|\beta|}{1+\gamma+2\delta}. \tag{2.10}$$

By using (1.3) and (2.5) in (2.9), we obtain

$$|a_3| \leq \frac{(4t^2+2t-1)|\beta|}{1+2\gamma+6\delta} \tag{2.11}$$

which completes the proof of Theorem 1.

For $\beta = 1$ in Theorem 1, we obtain the following corollary.

Corollary 1. *Let* $f \in M(\gamma, 1, t, \delta)$. *Then*

$$|a_2| \leq \frac{2t}{1+\gamma+2\delta}$$

and

$$|a_3| \leq \frac{4t^2+2t-1}{1+2\gamma+6\delta}.$$

If we choose $\gamma = 0$ in Theorem 1, we get the following corollary.

Corollary 2. *Let* $f \in M(0, \beta, t, \delta)$. *Then*

$$|a_2| \leq \frac{2t|\beta|}{1+2\delta}$$

and

$$|a_3| \leq \frac{(4t^2+2t-1)|\beta|}{1+6\delta}.$$

Putting $\gamma = 0$ and $\delta = 0$ in Corollary 1, we have the following corollary.

Corollary 3. *Let* $f \in M(0,1, t, 0)$. *Then*

$$|a_2| \leq 2t$$

and

$$|a_3| \leq 4t^2+2t-1.$$

For $\beta = 1, \gamma = 1$ and $\delta = 1$ in Theorem 1, we obtain the following corollary.

Corollary 4. *Let the function* $f(z)$ *given by (1.1) be in the class* $M(1,1, t, 1)$. *Then*

$$|a_2| \leq \frac{t}{2}$$

and

$$|a_3| \leq \frac{4t^2+2t-1}{9}.$$

3. FEKETE-SZEGÖ INEQUALITY FOR THE FUNCTION CLASS $M(\gamma, \beta, t, \delta)$

Now, we find the bounds of Fekete-Szegö functional $|a_3 - \mu a_2^2|$ defined for $M(\gamma, \beta, t, \delta)$.

Theorem 2. *Let the function $f(z)$ given by (1.1) be in the class $M(\gamma, \beta, t, \delta)$. Then for some $\mu \in \mathbb{R}$,*

$$|a_3 - \mu a_2^2| \leq \begin{cases} \dfrac{2t|\beta|}{1+2\gamma+6\delta}, & \mu \in [\mu_1, \mu_2], \\ \dfrac{2t|\beta|}{1+2\gamma+6\delta}\left|\dfrac{4t^2-1}{2t} - \mu\dfrac{2t\beta(1+2\gamma+6\delta)}{(1+\gamma+2\delta)^2}\right|; & \mu \notin [\mu_1, \mu_2], \end{cases} \tag{3.1}$$

where $\mu_1 = \frac{(1+\gamma+2\delta)^2(4t^2-2t-1)}{4t^2|\beta|(1+2\gamma+6\delta)}$ *and* $\mu_2 = \frac{(1+\gamma+2\delta)^2(4t^2+2t-1)}{4t^2|\beta|(1+2\gamma+6\delta)}$.

Proof. Let $f \in M(\gamma, \beta, t, \delta)$. By using (2.8) and (2.9) for some $\mu \in \mathbb{R}$, we have

$$|a_3 - \mu a_2^2| = \frac{|\beta|U_1(t)}{1+2\gamma+6\delta}\left|c_2 + \left\{\frac{U_2(t)}{U_1(t)} - \mu\frac{\beta(1+2\gamma+6\delta)U_1(t)}{(1+\gamma+2\delta)^2}\right\}c_1^2\right|. \tag{3.2}$$

Then, in view of (2.6), we conclude that

$$|a_3 - \mu a_2^2| \leq \frac{|\beta|U_1(t)}{1+2\gamma+6\delta}\max\left\{1, \left|\frac{U_2(t)}{U_1(t)} - \mu\frac{\beta(1+2\gamma+6\delta)U_1(t)}{(1+\gamma+2\delta)^2}\right|\right\}. \tag{3.3}$$

Finally, by using (1.3) in (3.3), we get

$$|a_3 - \mu a_2^2| \leq \frac{2t|\beta|}{1+2\gamma+6\delta}\max\left\{1, \left|\frac{4t^2-1}{2t} - \mu\frac{2t\beta(1+2\gamma+6\delta)}{(1+\gamma+2\delta)^2}\right|\right\}.$$

Because $t > 0$, we obtain

$$\left|\frac{4t^2-1}{2t} - \mu\frac{2t\beta(1+2\gamma+6\delta)}{(1+\gamma+2\delta)^2}\right| \leq 1$$

$$\Leftrightarrow \left\{\frac{(1+\gamma+2\delta)^2(4t^2-2t-1)}{4t^2|\beta|(1+2\gamma+6\delta)} \leq \mu \leq \frac{(1+\gamma+2\delta)^2(4t^2+2t-1)}{4t^2|\beta|(1+2\gamma+6\delta)}\right\}$$

$$\Leftrightarrow \mu_1 \leq \mu \leq \mu_2.$$

This proves Theorem 2.

For $\beta = 1$ in Theorem 2, we obtain the following corollary.

Corollary 5. *Let $f \in M(\gamma, 1, t, \delta)$. Then for some $\mu \in \mathbb{R}$,*

$$|a_3 - \mu a_2^2| \leq \begin{cases} \dfrac{2t}{1+2\gamma+6\delta}, & \mu \in [\mu_1, \mu_2], \\ \dfrac{2t}{1+2\gamma+6\delta}\left|\dfrac{4t^2-1}{2t} - \mu\dfrac{2t(1+2\gamma+6\delta)}{(1+\gamma+2\delta)^2}\right|; & \mu \notin [\mu_1, \mu_2], \end{cases}$$

where $\mu_1 = \frac{(1+\gamma+2\delta)^2(4t^2-2t-1)}{4t^2(1+2\gamma+6\delta)}$ *and* $\mu_2 = \frac{(1+\gamma+2\delta)^2(4t^2+2t-1)}{4t^2(1+2\gamma+6\delta)}$.

If we choose $\gamma = 0$ in Theorem 2, we get the following corollary.

Corollary 6. *Let* $f \in M(0, \beta, t, \delta)$. *Then for some* $\mu \in \mathbb{R}$,

$$|a_3 - \mu a_2^2| \leq \begin{cases} \dfrac{2t|\beta|}{1+6\delta}, & \mu \in [\mu_1, \mu_2], \\ \dfrac{2t|\beta|}{1+6\delta}\left|\dfrac{4t^2-1}{2t} - \mu\dfrac{2t\beta(1+6\delta)}{(1+2\delta)^2}\right|; & \mu \notin [\mu_1, \mu_2], \end{cases}$$

where $\mu_1 = \frac{(1+2\delta)^2(4t^2-2t-1)}{4t^2|\beta|(1+6\delta)}$ *and* $\mu_2 = \frac{(1+2\delta)^2(4t^2+2t-1)}{4t^2|\beta|(1+6\delta)}$.

Putting $\gamma = 0$ and $\delta = 0$ in Corollary 5, we have the following corollary.

Corollary 7. *Let the function* $f(z)$ *given by (1.1) be in the class* $M(0,1,t,0)$. *Then for some* $\mu \in \mathbb{R}$,

$$|a_3 - \mu a_2^2| \leq \begin{cases} 2t, & \mu \in [\mu_1, \mu_2], \\ 2t\left|\dfrac{4t^2-1}{2t} - 2\mu t\right|; & \mu \notin [\mu_1, \mu_2], \end{cases}$$

where $\mu_1 = \frac{4t^2-2t-1}{4t^2}$ *and* $\mu_2 = \frac{4t^2+2t-1}{4t^2}$.

For $\beta = 1, \gamma = 1$ and $\delta = 1$ in Theorem 2, we obtain the following corollary.

Corollary 8. *Let the function* $f(z)$ *given by (1.1) be in the class* $M(1,1,t,1)$. *Then for some* $\mu \in \mathbb{R}$,

$$|a_3 - \mu a_2^2| \leq \begin{cases} \dfrac{2t}{9}, & \mu \in [\mu_1, \mu_2], \\ \dfrac{2t}{9}\left|\dfrac{4t^2-1}{2t} - \mu\dfrac{9t}{8}\right|; & \mu \notin [\mu_1, \mu_2], \end{cases}$$

where $\mu_1 = \frac{16t^2-8t-4}{9t^2}$ *and* $\mu_2 = \frac{16t^2+8t-4}{9t^2}$.

REFERENCES

1. S. Altınkaya and S. Yalçın, On the Chebyshev polynomial bounds for classes of univalent functions, Khayyam Journal of Mathematics, 2(1) (2016), 1-5.
2. S. Altınkaya and S. Y. Tokgöz, On the Chebyshev coefficients for a general subclass of univalent functions, Turkish Journal of Mathematics, 42(6) (2018), 2885-2890.
3. S. Bulut, N. Magesh and V. K. Balaji, Certain subclasses of analytic functions associated with the Chebyshev polynomials, Honam Mathematical Journal, 40(4) (2018), 611-619.
4. M. Çağlar, Chebyshev polynomial coefficient bounds for a subclass of bi-univalent functions, Comptes Rendus De L'Academie Bulgare Des Sciences, 72(12) (2019), 1608-1615.
5. M. Çağlar, H. Orhan and M. Kamali, Fekete-Szegö problem for a subclass of analytic functions associated with Chebyshev polynomials, Bol. Soc. Paran. Mat., doi: 10.5269/bspm.51024 (in press).
6. E. H. Doha, The first and second kind Chebyshev coefficients of the moments of the general-order derivative of an infinitely differentiable function, Int. J. Comput. Math., 51 (1994), 21-35.
7. J. Dziok, R. K. Raina and J. Sokol, Application of Chebyshev polynomials to classes of analytic functions, C.

R. Math. Acad. Sci. Paris, 353(5) (2015), 433-438.
8. M. Fekete and G. Szegö, Eine Bemerkung über ungerade schlichte Funktionen, J. London Math. Soc., 8 (1933), 85-89.
9. S. Kazımoğlu and E. Deniz, Fekete-Szegö problem for generalized bi-subordinate functions of complex order, Hacet. J. Math. Stat., 49 (2020), 1695-1705.
10. J. C. Mason, Chebyshev polynomial approximations for the L-membrane eigenvalue problem, SIAM J. Appl. Math., 15 (1967), 172-186.
11. N. Mustafa and E. Akbulut, Application of the second Chebyshev polinomials to coefficient estimates of analytic functions, Journal of Scientific and Engineering Research, 5(6) (2018), 143-148.
12. N. Mustafa and E. Akbulut, Application of the second kind Chebyshev polinomial to the Fekete-Szegö problem of certain class analytic functions, Journal of Scientific and Engineering Research, 6(2) (2019), 154-163.
13. N. Mustafa and E. Akbulut, Application of the second kind Chebyshev polynomials to coefficient estimates of certain class analytic functions, International Journal of Applied Science and Mathematics, 6(2) (2019), 44-49.

Some Inequalities of Grüss Type for a Weighted Fractional Integral Operator

Mustafa GÜRBÜZ[1] and Çetin YILDIZ[2]

[1]*Department of Elementary Mathematics Education, Faculty of Education, Ağrı İbrahim Çeçen University, Ağrı-TURKEY*
[2]*Department of Mathematics Education, K.K. Education Faculty, Atatürk University, Erzurum-TURKEY*

mgurbuz@agri.edu.tr
cetin@atauni.edu.tr

Abstract. Studies on fractional calculus is growing rapidly in recent years. However, the application areas of the findings are increasing day by day. In order to contribute to this field, in this study, new lemma and theorems are obtained with the weighted fractional integrals of a function with respect to another function.

Keywords: Weighted fractional integral operator, Grüss type inequality.

1. INTRODUCTION

G. Grüss proved a useful and interesting inequality that gives and upper bound for difference between the mean value of product of two bounded functions (f and g) and product of mean value's of those functions. This precious inequality is as follows:

Theorem 1. *(See [2]) Let f and g are defined and integrable functions on $[a,b]$. Also let those functions be bounded as*

$$m_f \le f(x) \le M_f$$

and

$$m_g \le g(x) \le M_g$$

for all $x \in [a,b]$. Then the following inequality holds:

$$\left|\frac{1}{b-a}\int_a^b f(x)g(x)dx - \frac{1}{b-a}\int_a^b f(x)dx\,\frac{1}{b-a}\int_a^b g(x)dx\right| \le \frac{(M_f-m_f)(M_g-m_g)}{4} \tag{1.1}$$

Many researchers continue to study and find new upper bounds for Grüss inequality(see [3]-[5]). On the other hand studies on fractional calculations have been increasing rapidly in recent years. The increase in the application areas of fractional calculus also plays an important role in this increase. For some recent results about fractional calculus, particularly inequalities obtained by using different fractional integral operators, see [3]-[10] and the references therein. The weighted versions of the fractional integral operators also help to bring a different perspective to the literature. One of them in given in the following which is put forward by Jarad et al.

Definition 1. *(See [1]) Let $(a,b) \subseteq \mathbb{R}$ and h be a monotonic, increasing and positive function on $(a,b]$. Also let h be a continuously differentiable function on $(a,b]$ with $h(0) = 0$, $0 \in [a,b]$. Then the left and right-side of the weighted fractional integrals of a function f with respect to h on $[a,b]$ are given in the following respectively*

$$({}_{a+}\Im_w^k f)(x) = \frac{\omega^{-1}(x)}{\Gamma(k)}\int_a^x \big(h(x)-h(t)\big)^{k-1}\omega(t)f(t)h'(t)dt,$$

$$\left({}_w\Im_{b-}^k f\right)(x) = \frac{\omega^{-1}(x)}{\Gamma(k)} \int_x^b \left(h(t) - h(x)\right)^{k-1} \omega(t) f(t) h'(t) dt$$

where $a < x < b$, $k > 0$, $\omega^{-1}(x) = \frac{1}{\omega(x)}$ *and* $\omega(x) \neq 0$.

In this study new inequalities are obtained by the weighted fractional operator mentioned above.

2. MAIN RESULTS

Theorem 2. *Let* f *be an integrable function on* $[a, b] \subseteq [0, \infty)$. *Assume that there exist two integrable functions* m_1 *and* M_1 *on* $[0, \infty)$ *such that*

$$m_1(t) \leq f(t) \leq M_1(t) \tag{2.1}$$

for every $t \in [a, b]$. *Then for all* $\xi > 0$ *and* $k > 0$ *we have the following inequality*

$$\begin{aligned} &\left({}_{a+}\Im_w^k M_1\right)(\xi)\left({}_w\Im_{b-}^k f\right)(\xi) + \left({}_{a+}\Im_w^k f\right)(\xi)\left({}_w\Im_{b-}^k m_1\right)(\xi) \\ &\geq \left({}_{a+}\Im_w^k M_1\right)(\xi)\left({}_w\Im_{b-}^k m_1\right)(\xi) + \left({}_{a+}\Im_w^k f\right)(\xi)\left({}_w\Im_{b-}^k f\right)(\xi). \end{aligned}$$

Proof. Since f is bounded function as stated in (2.1) we have

$$\begin{aligned} &\left(M_1(x) - f(x)\right)\left(f(y) - m_1(y)\right) \geq 0 \\ &M_1(x) f(y) + f(x) m_1(y) \geq M_1(x) m_1(y) + f(x) f(y). \end{aligned} \tag{2.2}$$

Multiplying both sides of (2.2) with

$$\frac{w^{-1}(\xi)}{\Gamma(k)} h'(x)\left(h(\xi) - h(x)\right)^{k-1} w(x)$$

where h is a monotone increasing, continuously differentiable and positive function on $(a, b]$ with $h(0) = 0$, then integrating the resulting inequality with respect to x from a to ξ we have

$$\begin{aligned} &\frac{w^{-1}(\xi) f(y)}{\Gamma(k)} \int_a^\xi h'(x)\left(h(\xi) - h(x)\right)^{k-1} w(x) M_1(x) dx \\ &+ \frac{w^{-1}(\xi) m_1(y)}{\Gamma(k)} \int_a^\xi h'(x)\left(h(\xi) - h(x)\right)^{k-1} w(x) f(x) dx \\ &\geq \frac{w^{-1}(\xi) m_1(y)}{\Gamma(k)} \int_a^\xi h'(x)\left(h(\xi) - h(x)\right)^{k-1} w(x) M_1(x) dx \\ &+ \frac{w^{-1}(\xi) f(y)}{\Gamma(k)} \int_a^\xi h'(x)\left(h(\xi) - h(x)\right)^{k-1} w(x) f(x) dx. \end{aligned}$$

By using the definition of the weighted fractional integral of a function with respect to another function on $[a, \xi]$ we get

$$f(y)\left({}_{a+}\Im_w^k M_1\right)(\xi) + m_1(y)\left({}_{a+}\Im_w^k f\right)(\xi) \geq m_1(y)\left({}_{a+}\Im_w^k M_1\right)(\xi) + f(y)\left({}_{a+}\Im_w^k f\right)(\xi). \tag{2.3}$$

Multiplying both sides of (2.3) with

$$\frac{w^{-1}(\xi)}{\Gamma(k)} h'(y)\left(h(y) - h(\xi)\right)^{k-1} w(y)$$

then integrating the resulting inequality with respect to y from ξ to b we have

$$\begin{aligned} &\left({}_{a+}\Im_w^k M_1\right)(\xi) \frac{w^{-1}(\xi)}{\Gamma(k)} \int_\xi^b h'(y)\left(h(y) - h(\xi)\right)^{k-1} w(y) f(y) dy \\ &+ \left({}_{a+}\Im_w^k f\right)(\xi) \frac{w^{-1}(\xi)}{\Gamma(k)} \int_\xi^b h'(y)\left(h(y) - h(\xi)\right)^{k-1} w(y) m_1(y) dy \end{aligned}$$

$$\geq \left({}_{a+}\mathfrak{I}_w^k M_1\right)(\xi)\frac{w^{-1}(\xi)}{\Gamma(k)}\int_\xi^b h'(y)\big(h(y)-h(\xi)\big)^{k-1}w(y)m_1(y)dy$$

$$+\left({}_{a+}\mathfrak{I}_w^k f\right)(\xi)\frac{w^{-1}(\xi)}{\Gamma(k)}\int_\xi^b h'(y)\big(h(y)-h(\xi)\big)^{k-1}w(y)f(y)dy.$$

Again by using the definition of the weighted fractional integral of a function with respect to another function on $[\xi, b]$ we get

$$\left({}_{a+}\mathfrak{I}_w^k M_1\right)(\xi)\left({}_{w}\mathfrak{I}_{b-}^k f\right)(\xi) + \left({}_{a+}\mathfrak{I}_w^k f\right)(\xi)\left({}_{w}\mathfrak{I}_{b-}^k m_1\right)(\xi)$$

$$\geq \left({}_{a+}\mathfrak{I}_w^k M_1\right)(\xi)\left({}_{w}\mathfrak{I}_{b-}^k m_1\right)(\xi) + \left({}_{a+}\mathfrak{I}_w^k f\right)(\xi)\left({}_{w}\mathfrak{I}_{b-}^k f\right)(\xi)$$

Theorem 3. *Let f and g be integrable functions on $[a, b] \subseteq [0, \infty)$. Assume that there exist integrable functions m_1, m_2, M_1 and M_2 on $[a, b]$ such that*

$$m_1(t) \leq f(t) \leq M_1(t) \tag{2.4}$$

$$m_2(t) \leq g(t) \leq M_2(t) \tag{2.5}$$

for every $t \in [a, b]$. Then for all $\xi > 0$ and $k > 0$ we have the following inequalities

$$\left({}_{a+}\mathfrak{I}_w^k M_1\right)(\xi)\left({}_{w}\mathfrak{I}_{b-}^k g\right)(\xi) + \left({}_{a+}\mathfrak{I}_w^k f\right)(\xi)\left({}_{w}\mathfrak{I}_{b-}^k m_2\right)(\xi) \tag{2.6}$$

$$\geq \left({}_{a+}\mathfrak{I}_w^k M_1\right)(\xi)\left({}_{w}\mathfrak{I}_{b-}^k m_2\right)(\xi) + \left({}_{a+}\mathfrak{I}_w^k f\right)(\xi)\left({}_{w}\mathfrak{I}_{b-}^k g\right)(\xi)$$

$$\left({}_{a+}\mathfrak{I}_w^k M_1\right)(\xi)\left({}_{w}\mathfrak{I}_{b-}^k M_2\right)(\xi) + \left({}_{a+}\mathfrak{I}_w^k f\right)(\xi)\left({}_{w}\mathfrak{I}_{b-}^k g\right)(\xi) \tag{2.7}$$

$$\geq \left({}_{a+}\mathfrak{I}_w^k M_1\right)(\xi)\left({}_{w}\mathfrak{I}_{b-}^k g\right)(\xi) + \left({}_{a+}\mathfrak{I}_w^k f\right)(\xi)\left({}_{w}\mathfrak{I}_{b-}^k M_2\right)(\xi)$$

$$\left({}_{a+}\mathfrak{I}_w^k f\right)(\xi)\left({}_{w}\mathfrak{I}_{b-}^k g\right)(\xi) + \left({}_{a+}\mathfrak{I}_w^k m_1\right)(\xi)\left({}_{w}\mathfrak{I}_{b-}^k m_2\right)(\xi) \tag{2.8}$$

$$\geq \left({}_{a+}\mathfrak{I}_w^k f\right)(\xi)\left({}_{w}\mathfrak{I}_{b-}^k m_2\right)(\xi) + \left({}_{a+}\mathfrak{I}_w^k m_1\right)(\xi)\left({}_{w}\mathfrak{I}_{b-}^k g\right)(\xi)$$

$$\left({}_{a+}\mathfrak{I}_w^k f\right)(\xi)\left({}_{w}\mathfrak{I}_{b-}^k M_2\right)(\xi) + \left({}_{a+}\mathfrak{I}_w^k m_1\right)(\xi)\left({}_{w}\mathfrak{I}_{b-}^k g\right)(\xi) \tag{2.9}$$

$$\geq \left({}_{a+}\mathfrak{I}_w^k f\right)(\xi)\left({}_{w}\mathfrak{I}_{b-}^k g\right)(\xi) + \left({}_{a+}\mathfrak{I}_w^k m_1\right)(\xi)\left({}_{w}\mathfrak{I}_{b-}^k M_2\right)(\xi)$$

Proof. Since f and g are bounded functions as stated in (2.4) and (2.5) we have

$$\big(M_1(x)-f(x)\big)\big(g(y)-m_2(y)\big) \geq 0$$

$$M_1(x)g(y) + f(x)m_2(y) \geq M_1(x)m_2(y) + f(x)g(y) \tag{2.10}$$

Multiplying both sides of (2.10) with

$$\frac{w^{-1}(\xi)}{\Gamma(k)}h'(x)\big(h(\xi)-h(x)\big)^{k-1}w(x)$$

where h is a monotone increasing, continuously differentiable and positive function on $(a, b]$ with $h(0) = 0$, then integrating the resulting inequality with respect to x from a to ξ we have

$$\frac{w^{-1}(\xi)g(y)}{\Gamma(k)}\int_a^\xi h'(x)\big(h(\xi)-h(x)\big)^{k-1}w(x)M_1(x)dx$$

$$+\frac{w^{-1}(\xi)m_2(y)}{\Gamma(k)}\int_a^\xi h'(x)\big(h(\xi)-h(x)\big)^{k-1}w(x)f(x)dx$$

$$\geq \frac{w^{-1}(\xi)m_2(y)}{\Gamma(k)}\int_a^\xi h'(x)\big(h(\xi)-h(x)\big)^{k-1}w(x)M_1(x)dx$$

$$+\frac{w^{-1}(\xi)g(y)}{\Gamma(k)}\int_a^{\xi} h'(x)\big(h(\xi)-h(x)\big)^{k-1}w(x)f(x)dx.$$

By using the definition of the weighted fractional integral of a function with respect to another function on $[a,\xi]$ we get

$$g(y)({}_{a+}\mathfrak{I}_w^k M_1)(\xi)+m_2(y)({}_{a+}\mathfrak{I}_w^k f)(\xi)\geq m_2(y)({}_{a+}\mathfrak{I}_w^k M_1)(\xi)+g(y)({}_{a+}\mathfrak{I}_w^k f)(\xi) \tag{2.11}$$

Multiplying both sides of (2.11) with

$$\frac{w^{-1}(\xi)}{\Gamma(k)}h'(y)\big(h(y)-h(\xi)\big)^{k-1}w(y)$$

then integrating the resulting inequality with respect to y from ξ to b we have

$$\begin{aligned}
&({}_{a+}\mathfrak{I}_w^k M_1)(\xi)\frac{w^{-1}(\xi)}{\Gamma(k)}\int_{\xi}^{b} h'(y)\big(h(y)-h(\xi)\big)^{k-1}w(y)g(y)dy\\
&+({}_{a+}\mathfrak{I}_w^k f)(\xi)\frac{w^{-1}(\xi)}{\Gamma(k)}\int_{\xi}^{b} h'(y)\big(h(y)-h(\xi)\big)^{k-1}w(y)m_2(y)dy\\
&\geq({}_{a+}\mathfrak{I}_w^k M_1)(\xi)\frac{w^{-1}(\xi)}{\Gamma(k)}\int_{\xi}^{b} h'(y)\big(h(y)-h(\xi)\big)^{k-1}w(y)m_2(y)dy\\
&+({}_{a+}\mathfrak{I}_w^k f)(\xi)\frac{w^{-1}(\xi)}{\Gamma(k)}\int_{\xi}^{b} h'(y)\big(h(y)-h(\xi)\big)^{k-1}w(y)g(y)dy.
\end{aligned}$$

Again by using the definition of the weighted fractional integral of a function with respect to another function on $[\xi,b]$ we get

$$\begin{aligned}
&({}_{a+}\mathfrak{I}_w^k M_1)(\xi)\big({}_{w}\mathfrak{I}_{b-}^k g\big)(\xi)+({}_{a+}\mathfrak{I}_w^k f)(\xi)\big({}_{w}\mathfrak{I}_{b-}^k m_2\big)(\xi)\\
&\geq({}_{a+}\mathfrak{I}_w^k M_1)(\xi)\big({}_{w}\mathfrak{I}_{b-}^k m_2\big)(\xi)+({}_{a+}\mathfrak{I}_w^k f)(\xi)\big({}_{w}\mathfrak{I}_{b-}^k g\big)(\xi)
\end{aligned}$$

which is the desired result. To prove (2.7), (2.8) and (2.9) one can choose the statements given in (2.12), (2.13) and (2.14) respectively.

$$\big(M_1(x)-f(x)\big)\big(M_2(y)-g(y)\big)\geq 0 \tag{2.12}$$

$$\big(f(x)-m_1(x)\big)\big(g(y)-m_2(y)\big)\geq 0 \tag{2.13}$$

$$\big(f(x)-m_1(x)\big)\big(M_2(y)-g(y)\big)\geq 0 \tag{2.14}$$

Lemma 1. *Let f be an integrable function on $[a,b]\subseteq[0,\infty)$. Assume that there exist two integrable functions m_1 and M_1 on $[0,\infty)$ such that*

$$m_1(t)\leq f(t)\leq M_1(t) \tag{2.15}$$

for every $t\in[a,b]$. Then for all $\xi>0$ and $k>0$ we have the following identity

$$\begin{aligned}
&({}_{a+}\mathfrak{I}_w^k f^2)(\xi)\big({}_{w}\mathfrak{I}_{b-}^k 1\big)(\xi)+\big({}_{w}\mathfrak{I}_{b-}^k f^2\big)(\xi)({}_{a+}\mathfrak{I}_w^k 1)(\xi)\\
&=\big({}_{a+}\mathfrak{I}_w^k (M_1 f)\big)(\xi)\big({}_{w}\mathfrak{I}_{b-}^k 1\big)(\xi)-({}_{a+}\mathfrak{I}_w^k m_1 M_1)(\xi)\big({}_{w}\mathfrak{I}_{b-}^k 1\big)(\xi)\\
&+\big({}_{a+}\mathfrak{I}_w^k (m_1 f)\big)(\xi)\big({}_{w}\mathfrak{I}_{b-}^k 1\big)(\xi)+\big({}_{w}\mathfrak{I}_{b-}^k M_1 f\big)(\xi)({}_{a+}\mathfrak{I}_w^k 1)(\xi)\\
&-\big({}_{w}\mathfrak{I}_{b-}^k m_1 M_1\big)(\xi)({}_{a+}\mathfrak{I}_w^k 1)(\xi)+\big({}_{w}\mathfrak{I}_{b-}^k m_1 f\big)(\xi)({}_{a+}\mathfrak{I}_w^k 1)(\xi)\\
&-\big({}_{a+}\mathfrak{I}_w^k (M_1-f)(f-m_1)\big)(\xi)\big({}_{w}\mathfrak{I}_{b-}^k 1\big)(\xi)\\
&-\Big({}_{w}\mathfrak{I}_{b-}^k (M_1-f)(f-m_1)\Big)(\xi)({}_{a+}\mathfrak{I}_w^k 1)(\xi).
\end{aligned}$$

Proof. Since f is bounded function as stated in (2.15) we have

$$\begin{aligned}
&\big(M_1(y)-f(y)\big)\big(f(x)-m_1(x)\big)+\big(M_1(x)-f(x)\big)\big(f(y)-m_1(y)\big)\\
&-\big(M_1(x)-f(x)\big)\big(f(x)-m_1(x)\big)-\big(M_1(y)-f(y)\big)\big(f(y)-m_1(y)\big)\\
&=f^2(x)+f^2(y)-2f(x)f(y)+M_1(y)f(x)+m_1(x)f(y)-m_1(x)M_1(y)\\
&+M_1(x)f(y)+m_1(y)f(x)-m_1(y)M_1(x)-M_1(x)f(x)+m_1(x)M_1(x)\\
&-m_1(x)f(x)-M_1(y)f(y)+m_1(y)M_1(y)-m_1(y)f(y). \qquad (2.16)
\end{aligned}$$

Multiplying both sides of (2.16) with

$$\frac{w^{-1}(\xi)}{\Gamma(k)}h'(x)\big(h(\xi)-h(x)\big)^{k-1}w(x)$$

where h is a monotone increasing, continuously differentiable and positive function on $(a,b]$ with $h(0)=0$. Then integrating the resulting inequality with respect to x from a to ξ we have

$$\begin{aligned}
&\big(M_1(y)-f(y)\big)\big(({}_{a+}\mathfrak{I}_w^k f)(\xi)-({}_{a+}\mathfrak{I}_w^k m_1)(\xi)\big)\\
&+\big(({}_{a+}\mathfrak{I}_w^k M_1)(\xi)-({}_{a+}\mathfrak{I}_w^k f)(\xi)\big)\big(f(y)-m_1(y)\big)\\
&-\big({}_{a+}\mathfrak{I}_w^k(M_1-f)(f-m_1)\big)(\xi)\\
&-\big(M_1(y)-f(y)\big)\big(f(y)-m_1(y)\big)({}_{a+}\mathfrak{I}_w^k 1)(\xi) \qquad (2.17)\\
&=({}_{a+}\mathfrak{I}_w^k f^2)(\xi)+f^2(y)({}_{a+}\mathfrak{I}_w^k 1)(\xi)-2f(y)({}_{a+}\mathfrak{I}_w^k f)(\xi)\\
&+M_1(y)({}_{a+}\mathfrak{I}_w^k f)(\xi)+f(y)({}_{a+}\mathfrak{I}_w^k m_1)(\xi)-M_1(y)({}_{a+}\mathfrak{I}_w^k m_1)(\xi)\\
&+f(y)({}_{a+}\mathfrak{I}_w^k M_1)(\xi)+m_1(y)({}_{a+}\mathfrak{I}_w^k f)(\xi)-m_1(y)({}_{a+}\mathfrak{I}_w^k M_1)(\xi)\\
&-\big({}_{a+}\mathfrak{I}_w^k(M_1 f)\big)(\xi)+({}_{a+}\mathfrak{I}_w^k m_1 M_1)(\xi)\\
&-\big({}_{a+}\mathfrak{I}_w^k(m_1 f)\big)(\xi)-M_1(y)f(y)({}_{a+}\mathfrak{I}_w^k 1)(\xi)\\
&+m_1(y)M_1(y)({}_{a+}\mathfrak{I}_w^k 1)(\xi)-m_1(y)f(y)({}_{a+}\mathfrak{I}_w^k 1)(\xi)
\end{aligned}$$

Multiplying both sides of (2.17) with

$$\frac{w^{-1}(\xi)}{\Gamma(k)}h'(y)\big(h(y)-h(\xi)\big)^{k-1}w(y)$$

then integrating the resulting inequality with respect to y from ξ to b we have

$$\begin{aligned}
&\Big(({}_{w}\mathfrak{I}_{b-}^k M_1)(\xi)-({}_{w}\mathfrak{I}_{b-}^k f)(\xi)\Big)\big(({}_{a+}\mathfrak{I}_w^k f)(\xi)-({}_{a+}\mathfrak{I}_w^k m_1)(\xi)\big)\\
&+\big(({}_{a+}\mathfrak{I}_w^k M_1)(\xi)-({}_{a+}\mathfrak{I}_w^k f)(\xi)\big)\Big(({}_{w}\mathfrak{I}_{b-}^k f)(\xi)-({}_{w}\mathfrak{I}_{b-}^k m_1)(\xi)\Big)\\
&-\big({}_{a+}\mathfrak{I}_w^k(M_1-f)(f-m_1)\big)(\xi)\big({}_{w}\mathfrak{I}_{b-}^k 1\big)(\xi)\\
&-\Big({}_{w}\mathfrak{I}_{b-}^k(M_1-f)(f-m_1)\Big)(\xi)({}_{a+}\mathfrak{I}_w^k 1)(\xi)\\
&=({}_{a+}\mathfrak{I}_w^k f^2)(\xi)\big({}_{w}\mathfrak{I}_{b-}^k 1\big)(\xi)+\big({}_{w}\mathfrak{I}_{b-}^k f^2\big)(\xi)({}_{a+}\mathfrak{I}_w^k 1)(\xi)-2\big({}_{w}\mathfrak{I}_{b-}^k f\big)(\xi)({}_{a+}\mathfrak{I}_w^k f)(\xi)\\
&+\big({}_{w}\mathfrak{I}_{b-}^k M_1\big)(\xi)({}_{a+}\mathfrak{I}_w^k f)(\xi)+\big({}_{w}\mathfrak{I}_{b-}^k f\big)(\xi)({}_{a+}\mathfrak{I}_w^k m_1)(\xi)-\big({}_{w}\mathfrak{I}_{b-}^k M_1\big)(\xi)({}_{a+}\mathfrak{I}_w^k m_1)(\xi)\\
&+\big({}_{w}\mathfrak{I}_{b-}^k f\big)(\xi)({}_{a+}\mathfrak{I}_w^k M_1)(\xi)+\big({}_{w}\mathfrak{I}_{b-}^k m_1\big)(\xi)({}_{a+}\mathfrak{I}_w^k f)(\xi)-\big({}_{w}\mathfrak{I}_{b-}^k m_1\big)(\xi)({}_{a+}\mathfrak{I}_w^k M_1)(\xi)\\
&-\big({}_{a+}\mathfrak{I}_w^k(M_1 f)\big)(\xi)\big({}_{w}\mathfrak{I}_{b-}^k 1\big)(\xi)+({}_{a+}\mathfrak{I}_w^k m_1 M_1)(\xi)\big({}_{w}\mathfrak{I}_{b-}^k 1\big)(\xi)\\
&-\big({}_{a+}\mathfrak{I}_w^k(m_1 f)\big)(\xi)\big({}_{w}\mathfrak{I}_{b-}^k 1\big)(\xi)-\big({}_{w}\mathfrak{I}_{b-}^k M_1 f\big)(\xi)({}_{a+}\mathfrak{I}_w^k 1)(\xi)
\end{aligned}$$

$$+\left({}_w\mathfrak{I}_{b-}^k m_1 M_1\right)(\xi)\left({}_{a+}\mathfrak{I}_w^k 1\right)(\xi) - \left({}_w\mathfrak{I}_{b-}^k m_1 f\right)(\xi)\left({}_{a+}\mathfrak{I}_w^k 1\right)(\xi)$$

which is the desired result.

Theorem 4. *Let f and g be integrable functions on $[a,b] \subseteq [0,\infty)$. Assume that there exist integrable functions m_1, m_2, M_1 and M_2 on $[a,b]$ such that*

$$m_1(t) \le f(t) \le M_1(t) \tag{2.18}$$

$$m_2(t) \le g(t) \le M_2(t) \tag{2.19}$$

for every $t \in [a,b]$. Then for all $\xi > 0$ and $k > 0$ we have the following inequality

$$\begin{bmatrix}\left({}_{a+}\mathfrak{I}_w^k(fg)\right)(\xi)\left({}_w\mathfrak{I}_{b-}^k 1\right)(\xi) - \left({}_{a+}\mathfrak{I}_w^k f\right)(\xi)\left({}_w\mathfrak{I}_{b-}^k g\right)(\xi) \\ -\left({}_{a+}\mathfrak{I}_w^k g\right)(\xi)\left({}_w\mathfrak{I}_{b-}^k f\right)(\xi) + \left({}_{a+}\mathfrak{I}_w^k 1\right)(\xi)\left({}_w\mathfrak{I}_{b-}^k(fg)\right)(\xi)\end{bmatrix}^2$$

$$\le R(f,m_1,M_1) \times R(g,m_2,M_2)$$

where $R(u,m_i,M_i)$ is defined by

$$R(u,m_i,M_i) = \left({}_{a+}\mathfrak{I}_w^k(M_i u)\right)(\xi)\left({}_w\mathfrak{I}_{b-}^k 1\right)(\xi) + \left({}_{a+}\mathfrak{I}_w^k(m_i u)\right)(\xi)\left({}_w\mathfrak{I}_{b-}^k 1\right)(\xi)$$
$$+\left({}_w\mathfrak{I}_{b-}^k M_i u\right)(\xi)\left({}_{a+}\mathfrak{I}_w^k 1\right)(\xi) + \left({}_w\mathfrak{I}_{b-}^k m_i u\right)(\xi)\left({}_{a+}\mathfrak{I}_w^k 1\right)(\xi)$$
$$-2\left({}_{a+}\mathfrak{I}_w^k u\right)(\xi)\left({}_w\mathfrak{I}_{b-}^k u\right)(\xi).$$

Proof. Let f and g be two integrable functions defined on $[0,\infty)$ satisfying (2.18) and (2.19). We define

$$H(x,y) := \big(f(x)-f(y)\big)\big(g(x)-g(y)\big), \quad x,y \in [a,\xi] \subseteq [0,\infty).$$

Multiplying both sides with

$$\left(\frac{w^{-1}(\xi)}{\Gamma(k)}\right)^2 h'(x)h'(y)\left(\big(h(\xi)-h(x)\big)\big(h(y)-h(\xi)\big)\right)^{k-1} w(x)w(y)$$

and integrating the resulting identity with respect to x and y from a to ξ and from ξ to b respectively, we obtain

$$\left(\frac{w^{-1}(\xi)}{\Gamma(k)}\right)^2 \int_\xi^b \int_a^\xi h'(x)h'(y)\left(\big(h(\xi)-h(x)\big)\big(h(y)-h(\xi)\big)\right)^{k-1}$$
$$\times w(x)w(y)H(x,y)dxdy$$
$$= \left(\frac{w^{-1}(\xi)}{\Gamma(k)}\right)^2 \int_\xi^b h'(y)\big(h(y)-h(\xi)\big)^{k-1} w(y)$$
$$\times \left(\begin{matrix}\int_a^\xi h'(x)\left(\big(h(\xi)-h(x)\big)\right)^{k-1} w(x) \\ \times [f(x)g(x) - f(x)g(y) - f(y)g(x) + f(y)g(y)]dx\end{matrix}\right) dy$$
$$= \left({}_{a+}\mathfrak{I}_w^k(fg)\right)(\xi)\left({}_w\mathfrak{I}_{b-}^k 1\right)(\xi) - \left({}_{a+}\mathfrak{I}_w^k f\right)(\xi)\left({}_w\mathfrak{I}_{b-}^k g\right)(\xi)$$
$$-\left({}_{a+}\mathfrak{I}_w^k g\right)(\xi)\left({}_w\mathfrak{I}_{b-}^k f\right)(\xi) + \left({}_{a+}\mathfrak{I}_w^k 1\right)(\xi)\left({}_w\mathfrak{I}_{b-}^k(fg)\right)(\xi) \tag{2.20}$$

where h is a monotone increasing, continuously differentiable and positive function on $(a,b]$ with $h(0) = 0$. Applying the Cauchy-Schwarz inequality to (2.20) we get

$$\begin{bmatrix}\left({}_{a+}\mathfrak{I}_w^k(fg)\right)(\xi)\left({}_w\mathfrak{I}_{b-}^k 1\right)(\xi) - \left({}_{a+}\mathfrak{I}_w^k f\right)(\xi)\left({}_w\mathfrak{I}_{b-}^k g\right)(\xi) \\ -\left({}_{a+}\mathfrak{I}_w^k g\right)(\xi)\left({}_w\mathfrak{I}_{b-}^k f\right)(\xi) + \left({}_{a+}\mathfrak{I}_w^k 1\right)(\xi)\left({}_w\mathfrak{I}_{b-}^k(fg)\right)(\xi)\end{bmatrix}^2$$

$$\leq \begin{bmatrix} ({}_{a+}\mathfrak{I}_w^k f^2)(\xi)({}_w\mathfrak{I}_{b-}^k 1)(\xi) - ({}_{a+}\mathfrak{I}_w^k f)(\xi)({}_w\mathfrak{I}_{b-}^k f)(\xi) \\ -({}_{a+}\mathfrak{I}_w^k f)(\xi)({}_w\mathfrak{I}_{b-}^k f)(\xi) + ({}_{a+}\mathfrak{I}_w^k 1)(\xi)({}_w\mathfrak{I}_{b-}^k f^2)(\xi) \end{bmatrix}$$

$$\times \begin{bmatrix} ({}_{a+}\mathfrak{I}_w^k g^2)(\xi)({}_w\mathfrak{I}_{b-}^k 1)(\xi) - ({}_{a+}\mathfrak{I}_w^k g)(\xi)({}_w\mathfrak{I}_{b-}^k g)(\xi) \\ -({}_{a+}\mathfrak{I}_w^k g)(\xi)({}_w\mathfrak{I}_{b-}^k g)(\xi) + ({}_{a+}\mathfrak{I}_w^k 1)(\xi)({}_w\mathfrak{I}_{b-}^k g^2)(\xi) \end{bmatrix}$$

$$= \begin{bmatrix} ({}_{a+}\mathfrak{I}_w^k f^2)(\xi)({}_w\mathfrak{I}_{b-}^k 1)(\xi) - 2({}_{a+}\mathfrak{I}_w^k f)(\xi)({}_w\mathfrak{I}_{b-}^k f)(\xi) \\ +({}_{a+}\mathfrak{I}_w^k 1)(\xi)({}_w\mathfrak{I}_{b-}^k f^2)(\xi) \end{bmatrix}$$

$$\times \begin{bmatrix} ({}_{a+}\mathfrak{I}_w^k g^2)(\xi)({}_w\mathfrak{I}_{b-}^k 1)(\xi) - 2({}_{a+}\mathfrak{I}_w^k g)(\xi)({}_w\mathfrak{I}_{b-}^k g)(\xi) \\ +({}_{a+}\mathfrak{I}_w^k 1)(\xi)({}_w\mathfrak{I}_{b-}^k g^2)(\xi) \end{bmatrix}. \tag{2.21}$$

From Lemma 1 we have

$$({}_{a+}\mathfrak{I}_w^k f^2)(\xi)({}_w\mathfrak{I}_{b-}^k 1)(\xi) + ({}_w\mathfrak{I}_{b-}^k f^2)(\xi)({}_{a+}\mathfrak{I}_w^k 1)(\xi)$$
$$\leq ({}_{a+}\mathfrak{I}_w^k (M_1 f))(\xi)({}_w\mathfrak{I}_{b-}^k 1)(\xi) + ({}_{a+}\mathfrak{I}_w^k (m_1 f))(\xi)({}_w\mathfrak{I}_{b-}^k 1)(\xi)$$
$$+({}_w\mathfrak{I}_{b-}^k M_1 f)(\xi)({}_{a+}\mathfrak{I}_w^k 1)(\xi) + ({}_w\mathfrak{I}_{b-}^k m_1 f)(\xi)({}_{a+}\mathfrak{I}_w^k 1)(\xi)$$

since

$$({}_{a+}\mathfrak{I}_w^k m_1 M_1)(\xi)({}_w\mathfrak{I}_{b-}^k 1)(\xi) \geq 0$$
$$({}_w\mathfrak{I}_{b-}^k m_1 M_1)(\xi)({}_{a+}\mathfrak{I}_w^k 1)(\xi) \geq 0$$
$${}_{a+}\mathfrak{I}_w^k \left((M_1(\xi) - f(\xi))(f(\xi) - m_1(\xi))\right)({}_w\mathfrak{I}_{b-}^k 1)(\xi) \geq 0$$
$${}_w\mathfrak{I}_{b-}^k \left((M_1(\xi) - f(\xi))(f(\xi) - m_1(\xi))\right)({}_{a+}\mathfrak{I}_w^k 1)(\xi) \geq 0.$$

So we have

$$({}_{a+}\mathfrak{I}_w^k f^2)(\xi)({}_w\mathfrak{I}_{b-}^k 1)(\xi) - 2({}_{a+}\mathfrak{I}_w^k f)(\xi)({}_w\mathfrak{I}_{b-}^k f)(\xi)$$
$$+({}_{a+}\mathfrak{I}_w^k 1)(\xi)({}_w\mathfrak{I}_{b-}^k f^2)(\xi)$$
$$\leq ({}_{a+}\mathfrak{I}_w^k (M_1 f))(\xi)({}_w\mathfrak{I}_{b-}^k 1)(\xi) + ({}_{a+}\mathfrak{I}_w^k (m_1 f))(\xi)({}_w\mathfrak{I}_{b-}^k 1)(\xi)$$
$$+({}_w\mathfrak{I}_{b-}^k M_1 f)(\xi)({}_{a+}\mathfrak{I}_w^k 1)(\xi) + ({}_w\mathfrak{I}_{b-}^k m_1 f)(\xi)({}_{a+}\mathfrak{I}_w^k 1)(\xi)$$
$$-2({}_{a+}\mathfrak{I}_w^k f)(\xi)({}_w\mathfrak{I}_{b-}^k f)(\xi)$$
$$= R(f, m_1, M_1) \tag{2.22}$$

and similarly

$$({}_{a+}\mathfrak{I}_w^k g^2)(\xi)({}_w\mathfrak{I}_{b-}^k 1)(\xi) - 2({}_{a+}\mathfrak{I}_w^k g)(\xi)({}_w\mathfrak{I}_{b-}^k g)(\xi)$$
$$+({}_{a+}\mathfrak{I}_w^k 1)(\xi)({}_w\mathfrak{I}_{b-}^k g^2)(\xi)$$
$$\leq ({}_{a+}\mathfrak{I}_w^k (M_2 g))(\xi)({}_w\mathfrak{I}_{b-}^k 1)(\xi) + ({}_{a+}\mathfrak{I}_w^k (m_2 g))(\xi)({}_w\mathfrak{I}_{b-}^k 1)(\xi)$$
$$+({}_w\mathfrak{I}_{b-}^k M_2 g)(\xi)({}_{a+}\mathfrak{I}_w^k 1)(\xi) + ({}_w\mathfrak{I}_{b-}^k m_{21} g)(\xi)({}_{a+}\mathfrak{I}_w^k 1)(\xi)$$
$$-2({}_{a+}\mathfrak{I}_w^k g)(\xi)({}_w\mathfrak{I}_{b-}^k g)(\xi)$$
$$= R(g, m_2, M_2). \tag{2.23}$$

Using (2.21), (2.22) and (2.23) we get the desired result.

REFERENCES

1. F. Jarad, T. Abdeljawad and K. Shah, On the Weighted Fractional operators of a function with respect to another function. Fractals 2020. https://doi.org/10.1142/S0218348X20400113
2. G. Grüss, "Uber das maximum des absoluten betrages von $\frac{1}{b-a}\int_a^b f(x)g(x)dx - \frac{1}{(b-a)^2}\int_a^b f(x)dx \int_a^b g(x)dx$, Math. Z. 39 (1935), 215–226.
3. G. Rahman, K. S. Nisar, S. Rashid and T. Abdeljawad, Certain Grüss-type inequalities via tempered fractional integrals concerning another function. J. Ineq.& App., 2020 (1), 1-18.
4. S. Iqbal, M. Adil Khan and T. Abdeljawad, New general Grüss-type inequalities over σ-finite measure space with applications. Adv. Differ. Equ. 2020, 468 (2020). https://doi.org/10.1186/s13662-020-02933-1
5. S. Rashid, F. Jarad and M. A. Noor, Grüss-type integrals inequalities via generalized proportional fractional operators. RACSAM 114, 93 (2020). https://doi.org/10.1007/s13398-020-00823-5
6. M. Gürbüz, A. O. Akdemir, S. Rashid and E. Set, Hermite–Hadamard inequality for fractional integrals of Caputo–Fabrizio type and related inequalities. J. Ineq.& App., 2020(1), 1-10.
7. E. Set, A. O. Akdemir and M. E. Özdemir, Simpson type integral inequalities for convex functions via Riemann-Liouville integrals. Filomat, 31(14), 4415-4420, 2017.
8. B. Bayraktar, Some new generalizations of Hadamard-type midpoint inequalities involving fractional integrals. Probl. Anal. Issues Anal. 2020, 9 (27), No 3.
9. T. Toplu, E. Set, İ. İşcan and S. Maden, Hermite-Hadamard type inequalities for p −convex functions via Katugampola fractional integrals. Facta Univ. Ser. Math. Inform, 34, 149-164, 2019.
10. F. Qi, G. Rahman, S. M. Hussain, W. S. Du and K. S. Nisar, Some inequalities of Čebyšev type for conformable k −fractional integral operators. Symmetry, 10(11), 614, 2018.

On Subclasses of Analytic Functions Defined by q - Derivative and their Some Geometric Properties

Nizami MUSTAFA[1], Veysel NEZİR[2]

[1,2] *Department of Mathematics, Faculty of Science and Letters, Kafkas University, Kars, Turkey*

nizamimustafa@gmail.com
veyselnezir@yahoo.com

Abstract. Recently, the q - derivative operator has been used to investigate several subclasses of analytic functions in different ways with different perspectives by many researchers and their interesting results are too voluminous to discuss. For example, the extension of the theory of univalent functions can be used to describe the theory of q - derivative. The q - derivative operator are also used to construct subclasses of analytic functions and so on.

In this study, we introduce certain subclasses of analytic and univalent functions on the open unit disk in the complex plane defined by q - derivative. Here, we aim to find conditions for analytic and univalent functions to belonging to these classes.

1. INTRODUCTION

Let A be the class of analytic functions f on the open unit disk $U=\{z\in\mathbb{C}:\ |z|<1\}$ in the complex plane, normalized by $f(0)=0=f'(0)-1$ of the form

$$f(z)=z+a_2z^2+a_3z^3+\cdots+a_nz^n+\cdots=z+\sum_{n=2}^{\infty}a_nz^n,\ a_n\in\mathbb{C}. \tag{1.1}$$

Also, let's S be the family of all functions in A which are univalent in U.
Furthermore, we will denote by T the subclass of all functions f in A of the form

$$f(z)=z-a_2z^2-a_3z^3-\cdots-a_nz^n-\cdots=z-\sum_{n=2}^{\infty}a_nz^n,\ a_n\geq 0. \tag{1.2}$$

As well-known that some of the important and well-investigated subclasses of the univalent functions class S include the classes $S^*(\alpha)$ and $C(\alpha)$, respectively, starlike and convex functions of order α $(\alpha\in[0,1))$ on the open unit disk U.

By definition, we have (see for details, [2, 3], also [8])

$$S^*(\alpha)=\left\{f\in S:\ \mathrm{Re}\left(\frac{zf'(z)}{f(z)}\right)>\alpha,\ z\in U\right\},\ C(\alpha)=\left\{f\in S:\ \mathrm{Re}\left(1+\frac{zf''(z)}{f'(z)}\right)>\alpha,\ z\in U\right\}.$$

For $\beta \in [0,1)$, interesting generalization of the function classes $S^*(\alpha)$ and $C(\alpha)$ are the classes $S^*(\alpha,\beta)$ and $C(\alpha,\beta)$, which are defined as follows

$$S^*(\alpha,\beta)=\left\{ f \in S:\ \mathrm{Re}\left(\frac{zf'(z)}{\beta zf'(z)+(1-\beta) f(z)} \right) > \alpha,\ z \in U \right\},$$

$$C(\alpha,\beta)=\left\{ f \in S:\ \mathrm{Re}\left(\frac{f'(z)+zf''(z)}{f'(z)+\beta zf''(z)} \right) > \alpha,\ z \in U \right\}.$$

We will use $TS^*(\alpha,\beta)=T \cap S^*(\alpha,\beta)$ and $TC(\alpha,\beta)=T \cap C(\alpha,\beta)$.

The classes $TS^*(\alpha,\beta)$ and $TC(\alpha,\beta)$ were extensively studied by Altintaş and Owa [1] and certain conditions for hypergeometric functions and generalized Bessel functions for these classes were studied Moustafa [5] and Porwal and Dixit [7].

A generalization of the function classes $S^*(\alpha,\beta)$ and $C(\alpha,\beta)$ is the class $S^*C(\alpha,\beta;\gamma)$ for $\gamma \in [0,1]$, which defined as follows

$$S^*C(\alpha,\beta;\gamma)=\left\{ f \in S:\mathrm{Re}\left(\frac{zf'(z)+\gamma z^2 f''(z)}{\gamma z\left(f'(z)+\beta zf''(z)\right)+(1-\gamma)\left(\beta zf'(z)+(1-\beta) f(z)\right)} \right) > \alpha \right\}, z \in U.$$

Also, let's $TS^*C(\alpha,\beta;\gamma)=T \cap S^*C(\alpha,\beta;\gamma)$.

In his fundamental paper [4] Jackson, for $q \in (0,1)$ introduced the q - derivative operator D_q of the an analytic function f as follows

$$D_q f(z)=\begin{cases} \dfrac{f(z)-f(qz)}{(1-q)z}, & if \quad z \neq 0, \\ f'(0), & if \quad z=0. \end{cases}$$

The formulas for the q - derivative of a product and a quotient of functions are

$$D_q z^n=[n]_q z^{n-1},\ n \in \square,$$

where

$$[n]_q=\frac{1-q^n}{1-q}=\sum_{k=1}^{n} q^{k-1}$$

is the q - analogue of the natural numbers n.

It is clear that

$$[0]_q = 0,\ [1]_q = 1,\ \lim_{q\to 1^-}[n]_q = n$$

and

$$\lim_{q\to 1^-} D_q f(z) = f'(z)$$

for the function $f \in A$.

For $q \in (0,1)$ and $\alpha \in [0,1)$, we define by $S_q^*(\alpha)$ and $C_q(\alpha)$ the subclasses of A which we will call, respectively, q - starlike and q - convex functions of order α

$$S_q^*(\alpha) = \left\{ f \in S:\ \operatorname{Re}\frac{zD_q f(z)}{f(z)} > \alpha, z \in U \right\},\ C_q(\alpha) = \left\{ f \in S:\ \operatorname{Re}\frac{D_q\left(zD_q f(z)\right)}{D_q f(z)} > \alpha, z \in U \right\}.$$

Also, let's $TS_q^*(\alpha) = T \cap S_q^*(\alpha)$ and $TC_q(\alpha) = T \cap C_q(\alpha)$.

Interesting generalization of the function classes $S_q^*(\alpha)$ and $C_q(\alpha)$ for $\beta \in [0,1)$ are the classes $S_q^*(\alpha,\beta)$ and $C_q(\alpha,\beta)$, which we give as follows

$$S_q^*(\alpha,\beta) = \left\{ f \in A:\ \operatorname{Re}\left(\frac{zD_q f(z)}{\beta zD_q f(z) + (1-\beta) f(z)} \right) > \alpha,\ z \in U \right\},$$

$$C_q(\alpha,\beta) = \left\{ f \in A:\ \operatorname{Re}\left(\frac{D_q f(z) + zD_q^2 f(z)}{D_q f(z) + \beta zD_q^2 f(z)} \right) > \alpha,\ z \in U \right\}.$$

Let use $TS_q^*(\alpha,\beta) = T \cap S_q^*(\alpha,\beta)$ and $TC_q(\alpha,\beta) = T \cap C_q(\alpha,\beta)$.

Inspired by the studies mentioned above, we define a generalization of the function classes $S_q^*(\alpha,\beta)$ and $C_q(\alpha,\beta)$ as follows.

Definition 1. *A function f given by (1.1) is said to be in the class $S_q^* C_q(\alpha,\beta;\gamma)$, $\alpha,\beta \in [0,1)$, $\gamma \in [0,1]$ if the following condition is satisfied*

$$\operatorname{Re}\left(\frac{zD_q f(z) + \gamma z^2 D_q^2 f(z)}{\gamma z\left(D_q f(z) + \beta zD_q^2 f(z)\right) + (1-\gamma)\left(\beta zD_q f(z) + (1-\beta) f(z)\right)} \right) > \alpha, z \in U.$$

Also, we will use $TS_q^* C_q(\alpha,\beta;\gamma) = T \cap S_q^* C_q(\alpha,\beta;\gamma)$.

It is clear that $S_q^* C_q(\alpha,\beta;0) = S_q^*(\alpha,\beta)$, $S_q^* C_q(\alpha,\beta;1) = C_q(\alpha,\beta)$, $\lim_{q\to 1^-} S_q^* C_q(\alpha,\beta;\gamma) = S^* C(\alpha,\beta;\gamma)$ and $\lim_{q\to 1^-} TS_q^* C_q(\alpha,\beta;\gamma) = TS^* C(\alpha,\beta;\gamma)$.

So, function classes $S_q^* C_q(\alpha,\beta;\gamma)$ and $TS_q^* C_q(\alpha,\beta;\gamma)$ are generalization of the previously known function classes $S_q^*(\alpha,\beta)$, $C_q(\alpha,\beta)$, $S^* C(\alpha,\beta;\gamma)$ and $TS^* C(\alpha,\beta;\gamma)$ of analytic functions, respectively.

The object of this study is to examine characteristic properties of the classes $S_q^* C_q(\alpha,\beta;\gamma)$ and $TS_q^* C_q(\alpha,\beta;\gamma)$. Here, we give some conditions for an analytic and univalent function to belonging to these classes.

2. MAIN RESULTS

In this section, we will give a sufficient condition for the functions to belonging to the class $S_q^* C_q(\alpha,\beta;\gamma)$, and necessary and sufficient conditions for the functions to belonging to the class $TS_q^* C_q(\alpha,\beta;\gamma)$.

This conditions are given in the following Theorem 1 and Theorem 2, respectively.

Theorem 1. Let $f \in A$. Then, $f \in S_q^* C_q(\alpha,\beta;\gamma)$ if the following condition is satisfied

$$\sum_{n=2}^{\infty} \left\{ [n]_q \left[(1-\alpha\beta)\left(1+\gamma[n-1]_q\right) - (1-\beta)\alpha\gamma \right] - \alpha(1-\beta)(1-\gamma) \right\} |a_n| \le 1-\alpha . \tag{2.1}$$

The result obtained here is sharp.

Proof. Suppose that satisfied the condition (2.1). Let us show that $f \in S_q^* C_q(\alpha,\beta;\gamma)$.

From the Definition 1, as known that $f \in S_q^* C_q(\alpha,\beta;\gamma)$, $\alpha,\beta \in [0,1)$, $\gamma \in [0,1]$ if and only if

$$\operatorname{Re}\left(\frac{zD_q f(z) + \gamma z^2 D_q^2 f(z)}{\gamma z\left(D_q f(z) + \beta z D_q^2 f(z)\right) + (1-\gamma)\left(\beta z D_q f(z) + (1-\beta) f(z)\right)} \right) > \alpha, z \in U . \tag{2.2}$$

It can be easily shown that the condition (2.2) holds true if

$$\left| \frac{zD_q f(z) + \gamma z^2 D_q^2 f(z)}{\gamma z\left(D_q f(z) + \beta z D_q^2 f(z)\right) + (1-\gamma)\left(\beta z D_q f(z) + (1-\beta) f(z)\right)} - 1 \right| \le 1-\alpha . \tag{2.3}$$

So, $f \in S_q^* C_q(\alpha,\beta;\gamma)$ if satisfied the condition (2.3). Accordingly, it will be sufficient to show that the condition (2.3) is fulfilled within the scope of the theorem's hypothesis.

By simple computation, we write

$$\left|\frac{zD_q f(z)+\gamma z^2 D_q^2 f(z)}{\gamma z\left(D_q f(z)+\beta z D_q^2 f(z)\right)+(1-\gamma)\left(\beta z D_q f(z)+(1-\beta) f(z)\right)}-1\right|$$

$$=\left|\frac{\sum_{n=2}^{\infty}\left[\gamma[n]_q[n-1]_q+(1-\gamma)\left([n]_q-1\right)\right](1-\beta)a_n z^n}{z+\sum_{n=2}^{\infty}\left[\gamma\left(1+\beta[n-1]_q\right)[n]_q+(1-\gamma)\left(1+[n]_q-1\right)\beta\right]a_n z^n}\right|$$

$$\leq\frac{\sum_{n=2}^{\infty}\left[\gamma[n]_q[n-1]_q+(1-\gamma)\left([n]_q-1\right)\right](1-\beta)|a_n|}{1-\sum_{n=2}^{\infty}\left[\gamma\left(1+\beta[n-1]_q\right)[n]_q+(1-\gamma)\left(1+[n]_q-1\right)\beta\right]|a_n|}.$$

It can be easily seen that last expression of the above inequality is bounded by $1-\alpha$ if and only if satisfied the condition (2.1). Also, we can easily see that the condition (2.3) is satisfied if last expression of the above inequality is bounded by $1-\alpha$, which equivalent to the condition (2.1). With this, the desired result in the theorem has been proved.

Also, it is clear that the result obtained in the theorem is sharp for the functions

$$f_n(z)=z+\frac{1-\alpha}{[n]_q\left[(1-\alpha\beta)\left(1+\gamma[n-1]_q\right)-(1-\beta)\alpha\gamma\right]-\alpha(1-\beta)(1-\gamma)}z^n,\ z\in U,\ n=2,3,\ldots.$$

Thus, the proof of Theorem 1 is completed.

From the Theorem 1, we can readily deduce the following results.

Corollary 1. *Let* $f\in A$. *Then,* $f\in S_q^*(\alpha,\beta)$ *if the following condition is satisfied*

$$\sum_{n=2}^{\infty}\left([n]_q-\alpha-\left([n]_q-1\right)\alpha\beta\right)|a_n|\leq 1-\alpha.$$

The result obtained here is sharp for the functions

$$f_n(z)=z+\frac{1-\alpha}{[n]_q-\alpha-\left([n]_q-1\right)\alpha\beta}z^n,\ z\in U,\ n=2,3,\ldots.$$

Corollary 2. *Let* $f\in A$. *Then,* $f\in C_q(\alpha,\beta)$ *if the following condition is satisfied*

$$\sum_{n=2}^{\infty}\left[1-\alpha+(1-\alpha\beta)[n-1]_q\right][n]_q|a_n|\leq 1-\alpha.$$

The result obtained here is sharp for the functions

$$f_n(z) = z - \frac{1-\alpha}{[n]_q - \alpha - \left([n]_q - 1\right)\alpha\beta} z^n,\ z \in U,\ n = 2,3,\ldots .$$

As can be seen from the following theorem, for the function $f \in TS_q^* C_q(\alpha, \beta; \gamma)$ the converse of Theorem 1 is also true.

Theorem 2. *Let* $f \in T$. *Then,* $f \in TS_q^* C_q(\alpha, \beta; \gamma)$ *if and only if satisfied the following condition*

$$\sum_{n=2}^{\infty} \left\{ [n]_q \left[(1-\alpha\beta)\left(1+\gamma[n-1]_q\right) - (1-\beta)\alpha\gamma \right] - \alpha(1-\beta)(1-\gamma) \right\} |a_n| \le 1-\alpha . \qquad (2.1)$$

The result obtained here is sharp.

Proof. The proof of the sufficiency of the theorem can be proved similarly to the proof of Theorem 1. We will prove only the necessity of the theorem.

Assume that $f \in TS_q^* C_q(\alpha, \beta; \gamma)$, $\alpha, \beta \in [0,1), \gamma \in [0,1], q \in (0,1)$. That is,

$$\operatorname{Re}\left\{ \frac{zD_q f(z) + \gamma z^2 D_q^2 f(z)}{\gamma z\left(D_q f(z) + \beta z D_q^2 f(z)\right) + (1-\gamma)\left(\beta z D_q f(z) + (1-\beta) f(z)\right)} \right\} > \alpha,\ z \in U .$$

Then, by simple computation, we write

$$\operatorname{Re}\left\{ \frac{zD_q f(z) + \gamma z^2 D_q^2 f(z)}{\gamma z\left(D_q f(z) + \beta z D_q^2 f(z)\right) + (1-\gamma)\left(\beta z D_q f(z) + (1-\beta) f(z)\right)} \right\}$$

$$= \operatorname{Re}\left\{ \frac{z - \sum_{n=2}^{\infty} [n]\left(1+[n-1]\gamma\right) a_n z^n}{z - \sum_{n=2}^{\infty} (1-\beta)\left(\gamma[n]+1-\gamma\right) a_n z^n - \sum_{n=2}^{\infty} \beta[n]\left(\gamma[n-1]+1\right) a_n z^n} \right\} > \alpha.$$

The last expression in the brackets of the above inequality is real if choose z real. Hence, from the previous inequality letting $z \to 1$ through real values, we can write

$$1 - \sum_{n=2}^{\infty} [n]\left(1+[n-1]\gamma\right) a_n \ge \alpha \left\{ 1 - \sum_{n=2}^{\infty} (1-\beta)\left(\gamma[n]+1-\gamma\right) a_n - \sum_{n=2}^{\infty} \beta[n]\left(\gamma[n-1]+1\right) a_n \right\}.$$

This follows

$$\sum_{n=2}^{\infty}\left\{[n]_q\left[(1-\alpha\beta)\left(1+\gamma[n-1]_q\right)-(1-\beta)\alpha\gamma\right]-\alpha(1-\beta)(1-\gamma)\right\}|a_n|\le 1-\alpha\,,$$

which is the same as the condition (2.1). With this the result of the theorem was proven.

Furthermore, it is clear that the result obtained in the theorem is sharp for the functions

$$f_n(z)=z-\frac{1-\alpha}{[n]_q\left[(1-\alpha\beta)\left(1+\gamma[n-1]_q\right)-(1-\beta)\alpha\gamma\right]-\alpha(1-\beta)(1-\gamma)}z^n,\ z\in U,\ n=2,3,\ldots\,.$$

Thus, the proof of Theorem 2 is completed.

From the Theorem 2, we can readily deduce the following results.

Corollary 3. *Let* $f\in T$ *. Then,* $f\in TS_q^*(\alpha,\beta)$ *if and only if satisfied the following condition*

$$\sum_{n=2}^{\infty}\left([n]_q-\alpha-\left([n]_q-1\right)\alpha\beta\right)|a_n|\le 1-\alpha\,.$$

The result obtained here is sharp.

Corollary 4. *Let* $f\in T$ *. Then,* $f\in TC_q(\alpha,\beta)$ *if and only if satisfied the following condition*

$$\sum_{n=2}^{\infty}\left[1-\alpha+(1-\alpha\beta)[n-1]_q\right][n]_q|a_n|\le 1-\alpha\,.$$

The result obtained here is sharp.

Remark 1. *The results obtained in Theorem 1, Theorem 2 and Corollary 1-4 are generalization of the results obtained in Theorem 1,2 and Corollary 1-4 in [6].*

REFERENCES

1. O. Altintaş and S. Owa, On subclasses of univalent functions with negative coefficients, Pusan Kyongnam Mathematical Journal, vol. 4, pp. 41-56, 1988.
2. P. L. Duren, Univalent Functions, Grundlehren der Mathematischen Wissenshaften, Bd. 259, New York, Springer-Verlag, Tokyo, 1983, 382p.
3. A. W. Goodman, Univalent Functions, Volume I, Polygonal, Washington, 1983, 246p.
4. F. H. Jackson, On q - functions and a certain difference operatör, Trans. Roy. Soc. Edin, vol. 46, 1908, 253-281.
5. A. O. Moustafa, A study on starlike and convex properties for hypergeometric functions, Journal of Inequalities in Pure and Applied Mathematics, vol. 10, no. 3, article 87, pp. 1-16, 2009.
6. N. Mustafa and S. Korkmaz, Analytic Functions Expressed with Poisson Distribution Series and their Some Properties, Journal of Contemporary Applied Mathematics, (submitted) 2020.
7. S. Porwal and K. K. Dixit, An application of generalized Bessel functions on certain analytic functions, Acta Universitatis Matthiae Belii. Series Mathematics, pp. 51-57, 2013.
8. H. M. Srivastava and S. Owa, Current Topics in Analytic Function Theory, World Scientific, Singapore, 1992, 456p.

The Pell-Fibonacci Sequence in Finite Groups

Özgür ERDAĞ[1] and Ömür DEVECİ[1]

[1]*Department of Mathematics, Faculty of Science and Letters,*
Kafkas University, Kars-TURKEY

ozgur_erdag@hotmail.com
odeveci36@hotmail.com

Abstract. In this work, we extend the Pell-Fibonacci sequence to groups and we redefine the Pell-Fibonacci sequence by means of the elements of groups which is called the Pell-Fibonacci orbit. Also, we consider the Dihedral groups D_{2n}, $(n \geq 2)$ and then, we give the lengths of the periods of the Pell-Fibonacci orbit in the Dihedral groups D_{2n}, $(n \geq 2)$ as applications of the results obtained.

1. INTRODUCTION

In [5], Deveci defined the Pell-Fibonacci sequence which is directly related to the Pell and Fibonacci numbers as follows:

$$P-F(n+4)=3P-F(n+3)-3P-F(n+1)-P-F(n) \tag{1}$$

for $n \geq 0$ with initial constants $P-F(0)=P-F(1)=P-F(2)=0$ and $P-F(3)=1$.

By the equation (1), we can write the following companion matrix:

$$M_3=\begin{bmatrix} 3 & 0 & -3 & -1 \\ 1 & 0 & 0 & 0 \\ 0 & 1 & 0 & 0 \\ 0 & 0 & 1 & 0 \end{bmatrix}.$$

Also, by an inductive argument, he obtained that

$$(M_3)^n=\begin{bmatrix} x_{n+4}^3 & F_{n+2}+x_{n+3}^3-x_{n+4}^3 & F_{n+3}+x_{n+4}^3-x_{n+5}^3 & -x_{n+3}^3 \\ x_{n+3}^3 & F_{n+1}+x_{n+2}^3-x_{n+3}^3 & F_{n+2}+x_{n+3}^3-x_{n+4}^3 & -x_{n+2}^3 \\ x_{n+2}^3 & F_n+x_{n+1}^3-x_{n+2}^3 & F_{n+1}+x_{n+2}^3-x_{n+3}^3 & -x_{n+1}^3 \\ x_{n+1}^3 & F_{n-1}+x_n^3-x_{n+1}^3 & F_n+x_{n+1}^3-x_{n+2}^3 & -x_n^3 \end{bmatrix}$$

for $n \geq 1$. It is important to note that $\det M_3 = 1$.

Definition 1.1. The dihedral group D_{2n} of order $2n$ is defined by the presentation

$$D_{2n}=\langle x, y : x^n = y^2 = (xy)^2 = e \rangle$$

for $n \geq 2$.

It is well-known that a sequence is periodic if, after certain points, it consists only of repetitions of a fixed subsequence. The number of elements in the repeating subsequence is the period of the sequence. A sequence is simply periodic with period *k* if the first *k* elements in the sequence form a repeating subsequence.

The study of the linear recurrence sequences in groups began with the earlier work of Wall [10] where the ordinary Fibonacci sequences in cyclic groups were investigated. In the mid-eighties, Wilcox [11] extended the problem to abelian groups. The concept extended to some special linear recurrence sequences by several authors; see for example, [1-4, 6-9]. In this work, we study the Pell-Fibonacci sequence in groups and then we define the the Pell-Fibonacci orbit. Finally, we obtain the lengths of the periods of the Pell-Fibonacci orbit in the dihedral group D_{2n}, $(n \geq 2)$ as applications of the results obtained.

2. MAIN RESULTS

Let G be a finite j-generator group and let X be the subset of $\underbrace{G \times G \times G \cdots \times G}_{j}$ such that $(x_0, x_1, \ldots, x_{j-1}) \in X$ if and only if G is generated by $x_0, x_1, \ldots, x_{j-1}$. We call $(x_0, x_1, \ldots, x_{j-1})$ a generating j-tuple for G.

Definition 2.1. For a generating j-tuple $(x_0, x_1, \ldots, x_{j-1}) \in X$ we define the Pell-Fibonacci orbit as shown:

$$PF(n+4) = (PF(n))^{-1} (PF(n+1))^{-3} (PF(n+3))^{3}$$

for $n \geq 0$, with initial conditions

$$\begin{cases} PF(0) = x_1, PF(1) = x_2, PF(2) = x_3, PF(4) = x_4 & \text{if } j = 4, \\ PF(0) = x_1, PF(1) = x_2, PF(2) = x_3, PF(4) = e & \text{if } j = 3, \\ PF(0) = x_1, PF(1) = x_2, PF(2) = e, PF(4) = e & \text{if } j = 2. \end{cases}$$

For a generating j-tuple $(x_0, x_1, \ldots, x_{j-1}) \in X$, the Pell-Fibonacci orbit is denoted by $PF_{(G:x_0, x_1, \ldots, x_{j-1})}$.

Theorem 2.1. *A Pell-Fibonacci orbit $PF_{(G:x_0, x_1, \ldots, x_{j-1})}$ of a finite group G is simply periodic.*

Proof. Let k be the order of the group G, then it is clear that there are n^4 distinct 4-tuples of elements of G. Then, it is easy to see that at least one of the 4-tuples appears twice in the Pell-Fibonacci orbit $PF_{(G:x_0, x_1, \ldots, x_{j-1})}$. Because of the repeating, the Pell-Fibonacci orbit of the group G is periodic. Since the Pell-Fibonacci orbit $PF_{(G:x_0, x_1, \ldots, x_{j-1})}$ is periodic, there exist natural number u and v with $u \equiv v \pmod 4$, such that

$$PF(u) = PF(v), PF(u+1) = PF(v+1), PF(u+2) = PF(v+2), PF(u+3) = PF(v+3)$$

By the definition of the Pell-Fibonacci orbit $PF_{(G:x_0, x_1, \ldots, x_{j-1})}$, we can easily derive

$$PF(n+4) = (PF(n))^{-1} (PF(n+1))^{-3} (PF(n+3))^{3}.$$

Therefore, we obtain $PF(u) = PF(v)$, and it then follows that

$$PF(u-v) = PF(0), PF(u-v+1) = PF(1), PF(u-v+2) = PF(2), PF(u-v+3) = PF(3).$$

which implies that the Pell-Fibonacci orbit $PF_{(G:x_0, x_1, \ldots, x_{j-1})}$ is simply periodic.

□

Let the notation $LPF_{(G:x_0, x_1, \ldots, x_{j-1})}$ denote the length of the period of the Pell-Fibonacci orbit $PF_{(G:x_0, x_1, \ldots, x_{j-1})}$.

Corollary 2.1. *The lengths of the periods of the Pell-Fibonacci orbit in some the Dihedral groups* D_{2n} *are given in following table.*

$n=2$	$LPF_{(D_{2n}:x,y)}=6$
$n=3$	$LPF_{(D_{2n}:x,y)}=18$
$n=4$	$LPF_{(D_{2n}:x,y)}=12$
$n=5$	$LPF_{(D_{2n}:x,y)}=12$
$n=6$	$LPF_{(D_{2n}:x,y)}=18$
$n=7$	$LPF_{(D_{2n}:x,y)}=24$
$n=8$	$LPF_{(D_{2n}:x,y)}=24$
$n=9$	$LPF_{(D_{2n}:x,y)}=18$
$n=10$	$LPF_{(D_{2n}:x,y)}=12$
$n=11$	$LPF_{(D_{2n}:x,y)}=18$
$n=12$	$LPF_{(D_{2n}:x,y)}=36$
$n=13$	$LPF_{(D_{2n}:x,y)}=42$
$n=14$	$LPF_{(D_{2n}:x,y)}=24$
$n=15$	$LPF_{(D_{2n}:x,y)}=36$
$n=16$	$LPF_{(D_{2n}:x,y)}=48$
$n=17$	$LPF_{(D_{2n}:x,y)}=54$

Example 2.1. For $n=10$, we consider the length of the period of Pell-Fibonacci orbit in the Dihedral group D_{20}. Using the relations of Dihedral group D_{20}, we have the sequence

$$PF(0)=x, PF(1)=y, PF(2)=e, PF(3)=e, PF(4)=x^{-1}y, PF(5)=x,$$
$$PF(6)=x^3, PF(7)=y, PF(8)=x^2, PF(9)=x^{-4}, PF(10)=x^{-1}y, PF(11)=x^7,$$
$$PF(12)=x, PF(13)=y, PF(14)=e, PF(15)=e.$$

Since $PF(0)=PF(12)=x$, $PF(1)=PF(13)=y$, $PF(2)=PF(14)=e$ and $PF(3)=PF(15)=e$ the length of the period of the Pell-Fibonacci orbit $LPF_{(D_{20}:x,y)}$ is 12.

Example 2.2. For $n=17$, we consider the length of the period of Pell-Fibonacci orbit in the Dihedral group D_{34}. Using the relations of Dihedral group D_{34}, we have the sequence

$$PF(0)=x, PF(1)=y, PF(2)=e, PF(3)=e, PF(4)=x^{-1}y, PF(5)=x,$$

$$PF(6)=x^3,\ PF(7)=x^7y,\ PF(8)=x^{-5},\ PF(9)=x^{-8},\ PF(10)=x^{-6}y,\ PF(11)=x^{-2},$$
$$PF(12)=x^6,\ PF(13)=xy,\ PF(14)=x^4,\ PF(15)=x^{-4},\ PF(16)=x^7y,\ PF(17)=x^6,$$
$$PF(18)=x^{-8},\ PF(19)=xy,\ PF(20)=x^7,\ PF(21)=x^5,\ PF(22)=x^{-6}y,\ PF(23)=x^{-6},$$
$$PF(24)=x^{-6},\ PF(25)=x^7y,\ PF(26)=x^3,\ PF(27)=x^{-1},\ PF(28)=x^{-1}y,\ PF(29)=e,$$
$$PF(30)=e,\ PF(31)=y,\ PF(32)=x^{-1},\ PF(33)=x^{-3},\ PF(34)=x^{-8}y,\ PF(35)=x^5,$$
$$PF(36)=x^8,\ PF(37)=x^5y,\ PF(38)=x^2,\ PF(39)=x^{-6},\ PF(40)=x^{-2}y,\ PF(41)=x^{-4},$$
$$PF(42)=x^4,\ PF(43)=x^{-8}y,\ PF(44)=x^{-6},\ PF(45)=x^8,\ PF(46)=x^{-2}y,\ PF(47)=x^{-7},$$
$$PF(48)=x^{-5},\ PF(49)=x^5y,\ PF(50)=x^6,\ PF(51)=x^6,\ PF(52)=x^{-8}y,\ PF(53)=x^{-3},$$
$$PF(54)=x,\ PF(55)=y,\ PF(56)=e,\ PF(57)=e.$$

Since $PF(0)=PF(54)=x$, $PF(1)=PF(55)=y$, $PF(2)=PF(56)=e$ and $PF(3)=PF(57)=e$ the length of the period of the Pell-Fibonacci orbit $LPF_{(D_{34};x,y)}$ is 54.

REFERENCES

1. H. Aydin and G.C. Smith, Finite *p*-Quotients of Some Cyclically Presented Groups, Journal of the London Mathematical Society, 49 (1994), 83-92.
2. C.M. Campbell, H. Doostie and E.F. Robertson, Fibonacci Length of Generating Pairs in Groups, in Applications of Fibonacci Numbers, Vol. 3 Eds. G. E. Bergum et al. Kluwer Academic Publishers, (1990), 27-35.
3. C.M. Campbell and P.P. Campbell, The Fibonacci Lengths of Binary Polyhedral Groups and Related Groups, Congressus Numerantium, 194 (2009), 95-102.
4. O. Deveci and E. Karaduman, The Pell Sequences in Finite Groups, Utilitas Mathematica, 96 (2015), 263-276.
5. O. Deveci, The Connections Between Fibonacci, Pell, Jacobsthal and Padovan Numbers, is submitted.
6. R. Dikici and G.C. Smith, Fibonacci Sequences in Finite Nilpotent Groups, Turkish Journal of Mathematics, 21 (1997), 133-142.
7. D.L. Johnson, J.W. Wamsley and D. Wright, The Fibonacci Groups, Proceedings of the London Mathematical Society, 3 (1974), 577-592.
8. S.W. Knox, Fibonacci Sequences in Finite Groups, Fibonacci Quarterly, 30(2) (1992), 116-120.
9. K. Lü and J. Wang, *k*-step Fibonacci Sequence Modulo m, Utilitas Mathematica, 71 (2007), 169-178.
10. D.D. Wall, Fibonacci Series Modulo m, The American Mathematical Monthly, 67 (1960), 525-532.
11. H.J. Wilcox, Fibonacci Sequences of Period n in Groups, Fibonacci Quarterly, 24 (1986), 356-361.

The Laplace Transform of Distribution Functions of A Semi-Markovian Random Walk Process with Positive Tendency and Negative Jumps

Selahattin MADEN[1] and Ulviyya Y. KARIMOVA[2]

[1]*Department of Mathematics, Faculty of Arts and Sciences, Ordu University, 52200, Ordu, TURKEY,* selahattinmaden55@gmail.com

[2]*Department of İnternational Relations and Economy, Baku State University, Baku, AZERBAIJAN,* ulviyye_kerimova@yahoo.com

Abstract: One of the important problems of stochastic process theory is to define the Laplace transformations for the distribution of this process. With this purpose, we will investigate a semi-Markovian random walk process with positive tendency and negative jumps in this article. The first falling moment to a certain level of this process is constructed as mathematically and the Laplace transform of this random variable is obtained.

Keywords: Semi-Markovian Random Walk, Laplace Transform, Erlang Distribution.

MSC Subject Classification: 60A10, 60J25, 60G50

1. INTRODUCTION

In recent years, random walks with one or two barriers are being used to solve a number of very interesting problems in the fields of inventory, queues and reliability theories, mathematical biology etc. Many good monographs in this field exist in literature (see references [1]-[3] and etc.).

In particular, a number of very interesting problems of stock control, queues and reliability theories can be expressed by means of random walks with two barriers. These barriers can be reflecting, delaying, absorbing, elastic, etc., depending on concrete problems at hand. For instance, it is possible to express random levels of stock in a warehouse with finite volumes or queueing systems with finite waiting time or sojourn time by means of random walks with two delaying barriers. Furthermore, the functioning of stochastics systems with spare equipment can be given by random walks with two barriers, one of them is delaying and the other one is any type barrier.

It is known that the most of the problems of stock control theory is often given by means of random walks or random walks with delaying barriers (see References 1-2 etc.). Numerous studies have been done about step processes of semi-Markovian random walk with two barriers of their practical and theoretical importance. But in the most of these studies the distribution of the process has free distribution. Therefore the obtained results in this case are cumbersome and they will not be useful for applications ([1]-[4] and etc.).

The investigations of the distributions for the processes of semi-Markovian random process have an important value in the random process theory. There are number of works devoted to definition of the Laplace transforms for the distribution of the first passage time of the zero level. Some authors are used the asymptotic, factorization and etc. methods (see references [1], [2] and [5]). But other authors narrowing the class of distributions of walking are found the evident form for Laplace transforms for distributions and its main characteristics (see [3], [4]).

The purpose of the present article is to find the Laplace transforms for Erlang distribution of the semi-Markovian random processes with positive tendency and negative jumps. The first passage of the zero level of the semi-Markovian process with positive tendency and negative jumps will be included as a random variable. The Laplace transform for the distribution of this random variable is defined.

2. MAIN RESULTS

Suppose that $\{(\xi_i, \zeta_i)\}$, $i = 1,2,3,\ldots$ is a sequence of identically and independently distributed pairs of random variables, defined on any probability space $(\Omega, \mathcal{F}, P)$ such that ξ_i's are positive valued, i.e., $P\{\xi_i > 0\} = 1$, $i = 1,2,3,\ldots$. In addition, the random variables ξ_i and ζ_i are mutually independent as well.

Also let us denote the distribution function of ξ_1 and ζ_1

$$\Phi(t) = P\{\xi_1 < t\}, \quad \mathrm{F}(x) = P\{\zeta_1 < x\}, t \in \mathbb{R}^+, x \in \mathbb{R}, \qquad (2.1)$$

respectively. By using the random pairs (ξ_i, ζ_i) we can construct the following process of a semi-Markovian random walk

$$X(t) = z + t.tan\alpha - \sum_{i=1}^{k} \zeta_i, \ if \ \sum_{i=1}^{k} \xi_i \le t < \sum_{i=1}^{k+1} \xi_i, \ k = 0,1,2,\ldots, \ t > 0, \qquad (2.2)$$

where the number $X(0) = z > 0$ is given. $X(t)$ process is called as a semi-Markovian random walk process with positive tendency and negative jumps. One of the realizations of the process $X(t)$ will be in the following form:

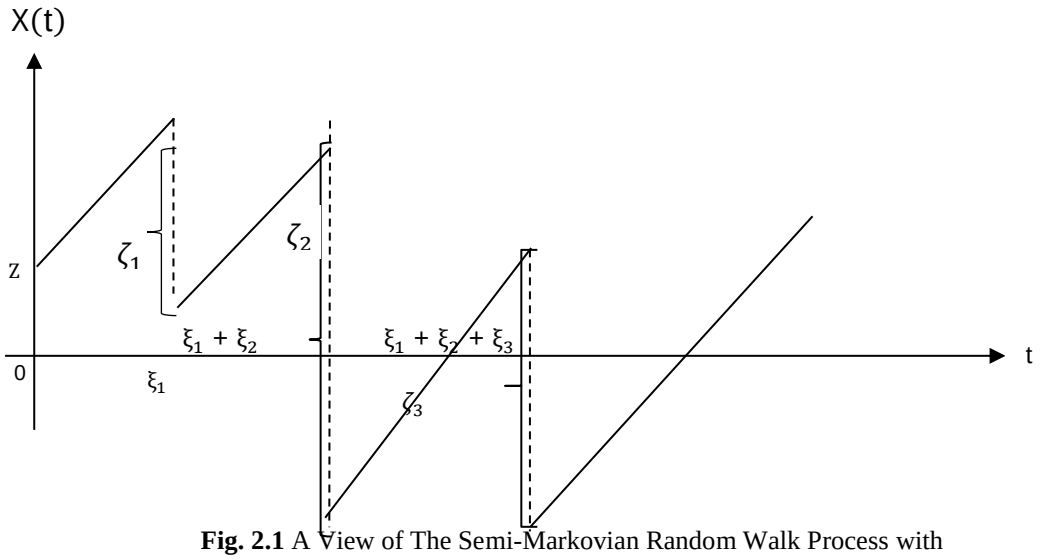

Fig. 2.1 A View of The Semi-Markovian Random Walk Process with positive tendency and negative jumps.

Now, we introduce the random variables τ_a and γ_a as follows:

$$\tau_a = inf\{k: X(t) \geq a\},\ k = 0,1,2,\ldots \tag{3.1}$$

$$\gamma_a = X(\tau_a) - a\ . \tag{3.2}$$

In this case, random variable τ_a denotes the first falling time to $a(a > 0)$ -level of the process $X(t)$. Furthermore, we get $\tau_a = +\infty$ when $X(t) < a$ for every t. Also, the random variable γ_a denotes the first jumping time from $a(a > 0) -$ level of the process $X(t)$. This random variables play an important role in solving of most probability problems arising in control of random levels of stocks in a warehouse which is functioning according to the process $X(t)$. For this reason, the consideration with detailed of random variables τ_a and γ_a seems very interesting from scientific and practical point of view.

The aim of the present work is to determine the Laplace-Stieltjes transform of the common distribution function of the random variables τ_a and γ_a. Denote the Laplace transform of the common distribution function of the random variables τ_a and γ_a by

$$E\left[e^{-\theta\tau_a - \mu\gamma_a}|X(0) = z\right],\quad \theta > 0, \mu > 0.$$

Now, let us give an analytical expression for random variable (τ_a, γ_a):

$$\xi_i^0 = \xi_i.tan\alpha, \qquad i = 0,1,2,\ldots$$

We can interprete random variable $\gamma_a -$ the number of jumps during the first passing time to $a(a > 0)$ -level of the process $X(t)$. Note that the process $X(t)$ can be pass from $a(a > 0)$ -level on the time of any step, for example, first, second or etc. Therefore we can write (τ_a, γ_a) as follows:

$$(\tau_a, \gamma_a) = \begin{cases} \tau_a = (a - z)cot\alpha, \quad \gamma_a = z + \xi_i^0 - a, & z + \xi_i^0 > a \\ \tau_a = \xi_1 + T,\ \gamma_a = z + \sum_{i=1}^{\nu_a} \xi_i^0 - \sum_{i=1}^{\nu_a - 1} \zeta_i - a\ , & z + \xi_i^0 < a \end{cases}$$

where τ_a and T are identically and independently distributed random variables. Denote the Laplace transform of the conditional common distribution of the random variable (τ_a, γ_a) by

$$\mathrm{L}(\theta, \mu|z) = E\left[e^{-\theta\tau_a - \mu\gamma_a}|X(0) = z\right],\quad \theta > 0,\ \mu > 0 \tag{3.3}$$

Now, we can give an integral equation for the Laplace transform of the conditional common distribution of the random variable (τ_a, γ_a). According to the total probability formula, we can write

$$\mathrm{L}(\theta, \mu|z) = E\left[e^{-\theta\tau_a - \mu\gamma_a}|X(0) = z\right]$$

$$= \int_{z+\xi_1^0 > a} e^{-\theta(a-z)cot\alpha - \mu(z+\xi_i^0 - a)} P(d\omega) \tag{3.4}$$

$$+\int_{z+\xi_1^0<a}^{a} e^{-\theta(\xi_1+T)-\mu\left(z+\sum_{i=1}^{\gamma_a}\xi_i^0-\sum_{i=1}^{\gamma_a-1}\zeta_i-a\right)}P(d\omega|X(0)=z+\xi_1^0-\zeta_1)$$

by using (2.2). Applying some substitutions, we obtain that

$$\mathrm{L}(\theta,\mu|z)=e^{(\mu-\theta cot\alpha)(a-z)}\int_{z+\xi_1^0>a}e^{-\mu\xi_1^0}P(d\omega)+e^{\mu(a-z)} \tag{3.5}$$

$$\cdot\int_{z+\xi_1^0<a}e^{-\theta(\xi_1+T)-\mu\sum_{i=1}^{\gamma_a}\xi_i^0+\mu\sum_{i=1}^{\gamma_a-1}\zeta_i}P(d\omega|X(0)=z+\xi_1^0-\zeta_1).$$

On the other hand, since γ_a can be the numbers $1,2,\ldots$ and etc., according to the total probability formula, we can write

$$\mathrm{L}(\theta,\mu|z)=e^{(\mu-\theta cot\alpha)(a-z)}\int_{z+\xi_1^0>a}e^{-\mu\xi_1^0}P(d\omega)$$

$$+e^{\mu(a-z)}\sum_{k=1}^{\infty}\int_{z+\xi_1^0<a}e^{-\theta(\xi_1+T)-\varkappa\sum_{i=1}^{k}\xi_i^0+\mu\sum_{i=1}^{k-1}\zeta_i}$$

$$\cdot P(d\omega|X(0)=z+\xi_1^0-\zeta_1)P(\gamma_a=k|X(0)=z) \tag{3.6}$$

from the expression (3.4). By substituting $\xi_i=t_i$, $\zeta_i=h_i$, $i\geq 1$ and $T=u$, we get the following integral equation for $\mathrm{L}(\theta,\mu|z)$:

$$\mathrm{L}(\theta,\mu|z)=e^{(\varkappa-\theta cot\alpha)(a-z)}\int_{t=(a-z)cot\alpha}^{\infty}e^{-\mu t.tan\alpha}dP(\xi_1<\mathrm{t})+e^{\mu(a-z)}$$

$$\cdot\int_{t_1=0}^{a-z}e^{-(\theta+\mu.tan\alpha)t_1}\,\mathrm{L}(\theta|z+t_1.tan\alpha-h_1).\ dP(\xi_1<t_1)dP\{\zeta_1<h_1\}$$

$$\cdot\sum_{k=1}^{\infty}\int_{t_2=0}^{\infty}e^{-\mu t_2\,tan\alpha}dP\{\xi_2<t_2\}\ldots\int_{t_k=0}^{\infty}e^{-\mu t_k\,tan\alpha}\,dP\{\xi_k<t_k\} \tag{3.7}$$

$$\cdot\int_{h_1=0}^{\infty}e^{\mu h_1}\,dP\{\zeta_1<h_1\}\ldots\int_{h_{k-1}}^{\infty}e^{\mu h_{k-1}}\,dP\{\zeta_{k-1}<h_{k-1}\}P\{\gamma_a=k|X(0)=z\}$$

In this case, $\mathrm{L}(\theta|z+t_1.tan\alpha-h)$ –is the Laplace-Stieltjes transform of the first passing time from $a(a>0)-$ level of the process $X(t)$. Therefore we can get $z+t_1.tg\alpha-h$ as the initial position of the process $X(t)$.

Let us denote

$$\varphi_{\xi_1}(\mu.tan\alpha)=\int_{t=0}^{\infty}e^{-\mu t.tan\alpha}dP\{\xi_1<\mathrm{t}\}$$

$$\varphi_{\zeta_1}(\mu)=\int_{h=0}^{\infty}e^{\mu h}dP\{\zeta_1<h\ \}.$$

Then, it is rewritten (3.7) as follows

$$\mathrm{L}(\theta,\mu|z) = e^{-(\mu-\theta cot\alpha)(a-z)}\int_{t=(a-z)cot\alpha}^{\infty} e^{-\theta t.tan\alpha}dP(\xi_1 < \mathrm{t}) + e^{\mu(a-z)}$$

$$\cdot\int_{h=0}^{\infty}\int_{\mathrm{t}=0}^{(a-z)cot\alpha} e^{-(\theta+\mu.tan\alpha)\mathrm{t}}\mathrm{L}(\theta|z+\mathrm{t}.tan\alpha-h)dP(\xi_1<\mathrm{t})dP\{\zeta_1<\mathrm{h}\}$$

$$\cdot\sum_{k=1}^{\infty}\left[\varphi_{\xi_1}(\mu.tan\alpha)\right]^{k-1}\left[\varphi_{\zeta_1}(\mu)\right]^{k-1} \qquad (3.8)$$

since random variables ξ_i and ζ_i, $i \geq 1$, are independent.

Now, assume that there are the following functions for the random variable ζ_1:

$$\varphi_{\xi_1}(\mu.\tan\alpha)\varphi_{\zeta_1}(\mu) < 1.$$

$$\psi(\mu) = \sum_{k=1}^{\infty}\left[\varphi_{\xi_1}(\mu tan\alpha)\varphi_{\zeta_1}(\mu)\right]^{k-1}. \qquad (3.9)$$

Therefore, we can write the Laplace-Stieltjes transform of the conditional common distribution of random variable (τ_a, γ_a) as the following integral equation:

$$\mathrm{L}(\theta,\mu|z) = e^{-(\mu-\theta cot\alpha)(a-z)}$$

$$\cdot\int_{t=(a-z)cot\alpha}^{\infty} e^{-\theta t.tan\alpha}dP(\xi_1<\mathrm{t}) + e^{-\mu(a-z)}\psi(\mu) \qquad (3.10)$$

$$\cdot\int_{h=0}^{\infty}\int_{\mathrm{u}=z-h}^{a-h} e^{-(\theta+\mu.tan\alpha)(u+h-z)cot\alpha}\mathrm{L}(\theta|u)\,dP(\xi_1<(u+h-z)cot\alpha)dP\{\zeta_1<\mathrm{h}\}$$

from (3.8) by substituting $u = z + \mathrm{t}.tan\alpha - h \implies t = (u+h-z)cot\alpha$. The integral equation given in (3.10) for $\mathrm{L}(\theta,\mu|z)$ can be solved by method of successive approximations for arbitrarily distributed random variables ξ_i and η_i, $i \geq 1$, but it is unsuitable for applications. On the other hand, this equation has a solution in explicit form in the classes of Erlang distributions. Therefore, this integral equation will be solved in the cases that the random variables ξ_1 and ζ_1 have an Erlang distribution of first order with the parameters λ_1 and λ_2 respectively. In this case, we have

$$P\{\xi_1 < \mathrm{t}\} = \left[1 - e^{-\lambda_1 t}\right]\varepsilon(t), \quad \lambda_1 > 0$$

$$P\{\zeta_1 < \mathrm{t}\} = \left[1 - e^{-\lambda_2 t}\right]\varepsilon(t), \quad \lambda_2 > 0 \qquad (3.11)$$

where $\varepsilon(t) = \begin{cases} 0, & \mathrm{t} < 0, \\ 1, & \mathrm{t} > 0. \end{cases}$

Therefore, aaccording to the total probability formula, we have the following integral equation for the Laplace transform of the conditional distribution of random variables ξ_1 and ζ_1

$$\varphi_{\xi_1}(\mu tan\alpha) = \lambda_1\int_{t=0}^{\infty} e^{-\mu tan\alpha.t}e^{-\lambda_1 t}dt = \frac{\lambda_1}{\lambda_1+\mu tan\alpha},$$

$$\varphi_{\zeta_1}(\mu) = \lambda_2 \int_{t=0}^{\infty} e^{\mu t} e^{-\lambda_2 t} dt = \frac{\lambda_2}{\lambda_2 - \mu}, \qquad \lambda_2 > \mu \ .$$

So, the general solution of integral equation (3.10) will be as follows:

$$\psi(\mu) = \frac{(\lambda_1 + \mu tan\alpha)(\lambda_2 - \mu)}{-\lambda_1 \mu + (\lambda_1 + \mu tan\alpha)\lambda_2},$$

$$L(\theta, \mu | z) = \frac{\lambda_1}{\lambda_1 + \theta tan\alpha} e^{-(\mu + \theta cot\alpha (tg\alpha - 1) + \lambda_1)(a - z)} +$$

$$+ \frac{\lambda_1 \lambda_2 e^{\mu(a-z)}}{\lambda_2 + K_1(\theta)} \psi(\mu). \frac{e^{-K_1(\theta)(a-z)} - e^{-(\lambda_1 + \theta + \mu . tan\alpha) cot\alpha (a-z)}}{(\lambda_1 + \theta + \mu . tan\alpha) cot\alpha - K_1(\theta)}$$

Conclusion: In this article we have defined Laplace transforms for Erlang distribution of the first falling time to zero level of semi-Markovian random process with positive tendency and negative jump. The obtained results can be applied in the theores of queuing, insurance, finance, and inventory management.

REFERENCES

1. Borovkov, A. A., *Stochastic Processes in The Theory of Queues*, Nauka, Moscow 1972.
2. Borovkov A. A., 'On the asymptotic behaviour of the distributions of the first passage', Mat. Zametki, Vol.75, No.1, pp.24–39, (2004).
3. Lotov, V. I., On some boundary crossing problems for gaussian random walks, The Annals of Probab., 24, 1996, pp.2154–2171, (1996).
4. Nasirova, T. I. (1984). Processes of Semi-Markovian Random Walk, ELM, Baku, 165p.
5. Nasirova T. I. and Kerimova U. Y., (2011). Definition of Laplace Transforms for the Distribution of the First Passage of Zero Level of the Semi-Markovian Random Process with Positive Tendency and Negative Jump Applied Mathematics, No:2, 908-917.
6. Maden, S., (2018). Distribution of the Lower Boundary Functional of the Step Process of Semi-Markovian Random Walk with Delaying Barrier, Karaelmas Science and Engineering Journal, 8(2):491-495.
7. Maden, S. and Karimova, U. Y., (2017). Determination of the laplace transform for the first falling moment to zero level of a semi-Markovian random process New Trends in Mathematical Sciences 4(5):165-171.
8. Nasirova, T. I., and Shamilova, B. G., (2014).Investigation of Some Probabilistic Characteristics of One Class of Semi Markovian Wandering with Delaying Screens, Automatic Control and Computer Sciences, Vol. 48, No. 2, 109–119.
9. Nasirova, T. I., Sadikova, R. I., and Ibaev, E. A.,(2015). Determination of the Mean and Mean Square Deviations of the System Level, Automatic Control and Computer Sciences, 49(1), 37–45.
10. Omarova, K. K., Bakhshiev, S. B., (2010). The Laplace Transform for Distribution of the Lower Bound Functional in a Semi Markovian Walk Process with a Delay Screen at Zero, Automatic Control and Computer Sciences, 44(4), 246-252.

Integral Operators Involving q - Poisson Distribution Series

Semra KORKMAZ[1], Nizami MUSTAFA[2], Veysel NEZİR[3]

[1,2,3] *Department of Mathematics, Faculty of Science and Letters, Kafkas University, Kars, Turkey*

korkmazsemra36@outlook.com; nizamimustafa@gmail.com; veyselnezir@yahoo.com

Abstract. The q - derivative operator has been used to investigate several subclasses of analytic functions in different ways with different perspectives by many researchers and their interesting results are too voluminous to discuss. For example, the extension of the theory of univalent functions can be used to describe the theory of q - derivative. The q - derivative operator are also used to construct subclasses of analytic functions and so on.

In this study, we introduce and investigate certain subclasses of analytic and univalent functions defined by q - derivative. Here, we give some conditions for an analytic and univalent function to belong to these classes. Also, in the study, we define two integral operators involving analytic functions, which defined by q – Poisson Distortion series. Here, we aim to find the conditions for this operators to belong to these subclasses of analytic functions.

1. INTRODUCTION

Let A be the class of analytic functions f on the open unit disk $U=\{z\in\mathbb{C}:\ |z|<1\}$ in the complex plane, normalized by $f(0)=0=f'(0)-1$ of the form

$$f(z)=z+a_2z^2+a_3z^3+\cdots+a_nz^n+\cdots=z+\sum_{n=2}^{\infty}a_nz^n,\ a_n\in\mathbb{C}. \tag{1.1}$$

Also, by S we will denote the family of all functions in A which are univalent in U.
Let T denote the subclass of all functions f in A of the form

$$f(z)=z-a_2z^2-a_3z^3-\cdots-a_nz^n-\cdots=z-\sum_{n=2}^{\infty}a_nz^n,\ a_n\geq 0. \tag{1.2}$$

Some of the important and well-investigated subclasses of the univalent functions class S include the classes $S^*(\alpha)$ and $C(\alpha)$, respectively, starlike and convex functions of order α $(\alpha\in[0,1))$ on the open unit disk U in the complex plane.

By definition, we have (see for details, [2, 3], also [8])

$$S^*(\alpha)=\left\{f\in A:\ \mathrm{Re}\left(\frac{zf'(z)}{f(z)}\right)>\alpha,\ z\in U\right\},\ C(\alpha)=\left\{f\in A:\ \mathrm{Re}\left(1+\frac{zf''(z)}{f'(z)}\right)>\alpha,\ z\in U\right\}.$$

For $\beta\in[0,1)$, interesting generalization of the function classes $S^*(\alpha)$ and $C(\alpha)$ are the classes $S^*(\alpha,\beta)$ and $C(\alpha,\beta)$, which defined as follows

$$S^*(\alpha,\beta)=\left\{f\in S:\ \mathrm{Re}\left(\frac{zf'(z)}{\beta zf'(z)+(1-\beta)f(z)}\right)>\alpha,\ z\in U\right\},$$

$$C(\alpha,\beta)=\left\{f\in S:\ \mathrm{Re}\left(\frac{f'(z)+zf''(z)}{f'(z)+\beta zf''(z)}\right)>\alpha,\ z\in U\right\}.$$

Let us $TS^*(\alpha,\beta)=T\cap S^*(\alpha,\beta)$ and $TC(\alpha,\beta)=T\cap C(\alpha,\beta)$.

The classes $TS^*(\alpha,\beta)$ and $TC(\alpha,\beta)$ were extensively studied by Altintaş and Owa [1] and certain conditions for hypergeometric functions and generalized Bessel functions for these classes were studied Moustafa [5] and Porwal and Dixit [7].

A generalization of the function classes $S^*(\alpha,\beta)$ and $C(\alpha,\beta)$ is the function class $S^*C(\alpha,\beta;\gamma)$ for $\gamma\in[0,1]$, which defined as follows

$$S^*C(\alpha,\beta;\gamma)=\left\{f\in S:\mathrm{Re}\left(\frac{zf'(z)+\gamma z^2f''(z)}{\gamma z\left(f'(z)+\beta zf''(z)\right)+(1-\gamma)\left(\beta zf'(z)+(1-\beta)f(z)\right)}\right)>\alpha\right\},\ z\in U.$$

In his fundamental paper [4] Jackson introduced the q - derivative operator D_q of the function f, for $q\in(0,1)$. The formulas for the q - derivative D_q of a product and a quotient of functions are

$$D_qz^n=[n]_qz^{n-1},\ n\in\square,$$

where

$$[n]_q=\frac{1-q^n}{1-q}=\sum_{k=1}^{n}q^{k-1}$$

is the q - analogue of the natural numbers n.
It is clear that

$$[0]_q=0,\ [1]_q=1,\ \lim_{q\to1^-}[n]_q=n$$

and

$$\lim_{q\to1^-}D_qf(z)=f'(z)$$

for the function $f\in A$.

For $q\in(0,1)$ and $\alpha\in[0,1)$, we define by $S_q^*(\alpha)$ and $C_q(\alpha)$ the subclasses of A which we will call, respectively, q - starlike and q - convex functions of order α

$$S_q^*(\alpha)=\left\{ f\in S:\ \operatorname{Re}\frac{zD_q f(z)}{f(z)}>\alpha, z\in U\right\},\ C_q(\alpha)=\left\{ f\in S:\ \operatorname{Re}\frac{D_q\left(zD_q f(z)\right)}{D_q f(z)}>\alpha, z\in U\right\}.$$

Also, let's $TS_q^*(\alpha)=T\cap S_q^*(\alpha)$ and $TC_q(\alpha)=T\cap C_q(\alpha)$.

Interesting generalization of the function classes $S_q^*(\alpha)$ and $C_q(\alpha)$ for $\beta\in[0,1)$ are the classes $S_q^*(\alpha,\beta)$ and $C_q(\alpha,\beta)$, which we define as follows

$$S_q^*(\alpha,\beta)=\left\{ f\in A:\ \operatorname{Re}\left(\frac{zD_q f(z)}{\beta zD_q f(z)+(1-\beta)f(z)}\right)>\alpha,\ z\in U\right\},$$

$$C_q(\alpha,\beta)=\left\{ f\in A:\ \operatorname{Re}\left(\frac{D_q f(z)+zD_q^2 f(z)}{D_q f(z)+\beta zD_q^2 f(z)}\right)>\alpha,\ z\in U\right\}.$$

Inspired by the studies mentioned above, we introduce a generalization of the function classes $S_q^*(\alpha,\beta)$ and $C_q(\alpha,\beta)$ by the following definition.

Definition 1. *A function* f *given by (1.1) is said to be in the class* $S_q^*C_q(\alpha,\beta;\gamma)$, $\alpha,\beta\in[0,1)$, $\gamma\in[0,1]$ *if the following condition is satisfied*

$$\operatorname{Re}\left(\frac{zD_q f(z)+\gamma z^2 D_q^2 f(z)}{\gamma z\left(D_q f(z)+\beta zD_q^2 f(z)\right)+(1-\gamma)\left(\beta zD_q f(z)+(1-\beta)f(z)\right)}\right)>\alpha, z\in U.$$

We will use $TS_q^*C_q(\alpha,\beta;\gamma)=T\cap S_q^*C_q(\alpha,\beta;\gamma)$.

It is clear that $S_q^*C_q(\alpha,\beta;0)=S_q^*(\alpha,\beta)$, $S_q^*C_q(\alpha,\beta;1)=C_q(\alpha,\beta)$, $\lim_{q\to 1^-}S_q^*C_q(\alpha,\beta;\gamma)=S^*C(\alpha,\beta;\gamma)$ and $\lim_{q\to 1^-}TS_q^*C_q(\alpha,\beta;\gamma)=TS^*C(\alpha,\beta;\gamma)$. So, function classes $S_q^*C_q(\alpha,\beta;\gamma)$ and $TS_q^*C_q(\alpha,\beta;\gamma)$ are generalization of the previously known function classes $S_q^*(\alpha,\beta)$, $C_q(\alpha,\beta)$, $S^*C(\alpha,\beta;\gamma)$ and $TS^*C(\alpha,\beta;\gamma)$ of analytic functions, respectively.

A variable x is said to have q - Poisson Distribution if it takes the values 0,1,2,3,… with probabilities e_q^{-p}, $\frac{p}{1!}e_q^{-p}$, $\frac{p^2}{2!}e_q^{-p}$, $\frac{p^3}{3!}e_q^{-p},\ldots$, respectively, where p a parameter and

$$e_q^x=1+x+\frac{x^2}{[2]_q!}+\frac{x^3}{[3]_q!}+\cdots+\frac{x^n}{[n]_q!}+\cdots=\sum_{n=0}^{\infty}\frac{x^n}{[n]_q!}$$

is q - exponential function and

$$[n]_q ! = [1]_q \cdot [2]_q \cdot [3]_q \cdots [n]_q$$

is the q - analogue of factorial

$$n! = 1 \cdot 2 \cdot 3 \cdots n .$$

Thus, for q - Poisson Distribution, we have

$$P_q(x = n) = \frac{p^n}{[n]_q !} e_q^{-p}, \ n = 0,1,2,3,\ldots .$$

Now, we introduce a q - Poisson Distribution series as follows

$$z + \sum_{n=2}^{\infty} \frac{p^{n-1} e_q^{-p}}{[n-1]_q !} z^n, \ z \in U . \tag{1.3}$$

We can easily show that series (1.3) is convergent and the radius of convergence is infinity.

Let us, we define function $F_q : \square \to \square$ by

$$F_q(z) = z + \sum_{n=2}^{\infty} \frac{p^{n-1} e_q^{-p}}{[n-1]_q !} z^n, \ z \in U . \tag{1.4}$$

Let's

$$G_q(z) = 2z - F_q(z) = z - \sum_{n=2}^{\infty} \frac{p^{n-1} e_q^{-p}}{[n-1]_q !} z^n, \ z \in U . \tag{1.5}$$

It is clear that $F_q \in A$ and $G_q \in T$, respectively.

Now, we introduce two integral operators involving these functions F_q and G_q, respectively, as follows

$$\hat{F}_q(z) = \int_0^z \frac{F_q(t)}{t} d_q t \tag{1.6}$$

and

$$\hat{G}_q(z) = \int_0^z \frac{G_q(t)}{t} d_q t . \tag{1.7}$$

In this study, using q - derivative we introduce certain subclasses of analytic and univalent functions on the open unit disk in the complex plane. Here, we give some conditions for an analytic and univalent function to belong to these classes. Applications of a q - Poisson Distribution series on the analytic functions are also given. In the study, we introduce two integral operators $\hat{F}_q$ and $\hat{G}_q$ involving functions F_q and G_q defined, respectively, by (1.4) and (1.5), and we aim to find the conditions for this integral operators to belonging to subclasses of analytic functions defined above.

2. MAIN RESULTS

In this section, we will give sufficient condition for the integral operator $\hat{F}_q$ defined by (1.6), belonging to the class $S_q^* C_q(\alpha,\beta;\gamma)$, and necessary and sufficient condition for the integral operator $\hat{G}_q$ defined by (1.7), belonging to the class $TS_q^* C_q(\alpha,\beta;\gamma)$, respectively.

In order to prove our main results, we need the following theorems, which one can be proved easily.

Theorem 1. *Let* $f \in A$. *Then,* $f \in S_q^* C_q(\alpha,\beta;\gamma)$ *if the following condition is satisfied*

$$\sum_{n=2}^{\infty}\left\{[n]_q\left[(1-\alpha\beta)\left(1+\gamma[n-1]_q\right)-(1-\beta)\alpha\gamma\right]-\alpha(1-\beta)(1-\gamma)\right\}|a_n|\le 1-\alpha .$$

The result obtained here is sharp.

Theorem 2. *Let* $f \in T$. *Then,* $f \in TS_q^* C_q(\alpha,\beta;\gamma)$ *if and only if*

$$\sum_{n=2}^{\infty}\left\{[n]_q\left[(1-\alpha\beta)\left(1+\gamma[n-1]_q\right)-(1-\beta)\alpha\gamma\right]-\alpha(1-\beta)(1-\gamma)\right\}|a_n|\le 1-\alpha .$$

The result obtained here is sharp.

A sufficient condition for the function $\hat{F}_q$ defined by (1.6) to belonging to the class $S_q^* C_q(\alpha,\beta;\gamma)$ is given by the following theorem.

Theorem 3. *Let* $p>0$ *and the following condition is satisfied*

$$\left[(1-\alpha\beta)\gamma p+\alpha(1-\beta)(1-\gamma)\left(1-\left(1-e_q^{-p}\right)p^{-1}\right)\right]e_q^p \le 1-\alpha . \tag{2.1}$$

Then, the function $\hat{F}_q$ *defined by (1.6) belongs to the class* $S_q^* C_q(\alpha,\beta;\gamma)$.

Proof. Since

$$\hat{F}_q(z) = z + \sum_{n=2}^{\infty} \frac{p^{n-1}}{[n]_q!} e_q^{-p} z^n,\ z \in U$$

according to Theorem 1, the function $\hat{F}_q$ belongs to the class $S_q^* C_q(\alpha, \beta; \gamma)$ if the following condition is satisfied

$$\sum_{n=2}^{\infty} \left\{ [n]_q \left[(1-\alpha\beta)\left(1+\gamma[n-1]_q\right) - (1-\beta)\alpha\gamma \right] - \alpha(1-\beta)(1-\gamma) \right\} \frac{p^{n-1}}{[n]_q!} e_q^{-p} \le 1-\alpha. \quad (2.2)$$

Let

$$L_q(\alpha, \beta; \gamma) = \sum_{n=2}^{\infty} \left\{ [n]_q \left[(1-\alpha\beta)\left(1+\gamma[n-1]_q\right) - (1-\beta)\alpha\gamma \right] - \alpha(1-\beta)(1-\gamma) \right\} \frac{p^{n-1}}{[n]_q!} e_q^{-p}.$$

Setting

$$\begin{aligned} &[n]_q \left[(1-\alpha\beta)\left(1+\gamma[n-1]_q\right) - (1-\beta)\alpha\gamma \right] - \alpha(1-\beta)(1-\gamma) \\ &= [n]_q \left[1-\alpha\beta-(1-\beta)\alpha\gamma \right] + [n]_q [n-1]_q (1-\alpha\beta)\gamma - \alpha(1-\beta)(1-\gamma) \end{aligned}$$

and by simple computation, we write

$$\begin{aligned} L_q(\alpha, \beta; \gamma) &= \sum_{n=2}^{\infty} \left\{ [n]_q \left[1-\alpha\beta-(1-\beta)\alpha\gamma \right] + [n]_q [n-1]_q (1-\alpha\beta)\gamma - \alpha(1-\beta)(1-\gamma) \right\} \frac{p^{n-1}}{e^p [n]_q!} \\ &= (1-\alpha\beta)\gamma p + \alpha(1-\beta)(1-\gamma)\left(1-\left(1-e_q^{-p}\right)p^{-1}\right) + (1-\alpha)\left(1-e_q^{-p}\right). \end{aligned}$$

Therefore, condition (2.2) holds true if

$$(1-\alpha\beta)\gamma p + \alpha(1-\beta)(1-\gamma)\left(1-\left(1-e_q^{-p}\right)p^{-1}\right) + (1-\alpha)\left(1-e_q^{-p}\right) \le 1-\alpha,$$

which is equivalent to (2.1).
Thus, the proof of Theorem 3 is completed.

From the Theorem 3, we can readily deduce the following results.

Corollary 1. *If* $p > 0$ *and satisfied the following condition*

$$\alpha(1-\beta)\left(1-\left(1-e_q^{-p}\right)p^{-1}\right)e_q^p \le 1-\alpha,$$

then the function $\hat{F}_q$ *defined by (1.6) belongs to the class* $S_q^*(\alpha, \beta)$.

Corollary 2. *If* $p>0$ *and satisfied the following condition*

$$(1-\alpha\beta)\,pe^{p}\le 1-\alpha$$

then the function $\hat{F}_q$ *defined by (1.6) belongs to the class* $C_q(\alpha,\beta)$.

Now, we give necessary and sufficient condition for the function $\hat{G}_q$ defined by (1.7), to belonging to the class $TS_q^{*}C_q(\alpha,\beta;\gamma)$ with the following theorem.

Theorem 4. *If* $p>0$, *then the function* $\hat{G}_q$ *defined by (1.7) belongs to the class* $TS_q^{*}C_q(\alpha,\beta;\gamma)$ *if and only if satisfied the following condition*

$$\left[(1-\alpha\beta)\gamma p+\alpha(1-\beta)(1-\gamma)\left(1-\left(1-e_q^{-p}\right)p^{-1}\right)\right]e_q^{p}\le 1-\alpha\,. \tag{2.3}$$

Proof. Firstly, let us prove the sufficiency of the theorem.
First of all, let us state that we will use Theorem 2 to prove the theorem.
It is clear that $\hat{G}_q\in T$. Let us show that the function $\hat{G}_q$ satisfies the sufficiency condition of Theorem 2.
From process of the proof of Theorem 3, we write

$$\begin{aligned}&\sum_{n=2}^{\infty}\left\{[n]_q\left[(1-\alpha\beta)\left(1+\gamma[n-1]_q\right)-(1-\beta)\alpha\gamma\right]-\alpha(1-\beta)(1-\gamma)\right\}\frac{p^{n-1}}{[n]_q!}e^{-p}\\&=(1-\alpha\beta)\gamma p+\alpha(1-\beta)(1-\gamma)\left(1-\left(1-e_q^{-p}\right)p^{-1}\right)+(1-\alpha)\left(1-e_q^{-p}\right).\end{aligned} \tag{2.4}$$

Now, suppose that condition (2.3) is satisfied. It follows that

$$(1-\alpha\beta)\gamma p+\alpha(1-\beta)(1-\gamma)\left(1-\left(1-e_q^{-p}\right)p^{-1}\right)\le(1-\alpha)e_q^{-p},$$

which is equivalent to

$$(1-\alpha\beta)\gamma p+\alpha(1-\beta)(1-\gamma)\left(1-\left(1-e_q^{-p}\right)p^{-1}\right)+(1-\alpha)\left(1-e_q^{-p}\right)\le 1-\alpha\,.$$

Hence, from (2.4), we have

$$\sum_{n=2}^{\infty}\left\{[n]_q\left[(1-\alpha\beta)\left(1+\gamma[n-1]_q\right)-(1-\beta)\alpha\gamma\right]-\alpha(1-\beta)(1-\gamma)\right\}\frac{p^{n-1}}{[n]_q!}e^{-p}\le 1-\alpha\,. \tag{2.5}$$

Thus, the function $\hat{G}_q$ satisfies the sufficiency condition of Theorem 2. Hence, the function $\hat{G}_q$ belongs to the class $TS_q^{*}C_q(\alpha,\beta;\gamma)$.

With this, the proof of the sufficiency of theorem is completed.

Now, let us we prove of the necessity of theorem.

Assume that $\hat{G}_q \in TS_q^* C_q(\alpha,\beta;\gamma)$. Then, from Theorem 2, we can write that condition (2.5) is satisfied.
It follows from (2.4) that

$$(1-\alpha\beta)\gamma p+\alpha(1-\beta)(1-\gamma)\left(1-\left(1-e_q^{-p}\right)p^{-1}\right)+(1-\alpha)\left(1-e_q^{-p}\right)\leq 1-\alpha,$$

which is equivalent to the condition (2.3).
This completes proof of the necessity of theorem.
So, the proof of Theorem 4 is completed.

From the Theorem 4, we can readily deduce the following results.

Corollary 3. *If* $p>0$, *then the function* $\hat{G}_q$ *defined by (1.7) belongs to the class* $TS_q^*(\alpha,\beta)$ *if and only if satisfied the following condition*

$$(1-\beta)\alpha\left((1-p^{-1})e_q^p+p^{-1}\right)\leq 1-\alpha\,.$$

Corollary 4. *If* $p>0$, *then the function* $\hat{G}_q$ *defined by (1.7) belongs to the class* $TC_q(\alpha,\beta)$ *if and only if satisfied the following condition*

$$(1-\alpha\beta)\,pe_q^p\leq 1-\alpha\,.$$

Remark 1. *The results obtained in Theorem 3, Theorem 4 and Corollary 1-4 are generalization of the results obtained in Theorem 5,6 and Corollary 9-12 in [6].*

REFERENCES

1. O. Altintaş and S. Owa, On subclasses of univalent functions with negative coefficients, Pusan Kyongnam Mathematical Journal, vol. 4, pp. 41-56, 1988.
2. P. L. Duren, Univalent Functions, Grundlehren der Mathematischen Wissenshaften, Bd. 259, New York, Springer-Verlag, Tokyo, 1983, 382p.
3. A. W. Goodman, Univalent Functions, Volume I, Polygonal, Washington, 1983, 246p.
4. F. H. Jackson, On q-functions and a certain difference operatör, Trans. Roy. Soc. Edin, vol. 46, 1908, 253-281.
5. A. O. Moustafa, A study on starlike and convex properties for hypergeometric functions, Journal of Inequalities in Pure and Applied Mathematics, vol. 10, no. 3, article 87, pp. 1-16, 2009.
6. N. Mustafa and S. Korkmaz, Analytic Functions Expressed with Poisson Distribution Series and their Some Properties, Journal of Contemporary Applied Mathematics, (submitted) 2020.
7. S. Porwal and K. K. Dixit, An application of generalized Bessel functions on certain analytic functions, Acta Universitatis Matthiae Belii. Series Mathematics, pp. 51-57, 2013.
8. H. M. Srivastava and S. Owa, Current Topics in Analytic Function Theory, World Scientific, Singapore, 1992, 456p.

Some Structures on Pythagorean Fuzzy Soft Topological Spaces

Taha Yasin ÖZTÜRK[1] and Adem YOLCU[2]

[1,2]*Department of Mathematics, Faculty of Science and Letters, Kafkas University, Kars-TURKEY*

taha36100@hotmail.com
yolcu.adem@gmail.com

Abstract. In this paper, along with the investigation of their many attributes, the concept of neighborhood, connectedness and compactness on pythagorean fuzzy soft topological space has been investigated. Some related theorems have been established as well.

1. INTRODUCTION

The most popular theories dealing with uncertainty are fuzzy set theory [27], intuitionistic fuzzy set theory [1], soft set theory [13], and rough set theory [16]. One of these theories, soft set theory, introduced by Molodtsov [13], and is distinct from other established theories due to its parametrization tools. Soft set theory is free from fuzzy set theory, rough set theory, underlying complexities and unclear information. Molodtsov introduced the basic findings of the new theory and successfully applied it in a variety of ways, such as smoothness of functions, game theory, operational analysis, Riemann integration, Peron integration, probability theory, etc. Maji et al. [10, 11, 12] focused on soft set theory and introduced the application of soft sets to decision-making problems.

Applications of these ideas occur in topology and many fields of mathematics. Chang [3], Shabir and Naz [21], Tanay et al.[23], D. Coker [4] and Z. Li et al. [9] were introduced the topological concepts of fuzzy, soft, fuzzy soft, intuitionistic fuzzy and intuitionistic fuzzy soft, respectively. Also, Karatas and Akdag [7] studied intuitionistic fuzzy soft continuous mapping, Osmanoglu and Tokat [15] studied intutionistic fuzzy soft topology, compactness and connectedness.

Defining intuitionistic fuzzy sets as $\mu + \nu \leq 1$ causes it to be useless in some problems. Therefore, pythagorean fuzzy set (PFS) proposed in Yager [24, 25] is a new method for dealing with vagueness given membership grade μ and non-membership grade ν satisfying condition $\mu^2 + \nu^2 \leq 1$. Pythagorean fuzzy set theory has a very similar relationship with intuitionistic fuzzy set theory. To define unclear information more adequately and reliably than intuitionistic fuzzy sets, the notion of pythagorean fuzzy sets can be used. This theory has recently attracted the attention of researcher [2, 6, 17, 19, 22, 28]. The Pythagorean fuzzy soft set theory was defined by Peng et al. [18], and its significant properties were studied. The Pythagorean fuzzy soft matrix and its different potential forms were investigated by Guleria and Bajaj [5]. M. Kirisci [8] defined the current Pythagorean fuzzy soft set form and suggested a decision-making problem solution. Pythagorean fuzzy topology was introduced by Olgun et al [14]. Riaz et al. [20] and Yolcu and Ozturk [26] investigated Pythagorean fuzzy soft topological spaces.

In this paper, we will discuss the concept of neighbourhood in a pythagorean fuzzy soft topological space, pythagorean fuzzy soft compactness and pythagorean fuzzy soft connectedness with some simple theorems.

2. PRELIMINARIES

Definition 1 [27] Let X be a universe. A fuzzy set F in X, $F = \{(x, \mu_F(x)) : x \in X\}$, where $\mu_F : X \to [0,1]$ is the membership function of the fuzzy set F; $\mu_F(x) \in [0,1]$ is the membership of $x \in X$ in f. The set of all fuzzy sets over X will be denoted by $FS(X)$.

Definition 2. [1] An intuitionistic fuzzy set F in X is $F = \{(x, \mu_F(x), \nu_F(x)) : x \in X\}$, where $\mu_F : X \to [0,1]$, $\nu_F : X \to [0,1]$ with the condition $0 \leq \mu_F(x) + \nu_F(x) \leq 1, \forall x \in X$. The numbers $\mu_F, \nu_F \in [0,1]$ denote the degree of membership and non-membership of x to F, respectively. The set of all intuitionistic fuzzy sets over X will be denoted by $IFS(X)$.

Definition 3. [13] Let E be a set of parameters and X be the universal set. A pair (F, E) is called a soft set over X, where F is a mapping $F: E \to \mathcal{P}(X)$. In other words, the soft set is a parameterized family of subsets of the set X.

Definition 4. [10] Let E be a set of parameters and X be the universal set. A pair (F, E) is called a fuzzy soft set over X, If $F: E \to FS(X)$ is a mapping from E into $FS(X)$ where $FS(X)$ is the set of all fuzzy subset of X.

Definition 5. [11] Let X be an initial universe E be a set of parameters. A pair (F, E) is called an intuitionistic fuzzy soft set over X, where F is a mapping given by, $F: E \to IFS(X)$.

In general, for every $e \in E$, $F(e)$ is an intuitionistic fuzzy set of X and it is called intuitionistic fuzzy value set of parameter e. Clearly, $F(e)$ can be written as a intuitionistic fuzzy set such that $F(e) = \{(x, \mu_F(x), v_F(x)) : x \in X\}$

Definition 6. [24] Let X be a universe of discourse. A pythagorean fuzzy set (PFS) in X is given by, $P = \{(x, \mu_P(x), v_P(x)) : x \in X\}$ where, $\mu_P : X \to 0,1]$ denotes the degree of membership and $v_p : X \to 0,1]$ denotes the degree of nonmembership of the element $x \in X$ to the set P with the condition that $0 \leq (\mu_P(x))^2 + (v_P(x))^2 \leq 1$.

Definition 7. [18] Let X be a universal set and E be a set of parameters. The pythagorean fuzzy soft set is defined as the pair (F, E) where, $F: E \to PFS(X)$ and $PFS(X)$ is the set of all Pythagorean fuzzy subsets of X. If $\mu_F^2(x) + v_F^2(x) \leq 1$ and $\mu_F(x) + v_F(x) \leq 1$, then pythagorean fuzzy soft sets degenerate into intuitionistic fuzzy soft sets.

Definition 8. [18] Let $A, B \subseteq E$ and $(F, A), (G, B)$ be two pythagorean fuzzy soft sets over X. (F, A) is said to be pythagorean fuzzy soft subset of (G, B) denoted by $(F, A) \tilde{\subseteq} (G, B)$ if,

1. $A \subseteq B$
2. $\forall e \in A$, $F(e)$ is a pythagorean fuzzy subset of $G(e)$ that is, $\forall x \in U$ and $\forall e \in A$, $\mu_{F(e)}(x) \leq \mu_{G(e)}(x)$ and $v_{F(e)}(x) \geq v_{G(e)}(x)$. If $(F, A) \tilde{\subseteq} (G, B)$ and $(G, B) \tilde{\subseteq} (F, A)$ then $(F, A), (G, B)$ are said to be equal.

Definition 9. [18] Let X be an initial universe E be a set of parameters and (F, E) be pythagorean fuzzy soft sets over X. The complement of (F, E) is denoted by $(F, E)^c$ and is defined by

$$(F, E)^c = \{(e, (x, v_{F(e)}(x), \mu_{F(e)}(x)) : x \in X) : e \in E\}$$

Definition 10. [8]

a) A pythagorean fuzzy soft set (F, E) over the universe X is said to be a null pythagorean fuzzy soft set if $\mu_{F(e)}(x) = 0$ and $v_{F(e)}(x) = 1$; $\forall e \in E, \forall x \in X$. It is denoted by $\tilde{0}_{(X,E)}$.

b) A pythagorean fuzzy soft set (F, E) over the universe X is said to be an absolute pythagorean fuzzy soft set if $\mu_{F(e)}(x) = 1$ and $v_{F(e)}(x) = 0$; $\forall e \in E, \forall x \in X$. It is denoted by $\tilde{1}_{(X,E)}$.

Definition 11. [8] Let (F, A) and (G, B) be two pythagorean fuzzy soft sets over the universe set X and E be a parameter set and $A, B \subseteq E$. Then,

a) Extended union of (F, A) and (G, B) is denoted by $(F, E) \tilde{\cup}_E (G, B) = (H, C)$ where $C = A \cup B$ and (H, C) defined by

$$(H, C) = \{(e, (x, \mu_{H(e)}(x), v_{H(e)}(x)) : x \in X) : e \in E\}$$

where

$$\mu_{H(e)}(x) = \begin{cases} \mu_{F(e)}(x) & , \text{if } e \in A - B \\ \mu_{G(e)}(x) & , \text{if } e \in B - A \\ \max\{\mu_{F(e)}(x), \mu_{G(e)}(x)\} & , \text{if } e \in A \cap B \end{cases}$$

$$v_{H(e)}(x) = \begin{cases} v_{F(e)}(x) & , \text{if } e \in A - B \\ v_{G(e)}(x) & , \text{if } e \in B - A \\ \min\{\mu_{F(e)}(x), \mu_{G(e)}(x)\} & , \text{if } e \in A \cap B \end{cases}$$

b) Extended intersection of (F,A) and (G,B) is denoted by $(F,E)\,\tilde{\cap}_E\,(G,B) = (H,C)$ where $C = A \cup B$ and (H,C) defined by

$$(H,C) = \{(e,(x,\mu_{H(e)}(x),\nu_{H(e)}(x)) : x \in X) : e \in E\}$$

where

$$\mu_{H(e)}(x) = \begin{cases} \mu_{F(e)}(x) & , \text{if } e \in A - B \\ \mu_{G(e)}(x) & , \text{if } e \in B - A \\ \min\{\mu_{F(e)}(x), \mu_{G(e)}(x)\}, & \text{if } e \in A \cap B \end{cases}$$

$$\nu_{H(e)}(x) = \begin{cases} \nu_{F(e)}(x) & , \text{if } e \in A - B \\ \nu_{G(e)}(x) & , \text{if } e \in B - A \\ \max\{\mu_{F(e)}(x), \mu_{G(e)}(x)\}, & \text{if } e \in A \cap B \end{cases}$$

Let X be an initial universe and $PFS(X)$ denote the family of pythagorean fuzzy sets over X and $PFSS(X,E)$ the family of all pythagorean fuzzy soft sets over X with parameters in E.

Definition 12. [26]Let $X \neq \emptyset$ be a universe set and $\tilde{\tau} \subset PFSS(X,E)$ be a collection of pythagorean fuzzy soft sets over X, then τ is said to be on pythagorean fuzzy soft topology on X if

(i) $\tilde{0}_{(X,E)}$, $\tilde{1}_{(X,E)}$ belong to $\tilde{\tau}$,
(ii) The union of any number of pythagorean fuzzy soft sets in $\tilde{\tau}$ belongs to $\tilde{\tau}$,
(iii) The intersection of any two pythagorean fuzzy soft sets in $\tilde{\tau}$ belongs to $\tilde{\tau}$.

The triple $(X,\tilde{\tau},E)_p$ is called an pythagorean fuzzy soft topological space over X. Every member of τ is called a pythagorean fuzzy soft open set in X.

Definition 13. [26]
a) Let X be an initial universe set, E be the set of parameters and $\tilde{\tau} = \{\tilde{0}_{(X,E)}, \tilde{1}_{(X,E)}\}$. Then $\tilde{\tau}$ is called a pythagorean fuzzy soft indiscrete topology on X and $(X,\tilde{\tau},E)_p$ is said to be a pythagorean fuzzy soft indiscrete space over X.
b) Let X be an initial universe set and E be the set of parameters and $\tilde{\tau}$ be the collection of all pythagorean fuzzy soft sets which can be defined over X. Then $\tilde{\tau}$ is called a pythagorean fuzzy soft discrete topology on X and $(X,\tilde{\tau},E)_p$ is said to be a pythagorean fuzzy soft discrete space over X.

Definition 14. [26] Let $(X,\tilde{\tau},E)_p$ be a pythagorean fuzzy soft topological space over X. A pythagorean fuzzy soft set (F,E) over X is said to be a pythagorean fuzzy soft closed set in X, if its complement $(F,E)^c$ belongs to $\tilde{\tau}$.

Proposition 1. [26] Let $(X,\tilde{\tau},E)_p$ be a pythagorean fuzzy soft topological space over X. Then, the following properties hold.

(i) $\tilde{0}_{(X,E)}$, $\tilde{1}_{(X,E)}$ are pythagorean fuzzy soft closed sets over X.
(ii) The intersection of any number of pythagorean fuzzy soft closed sets is a pythagorean fuzzy soft closed set over X.
(iii) The union of any two pythagorean fuzzy soft closed sets is a pythagorean fuzzy soft closed set over X.

Definition 15. [26] Let $(X,\tilde{\tau},E)_p$ be a pythagorean fuzzy soft topological space over X and (F,E) be a pythagorean fuzzy soft set over X. The pythagorean fuzzy soft closure of (F,E) denoted by $pcl(F,E)$ is the intersection of all pythagorean fuzzy soft closed supersets of (F,E).

Clearly $pcl(F,E)$ is the smallest pythagorean fuzzy soft closed set over X which contains (F,E).

Definition 16. [26] Let $(X,\tilde{\tau},E)_p$ be a pythagorean fuzzy soft topological space over X and $(H,E) \in PFSS(X,E)$. The pythagorean fuzzy soft interior of (H,E), denoted by $pint(H,E)$, is the union of all the pythagorean fuzzy soft open sets contained in (H,E).

Definition 17. [26] Let $(X,\tilde{\tau}_1,E)_p$, $(Y,\tilde{\tau}_2,E')_p$ be two pythagorean fuzzy soft topological spaces and $\psi: X \to Y$, $\sigma: E \to E'$ be mappings. Then a mapping $f = (\psi,\sigma): PFSS(X,E) \to PFSS(Y,E')$ is defined as: for $(H,A) \in PFSS(X,E)$, the image of (H,A) under f, denoted by $f((H,A))$, is a pythagorean fuzzy soft set in $PFSS(Y,E')$ given by

$$\mu_{\psi(H)}(e')(y) = \begin{cases} \sup\limits_{e\in\sigma^{-1}(e')\cap A, x\in\psi^{-1}(y)} \mu_{H(e)}(x) & , \quad \text{if} \quad \psi^{-1}(y) \neq \emptyset \\ 0 & , \quad \text{otherwise} \end{cases}$$

$$v_{\psi(H)}(e')(y) = \begin{cases} \inf\limits_{e\in\sigma^{-1}(e')\cap A, x\in\psi^{-1}(y)} v_{H(e)}(x) & , \quad \text{if} \quad \psi^{-1}(y) \neq \emptyset \\ 1 & , \quad \text{otherwise} \end{cases}$$

For $(F,B) \in PFSS(Y,E')$, the inverse image of (F,B) under f, denoted by $f^{-1}((F,B))$, is a pythagorean fuzzy soft set in $PFSS(X,E)$ given by:

$$\mu_{\psi^{-1}(F)}(e)(x) = \mu_{F(\sigma(e))}(\psi(x)),$$
$$v_{\psi^{-1}(F)}(e)(x) = v_{F(\sigma(e))}(\psi(x))$$

for all $e \in E$ and $x \in X$.

Definition 18. [26] Let $(X,\tilde{\tau}_1,E)_p$ and $(Y,\tilde{\tau}_2,E')_p$ be two pythagorean fuzzy soft topological spaces, a pythagorean fuzzy soft mapping $f = (\psi,\sigma): PFSS(X,E) \to PFSS(Y,E')$ is called a pythagorean fuzzy soft continuous if $f^{-1}((G,B)) \in \tilde{\tau}_1$ for all $(G,B) \in \tilde{\tau}_2$.

Definition 19. [20] A pythagorean fuzzy set (F,E) is called pyhagorean fuzzy soft point (PFS point), denoted as e_F, if for the element $e \in E$,

1. $F(e) = \tilde{0}_{(X,E)}$
2. $F(e') = \tilde{1}_{(X,E)}$ for all $e' \in E\backslash\{e\}$.

3. MAIN RESULTS

Definition 20. Let $(X,\tilde{\tau},E)_p$ be pythagorean fuzzy soft topological space over X. A pythagorean fuzzy soft set (F,E) in $(X,\tilde{\tau},E)_p$ is called a pythagorean fuzzy soft neighbourhood of the pythagorean fuzzy soft point $e_H \in (F,E)$, if there exists a pythagorean fuzzy soft open set (G,E) such that $e_H \in (G,E) \tilde{\subseteq} (F,E)$.

Theorem 1. Let $(X,\tilde{\tau},E)_p$ be pythagorean fuzzy soft topological space and $(F,E) \in PFSS(X,E)$. Then (F,E) is a pythagorean fuzzy soft open set if and only if (F,E) is a pythagorean fuzzy soft neighbourhood of its pythagorean fuzzy soft points.

Proof. Let (F,E) be a pythagorean fuzzy soft open set and $e_H \in (F,E)$. Then $e_H \in (F,E) \tilde{\subseteq} (F,E)$. Therefore, (F,E) is a pythagorean fuzzy soft neighbourhood of e_H.

Conversely, let (F,E) be a pythagorean fuzzy soft neighbourhood of its pythagorean fuzzy soft points and $e_H \in (F,E)$. Since (F,E) is a pythagorean fuzzy soft neighbourhood of the pythagorean fuzzy soft point e_H, there exist $(G,E) \in \tilde{\tau}$ such that $e_H \in (G,E) \tilde{\subseteq} (F,E)$. Since $(F,E) = \cup\{e_H : e_H \in (F,E)\}$, it follows that.$(F,E)$ is a union of pythagorean fuzzy soft open sets and hence (F,E) is a pythagorean fuzzy soft open set.

3.1 Compactness

Definition 21. A family Ω of $PFSS(X,E)$ is a cover of a pythagorean fuzzy soft set (F,E) if

$$(F,E) \tilde{\subseteq} \cup\{(F_i,E) : (F_i,E) \in \Omega, i \in I\}.$$

It is a pythagorean fuzzy soft open cover if each member of Ω is a pythagorean fuzzy soft open set. A subcover of Ω is a subfamily of Ω which is also cover.

Definition 22. Let $(X,\tilde{\tau},E)_p$ be pythagorean fuzzy soft topological space and $(F,E)\in PFSS(X,E)$. (F,E) is called compact if each pythagorean fuzzy soft open cover of (F,E) has a finite subcover. Also $(X,\tilde{\tau},E)_p$ is called pythagorean fuzzy soft compact spaces if each pythagorean fuzzy soft open cover of (X,E) has a finite subcover.

Example 1. If X is finite then $(X,\tilde{\tau},E)_p$ is pythagorean fuzzy soft compact space.

Example 2. Let $(X,\tilde{\tau}_1,E)_p$ and $(Y,\tilde{\tau}_2,E)_p$ be two pythagorean fuzzy soft topological spaces and $\tilde{\tau}_1\subset\tilde{\tau}_2$. Then, $(X,\tilde{\tau}_1,E)_p$ is pythagorean fuzzy soft compact space if $(Y,\tilde{\tau}_2,E)_p$ is pythagorean fuzzy soft compact space.

Theorem 2. Let $(X,\tilde{\tau},E)_p$ be pythagorean fuzzy soft topological space and $(F,E)\in PFSS(X,E)$. (F,E) is a pythagorean fuzzy soft compact set if and only if every pythagorean fuzzy soft open cover of (F,E) has a finite pythagorean fuzzy soft subcover.

Proof. Let $(F,E)\in PFSS(X,E)$ be a pythagorean fuzzy soft compact set and the family $\Omega=\{(F_i,E):i\in I\}$ is a pythagorean fuzzy soft open cover of (F,E). Then we obtain

$$(F,E)\,\tilde{\subseteq}\,\underset{i\in I}{\tilde{\cup}}(F_i,E)\Rightarrow(F,E)=\underset{i\in I}{\tilde{\cup}}((F,E)\,\tilde{\cap}_E\,(F_i,E)).$$

For each $i\in I$, $((F,E)\,\tilde{\cap}_E\,(F_i,E))\in\tilde{\tau}$, $\{(F,E)\,\tilde{\cap}_E\,(F_i,E)\}_{i\in I}$ is a pythagorean fuzzy soft open cover of (F,E) and $(X,\tilde{\tau},E)_p$ is pythagorean fuzzy soft compact space for

$$\exists i_1,\dots,i_n\ (F,E)=\underset{j=1}{\overset{n}{\tilde{\cup}}}\left((F,E)\,\tilde{\cap}_E\,(F_{i_j},E)\right)\,\tilde{\subseteq}\,\underset{j=1}{\overset{n}{\tilde{\cup}}}\left(F_{i_j},E\right)$$

is obtained. That is $\{(F_{i_j},E)\}_{j=\overline{1,n}}$ is a pythagorean fuzzy soft finite subcover of (F,E).

Conversely, Let $\{(G_{i_j},E)\}_{j=\overline{1,n}}$ be a pythagorean fuzzy soft open cover of $(X,\tilde{\tau},E)_p$. Since each $i\in I$, $(G_i,E)\in\tilde{\tau}$ there is $(F_i,E)\in\tilde{\tau}$ such that $(G_i,E)=(F,E)\,\tilde{\cap}_E\,(F_{i_j},E)$. Thus $\{(F_i,E):i\in I\}$ is a pythagorean fuzzy soft open cover of (F,E) in $(X,\tilde{\tau},E)_p$ and

$$\exists(F_{i_1},E),\dots,(F_{i_n},E):(F,E)\,\tilde{\subseteq}\,\underset{j=1}{\overset{n}{\tilde{\cup}}}\left(F_{i_j},E\right)\Rightarrow(F,E)=(F,E)\,\tilde{\cap}_E\,\underset{j=1}{\overset{n}{\tilde{\cup}}}\left(F_{i_j},E\right)$$
$$=\underset{j=1}{\overset{n}{\tilde{\cup}}}(F,E)\,\tilde{\cap}_E\left(F_{i_j},E\right)=\underset{j=1}{\overset{n}{\tilde{\cup}}}\left(G_{i_j},E\right)$$

So, we obtain from the condition of theorem.

Theorem 3. Let $(X,\tilde{\tau},E)_p$ be pythagorean fuzzy soft compact space and (F,E) be a pythagorean fuzzy soft closed set over X. Then (F,E) is also pythagorean fuzzy soft compact.

Proof. Suppose that (G_i,E) be any open cover of (F,E). Then $(X,E)\,\tilde{\subseteq}\left(\underset{i\in I}{\tilde{\cup}}(G_i,E)\right)\tilde{\cup}\,(F,E)^c$, that is (G_i,E) together with pythagorean fuzzy soft open set $(F,E)^c$ is a open cover of (X,E). Therefore there exist a finite subcover $(G_1,E),(G_2,E),\dots,(G_n,E),(F,E)^c$. So

$$(X,E)\,\tilde{\subseteq}\,(G_1,E)\,\tilde{\cup}_E\,(G_2,E)\,\tilde{\cup}_E\dots\tilde{\cup}_E\,(G_n,E)\,\tilde{\cup}_E\,(F,E)^c.$$

Therefore

$$(F,E)\,\tilde{\subseteq}\,(G_1,E)\,\tilde{\cup}_E\,(G_2,E)\,\tilde{\cup}_E\dots\tilde{\cup}_E\,(G_n,E)\,\tilde{\cup}_E\,(F,E)^c$$

which clear implies

$$(F,E)\,\tilde{\subseteq}\,(G_1,E)\,\tilde{\cup}_E\,(G_2,E)\,\tilde{\cup}_E\dots\tilde{\cup}_E\,(G_n,E)$$

since $(F,E)\,\tilde{\cap}_E\,(F,E)^c=\tilde{0}_{(X,E)}$. Hence (F,E) has a finite subcover and so is pythagorean fuzzy compact.

Theorem 4. $(X,\tilde{\tau},E)_p$ is pythagorean fuzzy soft compact space if and only if each family of pythagorean fuzzy soft closed sets with the finite intersection property has a non-null intersection.

Proof. $(\Rightarrow)$ Let Ω be any family of pythagorean fuzzy soft closed set such that $\cap\{(F_i,E):(F_i,E)\in\Omega,i\in I\}=\tilde{0}_{(X,E)}$. Consider $\Psi=\{(F_i,E)^c:(F_i,E)\in\Omega,i\in I\}$. So Ψ is a pythagorean fuzzy soft open cover of $(X,\tilde{\tau},E)_p$. As pythagorean

fuzzy soft topological space is compact, there exist a finite subcovering $(F_1,E)^c,(F_2,E)^c,\ldots,(F_i,E)$. Then $\bigcap_{i=1}^{n}(F_i,E)=(X,E)\setminus\bigcup_{i=1}^{n}(F_i,E)^c=(X,E)\setminus(X,E)=\tilde{0}_{(X,E)}$. Hence Ω cannot have finite intersection property.

$(\Leftarrow)$ Suppose that a pythagorean fuzzy soft topological space is not compact. Then any pythagorean fuzzy soft open cover of (X,E) has not a finite subcover. Let $\{(F_i,E):i\in I\}$ be an open cover of (X,E). So $\bigcup_{i=1}^{n}(F_i,E)\neq(X,E)$. Therefore $\bigcap_{i=1}^{n}(F_i,E)^c\neq\tilde{0}_{(X,E)}$. Thus $\{(F_i,E):i=1,\ldots,n\}$ have finite intersection property. By using hypothesis, $\cap(F_i,E)^c\neq\tilde{0}_{(X,E)}$ and so $\cup(F_i,E)\neq(X,E)$. This is a contradiction. Thus pythagorean fuzzy soft topological space is compact.

3.2 Connectedness

Definition 23. Let $(X,\tilde{\tau},E)_p$ be pythagorean fuzzy soft compact space over X. A pythagorean fuzzy soft separation of $\tilde{1}_{(X,E)}$ is a pair $(F,E),(G,E)$ of no-null pythagorean fuzzy soft open sets such that

$$\tilde{1}_{(X,E)}=(F,E)\,\tilde{\cup}_E\,(G,E),\ (F,E)\,\tilde{\cap}_E\,(G,E)=\tilde{0}_{(X,E)}$$

Definition 24. A pythagorean fuzzy soft topological spaces $(X,\tilde{\tau},E)_p$ is said to be pythagorean fuzzy soft connected if there does not exist a pythagorean fuzzy soft separation of (X,E). Otherwise, $(X,\tilde{\tau},E)_p$ is called a disconnected.

Example 3. Let $X=\{x_1,x_2\}$, $E=\{e_1,e_2\}$ and $\tilde{\tau}=\{\tilde{0}_{(X,E)},\tilde{1}_{(X,E)},(F_1,E),(F_2,E)\}$ where pyhagorean fuzzy soft set $(F_1,E),(F_2,E)$ are defined as following:

$$(F_1,E)=\begin{Bmatrix}(e_1,\{(x_1,1,0),(x_2,0,0)\})\\(e_2,\{(x_1,0,1),(x_2,1,0)\})\end{Bmatrix}$$
$$(F_2,E)=\begin{Bmatrix}(e_1,\{(x_1,0,1),(x_2,1,0)\})\\(e_2,\{(x_1,1,0),(x_2,0,1)\})\end{Bmatrix}$$

The pair (F_1,E) and (F_2,E) are pythagorean fuzzy soft separation of $\tilde{1}_{(X,E)}$. Therefore $(X,\tilde{\tau},E)_p$ is pythagorean fuzzy soft disconnected spaces.

Theorem 5. A pythagoren fuzzy soft topological space $(X,\tilde{\tau},E)_p$ is pythagorean fuzzy soft connected if and only if the only soft sets in $PFSS(X,E)$ that are both pythagorean fuzzy soft open and pythagorean fuzzy soft closed are only $\tilde{0}_{(X,E)}$ *and* $\tilde{1}_{(X,E)}$.

Proof. Let $(X,\tilde{\tau},E)_p$ be pythagorean fuzzy soft connected space. On the contrary, we suppose that (F,E) is both pythagorean fuzzy soft open and closed different from $\tilde{0}_{(X,E)},\tilde{1}_{(X,E)}$. Then $(F,E)^c$ is also bouth pythagorean fuzzy soft open and closed different from $\tilde{0}_{(X,E)},\tilde{1}_{(X,E)}$. Also $(F,E)\,\tilde{\cap}_E\,(F,E)^c=\tilde{1}_{(X,E)}$.Therefore $(F,E),(F,E)^c$ is a pythagorean fuzzy soft separation of $\tilde{1}_{(X,E)}$. This is a contradiction. So, the only pythagorean fuzzy soft closed and open sets in $PFSS(X,E)$ are $\tilde{0}_{(X,E)}$ and $\tilde{1}_{(X,E)}$.

Conversely, let $(F,E),(G,E)$ be a pythagorean fuzzy soft separation of $(X,\tilde{\tau},E)_p$. Then $(F,E)\neq(G,E)$ i.e, $(F,E)=(G,E)^c$. This shows that (G,E) is both pythagorean fuzzy soft open and pythagorean fuzzy soft closed different from $\tilde{0}_{(X,E)},\tilde{1}_{(X,E)}$. This is a contradiction. Hence, $(X,\tilde{\tau},E)_p$ is connected.

Example 4. Since the only pythagorean fuzzy soft sets in $PFSS(X,E)$ that are both pythagorean fuzzy soft open and pythagorean fuzzy soft closed are $\tilde{0}_{(X,E)},\tilde{1}_{(X,E)}$, pythagorean fuzzy soft indiscrete topological space $(X,\tilde{\tau},E)_p$ is pythagorean fuzzy soft connected.

Example 5. Pythagorean fuzzy soft discrete topological space $(X,\tilde{\tau},E)_p$ is pythagorean fuzzy soft disconnected. Because for at least one pythagorean fuzzy soft set (F,E) in $PFSS(X,E)$, pythagorean fuzzy soft set (F,E) is both pythagorean fuzzy soft open and pythagorean fuzzy soft closed.

Corollary 1. Let $(X,\tilde{\tau},E)_p$ be pythagorean fuzzy soft compact space over X. Then following statements are equivalent.

1. $(X,\tilde{\tau},E)_p$ is pythagorean fuzzy soft connected,
2. No-null pythagorean fuzzy soft open sets (F,E),$(G,E)$and $\tilde{1}_{(X,E)} = (F,E)\ \tilde{\cup}_E\ (G,E)$, $(F,E)\ \tilde{\cap}_E\ (G,E) = \tilde{0}_{(X,E)}$.
3. The only pythagorean fuzzy soft sets in $PFSS(X,E)$ that are both pythagorean fuzzy soft open and pythagorean fuzzy soft closed in $\tilde{0}_{(X,E)}$ and $\tilde{1}_{(X,E)}$.

4. CONCLUSION

In this study, we introduced pythagorean fuzzy soft neighbourhood, pythagorean fuzzy soft compactness and pythagorean fuzzy soft connectedness. Also we gave some basic properties of these concepts. We hope this study will be useful.

REFERENCES

1. K. Atanassov, Intuitionistic fuzzy sets, Fuzzy Sets and Systems, 20 (1986), pp. 87-96.
2. T. M. Athira, S. J. John and H. Garg, Entropy and distance measures of Pythagorean fuzzy soft sets and their applications, Journal of Intelligent & Fuzzy Systems vol. 37 (2019) pp. 4071–4084, Doi:10.3233/JIFS-190217
3. C. Chang, Fuzzy topological spaces, J. Math. Anal. Appl., vol. 24 (1968), pp. 182–190.
4. D. Coker, An introduction of intuitionistic fuzzy topological spaces, Fuzzy Sets and Systems, 88(1997), 81-89.
5. A. Guleria, R. K. Bajaj, On pythagorean fuzzy soft matrices, operations and their applications in decision making and medical diagnosis, Soft Computing, vol. 23 (2019), pp. 1889–7900, Doi:10.1007/s00500-018-3419-z.
6. A. Hussain, M. I. Ali and T. Mahmood, Pythagorean fuzzy soft rough sets and their applications in decision-making, Journal of Taibah University for Science, vol.14 No.1 (2020) , pp. 101-113, doi: 10.1080/16583655.2019.1708541
7. S. Karatas, M. Akdag, On intuitionistic fuzzy soft continuous mappings, Journal of New Results in Science, vol. 4 (2014), pp. 55–70.
8. M. Kirisci, New type pythagorean fuzzy soft set and decision-making application, arXiv preprint arXiv:1904.04064, (2019).
9. Z. Li and R. Cui, On the topological structure of intuitionistic fuzzy soft sets, Ann. Fuzzy Math. Inform, vol. 5 No. 1 (2013), pp. 229-239.
10. P. K. Maji, R. Biswas, A. R. Roy, Fuzzy soft sets, Journal of Fuzzy Mathematics vol. 9 No. 3 (2001), pp. 589–602.
11. P. K. Maji, R. Biswas, A. R. Roy, Intuitionistic fuzzy soft sets, Journal of fuzzy mathematics Vol. 9 No. 3 (2001), pp. 677–692.
12. P. Maji, R. Biswas, A. Roy, Soft set theory, Comput. Math. Appl., vol. 45 No. (4-5) (2003), pp. 555–562.
13. D. Molodtsov, Soft set theory-first results, Comput. Math. Appl., vol. 37 no. (4-5) (1999), pp. 19–31.
14. M. Olgun, M. Unver, S. Yardımcı, Complex and Intelligent Systems, (2019).
15. I. Osmanoglu, D. Tokat, On intuitionistic fuzzy soft Topology, Gen. Math. Notes, vol. 19 no.2 (2013), pp.59–70.
16. Z. Pawlak, Rough sets, Int. J. Comput. Sci., vol.11 (1982), pp.341–356.
17. X. Peng, Y. Yang, Some results for pythagorean fuzzy sets, International Journal of Intelligent Systems vol. 30 no. 11 (2015), pp. 1133–1160.
18. X. Peng, Y. Yang, J. Song, Y. Jiang, Pythagoren fuzzy soft set and its application, Computer Engineering vol. 41 no. 7 (2015), pp. 224–229.

19. X. Peng, New operations for interval-valued pythagorean fuzzy set, Scientia Iranica E, vol. 26 no.2 (2019), pp. 1049–1076.
20. M. Riaz, K. Naeem, M. Aslam, D. Afzal, F. Ahmahdi and S.S. Jamal Multi-criteria Group Decision Making with Pythagorean Fuzzy Soft Topology. Journal of Intelligent and Fuzzy Systems, (2020) pp. 1–18, Doi:10.3233/JIFS-190854.
21. M. Shabir, M. Naz, On soft topological spaces, Comput. Math. Appl., vol. 61 (2011), pp. 1786-1799.
22. G. Shahzadi and M. Akram, Hypergraphs based on pythagorean fuzzy soft model, Math. Comput. Appl., vol. 24 no. 100 (2019) doi:10.3390/mca24040100
23. B. Tanay, M. B. Kandemir, Topological structure of fuzzy soft sets, Comput. Math. Appl., vol. 61 (2011), pp. 2952–2957.
24. R. R. Yager, Pythagorean fuzzy subsets, Proc. Joint IFSA World Congress NAFIPS Annual Meet., 1, Edmonton, Canada, (2013) pp. 57-61.
25. R.R. Yager and A.M. Abbasov, Pythagorean membership grades, complex numbers, and decision making, Int. J. Intell. Syst., vol. 28 no.5, (2014) pp. 436-452.
26. A. Yolcu and T.Y. Ozturk, Some New Results on Pythagorean Fuzzy Soft Topological Spaces, TWMS J. App. Eng. Math. Accepted.
27. L. A. Zadeh, Fuzzy Sets, Information and Control, vol. 8 (1965), pp. 338-353.
28. S. Zeng, J. Chen and X. Li, A Hybrid Method for Pythagorean Fuzzy Multiple-Criteria Decision Making, International Journal of Information Technology and Decision Making, Vol. 15, No. 2 (2016) pp. 403–422, Doi: 10.1142/S0219622016500012.

Mathematical Modeling of the Effect of Laser Scan Speed on Size of Texture Created on Polyvinyl Chloride (PVC) Plate

Timur CANEL[1]and İrem BAĞLAN[2]

[1]Department of Physics, Faculty of Science and Arts,
Kocaeli University, Kocaeli-TURKEY
[2]Department of Mathematics, Faculty of Science and Arts,
Kocaeli University, Kocaeli-TURKEY

tcanel@ kocaeli.edu.tr
isakinc@kocaeli.edu.tr

Abstract. The objective of this study is to determine the mathematical model to apply the effect of the laser scan speed on groove size that is created on polyvinyl chloride (PVC). Polyvinyl chloride (PVC) which is a polymer is widely used in several industrial segments [1]. Polyvinyl chloride (PVC) plates can be used as a dust collecting material of WMESP with its good chemical stability, high strength, high corrosion and ageing resistance, insulation performance, and smooth surface [2]. When the scan speed is increased, the interaction time between the laser beam and the material decreases. In this mathematical model obtained, the change to groove size depending on the laser scan speed was modeled. To validate the mathematical model, the surfaces of the PVC plate with 4.5 mm thickness were ablated with different scan speed at constant power. Since the CO_2 lasers are more widely used in the industry, the CO_2 laser that has 10600 nm wavelengths and 130 Watts maximum power was used in the ablation. The images of ablated PVC surfaces were taken with a Leica stereo microscope. Size measurements were made from top view images obtained with optical microscope.
Keywords: Polyvinyl chloride (PVC), Laser ablation, CO_2 lasers, Surface texture, Polymers.

1. INTRODUCTION

Polymer surfaces can be modified by chemical modification and physical modification. Surface texturing is used for many applications such as changing the tribology properties of surface, increasing the wettability, manipulating the adhesion property and hydrofobization. Numerous methods have been designed and used commercially, especially for modifying polymer surfaces [3]. Chemical and mechanical methods used before laser processing of polymer surfaces have many disadvantages. Chemical surface treatment has very limited use due to the difficulty of controlling chemical reactions, especially environmental pollution. The main disadvantages in the processing of polymer surfaces by mechanical methods are the wear of the tools used and the process precision is not continuous.

The use of a laser in material machining has many advantages. Since the laser beam can be adjusted with suitable lenses to the desired focus, the laser beam of the desired beam intensity can be obtained. The laser with a suitable wavelength of selection can be made according to each material and desired product type. Other important advantages of using laser in material processing are that it can be processed precisely and the precision of the processes is continuous. Although the ablation mechanism in laser material processing has not been fully explained, it is strictly dependent on material properties and process parameters. The thermophysical properties of the material such as specific heat, absorption coefficient, and thermal conduction are effective in the ablation mechanism. Besides the laser properties such as the wavelength, frequency and power of the laser used, process parameters such as scan speed, overlap rate, number of pulses and beam size determine the ablation and therefore the quality of the processed material.

In order to obtain surface textures such as grooves and dimples with the desired shape and size, the effects of laser parameters on the surface texture were investigated in many studies [4,5]. Many optimization studies have been carried out to determine the effects of process parameters for different materials and different purposes on material quality and to obtain optimum parameters [6,7,8].
Mathematical modeling of the ablation mechanism and heat dissipation within the material in polymer processing with laser are quite compatible with experimental studies [9,10,11]. This shows that mathematical modeling is applicable in laser material processing.
In this study, the mathematical modeling of the width of the grooves created by laser on the PVC plate is made. In the mathematical model, the Fourier method with a homogenous approach is used. To obtain a numerical model, the effects of the laser scan speed on the groove size of PVC sheet were investigated and a simple mathematical model of the heat distribution on surface is proposed. The initial conditions and boundary conditions

The heat distribution equation on surface can be written as below;

$$\frac{\partial T(x,t)}{\partial t} = \alpha^2 \frac{\partial^2 T(x,t)}{\partial x^2} \tag{1}$$

where, T is the temperature as a function of time "t" and distance "x", α is the thermal diffusivity of the investigate material. The initial condition can be defined as; $T(x,0) = T_0,\ 0 < x < l.$ The boundary condition is; $\frac{\partial T(0,t)}{\partial x} = 0$, $\frac{\partial T(l,t)}{\partial x} = 0 \quad (t > 0)$. The boundary condition is homogeneous.

The temperature distribution as a function was obtained as given below;

$$T(x,t) = \sum_{k=1}^{\infty}\left(\varphi_{ck}\, e^{-\left(\frac{2\pi\alpha k}{l}\right)^2 t} + \int_0^t\int_0^l S(x,t)\cos\frac{2\pi k}{l}x e^{-\left(\frac{2\pi\alpha k}{l}\right)^2 (t-\tau)}dxd\tau\right)\cos\frac{2\pi k}{l}x + \sum_{k=1}^{\infty}\left(\varphi_{sk}\, e^{-\left(\frac{2\pi\alpha k}{l}\right)^2 t} + \int_0^t\int_0^l S(x,t)\sin\frac{2\pi k}{l}x e^{-\left(\frac{2\pi\alpha k}{l}\right)^2 (t-\tau)}dxd\tau\right)\sin\frac{2\pi k}{l}x - \frac{xH}{l\lambda} \tag{2}$$

Where S(x,t) is the heat source obtained from laser beam.

2. MATERIAL AND EXPERIMENTAL SETUP

The surfaces of 10 mm thick PVC sheets to be used were polished before ablation to cleaning and increase the transparency of the surfaces. Some physical and thermal properties of PVC sheet which were used in ablation and mathematical modeling have been listed in Table 1.

In the ablation process commercial 130 W CO_2 laser was used with different scan speeds at constant power. Laser spot diameter is 160 μm the laser beam intensity 6.5×10^9 W/m^2.

Table 1
Some physical and thermal properties of PVC

Properties	Value	Unit
Density	1350	kg/m^3
Coefficient of Thermal Expansion	5	cm / (cm °C)
Melting point	200	°C

Heat Deflection Temperature at 0.5 MPa	70	°C
Heat Deflection Temperature at 1.8 MPa	69	°C
Thermal Conductivity x 10^{-5}	0.15	W/mK

3. RESULTS AND DISCUSSION

In this study, mathematical model has been proposed for the groove formation on PVC sheet with various scan speeds and constant power. Groove sizes were measured from optical microscope images of ablated surfaces of PVC sheets.

Then we calculated Heat Deflection Zone boundary and molten zone boundary distances as 1648 μm and 1432 μm respectively. Temperatures at Heat Deflection boundary and molten zone boundary are 343 K and 473 K respectively. These values are used in temperature distribution equation obtain the Fourier coefficients which are depends on the material properties. The sizes of grooves were used in the calculation of coefficients. The groove widths were measured from images as seen in Table 2.

The coefficients in the temperature distribution equation (2) were calculated as φ_c (=221,7) and φ_s (-315.4). These are the coefficients depend on the PVC. Then, in order to verify the validity of mathematical model, new grooves were obtained using 200, 300, 400, 500 mm/s scan speeds. These coefficients were used to calculate temperature distribution for the same material and different scan speed.

Table 2 Laser scan speeds and groove widths measured from images.

Scan Speed mm/s	**Molten Zone width (μm)**	**Heat Deflection Zone (μm) Width**
100	1432	1648
200	1404	1604
300	1368	1570
400	1322	1520
500	1250	1430

Each laser scan speed and the coefficients obtained previously were used in the temperature distribution equation to calculate the temperatures for each speed of laser beam. The calculated temperatures for boundaries are given in Table 3.

Table 3. The theoretical and calculated temperatures for boundaries.

Scan speed mm/s		T(x,t) (K)	T(x,t) (K) (calculated)	% error
200	Melting	473	475.416	0.51
200	Heat Deflection	343	342.215	0.23
300	Melting	473	469.335	0.77
300	Heat Deflection	343	340.854	0.63
400	Melting	473	465.119	1.67
400	Heat Deflection	343	332.108	3.18
500	Melting	473	456.058	3.58
500	Heat Deflection	343	330,217	3.73

4. CONCLUSION

Grooves were formed on the PVC material surface with different scanning speeds by laser. The geometries of the formed grooves were examined with an optical microscope. Groove widths were measured from optical microscope images. The heat distribution that causes the formation of grooves is modeled with the Fourier method. First, material-specific coefficients were calculated with the proposed mathematical model. In order to prove the validity of these coefficients, 3 different grooves obtained with 3 different scanning speeds were examined. The results obtained show that the proposed mathematical model is reliable.

REFERENCES

1. M. Barletta, V. Tagliaferri, F. Trovalusci, F. Veniali, A. Gisario, The mechanisms of material removal in the fluidized bed machining (FBM) of polyvinyl chloride (PVC) substrates, Journal of Manufacturing Science and Engineering, 2013, 135(1): 011003-1-14 DOI: 10.1115/1.4007956
2. C. Huang, X. Ma, M. Wang, Y. Sun, C. Zhang, H. Tong, Property of the PVC Dust Collecting Plate Used in Wet Membrane Electrostatic Precipitator, IEEE Transactions on Plasma Science, 2014, 42(11), 3520-3528
3. V. Belaud, S. Valette, G. Stremsdoerfer, B. Beaugıraud, E. Audouard, And S. Benayoun, Femtosecond Laser Ablation of Polypropylene: A Statistical Approach of Morphological Data, Scanning 2014, Vol. 36, 209–217
4. S. Lazare, J. Lopez, F. Weisbuch, High-aspect-ratio microdrilling in olymericmaterials with intense KrF laser radiation, Appl. Phys. 1999, A 69 [Suppl.], S1–S6
5. S. Lazare And V. Tokarev, Recent Experimental and Theoretical Advances in Microdrilling of Polymers with Ultraviolet Laser Beams, Fifth International Symposium on Laser Precision Microfabrication, Proceedings of SPIE 2004, Vol. 5662, 221-231.
6. T. Canel, A.U. Kaya, B. Çelik, Parameter optimization of nanosecond laser for microdrilling on PVC by Taguchi method, Optics & Laser Technology, 2012, 44; 2347-2353
7. T. Canel, E. Kayahan, L. Candan, S. Fidan, T. Sınmazçelik, Influence of laser parameters in surface texturing of polyphenylene sulfide composites, J. Appl. Polym. Scı. 2019, Doi: 10.1002/App.47976
8. T. Canel, M. Zeren, T. Sınmazcelik, Laser parameters optimization of surface treating of Al 6082-T6 with Taguchi method, Optics & Laser Technology, 2019, 120; 105714
9. T. Canel, İ. Bağlan, T. Sinmazcelik, Mathematical modelling of laser ablation of random oriented short glass fiber reinforced Polyphenylene sulphide (PPS) polymer composite. Optics & Laser Technology, 2019, 115; 481-486
10. T. Canel, İ. Bağlan, T. Sınmazçelik, Mathematical modeling of heat distribution on carbon fiber Poly(etherether-ketone) (PEEK) composite during laser ablation, Optics & Laser Technology, 2020, 127; 106190
11. T. Canel, İ. Bağlan, Mathematical Modelling of One Dimensional Temperature Distribution As A Function Of Laser Intensity On Carbon Fiber Reinforced Poly(Ether-Ether-Ketone)-(Peek) Composite, TWMS J. App. and Eng. Math. 2020, V.10, N.3, pp. 769-777.

On Copies of c_0 and ℓ^1 and Failure of Fixed Point Property

Veysel NEZİR[1] and Nizami MUSTAFA[2]

[1,2]*Department of Mathematics, Faculty of Science and Letters, Kafkas University, Kars-TURKEY*
veyselnezir@yahoo.com
nizamimustafa@gmail.com

Abstract. James' Distortion theorems played a vital role to investigate Banach spaces containing nice copies of c_0 or ℓ^1 and their failure of the fixed point property for nonexpansive mappings. His tools leaded researchers to see that every classical nonreflexive Banach space contains an isomorphic copy of either c_0 or ℓ^1. There have been many researches done using these tools developed by James and followed by Dowling, Lennard and Turett mainly to see if a Banach space can be renormed to have the fixed point property for nonexpansive mappings when there is failure. Recently, in a study in preparation, the first author joined with his student Güven obtained alternative asymptotically isometric properties implying failure of the fixed point property inside copies of c_0 or ℓ^1. Inspired by their study, we investigate James' results and find relations with some new properties originated from their alternative asymptotically isometric properties. Then, we show that we get some properties that are alternative for Banach spaces to have isomorphic copies of c_0 or ℓ^1. So we obtain some results that imply failure of fixed point property besides nonreflexivity.

1. INTRODUCTION AND PRELIMINARIES

A Banach space is called to have the fixed point property for non-expansive mappings [fpp(n.e.)] if any non-expansive self-mappings defined on any non-empty closed, bounded and convex subset of the Banach space has a fixed point. It has been seen that most classical Banach spaces fail the fixed point property and especially there is a fact that if a Banach space is a non-reflexive Banach lattice then it fails the fixed point property if it contains either an isomorphic copy of c_0 or ℓ^1, Banach space of scalar sequences converging to 0, or an isomorphic copy of ℓ^1, Banach space of absolutely summable scalar sequences [6].

James [5] developed a tool which leaded researchers to understand if a Banach space contains an isomorphic copy of c_0 or ℓ^1. Strengthening James' Distortion theorems, Dowling et al. [2] obtained new tools to test if a Banach space contains an asymptotically isometric copy of ℓ^1 which implies the failure of the fixed point property for nonexpansive mappings. Considering the class of uniformly lipschitzian maps on closed, bounded, convex subsets of a Banach space, they saw that James's theorems can be used to get results concerning fixed points. Contiuning to investigate James' distortion theorems and their connection with fixed points, they also noticed that Banach spaces containing an isomorpic copy of c_0 fail the fixed point property for asymtotically nonexpansive mappings. Next, they worked on the concept of a Banach space containing an ai copy of ℓ^1 or c_0 which is used as an important tool in identifying Banach spaces failing FPP(n.e.).

Dowling et al. [4] showed an example of a Banach space such that their example and its all infinite dimensional subspaces fail the fixed point property while none does not contain any asymptotically isometric copy of c_0.

The notions of asymptotically isometric copies of the classical Banach spaces c_0 and ℓ^1 have applications in metric fixed point theory because they arise naturally in many places. For example, every non-reflexive subspace of $(\mathsf{L}_1[0,1], \|.\|_1)$, every infinite dimensional subspace of $(\ell^1\ \|.\|_1)$, and every equivalent renorming of ℓ^∞ contains an asymptotically isometric copy ℓ^1 and so all of these spaces fail the fixed point property [1, 3]. The concept of containing an asymptotically isometric copy ℓ^1 also arises in the isometric theory of Banach spaces in an intriguing

way: a Banach space X contains an asymptotically isometric copy ℓ^1 if and only if X^* contains an isometric copy of $(L_1[0,1], \|.\|_1)$ [3].

In a recent joint study under preparation, the first author and his student Güven recently introduced new properties for a Banach space to check if it fails the fixed point property. They proved that a Banach space contains an asymptotically isometric copy of ℓ^1 if and only if it has one of the properties they introduced. So they obtained equivalent properties. More importantly, in their study, they obtained alternative asymptotically isometric properties to the notion of asymptotically isometric copy of c_0. They also proved that if a Banach space has that alternative asymptotically isometric property, then it fails the fixed point property for nonexpansive mappings. Then, as their vital result, they showed that if a Banach space contains an asymptotically isometric copy of c_0 then it has the property he introduced but the converse is not true.

Inspired by their study, in this study, rather than the notions of asymptotic isometric copies of c_0 or ℓ^1, we consider the notion of isomorphic copy of c_0 or ℓ^1. We investigate James' results and find relations with some new properties originated from their alternative asymptotically isometric properties. Then, we show that we get some properties that are alternative for Banach spaces to have isomorphic copies of c_0 or ℓ^1. So we obtain some results that imply failure of fixed point property besides nonreflexivity.

Now we provide some preliminaries before giving our main results.

Definition 1. *Let K be a non-empty closed, bounded, convex subset of a Banach space $(X, \|\cdot\|)$. Let $T: K \to K$ be a mapping. We say T is nonexpansive if $\| T(x) - T(y) \| \leq \| x - y \|$ for all $x, y \in K$. Also, we say that K has the fixed point property for nonexpansive mappings [fpp(n.e.)] if for all nonexpansive mappings $T: K \to K$, there exists $z \in K$ with $T(z) = z$.*

As usual, $(c_0, \|\cdot\|_\infty)$ is given by $c_0 := \left\{x = (x_n)_{n\in\mathbb{N}} : \text{each } x_n \in \mathbb{R} \text{ and } \lim_{n\to\infty} x_n = 0\right\}$. Further, $\| x \|_\infty := \sup_{n\in\mathbb{N}} |x_n|$, for all $x = (x_n)_{n\in\mathbb{N}} \in c_0$. Also, c_{00} is the space of sequences with finetely many nonzero terms. Furthermore, $(\ell^1, \|\cdot\|_1)$ is the vector space of all absolutely summable scalar sequences such that $\| x \|_1 := \sum_{n=1}^{\infty} |x_n|$ for all $x = (x_n)_{n\in\mathbb{N}} \in \ell^1$.

Note that throughout the study, we will denote the sequence $s^* := (s_n{}^*)_{n\in\mathbb{N}}$ by decreasig rearrangement of the finite sequence $s = (s_j)_{j\in\mathbb{N}}$; that is, the squence whose terms contain all non-zero terms of $|s| = (|s_j|)_{j\in\mathbb{N}}$, arranged in non-increasing order, followed by infinitely many zeros when $|s|$ has only finitely many non-zero terms.

Definition 2. [5] *Let $(X, \|\cdot\|)$ be a Banach space. We say that if X contains an isomorphic copy of c_0 then there exist a sequence $(x_n)_n$ in X and scalars $0 < k \leq K < \infty$ such that for all finite sequences $(a_n)_n$,*

$$k \sup_n |a_n| \leq \left\| \sum_{n=1}^{\infty} a_n x_n \right\| \leq K \sup_n |a_n| \ .$$

Definition 3. [5] *Let $(X, \|\cdot\|)$ be a Banach space. We say that if X contains an isomorphic copy of ℓ^1 then there exist a sequence $(x_n)_n$ in X and scalars $0 < k \leq K < \infty$ such that for all $(a_n)_n \in \ell^1$,*

$$k \sum_{n=1}^{\infty} |a_n| \leq \left\| \sum_{n=1}^{\infty} a_n x_n \right\| \leq K \sum_{n=1}^{\infty} |a_n| \ .$$

Theorem 1. [5] *If a Banach space $(X, \|\cdot\|)$ contains an isomorphic copy of c_0, then there exists a sequence $(x_n)_n$ in X such that for every $\varepsilon > 0$ and for all $(a_n)_n \in c_0$,*

$$(1-\varepsilon)\sup_n|a_n| \le \left\|\sum_{n=1}^{\infty} a_n x_n\right\| \le \sup_n|a_n| \ .$$

Theorem 2. [5] *If a Banach space $(X,\|\cdot\|)$ contains an isomorphic copy of ℓ^1, then there exists a sequence $(x_n)_n$ in X such that for every $\varepsilon > 0$ and for all $(a_n)_n \in \ell^1$,*

$$(1-\varepsilon)\sum_{n=1}^{\infty}|a_n| \le \left\|\sum_{n=1}^{\infty} a_n x_n\right\| \le \sum_{n=1}^{\infty}|a_n| \ .$$

The following two theorems can be directly deduced from James' work [5].

Theorem 3. *A Banach space $(X,\|\cdot\|)$ contains an isomorphic copy of c_0 if and only if there exist a sequence $(x_n)_n$ in X and scalars $0 < k \le K < \infty$ such that for all finite sequences $(a_n)_n$,*

$$k\sup_n|a_n| \le \left\|\sum_{n=1}^{\infty} a_n x_n\right\| \le K\sup_n|a_n|$$

and $\lim_{n\to\infty} \| x_n \| = k$.

Theorem 4. *A Banach space $(X,\|\cdot\|)$ contains an isomorphic copy of ℓ^1 if and only if there exist a sequence $(x_n)_n$ in X and scalars $0 < k \le K < \infty$ such that for all $(a_n)_n \in \ell^1$,*

$$k\sum_{n=1}^{\infty}|a_n| \le \left\|\sum_{n=1}^{\infty} a_n x_n\right\| \le K\sum_{n=1}^{\infty}|a_n|$$

and $\lim_{n\to\infty} \| x_n \| = K$.

Theorem 5. [3] *A Banach space X contains an isomorphic copy of ℓ^1 if and only if there is a null sequence $(\varepsilon_n)_n$ in $(0,1)$ and a sequence $(x_n)_n$ in X so that*

$$(1-\varepsilon_k)\sum_{n=k}^{\infty}|t_n| \le \left\|\sum_{n=k}^{\infty} t_n x_n\right\| \le \sum_{n=k}^{\infty}|t_n| \ ,$$

for all $(t_n)_n \in \ell^1$ and for all $k \in \mathbb{N}$.

Theorem 6. [3] *A Banach space X contains an isomorphic copy of c_0 if and only if there is a decreasing null sequence $(\varepsilon_n)_n$ in $(0,1)$ and a sequence $(x_n)_n$ in X so that*

$$(1-\varepsilon_k)\sup_{n\ge k}|t_n| \le \left\|\sum_{n=k}^{\infty} t_n x_n\right\| \le (1+\varepsilon_k)\sup_{n\ge k}|t_n|,$$

for all $(t_n)_n \in c_0$ and for all $k \in \mathbb{N}$.

Theorem 7. [3] *A Banach space X contains an isomorphic copy of c_0 if and only if there is a null sequence $(\varepsilon_n)_n$ in $(0,1)$ and a sequence $(x_n)_n$ in X so that*

$$\sup_{n\ge k}|t_n| \le \left\|\sum_{n=k}^{\infty} t_n x_n\right\| \le (1+\varepsilon_k)\sup_{n\ge k}|t_n| \ ,$$

for all $(t_n)_n \in c_0$ and for all $k \in \mathbb{N}$.

Theorem 8. [3] *If a Banach space X contains an isomorphic copy of c_0, then X fails the fixed point property for asymptotically nonexpansive mappings on closed bounded convex subsets of X. (A mapping $T: C \to C$ is said to be asymptotically nonexpansive if $\| T^n x - T^n y \| \le k_n \| x - y \|$ for all $x, y \in C$ and for all $n \in \mathbb{N}$, where $(k_n)_n$ is a sequence of real numbers converging to 1.)*

Theorem 9. [3] *If a Banach space X contains an isomorphic copy of ℓ^1, then X fails the fixed point property for uniformly Lipschitzian mappings on closed bounded convex subsets of X. (A mapping $T: C \to C$ is said to be uniformly Lipschitzian if there exists $k \in [1, \infty)$ such that $\| T^n x - T^n y \| \leq k^n \| x - y \|$ for all $x, y \in C$ and for all $n \in N$.)*

Theorem 10. [6] *The following properties are equivalent for every Banach lattice X .*

1. *X is reflexive*
2. *No subspace of X is isomorphic to ℓ^1 or c_0.*

2. MAIN RESULTS

In this section, define a new property that implies the failure of the fixed point property for some classes of nonexpansive mappings. That is, we show that if a Banach space has the property we introduce then it fails to have the fixed point property for those classes of nonexpansive mappings. But firstly we show the relations of our properties with the notions of copies of ℓ^1 or c_0. We show that we get equivalent properties for Banach spaces to contain isomorphic copies of ℓ^1 or c_0 so the properties we show also imply nonreflexivity of Banach lattices. Now, let's see the properties we are interested in. Note that from the properties below, the alternative asymptotically idometric properties have been derived by Nezir and Güven in their recent study under preparation.

Definition 4. *We will say a Banach space $(X, \|\cdot\|)$ has property N-AIP-$\ell^1 - 1$ (which stands for new alternative isomorphic property for spaces in a copy of ℓ^1) if there exist a sequence $(x_n)_n$ in X and scalars $0 < k \leq K < \infty$ such that for all $(a_n)_n \in \ell^1$,*

$$k\left(\sum_{n=1}^{\infty} |a_n| + \sum_{n=1}^{\infty} \frac{|a_n|}{2^n}\right) \leq \left\|\sum_{n=1}^{\infty} a_n x_n\right\| \leq K\left(\sum_{n=1}^{\infty} |a_n| + \sum_{n=1}^{\infty} \frac{|a_n|}{2^n}\right)$$

and $\lim_{n\to\infty} \| x_n \| = K$.

Definition 5. *We will say a Banach space $(X, \|\cdot\|)$ has property N-AIP-$\ell^1 - 2$ if there exist a sequence $(x_n)_n$ in X and scalars $0 < k \leq K < \infty$ such that for all $(a_n)_n \in \ell^1$,*

$$k\sqrt{\left[\sum_{n=1}^{\infty} |a_n|\right]^2 + \left[\sum_{n=1}^{\infty} \frac{|a_n|}{2^n}\right]^2} \leq \left\|\sum_{n=1}^{\infty} a_n x_n\right\| \leq K\sqrt{\left[\sum_{n=1}^{\infty} |a_n|\right]^2 + \left[\sum_{n=1}^{\infty} \frac{|a_n|}{2^n}\right]^2}$$

and $\lim_{n\to\infty} \| x_n \| = K$.

Definition 6. *We will say a Banach space $(X, \|\cdot\|)$ has property N-AIP-$c_0 - 1$ (which stands for new alternative isomorphic property for spaces in a copy of c_0) if there exist a sequence $(x_n)_n$ in X and scalars $0 < k \leq K < \infty$ such that for all finite sequences $(a_n)_n$,*

$$k\left(\sup_n |a_n| + \sum_{n=1}^{\infty} \frac{|a_n|}{2^n}\right) \leq \left\|\sum_{n=1}^{\infty} a_n x_n\right\| \leq K\left(\sup_n |a_n| + \sum_{n=1}^{\infty} \frac{|a_n|}{2^n}\right)$$

and $\lim_{n\to\infty} \| x_n \| = k$.

Definition 7. *We will say a Banach space $(X, \|\cdot\|)$ has property N-AIP-$c_0 - 2$ if there exist a sequence $(x_n)_n$ in X and scalars $0 < k \leq K < \infty$ such that for all finite sequences $(a_n)_n$,*

$$k\sum_{n=1}^{\infty}\frac{a_n^*}{2^{n-1}} \le \left\|\sum_{n=1}^{\infty} a_n x_n\right\| \le K\sum_{n=1}^{\infty}\frac{a_n^*}{2^{n-1}}$$

and $\lim_{n\to\infty} \| x_n \| = k$.

Theorem 11. *A Banach space* $(X, \|\cdot\|)$ *has property N-AIP-*$\ell^1 - 1$ *if and only if it contains an isomorphic copy of* ℓ^1.

Proof. Assume that a Banach space $(X, \|\cdot\|)$ has property N-AIP-$\ell^1 - 1$. Then, there exist a sequence $(x_n)_n$ in X and scalars $0 < k \le K < \infty$ such that for all $(a_n)_n \in \ell^1$,

$$k\left(\sum_{n=1}^{\infty}|a_n| + \sum_{n=1}^{\infty}\frac{|a_n|}{2^n}\right) \le \left\|\sum_{n=1}^{\infty} a_n x_n\right\| \le K\left(\sum_{n=1}^{\infty}|a_n| + \sum_{n=1}^{\infty}\frac{|a_n|}{2^n}\right)$$

and $\lim_{n\to\infty} \| x_n \| = K$. Now for each $n \in \mathbb{N}$, define $y_n := \frac{2^n}{1+2^n} x_n$. Then, for all $(a_n)_n \in \ell^1$,

$$k\sum_{n=1}^{\infty}|a_n| \le \left\|\sum_{n=1}^{\infty} a_n y_n\right\| \le K\sum_{n=1}^{\infty}|a_n|$$

and $\lim_{n\to\infty} \| y_n \| = K$. Thus, by Theorem 4, X contains an isomorphic copy of ℓ^1.

Now, conversely, assume that X contains an isomorphic copy of ℓ^1. Then, there exist a sequence $(x_n)_n$ in X and scalars $0 < k \le K < \infty$ such that for all $(a_n)_n \in \ell^1$,

$$k\sum_{n=1}^{\infty}|a_n| \le \left\|\sum_{n=1}^{\infty} a_n x_n\right\| \le K\sum_{n=1}^{\infty}|a_n|$$

and $\lim_{n\to\infty} \| x_n \| = K$. Thus,

$$\frac{2k}{3}\left(\sum_{n=1}^{\infty}|a_n| + \sum_{n=1}^{\infty}\frac{|a_n|}{2^n}\right) \le \left\|\sum_{n=1}^{\infty} a_n x_n\right\| \le K\left(\sum_{n=1}^{\infty}|a_n| + \sum_{n=1}^{\infty}\frac{|a_n|}{2^n}\right)$$

and $\lim_{n\to\infty} \| x_n \| = K$. Therefore, X has property N-AIP-$\ell^1 - 1$ by Definition 4.

Theorem 12. *A Banach space* $(X, \|\cdot\|)$ *has property N-AIP-*$\ell^1 - 1$ *if and only if there is a null sequence* $(\varepsilon_n)_n$ *in* $(0,1)$ *and a sequence* $(x_n)_n$ *in X so that*

$$(1-\varepsilon_k)\left(\sum_{n=k}^{\infty}|t_n| + \sum_{n=k}^{\infty}\frac{|t_n|}{2^n}\right) \le \left\|\sum_{n=k}^{\infty} t_n x_n\right\| \le \sum_{n=k}^{\infty}|t_n| + \sum_{n=k}^{\infty}\frac{|t_n|}{2^n},$$

for all $(t_n)_n \in \ell^1$ *and for all* $k \in \mathbb{N}$.

Proof. Assume that a Banach space $(X, \|\cdot\|)$ has property N-AIP-$\ell^1 - 1$. Let $(t_n)_n \in \ell^1$ and fix $k \in \mathbb{N}$. Then, by the previous theorem and by Theorem 5, there is a null sequence $(\varepsilon_n)_n$ in $(0,1)$ and a sequence $(x_n)_n$ in X so that

$$(1-\varepsilon_k)\sum_{n=k}^{\infty}|t_n|\frac{1+2^n}{2^n} \le \left\|\sum_{n=k}^{\infty} t_n\frac{1+2^n}{2^n}x_n\right\| \le \sum_{n=k}^{\infty}|t_n|\frac{1+2^n}{2^n}.$$

Now define for each $n \in \mathbb{N}$, $y_n := \frac{1+2^n}{2^n} x_n$, then we get

$$(1-\varepsilon_k)\left(\sum_{n=k}^{\infty}|t_n| + \sum_{n=k}^{\infty}\frac{|t_n|}{2^n}\right) \le \left\|\sum_{n=k}^{\infty} t_n y_n\right\| \le \sum_{n=k}^{\infty}|t_n| + \sum_{n=k}^{\infty}\frac{|t_n|}{2^n}.$$

Conversely, assume that there is a null sequence $(\varepsilon_n)_n$ in $(0,1)$ and a sequence $(x_n)_n$ in X so that

$$(1-\varepsilon_k)\left(\sum_{n=k}^{\infty}|t_n|+\sum_{n=k}^{\infty}\frac{|t_n|}{2^n}\right)\leq\left\|\sum_{n=k}^{\infty}t_nx_n\right\|\leq\sum_{n=k}^{\infty}|t_n|+\sum_{n=k}^{\infty}\frac{|t_n|}{2^n},$$

for all $(t_n)_n\in\ell^1$ and for all $k\in N$. Then, pick $(t_n)_n\in\ell^1$ and $k\in\mathbb{N}$. Next for each $n\in\mathbb{N}$, define $y_n:=\frac{2^n}{1+2^n}x_n$. Then,

$$(1-\varepsilon_k)\sum_{n=k}^{\infty}|t_n|\leq\left\|\sum_{n=k}^{\infty}t_ny_n\right\|\leq\sum_{n=k}^{\infty}|t_n|.$$

Hence, by Theorem 5, X contains an isomorphic copy of ℓ^1. Then, by the previous theorem, X has property N-AIP-ℓ^1-1.

Theorem 13. *A Banach space $(X,\|\cdot\|)$ has property N-AIP-ℓ^1-2 if and only if it contains an isomorphic copy of ℓ^1.*

Proof. Assume that a Banach space $(X,\|\cdot\|)$ has property N-AIP-ℓ^1-2. Then, there exist a sequence $(x_n)_n$ in X and scalars $0<k\leq K<\infty$ such that for all $(a_n)_n\in\ell^1$,

$$k\sqrt{\left[\sum_{n=1}^{\infty}|a_n|\right]^2+\left[\sum_{n=1}^{\infty}\frac{|a_n|}{2^n}\right]^2}\leq\left\|\sum_{n=1}^{\infty}a_nx_n\right\|\leq K\sqrt{\left[\sum_{n=1}^{\infty}|a_n|\right]^2+\left[\sum_{n=1}^{\infty}\frac{|a_n|}{2^n}\right]^2}$$

and $\lim_{n\to\infty}\|x_n\|=K$. Now for each $n\in\mathbb{N}$, define $y_n:=\frac{2^n}{1+2^n}x_n$. Then, for all $(a_n)_n\in\ell^1$,

$$\frac{2k}{3}\sum_{n=1}^{\infty}|a_n|\leq\left\|\sum_{n=1}^{\infty}a_ny_n\right\|\leq K\sum_{n=1}^{\infty}|a_n|$$

and $\lim_{n\to\infty}\|y_n\|=K$. Thus, by Theorem 4, X contains an isomorphic copy of ℓ^1.

Now, conversely, assume that X contains an isomorphic copy of ℓ^1. Then, there exist a sequence $(x_n)_n$ in X and scalars $0<k\leq K<\infty$ such that for all $(a_n)_n\in\ell^1$,

$$k\sum_{n=1}^{\infty}|a_n|\leq\left\|\sum_{n=1}^{\infty}a_nx_n\right\|\leq K\sum_{n=1}^{\infty}|a_n|$$

and $\lim_{n\to\infty}\|x_n\|=K$. Thus,

$$\frac{2k}{3}\sqrt{\left[\sum_{n=1}^{\infty}|a_n|\right]^2+\left[\sum_{n=1}^{\infty}\frac{|a_n|}{2^n}\right]^2}\leq\left\|\sum_{n=1}^{\infty}a_nx_n\right\|\leq K\sqrt{\left[\sum_{n=1}^{\infty}|a_n|\right]^2+\left[\sum_{n=1}^{\infty}\frac{|a_n|}{2^n}\right]^2}$$

and $\lim_{n\to\infty}\|x_n\|=K$. Therefore, X has property N-AIP-ℓ^1-2 by Definition 5.

Theorem 14. *A Banach space $(X,\|\cdot\|)$ has property N-AIP-ℓ^1-2 if and only if there is a null sequence $(\varepsilon_n)_n$ in $(0,1)$ and a sequence $(x_n)_n$ in X so that*

$$(1-\varepsilon_k)\sqrt{\left[\sum_{n=k}^{\infty}|t_n|\right]^2+\left[\sum_{n=k}^{\infty}\frac{|t_n|}{2^n}\right]^2}\leq\left\|\sum_{n=k}^{\infty}t_nx_n\right\|\leq\sqrt{\left[\sum_{n=k}^{\infty}|t_n|\right]^2+\left[\sum_{n=k}^{\infty}\frac{|t_n|}{2^n}\right]^2},$$

for all $(t_n)_n\in\ell^1$ and for all $k\in\mathbb{N}$.

Proof. Assume that a Banach space $(X,\|\cdot\|)$ has property N-AIP-ℓ^1-2. Let $(t_n)_n\in\ell^1$ and fix $k\in\mathbb{N}$. Then, by the previous theorem and by Theorem 5, there is a null sequence $(\varepsilon_n)_n$ in $(0,1)$ and a sequence $(x_n)_n$ in X so that

$$(1-\varepsilon_k)\sum_{n=k}^{\infty}|t_n| \le \left\|\sum_{n=k}^{\infty} t_n x_n\right\| \le \sum_{n=k}^{\infty}|t_n| \ .$$

Then, take for each $k \in \mathbb{N}$, $\delta_k := 1-(1-\varepsilon_k)\frac{2^k}{1+2^k}$. So

$$(1-\delta_k)\frac{1+2^k}{2^k}\sum_{n=k}^{\infty}|t_n| \le \left\|\sum_{n=k}^{\infty} t_n x_n\right\| \le \sum_{n=k}^{\infty}|t_n| \le \sqrt{\left[\sum_{n=k}^{\infty}|t_n|\right]^2+\left[\sum_{n=k}^{\infty}\frac{|t_n|}{2^n}\right]^2} \ .$$

But since for each $n \ge k$,

$$(1-\delta_k)\sum_{n=k}^{\infty}|t_n|\frac{1+2^n}{2^n} \le (1-\delta_k)\sum_{n=k}^{\infty}|t_n|\frac{1+2^k}{2^k},$$

we have

$$(1-\delta_k)\sqrt{\left[\sum_{n=k}^{\infty}|t_n|\right]^2+\left[\sum_{n=k}^{\infty}\frac{|t_n|}{2^n}\right]^2} \le \left\|\sum_{n=k}^{\infty} t_n x_n\right\| \le \sqrt{\left[\sum_{n=k}^{\infty}|t_n|\right]^2+\left[\sum_{n=k}^{\infty}\frac{|t_n|}{2^n}\right]^2}.$$

Conversely, assume that there is a null sequence $(\varepsilon_n)_n$ in $(0,1)$ and a sequence $(x_n)_n$ in X so that

$$(1-\varepsilon_k)\sqrt{\left[\sum_{n=k}^{\infty}|t_n|\right]^2+\left[\sum_{n=k}^{\infty}\frac{|t_n|}{2^n}\right]^2} \le \left\|\sum_{n=k}^{\infty} t_n x_n\right\| \le \sqrt{\left[\sum_{n=k}^{\infty}|t_n|\right]^2+\left[\sum_{n=k}^{\infty}\frac{|t_n|}{2^n}\right]^2},$$

for all $(t_n)_n \in \ell^1$ and for all $k \in N$. Fix an increasing sequence $(m_i)_i$ in $\mathbb{N}$ and define for each $k \in \mathbb{N}$, $M_k := \sum_{i=1}^{k} m_i$ with $M_0 := 0$ and $y_k = \frac{1}{1+m_k}\sum_{n=M_{k-1}+1}^{M_k} x_n$.

Then, we get for each $k \in \mathbb{N}$,

$$\| y_k \| \le \frac{1}{m_k+1}(m_k+1) = 1$$

and thus, for all $(t_n)_n \in \ell^1$,

$$\left\|\sum_{n=k}^{\infty} t_n y_n\right\| \le \sum_{n=k}^{\infty}|t_n|$$

$$\left\|\sum_{n=k}^{\infty} t_n y_n\right\| = \left\| t_k\frac{1}{m_k+1}\sum_{j=M_{k-1}+1}^{M_k} x_j + t_{k+1}\frac{1}{m_{k+1}+1}\sum_{j=M_k+1}^{M_{k+1}} x_j + t_{k+2}\frac{1}{m_{k+2}+1}\sum_{j=M_{k+1}+1}^{M_{k+2}} x_j + \cdots + t_n\frac{1}{m_n+1}\sum_{j=M_{n-1}+1}^{M_n} x_j + \cdots \right\|$$

$$\ge \sqrt{\left(\sum_{n=k}^{\infty}|t_n|\frac{m_n}{m_n+1}\right)^2+\left(\sum_{n=k}^{\infty}\frac{|t_n|}{2^n}\frac{m_n}{m_n+1}\right)^2} \ge (1-\varepsilon_k)\frac{m_k}{m_k+1}\sum_{n=k}^{\infty}|t_n|$$

Then, for each $k \in \mathbb{N}$, define $\delta_k := 1-(1-\varepsilon_k)\frac{m_k}{m_k+1}$. Then,

$$(1-\delta_k)\sum_{n=k}^{\infty}|t_n| \le \left\|\sum_{n=k}^{\infty} t_n y_n\right\| \le \sum_{n=k}^{\infty}|t_n| \ .$$

Hence, by Theorem 5, X contains an isomorphic copy of ℓ^1. Then, by the previous theorem, X has property N-AIP-ℓ^1-2.

Theorem 15. *If a Banach space X has property N-AIP-ℓ^1-1 or if it has property N-AIP-ℓ^1-1, then X fails the*

fixed point property for uniformly Lipschitzian mappings on closed bounded convex subsets of X.

Proof. If a Banach space X has property N-AIP-ℓ^1-1 or if it has property N-AIP-ℓ^1-1, then X contains an isomorphic copy of ℓ^1 so X fails the fixed point property for uniformly Lipschitzian mappings on closed bounded convex subsets of X.

Theorem 16. *If a Banach space $(X,\|\cdot\|)$ has property N-AIP-c_0-1 then it contains an isomorphic copy of c_0 .*

Proof. Assume that a Banach space $(X,\|\cdot\|)$ has property *N-AIP-c_0-1*. Then, *there exist a sequence $(x_n)_n$ in X and scalars $0<k\leq K<\infty$ such that for all finite sequences $(a_n)_n$,*

$$k\left(\sup_n|a_n|+\sum_{n=1}^{\infty}\frac{|a_n|}{2^n}\right)\leq\left\|\sum_{n=1}^{\infty}a_nx_n\right\|\leq K\left(\sup_n|a_n|+\sum_{n=1}^{\infty}\frac{|a_n|}{2^n}\right)$$

and $\lim_{n\to\infty}\|x_n\|=k$. Hence,

$$k\sup_n|a_n|\leq\left\|\sum_{n=1}^{\infty}a_nx_n\right\|\leq\frac{3K}{2}\sup_n|a_n|$$

and $\lim_{n\to\infty}\|x_n\|=k$.

Theorem 17. *If a Banach space $(X,\|\cdot\|)$ has property N-AIP-c_0-2 then it contains an isomorphic copy of c_0.*

Proof. Assume that a Banach space $(X,\|\cdot\|)$ has property *N-AIP-c_0-2*. Then, *there exist a sequence $(x_n)_n$ in X and scalars $0<k\leq K<\infty$ such that for all finite sequences $(a_n)_n$,*

$$k\sum_{n=1}^{\infty}\frac{a_n^*}{2^{n-1}}\leq\left\|\sum_{n=1}^{\infty}a_nx_n\right\|\leq K\sum_{n=1}^{\infty}\frac{a_n^*}{2^{n-1}}$$

and $\lim_{n\to\infty}\|x_n\|=k$. Hence,

$$k\sup_n|a_n|\leq\left\|\sum_{n=1}^{\infty}a_nx_n\right\|\leq 2K\sup_n|a_n|$$

and $\lim_{n\to\infty}\|x_n\|=k$.

Theorem 18. *If a Banach space X has property N-AIP-c_0-1 or if it has property N-AIP-c_0-2, then X fails the fixed point property for asymptotically nonexpansive mappings on closed bounded convex subsets of X.*

Proof. If a Banach space X *has property N-AIP-c_0-1 or if it has property N-AIP-c_0-2*, then X contains an isomorphic copy of c_0 so X fails the fixed point property for asymptotically nonexpansive mappings on closed bounded convex subsets of X.

Theorem 19. *Let X be a Banach lattice. If X has one of the properties N-AIP-c_0-1, N-AIP-c_0-2, N-AIP-ℓ^1-1 or N-AIP-ℓ^1-2 then X is nonreflexive.*

Proof. If X *has property N-AIP-c_0-1 or if it has property N-AIP-c_0-2*, then X contains an isomorphic copy of c_0. But if *has property N-AIP-ℓ^1-1 or if it has property N-AIP-ℓ^1-2*, then X contains an isomorphic copy of ℓ^1. So, it contains either c_0 or ℓ^1. Then, by Theorem 10, X is nonreflexive.

REFERENCES

1. P.N. Dowling, C.J. Lennard, Every nonreflexive subspace of $L_1[0,1]$ fails the fixed point property, Proc. Amer. Math. Soc., 1997, 125: 443–446.
2. P.N. Dowling, C.J. Lennard, B. Turett, Reflexivity and the fixed-point property for nonexpansive maps, J. Math. Anal. Appl., 1996, 200(3): 653–662.

3. P.N. Dowling, C.J. Lennard, B. Turett, Renormings of l^1 and c_0 and fixed point properties, in: Handbook of Metric Fixed Point Theory, Springer, Netherlands, 2001, pp. 269–297.
4. P.N. Dowling, C.J. Lennard, B. Turett, Failure of the FPP inside an asymptotically isometric-free copy of c_0, Nonlinear Anal., 2010, 73(5): 1175-1179.
5. R.C. James, Uniformly non-square Banach spaces. Ann. of Math. (2), 1964, 542–550.
6. J. Lindenstrauss, L. Tzafriri, Classical Banach spaces I: sequence spaces, ergebnisse der mathematik und ihrer grenzgebiete, Vol. 92, Springer-Verlag, New York, 1977.

Subordination and Superordination of the Multiplier Transformation for Meromorphic Functions

Xiao-Yuan WANG[1] and Nan-Nan CHEN[2]

[1,2]*Institute of Sponge City Research,Pingxiang University, Jiangxi, P. R. China*

mewangxiaoyuan@163.com
1937004849@qq.com

Abstract. In the paper, the authors introduce and investigate a new subclasses of meromorphic functions, which by making use of the principle of subordination between analytic functions and a family of multiplier transforms. Some subordination and superordination results associated with the multiplier transforms are proved and several sandwich-type results are also obtained.

1. INTRODUCTION

Let Σ denote the class of functions of the form

$$f(z) = z^{-1} + \sum_{k=0}^{\infty} a_k z^k, \tag{1.1}$$

which are *analytic* in the *punctured* open unit disk

$$\mathbb{U}^* := \{z : z \in \mathbb{C} \text{ and } 0 < |z| < 1\} =: \mathbb{U}\setminus\{0\}.$$

Let $\mathcal{H}(\mathbb{U})$ be the linear space of all analytic functions in $\mathbb{U}$. For $n \in \mathbb{N}$ and $a \in \mathbb{C}$, we let

$$\mathcal{H}[a,n] := \{f \in \mathcal{H}(\mathbb{U}) : f(z) = a + a_n z^n + a_{n+1} z^{n+1} + \cdots\}.$$

Let $f, g \in \Sigma$, where f is given by (1.1) and g is defined by

$$g(z) = z^{-1} + \sum_{k=0}^{\infty} b_k z^k.$$

Then the functions f and g with the Hadamard product (or convolution) $f * g$ can be defined by

$$(f * g)(z) := z^{-1} + \sum_{k=0}^{\infty} a_k b_k z^k =: (g * f)(z).$$

For two functions f and g, analytic in $\mathbb{U}$, we say that the function f is subordinate to g in $\mathbb{U}$, and write

$$f(z) \prec g(z) \quad (z \in \mathbb{U}),$$

if there exists a Schwarz function ω, which is analytic in $\mathbb{U}$ with

$$\omega(0) = 0 \text{ and } |\omega(z)| < 1 \, (z \in \mathbb{U})$$

such that

$$f(z) = g(\omega(z)) \quad (z \in \mathbb{U}).$$

As is known to all that

$$f(z) \prec g(z) \quad (z \in \mathbb{U}) \Rightarrow f(0) = g(0) \text{ and } f(\mathbb{U}) \subset g(\mathbb{U}).$$

Furthermore, we have the following equivalence if the function g is univalent in $\mathbb{U}$,

$$f(z) \prec g(z) \quad (z \in \mathbb{U}) \Leftrightarrow f(0) = g(0) \text{and } f(\mathbb{U}) \subset g(\mathbb{U}).$$

For the functions $f \in \Sigma$, the multiplier transform $\mathsf{D}_{\lambda}^{n,l}$ can be defined as follows [4]

$$\mathsf{D}_{\lambda}^{n,l} f(z) := z^{-1} + \sum_{k=0}^{\infty} \left(\frac{\lambda + l(k+1)}{\lambda} \right)^{n} a_k z^k \tag{1.2}$$
$$(z \in \mathsf{U}^{*}; \lambda > 0; l0; n \in \mathsf{N}_0 := \mathsf{N} \cup \{0\};).$$

We can note that the multiplier transforms $\mathsf{D}_{\lambda}^{n,1}$ and $\mathsf{D}_{1}^{n,1}$ are the operators introduced and studied by Sarangi and Uralegaddi [13], and Uralegaddi and Somanatha [17, 18], respectively. Inspired by Wang and Wang[19], we can easily find from the multiplier transforms that

$$\mathsf{I}_{\lambda,\mu}^{n,l} f(z) = z^{-1} + \sum_{k=0}^{\infty} \frac{(\mu)_{k+1}}{(k+1)!} \left(\frac{\lambda}{\lambda + l(k+1)} \right)^{n} a_k z^k \quad (z \in \mathsf{U}^{*}), \tag{1.3}$$

where $(\mu)_k$ is the Pochhammer symbol defined by

$$(\mu)_k := \begin{cases} 1 & (k = 0), \\ \mu(\mu+1)\cdots(\mu+k-1) & (k \in \mathsf{N}). \end{cases}$$

Obviously, the multiplier transforms $\mathsf{I}_{\lambda,\mu}^{n,1}$ $(n \in \mathsf{N}_0)$ is the well-known Cho-Kwon-Srivastava operator (see, for more details, [2, 3, 5, 11, 14, 15] and references cited in).

It is readily verified from (1.3) that

$$z\left(\mathsf{I}_{\lambda,\mu}^{n,l} f\right)(z) = \mu \mathsf{I}_{\lambda,\mu+1}^{n,l} f(z) - (\mu+1)\mathsf{I}_{\lambda,\mu}^{n,l} f(z), \tag{1.4}$$

and

$$lz\left(\mathsf{I}_{\lambda,\mu}^{n+1,l} f\right)(z) = \lambda \mathsf{I}_{\lambda,\mu}^{n,l} f(z) - (\lambda+l)\mathsf{I}_{\lambda,\mu}^{n+1,l} f(z). \tag{1.5}$$

with $n0; l > 0, \lambda > 0 \, and \, \mu > 0.$

2. PRELIMINARIES RESULTS

In order to prove our main results, we need the following definitions and lemmas.

Definition 1 ([1, p.440, Definition 1]) Let $\psi : \mathsf{C}^4 \times \mathsf{U} \to \mathsf{C}$, $q(z)$ and $h(z)$ be univalent in U. If $p(z)$ is analytic in U and satisfies the third-order differential subordination

$$\psi(p(z), zp'(z), z^2 p''(z), z^3 p'''(z); z) \prec h(z), \tag{2.1}$$

then $p(z)$ is called a solution of the differential subordination. is called a dominant of the solutions of the differential subordination or more simply a dominant if $p(z) \prec q(z)$ for all $p(z)$ satisfying (2.1). A dominant $q(z)$ that satisfies

$$q(z) \prec q(z),$$

for all dominants of (2.1) is called the best dominant of (2.1).

Be similar to the second order differential superordinations studied by Miller and Mocanu [8], Tang *et al.* [16] defined the following third order differential superordinations.

Definition 2 ([16, p.3, Definition 5]) Let $\psi : \mathbb{C}^4 \times \mathbb{U} \to \mathbb{C}$ and the function $h(z)$ be analytic in $\mathbb{U}$. If the function $p(z)$ and

$$\psi(p(z), zp'(z), z^2p''(z), z^3p'''(z); z)$$

are univalent in $\mathbb{U}$ and satisfies the third order differential superordination

$$h(z) \prec \psi(p(z), zp'(z), z^2p''(z), z^3p'''(z); z), \tag{2.2}$$

then $p(z)$ is called a solution of the differential superordination.An analytic function $q(z)$ is called a subordinant of the solutions of the differential superordination or more simply a subordinant if $q(z) \prec p(z)$ satisfies (2.2) for

$p(z)$ satisfies (2.2), A univalent subordinant $q(z)$ that satisfies

$$q(z) \prec q(z)$$

for all superordinants $q(z)$ of (2.2) is said to be the best superordinant.

Lemma 1 *(See [4]) Let q be convex univalent in $\mathbb{U}$ and $\psi, \gamma \in \mathbb{C}$ with*

$$\Re\left(1 + \frac{zq''(z)}{q'(z)}\right) > \max\left\{0, -\Re\left(\frac{\psi}{\gamma}\right)\right\}.$$

If p is analytic in $\mathbb{U}$ and

$$\psi p(z) + \gamma z p'(z) \prec \psi q(z) + \gamma z q'(z),$$

then $p \prec q$, and q is the best dominant.

Lemma 2 ([8, p.132],[9, p.190]) *Let $q \in \mathbb{U}$ be univalent and θ, ϕ be analytic in a domain $\mathbb{D}$ containing $q(\mathbb{U})$ with $\phi(\omega) \neq 0$ when $\omega \in q(\mathbb{U})$. Set $Q(z) = zq'(z)\phi(q(z))$, and $h(z) = \theta(q(z)) + \sigma(z)$. Suppose that*

1. $Q(z)$ *is starlike in* $\mathbb{U}$,
2. $\Re\left(\frac{zh'(z)}{Q(z)}\right) > 0.$

If $p \in \mathbb{H}[q(0), 1]$ for some $n \in \mathbb{N}$ with $p(\mathbb{U}) \subset \mathbb{D}$ and

$$\theta(p(z)) + zp'(z)\phi(p(z)) \prec \theta(q(z)) + zq'(z)\phi(q(z)), \tag{2.3}$$

then $p \prec q$ and q is the best dominant.

Lemma 3 ([6, p.332]) *Let q be univalent in $\mathbb{U}$ and θ, ϕ be analytic in a domain $\mathbb{D}$ containing $q(\mathbb{U})$. Suppose that*

1. $zq'(z)\phi(q(z))$ *is starlike in* $\mathbb{U}$,
2. $\Re\left(\frac{\theta'(q(z))}{\phi(q(z))}\right) > 0.$

If $p \in \mathbb{H}[q(0), 1] \cap Q$, with $p(\mathbb{U}) \subseteq \mathbb{D}$; $\theta(p(z)) + zp'(z)\phi(p(z))$ is univalent in $\mathbb{U}$ and

$$\theta(q(z)) + zq'(z)\phi(q(z)) \prec \theta(p(z)) + zp'(z)\phi(p(z)),$$

then $q \prec p$ and q is the best dominant.

Lemma 4 ([7, p.822]) *Let* $q \in \mathcal{U}$ *be univalent and* $\gamma \in \mathbb{C}$ *, with* $\Re(\gamma) > 0$ *. If* $p \in \mathcal{H}[q(0),1] \cap Q$, $p(z) + \gamma z p'(z)$ *is univalent in* $\mathcal{U}$ *and*

$$q(z) + \gamma z q'(z) \prec p(z) + \gamma z p'(z) \quad (z \in \mathcal{U}),$$

then $q \prec p$ and q is the best dominant.

Lemma 5 *(See [12]) The function*

$$(1-z)^{\nu} \equiv e^{\nu \log(1-z)} \quad (\nu \neq 0)$$

is univalent in $\mathcal{U}$ if and only if ν is either in the closed disk $|\nu - 1| 1$ or in the closed disk $|\nu + 1| 1$.

The main purpose of the present paper is to investigate subordination, superordination and double sandwich theorems results involving the multiplier transformation $\mathrm{I}_{\lambda,\mu}^{n,l} f(z)$.

3. THE MAIN RELATIONSHIPS

Throughout this section unless otherwise mentioned the parameters $\gamma, \xi, n, \lambda, \mu, l, \sigma, \delta,$ and a, b are constrained as follows:

$$\gamma \neq 0, \xi \neq 0, n0; \lambda > 0, \mu > 0, l > 0, \sigma, \delta, a, b \in \mathbb{C} \ \text{ with } \ a + b \neq 0.$$

Firstly, we present following result.

Theorem 1 *Let* q *be convex univalent in* $\mathcal{U}$ *with*

$$\Re\left(1 + \frac{z q''(z)}{q'(z)}\right) > \max\left\{0, -\Re\left(\frac{\mu}{\eta}\right)\right\} \quad (\eta \neq 0). \tag{3.1}$$

If $f \in \Sigma$ satisfies the subordination

$$\eta z \mathrm{I}_{\lambda,\mu+1}^{n,l} f(z) + (1-\eta) z \mathrm{I}_{\lambda,\mu}^{n,l} f(z) \prec q(z) + \frac{\eta z q'(z)}{\mu}, \tag{3.2}$$

then

$$z \mathrm{I}_{\lambda,\mu}^{n,l} f(z) \prec q(z), \tag{3.3}$$

and q is the best dominant.

Proof. Suppose that the function h given by

$$\mathrm{h}(z) := z \mathrm{I}_{\lambda,\mu}^{n,l} f(z). \tag{3.4}$$

Taking logarithm derivative on both sides both sides of (3.4), we can get

$$\frac{z \mathrm{h}'(z)}{\mathrm{h}(z)} = 1 + \frac{z\left(\mathrm{I}_{\lambda,\mu}^{n,l} f\right)'(z)}{\mathrm{I}_{\lambda,\mu}^{n,l} f(z)}. \tag{3.5}$$

By virtue of (1.4), (3.2) and (3.4), we have

$$\mathrm{h}(z) + \frac{\eta z \mathrm{h}'(z)}{\mu} \prec q(z) + \frac{\eta z q'(z)}{\mu}.$$

According to Lemma 1, with $\gamma = \frac{\eta}{\mu}$ and $\psi = 1$ leads to (3.3).

Corollary 1 *Let* $-1 \quad B < A1$ *and*

$$\Re\left(\frac{1-Bz}{1+Bz}\right) > \max\left\{0,-\Re\left(\frac{\mu}{\eta}\right)\right\} \quad (\eta \neq 0).$$

If $f \in \Sigma$ satisfies the subordination

$$\eta z\mathrm{I}^{n,l}_{\lambda,\mu+1} f(z) + (1-\eta) z\mathrm{I}^{n,l}_{\lambda,\mu} f(z) \prec \frac{1+Az}{1+Bz} + \frac{\eta}{\mu}\frac{(A-B)z}{(1+Bz)^2},$$

then

$$z\mathrm{I}^{n,l}_{\lambda,\mu} f(z) \prec \frac{1+Az}{1+Bz},$$

and $\dfrac{1+Az}{1+Bz}$ is the best dominant.

On the basis of the method proving Theorem 1, considering (1.5) and Lemma 1, we easily get the following results.

Corollary 2 *Let* q *be convex univalent in* $\cup$ *with*

$$\Re\left(1+\frac{zq''(z)}{q'(z)}\right) > \max\left\{0,-\Re\left(\frac{\lambda}{\eta l}\right)\right\} \quad (\eta \neq 0). \tag{3.6}$$

If $f \in \Sigma$ satisfies the subordination

$$\eta z\mathrm{I}^{n,l}_{\lambda,\mu} f(z) + (1-\eta) z\mathrm{I}^{n+1,l}_{\lambda,\mu} f(z) \prec q(z) + \frac{\eta l z q'(z)}{\lambda},$$

then

$$z\mathrm{I}^{n+1,l}_{\lambda,\mu} f(z) \prec q(z),$$

and $q(z)$ is the best dominant.

Corollary 3 *Let* $-1 \quad B < A1$ *and*

$$\Re\left(\frac{1-Bz}{1+Bz}\right) > \max\left\{0,-\Re\left(\frac{\mu}{\eta}\right)\right\} \quad (\eta \neq 0).$$

If $f \in \Sigma$ satisfies the subordination

$$\eta z\mathrm{I}^{n,l}_{\lambda,\mu} f(z) + (1-\eta) z\mathrm{I}^{n+1,l}_{\lambda,\mu} f(z) \prec \frac{1+Az}{1+Bz} + \frac{\eta l}{\lambda}\frac{(A-B)z}{(1+Bz)^2},$$

then

$$z\mathrm{I}^{n+1,l}_{\lambda,\mu} f(z) \prec \frac{1+Az}{1+Bz},$$

and $\dfrac{1+Az}{1+Bz}$ is the best dominant.

Theorem 2 *Let* q *be univalent in* $\cup$. *Suppose that* q *satisfies*

$$\Re\left(1+\frac{zq''(z)}{q'(z)}-\frac{zq'(z)}{q(z)}\right)>0. \tag{3.7}$$

Let

$$\kappa(z)=1+\gamma\xi\left(1+\frac{az\left(\mathrm{I}^{n,l}_{\lambda,\mu+1}f\right)'(z)+bz\left(\mathrm{I}^{n,l}_{\lambda,\mu}f\right)'(z)}{a\mathrm{I}^{n,l}_{\lambda,\mu+1}f(z)+b\mathrm{I}^{n,l}_{\lambda,\mu}f(z)}\right). \tag{3.8}$$

If

$$\kappa(z)\prec 1+\gamma\frac{zq'(z)}{q(z)},$$

then

$$\left(\frac{az\mathrm{I}^{n,l}_{\lambda,\mu+1}f(z)+bz\mathrm{I}^{n,l}_{\lambda,\mu}f(z)}{a+b}\right)^{\xi}\prec q(z), \tag{3.9}$$

and q is the best dominant.

Proof. Defined the function p by

$$\rho(z):=\left(\frac{az\mathrm{I}^{n,l}_{\lambda,\mu+1}f(z)+bz\mathrm{I}^{n,l}_{\lambda,\mu}f(z)}{a+b}\right)^{\xi}\quad(\xi\neq 0;a+b\neq 0). \tag{3.10}$$

Then, differentiating both sides of (3.10) with respect to z logarithmically, we have

$$\frac{z\rho'(z)}{\rho(z)}=\xi\left(1+\frac{az\left(\mathrm{I}^{n,l}_{\lambda,\mu+1}f\right)'(z)+bz\left(\mathrm{I}^{n,l}_{\lambda,\mu}f\right)'(z)}{a\mathrm{I}^{n,l}_{\lambda,\mu+1}f(z)+b\mathrm{I}^{n,l}_{\lambda,\mu}f(z)}\right).$$

If we take

$$\theta(\omega)=1\quad\text{and}\quad\phi(\omega)=\frac{\gamma}{\omega},$$

such that $\theta(\omega)$ is analytic in $\mathbb{C}$ and that $\phi(\omega)\neq 0$ is analytic in $\mathbb{C}\setminus\{0\}$. Also let

$$Q(z):=zq'(z),\ \phi(q(z))=\gamma\frac{zq'(z)}{q(z)}$$

and

$$h(z):=\theta(q(z))+Q(z)=1+\gamma\frac{zq'(z)}{q(z)}.$$

From (3.7), we find that $Q(z)$ is starlike univalent in $\mathbb{U}$, and

$$\Re\left(\frac{zh'(z)}{Q(z)}\right)=\Re\left(1+\frac{zq''(z)}{q'(z)}-\frac{zq'(z)}{q(z)}\right)>0.$$

Thus, through Lemma 2 to (3.8), we obtain the desired result.

Taking $a=0,b=1,\gamma=1$ and $q(z)=\dfrac{1+Az}{1+Bz}$ in Theorem 2, we derive the following results.

Corollary 4 *Let* $-1\quad B<A1,\xi\neq 0$. *If* $f\in\Sigma$, *and*

$$1+\xi\left(1+\frac{z\left(\mathrm{I}_{\lambda,\mu}^{n,l}f\right)'(z)}{\mathrm{I}_{\lambda,\mu}^{n,l}f(z)}\right)\prec 1+\frac{(A-B)z}{(1+Az)(1+Bz)},$$

then

$$\left(z\mathrm{I}_{\lambda,\mu}^{n,l}f(z)\right)^{\xi}\prec\frac{1+Az}{1+Bz},$$

and $\dfrac{1+Az}{1+Bz}$ is the best dominant.

With the method of proof of Theorem 2, similarly, we easily get the following result.

Corollary 5 *Let* q *be univalent in* $\cup$. *Suppose that* q *satisfies (3.7). Let*

$$\rho(z)=1+\gamma\xi\left(1+\frac{az\left(\mathrm{I}_{\lambda,\mu}^{n,l}f\right)'(z)+bz\left(\mathrm{I}_{\lambda,\mu}^{n+1,l}f\right)'(z)}{a\mathrm{I}_{\lambda,\mu}^{n,l}f(z)+b\mathrm{I}_{\lambda,\mu}^{n+1,l}f(z)}\right). \tag{3.11}$$

If

$$\rho(z)\prec 1+\gamma\frac{zq'(z)}{q(z)}$$

then

$$\left(\frac{az\mathrm{I}_{\lambda,\mu}^{n,l}f(z)+bz\mathrm{I}_{\lambda,\mu}^{n+1,l}f(z)}{a+b}\right)^{\xi}\prec q(z),$$

and q is the best dominant.

Theorem 3 *Let* q *be univalent in* $\cup$. *Suppose that* q *satisfies*

$$\Re\left(1+\frac{zq''(z)}{q'(z)}\right)>\max\left\{0,-\Re\left(\frac{\sigma}{\gamma}\right)\right\}. \tag{3.12}$$

Let

$$\begin{aligned}\tau(z)=&\left(\frac{az\mathrm{I}_{\lambda,\mu+1}^{n,l}f(z)+bz\mathrm{I}_{\lambda,\mu}^{n,l}f(z)}{a+b}\right)^{\xi}\\&\cdot\left[\sigma+\gamma\mu\left(1+\frac{az\left(\mathrm{I}_{\lambda,\mu+1}^{n,l}f\right)'(z)+bz\left(\mathrm{I}_{\lambda,\mu}^{n,l}f\right)'(z)}{a\mathrm{I}_{\lambda,\mu+1}^{n,l}f(z)+b\mathrm{I}_{\lambda,\mu}^{n,l}f(z)}\right)\right]+\delta.\end{aligned} \tag{3.13}$$

If

$$\tau(z)\prec\sigma q(z)+\delta+\gamma zq'(z),$$

then

$$\left(\frac{az\mathrm{I}_{\lambda,\mu+1}^{n,l}f(z)+bz\mathrm{I}_{\lambda,\mu}^{n,l}f(z)}{a+b}\right)^{\xi}\prec q(z),$$

and q is the best dominant.

Proof. Let us consider a function Φ defined by

$$\Phi(z):=\left(\frac{az\mathrm{I}_{\lambda,\mu+1}^{n,l}f(z)+bz\mathrm{I}_{\lambda,\mu}^{n,l}f(z)}{a+b}\right)^{\xi}\quad(\xi\neq 0;a+b\neq 0). \tag{3.14}$$

Differentiating on both sides of (3.14) logarithmically, we get

$$\frac{z\Phi'(z)}{\Phi(z)}=\xi\left(1+\frac{az\left(\mathrm{I}_{\lambda,\mu+1}^{n,l}f\right)'(z)+bz\left(\mathrm{I}_{\lambda,\mu}^{n,l}f\right)'(z)}{a\mathrm{I}_{\lambda,\mu+1}^{n,l}f(z)+b\mathrm{I}_{\lambda,\mu}^{n,l}f(z)}\right)$$

and therefore

$$z\Phi'(z)=\xi\Phi(z)\left(1+\frac{az\left(\mathrm{I}_{\lambda,\mu+1}^{n,l}f\right)'(z)+bz\left(\mathrm{I}_{\lambda,\mu}^{n,l}f\right)'(z)}{a\mathrm{I}_{\lambda,\mu+1}^{n,l}f(z)+b\mathrm{I}_{\lambda,\mu}^{n,l}f(z)}\right).$$

Setting

$$\theta(\omega)=\sigma\omega+\delta\quad\text{and}\quad\phi(\omega)=\gamma.$$

Also taking

$$Q(z)=zq'(z)\phi(q(z))=\gamma zq'(z)$$

and

$$h(z)=\theta(q(z))+Q(z)=\sigma q(z)+\delta+\gamma zq'(z).$$

From (3.12), we find that $Q(z)$ is starlike in U, and

$$\Re\left(\frac{zh'(z)}{Q(z)}\right)=\Re\left(\frac{\sigma}{\gamma}+1+\frac{zq''(z)}{q'(z)}\right)>0.$$

Thus, the result follows from Lemma 2, immediately.

Taking $a=0,b=\gamma=1$ and $q(z)=\dfrac{1+Az}{1+Bz}$ in Theorem 3, we derive the following corollary.

Corollary 6 *Let*

$$\Re\left(\frac{1+Az}{1+Bz}\right)>\max\{0,-\Re(\sigma)\}.$$

If

$$\left(z\mathrm{I}_{\lambda,\mu}^{n,l}f(z)\right)^{\xi}\left[\sigma+\xi\left(1+\frac{z\left(\mathrm{I}_{\lambda,\mu}^{n,l}f\right)'(z)}{\mathrm{I}_{\lambda,\mu}^{n,l}f(z)}\right)\right]+\delta\prec\sigma\frac{1+Az}{1+Bz}+\delta+\frac{(A-B)z}{(1+Bz)^2},$$

then

$$\left(z\mathrm{I}_{\lambda,\mu}^{n,l}f(z)\right)^{\xi}\prec\frac{1+Az}{1+Bz},$$

and $\dfrac{1+Az}{1+Bz}$ is the best dominant.

By applying the method of proof of Theorem 3, similarly, we easily obtain the following result.

Corollary 7 *Let* q *be univalent in U. Suppose that* q *satisfies (3.12) and*

$$\varpi(z)=\left(\frac{az\mathrm{I}_{\lambda,\mu}^{n,l}f(z)+bz\mathrm{I}_{\lambda,\mu}^{n+1,l}f(z)}{a+b}\right)^{\xi}\cdot\left[\sigma+\gamma\xi\left(1+\frac{az\left(\mathrm{I}_{\lambda,\mu}^{n,l}f\right)'(z)+bz\left(\mathrm{I}_{\lambda,\mu}^{n+1,l}f\right)'(z)}{a\mathrm{I}_{\lambda,\mu}^{n,l}f(z)+b\mathrm{I}_{\lambda,\mu}^{n+1,l}f(z)}\right)\right]+\delta. \tag{3.15}$$

If

$$\varpi(z)\prec\sigma q(z)+\delta+\gamma zq'(z),$$

then

$$\left(\frac{az\mathrm{I}_{\lambda,\mu}^{n,l}f(z)+bz\mathrm{I}_{\lambda,\mu}^{n+1,l}f(z)}{a+b}\right)^{\xi}\prec q(z),$$

and q is the best dominant.

In view of Lemma 2 and Lemma 5, we get the following results.

Theorem 4 *Let* $0\quad\alpha<1$. *Suppose that* $\gamma\in\mathbb{C}$ *with* $\gamma\neq0$ *and satisfy either* $|2\mu\gamma(1-\alpha)+1|1$ *or* $|2\mu\gamma(1-\alpha)-1|1$. *If* f *satisfies*

$$\Re\left(\frac{\mathrm{I}_{\lambda,\mu+1}^{n,l}f(z)}{\mathrm{I}_{\lambda,\mu}^{n,l}f(z)}\right)>\alpha, \tag{3.16}$$

then

$$\left(z\mathrm{I}_{\lambda,\mu}^{n,l}f(z)\right)^{\gamma}\prec\frac{1}{(1-z)^{2\mu\gamma(1-\alpha)}}=q(z),$$

and q is the best dominant.

Proof. Let

$$\Psi(z)=\left(z\mathrm{I}_{\lambda,\mu}^{n,l}f(z)\right)^{\gamma}\quad(z\in\mathsf{U}). \tag{3.17}$$

Combining (1.4),(3.16) and (3.17), we derive

$$1+\frac{z\Psi'(z)}{\mu\gamma\Psi(z)}\prec\frac{1+(1-2\alpha)z}{1-z}\quad(z\in\mathsf{U}). \tag{3.18}$$

If we set

$$q(z)=\frac{1}{(1-z)^{2\mu\gamma(1-\alpha)}},\quad\theta(\omega)=1\quad\text{and}\quad\phi(\omega)=\frac{1}{\mu\gamma\omega},$$

then q is univalent by the condition of the theorem and Lemma 5. Furthermore, it is easy to show that $q,\theta(\omega)$ and $\phi(\omega)$ satisfy the conditions of Lemma 2. Since

$$Q(z)=zq'(z)\phi(q(z))=\frac{2(1-\alpha)z}{1-z}$$

is univalent starlike in U and

$$h(z)=\theta(q(z))+Q(z)=\frac{1+(1-2\alpha)z}{1-z}$$

satisfy the conditions of Lemma 2. Thus we redily arrive at the result follows from (3.18) immediately.

Corollary 8 *Let* $0 \quad \alpha < 1$ *and* $\gamma 1$. *If* $f \in \Sigma$ *satisfies the condition (3.16) then*

$$\Re\left(z\mathrm{I}_{\lambda,\mu}^{n,l} f(z)\right)^{2\mu\gamma(1-\alpha)} > 2^{-1/\gamma}$$

and the bound $2^{-1/\gamma}$ is the best possible.

By similarly applying the method of proof of Theorem 4 we easily get the following results.

Corollary 9 *Let* $0 \quad \alpha < 1$. *Suppose that* $\gamma \in \mathbb{C}$ *with* $\gamma \neq 0$ *and satisfy either* $|2\gamma\lambda(1-\alpha)/l + 1| 1$ *or* $|2\gamma\lambda(1-\alpha)/l - 1| 1$. *If* f *satisfies*

$$\Re\left(\frac{\mathrm{I}_{\lambda,\mu}^{n,l} f(z)}{\mathrm{I}_{\lambda,\mu}^{n+1,l} f(z)}\right) > \alpha, \tag{3.19}$$

then

$$\left(z\mathrm{I}_{\lambda,\mu}^{n+1,l} f(z)\right)^{\gamma} \prec \frac{l}{(1-z)^{2\gamma\lambda(1-\alpha)}} = q(z),$$

and q is the best dominant.

Corollary 10 *Let* $0 \quad \alpha < 1$ *and* $\gamma 1$. *If* $f \in \Sigma$ *satisfies the condition (3.19), then*

$$\Re\left(z\mathrm{I}_{\lambda,\mu}^{n+1,l} f(z)\right)^{2\gamma\lambda(1-\alpha)/l} > 2^{-1/\gamma}$$

and the bound $2^{-1/\gamma}$ is the best possible.

Next, we present some superordination results involving the multiplier transformation $\mathrm{I}_{\lambda,\mu}^{n,l} f(z)$.

Theorem 5 *Let* q *be convex univalent in* U *and* $\Re(\eta) > 0$. *Also let*

$$z\mathrm{I}_{\lambda,\mu}^{n,l} f(z) \in \mathrm{H}[q(0),1] \cap Q$$

and

$$\eta z\mathrm{I}_{\lambda,\mu+1}^{n,l} f(z) + (1-\eta) z\mathrm{I}_{\lambda,\mu}^{n,l} f(z)$$

is univalent in U. If

$$q(z) + \frac{\eta z q'(z)}{\mu} \prec \eta z\mathrm{I}_{\lambda,\mu+1}^{n,l} f(z) + (1-\eta) z\mathrm{I}_{\lambda,\mu}^{n,l} f(z), \tag{3.20}$$

then

$$q(z) \prec z\mathrm{I}_{\lambda,\mu}^{n,l} f(z), \tag{3.21}$$

and q is the best subordinant.

Proof. Let

$$\varepsilon(z) = z\mathrm{I}_{\lambda,\mu}^{n,l} f(z).$$

We easily get that

$$\varepsilon(z) + \frac{\eta z \varepsilon'(z)}{\mu} = \eta z\mathrm{I}_{\lambda,\mu+1}^{n,l} f(z) + (1-\eta) z\mathrm{I}_{\lambda,\mu}^{n,l} f(z) \tag{3.22}$$

Next, combining (3.20), (3.22) and Lemma 4, we easily derive the assertion (3.21) of Theorem 5.

With the aid of (1.5) and Lemma 4 and by similarly applying the method of proof of Theorem 5, we can get the following result.

Corollary 11 *Let* q *be convex univalent in* U *and* $\Re(\eta) > 0$. *Also let*

$$zI_{\lambda,\mu}^{n+1,l} f(z) \in H[q(0),1] \cap Q$$

and

$$\eta zI_{\lambda,\mu}^{n,l} f(z) + (1-\eta) zI_{\lambda,\mu}^{n+1,l} f(z)$$

is univalent in U. If

$$q(z) + \frac{\eta l z q'(z)}{\lambda} \prec \eta zI_{\lambda,\mu}^{n,l} f(z) + (1-\eta) zI_{\lambda,\mu}^{n+1,l} f(z),$$

then

$$q(z) \prec zI_{\lambda,\mu}^{n+1,l} f(z),$$

and q is the best subordinant.

By virtue of Lemma 3, and with similarly applying the method of proof of Theorem 5, we get the following results.

Corollary 12 *Let* q *be convex univalent in* U. *Also let*

$$\left(\frac{azI_{\lambda,\mu+1}^{n,l} f(z) + bzI_{\lambda,\mu}^{n,l} f(z)}{a+b} \right)^{\xi} \in H[q(0),1] \cap Q,$$

and κ be defined by (3.8) is univalent in U. If

$$1 + \gamma \frac{zq'(z)}{q(z)} \prec \kappa(z),$$

then

$$q(z) \prec \left(\frac{azI_{\lambda,\mu+1}^{n,l} f(z) + bzI_{\lambda,\mu}^{n,l} f(z)}{a+b} \right)^{\xi},$$

and q is the best subordinant.

Corollary 13 *Let* q *be convex univalent in* U. *Also let*

$$\left(\frac{azI_{\lambda,\mu}^{n,l} f(z) + bzI_{\lambda,\mu}^{n+1,l} f(z)}{a+b} \right)^{\xi} \in H[q(0),1] \cap Q,$$

and ρ be defined by ((3.11) is univalent in U. If

$$1 + \gamma \frac{zq'(z)}{q(z)} \prec \rho(z),$$

then

$$q(z) \prec \left(\frac{azI_{\lambda,\mu}^{n,l} f(z) + bzI_{\lambda,\mu}^{n+1,l} f(z)}{a+b} \right)^{\xi},$$

and q is the best subordinant.

Corollary 14 *Let* q *be convex univalent in* U. *Also let*

$$zI_{\lambda,\mu}^{n,l} f(z) \in H[q(0),1] \cap Q,$$

and τ be defined by (3.13) is univalent in $\cup$. If q satisfies

$$\Re\left(\frac{\sigma q'(z)}{\gamma}\right) > 0 \tag{3.23}$$

and

$$\sigma q(z) + \delta + \gamma z q'(z) \prec \tau(z),$$

then

$$q(z) \prec \left(\frac{a z I_{\lambda,\mu+1}^{n,l} f(z) + b z I_{\lambda,\mu}^{n,l} f(z)}{a+b}\right)^{\xi},$$

and q is the best subordinant.

Corollary 15 *Let q be convex univalent in $\cup$. Also let*

$$z I_{\lambda,\mu}^{n+1,l} f(z) \in H[q(0),1] \cap Q,$$

and ϖ be defined by (3.15) is univalent in $\cup$. If q satisfies (3.25) and

$$\sigma q(z) + \delta + \gamma z q'(z) \prec \varphi(z),$$

then

$$q(z) \prec \left(\frac{a z I_{\lambda,\mu}^{n,l} f(z) + b z I_{\lambda,\mu}^{n+1,l} f(z)}{a+b}\right)^{\xi},$$

and q is the best subordinant.

Finally, combining the results of subordination and superordination mentioned above, we get the following sandwich-type results.

Corollary 16 *Let q_1 and q_2 be convex univalent in $\cup$, and $\Re(\eta) > 0$. Suppose that q_2 satisfies (3.1) and $z I_{\lambda,\mu}^{n,l} f(z) \in H[q(0),1] \cap Q$. Let*

$$\eta z I_{\lambda,\mu+1}^{n,l} f(z) + (1-\eta) z I_{\lambda,\mu}^{n,l} f(z)$$

is univalent in $\cup$. If

$$q_1(z) + \frac{\eta z q_1'(z)}{\mu} \prec \eta z I_{\lambda,\mu+1}^{n,l} f(z) + (1-\eta) z I_{\lambda,\mu}^{n,l} f(z) \prec q_2(z) + \frac{\eta z q_2'(z)}{\mu},$$

then

$$q_1(z) \prec z I_{\lambda,\mu}^{n,l} f(z) \prec q_2(z),$$

and q_1 and q_2 are, respectively, the best subordinant and the best dominant.

Corollary 17 *Let q_3 and q_4 be convex univalent in $\cup$, and $\Re(\eta) > 0$. Suppose that q_4 satisfies (3.6) and $z I_{\lambda,\mu}^{n+1,l} f(z) \in H[q(0),1] \cap Q$. Let*

$$\eta z I_{\lambda,\mu}^{n,l} f(z) + (1-\eta) z I_{\lambda,\mu}^{n+1,l} f(z)$$

is univalent in U. If

$$q_3(z) + \frac{\eta l z q_3'(z)}{\lambda} \prec \eta z I_{\lambda,\mu}^{n,l} f(z) + (1-\eta) z I_{\lambda,\mu}^{n+1,l} f(z) \prec q_4(z) + \frac{\eta l z q_4'(z)}{\lambda},$$

then

$$q_3(z) \prec zI_{\lambda,\mu}^{n+1,l} f(z) \prec q_4(z),$$

and q_3 and q_4 are, respectively, the best subordinant and the best dominant.

Corollary 18 *Let q_5 be convex univalent and q_6 be univalent in $\cup$. Suppose that If q_6 satisfies (3.7) and*

$$\left(\frac{azI_{\lambda,\mu+1}^{n,l} f(z) + bzI_{\lambda,\mu}^{n,l} f(z)}{a+b}\right)^{\xi} \in H[q(0),1] \cap Q.$$

Let κ be defined by (3.8) is univalent in $\cup$. If

$$1+\gamma\frac{zq_5'(z)}{q_5(z)} \prec \kappa(z) \prec 1+\gamma\frac{zq_6'(z)}{q_6(z)},$$

then

$$q_5(z) \prec \left(\frac{azI_{\lambda,\mu+1}^{n,l} f(z) + bzI_{\lambda,\mu}^{n,l} f(z)}{a+b}\right)^{\xi} \prec q_6(z),$$

and q_5 and q_6 are, respectively, the best subordinant and the best dominant.

Corollary 19 *Let q_7 be convex univalent and q_8 be univalent in $\cup$. Suppose that q_8 satisfies (3.7) and*

$$\left(\frac{azI_{\lambda,\mu}^{n,l} f(z) + bzI_{\lambda,\mu}^{n+1,l} f(z)}{a+b}\right)^{\xi} \in H[q(0),1] \cap Q.$$

Let ρ be defined by (3.11) is univalent in $\cup$. If

$$1+\gamma\frac{zq_7'(z)}{q_7(z)} \prec \rho(z) \prec 1+\gamma\frac{zq_8'(z)}{q_8(z)},$$

then

$$q_7(z) \prec \left(\frac{azI_{\lambda,\mu}^{n,l} f(z) + bzQ_{\alpha+1,\beta}^{\lambda} f(z)}{a+b}\right)^{\xi} \prec q_8(z),$$

and q_7 and q_8 are, respectively, the best subordinant and the best dominant.

Corollary 20 *Let q_9 be convex univalent and q_{10} be univalent in $\cup$. Suppose that q_9 satisfies (3.23), q_{10} satisfies (3.12) and*

$$zI_{\lambda,\mu}^{n,l} f(z) \in H[q(0),1] \cap Q.$$

Let τ be defined by (3.13) is univalent in $\cup$. If

$$\sigma q_9(z) + \delta + \gamma z q_9'(z) \prec \tau(z) \prec \sigma q_{10}(z) + \delta + \gamma z q_{10}'(z),$$

then

$$q_9(z) \prec \left(\frac{azI_{\lambda,\mu+1}^{n,l} f(z) + bzI_{\lambda,\mu}^{n,l} f(z)}{a+b}\right)^{\xi} \prec q_{10}(z),$$

and q_9 and q_{10} are, respectively, the best subordinant and the best dominant.

Corollary 21 *Let* q_{11} *be convex univalent and* q_{12} *be univalent in* U. *Suppose that* q_{11} *satisfies (3.23),* q_{12} *satisfies* (3.12), *and*

$$z\mathsf{I}_{\lambda,\mu}^{n+1,l} f(z) \in \mathsf{H}[q(0),1] \cap Q.$$

Let ϖ be defined by (3.15) is univalent in U. If

$$\sigma q_{11}(z) + \delta + \gamma z q_{11}^{'}(z) \prec \varpi(z) \prec \sigma q_{12}(z) + \delta + \gamma z q_{12}^{'}(z),$$

then

$$q_{11}(z) \prec \left(\frac{az\mathsf{I}_{\lambda,\mu}^{n,l} f(z) + bz\mathsf{I}_{\lambda,\mu}^{n+1,l} f(z)}{a+b} \right)^{\xi} \prec q_{12}(z),$$

and q_{11} and q_{12} are, respectively, the best subordinant and the best dominant.

ACKNOWLEDGMENTS

The project is supported by Youth Science Fund Research Project of Pingxiang University (Grant Nos. 2019D0202; 2018D0218) and the Scientific Research Fund of Jiangxi Provincial Department of Education (Grant No.GJJ191157).

REFERENCES

1. J. A. Antonino, S. S. Miller, Third-order differential inequalities and subordinations in the complex plane. *Complex Var. Elliptic Equ.* **56** (2011), no. 5, 439–454.
2. N. E. Cho, O. S. Kwon and H. M. Srivastava, Inclusion and argument properties for certain subclasses of meromorphic functions associated with a family of multiplier transformations, *J. Math. Anal. Appl.* **300** (2004), 505–520.
3. N. E. Cho, O. S. Kwon and H. M. Srivastava, Inclusion relationships for certain subclasses of meromorphic functions associated with a family of multiplier transformations, *Integral Transforms Spec. Funct.* **16** (2005), 647–659.
4. R. M. El-Ashwah, A note on certain meromorphic p -valent functions, *Appl. Math. Lett.* **22** (2009), 1756–1759.
5. S. Hussain, Z. Shareef and M. Darus, On a class of functions associated with S ă l ă gean operator, *Rev. R. Acad. Cienc. Exactas Fs. Nat. Ser. A Math. RACSAM* **111** (2017), 213–222.
6. S. S. Miller and P. T. Mocanu, Briot-Boquet differential superordinations and sandwich theorems, *J. Math. Anal. Appl.* **329** (2007), 327–335.
7. S. S. Miller and P. T. Mocanu, Subordinants of differential superordinations, *Complex Var. Theory Appl.* **48** (2003), 815–826.
8. S. S. Miller and P. T. Mocanu, Differential Subordinations: Theory and Applications, Series on Monographs and Textbooks in Pure and Applied Mathematics. No. 225, Marcel Dekker, New York, (2000).
9. S. S. Miller and P. T. Mocanu, Univalent solutions of Briot-Bouquet differential equations, *J. Differential Equations* **56** (1985), 297–309.
10. M. H. Mohd, R. M. Ali, L. S. Keong and V. Ravichandran, Subclasses of meromorphic functions associated with convolution, *J. Inequal. Appl.* **2009** (2009), Article ID 190291, pp. 1–10.
11. K. Piejko and J. Sokó ł, Subclasses of meromorphic functions associated with the Cho-Kwon-Srivastava operator, *J. Math. Anal. Appl.* **337** (2008), 1261–1266.
12. M. S. Robertson, Certain classes of starlike functions, *Michigan Math. J.* **32** (1985), 135–140.
13. S. M. Sarangi and S. B. Uralegaddi, Certain differential operators for meromorphic functions, *Bull. Calcutta Math. Soc.* **88** (1996), 333–336.
14. H. M. Srivastava, Operators of basic (or q-) calculus and fractional q-calculus and their applications in geometric function theory of complex analysis, *Iran. J. Sci. Technol. Trans. A: Sci.* **44** (2020), 327-344.

15. S. Supramaniam, R. Chandrashekar,¡¤ S. K. Lee and K. G. Subramanian, Convexity of functions defined by differential inequalities and integral operators, *Rev. R. Acad. Cienc. Exactas Fs. Nat. Ser. A Math. RACSAM* **111** (2017), 147–157.
16. H. Tang, H. M. Srivastava, S.-H. Li, L.-N. Ma, Third-order differential subordination and superordination results for meromorphically multivalent functions associated with the Liu-Srivastava operator. *Abstr. Appl. Anal.* 2014, Art. ID 792175, 11 pp.
17. B. A. Uralegaddi and C. Somanatha, Certain differential operators for meromorphic functions, *Houston J. Math.* **17** (1991), 279–284.
18. B. A. Uralegaddi and C. Somanatha, New criteria for meromorphic starlike functions, *Bull. Austral. Math. Soc.* **43** (1991), 137–140.
19. Z.-G. Wang, X.-Y. Wang. Some subclasses of meromorphic multivalent functions involving a family of multiplier transforms. *Ital. J. Pure Appl. Math.* **42** (2019), 863–879.

The Hadamard-type Padovan-*p* Sequences Modulo *m*

Yeşim AKÜZÜM[1] and Ömür DEVECİ [1]

[1]*Department of Mathematics, Faculty of Science and Letters,*
Kafkas University, Kars-TURKEY

yesim_036@hotmail.com
odeveci36@hotmail.com

Abstract. In [1], Akuzum defined the Hadamard-type Padovan-*p* sequence by using Hadamard-type product of characteristic polynomials of Padovan sequence and the Padovan-*p* sequence as shown:

$$P_{n+p+2}^h = P_{n+p}^h - P_{n+3}^h + P_{n+1}^h - P_n^h$$

for $p \geq 4$ and $n \geq 0$ with initial constants $P_0^h = P_1^h = \cdots = P_p^h = 0$ and $P_{p+1}^h = 1$. Also, Akuzum [1] obtained miscellaneous properties of the Hadamard-type Padovan-*p* sequence. The study of recurrence sequences in groups began with the earlier work of Wall [10] where the ordinary Fibonacci sequences in cyclic groups were investigated. In this work, we obtain the cyclic groups which are produced by generating matrix of the Hadamard-type Padovan-*p* sequence when read modulo m. Also, we study the Hadamard-type Padovan-*p* sequence modulo m, and then we derive the relationship between the order of the cyclic groups obtained and the periods of the Hadamard-type Padovan-*p* sequence modulo m.

1. INTRODUCTION

In [1], Akuzum defined the Hadamard-type Padovan-*p* sequence by using Hadamard-type product of characteristic polynomials of Padovan sequence and the Padovan-*p* sequence as shown:

$$P_{n+p+2}^h = P_{n+p}^h - P_{n+3}^h + P_{n+1}^h - P_n^h \tag{1}$$

for $p \geq 4$ and $n \geq 0$ with initial constants $P_0^h = P_1^h = \cdots = P_p^h = 0$ and $P_{p+1}^h = 1$.

Also in [1], the Hadamard-type Padovan-*p* matrix was given as:

$$M_p = \begin{bmatrix} 0 & 1 & 0 & L & 0 & -1 & 0 & 1 & -1 \\ 1 & 0 & 0 & L & 0 & 0 & 0 & 0 & 0 \\ 0 & 1 & 0 & 0 & L & 0 & 0 & 0 & 0 \\ 0 & 0 & 1 & 0 & 0 & L & 0 & 0 & 0 \\ 0 & 0 & 0 & 1 & 0 & 0 & L & 0 & 0 \\ M & O & O & O & O & O & O & M & M \\ 0 & L & 0 & 0 & 0 & 1 & 0 & 0 & 0 \\ 0 & 0 & L & 0 & 0 & 0 & 1 & 0 & 0 \\ 0 & 0 & 0 & L & 0 & 0 & 0 & 1 & 0 \end{bmatrix}_{(p+2)\times(p+2)}$$

Then the author in [1] obtained that

$$\left(M_p\right)^n = \begin{bmatrix} P_{n+p+1}^h & P_{n+p+2}^h & & P_{n+p-1}^h - P_{n+p-2}^h & P_{n+p}^h - P_{n+p-1}^h & -P_{n+p}^h \\ P_{n+p}^h & P_{n+p+1}^h & & P_{n+p-2}^h - P_{n+p-3}^h & P_{n+p-1}^h - P_{n+p-2}^h & -P_{n+p-1}^h \\ P_{n+p-1}^h & P_{n+p}^h & & P_{n+p-3}^h - P_{n+p-4}^h & P_{n+p-2}^h - P_{n+p-3}^h & -P_{n+p-2}^h \\ \mathrm{M} & \mathrm{M} & M_p^* & \mathrm{M} & \mathrm{M} & \mathrm{M} \\ P_{n+1}^h & P_{n+2}^h & & P_{n-1}^h - P_{n-2}^h & P_n^h - P_{n-1}^h & -P_n^h \\ P_n^h & P_{n+1}^h & & P_{n-2}^h - P_{n-3}^h & P_{n-1}^h - P_{n-2}^h & -P_{n-1}^h \end{bmatrix} \tag{2}$$

where M_p^* is a $(p-3)\times(p-3)$ matrix as follow:

$$\begin{bmatrix} P_{n+p+3}^h - P_{n+p+1}^h & P_{n+p+4}^h - P_{n+p+2}^h & \mathrm{L} & P_{n+2p-1}^h - P_{n+2p-3}^h \\ P_{n+p+2}^h - P_{n+p}^h & P_{n+p+3}^h - P_{n+p+1}^h & \mathrm{L} & P_{n+2p-2}^h - P_{n+2p-4}^h \\ P_{n+p+1}^h - P_{n+p-1}^h & P_{n+p+2}^h - P_{n+p}^h & \mathrm{L} & P_{n+2p-3}^h - P_{n+2p-5}^h \\ \mathrm{M} & \mathrm{M} & & \mathrm{M} \\ P_{n+3}^h - P_{n+1}^h & P_{n+4}^h - P_{n+2}^h & \mathrm{L} & P_{n+p-1}^h - P_{n+p-3}^h \\ P_{n+2}^h - P_n^h & P_{n+3}^h - P_{n+1}^h & \mathrm{L} & P_{n+p-2}^h - P_{n+p-4}^h \end{bmatrix}.$$

It is important to note that $\det M_p = (-1)^p$.

The study of recurrence sequences in groups began with the earlier work of Wall [10] where the ordinary Fibonacci sequences in cyclic groups were investigated. Then, the concept extended to some special linear recurrence sequences by many studies; see for example, [2-9, 11]. In most of these studies, the linear recurrence sequences were examined by modulo m and the cyclic groups via some special matrices were obtained. In this work, we obtain the cyclic groups which are produced by generating matrix of the Hadamard-type Padovan-p sequence when read modulo m. Also, we study the Hadamard-type Padovan-p sequence modulo m, and then we derive the relationship between the order of the cyclic groups obtained and the periods of the Hadamard-type Padovan-p sequence modulo m.

2. MAIN RESULTS

Given an integer matrix $H = \left[h_{ij}\right]$, $H\left(modm\right)$ means that all entries of H are modulo m, that is $H\left(modm\right) = \left(h_{ij}\left(modm\right)\right)$. Let us consider the set $\left\langle H\right\rangle_m = \left\{H^i \left(\mathrm{mod}\, m\right) \middle|\ i \geq 0\right\}$. If $\gcd\left(m, \det H\right) = 1$, then the set $\left\langle H\right\rangle_m$ is a cyclic group. Let the notation $\left|\left\langle H\right\rangle_m\right|$ denote the order of the set $\left\langle H\right\rangle_m$.

Since $\det M_p = (-1)^p$ it is clear that the set $\left\langle M_p\right\rangle_m$ is a cyclic group for every positive integer m.

Theorem 1. Let r be a prime number and k the largest positive integer such that $\left|\left\langle M_p\right\rangle_r\right| = \left|\left\langle M_p\right\rangle_{r^k}\right|$. Then $\left|\left\langle M_p\right\rangle_{r^w}\right| = r^{w-k}.\left|\left\langle M_p\right\rangle_r\right|$ for every $w \geq k$. In particular, if $\left|\left\langle M_p\right\rangle_r\right| \neq \left|\left\langle M_p\right\rangle_{r^2}\right|$, then $\left|\left\langle M_p\right\rangle_{r^w}\right| = r^{w-1}.\left|\left\langle M_p\right\rangle_r\right|$ for every $w \geq 2$.

Proof. Suppose that t is a positive integer and $\left|\left\langle M_p \right\rangle_{r^m}\right|$ is denoted by $hP\left(r^m\right)$. Since $M_p^{hP\left(r^{t+1}\right)} \equiv I \pmod{r^{t+1}}$, we can write $M_p^{hP\left(r^{t+1}\right)} \equiv I \pmod{r^t}$ where I is the $(p+2)\times(p+2)$ identity matrix. Thus we get that $hP\left(r^t\right)$ divides $hP\left(r^{t+1}\right)$. Also, writing $\left(M_p\right)^{hP\left(r^t\right)} = I + \left(m_{ij}^{(t)} r^t\right)$, we obtain

$$\left(M_p\right)^{hP\left(r^t\right)\cdot r} = \left(I + \left(m_{ij}^{(t)} r^t\right)\right)^r = \sum_{i=0}^{r} \binom{r}{i} \left(m_{ij}^{(t)} r^t\right)^i \equiv I \pmod{r^{t+1}}$$

by the binomial expansion. So we get that $hP\left(r^{t+1}\right)$ divides $hP\left(r^t\right)\cdot r$. Thus, $hP\left(r^{t+1}\right) = hP\left(r^t\right)$ or $hP\left(r^{t+1}\right) = hP\left(r^t\right)\cdot r$. It is clear that $hP\left(r^{t+1}\right) = hP\left(r^t\right)\cdot r$ holds if and only if there exists an $m_{ij}^{(t)}$ integer which is not divisible by r. Since k is the largest positive integer such that $hP\left(r\right) = hP\left(r^k\right)$, we have $hP\left(r^k\right) \neq hP\left(r^{k+1}\right)$. Then there is an $m_{ij}^{(k+1)}$ which is not divisible by r. So we get that $hP\left(r^{k+1}\right) \neq hP\left(r^{k+2}\right)$. The proof is finished by induction on k.

If we reduce the Hadamard-type Padovan-*p* sequence $\left\{P_n^h\right\}$ modulo m and denote $P_n^h \pmod{m}$ by $P_n^{h,m}$, then we obtain the following repeating sequence:

$$\left\{P_n^{h,m}\right\} = \left\{P_0^{h,m}, P_1^{h,m}, P_2^{h,m}, \text{K}, P_i^{h,m}, \text{K}\right\}$$

Note that it has the same recurrence relation as in (1).

A sequence is periodic if, after a certain point, it consists only of repetitions of a fixed subsequence. The number of elements in the shortest repeating subsequence is called the period of the sequence. For example, the sequence $a,b,c,d,b,c,d,b,c,d,\text{K}$ is periodic after the initial element a and has period 3. A sequence is simply periodic with period k if the first k elements in the sequence form a repeating subsequence. For example, the sequence $a,b,c,d,a,b,c,d,a,b,c,d,\text{K}$ is simply periodic with period 4.

Theorem 2. The sequence $\left\{P_n^{h,m}\right\}$ is simply periodic.

Proof. Let us consider set $G_p = \left\{\left(g_0, g_1, \text{K}, g_{p+1}\right) \middle|\ g_i\text{'s are integers such that } 0 \le g_i \le m-1\right\}$. Then, we have $\left|G_p\right| = g^{p+2}$. Since there are m^{p+2} distinct $p+2$-tuples of elements of Z_m, at least one of the $p+2$-tuples appears twice in the sequence $\left\{P_n^{h,m}\right\}$. So, the subsequence following this $p+2$-tuple repeats; hence, the sequence is periodic. Let

$$P_{i+1}^{h,m} \equiv P_{j+1}^{h,m}, P_{i+2}^{h,m} \equiv P_{j+2}^{h,m}, \text{K}, P_{i+p+1}^{h,m} \equiv P_{j+p+1}^{h,m}$$

such that $i > j$, then $i \equiv j \pmod{p+2}$. From the definition of the Hadamard-type Padovan-*p* sequence, we can easily get that

$$P_i^{h,m} \equiv P_j^{h,m}, P_{i-1}^{h,m} \equiv P_{j-1}^{h,m}, \mathrm{K}, P_{i-j}^{h,m} \equiv P_0^{h,m}$$

which implies that the $\left\{P_n^{h,m}\right\}$ is a simply periodic sequence.

The period of the sequence $\left\{P_n^{h,m}\right\}$ is denoted by $LP_p\left(m\right)$.

It is easily seen from equation (2) that $LP_p\left(m\right) = \left|\left\langle M_p \right\rangle_m\right|$.

Theorem 3. If *m* has the prime factorization $m = \prod_{i=1}^{k} \left(r_i\right)^{e_i}, \left(\mathrm{k} \geq 1\right)$, then $LP_p\left(m\right)$ equals the least common multiple of the $LP_p\left(\left(r_i\right)^{e_i}\right)$.

Proof. The statement, "$LP_p\left(\left(r_i\right)^{e_i}\right)$ is the length of the period of $\left\{P_n^{h,(r_i)^{e_i}}\right\}$," implies that the sequence $\left\{P_n^{h,(r_i)^{e_i}}\right\}$ repeats only after blocks of length $\lambda \cdot LP_p\left(\left(r_i\right)^{e_i}\right), \left(\lambda \in N\right)$; and the statement, "$LP_p\left(m\right)$ is the length of the period $\left\{P_n^{h,m}\right\}$," implies that $\left\{P_n^{h,(r_i)^{e_i}}\right\}$ repeats after $LP_p\left(m\right)$ terms for all values i. Thus, $LP_p\left(m\right)$ is of the form $\lambda \cdot LP_p\left(\left(r_i\right)^{e_i}\right)$ for all values of i, and since any such number gives a period of $\left\{P_n^{h,m}\right\}$, we easily obtain that

$$LP_p\left(m\right) = lcm\left[LP_p\left(\left(r_1\right)^{e_1}\right), LP_p\left(\left(r_2\right)^{e_2}\right), \mathrm{K}, LP_p\left(\left(r_k\right)^{e_k}\right)\right].$$

REFERENCES

1. Y. Akuzum, The Hadamard-type Padovan-p Sequences, Turkish J. Sci., 5 (2020), 102-109.
2. H. Aydin and G.C. Smith, Finite p-Quotients of Some Cyclically Presented Groups, J. London Math. Soc., 49 (1994), 83-92.
3. O. Deveci, Y. Akuzum and E. Karaduman, The Pell-Padovan p-Sequences and Its Applications, Util. Math., 98 (2015), 327-347.
4. O. Deveci and E. Karaduman, On The Padovan p-Numbers, Hacettepe J. Math. Stat., 46 (2017), 579-592.
5. O. Deveci and E. Karaduman, The Pell Sequences in Finite Groups, Util. Math., 96 (2015), 263-276.
6. H. Doostie and P. Campbell, On the Commutator Lengths of Certain Classes of Finitely Presented Groups, Int. J. Math. Math. Sci., (2006), 1-9.
7. S.W. Knox, Fibonacci sequences in finite groups, Fibonacci Quart., 30(2) (1992), 116-120.
8. K. Lü and J. Wang, k-step Fibonacci Sequence Modulo m, Util. Math., 71 (2007), 169-178.
9. E. Ozkan, H. Aydin and R. Dikici, 3-step Fibonacci series modulo m, Appl. Math. Comput., 143(1) (2003), 165-172.
10. D.D. Wall, Fibonacci series modulo m, Amer. Math. Monthly, 67 (1960), 525-532.
11. H.J. Wilcox, Fibonacci sequences of period n in groups**,** Fibonacci Quart., 24(1986), 356-361.

Renewed Concept of Neutrosophic Soft Graphs

Yıldıray ÇELİK

Department of Mathematics, Faculty of Science and Arts, Ordu University, Ordu-TURKEY

ycelik61@gmail.com

Abstract. In this study, we give renewed concepts of neutrosophic soft graph and neutrosophic soft subgraph, and present illustrative examples. We also define union and intersection operations on neutrosophic soft graphs and derive their basic properties.

1. INTRODUCTION

The concept of neutrosophic set which is a powerful mathematical tool to struggle incomplete, indeterminate and inconsistent information was firstly presented by Smarandache [36]. Neutrosophic sets are generalization of the theory of fuzzy sets [38], intuitionistic fuzzy sets [12] and interval-valued intuitionistic fuzzy sets [13]. The neutrosophic sets are characterized by a truth-membership function T, an indeterminacy-membership function I and a falsity membership function F independently. Some more work on neutrosophic sets and their applications may be found on [8, 9, 10, 19, 20, 21, 40, 41].

The concept of soft sets was firstly introduced by Molodtsov [34]. The applications on algebraic structure of soft set have been studied in more detail [1, 6, 7, 11, 17, 23, 26, 37]. Maji et al. [29] gave the notion of fuzzy soft sets and investigated some properties of it. Thereafter many researchers have applied this concept on different branches of mathematics in [14, 18, 24, 25, 27, 32]. The concept of neutrosophic soft sets was firstly given by Maji [31].

Euler [22] first introduced the concept of graph theory. A graph is used to create a relationship between a given set of elements. Each element can be represented by a vertex and the relationship between them can be represented by an edge. The theory of graph is extremely useful tool for solving combinatorial problems in different areas such as geometry, algebra, number theory, topology, operation research, optimization and computer science, etc.. Dhavaseelan et al. [21] gave the concept of neutrosophic graph and investigated some properties of this concept. Rosenfeld [35] introduced the concept of fuzzy graphs. Thereafter many researchers have studied the different notions of graph theory using the fuzzy sets. Some operations on fuzzy graphs were introduced in [15, 34]. Akram et al. [2, 3, 4, 5] introduced many new concepts such as interval valued fuzzy graphs, soft graphs, fuzzy soft graphs and neutrosophic soft graphs. In this paper, renewed concept of neutrosophic soft graphs is given. Also some new operations such as extended union, restricted union, restricted intersection and extended intersection on fuzzy soft graphs are defined and some related properties are investigated.

2. PRELIMINARIES

Definition 2.1 [22] A graph G^* consists of set of finite objects $V = \{v_1, v_2, v_3, \dots, v_n\}$ called vertices and other set $E = \{e_1, e_2, e_3, \dots, e_n\}$ whose elements are called edges. Usually a graph is denoted as $G^* = (V, E)$. Let G^* be a graph and $\{u, v\}$ and edge of G^*. We may write uv instead of $\{u, v\}$.

Definition 2.2 [33] Let X be an inital universe set, E be a set of parameters, $A \subseteq E$ and $\wp(X)$ be denote power set of X. Then, a pair (F, A) is called a soft set over X, where F is mapping given by $F: A \to \wp(X)$

Definition 2.3 [36] A neutrosophic set A on the universe of discourse X is defined as $A = \{\langle x, T_A(x), I_A(x), F_A(x)\rangle, x \in X\}$, where $T, I, F: X \to [0,1]$ and $0 \leq T_A(x) + I_A(x) + F_A(x) \leq 3$ for all $x \in X$.

Definition 2.4 [31] Let $N(X)$ be set of all neutrosophic sets on universal set X, E be the set of parameters and $A \subseteq E$. A pair (F, A) is called a neutrosophic soft set over X, where F is a mapping given by $F: A \to N(X)$.

Definition 2.5 [31] Let (G, A) be a neutrosophic soft set over X. Then,

i. (G, A) is called a null neutrosophic soft set if $T_{G(e)}(x) = 0$, $I_{G(e)}(x) = 1$ and $F_{G(e)}(x) = 1$ for all $e \in A$, $x \in X$.

ii. (G, A) is called a whole neutrosophic soft set if $T_{G(e)}(x) = 1$, $I_{G(e)}(x) = 0$ and $F_{G(e)}(x) = 0$ for all $e \in A$, $x \in X$.

Definition 2.6 [31] Let (G, A) and (H, B) be two neutrosophic soft sets over U, then (G, A) is said to be a neutrosophic soft subset of (H, B) if

i. $A \subseteq B$

ii. $T_{G(e)}(x) \leq T_{H(e)}(x)$, $I_{G(e)}(x) \geq I_{H(e)}(x)$, $F_{G(e)}(x) \geq F_{H(e)}(x)$ for all $e \in A$ and $x \in X$.

Definition 2.7 [21] A neutrosophic graph of a graph $G^* = (V, E)$ is given by a pair $G = (A, B)$, where $A = < T_A, I_A, F_A >$ is a neutrosophic set on V and $B = < T_B, I_B, F_B >$ is a neutrosophic relation on E such that

$T_B(v_i v_j) \leq min\{T_A(v_i), T_A(v_j)\}$

$I_B(v_i v_j) \geq max\{I_A(v_i), I_A(v_j)\}$

$F_B(v_i v_j) \geq max\{F_A(v_i), F_A(v_j)\}$

for all $v_i v_j \in E$.

3. RENEWED NEUTROSOPHIC SOFT GRAPHS WITH SOME NEW OPERATIONS

Definition 3.1 A neutrosophic soft graph is an order 4-tuple $G = (G^*, f, g, A)$ such that

i. $G^* = (V, E)$ is a simple graph

ii. A is non-empty set of parameters

iii. (f, A) is a neutrosophic soft set over V

iv. (g, A) is a neutrosophic soft set over $V \times V$

v. $(f(e), g(e))$ is a neutrosophic graph for all $e \in A$. That is

$T_{ge}(x, y) \leq min\{T_{fe}(x), T_{fe}(y)\}$,

$I_{ge}(x, y) \geq min\{I_{fe}(x), I_{fe}(y)\}$,

$F_{ge}(x, y) \geq max\{F_{fe}(x), F_{fe}(y)\}$ for all $e \in A$ and $x, y \in V$.

Note that (f, A) is called a neutrosophic soft vertex and (g, A) is called a neutrosophic soft edge. Thus, $((f, A), (g, A))$ is called a neutrosophic soft graph.

Throughout this paper, we denote $G^* = (V, E)$ a simple graph, $h(e) = (f(e), g(e))$ a neutrosophic graph and $G = (G^*, f, g, A) = ((f, A), (g, A))$ a neutrosophic soft graph.

Example 3.2 Let $G^* = (V, E)$ be a simple graph with $V = \{x_1, x_2, x_3\}$ and $E = \{x_1x_2, x_1x_3, x_2x_3\}$. Let $A = \{e_1, e_2, e_3\}$ be a set of parameters. Let consider neutrosophic soft sets f and g over V and E, respectively, as given in Table 1. Clearly $G = (G^*, f, g, A)$ is a neutrosophic soft graph over G^*.

Table 1: Neutrosophic soft graph G

f	x_1	x_2	x_3
e_1	(0.2,0.4,0.5)	(0.4,0.5,0.6)	(0,1,1)
e_2	(0.2,0.7,0.8)	(0.3,0.5,0.6)	(0.5,0.6,0.7)
e_3	(0.3,0.3,0.5)	(0.2,0.2,0.3)	(0.3,0.4,0.9)
g	(x_1x_2)	(x_2x_3)	(x_1x_3)
e_1	(0.1,0.6,0.7)	(0,1,1)	(0,1,1)
e_2	(0.1,0.5,0.9)	(0,1,1)	(0.2,0.8,0.9)

e_3	(0.2,0.4,0.6)	(0.1,0.5,0.9)	(0.3,0.5,0.9)

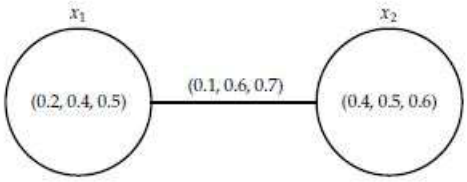

Figure 1: Neutrosophic graph $h(e_1) = (f(e_1), g(e_1))$

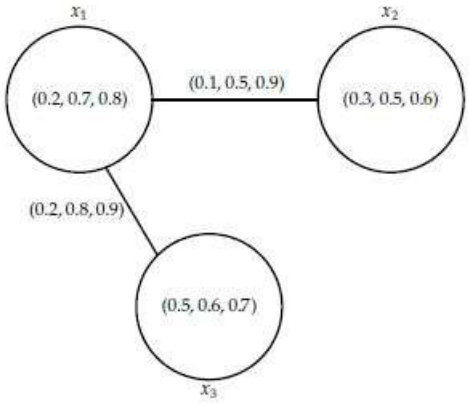

Figure 2: Neutrosophic graph $h(e_2) = (f(e_2), g(e_2))$

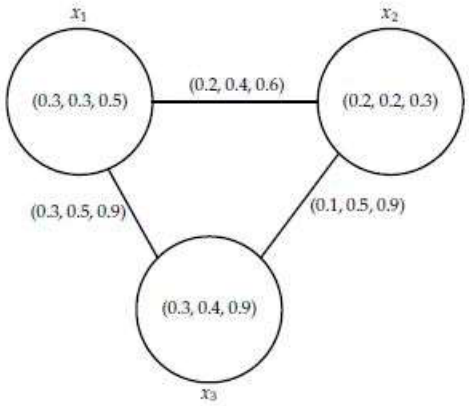

Figure 3: Neutrosophic graph $h(e_3) = (f(e_3), g(e_3))$

Definition 3.3 A neutrosophic soft graph $G' = (G^*, f', g', A')$ is called a neutrosophic soft subgraph of $G = (G^*, f, g, A)$ if

i. $A' \subseteq A$

ii. $f_e' \subseteq f_e$, that is $T_{f'e}(x) \leq T_{fe}(x)$, $I_{f'e}(x) \geq I_{fe}(x)$, $F_{f'e}(x) \geq F_{fe}(x)$

iii. $g_e' \subseteq g_e$, that is, $T_{g'e}(x) \leq T_{ge}(x)$, $I_{g'e}(x) \geq I_{ge}(x)$, $F_{g'e}(x) \geq F_{ge}(x)$

for all $e \in A'$, $xy \in E$.

Example 3.4 Let $G^* = (V, E)$ be a simple graph with $V = \{x_1, x_2, x_3\}$ and $E = \{x_1x_2, x_2x_3, x_1x_3\}$, and let $A' = \{e_1, e_2\}$ be a set of parameters. Let consider a neutrosophic soft graph $G = (G^*, f, g, A)$ as taken in Example 3.2. Now let consider another neutrosophic soft graph $G' = (G^*, f', g', A')$ as taken in Table 2.

Table 2: Neutrosophic soft graph G'

f'	x_1	x_2	x_3
e_1	(0.2,0.5,0.6)	(0.3,0.6,0.8)	(0,1,1)
e_2	(0.1,0.7,0.9)	(0.1,0.5,0.7)	(0.2,0.8,0.9)

g'	(x_1, x_2)	(x_2, x_3)	(x_1, x_3)
e_1	(0.1,0.7,0.8)	(0,1,1)	(0,1,1)
e_2	(0.1,0.9,0.9)	(0,1,1)	(0.1,0.8,0.9)

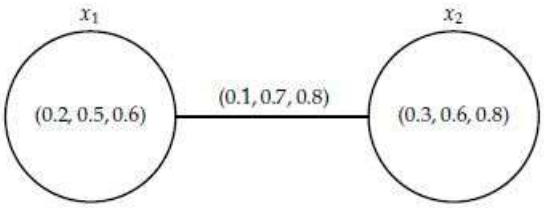

Figure 4: Neutrosophic graph $N'(e_1)$

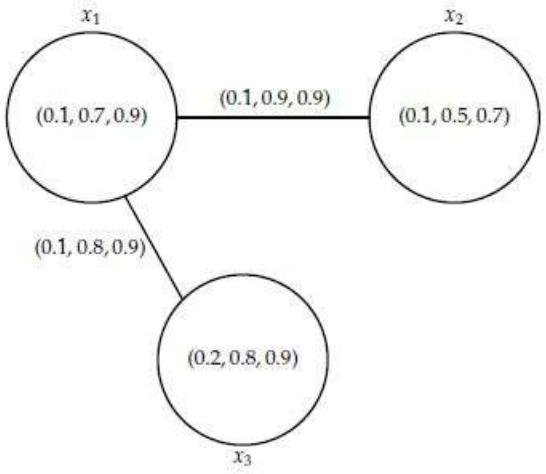

Figure 5: Neutrosophic graph $N'(e_2)$

It is clearly seen that $G' = (G^*, f', g', A')$ is a neutrosophic soft graph. Hence $G' = (G^*, f', g', A')$ is a neutrosophic soft subgraph of $G = (G^*, f, g, A)$.

Definition 3.5 Let $G^1 = (G^*, f^1, g^1, A_1)$ and $G^2 = (G^*, f^2, g^2, A_2)$ be two neutrosophic soft graphs over $G^* = (V, E)$. The union of G^1 and G^2 is denoted by $G^1 \cup G^2 = (G^*, f, g, A) = (G^*, f^1 \cup_N f^2, g^1 \cup_N g^2, A_1 \cup A_2)$. T, I and F membership values of vertices and edges of $G^1 \cup G^2$ are defined by as follow.

i. For all $e \in A = A_1 \cup A_2$ and $x \in V$

$$T_{f_e}(x) = \begin{cases} T_{f_e^1}(x) & e \in A_1 \backslash A_2 \\ T_{f_e^2}(x) & e \in A_2 \backslash A_1 \\ max\{T_{f_e^1}(x), T_{f_e^2}(x)\} & e \in A_1 \cap A_2 \end{cases}$$

$$I_{f_e}(x) = \begin{cases} I_{f_e^1}(x) & e \in A_1 \backslash A_2 \\ I_{f_e^2}(x) & e \in A_2 \backslash A_1 \\ min\{I_{f_e^1}(x), I_{f_e^2}(x)\} & e \in A_1 \cap A_2 \end{cases}$$

$$F_{f_e}(x) = \begin{cases} F_{f_e^1}(x) & e \in A_1 \backslash A_2 \\ F_{f_e^2}(x) & e \in A_2 \backslash A_1 \\ min\{F_{f_e^1}(x), F_{f_e^2}(x)\} & e \in A_1 \cap A_2 \end{cases}$$

ii. For all $e \in A$ and $xy \in E$

$$T_{g_e}(xy) = \begin{cases} T_{g_e^1}(xy) & e \in A_1 \backslash A_2 \\ T_{g_e^2}(xy) & e \in A_2 \backslash A_1 \\ max\{T_{g_e^1}(xy), T_{g_e^2}(xy)\} & e \in A_1 \cap A_2 \end{cases}$$

$$I_{g_e}(xy) = \begin{cases} I_{g_e^1}(xy) & e \in A_1 \backslash A_2 \\ I_{g_e^2}(xy) & e \in A_2 \backslash A_1 \\ min\{I_{g_e^1}(xy), I_{g_e^2}(xy)\} & e \in A_1 \cap A_2 \end{cases}$$

$$F_{g_e}(xy) = \begin{cases} T_{g_e^1}(xy) & e \in A_1 \backslash A_2 \\ T_{g_e^2}(xy) & e \in A_2 \backslash A_1 \\ min\{I_{g_e^1}(xy), I_{g_e^2}(xy)\} & e \in A_1 \cap A_2 \end{cases}$$

Example 3.6 Let $G^* = (V, E)$ be a simple graph with $V = \{x_1, x_2, x_3, x_4, x_5\}$ and $E = \{x_1x_2, x_1x_3, x_1x_4, x_1x_5, x_2x_3, x_2x_4, x_2x_5, x_3x_4, x_3x_5, x_4x_5\}$, and let $A_1 = \{e_1, e_2, e_3\}$ be a set of parameters. Let consider a neutrosophic soft graph $G^1 = (G^*, f^1, g^1, A_1)$ over $G^* = (V, E)$ as taken in Table 3.

Table 3: Neutrosophic soft graph G^1

f^1	x_1	x_2	x_3	x_4	x_5
e_1	(0.1,0.2,0.3)	(0,1,1)	(0.2,0.3,0.4)	(0.2,0.5,0.7)	(0,1,1)
e_2	(0.1,0.3,0.7)	(0,1,1)	(0.4,0.6,0.7)	(0.1,0.2,0.3)	(0,1,1)
e_3	(0.5,0.6,0.7)	(0,1,1)	(0.6,0.8,0.9)	(0.3,0.4,0.6)	(0,1,1)

g^1	(x_1x_2)	(x_1x_3)	(x_1x_4)	(x_1x_5)	(x_2x_3)
e_1	(0,1,1)	(0.1,0.4,0.5)	(0.1,0.6,0.7)	(0,1,1)	(0,1,1)
e_2	(0,1,1)	(0.1,0.7,0.8)	(0.1,0.4,0.8)	(0,1,1)	(0,1,1)
e_3	(0,1,1)	(0,1,1)	(0.2,0.7,0.9)	(0,1,1)	(0,1,1)
g^1	(x_2x_4)	(x_2x_5)	(x_3x_4)	(x_3x_5)	(x_4x_5)
e_1	(0,1,1)	(0,1,1)	(0.1,0.6,0.8)	(0,1,1)	(0,1,1)
e_2	(0,1,1)	(0,1,1)	(0.1,0.8,0.9)	(0,1,1)	(0,1,1)
e_3	(0,1,1)	(0,1,1)	(0.3,0.8,0.9)	(0,1,1)	(0,1,1)

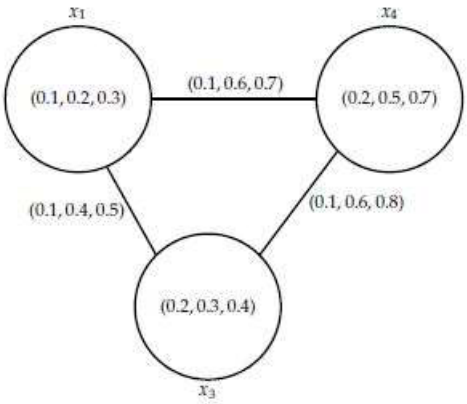

Figure 6: Neutrosophic graph $N_1(e_1)$

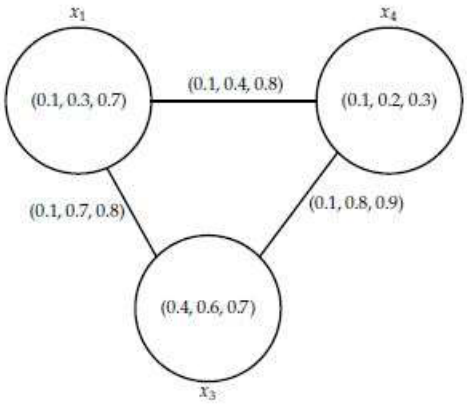

Figure 7: Neutrosophic graph $N_1(e_2)$

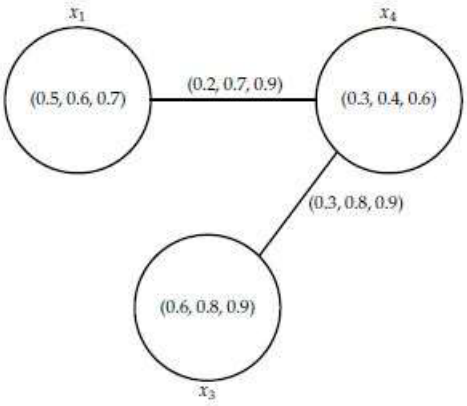

Figure 8: Neutrosophic graph $N_1(e_3)$

Now let consider another neutrosophic soft graph $G^2 = (G^*, f^2, g^2, A_2)$ with the parameter set $A_2 = \{e_2, e_4\}$ as taken in Table 4.

Table 4: Neutrosophic soft graph G^2

f^2	x_1	x_2	x_3	x_4	x_5
e_2	(0,1,1)	(0.1,0.2,0.4)	(0.2,0.3,0.4)	(0,1,1)	(0.4,0.6,0.7)
e_4	(0,1,1)	(0.3,0.6,0.8)	(0.5,0.7,0.9)	(0,1,1)	(0.3,0.4,0.5)

g^2	(x_1x_2)	(x_1x_3)	(x_1x_4)	(x_1x_5)	(x_2x_3)
e_2	(0,1,1)	(0,1,1)	(0,1,1)	(0,1,1)	(0.1,0.4,0.5)
e_4	(0,1,1)	(0,1,1)	(0,1,1)	(0,1,1)	(0.2,0.7,0.9)
g^2	(x_2x_4)	(x_2x_5)	(x_3x_4)	(x_3x_5)	(x_5x_6)
e_2	(0,1,1)	(0,1,1)	(0,1,1)	(0.2,0.8,0.9)	(0,1,1)
e_4	(0,1,1)	(0.2,0.6,0.8)	(0,1,1)	(0.3,0.9,0.9)	(0,1,1)

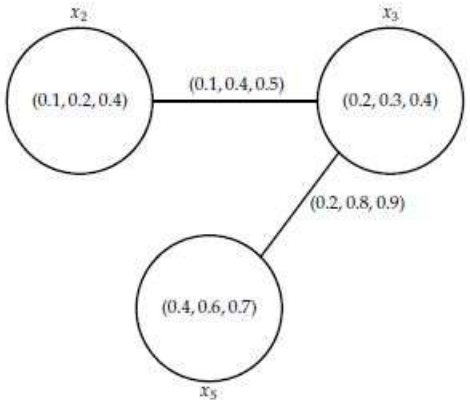

Figure 9: Neutrosophic graph $N_2(e_2)$

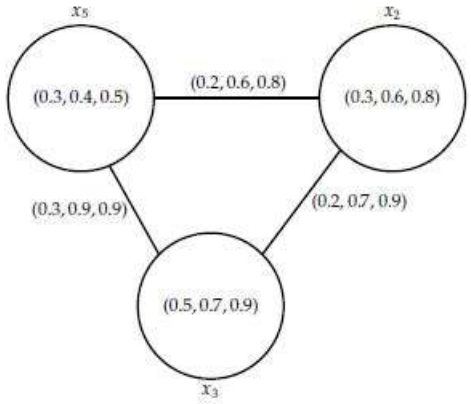

Figure 10: Neutrosophic graph $N_2(e_4)$

Clearly the parameter set of $G^1 \cup G^2 = (G^*, f, g, A)$ is $A = A_1 \cup A_2 = \{e_1, e_2, e_3, e_4\}$.

Hence the neutrosophic soft graph $G^1 \cup G^2 = (G^*, f, g, A)$ is obtained as in the Table 5.

Table 5: Neutrosophic soft graph $G^1 \cup G^2$

f	x_1	x_2	x_3	x_4	x_5
e_1	(0.1,0.2,0.3)	(0,1,1)	(0.2,0.3,0.4)	(0.2,0.5,0.7)	(0,1,1)
e_2	(0.1,0.3,0.7)	(0.1,0.2,0.4)	(0.4,0.3,0.4)	(0.1,0.2,0.3)	(0.4,0.6,0.7)
e_3	(0.5,0.6,0.7)	(0,1,1)	(0.6,0.8,0.9)	(0.3,0.4,0.6)	(0,1,1)
e_4	(0,1,1)	(0.3,0.6,0.8)	(0.5,0.7,0.9)	(0,1,1)	(0.3,0.4,0.5)

g	(x_1x_2)	(x_1x_3)	(x_1x_4)	(x_1x_5)	(x_2x_3)
e_1	(0,1,1)	(0.1,0.4,0.5)	(0.1,0.6,0.7)	(0,1,1)	(0,1,1)
e_2	(0,1,1)	(0.1,0.7,0.8)	(0.1,0.4,0.8)	(0,1,1)	(0.1,0.4,0.8)
e_3	(0,1,1)	(0,1,1)	(0.2,0.7,0.9)	(0,1,1)	(0,1,1)
e_4	(0,1,1)	(0,1,1)	(0,1,1)	(0,1,1)	(0.2,0.7,0.9)
g	(x_2x_4)	(x_2x_5)	(x_3x_4)	(x_3x_5)	(x_4x_5)
e_1	(0,1,1)	(0,1,1)	(0.1,0.6,0.8)	(0,1,1)	(0,1,1)
e_2	(0,1,1)	(0,1,1)	(0.1,0.8,0.9)	(0.2,0.8,0.9)	(0,1,1)
e_3	(0,1,1)	(0,1,1)	(0.3,0.9,0.9)	(0,1,1)	(0,1,1)
e_4	(0,1,1)	(0.2,0.6,0.8)	(0,1,1)	(0.3,0.4,0.6)	(0,1,1)

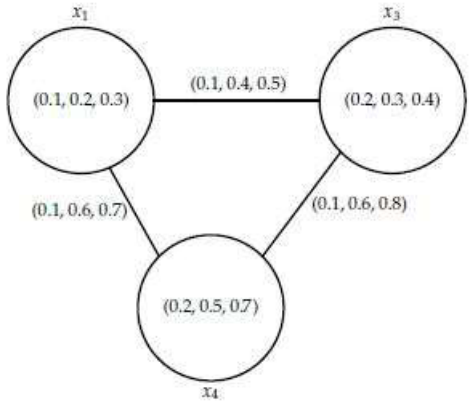

Figure 11: Neutrosophic graph $N(e_1)$

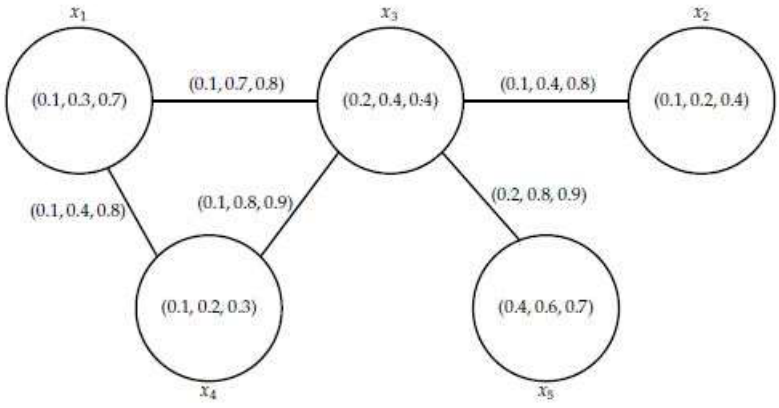

Figure 12: Neutrosophic graph $N(e_2)$

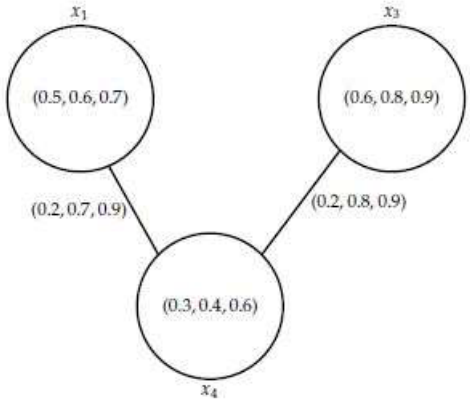

Figure 13: Neutrosophic graph $N(e_3)$

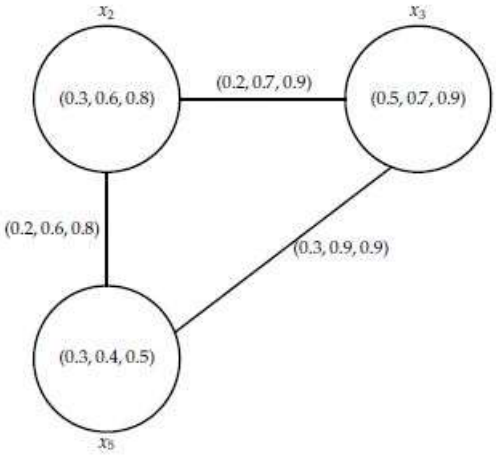

Figure 14: Neutrosophic graph $N(e_4)$

Theorem 3.7 Let $G^1 = (G^*, f^1, g^1, A_1)$ and $G^2 = (G^*, f^2, g^2, A_2)$ be two neutrosophic soft graph over $G^* = (V, E)$. Then $G^1 \cup G^2$ is a neutrosophic soft graph over $G^* = (V, E)$.

Definition 3.8 Let $G^1 = (G^*, f^1, g^1, A_1)$ and $G^2 = (G^*, f^2, g^2, A_2)$ be two neutrosophic soft graph over $G^* = (V, E)$. The intersection of G^1 and G^2 is denoted by $G^1 \cap G^2 = (G^*, f, g, A) = (G^*, f^1 \cap_N f^2, g^1 \cap_N g^2, A_1 \cap A_2)$. T, I and F membership values of vertices and edges of $G^1 \cap G^2$ are defined by as follow.

i. For all $e \in A = A_1 \cap A_2$ and $x \in V$
$T_{f_e}(x) = min\{T_{f_e^1}(x), T_{f_e^2}(x)\}$
$I_{f_e}(x) = max\{I_{f_e^1}(x), I_{f_e^2}(x)\}$
$F_{f_e}(x) = max\{F_{f_e^1}(x), F_{f_e^2}(x)\}$

ii. For all $e \in A = A_1 \cap A_2$ and $xy \in E$
$T_{g_e}(xy) = min\{T_{g_e^1}(xy), T_{g_e^2}(xy)\}$
$I_{g_e}(xy) = max\{I_{g_e^1}(xy), I_{g_e^2}(xy)\}$
$F_{g_e}(xy) = max\{F_{g_e^1}(xy), F_{g_e^2}(xy)\}$

Example 3.9 Let $G^* = (V, E)$ be a simple graph with $V = \{x_1, x_2, x_3, x_4\}$ and $E = \{x_1x_2, x_1x_3, x_1x_4, x_2x_3, x_2x_4, x_3x_4\}$, and let $A_1 = \{e_1, e_2\}$ be a set of parameters. Let consider a neutrosophic soft graph $G^1 = (G^*, f^1, g^1, A_1)$ over $G^* = (V, E)$ as taken in Table 6.

Table 6: Neutrosophic soft graph G^1

f^1	x_1	x_2	x_3	x_4
e_1	(0.1,0.2,0.3)	(0.2,0.4,0.5)	(0,1,1)	(0.1,0.5,0.7)
e_2	(0.2,0.3,0.7)	(0.4,0.6,0.7)	(0,1,1)	(0.3,0.4,0.6)

g^1	(x_1x_2)	(x_1x_3)	(x_1x_4)	(x_2x_3)	(x_2x_4)	(x_3x_4)
e_1	(0.1,0.5,0.6)	(0,1,1)	(0.1,0.5,0.7)	(0,1,1)	(0,1,1)	(0,1,1)
e_2	(0.2,0.7,0.8)	(0,1,1)	(0.1,0.6,0,7)	(0,1,1)	(0.2,0.7,0.9)	(0,1,1)

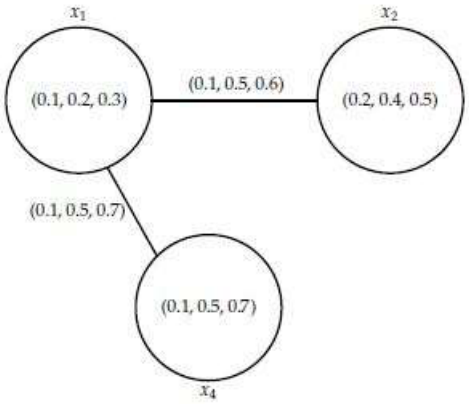

Figure 15: Neutrosophic graph $N_1(e_1)$

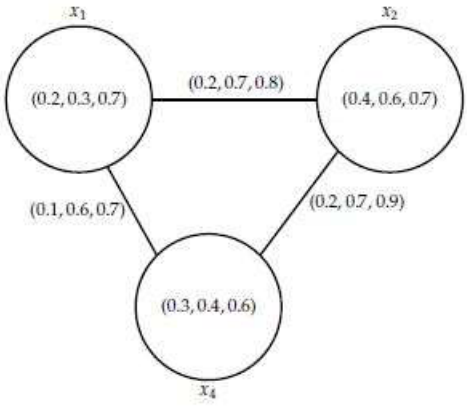

Figure 16: Neutrosophic graph $N_1(e_2)$

Now let consider another neutrosophic soft graph $G^2 = (G^*, f^2, g^2, A_2)$ with the parameter set $A_2 = \{e_2, e_3\}$ as taken in Table 7.

Table 7: Neutrosophic soft graph G^2

f^2	x_1	x_2	x_3	x_4
e_2	(0,1,1)	(0.3,0.5,0.6)	(0.2,0.4,0.5)	(0.4,0.5,0.9)
e_3	(0,1,1)	(0.2,0.4,0.5)	(0.1,0.2,0.6)	(0.1,0.5,0.7)

g^2	(x_1x_2)	(x_1x_3)	(x_1x_4)	(x_2x_3)	(x_2x_4)	(x_3x_4)
e_2	(0,1,1)	(0,1,1)	(0,1,1)	(0.1,0.6,0.7)	(0.2,0.6,0.9)	(0.2,0.7,0.9)
e_3	(0,1,1)	(0,1,1)	(0,1,1)	(0.1,0.5,0.8)	(0.1,0.7,0.8)	(0.1,0.8,0.9)

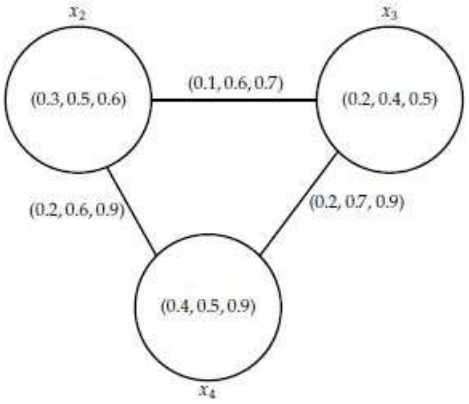

Figure 17: Neutrosophic graph $N_2(e_2)$

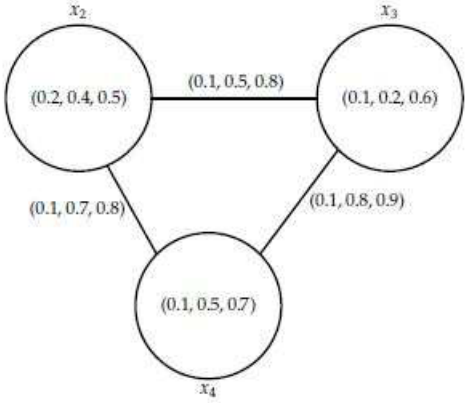

Figure 18: Neutrosophic graph $N_2(e_3)$

Clearly parameter set of G^1 and G^2 is $A = A_1 \cap A_2 = \{e_2\}$. Also the intersection of G^1 and G^2 is obtained as follow.

Table 10: Neutrosophic soft graph G^1G^2

f	x_1	x_2	x_3	x_4
e_2	(0,1,1)	(0.3,0.6,0.7)	(0,1,1)	(0.3,0.5,0.9)

g	(x_1x_2)	(x_1x_3)	(x_1x_4)	(x_2x_3)	(x_2x_4)	(x_3x_4)
e_2	(0,1,1)	(0,1,1)	(0,1,1)	(0,1,1)	(0.2,0.7,0.9)	(0,1,1)

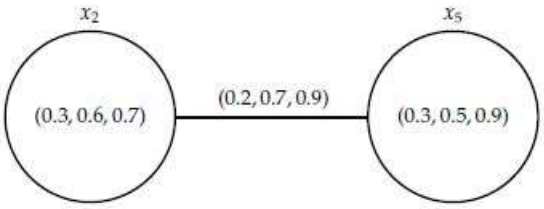

Figure 19: Neutrosophic graph $N(e_2)$

Theorem 3.10 Let $G^1 = (G^*, f^1, g^1, A_1)$ and $G^2(G^*, f^2, g^2, A_2)$ be two neutrosophic soft graph over $G^* = (V, E)$. Then $G^1 \cap G^2$ is a neutrosophic soft graph over $G^* = (V, E)$.

REFERENCES

1. U. Acar, F. Koyuncu and B. Tanay, Soft sets and soft rings, Computers and Mathematics with Applications, 59, 2010, 3458-3463.
2. M. Akram and S. Nawaz, Operations on Soft Graphs. Fuzzy Information and Engineering, 7(4), 2015, 423–449.
3. M. Akram and W.A. Dudek, Interval-valued Fuzzy Graphs. Computers and Mathematics with Applications, 61, 2011, 289-299.
4. M. Akram and S. Nawaz, Fuzzy Soft Graphs with Applications. Journal of Intelligent and Fuzzy Systems, 30(6), 2016, 3619-3632.
5. M. Akram and S. Sundas, Neutrosophic soft graphs with application, Journal of Intelligent and Fuzzy Systems, 32(1), 2017, 841-858.
6. H. Aktaş and N. Çağman, N. Soft sets and soft groups, Information Sciences, 177, 2007, 2726-2735.
7. M.I. Ali, F. Feng, X. Liu, W.K. Min and M. Shabir, On some new operations in soft set theory, Computers and Mathematics with Applications, 57, 2009, 1547-1553.
8. M. Ali and F. Smarandache, Complex Nuetrosophic Set, Neural Computing and Applications, 27(1), (2016), 1-18.
9. M. Ali, I. Deli and F. Smarandache, The Theory of Neutrosophic Cubic Sets and Their Applications in Pattern Recognition. Journal of Intelligent and Fuzzy Systems, 30(4), 2016, 1957-1963.
10. A.Q. Ansari, R. Biswas and S. Aggarwal, Neutrosophic classifier: An extension of fuzzy classifier, Applied Soft Computing, 13, 2013, 563-573.
11. A.O. Atagün and A. Sezgin, Soft substructures of rings, fields and modules, Computers and Mathematics with Applications, 61, 2011, 592-601.
12. K.T. Atanassov and G. Gargov, Intuitionistic Fuzzy Sets: Theory and Applications, Springer Physica-Verlag, Berlin, 1999.
13. K.T. Atanassov and G. Gargov, Interval valued intuitionistic fuzzy sets, Fuzzy Sets and Systems, 31, 1989, 343–349.
14. A. Aygünoğlu and H. Aygün, Introduction to fuzzy soft groups, Computers and Mathematics with Applications, 58, 2009, 1279-1286.
15. P. Bhattacharya, Some Remarks on Fuzzy Graphs, Pattern Recognition Letters, 6, 1987, 297-302.
16. S. Broumi, M. Talea, A. Bakali and F. Smarandache, Interval Valued Neutrosophic Graphs, Critical review, 12, 2016, 5–33.
17. Y. Çelik, C. Ekiz and S. Yamak, A new view on soft rings, Hacettepe Journal of Mathematics and Statistics, 40(2), 2011, 273-286.
18. Y. Çelik, A new approach to group theory via soft sets and L -fuzzy soft sets, International Journal of Pure and Applied Mathematics, 105(3), 2015, 459-475.
19. I. Deli, M. Ali and F. Smarandache, Bipolar neutrosophic sets and their application based on multicriteria decision making problems, Advanced Mechatronic Systems (ICAMechS), International Conference, 2015, 249-254.

20. I. Deli, Interval-valued neutrosophic soft sets and its decision making, International Journal of Machine Learning and Cybernetics, 8, 2015, 1-12.
21. R. Dhavaseelan, R. Vikramaprasad and V. Krishnaraj, Certain Types of Neutrosophic Graphs, International Journal of Mathematical Sciences and Applications, 5(2), 2015, 333-339.
22. L. Euler, Solutio problematis ad geometriam situs pertinentis, Commentarii Academiae Scientiarum Imperialis Petropolitanae, 8, 1736, 128-140.
23. F. Feng, Y.B. Jun and X. Zhao, Soft semirings, Computers and Mathematics with Applications, 56, 2008, 2621-2628.
24. E. İnan and M.A. Öztürk, Fuzzy soft rings and fuzzy soft ideals, Neural Computing and Applications, 21(1), 2012, 1-8.
25. P.P. John and P. Isaac, A study on fuzzy soft modules, Journal of Global Research in Mathematical Archives, 5(3), 2018, 139-145.
26. Y.B. Jun and C.H. Park, Applications of soft sets in ideal theory of BCK/BCI-algebras, Information Science, 178, 2008, 2466-2475.
27. Y.B. Jun, K.J. Lee and C.H. Park, Fuzzy soft set theory applied to BCK/BCI-algebras, Computers and Mathematics with Applications, 59, 2010, 3180-3192.
28. W.B. Kandasamy, K. Ilanthenral and F. Smarandache, Neutrosophic Graphs: A New Dimension to Graph Theory. EuropaNova, USA, 2015.
29. P.K. Maji, R. Biswas and A.R. Roy, Fuzzy Soft Sets, Journal of Fuzzy Mathematics, 9(3), 2001, 589-602.
30. P.K. Maji, R. Biswas and A.R. Roy, Soft set theory, Computers and Mathematics with Applications, 45, 2003, 555-562.
31. P.K. Maji, Neutrosophic soft set, Annals of Fuzzy Mathematics and Informatics, 5(1), 2013, 157-168.
32. P. Majumdar and S.K. Samanta, Generalised fuzzy soft sets, Computers and Mathematics with Applications, 59, 2010, 1425-1432.
33. D. Molodtsov, Soft set theory - first results, Computers and Mathematics with Applications, 37, 1999, 19-31.
34. J.N. Mordeson and C.S. Peng, Operations on fuzzy graphs. Information Sciences, 79, 1994, 159-170.
35. A. Rosenfeld, Fuzzy graphs, Fuzzy Sets and Their Applications to Cognitive and Decision Processes, Academic Press, New York, 1975.
36. F. Smarandache, Neutrosophic set-a generalization of the intuitionistic fuzzy set, Granular Computing, IEEE International Conference, USA, 2006.
37. Q.M. Sun, Z.L. Zhang and J. Liu, Soft Sets and Soft Modules, Lecture Notes in Computer Science, 5009, 2008, 403-409.
38. L.A. Zadeh, Fuzzy sets, Information and Control, 8, 1965, 338-353.
39. H. Zhang, J. Wang and X. Chen, An outranking approach for multi-criteria decision-making problems with interval-valued neutrosophic sets, Neural Computing and Applications, 27(3), 2015, 1-13.
40. H.Y. Zhang, P. Ji, J.Q. Wang and X.H. Chen, An Improved Weighted Correlation Coefficient Based on Integrated Weight for Interval Neutrosophic Sets and its Application in Multi-criteria Decision making Problems, International Journal of Computational Intelligence Systems, 8(6), 2015, 1027-1043.

Partial Sums of Generalized Dini Functions

Arda Anıl YILDIZ[1], Erhan DENİZ[1] and Murat ÇAĞLAR[1]

[1]*Department of Mathematics, Faculty of Science and Arts*
Kafkas University, Kars-TURKEY

arda_anil@windowslive.com
edeniz36@gmail.com
mcaglar25@gmail.com

Abstract. In the present investigation our main aim is to give lower bounds for the ratio of generalized Dini functions and their sequences of partial sums.

1. INTRODUCTION

Let us consider the following second-order linear homogenaus differential equation(see for details [7,13]):

$$z^2\omega''(z)+bz\omega'(z)+\left[cz^2-\nu^2+(1-b)\nu\right]\omega(z)=0 \quad (b,c,\nu\in\mathbb{C}). \tag{1.1}$$

The function $\omega_{\nu,b,c}(z)$ which is called the generalized Bessel function of the first kind of order ν, is defined as a particular solution of (1.1). We have the following familiar series representation for the function $\omega_{\nu,b,c}(z)$

$$\omega_{\nu,b,c}(z)=\sum_{n=0}^{\infty}\frac{(-c)^n}{n!\Gamma\left(\nu+n+(b+1)/2\right)}\left(\frac{z}{2}\right)^{2n+\nu} \qquad (z\in\mathbb{C}) \tag{1.2}$$

where Γ stands for the Euler gamma function. The series (1.2) permits the study of Bessel, modified Bessel and spherical Bessel functions in a unified manner. Each of these particular cases of the function $\omega_{\nu,b,c}(z)$ is worthy of mention here.

For $b=c=1$ in (1.2), we obtain the familiar Bessel function of the first kind of order ν defined by

$$J_\nu(z)=\sum_{n=0}^{\infty}\frac{(-1)^n}{n!\Gamma(n+\nu+1)}\left(\frac{z}{2}\right)^{2n+\nu} \qquad (z\in\mathbb{C}).$$

For $b=1$ and $c=-1$ in (1.2), we obtain the modified Bessel function of the first kind of order ν defined by

$$I_\nu(z)=\sum_{n=0}^{\infty}\frac{1}{n!\Gamma(\nu+n+1)}\left(\frac{z}{2}\right)^{2n+\nu} \qquad (z\in\mathbb{C}).$$

For $b=2$ and $c=-1$ in (1.2), the function $\omega_{\nu,b,c}(z)$ reduces to $\sqrt{2}j_\nu(z)/\sqrt{\pi}$, where j_ν is the spherical Bessel function of the first kind of order ν defined by

$$j_\nu(z)=\sqrt{\frac{\pi}{2}}\sum_{n=0}^{\infty}\frac{(-1)^n}{n!\Gamma(\nu+n+3/2)}\left(\frac{z}{2}\right)^{2n+\nu}\qquad(z\in\mathbb{C}).$$

Deniz et al. [4] considered the function $\psi_{\nu,b,c}(z)$ defined, in terms of the generalized and normalized Bessel function $\omega_{\nu,b,c}(z)$, by the transformation

$$\psi_{\nu,b,c}(z)=2^\nu\Gamma\left(\nu+\frac{b+1}{2}\right)z^{1-\nu/2}\omega_{\nu,b,c}\left(\sqrt{z}\right).\tag{1.3}$$

By using the well-known Pochhammer symbol (or the shifted factorial) $(\lambda)_\mu$ defined, for $\lambda,\mu\in\mathbb{C}$ and in terms of the Euler's function, by

$$(\lambda)_\mu=\frac{\Gamma(\lambda+\mu)}{\Gamma(\lambda)}=\begin{Bmatrix}1 & (\mu=0;\ \lambda\in\mathbb{C}-\{0\})\\ \lambda(\lambda+1)...(\lambda+n-1) & (\mu=n\in\mathbb{N};\ \lambda\in\mathbb{C})\end{Bmatrix}.$$

It is being understood conventionally that $(0)_0:=1$, and we obtain the following series representation for the function $\psi_{\nu,b,c}(z)$ given by (1.3)

$$\psi_{\nu,b,c}(z)=z+\sum_{n=1}^{\infty}\frac{(-c)^n}{4^n(\kappa)_n}\frac{z^{n+1}}{n!}$$

where $\mathbb{N}:=\{1,2,3,...\}$, $\mathbb{N}_0^-:=\{0,-1,-2,...\}$, and $\kappa:=\nu+\frac{b+1}{2}\notin\mathbb{N}_0^-$. In [5,6] authors defined and studied the generalized Dini functions $D_{\nu,a,b,c}:\mathbb{C}\to\mathbb{C}$ by

$$D_{\nu,a,b,c}(z)=(a-\nu)\omega_{\nu,b,c}(z)+z\omega'_{\nu,b,c}(z)\quad(a\in\mathbb{R}^+\text{ and }b,c,\nu\in\mathbb{C})$$

and its normalized form

$$\varphi_{\nu,a,b,c}(z)=\frac{2^\nu}{a}\Gamma\left(\nu+\frac{b+1}{2}\right)z^{1-\frac{\nu}{2}}D_{\nu,a,b,c}\left(\sqrt{z}\right)$$

where $\omega_{\nu,b,c}$ is the generalized Bessel function of first kind. From the definition of $\varphi_{\nu,a,b,c}(z)$ we obtain series representation as

$$\varphi_{\nu,a,b,c}(z)=z+\sum_{n=1}^{\infty}\frac{(-c)^n(2n+a)}{a4^n n!(\kappa)_n}z^{n+1}\tag{1.4}$$

Note that, the functions $D_{\nu,1,1,1}$ and $D_{\nu,2,1,1}$ are classical dini functions and the functions $D_{\nu,1,1,-1}$ and $D_{\nu,2,1,-1}$ are classical modified Dini functions.

Motivated by the papers of Silverman [11] and Silvia [12] in this paper we investigate the ratio of a function of the form (1.4) to its sequence of partial sums $\varphi_{\nu,a,b,c}(z)=z+\sum_{n=1}^{\infty}b_n z^{n+1}$ $\left(b_n=\frac{(-c)^n(2n+a)}{4^n an!(\kappa)_n}\right)$ in the unit disk

$\mathsf{U}=\{z:|z|<1\}$ when the coefficients of $\varphi_{\nu,a,b,c}$ satisfy some conditions. We will obtain some lower bounds for $\Re\left\{\frac{\varphi_{\nu,a,b,c}(z)}{(\varphi_{\nu,a,b,c})_m(z)}\right\}$, $\Re\left\{\frac{(\varphi_{\nu,a,b,c})_m(z)}{\varphi_{\nu,a,b,c}(z)}\right\}$, $\Re\left\{\frac{\varphi'_{\nu,a,b,c}(z)}{(\varphi_{\nu,a,b,c})'_m(z)}\right\}$ and $\Re\left\{\frac{(\varphi_{\nu,a,b,c})'_m(z)}{\varphi'_{\nu,a,b,c}(z)}\right\}$.

For interesting developments on the partial sums of some special functions and some classes of analytic functions, the readers can refer to the works of Sheil-Small [10], Brickman et al.[2], Silvia [12], Silverman [11], Owa et al. [9], Orhan and Yağmur [8], Çağlar and Deniz [3], Aktaş and Orhan [1].

The next result is a preliminary one, which will be used in the proof of the main results.

Lemma 1.1. If the parameter $a\in\mathbb{R}^+, b\in\mathbb{R}, c\in\mathbb{R}$ and $\nu\in\mathbb{R}-\mathbb{Z}_0^-$ are so constrained that $\kappa>\frac{|c|}{8}$ then the function

$$\varphi_{\nu,a,b,c}:\mathsf{U}\to\mathbb{R}$$

given by (1.4) satisfies the following inequalities:

i. $$|\varphi_{\nu,a,b,c}|\le 1+\frac{2|c|\left(8\kappa(a+2)-a|c|\right)}{a\left(8\kappa-|c|\right)^2}\quad(z\in\mathrm{U})$$

ii. $$|\varphi'_{\nu,a,b,c}(z)|\le 1+\frac{2|c|\left(128\kappa^2(a+2)-24a\kappa|c|+a|c|^2\right)}{a\left(8\kappa-|c|\right)^3}\quad(z\in\mathrm{U})$$

.

Proof. **i**. By using the inequalities:

$$|z_1+z_2|\le|z_1|+|z_2|,\ (\kappa)_n\ge\kappa^n \text{ and } n!\ge 2^{n-1}$$

and the equalities

$$\sum_{n=1}^{\infty}r^{n-1}=\frac{1}{1-r},$$

$$\sum_{n=1}^{\infty}nr^{n-1}=\frac{1}{(1-r)^2},$$

we have

$$\begin{aligned}
\left|\varphi_{v,a,b,c}(z)\right| &\leq \left|z+\sum_{n=1}^{\infty}\frac{(2n+a)(-c)^n}{a4^n n!(\kappa)_n}z^{n+1}\right| \leq 1+\sum_{n=1}^{\infty}\frac{(2n+a)|c|^n}{a4^n n!(\kappa)_n}\\
&= 1+\sum_{n=1}^{\infty}\frac{2n|c|^n}{a4^n n!(\kappa)_n}+\sum_{n=1}^{\infty}\frac{a|c|^n}{a4^n n!(\kappa)_n}\\
&= 1+\sum_{n=1}^{\infty}\frac{2n|c|^n}{a4^n 2^{n-1}\kappa^n}+\sum_{n=1}^{\infty}\frac{|c|^n}{4^n 2^{n-1}\kappa^n}\\
&= 1+\frac{|c|}{2\kappa a}\sum_{n=1}^{\infty}n\left(\frac{|c|}{8\kappa}\right)^{n-1}+\frac{|c|}{4\kappa}\sum_{n=1}^{\infty}\left(\frac{|c|}{8\kappa}\right)^{n-1}\\
&= 1+\frac{2|c|\left(8\kappa(a+2)-a|c|\right)}{a\left(8\kappa-|c|\right)^2} \qquad \left(\kappa>\frac{|c|}{8}\right).
\end{aligned}$$

ii. Similarly, by using the inequalities:

$$|z_1+z_2|\leq|z_1|+|z_2|,\ (\kappa)_n\geq\kappa^n \text{ and } n!\geq 2^{n-1}$$

and the equalities

$$\sum_{n=1}^{\infty}r^{n-1}=\frac{1}{1-r},$$
$$\sum_{n=1}^{\infty}nr^{n-1}=\frac{1}{(1-r)^2},$$
$$\sum_{n=1}^{\infty}n^2r^{n-1}=\frac{1+r}{(1-r)^3},$$

we have

$$\begin{aligned}
\left|\varphi'_{v,a,b,c}(z)\right| &= \left|1+\sum_{n=1}^{\infty}\frac{(n+1)(2n+a)(-c)^n}{a4^n n!(\kappa)_n}z^n\right| \leq 1+\sum_{n=1}^{\infty}\frac{\left(2n^2+n(a+2)+a\right)|c|^n}{a4^n n!(\kappa)_n}\\
&= 1+\sum_{n=1}^{\infty}\frac{2n^2|c|^n}{a4^n(n)!(\kappa)_n}+\sum_{n=1}^{\infty}\frac{(a+2)n|c|^n}{a4^n(n)!(\kappa)_n}+\sum_{n=1}^{\infty}\frac{|c|^n}{4^n\,n!(\kappa)_n}\\
&= 1+\sum_{n=1}^{\infty}\frac{2n^2|c|^n}{a4^n 2^{n-1}\kappa^n}+\sum_{n=1}^{\infty}\frac{(a+2)n|c|^n}{a4^n 2^{n-1}\kappa^n}+\sum_{n=1}^{\infty}\frac{|c|^n}{4^n 2^{n-1}\kappa^n}\\
&= 1+\frac{|c|}{2\kappa a}\sum_{n=1}^{\infty}n^2\left[\frac{|c|}{8\kappa}\right]^{n-1}+\left(\frac{a+2}{a}\right)\frac{|c|}{4\kappa}\sum_{n=1}^{\infty}n\left[\frac{|c|}{8\kappa}\right]^{n-1}+\frac{|c|}{4\kappa}\sum_{n=1}^{\infty}\left[\frac{|c|}{8\kappa}\right]^{n-1}\\
&= 1+\frac{2|c|\left(128\kappa^2(a+2)-24a\kappa|c|+a|c|^2\right)}{a\left(8\kappa-|c|\right)^3} \quad \left(\kappa>\frac{|c|}{8}\right).
\end{aligned}$$

Thus, the proof is completed.

2. MAIN RESULTS

Theorem 2.1. If the parameters $a \in \mathbb{R}^+, b \in \mathbb{R}, c \in \mathbb{C}$ and $\nu \in \mathbb{R} - \mathbb{R}_0^-$ and $\kappa := \nu + \frac{b+1}{2} \notin \mathbb{R}_0^-$ are so constrained that $\kappa > \frac{32|c|(a+1) + \sqrt{256|c|^2(a^2+8a+4)}}{128a}$, then

$$\Re\left\{\frac{\varphi_{\nu,a,b,c}(z)}{(\varphi_{\nu,a,b,c})_m(z)}\right\} \geq \frac{64a\kappa^2 - 32\kappa|c|(a+1) + 3a|c|^2}{a(8\kappa - |c|)^2} \quad (z \in \mathrm{U}), \tag{2.1}$$

and

$$\Re\left\{\frac{(\varphi_{\nu,a,b,c})_m(z)}{\varphi_{\nu,a,b,c}(z)}\right\} \geq \frac{a(8\kappa - |c|)^2}{64a\kappa^2 + 32\kappa|c| - a|c|^2} \quad (z \in \mathrm{U}). \tag{2.2}$$

Proof. We observe from part i. of Lemma 1.1 that

$$1 + \sum_{n=1}^{\infty} |b_n| \leq 1 + \frac{2|c|(8\kappa(a+2) - a|c|)}{a(8\kappa - |c|)^2},$$

which is equivalent to

$$\frac{a(8\kappa - |c|)^2}{2|c|(8\kappa(a+2) - a|c|)} \sum_{n=1}^{\infty} |b_n| \leq 1,$$

where $b_n = \frac{(-c)^n (2n+a)}{4^n an!(\kappa)_n}$. Now, we write

$$\begin{aligned} &\frac{a(8\kappa - |c|)^2}{2|c|(8\kappa(a+2) - a|c|)} \left[\frac{\varphi_{\nu,a,b,c}(z)}{(\varphi_{\nu,a,b,c})_n(z)} - \frac{64a\kappa^2 - 32\kappa|c|(a+1) + 3a|c|^2}{a(8\kappa - |c|)^2}\right] \\ &= \frac{1 + \sum_{n=1}^{m} b_n z^n + \frac{a(8\kappa - |c|)^2}{2|c|(8\kappa(a+2) - a|c|)} \sum_{n=m+1}^{\infty} b_n z^n}{1 + \sum_{n=1}^{m} b_n z^n} \\ &= \frac{1 + A(z)}{1 + B(z)}. \end{aligned}$$

Set $(1 + A(z))/(1 + B(z)) = (1 + w(z))/(1 - w(z))$, so that $w(z) = (A(z) - B(z))/(2 + A(z) + B(z))$. Then

$$w(z)=\frac{\frac{a(8\kappa-|c|)^2}{2|c|(8\kappa(a+2)-a|c|)}\sum_{n=m+1}^{\infty}b_n z^n}{2+2\sum_{n=1}^{m}b_n z^n+\frac{a(8\kappa-|c|)^2}{2|c|(8\kappa(a+2)-a|c|)}\sum_{n=m+1}^{\infty}b_n z^n}$$

and

$$|w(z)|\le\frac{\frac{a(8\kappa-|c|)^2}{2|c|(8\kappa(a+2)-a|c|)}\sum_{n=m+1}^{\infty}|b_n|}{2-2\sum_{n=1}^{m}|b_n|-\frac{a(8\kappa-|c|)^2}{2|c|(8\kappa(a+2)-a|c|)}\sum_{n=m+1}^{\infty}|b_n|}.$$

Now $|w(z)|\le 1$ if and only if

$$\frac{a(8\kappa-|c|)^2}{|c|(8\kappa(a+2)-a|c|)}\sum_{n=m+1}^{\infty}|b_n|\le 2-2\sum_{n=1}^{m}|b_n|,$$

which is equivalent to

$$\sum_{n=1}^{m}|b_n|+\frac{a(8\kappa-|c|)^2}{2|c|(8\kappa(a+2)-a|c|)}\sum_{n=m+1}^{\infty}|b_n|\le 1. \tag{2.3}$$

It suffices to show that the left hand side of (2.3) is bounded above by $\frac{a(8\kappa-|c|)^2}{2|c|(8\kappa(a+2)-a|c|)}\sum_{n=1}^{\infty}|b_n|$, which is equivalent to

$$\frac{64a\kappa^2-32\kappa|c|(a+1)+3a|c|^2}{2|c|(8\kappa(a+2)-a|c|)}\sum_{n=1}^{m}|b_n|\ge 0.$$

To prove the result (2.2), we write

$$\begin{aligned}&\frac{64a\kappa^2+32\kappa|c|-a|c|^2}{2|c|(8\kappa(a+2)-a|c|)}\left[\frac{(\varphi_{\nu,a,b,c})_n(z)}{\varphi_{\nu,a,b,c}(z)}-\frac{a(8\kappa-|c|)^2}{64a\kappa^2+32\kappa|c|-a|c|^2}\right]\\ &=\frac{1+\sum_{m=1}^{n}b_m z^m-\frac{a(8\kappa-|c|)^2}{2|c|(8\kappa(a+2)-a|c|)}\sum_{m=n+1}^{\infty}b_m z^m}{1+\sum_{m=1}^{\infty}b_m z^m}\\ &=\frac{1+w(z)}{1-w(z)}\end{aligned}$$

where

$$|w(z)| \le \frac{\frac{64a\kappa^2+32\kappa|c|-a|c|^2}{2|c|\left(8\kappa(a+2)-a|c|\right)}\sum_{m=n+1}^{\infty}|b_m|}{2-2\sum_{m=1}^{n}|b_m|-\frac{64a\kappa^2-32\kappa|c|(a+1)+3a|c|^2}{2|c|\left(8\kappa(a+2)-a|c|\right)}\sum_{m=n+1}^{\infty}|b_m|} \le 1$$

The last inequality is equivalent to

$$\sum_{m=1}^{n}|b_m|+\frac{a\left(8\kappa-|c|\right)^2}{2|c|\left(8\kappa(a+2)-a|c|\right)}\sum_{m=n+1}^{\infty}|b_m| \le 1 \tag{2.4}$$

Since the left hand side of (2.4) is bounded above by $\frac{a\left(8\kappa-|c|\right)^2}{2|c|\left(8\kappa(a+2)-a|c|\right)}\sum_{n=1}^{\infty}|b_n|$, the proof is completed.

Theorem 2.2. If the parametres $a \in \mathbb{R}^+, b \in \mathbb{R}, c \in \mathbb{C}$ and $\nu \in \mathbb{C}-\mathbb{Z}_0^-$ and $\kappa := \nu+\frac{b+1}{2} \notin \mathbb{Z}_0^-$ are so constrained that $512\kappa^3 a-64\kappa^2|c|(7a+8)+3a|c|^2\left(24\kappa-|c|\right) \ge 0,$ then

$$\Re\left\{\frac{\varphi'_{\nu,a,b,c}(z)}{\left(\varphi_{\nu,a,b,c}\right)'_m(z)}\right\} \ge \frac{512\kappa^3 a-64\kappa^2|c|(7a+8)+3a|c|^2\left(24\kappa-|c|\right)}{a\left(8\kappa-|c|\right)^3} \quad (z \in \mathrm{U}) \tag{2.5}$$

and

$$\Re\left\{\frac{\left(\varphi_{\nu,a,b,c}\right)'_m(z)}{\varphi'_{\nu,a,b,c}(z)}\right\} \ge \frac{a\left(8\kappa-|c|\right)^3}{512\kappa^3 a+64\kappa^2|c|(a+8)-a|c|^2\left(24\kappa-|c|\right)} \quad (z \in \mathrm{U}). \tag{2.6}$$

Proof. From part ii. of Lemma 1.1 we observe that

$$1+\sum_{n=1}^{\infty}(n+1)|b_n| \le 1+\frac{2|c|\left(128\kappa^2(a+2)-24a\kappa|c|+a|c|^2\right)}{a\left(8\kappa-|c|\right)^3},$$

which is equivalent to

$$\frac{a\left(8\kappa-|c|\right)^3}{2|c|\left(128\kappa^2(a+2)-24a\kappa|c|+a|c|^2\right)}\sum_{n=1}^{\infty}(n+1)|b_n| \le 1,$$

where $b_n = \frac{(-c)^n(2n+a)}{4^n an!(\kappa)_n}$. Now we write

$$\frac{a\left(8\kappa-|c|\right)^3}{2|c|\left(128\kappa^2(a+2)-24a\kappa|c|+a|c|^2\right)}\left[\frac{\varphi'_{\nu,a,b,c}(z)}{\left(\varphi_{\nu,a,b,c}\right)'_n(z)}-\frac{512\kappa^3 a-64\kappa^2|c|(7a+8)+3a|c|^2\left(24\kappa-|c|\right)}{a\left(8\kappa-|c|\right)^3}\right]$$

$$= \frac{1+\sum_{n=1}^{m}(n+1)b_n z^n + \dfrac{a\left(8\kappa-|c|\right)^3}{2|c|\left(128\kappa^2(a+2)-24a\kappa|c|+a|c|^2\right)}\sum_{n=m+1}^{\infty}(n+1)b_n z^n}{1+\sum_{n=1}^{m}(n+1)b_n z^n}$$

$$= \frac{1+w(z)}{1-w(z)},$$

where

$$|w(z)| \le \frac{\dfrac{a\left(8\kappa-|c|\right)^3}{2|c|\left(128\kappa^2(a+2)-24a\kappa|c|+a|c|^2\right)}\sum_{n=m+1}^{\infty}(n+1)|b_n|}{2-2\sum_{n=1}^{m}(n+1)|b_n|-\dfrac{a\left(8\kappa-|c|\right)^3}{2|c|\left(128\kappa^2(a+2)-24a\kappa|c|+a|c|^2\right)}\sum_{n=m+1}^{\infty}(n+1)|b_n|} \le 1.$$

The last inequality is equivalent to

$$\sum_{n=1}^{m}(n+1)|b_n| + \frac{a\left(8\kappa-|c|\right)^3}{2|c|\left(128\kappa^2(a+2)-24a\kappa|c|+a|c|^2\right)}\sum_{n=m+1}^{\infty}(n+1)|b_n| \le 1. \tag{2.7}$$

It suffices to show that the left hand side of (2.7) is bounded above by

$$\frac{a\left(8\kappa-|c|\right)^3}{2|c|\left(128\kappa^2(a+2)-24a\kappa|c|+a|c|^2\right)}\sum_{n=1}^{\infty}(n+1)|b_n|,$$

which is equivalent to

$$\frac{512\kappa^3 a-64\kappa^2|c|(7a+8)+3a|c|^2(24\kappa-|c|)}{2|c|\left(128\kappa^2(a+2)-24a\kappa|c|+a|c|^2\right)}\sum_{n=1}^{m}(n+1)|b_n| \ge 0.$$

To prove the result (2.6), we write

$$\frac{512\kappa^3 a+64\kappa^2|c|(a+8)-a|c|^2(24\kappa-|c|)}{2|c|\left(128\kappa^2(a+2)-24a\kappa|c|+a|c|^2\right)}\left[\frac{\left(\varphi_{\nu,a,b,c}\right)_n'(z)}{\varphi_{\nu,a,b,c}'(z)}-\frac{a\left(8\kappa-|c|\right)^3}{512\kappa^3 a+64\kappa^2|c|(a+8)-a|c|^2(24\kappa-|c|)}\right]$$

$$= \frac{1+\sum_{n=1}^{m}(n+1)b_n z^n + \dfrac{a\left(8\kappa-|c|\right)^3}{2|c|\left(128\kappa^2(a+2)-24a\kappa|c|+a|c|^2\right)}\sum_{n=m+1}^{\infty}(n+1)b_n z^n}{1+\sum_{n=1}^{m}(n+1)b_n z^n}$$

$$= \frac{1+w(z)}{1-w(z)},$$

where

$$|w(z)| \le \frac{\frac{512\kappa^3 a + 64\kappa^2 |c|(a+8) - a|c|^2 (24\kappa - |c|)}{2|c|\left(128\kappa^2 (a+2) - 24a\kappa|c| + a|c|^2\right)} \sum_{n=m+1}^{\infty} (n+1)|b_n|}{2 - 2\sum_{n=1}^{m} (n+1)|b_n| - \frac{512\kappa^3 a - 64\kappa^2 |c|(7a+8) + 3a|c|^2 (24\kappa - |c|)}{2|c|\left(128\kappa^2 (a+2) - 24a\kappa|c| + a|c|^2\right)} \sum_{n=m+1}^{\infty} (n+1)|b_n|} \le 1.$$

The last inequality is equivalent to

$$\sum_{n=1}^{m} (n+1)|b_n| + \frac{a(8\kappa - |c|)^3}{2|c|\left(128\kappa^2 (a+2) - 24a\kappa|c| + a|c|^2\right)} \sum_{n=m+1}^{\infty} (n+1)|b_n| \le 1. \tag{2.8}$$

Since the left hand side of (2.8) is bounded above by $\frac{a(8\kappa - |c|)^3}{2|c|\left(128\kappa^2 (a+2) - 24a\kappa|c| + a|c|^2\right)} \sum_{n=1}^{\infty} (n+1)|b_n|$, the proof is completed.

Remark 2.1. Taking $b = c = 1$ in Lemma 1.1, Theorem 2.1 and Theorem 2.2, we obtain the results of [1].

REFERENCES

1. İ. Aktaş, H. Orhan, *Partial sums of normalized Dini functions*, J. Classical Anal. Vol. 9, Number 2, 127-135 (2016).
2. L. Brickman, D. J. Hallenbeck, T. H. Macgragor, D. Wilken, *Convex hulls and extreme points of families of starlike and convex mappings*, Trans. Amer.Math. Soc. 185, 413–428, (1973).
3. M. Çağlar, E. Deniz, *Partial sums of the normalized Lommel functions*, Math. Inequal. Appl. 18,3, 1189–1199, (2015).
4. E. Deniz, H. Orhan and H. M. Srivastava, *Some su_cient conditions for univalence of certain families of integral operators involving generalized Bessel functions*, Taiwanese J. Math. 15(2), 883-917, (2011).
5. E. Deniz, Ş. Gören and M. Çağlar, *Starlikeness and convexity of the generalized Dini functions*, AIP Conference Proceedings 1833(020004) (2017), doi:10.1063/1.4981652.
6. E. Deniz and Ş. Gören, *Geometric Properties of Generalized Dini Functions*, Honam Mathematical J, 41, No.1, pp. 101-116, (2019).
7. F. W. J. Olver, D.W. Lozier, R.F. Boisvert, C.W. Clark (Eds.), *NIST Handbook of Mathematical Functions*, Cambridge Univ. Press, Cambridge, 2010.
8. H. Orhan, N. Yağmur, *Partial sums of Generilazed Bessel Functions*, J.Math. Inequal. 8, 4, 863–877, (2014).
9. S. Owa, H. M. Srivastava, N. Saito, *Partial sums of certain classes of analytic functions*, Int. J.Comput. Math. 81, 10, 1239–1256, (2004).
10. T. Sheill-Small, *A note on partial sums of convex schlicht functions*, Bull. London Math. Soc. 2, 165–168, (1970).
11. H. Silverman, *Partial sums of starlike and convex functions*, J. Math. Anal. Appl. 209, 221–227, (1997).
12. E. M. Silvia, *On partial sums of convex functions of order* α, Houston J. Math., 11, 397-404, (1985).
13. G. N. Watson, *A treatise on the theory of Bessel functions, Second edition*, Cambridge University Press, Cambridge, London and New York, 1944.

The Radii of $\alpha-$Convexity of the Function $az^2J_v''(z)+bzJ_v'(z)+cJ_v(z)$

Erhan DENİZ[1], Sercan KAZIMOĞLU[1] and Murat ÇAĞLAR[1]

[1]*Department of Mathematics, Faculty of Science and Arts,*
Kafkas University, Kars-TURKEY

edeniz36@gmail.com
srcnkzmglu@gmail.com
mcaglar25@gmail.com

Abstract. In this paper, our aim is to determine the radii of $\alpha-$convexity for three different kind of normalization of the function $N_v(z)=az^2J_v''(z)+bzJ_v'(z)+cJ_v(z)$, where $J_v(z)$ is the Bessel function of the first kind of order v. The key tools in the proof of our main results are the Mittag-Leffler expansion for function $N_v(z)$, properties of zeros of the function $N_v(z)$ and some inequalities for complex and real numbers.

1. INTRODUCTION

For $\mathrm{U}(r)=\{z\in\mathbb{C}:|z|<r\}$ denotes the disc of radius r centered at the origin. Let $f:\mathrm{U}(r_f)\to\mathbb{C}$ be the function defined by

$$f(z)=z+\sum_{n=2}^{\infty}a_nz^n, \qquad \textbf{(2.9)}$$

where r_f is the radius of convergence of the power series.

Let r be a real number with $r\in(0,r_f)$. We say that the function f defined by (1.1) is starlike in the disk $\mathrm{U}(r)$ if f univalent and $f(\mathrm{U}(r))$ is a starlike domain in $\mathbb{C}$ with respect to the origin. Analytically, the function f is starlike in $\mathrm{U}(r)$ if and only if $\mathrm{Re}\left(\frac{zf'(z)}{f(z)}\right)>0,\ z\in\mathrm{U}(r)$. For $\beta\in[0,1)$ we say that the function f is starlike of order β in $\mathrm{U}(r)$ if and only if $\mathrm{Re}\left(\frac{zf'(z)}{f(z)}\right)>\beta,\ z\in\mathrm{U}(r)$. We define by the real number

$$r_\beta^*(f)=\sup\left\{r\in(0,r_f):\mathrm{Re}\left(\frac{zf'(z)}{f(z)}\right)>\beta \text{ for all } z\in\mathrm{U}(r)\right\}$$

the radius of starlikeness of order β of the function f. Note that $r^*(f)=r_0^*(f)$ is the largest radius such that the imagine region $f(\mathrm{U}(r^*(f)))$ is a starlike domain with respect to the origin.

The function f defined by (1.1) is convex in the disk $\mathrm{U}(r)$ if f is univalent in $\mathrm{U}(r)$, and $f(\mathrm{U}(r))$ is a convex domain in $\mathbb{C}$. Analytically, the function f is convex in $\mathrm{U}(r)$ if and only if $\mathrm{Re}\left(1+\frac{zf''(z)}{f'(z)}\right)>0, z\in\mathrm{U}(r)$. For

$\beta \in [0,1)$ we say that the function f is convex of order β in $\mathrm{U}(r)$ if and only if $\mathrm{Re}\left(1+\frac{zf''(z)}{f'(z)}\right) > \beta, z \in \mathrm{U}(r)$.

The radius of convexity of order β of the function f is defined by the real number

$$r_\beta^{\,c}(f) = \sup\left\{r \in (0, r_f) : \mathrm{Re}\left(1+\frac{zf''(z)}{f'(z)}\right) > \beta \text{ for all } z \in \mathrm{U}(r)\right\}.$$

Note that $r^c(f) = r_0^{\,c}(f)$ is the largest radius such that the image region $f\left(\mathrm{U}\left(r^c(f)\right)\right)$ is a convex domain.

Let α and β be two real numbers with $\alpha \in$ □ and $\beta \in [0,1)$. We say that the function f is $\alpha-$convex of order β in $\mathrm{U}(r)$ if and only if

$$\mathrm{Re}\left((1-\alpha)\frac{zf'(z)}{f(z)} + \alpha\left(1+\frac{zf''(z)}{f'(z)}\right)\right) > \beta, \quad z \in \mathrm{U}(r).$$

The radius of $\alpha-$convex of order β of the function f is defined by the real number

$$r_{\alpha,\beta}(f) = \sup\left\{r \in (0, r_f) : \mathrm{Re}\left((1-\alpha)\frac{zf'(z)}{f(z)} + \alpha\left(1+\frac{zf''(z)}{f'(z)}\right)\right) > \beta \text{ for all } z \in \mathrm{U}(r)\right\}.$$

The radius of $\alpha-$convex of order β is the generalization of the radius of starlikeness of order β and of the radius of convexity of order β. We have $r_{0,\beta}(f) = r_\beta^{\,*}(f)$ and $r_{1,\beta}(f) = r_\beta^{\,c}(f)$. For more details on starlike, convex and α -convex functions, we refer to [7, 11, 12] and to the references therein.

The Bessel function of the first kind of order v is defined by [12, p. 217]

$$J_v(z) = \sum_{n=0}^{\infty} \frac{(-1)^n}{n!\Gamma(n+v+1)}\left(\frac{z}{2}\right)^{2n+v} \qquad (z \in \mathrm{C}) \qquad \textbf{(2.10)}$$

We know that it has all its zeros real for $v > -1$. In [10], Mercer introduced and studied the general function

$$N_v(z) = az^2 J_v''(z) + bzJ_v'(z) + cJ_v(z).$$

Here, as in [10], $q = b - a$ and

$$(c = 0 \text{ and } q \neq 0) \text{ or } (c > 0 \text{ and } q > 0).$$

From (1.2), we have the power series representation

$$N_v(z) = \sum_{n=0}^{\infty} \frac{Q(2n+v)(-1)^n}{n!\Gamma(n+v+1)}\left(\frac{z}{2}\right)^{2n+v} \qquad (z \in \mathrm{C}) \qquad \textbf{(2.11)}$$

where $Q(v)=av(v-1)+bv+c$ $(a,b,c\in\mathbb{R})$. There are three important works on the function N_v. First Mercer's paper [10] which it has been proved that the kth positive zero of N_v increases with v in $v>0$. Second, Ismail and Muldoon [8] showed that

(i). For $v>0$, the zeros of $N_v(z)$ are either real or purely imaginary.

(ii). For $v\geq\max\{0,v_0\}$, where v_0 is the largest real root of the quadratic $Q(v)=av(v-1)+bv+c$, the zeros of $N_v(z)$ are real.

(iii). If $v>0$, $\left(av^2+(b-a)v+c\right)/(b-a)>0$ and $a/(b-a)<0$, the zeros of $N_v(z)$ are all real except for a single pair which are conjugate purely imaginary

under the conditions $a,b,c\in\mathbb{R}$ such that $c=0$ and $b\neq a$ or $c>0$ and $b>a$. Last, in [4], Baricz, Çağlar and Deniz obtained sufficient and necessary conditions for the starlikeness of a normalized form of $N_v(z)$.

Note that N_v is not belongs to A. To prove the main results, we need normalization of the function N_v. In this paper we focus on the following normalized form

$$f_v(z)=\left[\frac{2^v\Gamma(v+1)}{Q(v)}N_v(z)\right]^{\frac{1}{v}},$$

$$g_v(z)=\frac{2^v\Gamma(v+1)z^{1-v}}{Q(v)}N_v(z),$$

$$h_v(z)=\frac{2^v\Gamma(v+1)z^{1-\frac{v}{2}}}{Q(v)}N_v\left(\sqrt{z}\right).$$

We also mention that the univalence, starlikeness, convexity and α-convex functions of Bessel functions of the first kind were studied extensively in several papers. We refer to [1-6, 9, 11] and to the references therein.

In this rest of this paper, the quadratic $Q(v)=av(v-1)+bv+c$ will always provide on $a,b,c\in\mathbb{R}$ and ($c=0$ and $a\neq b$) or ($c>0$ and $a<b$). Moreover, v_0 is largest real root of the quadratic $Q(v)$ defined according to the above conditions and we shall use the following notation

$$\mathrm{N}(\alpha,u(z))=(1-\alpha)\frac{zu'(z)}{u(z)}+\alpha\left(1+\frac{zu''(z)}{u'(z)}\right).$$

Theorem 1. Let $\alpha\geq 0$ and $\beta\in[0,1)$. The following statements hold:

a) If $v\geq\max\{0,v_0\}$, $v\neq 0$ then the radius of $\alpha-$convexity of order β of the function f_v is the smallest positive root of the equation

$$\alpha\left(1+\frac{rN_v''(r)}{N_v'(r)}\right)+\left(\frac{1}{v}-\alpha\right)\frac{rN_v'(r)}{N_v(r)}=\beta.$$

The radius of $\alpha-$convexity satisfies $r_{\alpha,\beta}(f_v)\leq\lambda'_{v,1}<\lambda_{v,1}$, where $\lambda_{v,1}$ and $\lambda'_{v,1}$ denote the first positive zeros of N_v and N_v', respectively.

b) If $v\geq\max\{0,v_0\}$, then the radius of $\alpha-$convexity of order β of the function g_v is the smallest positive root of the equation

$$1+(\alpha-1)\left(\nu-\frac{rN_\nu'(r)}{N_\nu(r)}\right)+\alpha\frac{r^2N_\nu''(r)+2(1-\nu)rN_\nu'(r)+(\nu^2-\nu)N_\nu(r)}{rN_\nu'(r)+(1-\nu)N_\nu(r)}=\beta.$$

c) If $\nu\geq\max\{0,\nu_0\}$ then the radius of $\alpha-$convexity of order β of the function h_ν is the smallest positive root of the equation

$$1+\left(\frac{\alpha-1}{2}\right)\left(\nu-\frac{\sqrt{r}N_\nu'(\sqrt{r})}{N_\nu(\sqrt{r})}\right)+\frac{\alpha}{2}\frac{rN_\nu''(\sqrt{r})+(3-2\nu)\sqrt{r}N_\nu'(\sqrt{r})+(\nu^2-\nu)N_\nu(\sqrt{r})}{\sqrt{r}N_\nu'(\sqrt{r})+(2-\nu)N_\nu(\sqrt{r})}=\beta.$$

Proof. a) We assume that $\alpha>0,$ the case $\alpha=0$ was proved already in [9]. Using the definition of the function f_ν, we have

$$\frac{zf_\nu'(z)}{f_\nu(z)}=\frac{1}{\nu}\frac{zN_\nu'(z)}{N_\nu(z)},\quad 1+\frac{zf_\nu''(z)}{f_\nu'(z)}=1+\frac{zN_\nu''(z)}{N_\nu'(z)}+\left(\frac{1}{\nu}-1\right)\frac{zN_\nu'(z)}{N_\nu(z)}$$

where $\nu\geq\max\{0,\nu_0\},\ \nu\neq0.$
In view of the following infinite product representations [9]

$$N_\nu(z)=\frac{Q(\nu)z^\nu}{2^\nu\Gamma(\nu+1)}\prod_{n\geq1}\left(1-\frac{z^2}{\lambda_{\nu,n}^2}\right),\quad N_\nu'(z)=\frac{Q(\nu)\nu z^{\nu-1}}{2^\nu\Gamma(\nu+1)}\prod_{n\geq1}\left(1-\frac{z^2}{\lambda_{\nu,n}'^2}\right),$$

where $\lambda_{\nu,n}$ and $\lambda_{\nu,n}'$ are the nth positive roots of N_ν and N_ν', respectively, logarithmic differentiation yields

$$\frac{zN_\nu'(z)}{N_\nu(z)}=\nu-\sum_{n\geq1}\frac{2z^2}{\lambda_{\nu,n}^2-z^2},\quad 1+\frac{zN_\nu''(z)}{N_\nu'(z)}=\nu-\sum_{n\geq1}\frac{2z^2}{\lambda_{\nu,n}'^2-z^2},$$

which implies that

$$\begin{aligned}\mathrm{N}(\alpha,f_\nu(z)) &= (1-\alpha)\frac{zf_\nu'(z)}{f_\nu(z)}+\alpha\left(1+\frac{zf_\nu''(z)}{f_\nu'(z)}\right)\\ &= \alpha+\left(\frac{1}{\nu}-\alpha\right)\frac{zN_\nu'(z)}{N_\nu(z)}+\alpha\frac{zN_\nu''(z)}{N_\nu'(z)}\\ &= 1-\left(\frac{1}{\nu}-\alpha\right)\sum_{n\geq1}\frac{2z^2}{\lambda_{\nu,n}^2-z^2}-\alpha\sum_{n\geq1}\frac{2z^2}{\lambda_{\nu,n}'^2-z^2}.\end{aligned}$$

On the other hand, we know (see [2, Lem. 2.1]) that if $a>b>0,\ z\in\mathbb{C}$ and $\lambda\leq1$, then for all $|z|<b$ we have

$$\lambda\,\mathrm{Re}\left(\frac{z}{a-z}\right)-\mathrm{Re}\left(\frac{z}{b-z}\right)\geq\lambda\frac{|z|}{a-|z|}-\frac{|z|}{b-|z|}. \qquad \textbf{(2.12)}$$

Using the inequality (1.4) for all $z\in\mathbb{U}\left(0,\lambda_{\nu,1}'\right)$, we obtain the inequality

$$\frac{1}{\alpha}\operatorname{Re}\mathrm{N}\left(\alpha, f_\nu(z)\right) \geq \frac{1}{\alpha}+\left(1-\frac{1}{\alpha\nu}\right)\sum_{n\geq 1}\frac{2r^2}{\lambda_{\nu,n}^2-r^2}-\sum_{n\geq 1}\frac{2r^2}{\lambda_{\nu,n}'^2-r^2}=\frac{1}{\alpha}\mathrm{N}\left(\alpha, f_\nu(r)\right),$$

where $|z|=r$. Here, we used the fact that the zeros $\lambda_{\nu,n}$ and $\lambda'_{\nu,n}$ interlace according to the inequalities [9]

$$\lambda'_{\nu,1}<\lambda_{\nu,1}<\lambda'_{\nu,2}<\lambda_{\nu,2}<\ldots. \qquad \textbf{(2.13)}$$

Now, the above deduced inequality implies that for $r\in\left(0,\lambda'_{\nu,1}\right)$ we have $\inf_{z\in\mathrm{U}(0,r)}\mathrm{N}\left(\alpha, f_\nu(z)\right)=\mathrm{N}\left(\alpha, f_\nu(r)\right)$. On other hand, the function $r\mapsto\mathrm{N}\left(\alpha, f_\nu(r)\right)$ is strictly decreasing on $\left(0,\lambda'_{\nu,1}\right)$ since

$$\begin{aligned}\frac{\partial}{\partial r}\left(\alpha, f_\nu(r)\right) &= -\left(\frac{1}{\nu}-\alpha\right)\sum_{n\geq 1}\frac{4r\lambda_{\nu,n}^2}{\left(\lambda_{\nu,n}^2-r^2\right)^2}-\alpha\sum_{n\geq 1}\frac{4r\lambda_{\nu,n}'^2}{\left(\lambda_{\nu,n}'^2-r^2\right)^2}\\ &< \alpha\sum_{n\geq 1}\frac{4r\lambda_{\nu,n}^2}{\left(\lambda_{\nu,n}^2-r^2\right)^2}-\alpha\sum_{n\geq 1}\frac{4r\lambda_{\nu,n}'^2}{\left(\lambda_{\nu,n}'^2-r^2\right)^2}<0\end{aligned}$$

for $\nu\geq\max\left\{0,\nu_0\right\}$, $\nu\neq 0$ and $r\in\left(0,\lambda'_{\nu,1}\right)$. Here, we used again the fact that the zeros $\lambda_{\nu,n}$ and $\lambda'_{\nu,n}$ interlace and for all $n\in\{1,2,3,\ldots\}$, $r<\sqrt{\lambda_{\nu,1}\lambda'_{\nu,1}}$ we have that

$$\lambda_{\nu,n}^2\left(\lambda_{\nu,n}'^2-r^2\right)^2<\lambda_{\nu,n}'^2\left(\lambda_{\nu,n}^2-r^2\right)^2.$$

We also have that $\lim_{r\to 0}\left(\alpha, f_\nu(r)\right)=1>\beta$ and $\lim_{r\to\lambda'_{\nu,1}}\left(\alpha, f_\nu(r)\right)=-\infty$, which means that for $z\in\mathrm{U}\left(0,r_1\right)$ we have $\operatorname{Re}\mathrm{N}\left(\alpha, f_\nu(z)\right)>\beta$ if and only if r_1 is the unique root of $\mathrm{N}\left(\alpha, f_\nu(z)\right)=\beta$, situated in $\left(0,\lambda'_{\nu,1}\right)$. Finally, once again, using the interlacing inequalities (1.5), we obtain the inequality

$$\frac{\partial}{\partial\alpha}\left(\alpha, f_\nu(r)\right)=\sum_{n\geq 1}\frac{2r^2}{\lambda_{\nu,n}^2-r^2}-\sum_{n\geq 1}\frac{2r^2}{\lambda_{\nu,n}'^2-r^2}<0$$

where $\nu\geq\max\left\{0,\nu_0\right\}$, $\nu\neq 0$, $\alpha\geq 0$ and $r\in\left(0,\lambda'_{\nu,1}\right)$. This implies that the function $\alpha\mapsto\left(\alpha, f_\nu(r)\right)$ is strictly decreasing on $[0,\infty)$ for all $\nu\geq\max\left\{0,\nu_0\right\}$, $\nu\neq 0$ and $r\in\left(0,\lambda'_{\nu,1}\right)$ fixed. Consequently, as a function of α the unique root of the equation $\mathrm{N}\left(\alpha, f_\nu(z)\right)=\beta$ is strictly decreasing, where $\beta\in[0,1)$, $\nu\geq\max\left\{0,\nu_0\right\}$, $\nu\neq 0$ and $r\in\left(0,\lambda'_{\nu,1}\right)$ are fixed. Thus, in the case when $\alpha\in(0,1)$ the radius of $\alpha-$convexity of the function f_ν will be between the radius of convexity and the radius of starlikeness of the function f_ν.

b) Similarly, as in the proof of Theorem 1-a, we assume that $\alpha>0$, the case $\alpha=0$ was proved in [9].
We know that following equalities (see [9])

$$\frac{zg_\nu'(z)}{g_\nu(z)}=(1-\nu)+\frac{zN_\nu'(z)}{N_\nu(z)},\quad 1+\frac{zg_\nu''(z)}{g_\nu'(z)}=1-\sum_{n\geq 1}\frac{2z^2}{\delta_{\nu,n}^2-z^2}$$

where $\delta_{\nu,n}$ is the n th positive zero of the function $g'(z)$. Thus, we have that

$$\begin{aligned}\mathrm{N}\left(\alpha, g_\nu(z)\right) &= (1-\alpha)\frac{zg_\nu'(z)}{g_\nu(z)}+\alpha\left(1+\frac{zg_\nu''(z)}{g_\nu'(z)}\right)\\ &= (1-\alpha)\left((1-\nu)+\frac{zN_\nu'(z)}{N_\nu(z)}\right)+\alpha\left(1+\frac{zg_\nu''(z)}{g_\nu'(z)}\right)\\ &= 1+(\alpha-1)\sum_{n\geq 1}\frac{2z^2}{\lambda_{\nu,n}^2-z^2}-\alpha\sum_{n\geq 1}\frac{2z^2}{\delta_{\nu,n}^2-z^2}.\end{aligned}$$

Applying the inequality (1.4), we have that

$$\frac{1}{\alpha}\mathrm{Re}\,\mathrm{N}\left(\alpha, g_\nu(z)\right)\geq\frac{1}{\alpha}+\left(1-\frac{1}{\alpha}\right)\sum_{n\geq 1}\frac{2r^2}{\lambda_{\nu,n}^2-r^2}-\sum_{n\geq 1}\frac{2r^2}{\lambda_{\nu,n}'^2-r^2}=\frac{1}{\alpha}\mathrm{N}\left(\alpha, g_\nu(r)\right),$$

where $|z|=r$. Here, we tacitly used the fact that for all $n\in\{1,2,3,\ldots\}$ we have $\delta_{\nu,n}\in\left(\lambda_{\nu,n-1},\lambda_{\nu,n}\right)$, where $\lambda_{\nu,n}$ is the n th positive zero of N_ν. Thus, for $r\in\left(0,\delta_{\nu,1}\right)$ we get $\inf_{z\in\mathrm{U}(0,r)}\mathrm{Re}\,\mathrm{N}\left(\alpha, g_\nu(r)\right)=\mathrm{N}\left(\alpha, g_\nu(r)\right)$, since according to the minimum principle of harmonic functions, the infimum is taken on boundary. On the other hand, the function $r\mapsto\mathrm{N}\left(\alpha, g_\nu(r)\right)$ is strictly decreasing on $\left(0,\delta_{\nu,1}\right)$ since

$$\begin{aligned}\frac{\partial}{\partial r}\square\left(\alpha, g_\nu(r)\right) &= (\alpha-1)\sum_{n\geq 1}\frac{4r\lambda_{\nu,n}^2}{\left(\lambda_{\nu,n}^2-r^2\right)^2}-\alpha\sum_{n\geq 1}\frac{4r\delta_{\nu,n}^2}{\left(\delta_{\nu,n}^2-r^2\right)^2}\\ &< \alpha\sum_{n\geq 1}\frac{4r\lambda_{\nu,n}^2}{\left(\lambda_{\nu,n}^2-r^2\right)^2}-\alpha\sum_{n\geq 1}\frac{4r\delta_{\nu,n}^2}{\left(\delta_{\nu,n}^2-r^2\right)^2}<0\end{aligned}$$

for $\nu\geq\max\{0,\nu_0\}$ and $r\in\left(0,\delta_{\nu,1}\right)$. Here, we again used the fact that the zeros $\lambda_{\nu,n}$ and $\delta_{\nu,n}$ interlace and for all $n\in\{1,2,3,\ldots\}$, $r<\sqrt{\lambda_{\nu,1}\delta_{\nu,1}}$ we have that

$$\lambda_{\nu,n}^2\left(\delta_{\nu,n}^2-r^2\right)^2<\delta_{\nu,n}^2\left(\lambda_{\nu,n}^2-r^2\right)^2.$$

We also have that $\lim_{r\square 0}\square\left(\alpha, g_\nu(r)\right)=1>\beta$ and $\lim_{r\square\delta_{\nu,1}}\square\left(\alpha, g_\nu(r)\right)=-\infty$, which means that for $z\in\mathrm{U}\left(0,r_2\right)$ we have $\mathrm{Re}\,\mathrm{N}\left(\alpha, g_\nu(z)\right)>\beta$ if and only if r_2 is the unique root of $\mathrm{N}\left(\alpha, g_\nu(z)\right)=\beta$, situated in $\left(0,\delta_{\nu,1}\right)$. Using the interlacing inequalities $\lambda_{\nu,n-1}<\delta_{\nu,n}<\lambda_{\nu,n}$, we obtain

$$\frac{\partial}{\partial\alpha}\square\left(\alpha, g_\nu(r)\right)=\sum_{n\geq 1}\frac{2r^2}{\lambda_{\nu,n}^2-r^2}-\sum_{n\geq 1}\frac{2r^2}{\delta_{\nu,n}^2-r^2}<0,$$

where $\nu\geq\max\{0,\nu_0\}$, $\alpha\geq 0$ and $r\in\left(0,\delta_{\nu,1}\right)$. This implies that the function $\alpha\mapsto\square\left(\alpha, g_\nu(r)\right)$ is strictly decreasing on $[0,\infty)$ for all $\nu\geq\max\{0,\nu_0\}$ and $r\in\left(0,\delta_{\nu,1}\right)$ fixed. Consequently, as a function of α the unique root of the equation $\mathrm{N}\left(\alpha, g_\nu(z)\right)=\beta$ is strictly decreasing, where $\beta\in[0,1)$, $\nu\geq\max\{0,\nu_0\}$ and $r\in\left(0,\delta_{\nu,1}\right)$ are fixed. Thus, for $\alpha\in(0,1)$ the radius of $\alpha-$convexity of the function g_ν is between the radius of convexity and the radius of starlikeness of the function g_ν.

c) We assume that $\alpha > 0$, the case $\alpha = 0$ was proved already in [9]. In [9], using the definition of the function h_ν, we have

$$\frac{zh_\nu'(z)}{h_\nu(z)} = \left(1-\frac{\nu}{2}\right) + \frac{1}{2}\frac{\sqrt{z}N_\nu'\left(\sqrt{z}\right)}{N_\nu\left(\sqrt{z}\right)}, \quad 1+\frac{zh_\nu''(z)}{h_\nu'(z)} = 1-\sum_{n\geq 1}\frac{z}{\gamma_{\nu,n}^2 - z}$$

where $\nu \geq \max\{0, \nu_0\}$, it follows that

$$\begin{aligned} \mathrm{N}\left(\alpha, h_\nu(z)\right) &= (1-\alpha)\frac{zh_\nu'(z)}{h_\nu(z)} + \alpha\left(1+\frac{zh_\nu''(z)}{h_\nu'(z)}\right) \\ &= (1-\alpha)\left(\left(1-\frac{\nu}{2}\right) + \frac{1}{2}\frac{\sqrt{z}N_\nu'\left(\sqrt{z}\right)}{N_\nu\left(\sqrt{z}\right)}\right) + \alpha\left(1+\frac{zh_\nu''(z)}{h_\nu'(z)}\right) \\ &= 1+(\alpha-1)\sum_{n\geq 1}\frac{z}{\lambda_{\nu,n}^2 - z} - \alpha\sum_{n\geq 1}\frac{z}{\gamma_{\nu,n}^2 - z}. \end{aligned}$$

Similarly, we can prove part c as in the proof of Theorems 1-a and 1-b. Thus, we omitted details.

Remark 1. Taking $\alpha = 0$ and $\alpha = 1$ in Theorem 1, we obtain the results in [9].

REFERENCES

1. Á. Baricz, Geometric properties of generalized Bessel functions of complex order, Mathematica, 48(71), (2006), 13–18.
2. Á. Baricz and R. Szász, The radius of convexity of normalized Bessel functions of the first kind, Anal. Appl. 12(5), (2014), 485–509.
3. Á. Baricz, H. Orhan and R. Szász, The radius of $\alpha-$convexity of normalized Bessel functions of the first kind, Comput. Methods Funct. Theory 16, (2016), 93–103.
4. A. Baricz, M. Çağlar, E. Deniz, Starlikeness of Bessel functions and their derivatives, Math. Inequal. Appl., 19(2) (2016), 439–449.
5. M. Çağlar, E. Deniz, R. Szasz, Radii of α-convexity of some normalized Bessel functions of the first kind, Results Math., 72(4) (2017), 2023–2035.
6. E. Deniz, S. Kazımoğlu and M. Çağlar, Radii of Uniform Convexity of Lommel and Struve Functions, Bull. Iran. Math. Soc. https://doi.org/10.1007/s41980-020-00457-8 (2020).
7. P. L. Duren, Univalent functions, Grundlehren Math. Wiss. vol. 259. Springer, New York (1983).
8. M. E. H. Ismail and M. E. Muldoon, Bounds for the small real and purely imaginary zeros of Bessel and related functions, Meth. Appl. Anal. 2(1), (1995), 1-21.
9. S. Kazımoğlu and E. Deniz, Geometric Properties of function $az^2J_\nu''(z)+bzJ_\nu'(z)+cJ_\nu(z)$, arXiv:2006. 13732v1, (2020).
10. A. McD. Mercer, The zeros of $az^2J_\nu''(z)+bzJ_\nu'(z)+cJ_\nu(z)$ as functions of order, Internat. J. Math. Math. Sci, 15, (1992), 319-322.
11. P. T. Mocanu and M. O. Reade, The radius of $\alpha-$convexity for the class of starlike univalent functions, α real, Proc. Am. Math. Soc. 51(2), (1975), 395-400.
12. F. W. J. Olver, D.W. Lozier, R.F. Boisvert, C.W. Clark (Eds.), *NIST Handbook of Mathematical Functions*, Cambridge Univ. Press, Cambridge, (2010).

Comparison of Kernels Function on Twin Support Vector Machines for Lung Cancer Classification

Alva Andhika SA'ID[1], Fildzah ZHAFARINA[1], and Zuherman Rustam[1]

[1]*Department of Mathematics, Faculty of Mathematics and Natural Sciences, University of Indonesia*

alva@sci.ui.ac.id
fildzah.zhafarina@sci.ui.ac.id
rustam@ui.ac.id

Abstract. Machine learning technology is needed in the medical field. Therefore, this research is useful for solving problems in the medical field by using machine learning. Many cases of lung cancer are diagnosed late. Early detection of lung cancer is the most promising way to enhance a patient's chance of survival. Machine learning is an approach that is part of artificial intelligence and can detect lung cancer early. Twin support vector machines aim to find two hyperplanes such that each plane has a distance close to one data class and as far as possible from another data class. This study discusses lung cancer classification using the twin support vector machines method based on the kernel function. Twin support vector machines is fast in building a model and has good generalizations. However, twin support vector machines require kernel functions to operate in the feature space. The kernel functions commonly used are the linear kernel, polynomial kernel, and radial basis function (RBF) kernel. This paper uses the twin support vector machines method with these kernels and compares the best kernel for use by twin support vector machines to classify lung cancer dataset. Our work will be performed on the lung cancer CT Scan dataset obtained by the Cipto Mangunkusumo Hospital, Indonesia. It consists of benign cases 69 and malignant cases 69. However, the best kernel obtained is the RBF kernel, which produces an accuracy of 100%, a precision of 100%, a recall of 100%, f1-score of 100%, and a running time of around 0.41 s.

1. INTRODUCTION

I. Lung Cancer

Lung cancer is known to be one of the most dangerous illnesses [1]. The right lung has 3 parts, which are called lobes, while the left lung has 2 lobes. Lung cancer is the leading cause of cancer-related deaths worldwide with 30%-40% occurring in developing countries. The prediction of the early stages will save many lives when there is an early-stage cancerous tumor. In addition to patient evaluation, a cancer diagnosis is followed by blood testing, X-ray, biopsy, and CT scan. For a radiologist, distinguishing the lung nodule from the chest radiograph picture is the most difficult component. In CT scans and X-ray imaging, the lung nodules can be understood as tiny tissue masses that are visible as white shadows [2]. Machine learning is an artificial intelligence technology that gives systems the ability to learn and develop from experience automatically without being specifically programmed [3]. The twin support vector machines is one method that is common because the learning output is very good [4]. The kernel method is a method that uses functions while the algorithm operates in a higher-dimensional feature space. Product operations between images, all feature pairs, are used in this method. This approach is used by a support vector machine and a twin support vector machines directly or indirectly to classify knowledge [5]. The kernel functions normally used to help classify data with twin support vector machines are the linear kernel, polynomial kernel, and RBF kernel. This paper proposes the dual help twin support vector machines as a unique method for the early detection of lung cancer. The kernel capabilities used are the linear kernel, polynomial kernel, and RBF kernel. This paper compares the overall performance of the dual help twin vector machines with every kernel to get the quality kernel for the detection of lung cancer.

II. Methodology

This research uses twin support vector machines to classify lung cancer dataset. This method is evaluated using 5-fold cross-validation, 45-random state, and later compared.

a. *Twin support vector machines*

Support Vector Machine is the method used to find a single hyperplane to identify samples. Jayadeva and Chandra projected a unique twin hyperplane-based variant twin SVM. The principles of the generalized proximal support vector machine (GEPSVM) are applied here, requiring for every category 2 non-parallel optimum hyperplanes. As in an exceedingly commonplace SVM, there are two quadratic programming (QP) issues optimized as TSVM pairs. Mathematically, by addressing the following two quadratic programming issues, the TSVM primary issue can be optimized. Equations of the two hyperplanes are as follows [6]:

$$\begin{aligned} w_1^T x_s + b_1 &= 0 \\ w_2^T x_s + b_2 &= 0 \end{aligned} \tag{1}$$

i-th parameters of the hyperlines shown by w_i and b_i. Each hyperline is nearest to the sample of its class, of non-parallel type, and farthest from the sample of the opposite class.

Assume a binary classification task with classes +1 and −1, and A ∈ $\mathbb{R}^{n_1 xd}$ and B ∈ $\mathbb{R}^{n_2 xd}$ indicate that with each class +1 and -1, each matrix has a sample. For each matrix row, one sample is shown based on the appropriate class. The two twin support vector machines hyperplanes obtained from equations (2) and (3) are [7]:

$$\min \frac{1}{2}(\boldsymbol{Aw_1} + \boldsymbol{e}b_1)^T(\boldsymbol{Aw_1} + \boldsymbol{e}b_1) + p_1 e^T \xi \tag{2}$$
$$s.t\ -(\boldsymbol{Bw_1} + \boldsymbol{e}b_1) + \xi \geq e, \xi \geq 0$$

$$\min \frac{1}{2}(\boldsymbol{Bw_2} + \boldsymbol{e}b_2)^T(\boldsymbol{Bw_2} + \boldsymbol{e}b_2) + p_2 e^T \xi \tag{3}$$
$$s.t - (\boldsymbol{Aw_2} + \boldsymbol{e}b_2) + \xi \geq e, \xi \geq 0$$

ξ is a non-negative part of the vector, so ξ ≥ 0. A vector represented by e for the scale slack variable n. The traditional method is to let the margin of choice produce a few errors. A standard approach is taken if no linear separation of the sampling service is feasible. (Some points are at or at the wrong margin, for instance). Every zero-zero element of the slack variable vector calculates the cost of the wrong-classified sample, which is proportional to the distance between the sample and the decision margin. Based on these equations, the penalty parameters are ρ_1 and ρ_2. In different fields, Twin SVM is in great demand with different versions of the proposed algorithm [8].

b. *Kernel function*

Kernel method is a way that uses kernel functions to work algorithms in feature areas that have higher dimensions. This method uses product operations between pictures of all image pairs within the feature area [9]. Accuracy for classifying objects in the right cluster is difficult to obtain in high dimensional data sets, measuring euclidean distances on k-means, c-means, or fuzzy c-medoids. Distribution data can be represented to validate the truly central cluster. This difficulty can be overcome by using the kernel method [10]. Let X^n be an input space; F is a feature space and ϕ : Xn →F

Linear Kernel

Deriving the feature vector inexplicit by a kernel is normally quite difficult, and solely doable if the kernel is Mercer. However, account a kernel from a feature vector is easy: we just use [11]:

$$K(x, x') = \varphi(x)^T \varphi(x') = \langle \varphi(x), \varphi(x') \rangle \tag{4}$$

If $\varphi(x) = x$, we get the linear kernel, defined by [11]:

$$K(x, x') = x^T x' \tag{5}$$

This is helpful if the first knowledge is already high dimensional, and if the original options are severally informative, e.g., a bag of words illustration wherever the vocabulary size is large, or the expression level of the many genes. In such a case, the choice boundary is probably going to be expressible as a linear combination of the original features, therefore it's not necessary to figure in another feature space. Of course, not all high dimensional issues are linearly separable. For example, pictures are high dimensional, however individual pixels aren't terribly informative, so image classification usually needs non-linear kernels.

Polynomial Kernel
The Polynomial kernel is defined as [12]:

$$K(x, x') = (x'^T x + C)^n \tag{6}$$

where n is that the "order" of the kernel and c may be a constant that enables to trade off the influence of the upper order and lower order terms. Second-order or quadratic kernels are a well-liked type of Polynomial kernel, widely utilized in Speech Recognition. Higher-order kernels tend to "overfit" the coaching knowledge and so don't generalize well.

RBF Kernel
The squared exponential kernel (SE kernel) or Gaussian kernel is defined by [13]:

$$K(x, x') = \exp(-\tfrac{1}{2}(x - x')^T \Sigma^{-1}(x - x') - \tfrac{1}{2}\textstyle\sum_{j=1}^{D} \frac{1}{\sigma_j{}^2}\left(x_j - x_j'\right)^2 \tag{7}$$

If Σ is diagonal, this can be written as [14]:

$$K(x, x') = \exp\left(-\frac{1}{2}\sum_{j=1}^{D} \frac{1}{\sigma_j{}^2}\left(x_j - x_j'\right)^2\right) \tag{8}$$

We can interpret the σ_j as defining the characteristic length scale of dimension j. If $\sigma_j = \infty$, the corresponding dimension is ignored; hence this is known as the ARD kernel. If Σ is spherical, we get the isotropic kernel [15]:

$$K(x, x') = \exp\left(-\frac{\|x - x'\|^2}{2\sigma^2}\right) \tag{9}$$

Here σ^2 is known as the bandwidth. Equation 14.3 is an example of a radial basis function or RBF kernel since it is only a function of $\|x - x'\|$.

c. *Confusion Matrix*

A misunderstanding matrix was used in this paper to assist in measuring the classification model's assessment parameters. The uncertainty matrix is used to test the Twin support vector machines classification model based on the kernel for lung cancer diagnosis. **Table 1** shown confusion matrix [16]:

Table 1. Confusion Matrix

		Predict	
		Cancer (Y)	**Non-Cancer (N)**
Actual	**Cancer (Y)**	TP	FN
	Non-Cancer (N)	FP	TN

TP (True Positive) : Many cases of lung cancer are predicted to be correct
TN (True Negative) : Many cases of non-lung cancer are predicted to be correct
FP (False Positive) : Many cases of non-lung cancer are predicted to be wrong (predicted as lung cancer)
FN (False Negative) : Many lung cancer cases are predicted to be wrong (predicted as not lung cancer)

Evaluation Parameters

Accuracy, precision, recall, f1-score, and required running time were the parameters for assessing the performance of the Twin support vector machines classification model. The formula for accuracy, precision, recall, f1-score shown in equation 10, 11, 12, 13 [17-19]:

$$Accuracy = \frac{(TN + TP)}{(FN + TP + FP + TN)} x\ 100\% \quad (10)$$

$$Precision = \frac{TP}{TP + FP} x\ 100\% \quad (11)$$

$$Recall = \frac{TP}{TP + FN}\ x\ 100\% \quad (12)$$

$$F1Score = 2\ x\ \frac{(\ Precision\ x\ Recall\ )}{(\ Precision + Recall\ )} x\ 100\% \quad (13)$$

2. MAIN RESULTS

V. Data

In this study, the data consisted of 138 samples and seven features. These seven features consist of area, min, max, average, SD, sum, and length. Diagnosis features become a target feature in detecting lung cancer. The data are lung cancer data obtained from Cipto Mangunkusumo Hospital, Jakarta, Indonesia with 69 samples of cancer diagnoses (1), and 69 samples of non-cancer (0). **Table 2** and **Table 3** represented part of the data :

Table 2. Lung cancer dataset variable

Attributes	Description
Area	The size of the lung cancer area
Min	The minimum score for lung cancer is a number of the lowest intensity present within the circled area
Max	The maximum value of lung cancer ie the highest intensity figure in the area which is circled
Average	The average score for lung cancer is a number of the average intensity that exists within that area circled
SD	Standard error value in lung cancer
Sum	Number of dots in lung cancer
Lenght	Length of lung cancer

Tabel 3. Sample of lung cancer data

Area	Min	Max	Average	SD	Sum	Length	Target
106.53	-926	-773	-863	29.5	-156324	36.6	0
76.07	-924	-755	-850	29.02	-121557	31.01	0
109.76	-42	88	28.45	24.68	5576	37.17	1
135.93	-917	-683	-875	41.11	-284527	41.34	0
97.55	-12	65	32.59	14.05	7562	35.01	1
103.04	-14	66	36.39	15.22	9025	35.98	1
106.07	-869	604	-762	40.48	-162501	36.51	0
129.01	-858	-418	-746	75.5	-194800	40.27	0
85.15	-7	129	54.85	26.35	8667	32.79	1
176.69	-879	-644	-814	49.22	-177463	47.16	0

Results

The performance evaluation of the Twin Support Vector Machines classification model with linear kernel, polynomial kernel, and RBF kernel is discussed in this section. The kernel-based Twin Support Vector Machines classification model detects lung cancer using the linear kernel, polynomial kernel, and RBF kernel. The highest accuracy, precision, recall, and f1-score in this analysis is from the RBF kernel when using $\sigma = 1$. This means that, when using twin support vector machines, the RBF kernel is a sufficient kernel for lung detection. In this paper, we developed the model of twin support vector machines classification for lung cancer detection with linear kernels, polynomial kernels, and radial basis function kernels. Table 4 provides a comparison of the linear kernel, polynomial kernel, and RBF kernel results of twin support vector machines. Accuracy, precision, recall, f1-score, and running time are the performance assessment metrics compared. **Table 4** demonstrates the outcome of the kernel-based twin support vector machines classification model.

TABLE 4. The Result of Lung Cancer Classification using Twin support vector machines

No.	Kernel Function	Accuracy(%)	Precision(%)	Recall (%)	F1-Score(%)	Running time
1.	Linear Kernel	97,8%	97%	98%	98%	0.16 s
2.	Polynomial Kernel	97,8%	97%	98%	98%	0.144 s
3.	**RBF Kernel**	**100%**	**100%**	**100%**	**100%**	**0.41 s**

Based on Tabel 4, that can be seen that twin support vector machine models the highest accuracy, precision, recall, and f1-score of 100% was recorded when using the RBF kernel at 0.41 seconds. While the lowest accuracy at 97,8% was recorded when linear and polynomial kernel with a running time of 0.16 seconds for linear kernel and 0.144 seconds for the polynomial kernel. The lowest precision at 97% was recorded when linear and polynomial kernel. The lowest recall at 98% was recorded when linear and polynomial kernel. The lowest f1-score at 98% was recorded when linear and polynomial kernel (using $n = 4$). For consideration of running time, the twin support vector machines model with polynomial kernel has the fastest running time compared to linear and RBF kernel which is around 0.16 seconds. The twin support vector machines model with the RBF kernel actually produces the longest-running time which is around 0.41 seconds. Based on the results obtained, the RBF kernel gets the best results in terms of accuracy, precision, recall, and f1-score. Thus, the RBF kernel is the best kernel for the twin support vector machines in detecting lung cancer dataset.

CONCLUSION

Lung cancer detection quickly is very important. it is useful for handling cancer quickly before being infected to all organs of the body. However, this is difficult because lung cancer has no specific symptoms. The Twin SVM method can help detect lung cancer based on CT scan data. The most appropriate kernel for the twin support vector machines method in detecting lung cancer is the RBF kernel which produces an accuracy, precision, recall, and f1-score of 100% and the required running time is 0.41 seconds.

ACKNOWLEDGMENT

This research is supported financially by The Indonesian Ministry of Research and Technology, with a KEMENRISTEK/BRIM 2021 research grant scheme.

REFERENCES

1. Chen, Z., Fillmore, C. M., Hammerman, P. S., Kim, C. F., & Wong, K. K. (2014). Non-small-cell lung cancers: a heterogeneous set of diseases. *Nature Reviews Cancer*, *14*(8), 535-546.
2. Nanglia, P., Kumar, S., Mahajan, A. N., Singh, P., & Rathee, D. (2020). A hybrid algorithm for lung cancer classification using SVM and Neural Networks. *ICT Express*.
3. Rustam, Z., & Ariantari, N. P. A. A. (2018, June). Support Vector Machines for Classifying Policyholders Satisfactorily in Automobile Insurance. In Journal of Physics: Conference Series (Vol. 1028, No. 1, p. 012005). IOP Publishing Ltd.

4. Huang, H., Wei, X., & Zhou, Y. (2018). Twin support vector machines: A survey. Neurocomputing, 300, 34-43.
5. Shawe-Taylor, J., & Cristianini, N. (2004). Kernel methods for pattern analysis. Cambridge university press.
6. Khemchandani, R., & Chandra, S. (2007). Twin support vector machines for pattern classification. *IEEE Transactions on pattern analysis and machine intelligence*, *29*(5), 905-910.
7. Kumar, M. A., & Gopal, M. (2009). Least squares twin support vector machines for pattern classification. *Expert systems with applications*, *36*(4), 7535-7543.
8. Ding, S., An, Y., Zhang, X., Wu, F., & Xue, Y. (2017). Wavelet twin support vector machines based on glowworm swarm optimization. Neurocomputing, 225, 157-163.
9. Sadewo, W., Rustam, Z., Hamidah, H., & Chusmarsyah, A. R. (2020). Pancreatic Cancer Early Detection Using Twin support vector machines Based on Kernel. Symmetry, 12(4), 667.
10. Rustam, Z., & Talita, A. S. (2017, July). Fuzzy kernel K-medoids algorithm for anomaly detection problems. In AIP Conference Proceedings (Vol. 1862, No. 1, p. 030154). AIP Publishing LLC.
11. Deisenroth, M. P., Faisal, A. A., & Ong, C. S. (2020). *Mathematics for machine learning*. Cambridge University Press
12. Pham, N., & Pagh, R. (2013, August). Fast and scalable polynomial kernels via explicit feature maps. In *Proceedings of the 19th ACM SIGKDD international conference on Knowledge discovery and data mining* (pp. 239-247).
13. Kuo, B. C., Ho, H. H., Li, C. H., Hung, C. C., & Taur, J. S. (2013). A kernel-based feature selection method for SVM with RBF kernel for hyperspectral image classification. *IEEE Journal of Selected Topics in Applied Earth Observations and Remote Sensing*, *7*(1), 317-326.
14. Han, S., Qubo, C., & Meng, H. (2012, June). Parameter selection in SVM with RBF kernel function. In *World Automation Congress 2012* (pp. 1-4). IEEE.
15. Smits, G. F., & Jordaan, E. M. (2002, May). Improved SVM regression using mixtures of kernels. In *Proceedings of the 2002 International Joint Conference on Neural Networks. IJCNN'02 (Cat. No. 02CH37290)* (Vol. 3, pp. 2785-2790). IEEE.
16. Townsend, J. T. (1971). Theoretical analysis of an alphabetic confusion matrix. *Perception & Psychophysics*, *9*(1), 40-50.
17. Story, M., & Congalton, R. G. (1986). Accuracy assessment: a user's perspective. *Photogrammetric Engineering and remote sensing*, *52*(3), 397-399.
18. Davis, J., & Goadrich, M. (2006, June). The relationship between Precision-Recall and ROC curves. In *Proceedings of the 23rd international conference on Machine learning* (pp. 233-240).
19. Chicco, D., & Jurman, G. (2020). The advantages of the Matthews correlation coefficient (MCC) over F1 score and accuracy in binary classification evaluation. *BMC genomics*, *21*(1), 6.

Convolutional Neural Networks and Support Vector Machines Applied to CT Scan in Ischemic Stroke Detection

Glori Stephani SARAGIH[1] and Zuherman RUSTAM[1]

[1]*Department of Mathematics, Faculty of Mathematics and Science, Universitas Indonesia, Depok-INDONESIA*

glori.stephani@sci.ui.ac.id

Abstract. Stroke is a disease that causes long-term disability and death, so it is important to be able to detect a stroke as early as possible. Stroke is divided into 2 types, namely ischemic stroke and hemorrhagic stroke, but 87% of stroke sufferers are ischemic strokes. CT scan is effective for accurate diagnosis of ischemic stroke. Technological developments in the health sector have played an important role in helping the management of ischemic stroke sufferers. In recent years, deep learning and machine learning have provided new directions for CT scan detection for ischemic stroke sufferers, due to their ability to provide highly accurate predictive results. So, the problem of long-term diagnosis that adds to doctor's fatigue and can lead to the wrong situation is no longer a worrying factor. In this paper, we build an ensemble method that helps improve the accuracy of ischemic stroke detection, we combine deep learning and machine learning. Convolutional Neural Network (CNN) is one of the methods commonly used for image classification, but in this study, we only used CNN to extract the CT scan image data into numeric, then the results of the convolution were classified with Support Vector Machines (SVM) classifier. A total of 92 CT scans were considered for this model, data obtained from the Radiology Department of the National General Hospital (RSCM) Cipto Mangunkusumo, Indonesia. The proposed method efficiently detects ischemic stroke with 100% accuracy, 100% precision, 100% specificity, 100% f-score and 8.19759 seconds running time by using CNN as feature extraction and SVM as a classifier, wherein the proposed method can be used to assist a doctor or radiologist in the decision-making process in the treatment of ischemic stroke.

Keywords: convolutional neural network; image classification; stroke ischemic; support vector machines

1. INTRODUCTION

Stroke is the main neurological disease in adulthood, based on the high incidence, emergencies, the main cause of disability, and death is from the stroke. According to the Global Burden of Disease Study, stroke is one of the diseases with the most deaths in the world. A stroke can be defined as an injury to the brain caused by a blockage of blood vessels and making inadequate blood supply that causes bleeding in the brain parenchyma [1]. This disease requires lifelong health services because stroke itself is a cardio-cerebrovascular disease that is classified as a catastrophic disease and requires therapy with special expertise using sophisticated medical devices [2]. Early detection of stroke needs to be given extra attention, so we able to reduce the number of cases from year to year. When a person experiences a symptom of paralysis in one part of his body, it is necessary to do a further examination so we could determine whether the cause of the symptoms is from stroke, infection, tumor, or something else.

The first step examination that medical use nowadays is Computerized Tomography Scan (CT scan). It is necessary before a patient gets treatment. But there is an alternative to CT scanning which is Magnetic Resonance Imaging (MRI), but MRI costs are more expensive, and the examination time is longer than CT scan therefore doctors will recommend the patient to CT scan [3]. CT scan is also useful to distinguish the type of stroke suffered by the patient. The stroke itself can be divided into two types, hemorrhagic and ischemic stroke. Hemorrhagic stroke is when there is a rupture of the intracerebral blood vessels in the brain, while if there is a blockage of blood vessels in the brain by thrombus or embolism will cause an ischemic stroke [1]. The majority of stroke is stroke ischemic, that is 87% and the rest are patients who experience intracerebral and subarachnoid hemorrhages which are pathologically hemorrhagic strokes [4]. In this paper, we will be focusing on ischemic stroke since this is the most common type of stroke in society. Ischemic stroke can be seen by the symptoms felt by the patient which are paralysis, trouble of speaking or understanding speech, dizziness, trouble walking, loss of balance or coordination and unexplained fails, loss of consciousness, sudden and severe headache. Early detection can help ischemic stroke new sufferers avoiding death and permanent injuries because there is a golden period in stroke management that is as long as 4.5 hours [5].

Ischemic stroke generally causes changes in density in the brain and we can see the changes on CT scan with result darker namely the hypodense area. Hypodense is intended for softer tissue, such as air or liquid. Be that as it may, the area of ischemic stroke on the CT examination isn't clear, so, the conclusion relies upon the doctors in evaluating the results. High mortality and disability bring issues to light on the significance of the early detection of ischemic stroke; therefore, research has been completed, particularly in the field of innovation.

In recent years, machine learning and deep learning had taken part in developing the CT scan accuracy for ischemic stroke sufferers because of their ability to provide predictive results. Machine learning is the design of algorithms that computers use to perform certain tasks without explicit command by using patterns and intervention instead [6]. On the other hand, deep learning is a branch of machine learning which consists of a high-level abstraction modeling algorithm in data using a set of non-linear transformation functions arranged in layers and depth [7]. One of the most widely used deep learning methods for image recognition and classification is Convolutional Neural Networks (CNN). Gautam and Raman [8] classify brain CT scan images into hemorrhagic, ischemic stroke and normal by using CNN, they used 2 datasets to check the robustness of their method, the accuracy of dataset 1 for the first experiment is 98.33% and the second experiment 98.77, while the dataset 2 for the first experiment is 92.22% and the second experiment 93.33%. The elapsed time to train the classification model is different based on the architecture used, the faster one is Alexnet with 1 min 38 second and the slowest is ResNet50 with 21 min 49 second for experiments with dataset 1. For dataset 2, the elapsed time required longer than the dataset 1, elapsed time of AlexNet and ResnNet50 are 2 min 15 second and 25 min 52 second, respectively [8]. The highest accuracy makes CNN the most widely used, but the computation time required is quite long and can even reach 25 minutes, making the authors change the approach in classification strokes.

There is another approach to classifying image data by combining two methods, namely the feature extraction method for converting images to numeric and machine learning for classification. Rajini and Bhavani [9] used Gray Level Co-Occurrence Matrix (GLCM) as a feature extraction and several machine learning methods as a classifier, these are K-means with 96% accuracy, KNN with 97% accuracy, and Support Vector Machines (SVM) with 98% accuracy. Kanchana and Menaka [10] used gray level run length matrix features, GLCM, and Hu's moment features are extracted. Then, the classification used logistic regression, SVM, random forest and neural network with classification accuracy 88.77%, 97.86%. 99.79%. and 99.79%, respectively. Sabut, et. al [11] used GLCM as a feature extraction and SVM as a classifier, the lesion area was classified effectively with accuracy 90.23%.

Based on two approaches before, deep learning and combining between extraction feature model and machine learning for classification, make the author create a new approach by combining deep learning and machine learning, which means that the extraction features that are already widely used such as GLCM will be replaced with deep learning method, that is CNN. It could also mean that the classification part on CNN, which is Neural Network will be replaced by other machine learning methods. Several studies [9][10][11] have used several classification methods and SVM is a method that is often used and also provides high accuracy, which is above 90%. SVM has been very widely used for several studies on different datasets and also sectors, such as the intrusion detection system classification [12][13][14], insolvency prediction in insurance company [15], policyholders' satisfactorily classification in automobile insurance [16], schizophrenia classification [17], and acute sinusitis classification [18]. Therefore, the machine learning method that will be used as a classifier is SVM. Thus, the proposed method in this research is to combine feature extraction, namely CNN and classification using SVM.

Convolutional Neural Networks

CNN is a widely used deep learning method. The CNN method has two stages, first feature extraction with convolutional layer and pooling layer, second is a trainable classifier or fully connected neural network [19]. Some of the important layers that have been used in the CNN architecture given below:

1. **Input**: the input layer where we insert the CT scan images data.
2. **Convolution**: the convolutional layer extracts features from the image layer where each image element is enclosed in a filter that has the same depth as the image [20]. In this research, five convolutional layers are used with the same size 3 x 3. The number of filters used in the first, second, third, fourth, and five are 32, 64,

32, 64, and 32, respectively. For considering the output size of flatten layer, the number of filters is chosen wisely.

3. **ReLU:** after the convolutional layer, this layer is placed, its point is to threshold all input values [21]. ReLU is an activation function that used for familiarizing non-linearities and made faster computation compared to tanh and sigmoid [22].
4. **Max Pooling:** the pooling layer is used to reduce the size of the feature maps, the widely used pooling layer is max pooling, where the use 2x2.
5. **Batch Normalization:** the normalization layer is used thereafter because aim of preventing model divergence [23], to normalize activation the previous layer in each batch is used this normalization layer.
6. **Dropout:** the dropout is used to generalize better the network and the influence of individual neurons on the resulting output reduced [24]. In this research, we used rate = 0.2.

The figure below is a detail of the CNN architecture used [25][26]:

(1) INPUT: 152 x 152 x 1
(2) Conv2D: 3x3 size, 32 filters, 1 stride
(3) ReLU: max(0, $h_\theta(x)$)
(4) MaxPooling: 2x2 size, 1 stride
(5) BatchNormalization
(6) Conv2D: 3x3 size, 64 filters, 1 stride
(7) ReLU: max(0, $h_\theta(x)$)
(8) MaxPooling: 2x2 size, 1 stride
(9) BatchNormalization
(10) Conv2D: 3x3 size, 96 filters, 1 stride
(11) ReLU: max(0, $h_\theta(x)$)
(12) MaxPooling: 2x2 size, 1 stride
(13) BatchNormalization
(14) Conv2D: 3x3 size, 64 filters, 1 stride
(15) ReLU: max(0, $h_\theta(x)$)
(16) MaxPooling: 2x2 size, 1 stride
(17) BatchNormalization
(18) Conv2D: 3x3 size, 32 filters, 1 stride
(19) ReLU: max(0, $h_\theta(x)$)
(20) MaxPooling: 2x2 size, 1 stride
(21) Dropout: rate=0.2
(22) Flatten output: 1 x 6273

Fig. 1. CNN architecture

Support Vector Machines

After the data is extracted by CNN, the process will be classified with SVM. SVM is supervise learning model, meaning that the dataset must be labeled [27], making it suitable for the task of distinguishing between density is changeable and unchanging density for CT scan images of the brain of ischemic stroke patients. The training data will be labeling into "1" for change in density and "0" for no change in density. The training data used to build a model are assumed to be separated by line. If we have data sample $A = \{(x_i, y_i)\}_{i=1,2,\dots,n}$, $x_i \in \Re^N$, $y_i \in \{0,1\}$, where N is the amount of data, w is a hyperplane, and b is a constant which showed the range of hyperplane to the center point, with the following equation [28]:

$$\boldsymbol{wx} + b = 0 \quad (1)$$

Find the minimum point in equation (1) then bring it into equation (2) to create the formula, namely is called the Quadratic Programming (QP) problem [29].

$$\min\left(\frac{1}{2}\|\boldsymbol{w}\|^2\right) \quad (2)$$

$$y_i(\boldsymbol{w} \cdot \boldsymbol{x}_i + b) \geq 1, \forall i = 1, \dots, N \quad (3)$$

Lagrange Multiplier is one of the various computational techniques that can solve this problem, for the search for maximum margin is equal to minimize $\|\boldsymbol{w}\|^2$ which is stated in equation (4) [29]:

$$minL(\boldsymbol{w}, b, \alpha) = \frac{1}{2}\|\boldsymbol{w}\|^2 - \sum_{i=1}^{n} \alpha_i [y_i(\boldsymbol{w}^{\mathrm{T}}\boldsymbol{x_i} + \boldsymbol{b}) - 1] \quad (4)$$

with the constraints in the following equation (5), (6), (7), (8).

$$\alpha_i \geq 0 \quad (5)$$

$$1 - y_i(\boldsymbol{w}^{\mathrm{T}}\boldsymbol{x_i} + b) \geq 0 \quad (6)$$

$$\alpha_i [1 - y_i(\boldsymbol{w}^{\mathrm{T}}\boldsymbol{x_i} + b)] = 0 \quad (7)$$

$$\forall i = 1,2, \dots, n \quad (8)$$

The final function is stated in following equation (9):

$$\boldsymbol{f}(\boldsymbol{x}) = \boldsymbol{w}.\boldsymbol{x} + b \quad (9)$$

Proposed Method

The flowchart of the proposed method CNN-SVM is given in Fig. 4. The proposed method has 5-step working structure, with the detail below:

Step 1 **Obtaining the CT scan images**

There are 92 brain CT Scan images consisting of 48 images with no change in density and 44 images with change in density in ischemic stroke patients that obtained from the Department of Radiology, Cipto Mangunkusumo National General Hospital (RSCM), Indonesia. CT scan data of the brain were observed as high as the third ventricle.

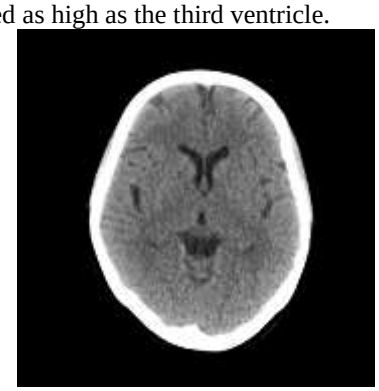

Fig. 2. No change in density

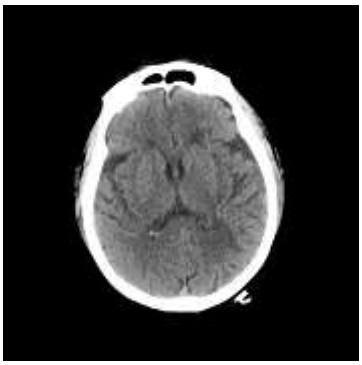

Fig. 3. Change in density

Step 2 **Cropping image**

The CT scan images are cropped, the dimensions of images used in this research is 512x512 pixels with type of file is jpg.

Step 3 **Conversion to grayscale**

In order to make the process faster, the CT scan images are converted to grayscale.

Step 4 **Extract features by using CNN**

In order to extract the feature of 92 brain CT scan images, the related images are given to CNN architecture.

Step 5 **SVM classifier**

The CT scan image is extracted using CNN architecture, then the output in the form of matrix data is forwarded to the SVM classifier.

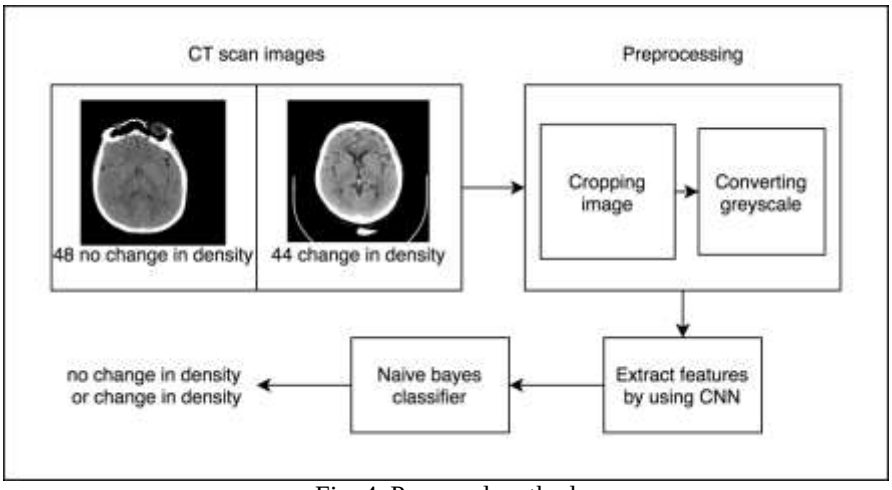

Fig. 4. Proposed method

2. MAIN RESULTS

After pre-processing, the CT scan images were converted into numeric data using CNN, the elapsed time of CNN process is 7.631490 sec. The result of feature extraction is in the form of matrix data to which we add a label for each of row, the matrix is shows in the table below:

TABLE VI
MATRIX INPUT

Data	y_1	y_2	…	y_{6272}	y_{6273}	y
x_1	2.34E-04	4.05E-01	…	2.38E-06	0.00E+00	1
x_2	5.35E-06	7.42E-07	…	4.77E-07	0.00E+00	1
…	…	…	…	…	…	
x_{91}	1.00E-06	8.71E-07	…	3.34E-06	2.86E-06	0
x_{92}	0.00E+00	7.94E-07	…	2.14E-06	1.91E-06	0

The matrix data is an input that used for classification. In this research, we used SVM as a classifier. The performance of purposed method is determined with confusion matrix, the Table II shows us the confusion matrix that used.

TABLE VIII
CONFUSION MATRIX

		Predicted Class	
		Change in Density	No Change in Density
Actual Class	Change in Density	TP	FN
	No Change in Density	FP	TN

The confusion matrix shows the number of incorrect and correct prediction that made by the model compared to the actual data. Based on the value of TP, FP, FN, and TN from the confusion matrix, these four categories help us assess the performance of the SVM classifier:

$$\text{Accuracy} = \frac{TP + TN}{TP + TN + FP + FN} \tag{10}$$

$$\text{Precision} = \frac{TP}{TP + FP} \tag{11}$$

$$\text{Specificity} = \frac{TN}{FP + TN} \tag{12}$$

$$F - \text{score} = \frac{TP}{TP + \frac{1}{2}(FP + FN)} \tag{13}$$

The Table III show us the performance of stroke ischemic classification by using Support Vector Machines, which the kernel function used for the Support Vector Machine in this research is linear kernel.

TABLE VIIIII
THE PERFORMANCE OF STROKE ISCHEMIC CLASSIFICATION USING SUPPORT VECTOR MACHINES AS A CLASSIFIER AND CONVOLUTIONAL NEURAL NETWORK AS A FEATURE EXTRACTION

%Training	Accuracy (%)	Precision (%)	Specificity (%)	F-score (%)	Running Time (sec)
10	47.61%	43.00%	48.00%	37.00%	0.5506
20	62.66%	64.00%	62.00%	62.00%	0.5055
30	75.75%	76.00%	76.00%	76.00%	0.5416
40	75.00%	75.00%	75.00%	75.00%	0.6738
50	74.47%	75.00%	75.00%	74.00%	0.6226
60	94.73%	95.00%	95.00%	95.00%	0.6027
70	100.00%	100.00%	100.00%	100.00%	0.5196
80	94.73%	95.00%	95.00%	95.00%	0.5323
90	100.00%	100.00%	100.00%	100.00%	0.5457
AVG	80.55%	80.33%	80.67%	79.33%	0.5661

Table III shows us the proposed method is resulting the best performance, when the composition of training data in 70% and 90%. The performance of classifier for 70% percentage of training dataset are 100% accuracy, 100% precision, 100% specificity, 100% f-score and 0.5196 sec running time. The performance of classifier for 90% percentage of training dataset are 100% accuracy, 100% precision, 100% specificity, 100% f-score and 0.5457 sec running time. The difference is only during running time, but it only differs very slightly, this is because the amount of data processed in training data is 90%, certainly more than 70%. The average value of performance of classifier method for all percentage of data training are 80.55% accuracy, 80.33% precision, 80.67% specificity, 79.33% f-score and 0.5661 sec running time. If we use the highest accuracy as the best performance, it means the proposed method we use can 100% correctly classify CT scan stroke ischemic images with a running time of only 8.19759 seconds. A very short time compared to the CNN-only method and the highest accuracy that CNN-only and combining extraction feature and machine learning approach.

CONCLUSION

In this research, which applied Convolutional Neural Network as the feature extraction and Support Vector Machines as the classification method by using brain CT scan images data of ischemic stroke patients that obtained from Department of Radiology, Cipto Mangunkusumo National General Hospital (RSCM), Indonesia. The proposed method gives the values of accuracy for each amount of data training. From the experimental results, it can be concluded that the performance of Support Vector Machines with CNN reaches a highest rate at 100% accuracy, 100% precision, 100% specificity, 100% f-score and 8.19759 sec running time when the amount of data training is

equal to 70%, wherein the proposed method can be used to assist a doctor or radiologist in the decision-making process in the treatment of ischemic stroke.

ACKNOWLEDGEMENT

This work was supported financially by Indonesia Ministry of Research and Technology/ National Research and Innovation Agency (RISTEK-BRIN) 2021 research grant scheme.

REFERENCES

1. J. Stein. *Essentials of Physical Medicine and Rehabilitation Chapter 159 Stroke*, Philadelphia: Elsevier, 2020.
2. Heniwati, and Thabrany, H. (2006). Perbandingan Klaim Penyakit Katastropik Peserta Jaminan Kesehatan Nasional di Provinsi DKI Jakarta dan Nusa Tenggara Timur tahun 2014. *Jurnal Ekonomi Kesehatan Indonesia*, vol. 1, no. 2.
3. C. Chin, et. al. (2017). An Automated Early Ischemic Stroke Detection System Using CNN Deep Learning Algorithm. *IEEE 8th International Conference on Awareness Science and Technology (iCAST)*, pp. 368-372.
4. American Stroke Association (2020). Let's talk about Ischemic Stroke. Dallas: American Heart Association.
5. Ministry of Health of the Republic of Indonesia. (2017). [Online]. Available: http://p2ptm.kemkes.go.id/artikel-sehat/germas-cegah-stroke
6. J. G. Lee, et. al. (2017). Deep Learning in Medical Imaging: General Review. *Korean Journal of Radiology*, vol. 18, no. 4, pp. 570-584.
7. I. Goodfellow, et. al. *Deep Learning*, England: The MIT Press Cambridge, 2016.
8. Gautam, A. and Raman, B. (2021). Towards effective classification of brain hemorrhagic and ischemic stroke using CNN. *Biomedical Signal Processing and Control*, vol 63, pp. 102178.
9. Rajini, N. H and Bhavani, R. (2013). Computer aided detection of ischemic stroke using segmentation and texture features. *Measurement*, vol. 46, no. 6, pp. 1865-1874.
10. Kanchana, R., Menaka, R. (2020). Ischemic stroke lesion detection, characterization and classification in CT images with optimal features selection. *Biomed. Eng. Lett*, vol. 10, pp. 333–344. https://doi.org/10.1007/s13534-020-00158-5
11. Sabut, S., et. al. (2018). Segmentation and Classification of Ischemic Stroke using Optimized Features in Brain MRI. *Biomedical Engineering: Application, Basis and Communication*, vol. 30, no 3, pp. 1850011.
12. Rustam, Z. and Zahras, D. (2017). Comparison between Support Vector Machine and Fuzzy C-Means as Classifier for Intrusion Detection System. *Journal of Physics: Conference Series*, vol 1028.
13. Rustam, Z. and Ariantari, N. P. A. A. (2018). Comparison between support vector machine and fuzzy kernel c-means as classifiers for intrusion detection system using chi-square feature selection. *American Insitute of Physics Inc*, vol 2023.
14. R. Vijayanand, D. Devaraj and B. Kannapiran. (2017). Support vector machine based intrusion detection system with reduced input features for advanced metering infrastructure of smart grid. *2017 4th International Conference on Advanced Computing and Communication Systems (ICACCS)*, Coimbatore, pp. 1-7. doi: 10.1109/ICACCS.2017.8014590
15. Rustam, Z. and Yaurita, F. (2018). Insolvency prediction in insurance companies using support vector machines and fuzzy kernel c-means. *Journal of Physics: Conferences Series*, vol 1028(1), pp. 012118.
16. Rustam, Z. and Ariantari, N. P. A. A. (2018). Support Vector Machines for Classifying Policyholders Satisfactorily in Automobile Insurance. *Journal of Physics: Conference Series*, vol 1028(1), pp. 012005.
17. Rampisela, T. V. and Rustam, Z. (2018). Classification of schizophrenia data using support vector machine (SVM). *Journal of Physics: Conference Series*, vol 1108(1), pp. 012044.
18. Arfiani, et. al. (2019). Kernel Spherical K-Means and Support Vector Machine for Acute Sinusitis Classification. *IOP Conference Series: Materials Science and Engineering*, vol 546.
19. Cao, G., et. al. (2013). A hybrid Cnn-Rf method for electron microscopy images segmentation. *Journal Biometrics Biomaterials and Tissue Engineering*, vol. 18, no. 114.
20. Krizhevsky, A., Sutskever, I., and Hinton, G. E. (2012). ImageNet classification with deep convolutional neural networks. *In: Proc Adv Neural Inf Process Syst*, pp. 1097-1105.

21. Nair, V. and Hinton, G.E. (2010). Rectified linear units improve restricted Boltzmann machines. *In: Proc 27th Int Conf Machine Learning (ICML),* pp. 807-814.
22. Nwankpa, C., Ijomah, W., Gachagan, A., and Marshall, S. (2018). Activation Functions: Comparison of trends in Practice and Research for Deep Learning. arXiv e-prints, p. arXiv:1811.03378. [Online]. Available: https://ui.adsabs.harvard.edu/abs/2018arXiv181103378N
23. Schilling, F. (2016). The effect of batch normalization on deep convolutional neural networks. Degree Project in Computer Science and Engineering, School of Computer Science and Communication, KTH Royal Institute of Technology, Stockholm, Sweden.
24. Srivastava, N., Hinton, G., Krizhevsky, A., Sutskever, I. and Salakhutdinov, R. (2014). Dropout: a simple way to prevent neural networks from overfitting. *J. Mach. Learn. Res.,* vol. 15, no. 1, pp. 1929–1958.
25. Rustam, Z., et. al. (2020). Analysis of Architecture Combining Convolutional Neural Network (CNN) and Kernel K-Means Clustering for Lung Cancer Diagnosis. *International Journal on Advanced Science Engineering Information Technology,* vol 10, no 3.
26. Saragih, G. S., et. al. (2020). Ischemic Stroke Classification using Random Forests Based on Feature Extraction of Convolutional Neural Networks. *International Journal on Advanced Science Engineering Information Technology,* vol 10, no 5.
27. Saragih, G. S., and Rustam, Z. (2018). Support Vector Machine with Fisher Score Feature Selection to Predict Disease-Resistant Gene in Rice. *Journal of Physics: Conference Series,* 1108.
28. Saragih, G.S. (2017). Prediction of Disease-Resistant Gene in Rice Based on Support Vector Machine and Fuzzy Kernel C-Means. *Advances in Social Science, Education and Humanities Research,* vol 218.
29. Rustam, Z., Utami, D. A., Hidayat, R., Pandelaki, J., and Nugroho, W. A. (2019). Hybrid Processing Method for Support Vector Machines for Classification of Imbalanced Cerebral Infraction Datasets. *International Journal on Advance Science Engineering Information Technology,* vol 9, no 2.

Inequalities for Geometrically Convex Functions

Saad Ihsan BUTT[1], Alper EKİNCİ[2], Ahmet Ocak AKDEMİR[3] and Sinan ASLAN[4]

[1] *COMSATS University of Islamabad, Lahore Campus, Lahore-PAKİSTAN*
[2] *Department of Foreign Trade, Bandirma Vocational High School,*
Bandirma Onyedi Eylul University, Balikesir-Bandırma-TURKEY
[3] *Department of Mathematics, Faculty of Science and Letters,*
Ağrı İbrahim Çeçen University, Ağrı-TURKEY
[4] *Graduate School of Natural and Applied Sciences,*
Giresun University, Giresun-TURKEY

saadihsanbutt@gmail.com
alperekinci@hotmail.com
aocakakdemir@gmail.com
sinanaslan0407@gmail.com

Abstract. In the present paper, we have recalled some definitions and well known results for the field of inequality theory. Then, some new integral inequalities have been established for geometrically convex functions via some well-known inequalities such that Young and Hölder inequality. Our results involve new upper bounds for product of geometrically convex functions that have applications in different branches of mathematics with statistics and convex analysis.

1. INTRODUCTION

The concept of convex function, which is widely used in inequality and is known with its applications in many fields of mathematics, has continued to be interesting even though its history dates back to ancient times. Differentiable or integrable convex functions have been the focus of many researchers and have been the subject of many articles in the field of inequality theory. Let's start with the definition of this aesthetics and useful functions.

Definition 1.1 *A function* $f:\mathbb{R}\to\mathbb{R}$ *is said to be convex on* I *if inequality*

$$f\left(tx+\left(1-t\right)y\right)\le tf\left(x\right)+\left(1-t\right)f\left(y\right) \tag{1.1}$$

holds for all $x,y\in I$ and $t\in[0,1]$

Some studies have been designed to form different types of convex function classes in order to carry the convex function classes to a new dimension. Many convex function types, especially the convex function definition, are closely related to the special means and contain the mean expressions in the definition. We will continue with some types of convex function types that come into prominence among convex function types and find application in statistics.

In [9], Niculescu mentioned definitions of geometrically convex functions as:

The arithmetic-geometric convex functions namely $\log-$ convex functions or AG-convex functions are defined as $f:I\subseteq\left(0,\infty\right)\to\left(0,\infty\right)$ and hold the following inequality:

$$x,y\in I \text{ and } \alpha\in[0,1]\Rightarrow f(\alpha x+(1-\alpha)y)\le[f(x)]^{\alpha}[f(y)]^{1-\alpha}. \tag{1.2}$$

i.e., for which $\log f$ is convex.

The geometric-geometric convex functions namely multiplicatively convex functions or GG-convex functions are defined as $f:I\subseteq\left(0,\infty\right)\to J\subseteq\left(0,\infty\right)$ and satisfy:

$$x, y \in I \text{ and } \alpha \in [0,1] \Rightarrow f\left(x^{\alpha} y^{1-\alpha}\right) \leq \left[f(x)\right]^{\alpha} \left[f(y)\right]^{1-\alpha}. \quad (1.3)$$

The class of all geometric-arithmetic convex functions or namely GA-convex functions are defined as $f : I \subseteq (0,\infty) \to (0,\infty)$ and hold:

$$x, y \in I \text{ and } \alpha \in [0,1] \Rightarrow f\left(x^{\alpha} y^{1-\alpha}\right) \leq \alpha f(x) + (1-\alpha) f(y). \quad (1.4)$$

Besides, recall that the criterion of $GA-$convexity is $x^2 f'' + x f' \geq 0$ which implies all twice differentiable non-decreasing convex functions are also $GA-$convex.
Examples of functions that contain some important statistical definitions and closely related to many other mathematical concepts are presented below.

Remark 1.1 *[4] Some examples of log-concave and concave functions*

1. The normal probability density function $f(x) = \frac{1}{\sqrt{2\pi}} e^{-x^2/2}$ is log-concave on $(0,1)$, which is also concave on $(0,1)$ since $\log f(x) = -x^2/2 \ln \frac{1}{\sqrt{2\pi}}$ is a concave function.

2. The probability density function of the beta distribution, for $0 \leq x \leq 1$, and shape parameters $\alpha_1, \alpha_2 > 0$, is a power function of the variable x and of its reflection $(1-x)$ like follows:

$$f(x;\alpha_1,\alpha_2) = \frac{1}{\beta(\alpha_1,\alpha_2)} x^{\alpha_1 - 1}(1-x)^{\alpha_2 - 1}$$

is concave and $\log$-concave function for $\alpha_1 = \alpha_2 = 2$, where β is Euler-Beta function. Namely $f(x) = \frac{\Gamma(4)}{\Gamma(2)\Gamma(2)} x(1-x) = 6(x - x^2)$ is concave and $\log$-concave function on $(0,1)$.

Hermite-Hadamard inequality, which suggests bounds for the mean value of a convex function, is given as follows.

Theorem 1.1. *(See [2], [3]) Let $f : I \subset \mathbb{R} \to \mathbb{R}$ be a convex function and $u, v \in I$ with $u < v$. The following double inequality:*

$$f\left(\frac{u+v}{2}\right) \leq \frac{1}{v-u} \int_u^v f(x)dx \leq \frac{f(u) + f(v)}{2} \quad (1.5)$$

is known in the literature as Hadamard's inequality (or Hermite-Hadamard inequality) for convex functions. If f is a positive concave function, then the inequality is reversed.

It is worth remembering some special means to be used in this study.The extended logarithmic mean L_p of $a, b > 0$ is given for $a = b$ by $L_p(a,a) = a$ and for $a \neq b$ by

$$L_p(a,b)=\begin{cases}\left[\dfrac{b^{p+1}-a^{p+1}}{(p+1)(b-a)}\right]^{\frac{1}{p}}, & p\neq -1,0\\ \dfrac{b-a}{\ln b-\ln a}, & p=-1\\ \dfrac{1}{e}\left(\dfrac{b^b}{a^a}\right)^{\frac{1}{(b-a)}}, & p=0\end{cases}.$$

It is obivous that $L_{-1}(a,b)$ is called the logarithmic mean $L(a,b)$. Two important averages subject to arithmetic geometric inequality are defined as follows.

$$G(a,b)=\sqrt{ab},$$

$$A(a,b)=\frac{a+b}{2}$$

are the geometric mean and arithmetic mean, respectively.

For more detailed information, inequalities, generalizations, and interesting new results for special means and geometric convex function classes, please refer to the papers [1],[5], [6],[8]-[17].

Many articles listed in the bibliography section have obtained results based on geometric convex function classes and special averages. Here we just want to remind you a few of these results. In [7] Yang et al. established the following results;

Theorem 1.2. *Let* $f,g:I\to(0,\infty)$ *be log-convex functions on* I *and* $a,b\in I$ *with* $a<b$ *and* $\alpha,\beta>0$ *with* $\alpha+\beta=1$. *Then the following inequality holds:*

$$\frac{1}{b-a}\int_a^b f(x)g(x)x\le\alpha\left[L_{\frac{1}{\alpha}-1}(f(a),f(b))\right]^{\frac{1-\alpha}{\alpha}}L(f(a),f(b))$$
$$+\beta\left[L_{\frac{1}{\beta}-1}(g(a),g(b))\right]^{\frac{1-\beta}{\beta}}L(g(a),g(b)).$$

Theorem 1.3. *Let* $f,g:I\to(0,\infty)$ *be log-concave functions on* I *and* $a,b\in I$ *with* $a<b$. *Further, let* $\alpha>1$ *with* $\alpha+\beta=1$ *(or* $\beta>1$ *with* $\alpha+\beta=1$*). Then the following inequality holds:*

$$\frac{1}{b-a}\int_a^b f(x)g(x)x\ge\alpha\left[L_{\frac{1}{\alpha}-1}(f(a),f(b))\right]^{\frac{1-\alpha}{\alpha}}L(f(a),f(b))$$
$$+\beta\left[L_{\frac{1}{\beta}-1}(g(a),g(b))\right]^{\frac{1-\beta}{\beta}}L(g(a),g(b)).$$

The goal of this paper is to establish some new integral inequalities for geometrically convex functions by using above-mentioned classical integral inequalities.

2. MAIN RESULTS

Theorem 2.1. *Let* $f, g: I \subseteq (0,\infty) \to (0,\infty)$ *are* $GA-$*convex functions and* f, g, fg *are integrable functions on* $[a,b]$ *such that* $a,b \in I$, $\frac{b}{a} \neq 1$. *Then, we point out the following new result:*

$$\frac{1}{\ln b - \ln a}\int_a^b f(x)g\left(\frac{ab}{x}\right)dx \leq T_1 f(b)g(a) + T_2 f(a)g(b) + T_3\left(f(a)g(a) + f(b)g(b)\right) \tag{2.1}$$

where

$$T_1 = \frac{b\ln^2\frac{b}{a} - 2b\ln\frac{b}{a} + 2b - 2a}{\ln^3\frac{b}{a}},$$

$$T_2 = \frac{a\ln^2\frac{b}{a} - 2a\ln\frac{b}{a} + 2\ln\frac{b}{a} - 2}{\ln^3\frac{b}{a}},$$

$$T_3 = \frac{2b\ln^2\frac{b}{a} - 3b\ln\frac{b}{a} + a\ln\frac{b}{a} + 2b - 2a}{\ln^3\frac{b}{a}}.$$

Proof. By using the functions f and g and conditions of Theorem, we can write

$$\frac{1}{\ln b - \ln a}\int_a^b f(x)g\left(\frac{ab}{x}\right)dx = \int_0^1 b^t a^{1-t} f\left(b^t a^{1-t}\right)g\left(a^t b^{1-t}\right)dt.$$

Here we have used the change of the variables as $x = b^t a^{1-t}$ and $dx = b^t a^{1-t}\ln\frac{b}{a}dt$. By taking into account $GA-$convexity of f and g, we get

$$\begin{aligned}
&\frac{1}{\ln b - \ln a}\int_a^b f(x)g\left(\frac{ab}{x}\right)dx \\
&\leq \int_0^1 b^t a^{1-t}\left[tf(b) + (1-t)f(a)\right]\left[tg(a) + (1-t)g(b)\right]dt \\
&= \int_0^1 b^t a^{1-t}\left[t^2 f(b)g(a) + t(1-t)\left(f(a)g(a) + f(b)g(b)\right) + (1-t)^2 f(a)g(b)\right]dt.
\end{aligned}$$

By computing the above integrals, we obtain

$$\begin{aligned}
&\frac{1}{\ln b - \ln a}\int_a^b f(x)g\left(\frac{ab}{x}\right)dx \\
&\leq \left[\frac{b\ln^2\frac{b}{a} - 2b\ln\frac{b}{a} + 2b - 2a}{\ln^3\frac{b}{a}}\right] f(b)g(a)
\end{aligned}$$

$$+\left[\frac{a\ln^2\frac{b}{a}-2a\ln\frac{b}{a}+2\ln\frac{b}{a}-2}{\ln^3\frac{b}{a}}\right]f(a)g(b)$$

$$+\left[\frac{2b\ln^2\frac{b}{a}-3b\ln\frac{b}{a}+a\ln\frac{b}{a}+2b-2a}{\ln^3\frac{b}{a}}\right]\left(f(a)g(a)+f(b)g(b)\right).$$

Thus, this complete the proof of the inequality (2.1).

Similar to this result can be easily obtained for $GG-$convex functions.

Theorem 2.2. *Let* $f,g:I\subseteq(0,\infty)\to(0,\infty)$ *are* $GG-$*convex functions and* f,g,fg *are integrable functions on* $[a,b]$ *such that* $a,b\in I$, $\frac{b}{a}\neq 1$. *Then, we have:*

$$\frac{1}{\ln b-\ln a}\int_a^b f(x)g\left(\frac{ab}{x}\right)dx\le L\left(af(a)g(b),bf(b)g(a)\right)$$

where $L(u,v)$ is the logarithmic mean of u and v.

Proof. Procedures similar to the proof of the previous theorem should be considered, but we only need to select the functions $GG-$convex. So, we can write

$$\frac{1}{\ln b-\ln a}\int_a^b f(x)g\left(\frac{ab}{x}\right)dx$$
$$=\int_0^1 b^t a^{1-t}f\left(b^t a^{1-t}\right)g\left(a^t b^{1-t}\right)dt$$
$$\le\int_0^1\left[bf(b)g(a)\right]^t\left[af(a)g(b)\right]^{1-t}dt.$$

By a simple calculation, we deduce

$$\frac{1}{\ln b-\ln a}\int_a^b f(x)g\left(\frac{ab}{x}\right)dx\le\frac{bf(b)g(a)-af(a)g(b)}{\ln bf(b)g(a)-\ln af(a)g(b)}.$$

The proof is completed.

Theorem 2.3. *Let* $f:I\subseteq(0,\infty)\to(0,\infty)$ *is* $GG-$*convex function and* f *is integrable function on* $[a,b]$ *such that* $a,b\in I$, $\frac{b}{a}\neq 1$. *Then, one has the following inequality:*

$$\frac{1}{\ln b-\ln a}\int_a^b f(x)f\left(\frac{ab}{x}\right)dx\le G^2\left(f(a),f(b)\right)L(a,b)$$

where $L(u,v)$ is the logarithmic mean of u and v and $G(u,v)$ is the geometric mean of u and v.

Proof. By using the definition of $GG-$convexity, we have

$$\frac{1}{\ln b-\ln a}\int_a^b f(x)f\left(\frac{ab}{x}\right)dx$$
$$=\int_0^1 b^t a^{1-t} f\left(b^t a^{1-t}\right)f\left(a^t b^{1-t}\right)dt$$
$$\leq f(a)f(b)\int_0^1 b^t a^{1-t}dt = f(a)f(b)\frac{b-a}{\ln b-\ln a}$$

which completes the proof.

Theorem 2.4. *Suppose that* $f:I\subseteq(0,\infty)\to(0,\infty)$ *be* $GA-$*convex function,* $g:I\subseteq(0,\infty)\to(0,\infty)$ *be* $GG-$*convex function and* f, g, fg *are integrable functions on* $[a,b]$ *such that* $a,b\in I$, $\frac{b}{a}\neq 1$. *Then, one has the following inequality:*

$$\frac{1}{\ln b-\ln a}\int_a^b f(x)g\left(\frac{ab}{x}\right)dx\leq\frac{L_p^p(f(a),f(b))}{p}+\frac{L\left((ag(b))^q,(bg(a))^q\right)}{q},$$

for $\frac{1}{p}+\frac{1}{q}=1$ where $L(u,v)$ is the logarithmic mean of u and v and $G(u,v)$ is the geometric mean of u and v.

Proof. The classical Young's inequality can be represented by (see [2]):

$$\alpha\beta\leq\frac{\alpha^p}{p}+\frac{\beta^q}{q},\ \text{for}\frac{1}{p}+\frac{1}{q}=1,\ \alpha,\beta>0.$$

Since f is $GA-$convex function and g is $GG-$convex function on I, we get

$$\frac{1}{\ln b-\ln a}\int_a^b f(x)g\left(\frac{ab}{x}\right)dx$$
$$=\int_0^1 b^t a^{1-t} f\left(b^t a^{1-t}\right)g\left(a^t b^{1-t}\right)dt$$
$$\leq\int_0^1 b^t a^{1-t}\left[tf(b)+(1-t)f(a)\right]\left[g(a)\right]^t\left[g(b)\right]^{1-t}dt.$$

By using the Young inequality, we can write

$$\frac{1}{\ln b-\ln a}\int_a^b f(x)g\left(\frac{ab}{x}\right)dx$$
$$\leq\int_0^1 b^t a^{1-t}\left[tf(b)+(1-t)f(a)\right]\left[g(a)\right]^t\left[g(b)\right]^{1-t}dt$$
$$\leq\frac{\int_0^1\left[tf(b)+(1-t)f(a)\right]^p dt}{p}+\frac{\int_0^1 b^{qt}a^{q(1-t)}\left[g(a)\right]^{qt}\left[g(b)\right]^{q(1-t)}dt}{q}.$$

By computing the above integrals, we obtain

$$\frac{1}{\ln b-\ln a}\int_a^b f(x)g\left(\frac{ab}{x}\right)dx$$

$$\leq \left(\frac{[f(b)]^{p+1} - [f(a)]^{p+1}}{f(b) - f(a)} \right) \left(\frac{1}{p(p+1)} \right) + \frac{(bg(a))^q - (ag(b))^q}{q\left(\ln(bg(a))^q - \ln(ag(b))^q\right)},$$

which completes the proof.

Theorem 2.5. *Suppose that* $f, g : I \subseteq (0,\infty) \to (0,\infty)$ *be two functions and* $|f|, |g|, |fg|$ *are integrable functions on* $[a,b]$ *such that* $a,b \in I$, $a < b$. *If* $|f|$ *is* $GA-$*convex and* $|g|$ *is* $GG-$*convex function, then, one has the following inequality:*

$$\frac{1}{\ln b - \ln a} \int_a^b |f(x)| \left| g\left(\frac{ab}{x}\right) \right| dx$$

$$\leq \left[\left(\frac{[|f(b)|]^{p+1} - [f(a)]^{p+1}}{|f(b)| - f(a)} \right) \left(\frac{1}{(p+1)} \right) \right]^{\frac{1}{p}} \left[\frac{(b|g(a)|)^q - (a|g(b)|)^q}{\ln(b|g(a)|)^q - (a|g(b)|)^q} \right]^{\frac{1}{q}}$$

for $\frac{1}{p} + \frac{1}{q} = 1, p > 1.$

Proof. By using the definition of $|f|$ and $|g|$ and changing of the variables, we have

$$\frac{1}{\ln b - \ln a} \int_a^b |f(x)| \left| g\left(\frac{ab}{x}\right) \right| dx$$

$$\leq \int_0^1 b^t a^{1-t} \left[t|f(b)| + (1-t)|f(a)| \right] \left[|g(a)| \right]^t \left[|g(b)| \right]^{1-t} dt.$$

By applying the well-known Hölder integral inequality, we get:

$$\frac{1}{\ln b - \ln a} \int_a^b |f(x)| \left| g\left(\frac{ab}{x}\right) \right| dx$$

$$\leq \left(\int_0^1 \left[t|f(b)| + (1-t)|f(a)| \right]^q dt \right)^{\frac{1}{p}} \left(\int_0^1 b^{qt} a^{q(1-t)} \left[|g(a)| \right]^{qt} \left[|g(b)| \right]^{q(1-t)} dt \right)^{\frac{1}{q}}.$$

By making use of necessary computations, we obtain;

$$\frac{1}{\ln b - \ln a} \int_a^b |f(x)| \left| g\left(\frac{ab}{x}\right) \right| dx$$

$$\leq \left[\left(\frac{\left[|f(b)| \right]^{p+1} - [f(a)]^{p+1}}{|f(b)| - f(a)} \right) \left(\frac{1}{(p+1)} \right) \right]^{\frac{1}{p}} \left[\frac{(b|g(a)|)^q - (a|g(b)|)^q}{\ln(b|g(a)|)^q - \ln(a|g(b)|)^q} \right]^{\frac{1}{q}}.$$

Which completes the proof.

Theorem 2.6 *Suppose that* $f, g : I \subseteq (0,\infty) \to (0,\infty)$ *be two functions and* $|f|, |g|, |fg|$ *are integrable functions on* $[a,b]$ *such that* $a,b \in I$, $a < b$. *If* $|f|$ *and* $|g|$ *are* $GG-$*convex function, then, one has the following inequality:*

$$\frac{1}{\ln b - \ln a} \int_a^b |f(x)| \left| g\left(\frac{ab}{x}\right) \right| dx$$

$$\leq \left[\frac{\left(\left|f(b)\right|\right)^p-\left(\left|f(a)\right|\right)^p}{\ln\left(\left|f(b)\right|\right)^p-\ln\left(\left|f(a)\right|\right)^p}\right]^{\frac{1}{p}}\left[\frac{\left(b\left|g(a)\right|\right)^q-\left(a\left|g(b)\right|\right)^q}{\ln\left(b\left|g(a)\right|\right)^q-\ln\left(a\left|g(b)\right|\right)^q}\right]^{\frac{1}{q}}$$

$$\leq L^{\frac{1}{p}}((|f(a)|)^p,(|f(b)|)^p)L^{\frac{1}{q}}((a|g(b)|)^q,(b|g(a)|)^q)$$

for $\frac{1}{p}+\frac{1}{q}=1, p>1,$ where $L(u,v)$ is the logarithmic mean of u and v.

Proof. By using the definition of $|f|$ and $|g|$ and changing of the variables, we have

$$\frac{1}{\ln b-\ln a}\int_a^b\left|f(x)\right|\left|g\left(\frac{ab}{x}\right)\right|dx$$

$$\leq \int_0^1 b^t a^{1-t}\left[\left|f(a)\right|\right]^t\left[\left|f(b)\right|\right]^{1-t}\left[\left|g(a)\right|\right]^t\left[\left|g(b)\right|\right]^{1-t}dt.$$

By applying the well-known Hölder integral inequality, we get:

$$\frac{1}{\ln b-\ln a}\int_a^b\left|f(x)\right|\left|g\left(\frac{ab}{x}\right)\right|dx$$

$$\leq\left(\int_0^1\left[\left|f(b)\right|\right]^{pt}\left[\left|f(a)\right|\right]^{p(1-t)}dt\right)^{\frac{1}{p}}\left(\int_0^1 b^{qt}a^{q(1-t)}\left[\left|g(a)\right|\right]^{qt}\left[\left|g(b)\right|\right]^{q(1-t)}dt\right)^{\frac{1}{q}}.$$

By making use of necessary computations, we obtain;

$$\frac{1}{\ln b-\ln a}\int_a^b\left|f(x)\right|\left|g\left(\frac{ab}{x}\right)\right|dx$$

$$\leq\left[\left(\frac{(|f(b)|)^p-(f(a))^p}{ln(|f(b)|)^p-ln(f(a))^p}\right)\right]^{\frac{1}{p}}\left[\frac{(b|g(a)|)^q-(a|g(b)|)^q}{ln(b|g(a)|)^q-ln(a|g(b)|)^q}\right]^{\frac{1}{q}}$$

which completes the proof.

3. CONCLUSION

In this study, we have proved some new integral inequalities for product of $GA-$ and $GG-$convex functions by using some integration techniques and elemantery analysis. The results have been established via some classical inequalities such as Hölder integral inequality and Young inequality. We presented the results for special means of real numbers. The results can be extended to fractional calculus by using some new fractional integral operators. Also, similar results can be found for more general convex function classes.

REFERENCES

1. S.S. Dragomir and C. E. M. Pearce, Selected Topics on Hermite-Hadamard Inequalities and Applications, RGMIA Monographs, Victoria University, 2000.
2. G.H. Hardy, J.E. Littlewood and G. Pólya, *Inequalities*, 2nd ed. Cambridge,England: Cambridge University Press, 1988.
3. D.S. Mitrinovic, J.E. Pecaric and A.M. Fink, *Classical and New Inequalties in Analysis*, Kluwer Academic Publisher, 1993.

4. C.P. Niculescu, *The Hermite-Hadamard inequality for log-convex functions*, Nonlinear Analysis **75** (2012), 662 -669.
5. C.P. Niculescu, L.E. Persson, *Convex Functions and their Applications*, A Contemporary Approach, in: CMS Books in Mathematics, Springer-Verlag, New York, **23** (2006**)**.
6. C.E.M. Pearce, J. Pecaric, V. Simic, *Stolarsky means and Hadamard's inequality*, J. Math.Anal. Appl. **220** (1998), 99-109.
7. G-S. Yang, K-L. Tseng and H-T. Wang, *A Note On Integral Inequalities Of Hadamard Type For Log-Convex And Log-Concave Functions*, Taiwenese Journal of Mathematics, **16(2)** (2012), 479 -496.
8. T-Y. Zhang, A-P. Ji and F. Qi, Sone inequalities of Hermite-Hadamard type for $GA-$convex functions with applications to means, Le Matematiche, Vol. LXVIII (2013) – Fasc. I, pp. 229–239, doi: 10.4418/2013.68.1.17.
9. C.P. Niculescu, Convexity according to the geometric mean, Math. Inequal. Appl., 3 (2) (2000), 155–167. Available online at http://dx.doi.org/10.7153/mia-03-19.
10. C.P. Niculescu, Convexity according to means, Math. Inequal. Appl. 6 (4) (2003), 571–579. Available online at http://dx.doi.org/10.7153/mia-06-53.
11. G.D. Anderson, M.K. Vamanamurthy and M. Vuorinen, Generalized convexity and inequalities, J. Math. Anal. Appl. 335 (2007) 1294–1308.
12. İ. İşcan, Some Generalized Hermite-Hadamard Type Inequalities for Quasi-Geometrically Convex Functions, American Journal of Mathematical Analysis 1, no. 3 (2013): 48-52. doi: 10.12691/ajma-1-3-5.
13. İ. İşcan, New general integral inequalities for some $GA-$convex and quasi-geometrically convex functions via fractional integrals, arXiv:1307.3265v1.
14. İ. İşcan, Hermite-Hadamard type inequalities for $GA-s-$convex functions, arXiv:1306.1960v2.
15. X-M. Zhang, Y-M. Chu, and X-H. Zhang, The Hermite-Hadamard type inequality of $GA-$convex functions and its application, Journal of Inequalities and Applications, Volume 2010, Article ID 507560, 11 pages, doi:10.1155/2010/507560.
16. R.A. Satnoianu, Improved $GA-$convexity inequalities, Journal of Inequalities in Pure and Applied Mathematics, Volume 3, Issue 5, Article 82, 2002.
17. M.A. Latif, New Hermite-Hadamard type integral inequalities for $GA-$convex functions with applications, Analysis, Volume 34, Issue 4, 379-389, 2014. Doi: 10.1515/anly-2012-1235.

Some Fractional Integral Inequalities for Geometrically Convex Functions

Saima RASHID[1], Ahmet Ocak AKDEMİR[2], Alper EKİNCİ[3] and Sinan ASLAN[4]

[1]*Government College University,*
Department of Mathematics, Faisalabad-PAKİSTAN
[2]*Department of Mathematics, Faculty of Science and Letters,*
Ağrı İbrahim Çeçen University, Ağrı-TURKEY
[3]*Department of Foreign Trade, Bandirma Vocational High School,*
Bandirma Onyedi Eylul University, Balikesir-Bandırma-TURKEY
[4] *Graduate School of Natural and Applied Sciences,*
Giresun University, Giresun-TURKEY

SaimaMoeed.gc@gmail.com
aocakakdemir@gmail.com
alperekinci@hotmail.com
sinanaslan0407@gmail.com

Abstract. In this paper some new inequalities of Hadamard-type are established for the classes of functions whose derivatives of absolute values are geometrically m-geometrically convex functions via Riemann-Liouville integrals.

1. INTRODUCTION

Let $f:I\subset\mathbb{R}\to\mathbb{R}$ be a convex function defined on the interval I of real numbers and $a,b\in I$ with $a<b$. The following inequality is well known in the literature as the Hermite–Hadamard inequality:

$$f\left(\frac{a+b}{2}\right)\le\frac{1}{b-a}\int_a^b f(x)dx\le\frac{f(a)+f(b)}{2}.$$

Let us recall some known definitions and results which will be used in this paper. The function $f:[a,b]\to\mathbb{R}$ is said to be convex, if we have

$$f\left(tx+(1-t)y\right)\le tf\left(x\right)+(1-t)f\left(y\right)$$

for all $x,y\in[a,b]$ and $t\in[0,1]$.
The concept of $m-$convexity has been introduced by Toader in [5] as following:

Definition 1. *The function $f:[0,b]\to\mathbb{R}$, $b>0$, is said to be $m-$convex, where $m\in[0,1]$, if we have*

$$f\left(tx+m(1-t)y\right)\le tf\left(x\right)+m(1-t)f\left(y\right)$$

for all $x,y\in[0,b]$ and $t\in[0,1]$. We say that f is $m-$concave if $-f$ is $m-$convex.

In [4], Miheşan gave definition of $(\alpha,m)-$convexity as following:

Definition 2. *The function $f:[a,b]\to\mathbb{R}$, $b>0$ is said to be $(\alpha,m)-$convex, where $(\alpha,m)\in[0,1]^2$, if we have*

$$f\left(tx+m(1-t)y\right)\le t^{\alpha}f\left(x\right)+m(1-t^{\alpha})f\left(y\right)$$

for all $x,y\in[a,b]$ and $t\in[0,1]$.

Denote by $K_m^{\alpha}(b)$ the class of all $(\alpha,m)-$convex functions on $[0,b]$ for which $f(0)\le 0$. If we choose $(\alpha,m)=(1,m)$, it can be easily seen that $(\alpha,m)-$convexity reduces to $m-$convexity and for $(\alpha,m)=(1,1)$, we have ordinary convex functions on $[0,b]$. For the recent results based on the above definitions see the papers [1]-[13].

In [12], authors introduce two new concepts called $m-$ and $(\alpha,m)-$ geometrically convex functions as followings:

Definition 3. *Let* $f(x)$ *be a positive function on* $[0,b]$ *and* $m\in(0,1]$. *If*

$$f\left(x^t y^{m(1-t)}\right)\le [f(x)]^t [f(y)]^{m(1-t)}$$

holds for all $x,y\in[0,b]$ and $t\in[0,1]$, then we say that the function $f(x)$ is $m-$geometrically convex on $[0,b]$.

Definition 4. *Let* $f(x)$ *be a positive function on* $[0,b]$ *and* $(\alpha,m)\in(0,1]\times(0,1]$. *If*

$$f\left(x^t y^{m(1-t)}\right)\le [f(x)]^{t^{\alpha}} [f(y)]^{m\left(1-t^{\alpha}\right)}$$

holds for all $x,y\in[0,b]$ and $t\in[0,1]$, then we say that the function $f(x)$ is $(\alpha,m)-$geometrically convex on $[0,b]$.

In [12], Xi *et al.* proved following inequalities of Hadamard type for $m-$ and $(\alpha,m)-$geometrically convex functions:

Theorem 1. *Let* $I\supset[0,\infty)$ *be an open interval and* $f:I\to(0,\infty)$ *is differentiable. If* $f'\in L([a,b])$ *and* $|f'|$ *is decreasing and* $(\alpha,m)-$*geometrically convex on* $[\min\{1,a\},b]$ *for* $a\in[0,\infty)$ $b\ge 1$, *and* $(\alpha,m)\in(0,1]\times(0,1]$, *then*

$$\left|\frac{f(a)+f(b)}{2}-\frac{1}{b-a}\int_a^b f(x)dx\right|\le\frac{b-a}{2}\left(\frac{1}{2}\right)^{1-\frac{1}{q}}|f'(b)|^m[G_1(\alpha,m,q)]^{\frac{1}{q}}$$

is valid for $q\ge 1$, where

$$G_1(\alpha,m,q)=\int_0^1\left|1-2t\right|\left(\frac{|f'(a)|}{|f'(b)|^m}\right)^{qt^{\alpha}}dt. \tag{1.1}$$

Corollary 1. *Let* $I\supset[0,\infty)$ *be an open interval and* $f:I\to(0,\infty)$ *is differentiable. If* $f'\in L([a,b])$ *and* $|f'|$ *is decreasing and* $m-$*geometrically convex on* $[\min\{1,a\},b]$ *for* $a,b\in[0,\infty)$ *with* $a<b$ *and* $b\ge 1$ *and* $m\in(0,1]$, *then*

$$\left|\frac{f(a)+f(b)}{2}-\frac{1}{b-a}\int_a^b f(x)dx\right|\le\frac{b-a}{2}\left(\frac{1}{2}\right)^{1-\frac{1}{q}}|f'(b)|^m[G_1(1,m,q)]^{\frac{1}{q}}$$

is valid for $q\ge 1$, where G_1 is defined by (1.1).

Theorem 2. *Let* $I \supset [0,\infty)$ *be an open interval and* $f: I \to (0,\infty)$ *is differentiable. If* $f' \in L([a,b])$ *and* $|f'|$ *is decreasing and* $(\alpha,m)-$*geometrically convex on* $[\min\{1,a\},b]$ *for* $a \in [0,\infty)$, $b \geq 1$, *and* $(\alpha,m) \in (0,1]\times(0,1]$, *then*

$$\left|f\left(\tfrac{a+b}{2}\right) - \tfrac{1}{b-a}\int_a^b f(x)dx\right| \leq \tfrac{b-a}{4}\left(\tfrac{1}{2}\right)^{1-\frac{3}{q}} |f'(b)|^m [G_2(\alpha,m,q)]^{\frac{1}{q}}$$

is valid for $q \geq 1$, where

$$G_2(\alpha,m,q) = \left[\int_0^{\frac{1}{2}} t\left(\frac{|f'(a)|}{|f'(b)|^m}\right)^{qt^\alpha} dt\right]^{\frac{1}{q}} + \left[\int_{\frac{1}{2}}^{1} (1-t)\left(\frac{|f'(a)|}{|f'(b)|^m}\right)^{qt^\alpha} dt\right]^{\frac{1}{q}}. \tag{1.2}$$

Corollary 2. *Let* $I \supset [0,\infty)$ *be an open interval and* $f: I \to (0,\infty)$ *is differentiable. If* $f' \in L([a,b])$ *and* $|f'|$ *is decreasing and* $m-$*geometrically convex on* $[\min\{1,a\},b]$ *for* $a \in [0,\infty)$, $b \geq 1$, *and* $m \in (0,1]$, *then*

$$\left|f\left(\tfrac{a+b}{2}\right) - \tfrac{1}{b-a}\int_a^b f(x)dx\right| \leq \tfrac{b-a}{4}\left(\tfrac{1}{2}\right)^{1-\frac{3}{q}} |f'(b)|^m [G_2(1,m,q)]^{\frac{1}{q}}$$

is valid for $q \geq 1$, where G_2 is defined by (1.2).

Definition 5. *Let* $f \in L_1[a,b]$. *The Riemann-Liouville integrals* $J^{\alpha}_{a^+} f$ *and* $J^{\alpha}_{b^-} f$ *of order* $\alpha > 0$ *with* $a \geq 0$ *are defined by*

$$J^{\alpha}_{a^+} f(x) = \frac{1}{\Gamma(\alpha)}\int_a^x (x-t)^{\alpha-1} f(t)dt, \quad x > a$$

and

$$J^{\alpha}_{b^-} f(x) = \frac{1}{\Gamma(\alpha)}\int_x^b (t-x)^{\alpha-1} f(t)dt, \quad x < b$$

where $\Gamma(n) = \int_0^\infty x^{n-1}e^{-x}dx$ here is $J^0_{a+} = J^0_{b-} = f(x)$

In the case of $\alpha = 1$, the fractional integral reduces to the classical integral. Properties of this operator can be found in the references [14]-[16].
The main purpose of this paper is to establish some new Hadamard type inequalities for m-geometrically convex functions by using Riemann-Liouville integrals.

2. MAIN RESULTS

We use the following lemma in order to prove our main results (See [13]).

Lemma 1. *Let* $f: [a,b] \to \mathbb{R}$ *be a differentiable mapping on* (a,b) *with* $a < b$. *If* $f' \in L[a,b]$, *then the following equality for fractional integrals holds:*

$$\frac{f(a)+f(b)}{2} - \frac{\Gamma(\mu+1)}{2(b-a)^{\alpha}}\left[J^{\mu}_{a^+} f(b) + J^{\mu}_{b^-} f(a)\right]$$

$$= \frac{b-a}{2}\int_0^1 \left[(1-t)^{\mu} - t^{\mu}\right] f'(ta+(1-t)b)dt.$$

A very helpful Lemma which is given as following by Xi *et al.* (see [12]):

Lemma 2. *For* $x, y \in [0,\infty)$ *and* $m,t \in (0,1]$, *if* $x < y$ *and* $y \geq 1$, *then*

$$x^t y^{m(1-t)} \leq tx + (1-t)y.$$

Theorem 3. *Let* $f : I \to (0,\infty)$, *be a differentiable mapping. If* $f' \in L[a,b]$ *and* $|f'|$ *is decreasing and* $m-$*geometrically convex on* $[\min\{1,a\},b]$ *for* $a \in [0,\infty)$, $b \geq 1$, *and* $m \in (0,1]$, *then the following inequality holds for fractional integrals with* $\mu > 0$ *;*

$$\left|\frac{f(a)+f(b)}{2} - \frac{\Gamma(\mu+1)}{2(b-a)^{\mu}}\left[J^{\mu}_{a^+} f(b) + J^{\mu}_{b^-} f(a)\right]\right|$$
$$\leq \frac{b-a}{2}|f'(b)|^m \left[\int_0^{\frac{1}{2}} ((1-t)^{\mu} - t^{\mu})\left(\frac{|f'(a)|}{|f'(b)|^m}\right)^t dt + \int_{\frac{1}{2}}^1 (t^{\mu} - (1-t)^{\mu})\left(\frac{|f'(a)|}{|f'(b)|^m}\right)^t dt\right]$$

where Γ is Euler Gamma function.

Proof. From Lemma 1-Lemma 2 and by using the properties of modulus, we have

$$\left|\frac{f(a)+f(b)}{2} - \frac{\Gamma(\mu+1)}{2(b-a)^{\mu}}\left[J^{\mu}_{a^+} f(b) + J^{\mu}_{b^-} f(a)\right]\right|$$
$$\leq \frac{b-a}{2}\int_0^1 \left[(1-t)^{\mu} - t^{\mu}\right] f'(ta+(1-t)b)dt$$
$$\leq \frac{b-a}{2}\int_0^1 \left[(1-t)^{\mu} - t^{\mu}\right] f'(a^t b^{m(1-t)})dt.$$

Since $|f'|$ is $m-$geometrically convex, we can write

$$\left|\frac{f(a)+f(b)}{2} - \frac{\Gamma(\mu+1)}{2(b-a)^{\mu}}\left[J^{\mu}_{a^+} f(b) + J^{\mu}_{b^-} f(a)\right]\right|$$
$$\leq \frac{b-a}{2}|f'(b)|^m \left[\int_0^{\frac{1}{2}} ((1-t)^{\mu} - t^{\mu})\left(\frac{|f'(a)|}{|f'(b)|^m}\right)^t dt + \int_{\frac{1}{2}}^1 (t^{\mu} - (1-t)^{\mu})\left(\frac{|f'(a)|}{|f'(b)|^m}\right)^t dt\right]$$

This completes the proof.

Corollary 3. *Under the assumptions of Theorem 3, the following inequality holds:*

$$\left|\frac{f(a)+f(b)}{2} - \frac{\Gamma(\alpha+1)}{2(b-a)^{\alpha}}\left[J^{\alpha}_{a^+} f(b) + J^{\alpha}_{b^-} f(a)\right]\right|$$
$$\leq \frac{b-a}{2} M^m \left[\int_0^{\frac{1}{2}} ((1-t)^{\mu} - t^{\mu}) M^{(1-m)t} dt + \int_{\frac{1}{2}}^1 (t^{\mu} - (1-t)^{\mu}) M^{(1-m)t} dt\right].$$

Proof. The proof is immediate follows from the fact that $|f'| \leq M$ in Theorem 3.

Theorem 4. *Let* $f:I\to(0,\infty)$ *be a differentiable mapping. If* $f'\in L[a,b]$ *and* $|f'|^q$ *is decreasing and* $(\alpha_1,m)-$*geometrically convex on* $[\min\{1,a\},b]$ *for* $a\in[0,\infty)$, $b\geq 1$ *and* $(\alpha_1,m)\in(0,1]\times(0,1]$, *then the following inequality holds for fractional integrals with* $\alpha>0$*:*

$$\left|\frac{f(a)+f(b)}{2}-\frac{\Gamma(\alpha+1)}{2(b-a)^{\alpha}}\left[J^{\alpha}_{a^+}f(b)+J^{\alpha}_{b^-}f(a)\right]\right| \tag{2.1}$$

$$\leq\frac{b-a}{2}|f'(b)|^m\left[\left(\int_0^{\frac{1}{2}}((1-t)^{\alpha}-t^{\alpha})^p dt\right)^{\frac{1}{p}}\left(\int_0^{\frac{1}{2}}\left(\frac{|f'(a)|}{|f'(b)|^m}\right)^{qt^{\alpha_1}}dt\right)^{\frac{1}{q}}\right.$$

$$\left.+\left(\int_{\frac{1}{2}}^1((t^{\alpha}-(1-t)^{\alpha})^p dt\right)^{\frac{1}{p}}\left(\int_{\frac{1}{2}}^1\left(\frac{|f'(a)|}{|f'(b)|^m}\right)^{qt^{\alpha_1}}dt\right)^{\frac{1}{q}}\right].$$

Where Γ is Euler Gamma function for $q>1$ and $p^{-1}+q^{-1}=1$.

Proof. From Lemma 1- Lemma 2 and by using the Hölder integral inequality, we have

$$\left|\frac{f(a)+f(b)}{2}-\frac{\Gamma(\alpha+1)}{2(b-a)^{\alpha}}\left[J^{\alpha}_{a^+}f(b)+J^{\alpha}_{b^-}f(a)\right]\right|$$

$$\leq\frac{b-a}{2}|f'(b)|^m\left[\left(\int_0^{\frac{1}{2}}((1-t)^{\alpha}-t^{\alpha})^p dt\right)^{\frac{1}{p}}\left(\int_0^{\frac{1}{2}}|f'(ta+(1-t)b)|^q dt\right)^{\frac{1}{q}}\right.$$

$$\left.+\left(\int_{\frac{1}{2}}^1((t^{\alpha}-(1-t)^{\alpha})^p dt\right)^{\frac{1}{p}}\left(\int_{\frac{1}{2}}^1|f'(ta+(1-t)b)|^q dt\right)^{\frac{1}{q}}\right]$$

$$\leq\frac{b-a}{2}|f'(b)|^m\left[\left(\int_0^{\frac{1}{2}}((1-t)^{\alpha}-t^{\alpha})^p dt\right)^{\frac{1}{p}}\left(\int_0^{\frac{1}{2}}|f'(a^t b^{m(1-t)})|^q dt\right)^{\frac{1}{q}}\right.$$

$$\left.+\left(\int_{\frac{1}{2}}^1((t^{\alpha}-(1-t)^{\alpha})^p dt\right)^{\frac{1}{p}}\left(\int_{\frac{1}{2}}^1|f'a^t b^{m(1-t)}|^q dt\right)^{\frac{1}{q}}\right].$$

Since $|f'|$ is $(\alpha_1,m)-$ geometrically convex, we can write

$$\left|\frac{f(a)+f(b)}{2}-\frac{\Gamma(\alpha+1)}{2(b-a)^{\alpha}}\left[J^{\alpha}_{a^+}f(b)+J^{\alpha}_{b^-}f(a)\right]\right|$$

$$\leq \frac{b-a}{2}|f'(b)|^m\left[\left(\int_0^{\frac{1}{2}}((1-t)^\alpha - t^\alpha)^p dt\right)^{\frac{1}{p}}\left(\int_0^{\frac{1}{2}}\left(\frac{|f'(a)|}{|f'(b)|^m}\right)^{qt^{\alpha_1}} dt\right)^{\frac{1}{q}}\right.$$
$$\left. + \left(\int_{\frac{1}{2}}^1 (t^\alpha - (1-t)^\alpha)^p dt\right)^{\frac{1}{p}}\left(\int_{\frac{1}{2}}^1\left(\frac{|f'(a)|}{|f'(b)|^m}\right)^{qt^{\alpha_1}} dt\right)^{\frac{1}{q}}\right].$$

By computing the above integrals the proof is completed.

Corollary 4. *Under the assumptions of Theorem 4, the following inequality holds:*

$$\left|\frac{f(a)+f(b)}{2} - \frac{\Gamma(\alpha+1)}{2(b-a)^\alpha}\left[J^\alpha_{a^+} f(b) + J^\alpha_{b^-} f(a)\right]\right|$$
$$\leq \frac{b-a}{2}|f'(b)|^m\left[\left(\int_0^{\frac{1}{2}}((1-t)^\alpha - t^\alpha)^p dt\right)^{\frac{1}{p}}\left(\int_0^{\frac{1}{2}} M^{(1-m)qt^{\alpha_1}} dt\right)^{\frac{1}{q}}\right.$$
$$\left. + \left(\int_{\frac{1}{2}}^1 (t^\alpha - (1-t)^\alpha)^p dt\right)^{\frac{1}{p}}\left(\int_{\frac{1}{2}}^1 M^{(1-m)qt^{\alpha_1}} dt\right)^{\frac{1}{q}}\right].$$

Proof. By taking $\left|f'\right| \leq M$ in (2.1), the proof is completed.

Corollary 5. *Under the assumptions of Theorem 4, the following inequality holds:*

$$\left|\frac{f(a)+f(b)}{2} - \frac{\Gamma(\alpha+1)}{2(b-a)^\alpha}\left[J^\alpha_{a^+} f(b) + J^\alpha_{b^-} f(a)\right]\right|$$

$$\leq \frac{b-a}{2}|f'(b)|^m\left[\left(\int_0^{\frac{1}{2}}((1-t)^\alpha - t^\alpha)^p dt\right)^{\frac{1}{p}}\left(\int_0^{\frac{1}{2}}\left(\frac{|f'(a)|}{|f'(b)|^m}\right)^{qt^{\alpha}} dt\right)^{\frac{1}{q}}\right.$$
$$\left. + \left(\int_{\frac{1}{2}}^1 (t^\alpha - (1-t)^\alpha)^p dt\right)^{\frac{1}{p}}\left(\int_{\frac{1}{2}}^1\left(\frac{|f'(a)|}{|f'(b)|^m}\right)^{qt^{\alpha}} dt\right)^{\frac{1}{q}}\right].$$

Proof. If we set $\alpha = \alpha_1$ with $\alpha, \alpha_1 \in (0,1]$ in (2.1), the proof is completed.

Corollary 6. *Let* $f: I \to (0,\infty)$, *be a differentiable mapping. If* $f' \in L[a,b]$ *and* $\left|f'\right|$ *is decreasing and* $m-$*geometrically convex on* $[\min\{1,a\},b]$ *for* $a \in [0,\infty)$, $b \geq 1$ *and* $m \in (0,1]$, *then the following inequality holds:*

$$\left|\frac{f(a)+f(b)}{2} - \frac{\Gamma(\alpha+1)}{2(b-a)^\alpha}\left[J^\alpha_{a^+} f(b) + J^\alpha_{b^-} f(a)\right]\right|$$

$$\leq \frac{b-a}{2}|f'(b)|^m\left[\left(\int_0^{\frac{1}{2}}((1-t)^\alpha - t^\alpha)^p dt\right)^{\frac{1}{p}}\left(\int_0^{\frac{1}{2}}\left(\frac{|f'(a)|}{|f'(b)|^m}\right)^{qt} dt\right)^{\frac{1}{q}}\right.$$
$$\left. + \left(\int_{\frac{1}{2}}^1 (t^\alpha - (1-t)^\alpha)^p dt\right)^{\frac{1}{p}}\left(\int_{\frac{1}{2}}^1\left(\frac{|f'(a)|}{|f'(b)|^m}\right)^{qt} dt\right)^{\frac{1}{q}}\right].$$

Corollary 7. *If we choose* $\alpha = 1$ *in our results, we obtain several integral inequalities for* $m-$*geometrically and* $(\alpha, m)-$*geometrically convex functions.*

REFERENCES

1. M.K. Bakula, M.E. Özdemir and J. Pecaric, Hadamard-type inequalities for m-convex and (α, m) −convex functions, J. Inequal. Pure and Appl. Math., 9, (4), (2007), Article 96.
2. M.K. Bakula, J. Pecaric and M. Ribibic, Companion inequalities to Jensen's inequality for m-convex and (α, m) −convex functions, J. Inequal. Pure and Appl. Math., 7 (5) (2006), Article 194.
3. S.S. Dragomir and G. Toader, Some inequalities for m-convex functions, Studia University Babes Bolyai, Mathematica, 38 (1) (1993), 21-28.
4. V.G. Miheşan, A generalization of the convexity, Seminar of Functional Equations, Approx. and Convex, Cluj-Napoca (Romania) (1993).
5. G. Toader, Some generalization of the convexity, Proc. Colloq. Approx. Opt., Cluj-Napoca, (1984), 329-338.
6. E. Set, M. Sardari, M.E. Özdemir and J. Rooin, On generalizations of the Hadamard inequality for (α, m) −convex functions, Kyungpook J. Math., (2011), Accepted.
7. M.E. Özdemir, M. Avci and E. Set, On some inequalities of Hermite-Hadamard type via m-convexity, Applied Mathematics Letters, 23 (2010), 1065-1070.
8. G. Toader, On a generalization of the convexity, Mathematica, 30 (53) (1988), 83-87.
9. S.S. Dragomir, On some new inequalities of Hermite-Hadamard type for m-convex functions, Tamkang Journal of Mathematics, 33 (1) (2002).
10. M.Z. Sarikaya, E. Set, M.E. Özdemir, Some new Hadamard's type inequalities for co-ordinated m-convex and (α, m) −convex functions, Hacettepe J. of. Math. and St., 40, 219-229, (2011).
11. M.E. Özdemir, M. Avc and H. Kavurmaci, Hermite–Hadamard-type inequalities via (α, m) −convexity, Computers and Mathematics with Applications, 61 (2011), 2614–2620.
12. B.Y. Xi, R.F. Bai and F. Qi, Hermite-Hadamard type inequalities for the m- and (α, m) −geometrically convex functions, Aequationes Mathematicae, Springer Basel AG 2012, doi: 10.1007/s00010-011-0114-x.
13. E. Set, M.Z. Sarikaya, M.E. Özdemir and H. Yildirim, The Hermite-Hadamard's Inequality for some convex functions via fractional integrals and related results, JAMSI 10 (2014) 2, 69-83.
14. R. Gorenflo, F. Mainardi, Fractional calculus: integral and differential equations of fractional order, Springer Verlag, Wien (1997), 223-276.
15. S. Miller and B. Ross, An introduction to the Fractional Calculus and Fractional Differential Equations, John Wiley and Sons, USA, 1993, p.2.
16. I. Podlubny, Fractional Differential Equations, Academic Press, San Diego, 1999.

3rd INTERNATIONAL CONFERENCE
ON MATHEMATICAL AND RELATED SCIENCES:
CURRENT TRENDS AND DEVELOPMENTS
ICMRS 2020

20-22 NOVEMBER, 2020

Classification of Hepatocellular Carcinoma (HCC) using An Extended Three-Way C-Means Based on Kernel

Zuherman RUSTAM[1] and Sri HARTINI[1]

[1]*Department of Mathematics, University of Indonesia, Depok 16424, INDONESIA*

rustam@ui.ac.id

Abstract. Three-way c-means based on the kernel function of classifying Hepatocellular Carcinoma (HCC) data was proposed in this paper. As the improvement version of the rough k-means, it will be integrated with the polynomial kernel function. One of the important benefits of the proposed method is its ability to handle the data that cannot be separated linearly. The method was evaluated using k-fold cross-validation with k = 3, 5, 7, 10. Its sensitivity, precision, and F1-Score were compared to the three-way c-means in classifying the HCC dataset from Al Islam Bandung Hospital Indonesia, which consists of 130 HCC and 73 non-HCC samples. The result confirms that the proposed method makes the increment up to 10 percent to the three-way c-means in sensitivity, precision, and F1-Score. Therefore, the method proposed in this paper can be used to provide a proper diagnosis because it has high sensitivity in the classification.

1. INTRODUCTION

Hepatocellular carcinoma (HCC) is the third most tumor diseases that causes death worldwide [1]. However, the diagnosis of this disease is still difficult and therefore make many patients are diagnosed when they are already in severe condition and are too late to be treated. Even for those patients who can obtain surgery or liver transplantation when their life could be saved by these treatment, their overall survival rates are still low [2]. Therefore, the early diagnosis of this disease is important to obtain higher survival rate for each patient.

The diagnosis of HCC can be obtained by histology for lesions lacking on the radiological features or contrast enhanced ultrasonography [3]. Serum markers as alpha-fetoprotein (AFP) assessment and hepatic imaging also have applied to early diagnosis and treatment for the patients with HCC [4]. Beside serum AFP, there are also cancer antigens (CA19-9) and carcinoembryonic antigen (CEA) that can be used to detect HCC in the early stage [5]. In this research, we used Serum CA19-9 blood tests to obtain an early diagnosis of HCC. According to Zhang et al [6], serum CA19-9 can be used as a good predictors of HCC and with CA19-9 levels > 37 ng/ml we can predict the overall survival in patients with HCC after resection.

There are several methods that have been done to provide HCC diagnosis. Machine learning is one of the powerful methods that can be used to obtain high accuracy in diagnosing HCC. Ciocchetta, Demichelis, and Sboner [7] achieved 97.2 accuracy used rule induction algorithm and decision tree with histopathological features from the patients who received liver transplantation. Meanwhile, Lin et al [8] used Convolutional Neural Network (CNN) based on VGG-16 in the combination of the excitation fluorescence and image data for achieving over 90% accuracy in diagnosing HCC. Liao et al [9] also used deep CNN in histopathological images to detect HCC and provided promising results. Moreover, Khairi, Rustam, and Utama [10] used Possibilistic C-Means (PCM) algorithm on Serum AFP blood test data and achieved about 92% accuracy. Therefore, machine learning algorithm is truly promising to develop in order to obtain higher accuracy in providing early diagnosing HCC patients.

In this paper, we proposed an extended version of three-way c-means algorithm that likely the existing three-way c-means algorithm but is in the frame work of k-means. The extended version is different in terms of distance measurement. Instead of using Euclidean distance, we used kernel trick and used polynomial kernel function to make the algorithm perform even better in nonlinearly separable data.

2. METHODOLOGY

A. Dataset

Serum CA 19-9 could be one of the determiners of HCC existence. Therefore, a dataset of serum CA 19-9 blood tests is used in this research. Hepatocellular Carcinoma (HCC) dataset used in this study was obtained from the Al Islam Bandung Hospital Indonesia. The dataset consists of 130 HCC and 73 non-HCC samples. Each sample was described by age, hemoglobin, hematocrit, leukocyte, platelet counts. Some of the samples are shown in Table 1 where HCC samples are labelled as class 1 and non-HCC samples are labelled as class 2.

Table 1. HCC Dataset Samples

Age	Hemoglobin	Hematocrit	Leukocyte	Platelet Counts	Class
48	11.3	7,600	38.6	298,000	1
37	13.1	7,100	40.1	382,000	1
40	10.5	21,600	32.4	361,000	1
27	11.4	97,500	34.7	265,000	2
45	13.4	18,600	41.6	361,000	2

B. Proposed Method

In this research, we proposed kernel three-way c-means algorithm that is an extended version of the former algorithm. Three-way c-means was proposed by Zhang K [11] in order to fix the problem in rough k-means clustering. In this method, there are three regions of clusters, namely positive region, boundary region, and negative region. The positive region $\underline{\mathbb{C}}$ of a clusters consists of the data points that belong to the cluster, the boundary region $\hat{\mathbb{C}}$ of a clusters consists of the data points that probably belong to the cluster, and the data points that do not belong to the cluster are taken as a part of the negative region $\tilde{\mathbb{C}}$ of a cluster. Then, a cluster $\mathbb{C}_i$ is represented as $(\underline{\mathbb{C}}, \hat{\mathbb{C}})$

Three-way c-means applied the three-way weight and three-way assignment. In order to calculate the three-way weight w_{ij} of data point x_j in cluster $\mathbb{C}_i$, the values of B_{x_j}, μ_{ij}, and M_{x_j} have to found first. B_{x_j} is the clusters where positive or boundary regions contain x_j. Then fuzzy membership μ_{ij} is defined by Bezdek [12] in Eq. (1). Meanwhile M_{x_j} is a multiset which its elements are the fuzzy membership of x_j in the clusters of B_{x_j}.

$$\mu_{ij} = \sum_{l=1}^{c} \left(\frac{d(x_i, x_j)}{d(x_l, x_j)} \right)^{-\frac{2}{m-1}}, 1 \le i \le c, 1 \le j \le n \tag{1}$$

As the extended version of three-way c-means, the distance formula inside Eq. (1) is replaced by the distance measurement in the feature space [13] according to the concept of kernel function used. As the result, the Eq. (1) becomes Eq. (2) and therefore the difference between both methods is only in fuzzy membership calculation.

$$\mu_{ij} = \sum_{l=1}^{c} \left(\frac{K(\mathbf{x_i}, \mathbf{x_i}) - 2K(\mathbf{x_i}, \mathbf{x_j}) + K(\mathbf{x_j}, \mathbf{x_j})}{K(\mathbf{x_l}, \mathbf{x_l}) - 2K(\mathbf{x_l}, \mathbf{x_j}) + K(\mathbf{x_j}, \mathbf{x_j})} \right)^{-\frac{1}{m-1}}, \quad 1 \le i \le c, \quad 1 \le j \le n \tag{2}$$

The kernel function used in Eq. (2) is polynomial kernel function where we will use the first tenth degree to evaluate the performance of the extended version. The formula of polynomial kernel function [14] is given in Eq. (3) where h denotes the polynomial degree.

$$K(\mathbf{x_i}, \mathbf{x_j}) = (1 + \mathbf{x_i} \cdot \mathbf{x_j})^{\mathbf{h}} \tag{3}$$

The proposed method also consists of update step and assignment step. Update step was used to calculate the means of the cluster; meanwhile, the assignment step was followed the three-way assignment rules to determine whether the data point belong to the positive region, boundary region, or negative region of the cluster. The algorithm of three-way c-means was given in Figure 1.

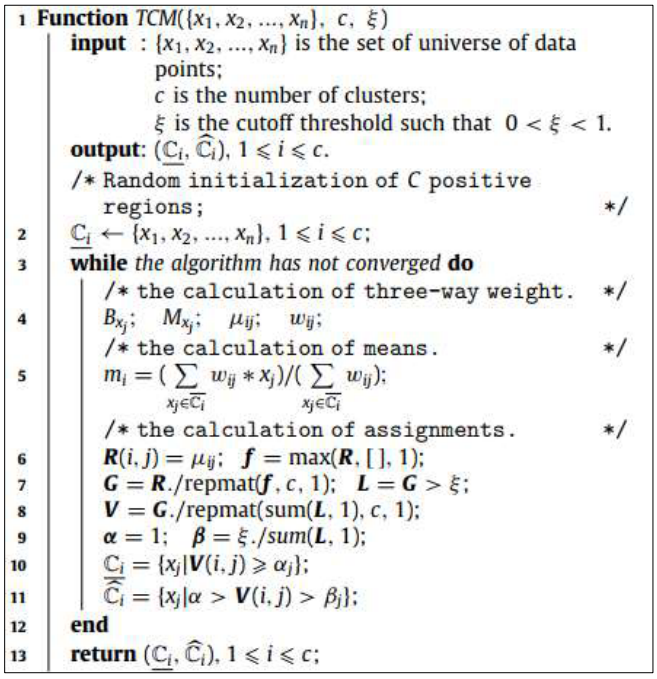

Figure 1. Algorithm of three-way c-means [11]

C. Performance Measurement

The performance of both three-way c-means and the proposed method was examined using the confusion matrix to calculate the sensitivity, precision, and F1-Score, which the formulas are given in Eqs. (4)-(6).

$$\text{Sensitivity} = \frac{TP}{TP + FN} \tag{4}$$

$$\text{Precision} = \frac{TP}{TP + FP} \tag{5}$$

$$\text{F1-Score} = \frac{2 * \text{sensitivity} * \text{precision}}{\text{sensitivity} + \text{precision}} \tag{6}$$

In those formula, TP (True Positive) is the number of HCC samples correctly diagnosed, FN (False Negative) is the number of HCC samples incorrecly diagnossed as non-HCC, and FP (False Positive) is the number of non-HCC samples incorrectly diagnosed as HCC.

3. RESULTS AND DISCUSSION

The performance of three-way c-means first evaluated using k-fold cross validation where k = 3, 5, 7, and 10. The result is shown in Table 2. From this table, based on the average of F1-Score, the performance of this method in classifying HCC is still below in 70 percent.

Table 2. Three-Ways C-Means Clustering Performance in Diagnosing HCC

k	The Average of Sensitivity	The Average of Precision	The Average of F1-Score
3	60.47	71.60	60.67
5	77.69	70.49	69.77
7	71.93	72.51	68.29
10	72.31	75.07	69.29

The performance of kernel three way c-means was also eevaluated used several k in k-fold cross validation. In Table 3, we can see the performance of kernel three-way c-means in different value of polynomial degree based on evaluation of 3-fold cross validation. There are some polynomial degrees that cause its performance still similar with

the method without kernel, but we can see that the ninth polynomial degree gives us the highest F1-Score among the other polynomial degrees.

Table 3. Kernel Three-Ways C-Means Clustering Performance in Diagnosing HCC using 3-fold cross validation

Polynomial Degree	The Average of Sensitivity	The Average of Precision	The Average of F1-Score
1	60.47	71.60	60.67
2	59.30	72.93	60.24
3	59.59	73.52	60.66
4	58.50	73.14	59.59
5	75.67	68.77	67.85
6	72.55	67.12	66.56
7	76.28	68.45	67.30
8	69.07	42.96	52.25
9	**63.29**	**63.45**	**75.01**
10	56.65	62.91	70.97

As the next discussion, the performance of kernel three-way c-means using 5-fold cross validation is given in Table 4. The highest F1-Score is delivered when used sixth polynomial degree with the lower value, but we can observe that the sensitivity and precision of this method is better than both tables that we have been discussed so far.

Table 4. Kernel Three-Ways C-Means Clustering Performance in Diagnosing HCC using 5-fold cross validation

Polynomial Degree	The Average of Sensitivity	The Average of Precision	The Average of F1-Score
1	77.69	71.81	70.08
2	76.41	72.09	69.03
3	76.84	72.46	69.51
4	76.27	72.20	68.93
5	76.17	72.15	68.84
6	**82.57**	**69.86**	**72.04**
7	57.99	58.57	49.77
8	67.36	51.33	58.36
9	81.74	69.51	71.88
10	64.26	55.30	53.07

In the next tables, we will discussed the performance of kernel three-way c-means using 7-fold cross validation (see Table 5) and 10-fold cross validation (see Table 6). Based on F1-Score, the performance of proposed method is still better when utilize 10-fold cross validation, but when use 7-fold cross validation, there is an improvement especially in many values of polynomial degree. However, we can choose the fifth polynomial degree in 7-fold cross validation as the highest F1-Score within the table and also the first polynomial degree in 10-fold cross validation.

Furthermore, not only the 7-fold cross validation gives the better F1-Score among the other k values in k-fold cross validation, but also provided better sensitivity. However, the proposed method that evaluated with 10-fold cross-validation still gives better precision than the other. It is very interesting how the k value in k-fold cross validation provides various performance and also affect the value of sensitivity, precision, and F1-Score of the proposed method.

Table 5. Kernel Three-Ways C-Means Performance in Diagnosing HCC using 7-fold cross validation

Polynomial Degree	The Average of Sensitivity	The Average of Precision	The Average of F1-Score
1	71.93	72.51	68.29
2	86.40	71.65	75.08
3	87.52	71.36	75.44
4	87.66	71.33	75.48
5	**87.68**	**71.32**	**75.49**
6	72.95	56.78	62.12
7	84.48	71.09	74.21
8	76.46	74.27	69.77
9	76.59	69.17	69.73
10	70.68	59.04	62.08

Table 6. Kernel Three-Ways C-Means Performance in Diagnosing HCC using 10-fold cross validation

Polynomial Degree	The Average of Sensitivity	The Average of Precision	The Average of F1-Score
1	**76.15**	**76.16**	**70.79**
2	74.76	77.08	70.30
3	73.93	76.96	69.71
4	73.85	76.95	69.66
5	73.85	76.94	69.66
6	75.94	75.27	69.93
7	77.53	75.50	70.51
8	70.68	64.81	63.19
9	70.06	63.50	62.50
10	64.41	55.35	57.39

After discussed each of kernel three-way c-means performance in different k value in k-fold cross validation, now we will compared the performance of three way c-means and the proposed method for each k-fold cross validation. From Table 7, we can see that the proposed method provides better performance in terms of sensitivity and F1-Score for all k-fold cross validation. Meanwhile, three-way c-means c-means is still better in precision except when 10-fold cross valdiation. In this table, we can also see the proposed method performs best when evaluated in 7-fold cross validation. Furthermore, if we compared the precision in the other evaluations, the precision of our proposed method in 7-fold cross validation is still the second highest precision. Therefore, as the result of comparison between three-way c-means and our proposed method, the latter is better than the former in order to diagnose HCC patients.

Table 7. The Comparison of Three Way C-Means and Proposed Method Performance in Diagnosing HCC

k	Method	The Average of Sensitivity	The Average of Precision	The Average of F1-Score
3	Three-way c-means	60.47	**71.60**	60.67
	Kernel three-way c-means (9th polynomial kernel)	**63.29**	63.45	**75.01**
5	Three-way c-means	77.69	**70.49**	69.77
	Kernel three-way c-means (6th polynomial kernel)	**82.57**	69.86	**72.04**
7	Three-way c-means	71.93	**72.51**	68.29
	Kernel three-way c-means (5th polynomial kernel)	**87.68**	71.32	**75.49**
10	Three-way c-means	72.31	75.07	69.29
	Kernel three-way c-means (1st polynomial kernel)	**76.15**	**76.16**	**70.79**

4. CONCLUSION

Hepatocellular carcinoma is the most common type of primary liver cancer in adults and also cause the death worldwide. The diagnosis system is still poor and therefore the development for early diagnosis of HCC patients is still an essensial issue. Serum CA 19-9 could be one of the determiners of HCC existence. Therefore, a dataset of serum CA 19-9 blood tests from the laboratory of Al Islam Bandung Hospital in Indonesia was used in this study. We proposed an extended version of three-way c-means based on polinomial kernel that called as kernel three-way c-means. The experiments using this dataset is conducted based on k-fold cross valdiation where k = 3, 5, 7, and 10. Based on the experiments, the sensitivity and F1-Score of our proposed method in HCC classification were obtained better for all k-fold cross-validation conducted than the method without kernel function. However, three-way c-means clustering is better when it comes to precision measurement. Moreover, the 10-fold cross-validation yields better performance in HCC classification than three-way c-means in sensitivity, precision, and F1-Score measurement. Overall, our proposed method performs best when evaluated in 7-fold cross validation with 87.68

sensitivity, 71.32 precision, and 75.49 F1-score. Therefore it can be an option to diagnose HCC patients. As the future works, there are a lot of space for improvement especially in order to improve the accuracy in diagnosing HCC patients using Serum CA 19-9 blood tests data.

ACKNOWLEDGEMENT

This work was supported financially by Indonesia Ministry of Research and Technology/ National Research and Innovation Agency (KEMENRISTEK/BRIN) 2021 research grant scheme. The authors are thankful for the kindness of the doctor and staff at the Al Islam Bandung Hospital Indonesia, in providing Hepatocellular Carcinoma (HCC) datasets.

REFERENCES

1. A. Gerbes *et al.*, "Gut roundtable meeting paper: selected recent advances in hepatocellular carcinoma," *Gut*, vol. 67, no. 2, p. 380, 2018, doi: 10.1136/gutjnl-2017-315068.
2. L. Qiu *et al.*, "Circular RNA Signature in Hepatocellular Carcinoma," *Journal of Cancer*, Research Paper vol. 10, no. 15, pp. 3361-3372, 2019, doi: 10.7150/jca.31243.
3. J. D. Yang and J. K. Heimbach, "New advances in the diagnosis and management of hepatocellular carcinoma," *BMJ*, vol. 371, p. m3544, 2020, doi: 10.1136/bmj.m3544.
4. A. Sangiovanni *et al.*, "Increased survival of cirrhotic patients with a hepatocellular carcinoma detected during surveillance," *Gastroenterology*, vol. 126, no. 4, pp. 1005-1014, 2004/04/01/ 2004, doi: 10.1053/j.gastro.2003.12.049.
5. M. I. A. Edoo *et al.*, "Serum Biomarkers AFP, CEA and CA19-9 Combined Detection for Early Diagnosis of Hepatocellular Carcinoma," (in eng), *Iran J Public Health*, vol. 48, no. 2, pp. 314-322, 2019. [Online]. Available: https://pubmed.ncbi.nlm.nih.gov/31205886.
6. J. Zhang *et al.*, "Overexpression of Epcam and CD133 Correlates with Poor Prognosis in Dual-phenotype Hepatocellular Carcinoma," (in eng), *Journal of Cancer*, vol. 11, no. 11, pp. 3400-3406, 2020, doi: 10.7150/jca.41090.
7. F. Ciocchetta, F. Demichelis, and A. Sboner, "Machine learning methods to understand hepatocellular carcinoma pathology," 01/01 2003.
8. H. Lin *et al.*, "Automated classification of hepatocellular carcinoma differentiation using multiphoton microscopy and deep learning," *Journal of Biophotonics*, vol. 12, no. 7, p. e201800435, 2019/07/01 2019, doi: 10.1002/jbio.201800435.
9. H. Liao *et al.*, "Deep learning-based classification and mutation prediction from histopathological images of hepatocellular carcinoma," *Clinical and Translational Medicine*, vol. 10, no. 2, p. e102, 2020/06/01 2020, doi: 10.1002/ctm2.102.
10. R. Khairi, Z. Rustam, and S. Utama, "Possibilistics C-Means (PCM) Algorithm for the Hepatocellular Carcinoma (HCC) Classification," in *IOP Conference Series: Materials Science and Engineering*, 2019, vol. 546, 5 ed., doi: 10.1088/1757-899X/546/5/052038.
11. K. Zhang, "A three-way c-means algorithm," *Applied Soft Computing*, vol. 82, p. 105536, 2019/09/01/ 2019, doi: 10.1016/j.asoc.2019.105536.
12. J. C. Bezdek, R. Ehrlich, and W. Full, "FCM: The fuzzy c-means clustering algorithm," *Computers & Geosciences*, vol. 10, no. 2, pp. 191-203, 1984/01/01/ 1984, doi: 10.1016/0098-3004(84)90020-7.
13. N. Cristianini and J. Shawe-Taylor, *An introduction to support Vector Machines: and other kernel-based learning methods*. Cambridge University Press, 1999.
14. L. Liu, B. Shen, and X. Wang, "Research on Kernel Function of Support Vector Machine," in *Advanced Technologies, Embedded and Multimedia for Human-centric Computing. Lecture Notes in Electrical Engineering*, vol. 260, Y. M. Huang, H. C. Chao, D. J. Deng, and J. Park Eds.: Springer, Dordrecht, 2013.

3rd INTERNATIONAL CONFERENCE
ON MATHEMATICAL AND RELATED SCIENCES:
CURRENT TRENDS AND DEVELOPMENTS
ICMRS 2020

20-22 NOVEMBER, 2020

Differential *LG*-game of Many Pursuers and One Evader

Bahrom SAMATOV[1], Mahmud HORILOV[1] and Ulmasjon SOYIBBOEV[1]

[1]*Department of Mathematical analysis, Faculty of Mathematics,*
Namangan State University, Namangan-UZBEKISTAN

samatov57@inbox.ru
mxorilov86@mail.ru
ulmasjonsoyibboev@gmail.com

Abstract. In this article, we have considered a simple motion differential game of m pursuers and one evader in R^n. Here controls of the pursuers are subjected to linear constraints which is the generalization of both integral and geometrical constraints, and control of the evader is subjected to a geometrical constraint. To solve a pursuit problem, the attainability domain of each pursuer has been constructed and therefore, necessary and sufficient conditions have been obtained by intersection of them.

1. INTRODUCTION

Differential games were initiated by Isaacs [23]. Fundamental results were obtained by Bercovitz [6]–[7], Basar [4]-[5], Chikrii [9], Elliot and Kalton [10], Fleming [11]–[12], Friedman [13], Hajek [15]–[16], Ho, Bryson and Baron [17], Pontryagin [27], Krasovskii [24], Petrosjan [26], Pshenichnyi [28]–[29], Subbotin [36]–[37] and others. The book of Isaacs [23] contains many specific game problems that were discussed in details and proposed for further study. One of them is the "Life-line" problem, which rather was comprehensively studied by Petrosjan [26] by approximating measurable controls with most efficient piecewise constant controls that presents the strategy of parallel approach. Later this strategy was called Π-strategy. The strategies proposed in [1], [26], [28] for a simple motion pursuit game with geometrical constraints became the starting point for the development of the pursuit methods in games with multiple pursuers (see e.g. [2], [14], [30]–[34]). A relay pursuit-evasion problem with two pursuers and one evader was studied [36]. The problem is reduced to one pursuer and one evader problem subject to a state constraint. To prolong the capture time, a suboptimal control strategy for the evader was proposed. A relay-pursuit strategy was applied in [3], according to which only one pursuer is assigned to go after the evader at every instant of time. The paper of [35] is devoted to capturing the evader in the shortest time. The Apollonius circles formed by the evader and each pursuer are used to analyze how the evader can find a better strategy to escape or prolong the capture time. The constructing of optimal strategies of players and finding the value of the game are difficult and important problems of differential games. Pashkov and Terekhov [25] studied a simple motion differential game of optimal approach of two pursuers and one evader. In the case where maximal speeds of pursuers are equal, optimal strategies of players were constructed. The works [19–23] are devoted to a simple motion differential game of k pursuers and one evader.

At the present time there are more than a hundred monographs on the theory. Nevertheless, completely solved samples of Differential Games are quite few. This work is devoted to the Pursuit problem when linear constraints which are the generalization of integral as well as geometrical constraints are imposed on the pursuers' control class and only a geometrical constraint is imposed on the evader's control class and here it is studied in the term of winning of the pursuer.

2. STATEMENT OF THE PROBLEM

Consider the differential game when Pursuer $\mathbf{X}_i$, $i=1,2,...,m$ and Evader $\mathbf{Y}$. having radius vectors x_i and y correspondingly move in R^n. If their velocity vectors are u_i and v then the game will be described by the equations:

$$\dot{x}_i = u_i, \quad x_i(0) = x_{i0}, \tag{2.1}$$

$$\dot{y} = v, \quad y(0) = y_0, \tag{2.2}$$

where $x_i, y, u_i, v \in R^n$, $n \geq 1$ and x_{i0}, y_0 are the initial positions of the objects $\mathbf{X}_i$ and $\mathbf{Y}$. Here the temporal variation of u_i must be a measurable function $u_i(\cdot):[0,\infty) \to R^n$, we impose a constraint of the form

$$\int_0^t |u_i(s)|^2 \, ds \leq L_i(t), \quad t \geq 0, \tag{2.3}$$

admitting a linear change $L_i(t) = k_i t + \rho_{i0}$ in the time t, where k_i is arbitrary and ρ_{i0} is a nonnegative numbers. From the physical point of view, the right-hand of inequality (2.3) corresponds to the linear change of the given resource depending on the time $t \geq 0$. Therefore, the linear function $L_i(t)$ can be called a current change of the given resource of the Pursuers $\mathbf{X}_i$. Clearly, this resource increases if $k_i > 0$, decreases if $k_i < 0$ and remains unchanged if $k_i = 0$. In the last case, constraint (2.3) is called an Integral constraint. If $\rho_{i0} = 0$ and $k_i > 0$, then constraint (2.3) can be called a Geometrical constraint.

We call inequality (2.3) as $L-$*constraint* (Linear constraint) and denote by U_L^i the class of admissible controls, i.e., of all measurable functions satisfying the $L-$constraint.

Similarly, the temporal variation of v must be a measurable function $v(\cdot):[0,\infty) \to R^n$, and on this vector-function, we impose a geometrical constraint (briefly, $G-$constraint)

$$|v(t)| \leq \beta \quad \text{for almost every } t \geq 0, \tag{2.4}$$

where β is a nonnegative parametric number which means the maximal velocity of the evader. We denote by V_G the class of the evader's admissible controls satisfying constraint (2.4).

In the *LG*-game (2.1)–(2.4), the objective of the Pursuer $\mathbf{X}_i$ is to catch the Evader $\mathbf{Y}$, i.e., reach the equality $x_i(t) = y(t)$, where $x_i(t)$ and $y(t)$ are trajectories generated during the game. The notion of a "trajectories generated during the game" requires clarification. the Evader $\mathbf{Y}$ tries to avoid an encounter, and if it is impossible, postpone the moment of the encounter as far as possible. Naturally, this is a preliminary problem setting.

Here we are going to study mainly the game with phase constraints for the Evader being given by a subset A of R^n which is called the "Life-line" [23] (for the Evader naturally). Notice that in the case $A = \varnothing$ we have a simple *LG*-game .

Definition 1. *By the equations and initial conditions in (2.1)–(2.2), any pairs* $(x_{i0}, u_i(\cdot))$, $u_i(\cdot) \in U_L^i$ *and* $(y_0, v(\cdot))$, $v(\cdot) \in V_G$ *generate the trajectories*

$$x_i(t) = x_{i0} + \int_0^t u_i(s)\, ds, \qquad y(t) = y_0 + \int_0^t v(s)\, ds \tag{2.5}$$

respectively. In this case $x_i(t)$ *is called the pursuer's motion trajectory and* $y(t)$ *is called the evader's motion trajectory.*

Definition 2. *For each triple* $(k_i, \rho_{i0}, u_i(\cdot))$, $u_i(\cdot) \in U_L^i$ *the scalar quantity*

$$\rho_i(t) = L_i(t) - \int_0^t |u_i(s)|^2 \, ds, \quad \rho_i(0) = \rho_{i0}, \quad t \geq 0 \tag{2.6}$$

is called the residual pursuer resource at a time moment t .

Definition 3. *The map* $u_i(\cdot): V_G \to U_L^i$ *is called the strategy for* $\mathbf{X}_i$ *if the following properties hold:*

1^o. *(Admissibility.) For every* $v(\cdot) \in V_G$, *the inclusion* $u_i(\cdot) = u_i[v(\cdot)] \in U_L^i$ *is valid.*

2^o. *(Volterranianity.) For every* $v_1(\cdot), v_2(\cdot) \in V_G$ *and* $t \geq 0$, *the equality* $v_1(s) = v_2(s)$ *a.e. on* $[0, t]$ *implies* $u_{i_1}(s) = u_{i_2}(s)$ *a.e. on* $[0, t]$ *with* $u_i(\cdot) = u_i[v(\cdot)] \in U_L^i$, $i = 1, 2, \ldots, m$.

Definition 4. *A strategy* $u_i(v)$ *is called winning for* $\mathbf{X}_i$ *on the interval* $[0,T]$ *in the LG-game, if for every* $v(\cdot)\in V_G$ *there exists a moment* t^* Î $[0,T]$ *that holds the equality* $x_i(t^*) = y(t^*)$.

Definition 5. *Assume that* y_0 Ï $\bar{A}$ Ì R^n *and a strategy* $u_i(v)$ *is winning for some* $\mathbf{X}_i$ *on the interval* $[0,T]$, *while* $\mathbf{Y}$ *stays in the zone* $R^n \setminus \bar{A}$ *i.e.,* $y_t(\cdot) = \{y(s): 0 \le s \le t\} \subset \bar{A}$ *and* $t \in [0,T]$. *Then the "Life-line" LG -game is called winning for the players* $\mathbf{X}_i$, $i = 1,2,...,m$ *on the interval* $[0,T]$.

Notice that $\bar{A}$ doesn't restrict any motion of $\mathbf{X}_i$. Here $\bar{A}$ is the closure of the set $A \subset R^n$.

Let $x_{i0} \neq y_0$ and the current value of control $v(t)$, $t \ge 0$ is given, where $v(\cdot)\in V_G$. Suppose that the triple (μ_{i0}, k_i, β) is a parametric state of the *LG*-game and denoted it by p_i. We find the following nonempty simply connected set of such states p_i

$$\mathbf{P}^i_{LG} = \mathbf{P}^i_1 \cup \mathbf{P}^i_2 \cup \mathbf{P}^i_3$$

where

$$\mathbf{P}^i_1 = \{p_i : \mu_{i0} \ge 0,\ k_i > \beta^2,\ \beta \ge 0\},$$
$$\mathbf{P}^i_2 = \{p_i : \mu_{i0} > 2\beta,\ k_i = \beta^2,\ \beta \ge 0\},$$
$$\mathbf{P}^i_3 = \{p_i : \mu_{i0} \ge 2\left(\beta + \sqrt{\beta^2 - k_i}\right),\ k_i < \beta^2,\ \beta \ge 0\}$$

and $\mathbf{P}^i_1$, $\mathbf{P}^i_2$, $\mathbf{P}^i_3$ are mutually disjoint sets.

Definition 6. *The function*

$$u_i(v) = v - \lambda_i(v)\xi_{i0} \qquad (2.7)$$

is called the strategy of parallel pursuit (*briefly,* $P^{\,i}_{LG}$*-strategy*) *for* $\mathbf{X}_i$ *in the LG-game, where* $\lambda_i(v) = \mu_{i0}/2 + \langle v, \xi_{i0}\rangle + \sqrt{\left(\mu_{i0}/2 + \langle v, \xi_{i0}\rangle\right)^2 + k_i - |v|^2}$, $\xi_{i0} = z_{i0}/|z_{i0}|$, $z_{i0} = x_{i0} - y_0$, $\mu_{i0} = \rho_{i0}/|z_{i0}|$.

Property 1. *The scalar function* $\lambda_i(v)$ *is positively determined and continious in* $|v| \le \beta$ *for every* $p_i \in \mathbf{P}^i_{LG}$.

Property 2. *If* $p_i \in \mathbf{P}^i_{LG}$, *then for* $P^{\,i}_{LG}$*-strategy, the equality*

$$|u_i(v)|^2 = k_i + \mu_{i0}\lambda_i(v). \qquad (2.8)$$

holds.

In [32], B.T.Samatov proved the following statements for the *LG* -game of one pursuer and one evader.

Theorem 1. *If in the LG -game,* $p \in \mathbf{P}_{LG}$ *and pursuer* $\mathbf{X}$ *apply* P_{LG}*-strategy then the equalities*

$$\rho(t) = \Lambda_{LG}(t, v(\cdot))\rho_0, \quad t \in [0, t^*], \qquad (2.9)$$
$$z(t) = x(t) - y(t) = \Lambda_{LG}(t, v(\cdot))z_0 \qquad (2.10)$$

hold, where $\Lambda_{LG}(t, v(\cdot)) = 1 - \frac{1}{|z_0|}\int_0^t \lambda(v(s))ds$ *is a scalar continuous monotone decreasing function with* t, $t \ge 0$, $t^* = min\{t : z(t) = 0\}$.

Theorem 2. *Let* $p \in \mathbf{P}_{LG}$ *in the LG –game. Then* P_{LG}*-strategy is winning on the time interval* $[0, T_{LG}]$, *where* $T_{LG} = |z_0|/\lambda_{LG}$ *and* $\lambda_{LG} = \mu_0/2 - \beta + \sqrt{(\mu_0/2 - \beta)^2 + k - \beta^2}$.

3. MAIN RESULTS

Let the conditions of Theorem 1 and Theorem 2 hold. We suppose that in the moment t, $t^3\ 0$ the evader $\mathbf{Y}$ moves from a position y holding a constant vector v, $|v|£\ b$. The pursuers $\mathbf{X}_i$ use Π^i_{LG} – strategy from a position x_i basing on the resource ρ_i, $\rho_i > 0$. Then w is a point where the pursuers $\mathbf{X}_i$ should meet the evader $\mathbf{Y}$. The set of all such points w will be given by relations:

$$|w-x_i| = T|u_i(v)|, \qquad |w-y| = T|v|, \qquad T|u_i(v)|^2 = k_i T + \rho_i, \quad T>0$$

and from these relations we find

$$W^i_{LG}(x_i, y, \rho_i) = \left\{w : |w-x_i|^2 \ge (k_i/\beta^2)|w-y|^2 + (\rho_i/\beta)|w-y|\right\}. \tag{3.1}$$

Theorem 3. *If* $p_i \in \mathbf{P}^i_{LG}$ *in the LG -game (2.1)-(2.4), then*

$$W^i_{LG}(t) = x_i(t) + \Lambda_i(t, v(\cdot))[W^i_{LG}(0) - x_{i0}], \quad t \in [0, t^*_i], \tag{3.2}$$

where $W^i_{LG}(t) = W^i_{LG}(x_i(t), y(t), r_i(t))$, $t^*_i = \min\{t : z_i(t) = 0\}$, $i = 1, 2, ..., m$ *and*

$$W^i_{LG}(0) = \left\{w : |w-x_{i0}|^2 \ge (k_i/\beta^2)|w-y_0|^2 + (\rho_{i0}/\beta)|w-y_0|\right\}.$$

Proof. Consider the situation when $\mathbf{X}_i$ holds the Π^i_{LG} – strategy while $\mathbf{Y}$ on $[0, t^*_i]$ applies any control $v(\cdot) \in V_G$. Assume that $x_i(t)$, $y(t)$ are the current positions of players and $\rho_i(t)$ is the current resource of the pursuer. Then from (2.9) and (3.1) we have

$$W^i_{LG}(t) - x_i(t) = \left\{w : |w|^2 \ge (k_i/\beta^2)|w + z_i(t)|^2 + (\rho_i(t)/\beta)|w + z_i(t)|\right\} =$$

$$= \left\{w : |w|^2 \ge (k_i/\beta^2)|w + \Lambda_i(t, v(\cdot))z_{i0}|^2 + (\Lambda_i(t, v(\cdot))\rho_{i0}/\beta)|w + \Lambda_i(t, v(\cdot))z_{i0}|\right\} =$$

$$= \left\{w : |w/\Lambda_i(t, v(\cdot))|^2 \ge (k_i/\beta^2)|w/\Lambda_i(t, v(\cdot)) + z_{i0}|^2 + \right.$$

$$\left. + (\rho_{i0}/\beta)|w/\Lambda_i(t, v(\cdot)) + z_{i0}|\right\} = \Lambda_i(t, v(\cdot))[W^i_{LG}(0) - x_{i0}].$$

Property 3. *If* $p_i \in \mathbf{P}^i_{LG}$, *then for* $W^i_{LG}(t)$ *is a convex set on* $[0, t^*_i]$.

Theorem 4. *Let* $p_i \in \mathbf{P}^i_{LG}$ *in the LG -game (2.1)-(2.4). Then the relation*

$$W^i_{LG}(t_2) \subset W^i_{LG}(t_1) \tag{3.3}$$

is true for $\forall t_1, t_2 \in [0, t^*]$, $0 \le t_1 \le t_2$.

P r o o f. From (2.8) we have

$$\left|v|z_{i0}| - \lambda_i(v)z_{i0}\right|^2 = k_i|z_{i0}|^2 + \lambda_i(v)\rho_{i0}|z_{i0}|.$$

Then from $|v(t)| \le \beta$ and Property 1 we obtain

$$\left|(v|z_{i0}|/\lambda_i(v) + y_0) - x_{i0}\right|^2 \ge (k_i/\beta^2)\left|(v|z_{i0}|/\lambda_i(v) + y_0) - y_0\right|^2 +$$

$$+ (\rho_{i0}/\beta)\left|(v|z_{i0}|/\lambda_i(v) + y_0) - y_0\right|$$

or

$$v|z_{i0}|/\lambda_i(v) + y_0 \in W^i_{LG}(0) \tag{3.4}$$

Using properties of the supporting function $F(W, p) = \sup_{w \in W} \langle w, p_i \rangle$ in [8] and from (3.4) we have

$$\langle v|z_{i0}|/\lambda_i(v) + y_0, \psi\rangle \le F(W^i_{LG}(0), \psi) \Rightarrow$$

$$\Rightarrow \langle v, \psi\rangle - \frac{1}{|z_{i0}|}\lambda_i(v)F(W^i_{LG}(0) - y_0, \psi) \le 0 \tag{3.5}$$

for all $\psi \in R^n$, $|\psi| = 1$. From (1.1), (1.7), (3.2) and (3.4) we have

$$F(W_{LG}^i(t), \psi) = \langle x_i(t), \psi \rangle + \Lambda_i(t, v(\cdot)) F(W_{LG}^i(0) - x_{i0}, \psi) \Rightarrow$$

$$\Rightarrow \frac{d}{dt} F(W_{LG}^i(t), \psi) = \langle \dot{x}_i(t), \psi \rangle - \frac{1}{|z_{i0}|} \lambda_i(v) F(W_{LG}^i(0) - x_{i0}, \psi) =$$

$$= \langle v - \lambda_i(v)\xi_{i0}, \psi \rangle - \frac{1}{|z_{i0}|} \lambda_i(v) F(W_{LG}^i(0) - x_{i0}, \psi) =$$

$$= \langle v, \psi \rangle - \frac{1}{|z_{i0}|} \lambda_i(v) F(W_{LG}^i(0) - y_0, \psi) \le 0 .$$

Property 4. *If* $p_i \in \mathbf{P}_{LG}^i$, *then inclusion* $y(t) \in W_{LG}^i(0)$ *is valid on the time interval* $t \in [0, t_i^*]$.

Theorem 5. *If in the LG -game* $p_i \in \mathbf{P}_{LG}^i$ *hold for some* $i = 1, 2, ..., m$, *then* $y(t) \in W_{LG}$ *on the time interval* $[0, T_{LG}]$, *where* $W_{LG} = \bigcap_{i=1}^{m} W_{LG}^i(0)$, $T_{LG} = d / \beta$, $d = \max\{|w_1 - w_2| : w_1, w_2 \in W_{LG}\}$.

P r o o f. This follows from Theorems 2-4 and Property 4.

Theorem 6. *If* $W_{LG} \cap A = \varnothing$, *then in the "Life-line" LG –game, the players* $\mathbf{X}_i$, $i = 1, 2, ..., m$ *win on the interval* $[0, T_{LG}]$.

P r o o f. This follows from Theorem 5.

4. GEOMETRICAL REPRESENTATIONS

We will show geometrical representation of the set boundary of attainability points of the LG -game for some $i = 1, 2, ..., m$ in some particular cases in R^2.

1. Let $p_i \in \mathbf{P}_1^i$, $x_{i0} = (0, 0)$, $y_0 = (1, 0)$, $k_i = 2$, $\beta = 1$, $\rho_{i0} = 1$, then we have the below equation for some $\mathbf{X}_i$ from (3.1) at $t = 0$

$$x_i^2 + y^2 = 2((x_i - 1)^2 + y^2) + \sqrt{(x_i - 1)^2 + y^2}$$

and its smooth line consists of Cartesian's oval (Picture-1).

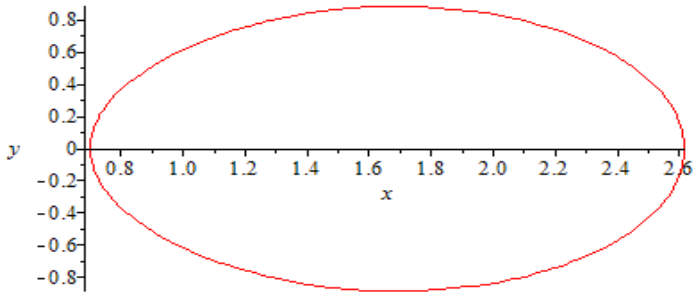

Picture-1

2. If $p_i \in \mathbf{P}_2^i$, $x_{i0} = (0, 0)$, $y_0 = (1, 0)$, $\beta = 1$, $\rho_{i0} = 3$, then its equation

$$(25/9) \cdot (x_i - 7/5)^2 + 5y^2 = 1$$

and its smooth line consists of Ellipse (Picture-2).

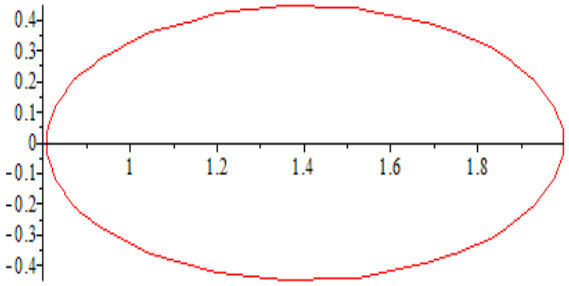

Picture-2

3. If $p_i \in \mathbf{P}_3^i$, $x_{i0} = (0,0)$, $y_0 = (1,0)$, $k_i = \frac{3}{4}$, $\beta = 1$, $\rho_{i0} = 3$, then its equation

$$x_i^2 + y^2 = \frac{3}{4}((x_i - 1)^2 + y^2) + 3\sqrt{(x_i - 1)^2 + y^2}$$

and its smooth line consists of the inner loop of Pascal's snail (Picture-3).

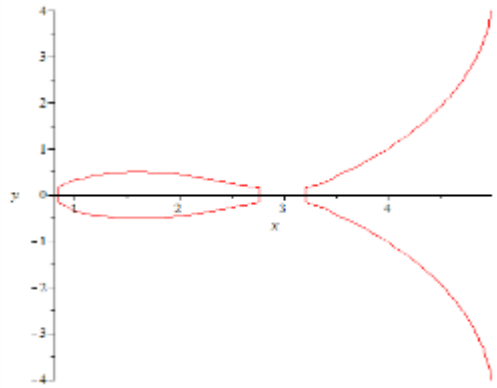

Picture-3

REFERENCES

1. A. A. Azamov, On the quality problem for simple pursuit games with constraint. Serdica Bulgariacaemath. Publ.Sofia, 1986, 12(1), 38–43.
2. A. A. Azamov and B.T.Samatov, The Π-Strategy: Analogies and Applications. The Fourth International Conference Game Theory and Management, St.Petersburg, 2010, 33–47.
3. E. Bakolas and P. Tsiotras, On the relay pursuit of a maneuvering target by a group of pursuers. In 50th IEEE Conference on Decision and Control and European Control Conference, Orlando, FL, 2011, pp. 4270–4275.
4. T. Basar, Stochastik differential games and intricacy of information structures. Dynamic Games in Economics- Springer, 2014, pp. 23-49.
5. T. Basar and P. Bernhard, H-infinity optimal control and related mini-max design problems: a dynamic game approach. - Boston: Birkhauser, pp. 428. 1995.
6. L. D. Berkovitz A Survey of Differential Games, Mathematical Theory of Control. New York, Academic Press 373–385. 1967.
7. L. D. Berkovitz, Differential game of generalized pursuit and evasion. SIAM J. Contr. 1986, 24(3), 361–373.
8. V. I. Blagodatskikh, Introduction to optimal control. Linear theory. Moscow. Graduate School. 2001.
9. A. A. Chikrii, Conflict-Controlled Processes. Kluwer, Dordrecht. 1997.

10. R. J. Elliot and N. J. Kalton, The Existence of Value for Differential Games. American Mathematical Soc. 1972.
11. W. H. Fleming, A note on differential games of prescribed duration. Contributions to the Theory of Games. 1957, Vol.3, 407–416.
12. W. F. Fleming, The convergence problem for differential games. J. Math. Anal. Appl. 1961, Vol.3, 102–116.
13. A. Friedman, Differential Games. Wiley Interscience, New York. 1971.
14. N. L. Grigorenko, Mathematical Methods of Control for Several Dynamic Processes. Izdat. Gos. Univ., Moscow. 1990.
15. O. Hajek, Pursuit games. New York, Academic Press. 1975.
16. O. Hajek, Pursuit Games: An Introduction to the Theory and Applications of Differential Games of Pursuit and Evasion, Dove. Pub. New York. 2008.
17. Ho Y. Bryson and A. S. Baron, Differential games and optimal pursuit-evasion strategies. IEEE Trans Autom Control, 1965, 10: 385-389.
18. G. I. Ibragimov, On the optimal pursuit game of several pursuers and one evader. Prikladnaya Matematika i Mekhanika. 2008, 62(2): 199–205.
19. G. I. Ibragimov, Optimal pursuit with countable many pursuers and one evader, Differential Equations, 2005, 41(5): 627–635.
20. G. I. Ibragimov, The optimal pursuit problem reduced to an infinite system of differential equations. J. Appl. Maths Mekhs. 2013, 77(5): 470–476.
21. G. I. Ibragimov, Optimal pursuit time for a differential game in the Hilbert space *l*2. ScienceAsia, 2013, 39S: 25– 30.
22. G. I. Ibragimov and N. Abd Rasid and A. Sh. Kuchkarov and F. Ismail, Multi pursuer differential game of optimal approach with integral constraints on controls of players. Taiwanese Journal of Mathematics, 19(3):963–976, Doi: 10.11650/tjm.19. 2015. 2288.
23. R. Isaacs, Differential games. John Wiley and Sons, New York. 1965.
24. N. N. Krasovskii, A. I. Subbotin, Positional Differential Games. Nauka, Moscow. (in Russian), 1974.
25. A. G. Pashkov and S. D. Terekhov, A differential game of approach with two pursuers and one evader. Journal of Optimization Theory and Applications, 1987, 55(2): 303–311.
26. L. A. Petrosjan, Differential games of pursuit. Series on optimization, Vol.2. World Scientific Poblishing, Singapore. 1993.
27. L. S. Pontryagin , Selected Works. MAKS Press, Moscow. 2004.
28. B. N. Pshenichnyi, Simple pursuit by several objects. Cybernetics and System Analysis. 1976, 12(3): 484-485. DOI 10.1007/BF01070036.
29. B. N. Pshenichnyi and A. A. Chikrii and J. S. Rappoport, An efficient method of solving differential games with many pursuers, Dokl. Akad. Nauk SSSR 1981, 256, 530–535. (in Russian).
30. B. T. Samatov, On a Pursuit-Evasion Problem under a Linear Change of the Pursuer Resource. Siberian Advances in Mathematics, Allerton Press, Inc.Springer. New York, 2013, 23(4): 294–302.
31. B. T. Samatov, The Pursuit- Evasion Problem under Integral-Geometric constraints on Pursuer controls. Automation and Remote Control, Pleiades Publishing, Ltd. New York. 2013, 74(7): 1072–1081.
32. B. T. Samatov, The Π-strategy in a differential game with linear control constraints. J. Appl. Maths and Mechs, Elsevier. Netherlands. 2014, 78(3): 258–263.
33. B. T. Samatov, Problems of group pursuit with integral constraints on controls of the players I. Cybernetics and Systems Analysis, 2013, 49(5): 756–767.
34. B. T. Samatov, Problems of group pursuit with integral constraints on controls of the players II. Cybernetics and Systems Analysis. 2013, 49(6): 907–924.
35. J. Shiyuan and Q. Zhihua, Pursuit-evasion games with multi-pursuer vs. one fast evader. Proceedings of the 8th World Congress on Intelligent Control and Automation: 2010, 3184–3189.
36. A. I. Subbotin and A. G. Chentsov, Optimization of Guaranteed Result in Control Problems. Nauka, Moscow. 1981.
37. A. I. Subbotin, Generalization of the Main Equation of Differential Game Theory, Journal of Optimization Theory and Applications, 1984, 43(1): 103–133.
38. W. Sun and P. Tsiotras, An optimal evader strategy in a two-pursuer one-evader problem, Proc. 53rd IEEE Conf. Decision and Control, Los Angeles, CA, 2014, 4266–4271.

Partial Sums of the Bessel-Struve Kernel Function

Sercan KAZIMOĞLU[1], Erhan DENİZ[1] and Murat ÇAĞLAR[1]

[1]*Department of Mathematics, Faculty of Science and Arts,*
Kafkas University, Kars-TURKEY

srcnkzmglu@gmail.com
edeniz36@gmail.com
mcaglar25@gmail.com

Abstract. Let $(B_\nu)_n(z) = z + \sum_{m=1}^{n} b_m z^{m+1}$ be the sequence of partial sums of normalized Bessel-Struve kernel function $B_\nu(z) = z + \sum_{m=1}^{\infty} b_m z^{m+1}$. The purpose of the present paper is to determine lower bounds for $\Re\left\{\frac{B_\nu(z)}{(B_\nu)_n(z)}\right\}$, $\Re\left\{\frac{(B_\nu)_n(z)}{B_\nu(z)}\right\}$, $\Re\left\{\frac{B'_\nu(z)}{(B_\nu)'_n(z)}\right\}$ and $\Re\left\{\frac{(B_\nu)'_n(z)}{B'_\nu(z)}\right\}$.

1. INTRODUCTION

Let A denote the class of functions of the form:

$$f(z) = z + \sum_{n=2}^{\infty} a_n z^n,$$

which are analytic in the open unit disk

$$U = \{z : |z| < 1\}.$$

We denote by S the class of all functions in A which are univalent in *U*.
The function J_ν, known as the Bessel function of the first kind of order ν, is a particular solution of the second order Bessel differential equation

$$z^2 y''(z) + z y'(z) + \left(z^2 - \nu^2\right) y(z) = 0.$$

This function has the power series representation

$$J_\nu(z) = \sum_{n=0}^{\infty} \frac{(-1)^n}{n!\Gamma(n+\nu+1)} \left(\frac{z}{2}\right)^{2n+\nu}. \tag{1.1}$$

On the other hand the modified Bessel function $I_\nu(z)$ is the particular solution of the differential equation

$$z^2 y''(z) + z y'(z) - \left(z^2 - \nu^2\right) y(z) = 0,$$

and have the series representation

$$I_\nu(z)=\sum_{n=0}^{\infty}\frac{1}{n!\Gamma(n+\nu+1)}\left(\frac{z}{2}\right)^{2n+\nu}, \tag{1.2}$$

The Struve function of order ν given by

$$H_\nu(z):=\sum_{n=0}^{\infty}\frac{(-1)^k}{\Gamma\left(n+\frac{3}{2}\right)\Gamma\left(n+\nu+\frac{3}{2}\right)}\left(\frac{z}{2}\right)^{2n+\nu+1} \tag{1.3}$$

is a particular solution of the non-homogeneous Bessel differential equation

$$z^2y''(z)+zy'(z)+\left(z^2-\nu^2\right)y(z)=\frac{4\left(\frac{z}{2}\right)^{\nu+1}}{\sqrt{\pi}\Gamma\left(\nu+\frac{1}{2}\right)}. \tag{1.4}$$

A solution of the non-homogeneous modified Bessel equation

$$z^2y''(z)+zy'(z)-\left(z^2+\nu^2\right)y(z)=\frac{4\left(\frac{z}{2}\right)^{\nu+1}}{\sqrt{\pi}\Gamma\left(\nu+\frac{1}{2}\right)}, \tag{1.5}$$

yields the modified Struve function

$$\begin{aligned} L_\nu(z) &= -ie^{\frac{i\nu\pi}{2}}H_\nu(iz) \\ &= \sum_{n=0}^{\infty}\frac{1}{\Gamma\left(n+\nu+\frac{3}{2}\right)\Gamma\left(n+\frac{3}{2}\right)}\left(\frac{z}{2}\right)^{2n+\nu+1}. \end{aligned} \tag{1.6}$$

The Struve functions occur in areas of physics and applied mathematics, for example, in water-wave and surface-wave problems [1], as well as in problems on unsteady aerodynamics [12]. The Struve functions are also important in particle quantum dynamical studies of spin decoherence [11] and nanotubes [10].

Consider the Bessel-Struve kernel function B_ν defined on the unit disk $U=\{z:|z|<1\}$ as

$$\mathrm{B}_\nu(z):=j_\nu(iz)-ih_\nu(iz),\quad \nu>-\frac{1}{2}, \tag{1.7}$$

where, $j_\nu(z):=2^\nu z^{-\nu}\Gamma(\nu+1)J_\nu(z)$ and $h_\nu(z):=2^\nu z^{-\nu}\Gamma(\nu+1)H_\nu(z)$ are respectively known as the normalized Bessel functions and the normalized Struve functions of first kind of order ν. The Bessel-Struve transformation and Bessel-Struve kernel functions are appeared in many article. In [6], Hamem et. al. studies an analogue of the Cowling's Price theorem for the Bessel-Struve transform defined on real domain and also provide Hardy type theorem associated with this transform. The Bessel-Struve intertwining operator on is considered in [4, 7]. The fock space of the Bessel-Struve kernel functions is discussed in [4, 8].

The kernel $z \mapsto \mathrm{B}_\nu(\gamma z),\ \gamma \in \square$ is the unique solution of the initial value problem

$$\mathrm{L}_\nu u(z) = \lambda^2 u(z), \quad u(0) = 1,\ u'(0) = \frac{\lambda \Gamma(\nu+1)}{\sqrt{\pi}\Gamma\left(\nu+\frac{3}{2}\right)}. \tag{1.8}$$

Here L_ν, $\nu > -1/2$ is the Bessel-Struve operator given by

$$\mathrm{L}_\nu\left(u(z)\right) := \frac{d^2u}{dz^2}(z) + \frac{2\nu+1}{z}\left(\frac{du}{dz}(z) - \frac{du}{dz}(0)\right). \tag{1.9}$$

Now from (1.1) and (1.6), it is evident that B_ν (taking $\gamma = 1$) possesses the power series

$$\mathrm{B}_\nu := \sum_{n=0}^{\infty} \frac{\Gamma(\nu+1)\Gamma\left(\frac{n+1}{2}\right)}{\sqrt{\pi}n!\Gamma\left(\frac{n}{2}+\nu+1\right)} z^n. \tag{1.10}$$

The identity (1.8) and (1.9) together imply that B_ν satisfy the differential equation

$$z^2 g_\nu''(z) + (2\nu+1) g_\nu'(z) - z g_\nu(z) = zM \tag{1.11}$$

where $M = \dfrac{2\Gamma(\nu+1)}{\sqrt{\pi}\Gamma(\nu+1/2)}$.

Another significance is that B_ν can be express as the sum of the modified Bessel and the modified Struve function of first kind of order ν. For the sake of completeness, in the following result we established this relation.

Proposition 1.1. For $\nu > 0$, the following identity holds:

$$z^\nu \mathrm{B}_\nu(z) = 2^\nu \Gamma(\nu+1)\left(I_\nu(z) + L_\nu(z)\right).$$

The function B_ν have the following recurrence relation which is useful in sequel.

Proposition 1.2. For $\nu > 0$, the following recurrence relation holds for B_ν:

$$z\mathrm{B}_\nu'(z) = 2\nu \mathrm{B}_{\nu-1}(z) - 2\nu \mathrm{B}(z). \tag{1.12}$$

Due to the function defined by (1.10) does not belong to the class A, we consider following normalized form of the Bessel-Struve kernel functions.
For $\nu > 0$, $z \in U$, in [2], authors studied some geometric properties of following normalized Bessel-Struve kernel function

$$B_\nu(z) = zB_\nu(z) = 2\left(\sum_{m=0}^{\infty}\frac{\Gamma(\nu+1)}{\Gamma(m+\nu+1)m!}\left(\frac{z}{2}\right)^{2m+1}+\sum_{m=0}^{\infty}\frac{\Gamma(\nu+1)}{\Gamma(m+3/2)\Gamma(m+\nu+3/2)}\left(\frac{z}{2}\right)^{2m+2}\right)$$
$$= \sum_{m=0}^{\infty}\frac{1}{2^{2m}m!(\nu+1)_m}z^{2m+1}+\sum_{m=0}^{\infty}\frac{1}{(3/2)_m\left(\nu+\frac{3}{2}\right)_m 2^{2m+1}}z^{2m+2}, \quad (1.13)$$

where $(\lambda)_\mu$ is Pochhammer symbol (or the shifted factorial) defined, for $\lambda,\mu\in\mathbb{C}$ and in terms of the Euler-Gamma function, by

$$(\lambda)_\mu = \frac{\Gamma(\lambda+\mu)}{\Gamma(\lambda)} = \begin{cases} 1 & (\mu=0;\ \lambda\in\mathbb{C}-\{0\}) \\ \lambda(\lambda+1)...(\lambda+n-1) & (\mu=n\in\mathbb{N};\ \lambda\in\mathbb{C}) \end{cases}.$$

For various interesting developments concerning partial sums of analytic univalent functions, the reader may be (for examples) refered to the works of Çağlar and Deniz [3], Orhan and Yağmur [9], Yağmur and Orhan [13].

In this note, we will determine lower bounds of $\Re\left\{\frac{B_\nu(z)}{(B_\nu)_n(z)}\right\}$, $\Re\left\{\frac{(B_\nu)_n(z)}{B_\nu(z)}\right\}$, $\Re\left\{\frac{B'_\nu(z)}{(B_\nu)'_n(z)}\right\}$ and $\Re\left\{\frac{(B_\nu)'_n(z)}{B'_\nu(z)}\right\}$.

Lemma 1.1. If the parameter $\nu\in\mathbb{C}$, then the function $B_\nu: U\to\mathbb{C}$ given by (1.13) satisfies the following inequalities:

iii. $$\left|B_\nu(z)\right| \le \frac{192\nu^2+480\nu+289}{128\nu^2+288\nu+154} \quad \left(\nu>-\frac{7}{8}\right).$$

iv. $$\left|B'_\nu(z)\right| \le \frac{32\nu^2+88\nu+56}{16\nu^2+32\nu+15} \quad \left(\nu<-\frac{7}{4}\right).$$

Proof. **i.** By using the well-known triangle inequality:

$$|z_1+z_2| \le |z_1|+|z_2|$$

and the inequalities

$$m!(\nu+1)_m \ge 2^{m-1}(\nu+1)^m \quad \text{and} \quad (3/2)_m(\nu+3/2)_m \ge 2^{m-1}(\nu+3/2)^m \quad (m\in\{1,2,...\})$$

we have

$$\begin{aligned}
\left|B_\nu(z)\right| = \left|z+\sum_{m=1}^{\infty} b_m z^{m+1}\right| &\le 1+\sum_{m=1}^{\infty}|b_m| \\
&\le \frac{3}{2}+\sum_{m=1}^{\infty}\frac{1}{2^{2m}\,m!(\nu+1)_m}+\sum_{m=1}^{\infty}\frac{1}{(3/2)_m\left(\nu+\frac{3}{2}\right)_m\,2^{2m+1}} \\
&\le \frac{3}{2}+\sum_{m=1}^{\infty}\frac{1}{2^{2m}2^{m-1}(\nu+1)^m}+\sum_{m=1}^{\infty}\frac{1}{2^{2m+1}2^{m-1}\left(\nu+\frac{3}{2}\right)^m} \\
&= \frac{3}{2}+2\sum_{m=1}^{\infty}\left(\frac{1}{8\nu+8}\right)^m+\sum_{m=1}^{\infty}\left(\frac{1}{8\nu+12}\right)^m \\
&= \frac{192\nu^2+480\nu+289}{128\nu^2+288\nu+154}\quad\left(\nu>-\frac{7}{8}\right),
\end{aligned}$$

where $b_m=\dfrac{\Gamma(\nu+1)\Gamma\left(\frac{m+1}{2}\right)}{\sqrt{\pi}\,m!\,\Gamma\left(\frac{m}{2}+\nu+1\right)}$.

ii. Similarly, suppose that $\nu<-\dfrac{7}{4}$, by using well-known triangle inequality and the following inequalities:

$$m!(\nu+1)_m \ge \frac{2m+1}{4}(\nu+1)^m \quad\text{and}\quad (3/2)_m(\nu+3/2)_m \ge \left(\frac{m+1}{2}\right)(\nu+3/2)^m \quad (m\in\mathbb{N})$$

we get

$$\begin{aligned}
\left|B_\nu'(z)\right| &= \left|\left(1+\sum_{m=1}^{\infty}\frac{(2m+1)}{4^m\,m!(\nu+1)_m}z^{2m}+z+\sum_{m=1}^{\infty}\frac{(2m+2)}{(3/2)_m\left(\nu+\frac{3}{2}\right)_m\,2^{2m+1}}z^{2m+1}\right)\right| \\
&\le 2+\sum_{m=1}^{\infty}\frac{2m+1}{4^m\,m!(\nu+1)_m}+\sum_{m=1}^{\infty}\frac{m+1}{(3/2)_m\left(\nu+\frac{3}{2}\right)_m\,4^m} \\
&\le 2+\sum_{m=1}^{\infty}\frac{2m+1}{4^m\left(\frac{2m+1}{4}\right)(\nu+1)^m}+\sum_{m=1}^{\infty}\frac{m+1}{4^m\left(\frac{m+1}{2}\right)\left(\nu+\frac{3}{2}\right)^m} \\
&= 2+4\sum_{m=1}^{\infty}\left(\frac{1}{4\nu+4}\right)^m+2\sum_{m=1}^{\infty}\left(\frac{1}{4\nu+6}\right)^m \\
&= \frac{32\nu^2+88\nu+56}{16\nu^2+32\nu+15}\quad\left(\nu<-\frac{7}{4}\right)
\end{aligned}$$

2. MAIN RESULTS

Theorem 2.1. If the parameter $\nu\in\mathbb{R}$ and $\nu\neq -1,-2,\ldots$ are so constrained that $\nu>\dfrac{-6+\sqrt{17}}{8}$, then

$$\Re\left\{\frac{B_\nu(z)}{(B_\nu)_n(z)}\right\}\geq\frac{64\nu^2+96\nu+19}{128\nu^2+288\nu+154}\quad(z\in\mathrm{U}),\tag{2.1}$$

and

$$\Re\left\{\frac{(B_\nu)_n(z)}{B_\nu(z)}\right\}\geq\frac{128\nu^2+288\nu+154}{192\nu^2+480\nu+289}\quad(z\in\mathrm{U}).\tag{2.2}$$

Proof. We observe from part i of Lemma 1.1 that

$$1+\sum_{m=1}^{\infty}|b_m|\leq\frac{192\nu^2+480\nu+289}{128\nu^2+288\nu+154},$$

which is equivalent to

$$\frac{128\nu^2+288\nu+154}{64\nu^2+192\nu+135}\sum_{m=1}^{\infty}|b_m|\leq 1,$$

Now, we write

$$\frac{128\nu^2+288\nu+154}{64\nu^2+192\nu+135}\left[\frac{B_\nu(z)}{(B_\nu)_n(z)}-\frac{64\nu^2+96\nu+19}{128\nu^2+288\nu+154}\right]=\frac{1+\sum_{m=1}^{n}b_mz^m+\frac{128\nu^2+288\nu+154}{64\nu^2+192\nu+135}\sum_{m=n+1}^{\infty}b_mz^m}{1+\sum_{m=1}^{n}b_mz^m}$$

$$=\frac{1+A(z)}{1+B(z)}.$$

Set $(1+A(z))/(1+B(z))=(1+w(z))/(1-w(z))$, so that $w(z)=(A(z)-B(z))/(2+A(z)+B(z))$. Then

$$w(z)=\frac{\frac{128\nu^2+288\nu+154}{64\nu^2+192\nu+135}\sum_{m=n+1}^{\infty}b_mz^m}{2+2\sum_{m=1}^{n}b_mz^m+\frac{128\nu^2+288\nu+154}{64\nu^2+192\nu+135}\sum_{m=n+1}^{\infty}b_mz^m}$$

and

$$|w(z)|\leq\frac{\frac{128\nu^2+288\nu+154}{64\nu^2+192\nu+135}\sum_{m=n+1}^{\infty}|b_m|}{2-2\sum_{m=1}^{n}|b_m|-\frac{128\nu^2+288\nu+154}{64\nu^2+192\nu+135}\sum_{m=n+1}^{\infty}|b_m|}$$

Now $|w(z)|\leq 1$ if and only if

$$\sum_{m=1}^{n}|b_m|+\frac{128\nu^2+288\nu+154}{64\nu^2+192\nu+135}\sum_{m=n+1}^{\infty}|b_m|\leq 1.\tag{2.3}$$

It suffices to show that the left hand side of (2.3) is bounded above by $\frac{128\nu^2+288\nu+154}{64\nu^2+192\nu+135}\sum_{m=1}^{\infty}|b_m|$, which is equivalent to

$$\frac{64\nu^2+96\nu+19}{64\nu^2+192\nu+135}\sum_{m=1}^{n}|b_m|\geq 0.$$

To prove the result (2.2), we write

$$\frac{192\nu^2+480\nu+289}{64\nu^2+192\nu+135}\left[\frac{(B_\nu)_n(z)}{B_\nu(z)}-\frac{128\nu^2+288\nu+154}{192\nu^2+480\nu+289}\right] = \frac{1+\sum_{m=1}^{n}b_m z^m-\frac{128\nu^2+288\nu+154}{64\nu^2+192\nu+135}\sum_{m=n+1}^{\infty}b_m z^m}{1+\sum_{m=1}^{\infty}b_m z^m}$$

$$= \frac{1+w(z)}{1-w(z)}$$

where

$$|w(z)|\leq\frac{\frac{192\nu^2+480\nu+289}{64\nu^2+192\nu+135}\sum_{m=n+1}^{\infty}|b_m|}{2-2\sum_{m=1}^{n}|b_m|-\frac{64\nu^2+96\nu+19}{64\nu^2+192\nu+135}\sum_{m=n+1}^{\infty}|b_m|}\leq 1$$

The last inequality is equivalent to

$$\sum_{m=1}^{n}|b_m|+\frac{128\nu^2+288\nu+154}{64\nu^2+192\nu+135}\sum_{m=n+1}^{\infty}|b_m|\leq 1 \qquad (2.4)$$

Since the left hand side of (2.4) is bounded above by $\frac{128\nu^2+288\nu+154}{64\nu^2+192\nu+135}\sum_{m=1}^{\infty}|b_m|$, the proof is completed.

Theorem 2.2. If the parameters $\nu\in\mathbb{R}$ and $\nu\neq -1,-2,\ldots$ are so constrained that $\nu<-\frac{7+2\sqrt{2}}{4}$, then

$$\Re\left\{\frac{B_\nu'(z)}{(B_\nu)'_n(z)}\right\}\geq\frac{-24\nu-26}{16\nu^2+32\nu+15}\quad(z\in\mathrm{U}) \qquad (2.5)$$

and

$$\Re\left\{\frac{(B_\nu)'_n(z)}{B_\nu'(z)}\right\}\geq\frac{16\nu^2+32\nu+15}{32\nu^2+88\nu+56}\quad(z\in\mathrm{U}). \qquad (2.6)$$

Proof. From part ii. of Lemma 1.1 we observe that

$$1+\sum_{m=1}^{\infty}(m+1)|b_m|\leq\frac{32\nu^2+88\nu+56}{16\nu^2+32\nu+15},$$

which is equivalent to

$$\frac{16\nu^2+32\nu+15}{16\nu^2+56\nu+41}\sum_{m=1}^{\infty}(m+1)|b_m|\leq 1,$$

where $b_m=\frac{\Gamma(\nu+1)\Gamma\left(\frac{m+1}{2}\right)}{\sqrt{\pi}m!\Gamma\left(\frac{m}{2}+\nu+1\right)}$. Now we write

$$\frac{16\nu^2+32\nu+15}{16\nu^2+56\nu+41}\left[\frac{B_\nu'(z)}{(B_\nu)_n'(z)}-\frac{-24\nu-26}{16\nu^2+32\nu+15}\right] = \frac{1+\sum_{m=1}^{n}(m+1)b_m z^m+\frac{16\nu^2+32\nu+15}{16\nu^2+56\nu+41}\sum_{m=n+1}^{\infty}(m+1)b_m z^m}{1+\sum_{m=1}^{n}(m+1)b_m z^m}$$

$$= \frac{1+w(z)}{1-w(z)},$$

where

$$|w(z)|\le\frac{\frac{16\nu^2+32\nu+15}{16\nu^2+56\nu+41}\sum_{m=n+1}^{\infty}(m+1)|b_m|}{2-2\sum_{m=1}^{n}(m+1)|b_m|-\frac{16\nu^2+32\nu+15}{16\nu^2+56\nu+41}\sum_{m=n+1}^{\infty}(m+1)|b_m|}\le 1.$$

The last inequality is equivalent to

$$\sum_{m=1}^{n}(m+1)|b_m|+\frac{16\nu^2+32\nu+15}{16\nu^2+56\nu+41}\sum_{m=n+1}^{\infty}(m+1)|b_m|\le 1. \qquad (2.7)$$

It suffices to show that the left hand side of (2.7) is bounded above by $\frac{16\nu^2+32\nu+15}{16\nu^2+56\nu+41}\sum_{m=1}^{\infty}(m+1)|b_m|$, which is equivalent to

$$\frac{-24\nu-26}{16\nu^2+56\nu+41}\sum_{m=1}^{n}(m+1)|b_m|\ge 0.$$

To prove the result (2.6), we write

$$\frac{32\nu^2+88\nu+56}{16\nu^2+56\nu+41}\left[\frac{(B_\nu)_n'(z)}{B_\nu'(z)}-\frac{16\nu^2+32\nu+15}{32\nu^2+88\nu+56}\right]=\frac{1+w(z)}{1-w(z)},$$

where

$$|w(z)|\le\frac{\frac{32\nu^2+88\nu+56}{16\nu^2+56\nu+41}\sum_{m=n+1}^{\infty}(m+1)|b_m|}{2-2\sum_{m=1}^{n}(m+1)|b_m|+\frac{24\nu+26}{16\nu^2+56\nu+41}\sum_{m=n+1}^{\infty}(m+1)|b_m|}\le 1.$$

The last inequality is equivalent to

$$\sum_{m=1}^{n}(m+1)|b_m|+\frac{16\nu^2+32\nu+15}{16\nu^2+56\nu+41}\sum_{m=n+1}^{\infty}(m+1)|b_m|\le 1. \qquad (2.8)$$

Since the left hand side of (2.8) is bounded above by $\frac{16\nu^2+32\nu+15}{16\nu^2+56\nu+41}\sum_{m=1}^{\infty}(m+1)|b_m|$, the proof is completed.

REFERENCES

1. A. R. Ahmadi and S. E. Widnall, Unsteady lifting-line theory as a singular-perturbation problem. J. Fluid Mech. 153, (1985), 59–81.
2. A. Bayır, Hardy Spaces of Some Special Functions, Kafkas University, Institute of Science, (2019).

3. M. Çağlar and E. Deniz, Partial sums of the normalized Lommel functions, Math. Inequal. Appl., 18(3), (2015), 1189-1199.
4. A. Gasmi and M. Sifi, The Bessel-Struve intertwining operator on and meanperiodic functions, Int. J. Math. Math. Sci. 57-60, 3171–3185, (2004).
5. A. Gasmi and F. Soltani, Fock spaces for the Bessel-Struve kernel, J. Anal. Appl. 3, 91–106, (2005).
6. S. Hamem, L. Kamoun and S. Negzaoui, Cowling-Price type theorem related to Bessel-Struve transform, Arab J. Math. Sci. 19, no. 2, 187–198, (2013).
7. L. Kamoun and M. Sifi, Bessel-Struve intertwining operator and generalized Taylor series on the real line, Integral Transforms Spec. Funct. 16, 39–55, (2005).
8. S. R. Mondal, On the geometrıc propertıes of the Bessel-Struve kernel functıon, arXiv:1601.08102v1, (2016).
9. H. Orhan and N. Yağmur, Partial sums of the generalized Bessel functions, J. Math. Inequal., 8(4), (2014), 863-877.
10. T. G. Pedersen, Variational approach to excitons in carbon nanotubes. Phys. Rev. B 67, no. 7, (0734011)–(0734014), (2003).
11. J. Shao, P. Haanggi, Decoherent dynamics of a two-level system coupled to a sea of spins. Phys. Rev. Lett. 81, no. 26, 5710–5713, (1998).
12. D. C. Shaw, Perturbational results for diffraction of water-waves by nearlyvertical barriers. IMA, J. Appl. Math. 34, no. 1, 99–117, (1985).
13. N. Yağmur and H. Orhan, Partial sums of the generalized Struve functions, Miskolc Mathematical Notes, 17(1), (2016), 657-670.

An Efficient and Robust Ischemic Stroke Detection Using a Combination of Convolutional Neural Network (CNN) and Kernel K-Means Clustering

Zuherman RUSTAM[1] and Sri HARTINI[1]

[1]*Department of Mathematics, University of Indonesia, Depok 16424, Indonesia*

rustam@ui.ac.id

Abstract. This paper introduces the combined widely-used Convolutional Neural Network (CNN) and Kernel K-Means clustering method for ischemic stroke detection from CT image. We propose an efficient and robust alternating classification scheme for overcoming the large time computation and noisy ischemic stroke image obtained from Cipto Mangunkusumo (RSCM) Hospital, Indonesia. This method used a bunch of convolutional layers resulted from CNN architecture and then vectorize the matrix output as the new input in Kernel K-Means clustering. According to several experiments that we conducted, our proposed method achieved 99% accuracy, 100% sensitivity, 98% precision, 98.04% specificity, and 98.99% F1-Score using 11-fold cross-validation with RBF kernel function (sigma=5×10-2). Therefore, our experiments show that the performance of the combination of CNN and Kernel K-Means clustering decisively competed with several other state-of-the-art methods in the deep learning field.

1. INTRODUCTION

Ischemic stroke is one of kind of stroke beside the hemorrhagic stroke. It is the most common type because it dominates 85 percent of stroke cases [1]. It is also ranked as the second leading cause of death worldwide, with an annual mortality rate of about 5.5 million [2]. This disease is usually caused by a blood clot that blocks or plugs a blood vessel in the brain that keeps blood from flowing to the brain. Therefore, the duration of cerebral ischemia is a critical factor in determining the severity of brain damage. Thus, accurate and timely observation of the ischemic process is highly critical to course the action [3].

Ischemic stroke can be detected from the analysis of its Computerized Tomographic (CT) scan and Magnetic Resonance Imaging (MRI) results. Several methods have been used in previous researches to detect an ischemic stroke. Some of them applied support vector machines [4–6], clustering [7–9], but most of them used the various architecture of neural networks. As the frequently used method, deep learning outperforms other techniques when it comes to complex problems such as image classification if the data size is large.

According to the Ischemic Stroke Lesion Segmentation 2017 (ISLES 2017) Challenge that provided dataset of MRI images to detect ischemic stroke, many researchers almost always employed deep learning tools, which were predominately convolutional neural networks (CNNs) to reach the optimal results [10]. However, even though deep learning, such as CNN, delivers impressive accuracy in detecting ischemic stroke, it takes much computational time to train the model. It depends on the number of epoch and batch size used so that the expected out-of-sample error can be reached without causing the model to become overfitting [11]. Meanwhile, machine learning methods such as Support Vector Machines (SVM) usually may become inefficient once it is given large number of feature vectors to process [12].

Therefore, in this research, we would like to explore a combination of the deep learning architecture and machine learning method to overcome those limitations. Specifically, we proposed an effective and robust method that is a combination of CNN and K-Means clustering based on kernel. The extensive input of images on CNN is reduced while passing the model layers. After that, using the flatten layer output of the last convolutional step in CNN, the data matrix of the different classes will be constructed as the input for Kernel K-Means clustering, which has a smaller size than the original input images. As a result, the centroid of each class was built to detect the class of the out-of-sample dataset.

2. METHODOLOGY

A. The Dataset

The dataset used in this research was collected from Cipto Mangunkusumo (RSCM) Hospital, Indonesia. It has 334 images that consist of 185 non-ischemic stroke and 149 ischemic stroke images. The phone camera with the specification 48-megapixel camera with an f/2.0 aperture took those images resulted from an CT scan. The average height of images is 3047 pixels with the maximum and minimum height are 4023 and 2225 pixels, respectively. Meanwhile, the average width of images is 2598 pixels with the maximum and minimum width are 3545 and 1902 pixels, respectively. However, the input of images that we used is 512 x 512 pixels so that the size of input images is not huge. However, all of the regions of the brain are still included.

The sample of the ischemic stroke CT image is shown in Figure 1(a). From the image, we can identify that the middle region of the brain is fueled by a dark area, which indicates the existence of the disease. Compared with Figure 1(b), the non-ischemic stroke MRI image shown in this figure has a clearer region. However, the non-ischemic stroke dataset has not only a healthy brain image. Indeed, it also consists the other brain diseases image that is not categorized as the ischemic stroke.

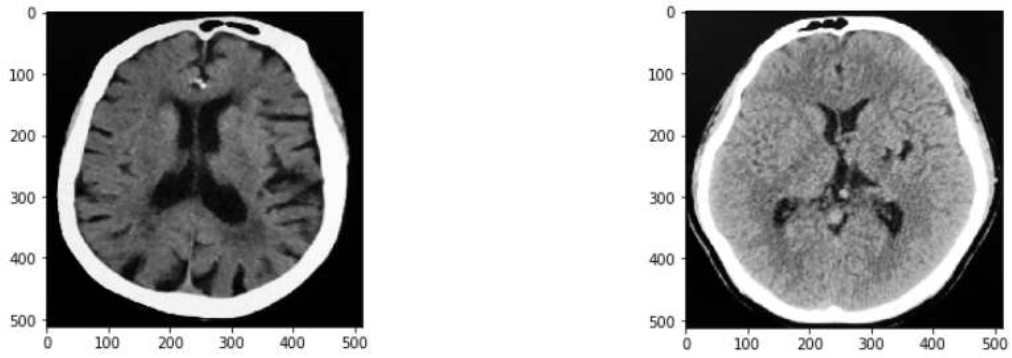

Fig. 1. The sample of the (a) ischemic and (b) non-ischemic stroke CT image

B. The Proposed Method

In this research, we proposed an effective and robust method that is a combination of CNN and K-Means clustering based on kernel. Convolutional Neural Network (CNN) is one of deep learning algorithms. It has many architecturess which mostly consists of convolutional layers, pooling layers, and fully connected layers. In this research, Keras, as the python deep learning library, is used to build the model architecture where the details were given in Figure 2. Consider an input grayscale image with a size of 152 x 152 x 1 pixels. This input image will be processed through a convolutional layer with the Rectified Linear Unit (ReLU) activation function, maximum pooling layer, and normalization layer, respectively, before finally be applied dropout and make the output flat.

Two-dimension convolutional layer (denoted by Conv2D) consists of the number of filters with size $3 \times 3 \times 1$ in this research. This layer constructs a convolution kernel that is convoluted with the layer input to produce a tensor of outputs through the dot product computation. Convolution operation extracts useful features from locally correlated data points. The output of the convolutional kernels is assigned to the non-linear processing unit (activation function), which not only helps in learning abstractions but also embeds non-linearity in the feature space [13].

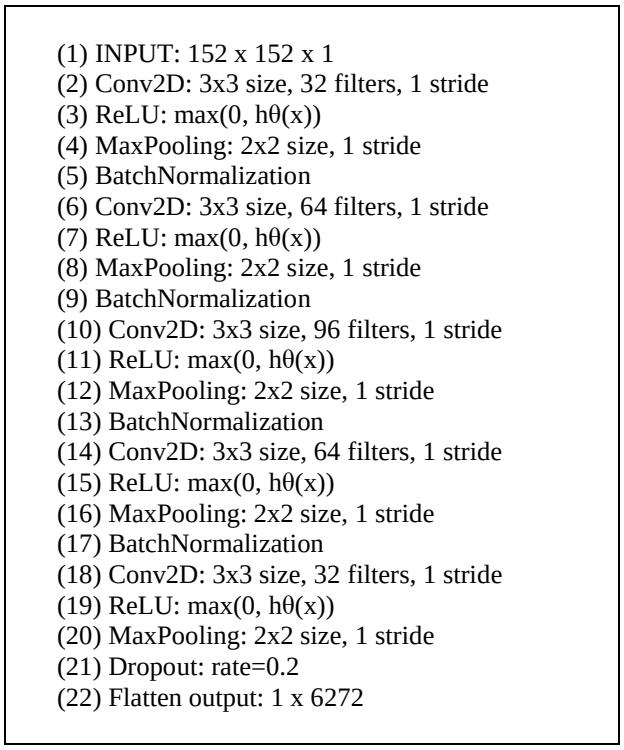

Fig. 2. The CNN architecture used in this paper

Consequently, Rectified Linear Unit (ReLU) activation function is used. Then, the maximum pooling layer (denoted by MaxPooling) used to reduces the size of input images from the convolutional layer using max-pooling operation. Lastly, the normalization layer used to normalize the activations of the previous layer at each batch. For example, it applied a transformation that maintains the mean activation close to 0 and the activation standard deviation close to 1. After the input image passed the bunch of convolutional layers, the information in every hidden neuron output will only keep 80 percent information because the dropout rate is 0.2. As the last step, the output obtained from this CNN is the vector with length 6272 for every input image.

Input:
$X = \{\mathbf{x}_1, \mathbf{x}_2, \ldots, \mathbf{x}_N\}$, C (the number of cluster), ε (epsilon), T (the maximum number of iterations).
Output:
$V = \{\mathbf{v}_1, \mathbf{v}_2, \ldots, \mathbf{v}_C\}$,
$U = [\, r_{nc} \,]$ where n = 1, 2, …, N and c = 1, 2, … C.

(1) Initialization: $V^0 = \{\mathbf{v}_1, \mathbf{v}_2, \ldots, \mathbf{v}_C\}$,
(2) Update membership of the data point $\mathbf{x}_i$ in j^{th}-cluster.
If $c = argmin_j\, (K(\boldsymbol{x}_n, \boldsymbol{x}_n) - 2\, K(\boldsymbol{x}_n, \boldsymbol{\mu}_c) + K(\boldsymbol{\mu}_c, \boldsymbol{\mu}_c))$, then $r_{nc} = 1$. Otherwise, $r_{nc} = 0$.
(3) Update cluster center V^t using:
$\boldsymbol{\mu}_c = (\Sigma_n\, r_{nc}\, \boldsymbol{x}_n) \,/\, \Sigma_n\, r_{nc}$
(4) Check the stop criteria. If $\| V^{(t-1)} - V^{(t)} \| < \varepsilon$ or T = t, then the iteration stops. Otherwise, t = t+1 and go back to step 2;
(5) End.

Fig. 3. The algorithm of Kernel K-Means Clustering

As the replacement of fully connected layer, we used Kernel K-Means clustering to classify the data. It was a modification method of K-Means (KM) clustering that formerly introduced by Lloyd [14]. The modification is based on the kernel function that proposed by Vapnik [15]. The algorithm of Kernel K-Means clustering is given in Figure 4. In this research, we used RBF kernel function that formula given in Eq. (1):

$$K(\mathbf{x}, \mathbf{y}) = \exp(-\|\mathbf{x} - \mathbf{y}\|^2/(2\sigma^2)) \quad (1)$$

C. Performance Measurement

As the input of CNN, we used all of 334 labeled images: 1 for ischemic stroke images and 0 for non-ischemic images. The images are resized to the same size 152 x 152 pixels. This input is then passed to the bunch of CNN layers, as described in Figure 2. As a result, every image 152 x 152 x 1 pixel became a vector with length 6272. Therefore, we now have matrix 334 x 6272, where the row index is indicated the image that we observed and the column index is indicated the feature map resulted by CNN.

The next step is then dividing the matrix data according to its label, whether it is included in class 1 (ischemic stroke) or class 0 (non-ischemic stroke). In this case, we have two matrices data with size 185 x 6272 for the non-ischemic stroke and 149 x 6272 for the ischemic stroke class. Those matrices were then used in k-fold cross-validation for evaluating KM clustering based on kernel algorithm. For example, when we used 5-fold cross-validation, the data is divided into five folds for each class. Therefore, we get the number of points in every fold as shown in Table I.

Table 1. The number of Data in Every 5 Folds of Ischemicand Non-Ischemic Stroke Data

Fold	The number of ischemic stroke data points	The number of non-ischemic stroke data points
1	30	37
2	30	37
3	30	37
4	30	37
5	29	37
Total	149	185

In this research, a fold was used to obtain the centroids of the clusters according to the algorithm in Figure 3, while the rest k−1 folds were used to evaluate the method by determining the class of every data point according to its nearest centroid. If the data point was nearer to the centroid of class 1, then the predicted class for this data point is 1. Meanwhile, if the data point was nearer to the centroid of class 0, then the predicted class is 0.

For measuring the performance of combined CNN and KM clustering based on kernel method, the confusion matrix (see Table II) is used to calculate the percentage of accuracy, sensitivity, precision, specificity, and F1-Score. There are four possible outcomes in the confusion matrix that we might obtain: True Positive (TP), False Positive (FP), True Negative (TN), and False Negative (FN).

Table II. Confusion Matrix for Ischemic Stroke Dataset

CONFUSION MATRIX	Predicted Class	
	Ischemic Stroke	Non-Ischemic Stroke

Actual Class	Ischemic Stroke	TP	FN
	Non-Ischemic Stroke	FP	TN

The condition where ischemic stroke data is correctly predicted as ischemic stroke counts as True Positive, while the condition where non-ischemic stroke data is correctly predicted as non-ischemic stroke counts as True Negative. Meanwhile, when ischemic stroke data is incorrectly diagnosed as non-ischemic stroke, it counts as False Negative. Lastly, when non-ischemic stroke data is incorrectly diagnosed as ischemic stroke, it counts as False Positive. Using the rule of the confusion matrix, we can examine the performance of combined CNN+KM clustering based on kernel using the formulas that were listed in Table III.

Table III. Performance Measure

Performance Measure	**Formula**
Accuracy	(TP + TN) / (TP + FP + TN + FN)
Sensitivity	TP / (TP + FN)
Precision	TP / (TP + FP)
Specificity	TN / (TN + FP)
F1-Score	(2 × Sensitivity × Precision) / (Sensitivity + Precision)

3. RESULTS AND DISCUSSION

As we have described in the previous section, the results of the last 2D-convolutional layer in CNN architecture were used as the new input for KM clustering based on kernel in the vector form. However, the convolutional result of Figure 1(a) in image form that can be seen in Figure 4(a). As a comparison, we also provided the convolutional result of Figure 1(b) in image form that can be seen in Figure 4(b). It might look similar in a glance, but they are different because they came from different kinds of images.

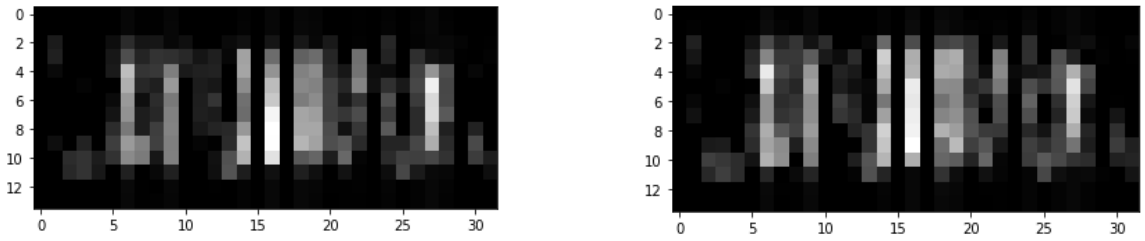

(a) (b)

Fig. 4. The result of the last convolutional layer for image: (a) in Figure 1a, and (b) in Figure 1b.

Because every image 152 x 152 x 1 pixel became vector with length 6272, we then obtained two matrices, each from class ischemic stroke and non-ischemic stroke.

Table IV. Matrix Input for Ischemic Stroke (Class 1)

Data	f_1	f_2	…	f_{6271}	f_{6272}
x_1	0.139936	0	…	0.045084	0.051006
x_2	0.153615	0	…	0.258974	0.633877
…	…	…	…	…	…
x_{148}	0.211017	0	…	0.143986	0.172800
x_{149}	0.439847	0	…	0.980306	5.199656

Table IV above provided the matrix input from class ischemic stroke, while Table V below provided the matrix input from a class non-ischemic stroke. Each column represents the feature map in the image after passing the bunch of convolutional operations.

Table V. Matrix Input for Non-Ischemic Stroke (Class 0)

Data	f_1	f_2	…	f_{6271}	f_{6272}
x_1	0.176003	0	…	0.107532	0.073519
x_2	0.158362	0	…	0.089604	0.091670
…	…	…	…	…	…
x_{184}	0.187925	0.013181	…	0.272290	0.502731
x_{185}	0.478123	0	…	1.752787	9.493455

Using both of those matrices in KM clustering based on RBF kernel on 5-fold cross-validation, the performance of this combined method is evaluated, which shown in Tabel VI. Given several RBF kernel parameter σ, it was obtained that $\sigma = 5\times10^{-2}$ delivered the highest performance measure among the others.

Table VI. The Performance of 5-fold Cross-Validation of CNN + K-Means Clustering Based on RBF Kernel Function for Ischemic Stroke Detection

σ	Accuracy	Sensitivity	Precision	Specificity	F1-Score
10^{-8}	97.00	97.96	96.00	96.08	96.97
10^{-4}	96.50	97.94	95.00	95.15	96.45
10^{-3}	96.50	96.97	96.00	96.04	96.48
5×10^{-2}	**97.50**	**97.98**	**97.00**	**97.03**	**97.49**
10^{-1}	95.50	95.96	95.00	95.05	95.48
1	95.50	95.05	96.00	95.96	95.52
10	95.50	94.17	97.00	96.91	95.57
10^{2}	96.50	96.97	96.00	96.04	96.48
10^{3}	95.00	95.00	95.00	95.00	95.00
10^{4}	95.50	95.05	96.00	95.96	95.52

Therefore, we then evaluated several values of k in k-fold cross-validation such as k = 3, 5, 7, 9, and 11 to see its behavior. As the results, we can see in Table VII that the performance of our proposed method was increasing in line with the increase in the value of k.

Table VII. The Performance of k-Fold Cross-Validation of CNN + K-Means Clustering Based on RBF Kernel Function with $\sigma = 5\times10^{-2}$ for Ischemic Stroke Detection

k	Accuracy	Sensitivity	Precision	Specificity	F1-Score
3	96.00	96.00	96.00	96.00	96.00
5	97.50	97.98	97.00	97.03	97.49
7	97.00	97.00	97.00	97.00	97.00
9	98.50	98.99	98.00	98.02	98.49
11	**99.00**	**100.00**	**98.00**	**98.04**	**98.99**

As the best results, we obtained when 11-fold cross-validation and RBF kernel parameter σ = 5×10-2 is used. For the time computational time that our proposed method needs, it takes less than 10 seconds for passing the dataset to the CNN model and 71 ± 0.098 seconds on average for running the k-fold cross-validation on KM clustering based on RBF kernel. Compared to the only used deep learning CNN model to test the model after training it with the number of epochs and batch sizes, our proposed method is more efficient in time. The performance measures, especially accuracy, are also competing with several state-of-art deep learning methods.

4. CONCLUSION

Detecting the ischemic stroke from the CT image is not an easy task. Considering the deep learning method, especially CNN, as the reliable method in image classification, we proposed an efficient and robust method that combined CNN with KM clustering based on kernel. From our experiments using the ischemic dataset from Cipto Mangunkusumo (RSCM) Hospital, Indonesia, it was concluded that our proposed method has more efficient in time computation and also delivers competing accuracy with the other deep learning methods.

ACKNOWLEDGEMENT

This work was supported financially by Indonesia Ministry of Research and Technology/ National Research and Innovation Agency (KEMENRISTEK/BRIN) 2021 research grant scheme. The authors are thankful for the kindness of the doctor and staff at the Department of Radiology, Cipto Mangunkusumo Hospital, in providing the ischemic stroke image datasets.

REFERENCES

1. T. D. Musuka, S. B. Wilton, M. Traboulsi, and M. D. Hill, “Diagnosis and management of acute ischemic stroke: speed is critical,” *CMAJ: Canadian Medical Association journal (journal de l'Association medicale Canadienne)*, vol. 187(12), pp. 887–893, September 2015.
2. E. S. Donkor, “Stroke in the 21st century: A snapshot of the burden, epidemiology, and quality of life,” *Stroke research and treatment*, vol. 2018(3238165), pp. 1–10, November 2018.
3. T. Savić, G. Gambino, V. S. Bokharaie, H. R. Noori, N. K. Logothetis, and G. Angelovski, “Early detection and monitoring of cerebral ischemia using calcium-responsive MRI probes,” *Proceedings of the National Academy of Sciences*, vol. 116(41), pp. 20666–20671, October 2019.
4. O. Maier, M. Wilms, J. v. d. Gablentz, U. Krämer, and H. Handels, "Ischemic stroke lesion segmentation in multi-spectral MR images with support vector machine classifiers," *Proceedings of SPIE-The International Society for Optical Engineering*, vol. 9035(903504), March 2014.
5. S. Sabut, K. S. Asit, P. K. Biswal, and S. Sahoo, “Segmentation and classification of ischemic stroke using optimized features in brain MRI,” *Biomedical Engineering Applications Basis and Communications*, January 2018.
6. N. D. Forkert, T. Verleger, B. Cheng, G. Thomalla, C. C. Hilgetag, and J. Fiehler, “Multiclass support vector machine-based lesion mapping predicts functional outcome in ischemic stroke patients,” *PLoS ONE*, vol. 10(6), June 2015.
7. N. Rajini and R. Bhavani, “Automatic detection and classification of ischemic stroke using k-means clustering and texture features,” *In book: Emerging Technologies in Intelligent Applications for Image and Video Processing*, January 2016.
8. F. Aboudi, C. Drissi, and T. Kraiem, “Brain ischemic stroke segmentation from brain MRI between clustering methods and region-based methods,” *In book: Heart Failure*, pp. 144–154, January 2019.
9. A. Vupputuri, S. Ashwal, B. Tsao, and N. Ghosh, “Ischemic stroke segmentation in multi-sequence MRI by symmetry determined superpixel based hierarchical clustering,” *Computers in Biology and Medicine*, vol. 116, January 2020.
10. S. Winzeck, A. Hakim, R. McKinley, J. Pinto, V. Alves, C. Silva, … M. Reyes, “ISLES 2016 and 2017-benchmarking ischemic stroke lesion outcome prediction based on multispectral MRI,” *Frontiers in neurology*, vol. 9(679), pp. 1–20, September 2018.
11. C. J. Shallue, J. Lee, J. Antognini, J. Sohl-Dickstein, R. Frostig, and G. E. Sahl, "Measuring the effects of data parallelism on neural network training," *Journal of Machine Learning Research*, vol. 20, pp. 1–49, July 2019.

12. Z. Xiao, R. Huang, Y. Ding, T. Lan, R-F. Dong, Z. Qin, X. Zhang, W. Wang, "A deep learning-based segmentation method for brain tumor in MR images," *IEEE 6th International Conference on Computational Advances in Bio and Medical Sciences (ICCABS)*, pp. 1–6, October 2016.
13. A. Khan, A. Sohail, U. Zahoora, and A. S. Qureshi, "A survey of the recent architectures of deep convolutional neural networks," *arXiv preprint arXiv*. 1901.06032, 2019.
14. S. P. Lloyd, "Least squares quantization in PCM," IEEE Transactions on Information Theory, vol. 28(2), pp. 129–137, March 1982.
15. V. N. Vapnik, "Statistical Learning Theory," New York: Wiley, 1998.

New Exact Solutions for Conformable Time Fractional Equation System Via IBSEFM

Volkan ALA[1], Ulviye DEMİRBİLEK[1], Khanlar R. MAMEDOV[1]

[1]*Department of Mathematics, Faculty of Science and Arts, Mersin University, Mersin-TURKEY*

volkanala@mersin.edu.tr
udemirbilek@mersin.edu.tr
hanlar@mersin.edu.tr

Abstract. The aim of this paper is to construct exact solutions for the time fractional equation system by using Improved Bernoulli Sub-Equation Function Method (IBSEFM). In this work, we consider nonlinear conformable time fractional coupled approximate long water wave equation. Applying the IBSEFM, we obtain new exact solutions with the help of computer software. This method is powerful, effective and straihghtforward for solving nonlinear partial differential equations to obtain more and new solitions with the integer and fractional order in mathematical physics.

Keywords: *Time fractional approximate long water wave equation, Improved Bernoulli Sub-Equation Function Method, Fractional derivative.*

1. INTRODUCTION

In recent years, fractional order differential equation is a topic that has played an important role in defining the complex dynamics of real world problems from various fields of science and engineering. The fractional differential equation is also widely used in various physical models such as physics, fluid mechanics, plasma physics, optical fibers, solid state physics, etc. [1–3] . With the rapid development of computer algebraic systems, many numerical methods have been developed to obtain solutions of fractional order differential equations. Some of these effective methods are fractional Riccati expansion [4], generalized projective Riccati equation [5], extended direct algebraic [6], modified expansion function [7] and improved Bernoulli sub-equation function method [8,9]. In 2014, Khalil et al. [10] introduced a new simple, significant definition of the fractional derivative called conformable fractional derivative. The conformable fractional derivative is theoretically easier than fractional derivative to handle. In addition, the conformable fractional derivative satisfies many known features that can't be satisfied by the existing fractional derivatives, for instance; the chain rule [11]. The conformable fractional derivative has the weakness that the fractional derivative of differentiable function at the point zero is equal to zero. So that in [12] it is proposed a suitable fractional derivative that allows us to escape the lack of the conformable fractional derivative.

The conformable derivative of order α according to the independent variable t is defined as [10]

$$D_t^\alpha\left(g(t)\right)=\lim_{\tau\to\infty}\frac{g\left(t+\tau t^{1-\alpha}\right)-g(t)}{\tau},\ t>0,\ \alpha\in(0,1],$$

for a function $g=g(t):[0,\infty)\to\mathbb{R}$.

Theorem 1. Assume that the order of the derivative $\alpha\in(0,1]$ and assume that $f=f(t)$ and $g=g(t)$ are $\alpha-$ differentiable for all positive t. Then,

i. $D_t^\alpha\left(c_1f+c_2g\right)=c_1D_t^\alpha(f)+c_2D_t^\alpha(g),\ \forall c_1,c_2\in\mathbb{R}$.

ii. $D_t^\alpha\left(t^k\right)=kt^{k-\alpha},\forall k\in\mathbb{R}$.

iii. For all constant function $f(t)=\lambda,\ D_t^\alpha(\lambda)=0.$

iv. $D_t^\alpha(fg)=fD_t^\alpha(g)+gD_t^\alpha(f).$

v. $D_t^\alpha\left(\frac{f}{g}\right)=\frac{gD_t^\alpha(f)-fD_t^\alpha(g)}{g^2},\ g\neq 0.$

Conformable fractional differential operator satisfies certain basic features like Laplace transform, the chain rule and Taylor series expansion.

Theorem2. Let $g,h:(0,\infty)\to$ be differentiable and also α conformable differentiable functions, then the following rule holds:

$$D_t^\alpha(f\circ g)=t^{1-\alpha}g'(t)\,f'(g(t)).$$

The proofs of these theorems are given in [12] and in [11] respectively.

Let us consider the coupled Whitham-Broer-Kaup (WBK) equation system which have been introduced by Whitham [13], Broer [14] and Kaup [15]. This equation system describes the propagation of shallow water waves with different dispersion relations. Consider the following conformable time fractional coupled Whitham-Broer-Kaup (WKB) equation system:

$$\left.\begin{aligned}D_t^\alpha u+uu_x+v_x+bu_{xx}=0,\\ D_t^\alpha v+(uv)_x-au_{xxx}-bv_{xx}=0,\end{aligned}\right\}$$

where $t>0,\ a$ is a parameter describing the order of the fractional time derivative and $0<\alpha\leq 1,$ In this equation system the field of horizontal field of horizontal velocity is represented by $u=u(x,t);\ v=v(x,t)$ which is the height that deviates from equilibrium position of liquid, and the constants a,b are represented in different diffusion power. If $a=0,b=\frac{1}{2},$ the fractional coupled WKB equation system reduces to the nonlinear time fractional approximate long wave (ALW) equation systems which are a special case of WKB equations.

In this study, we focus on the exact solutions of the following nonlinear conformable time fractional approximate long wave (ALW):

$$\left.\begin{aligned}D_t^\alpha u+uu_x+v_x+\frac{1}{2}u_{xx}=0,\\ D_t^\alpha v+(uv)_x-\frac{1}{2}bv_{xx}=0,\end{aligned}\right\}\qquad(1)$$

where $t>0,\ a$ is a parameter describing the order of the fractional time derivative and $0<\alpha\leq 1.$ Before beginning to the solution procedure, we should give the description of the proposed method.

2. DESCRIPTION OF THE IMPROVED BERNOULLI SUB-EQUATION FUNCTION METHOD (IBSEFM)

In this part, let us give the fundamental properties of the IBSEFM [8,9]. We present the six basic steps of the IBSEFM below the following:

Step 1: Let us take account of the following conformable time-fractional partial differential (PDE) of the style

$$P=\left(v,D_t^{(m)}v,D_x^{(m)}v,D_{xt}^{(2m)}v,D_{xxt}^{(3m)}v,\ldots\right)=0.\qquad\textbf{(2)}$$

where $D_t^{(m)}$ is the Conformable derivate operator, $v(x,t)$ is an unknown function, P is a polynomial in v and its partial derivatives contain fractional derivatives. The aim is to convert CFPDEs with a suitable fractional transformation into the ordinary differential equation (ODE). The wave transformation as:

$$v(x,t)=V(x),\quad x=(x-kt^a a^{-1}),\qquad\textbf{(3)}$$

where k is an arbitrary constant and not zero. Using the properties of Conformable derivate, it enables us to convert (3) into an ODE in the form:

$$N(V, V', V'', \ldots) = 0. \tag{4}$$

Step 2: If we integrate (4) term to term once or more, we acquire integration constant(s) which may be determined then.

Step 3: We hypothesize that the solution of (4) may be presented below:

$$V(x) = \frac{\sum_{i=0}^{n} a_i F^i(x)}{\sum_{i=0}^{m} b_i F^i(x)} = \frac{a_0 + a_1 F(x) + \ldots + a_n F^n(x)}{b_0 + b_1 F(x) + \ldots + b_m F^m(x)}, \tag{5}$$

where $a_0, a_1, \ldots, a_n$ and $b_0, b_1, \ldots, b_m$ are coefficients which will be determined later. $m \neq 0, n \neq 0$ are chosen arbitrary constants to balance principle and considering the form of Bernoulli differential equation below the following:

$$F'(x) = s F(x) + d F^M(x), \; d \neq 0, s \neq 0, \; M \in R / \{0, 1, 2\}, \tag{6}$$

where $F(x)$ is polynomial.

Step 4: The positive integer m, n, M (are not equal to zero) which is found by balance principle that is both nonlinear term and the highest order derivative term of (4).
Substituting (5) and (6) in (3) it gives us an equation of polynomial $\Theta(F)$ of F as following;

$$Q(F(x)) = r_s F(x)^s + \ldots + r_1 F(x) + r_0 = 0,$$

where $r_i, (i = \overline{0, j})$ are coefficients and will be determined later.

Step 5: The coefficients of $Q(F(x))$ which will give us a system of algebraic equations, whole be zero.

$$r_i = 0, \; i = \overline{0, j}.$$

Step 6: Once we solve (4), we get the following two cases with respect to σ and d :

a) For $E \in R$,

$$F(x) = \left[\frac{d e^{s(E-1)} + E s}{s e^{s(E-1)x}} \right]^{\frac{1}{1-E}}, \; d \neq s. \tag{7}$$

b) For $d = s$, $E \in R$,

$$F(x) = \left[\frac{(E-1) + (E+1)\tanh\left(s(1-E)\frac{x}{2}\right)}{1 - \tanh\left(s(1-E)\frac{x}{2}\right)} \right] \tag{8}$$

Using a complete discrimination system for polynomial of $F(x)$, we obtain the analytical solutions of (4) via software programme and categorize the exact solutions of (4). To achieve better results, we can plot two - three dimensional figures and contourplot of analytical solutions by considering proper values of parameters.

3. IMPLEMENTATION OF THE IBSFM

By taking the traveling wave transformation as:

$$u(x,t) = U(x),\ x = x - p(t^a a^{-1}), \tag{9}$$

where p is arbitrary constant (is not zero) to be determined later. Using the (9) into (1) the following equation is obtained [34]:

$$\begin{aligned} &-2pu + u^2 + 2v + u' = 0, \\ &-2pv + 2uv - v' = 0, \end{aligned} \tag{10}$$

From first equation, we reach

$$v = 2pu - u^2 - u'. \tag{11}$$

Substituting (11) into the second equation of (10), we obtain

$$-u''' + 4p^2 u' - 6p^2 u^2 + 2u^3 = 0. \tag{12}$$

When we apply the balance for the terms u^3 and u''', we obtain the relationship for m, n and M as below:

$$M + m = n + 1.$$

This relationship of m, n and M give us different types of the solutions of (12). Using homogeneous balance principle, for $M = n = 3$ and $m = 1$ in (1), then we get as follows:

$$u(x) = \frac{\sum_{i=0}^{3} a_i F^i(x)}{\sum_{i=0}^{1} b_i F^i(x)} = \frac{a_0 + a_1 F(x) + a_2 F^2(x) + a_3 F^3(x)}{b_0 + b_1 F(x)} = \frac{y}{j}, \tag{13}$$

$$u'(x) = \frac{y'(x)j(x) - y(x)j'(x)}{j^2(x)},$$

$$u''(x) = -\frac{[y(x)j'(x)]j^2(x) - 2y(x)[j(x)]^2 j'(x)}{j^4(x)} + \frac{y'(x)j(x) - y(x)j'(x)}{j^2(x)}. \tag{14}$$

Substituting (13) and (14) in (12), we get a system of algebraic system. When we equal to zero all the same power of F and solving the algebraic system of equations from coefficients of polynomial of F, it yields the following coefficients:

$$Const := 2a_0^3 - 6pa_0^2 b_0 + 4p^2 a_0 b_0^2 0,$$

$$F := 6a_0^2 a_1 - 12pa_0 a_1 b_0 + 4p^2 a_1 b_0^2 - s^2 a_1 b_0^2 - 6pa_0^2 b_1 + 8p^2 a_0 b_0 b_1 + s^2 a_0 b_0 b_1 = 0,$$

$$\begin{aligned} F^2 :\ & 6a_0 a_1^2 + 6a_0^2 a_2 - 6ma_1^2 b_0 - 12ma_0 a_2 b_0 + 4m^2 a_2 b_0^2 - 4\sigma^2 a_2 b_0^2 - 12ma_0 a_1 b_1 + 8m^2 a_1 b_0 b_1 \\ & + \sigma^2 a_1 b_0 b_1 + 4m^2 a_0 b_1^2 - \sigma^2 a_0 b_1^2 = 0, \end{aligned}$$

$$\vdots$$

$$F^9 : 6a_2^2 a_3 + 6a_1 a_3^2 - 15d^2 a_3 b_0^2 - 6pa_3^2 b_1 - 9d^2 a_2 b_0 b_1 - 12d\sigma a_3 b_1^2 = 0,$$

$$F^{10} : 6a_2 a_3^2 - 21d^2 a_3 b_0 b_1 - 3d^2 a_2 b_1^2 = 0,$$

$$F^{11} : 2a_3^3 - 8d^2 a_3 b_1^2 = 0.$$

Then, we solve the above system of equations and substitute in each case the obtained result of the coefficients to get the new solution(s) $u(x,t)$ and $v(x,t)$. By solving the above system with the aid of software, the coefficients are obtained as:

Case1: For $\sigma \neq d$, can be also considered the following coefficients obtained by software;

$$a_0 = 2pb_0;\ a_1 = 2pb_1;\ a_2 = 2db_0;\ a_3 = 2db_1;\ \sigma = p; \tag{15}$$

where d, p are different from zero.

Putting (15) along with (7) in (13)-(14), we acquire the exponential function solution as follow:

$$u(x,t) = \frac{2p^2E}{-de^{2p\left(x-\frac{pt^{\alpha}}{\alpha}\right)} + pE}. \tag{16}$$

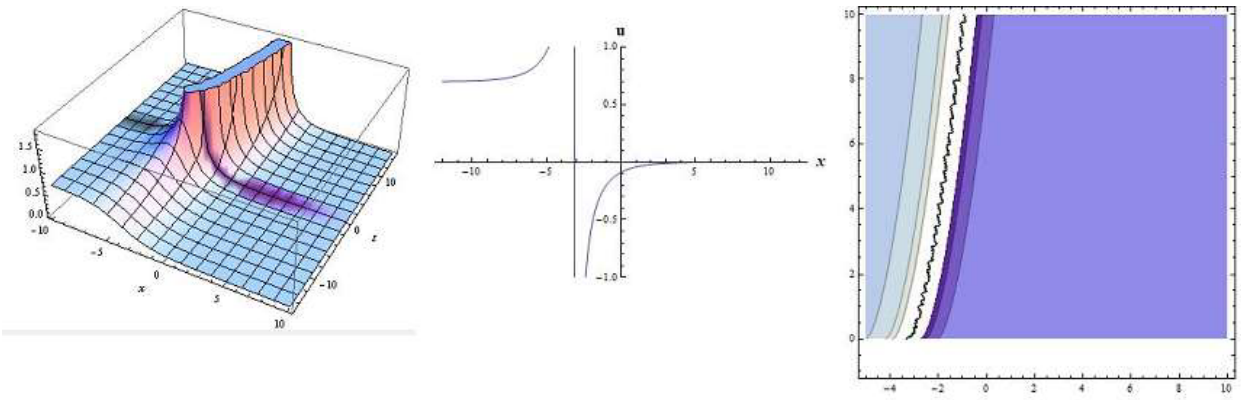

Figure 1: The 2D-3D surfaces and contourplot of the exact solution of $u(x,t)$ by considering the values:
$E = 0.2; p = 0.35; d = 0.7; a = 0.61;\ -10 < x < 10, -15 < t < 15$ for 3D surface,
$-12 < x < 12;\ t = 0.1$ for 2D surface,
$-5 < x < 10,\ -1 < t < 10$ **for contourplot.**

Substituting the solution (16) in Eq (11), we obtain

$$v(x,t) = -\frac{4de^{2p\left(x-\frac{pt^{\alpha}}{\alpha}\right)}p^3E}{\left(de^{2m\left(x-\frac{mt^{\alpha}}{\alpha}\right)} - pE\right)^2}.$$

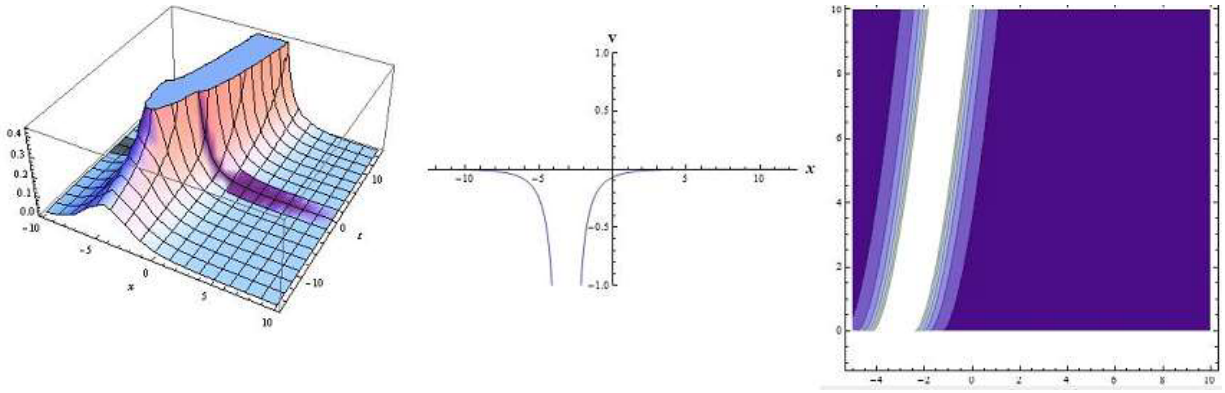

Figure 2: The 2D-3D surfaces and contourplot of the exact solution of $v(x,t)$ by considering the values: $E = 0.2; p = 0.35; d = 0.7; a = 0.61;\ -10 < x < 10, -15 < t < 15$ for 3D surface, $-12 < x < 12; t = 0.1$ for 2D surface, $-5 < x < 10,\ -1 < t < 10$ for contourplot.

4. CONCLUSION

The exact solutions of the fractional equation obtained using the IBSEFM method are presented in $u(x,t)$ and $v(x,t)$. Hence we obtain new solutions to the time fractional approximate long water wave equation. The IBSEFM is applied accurately to obtain the exact solutions for generalized form of the nonlinear conformable time fractional equation. The method is simple, reliable and very efficient in finding exact solutions for these nonlinear fractional evolution equations. Hence, the proposed technique may be taken as a new approach to find exact solutions to the models.

REFERENCES

1. A. Hasegawa, Plasma Instabilities and Nonlinear Effect (Springer-Verlag, Berlin, 1975.
2. K.S. Miller, B. Ross, An Introduction to the Fractional Calculus and Fractional Differential Equations, Wiley, New York, 1993.
3. A.A. Kilbas, H.M. Srivastava and J.J. Trujillo, Theory and Applications of Fractional Differential Equations, Elsevier, Amsterdam, 2006.
4. A. Emad, B.Abdel-Salam, A.Y. Eltayeb, Solution of nonlinear space-time fractional differential equations using the fractional Riccati expansion method. Math. Probl. Eng., vol. 2013, pp. 1--6, 2013.
5. H. Rezazadeh, A. Korkmaz, M. Eslami, J. Vahidi, R. Ashgari, Traveling wave solution of conformable fractional generalized reaction Duffing model by generalized projective Riccati equation method, Opt. Quant. Electron., vol. 50, no. 3, 2018.
6. A. Tozar, A. Kurt, O. Tasbozan, New Wave Solutions of Time Fractional Integrable Dispersive Wave Equation Arising in Ocean Engineering Models. Kuwait J. Sci., vol. 47, no. 2, pp.22-33, 2020.
7. G. Yel, H. M. Baskonus, Solitons in conformable time-fractional Wu-Zhang system arising in coastal design. Pramana, vol. 93, 2019.
8. V. Ala, U. Demirbilek, K. R. Mamedov, An application of improved Bernoulli sub-equation function method to the nonlinear conformable time-fractional SRLW equation. AIMS Mathematics, vol.5 no.4, pp.3751-3761, 2020.
9. H. Bulut, H. and M. Baskonus, Exponential prototype structures for (2+1)-dimensional BoitiLeon-Pempinelli systems in mathematical physics, Waves in Random and Complex Media, vol. 26, no. 2, pp.189--195, 2016.

10. R. Khalil, M. Al Horani, A. Yousef, M. Sababheh, A new definition of fractional derivative, J. Comput. Appl. Math, vol.264, pp.65--70, 2014.
11. T. Abdeljawad, On conformable fractional calculus, J. Comput. Appl. Math., vol. 279, pp.57--66, 2015.
12. A. Atangana, D. Baleanu, A. Alsaedi, New properties of conformable derivative, Open Math., vol.13, pp.1-10, 2015.
13. G. B. Whitham, Variational methods and applications to water waves, Proc. Royal Ser. A., vol. 299, pp. 6--25, 1967.
14. L. J. F. Broer, Approximate equations for long water waves, Applied Scientific Research, vol.31, pp. 377--395, 1975.
15. D. J. Kaup, A Higher order water-wave equation and the method for solving it, Progress of Theoretical Physics, vol. 54, pp. 396--408, 1975.

Some New Fractional Inequalities for Quasi-Convex Functions

Tahir Ullah KHAN[1], Sinan ASLAN[2], M. Emin ÖZDEMİR[3], and Alper EKİNCİ[4]

[1]*University of Peshawar, Peshawar-PAKİSTAN*
[2]*Graduate School of Natural and Applied Sciences,*
Giresun University, Giresun-TURKEY
[3]*Department of Mathematics Education, Faculty of Education,*
Bursa Uludağ University, Bursa-TURKEY
[4]*Department of Foreign Trade, Bandirma Vocational High School,*
Bandirma Onyedi Eylul University, Balikesir-Bandırma-TURKEY

tahirullah348@gmail.com
sinanaslan0407@gmail.com
eminozdemir@uludag.edu.tr
alperekinci@hotmail.com

Abstract. In this paper, some historical backgrounds and some earlier results have been given related to quasi-convexity, Riemann-Liouville fractional integral operators and general forms of proportional fractional integral operators. In the second part, some new integral inequalities have been established via the general forms of proportional fractional integral operators for integrable quasi-convex mappings.

1. INTRODUCTION

Let's first define the spaces we will use throughout this paper.

Definition 1.1 *[22, 34]* $f(\kappa)$ *be in* $L_{q,r}[0,\infty)$ *space if*

$$L_{q,r}[0,\infty)=\{f:\| f \|_{L_{q,r}[0,\infty)}=\left(\int_a^b | f(\kappa)|^q \kappa^r d\kappa\right)^{\frac{1}{q}}<\infty, 1\le q<\infty, r\ge 0\}.$$

For $r=0$,

$$L_q[0,\infty)=\{f:\| f \|_{L_{q,r}[0,\infty)}=\left(\int_a^b | f(\kappa)|^q d\kappa\right)^{\frac{1}{q}}<\infty, 1\le q<\infty\}.$$

Definition 1.2 *[21] Let* $f\in L_1[0,\infty)$ *and* h *be an increasing and positive monotone function on* $[0,\infty)$ *and also derivative* h' *is continuous on* $[0,\infty)$ *and* $h(0)=0$. *The space* $X_h^q(0,\infty)(1\le q<\infty)$ *of those real-valued Lebesgue measurable functions* f *on* $[0,\infty)$ *for which*

$$\| f \|_{X_h^q}=\left(\int_0^\infty | f(\kappa)|^q h'd\kappa\right)^{\frac{1}{q}}<\infty, 1\le q<\infty$$

and for the case $q=\infty$

$$\| f \|_{X_h^\infty}=ess\sup_{0\le\kappa<\infty}[h'(\kappa)f(\kappa)].$$

Specially, when $h(\varepsilon)=\varepsilon(1\le q<\infty)$ the space $X_h^q[0,\infty)$ coincides with the $L_q[0,\infty)$-space and also if we choose $h(\varepsilon)=ln\varepsilon(1\le q<\infty)$ the space $X_h^q[0,\infty)$ coincides with $L_{q,r}[1,\infty)$-space.

The fractional calculus, which is engaged in integral and differential operators of arbitrary orders, is as old as the conceptional calculus that deals with integrals and derivatives of non-negative integer orders. The fractional operators are excellent tools to use in modeling long-memory processes and many phenomena that appear in physics, chemistry, electricity, mechanics and many other disciplines. We will continue by remembering a few of the operators that fractional analysis brings to the world of mathematics, and with their unique applications for real world problems, allowing many researchers to conduct motivated studies. Now let's give some important fractional integral operator definitions.

Definition 1.3 *Let* $f \in L_1[a,b]$. *The Riemann-Liouville integrals* $J_{a+}^{\alpha} f$ *and* $J_{b-}^{\alpha} f$ *of order* $\alpha > 0$ *with* $a \geq 0$ *are defined by*

$$J_{a+}^{\alpha} f(\varepsilon) = \frac{1}{\Gamma(\alpha)} \int_a^{\varepsilon} (\varepsilon - \kappa)^{\alpha-1} f(\kappa) d\kappa, \quad \varepsilon > a$$

and

$$J_{b-}^{\alpha} f(\varepsilon) = \frac{1}{\Gamma(\alpha)} \int_{\varepsilon}^{b} (\kappa - \varepsilon)^{\alpha-1} f(\kappa) d\kappa, \quad \varepsilon < b$$

respectively. Here $\Gamma(\varepsilon)$ is the Gamma function and its definition is $\Gamma(\varepsilon) = \int_0^{\infty} e^{-\varepsilon} \varepsilon^{\kappa-1} d\kappa.$

It is to be noted that $J_{a+}^{0} f(\varepsilon) = J_{b-}^{0} f(\varepsilon) = f(\varepsilon)$ in the case of $\alpha = 1$, the fractional integral reduces to the classical integral.

Definition 1.4 *[24] Let* (a,b) *with* $-\infty \leq a < b \leq \infty$ *be a finite or infinite interval of the real line* $\mathbb{R}$ *and* α *a complex number with* $Re(\alpha) > 0$. *Also let* h *be a strictly increasing function on* (a,b), *having a continuous derivative* h' *on* (a,b). *The generalized left and right sided Riemann-Liouville fractional integrals of a function* f *with respect to another function* h *on* $[a,b]$ *defined as*

$${}_{a+}^{h} I^{\alpha} f(\varepsilon) = \frac{1}{\Gamma(\alpha)} \int_a^{\varepsilon} (h(\varepsilon) - h(\kappa))^{\alpha-1} f(\kappa) h'(\kappa) d\kappa, \quad \varepsilon > a$$

and

$${}_{b-}^{h} I^{\alpha} f(\varepsilon) = \frac{1}{\Gamma(\alpha)} \int_{\varepsilon}^{b} (h(\kappa) - h(\varepsilon))^{\alpha-1} f(\kappa) h'(\kappa) d\kappa, \quad \varepsilon < b.$$

In [16], Jarad et al. identified the generalized proportional fractional integrals that satisfy many important features as follows:

Definition 1.5 *The left and right generalized proportional fractional integral operators are respectively defined by*

$${}_{a+}\mathrm{J}^{\alpha,\zeta} f(\varepsilon) = \frac{1}{\zeta^{\alpha}\Gamma(\alpha)} \int_a^{\varepsilon} e^{\left[\frac{\zeta-1}{\zeta}(\varepsilon-\kappa)\right]} (\varepsilon - \kappa)^{\alpha-1} f(\kappa) d\kappa, \quad \varepsilon > a$$

and

$${}_{b-}\mathrm{J}^{\alpha,\zeta} f(\varepsilon) = \frac{1}{\zeta^{\alpha}\Gamma(\alpha)} \int_{\varepsilon}^{b} e^{\left[\frac{\zeta-1}{\zeta}(\kappa-\varepsilon)\right]} (\kappa - \varepsilon)^{\alpha-1} f(\kappa) d\kappa, \quad \varepsilon < b$$

where $\zeta \in (0,1]$ and $\alpha \in \mathbb{C}$ and $\mathrm{R}(\alpha) > 0$.

Definition 1.6 *[23] Let* a,b *be two nonnegative real numbers with* $a<b,\alpha,\rho$ *two positive real numbers, and* $f:[a,b]\to\mathbb{R}$ *be an integrable function. The left and right Katugampola fractional integrals defined as*

$$ {}_{a+}\mathrm{I}^{\alpha} f(\varepsilon)=\frac{1}{\Gamma(\alpha)}\int_a^{\varepsilon}\left(\frac{\varepsilon^{\rho}-\kappa^{\rho}}{\rho}\right)^{\alpha-1}\frac{f(\kappa)d\kappa}{\kappa^{1-\rho}},\quad \varepsilon>a $$

and

$$ {}_{b-}\mathrm{I}^{\alpha} f(\varepsilon)=\frac{1}{\Gamma(\alpha)}\int_{\varepsilon}^{b}\left(\frac{\kappa^{\rho}-\varepsilon^{\rho}}{\rho}\right)^{\alpha-1}\frac{f(\kappa)d\kappa}{\kappa^{1-\rho}},\quad \varepsilon<b. $$

Definition 1.7 *[30, 24] Let* a,b *be two reals with* $0<a<b$ *and* $f:[a,b]\to\mathbb{R}$ *be an integrable function. The left and right Hadamard fractional integrals of order* $\alpha>0$ *are defined as*

$$ {}_{a+}\mathrm{F}^{\alpha} f(\varepsilon)=\frac{1}{\Gamma(\alpha)}\int_a^{\varepsilon}\frac{f(\kappa)}{\kappa\left(\ln\frac{\varepsilon}{\kappa}\right)^{1-\alpha}}d\kappa,\quad \varepsilon>a $$

and

$$ {}_{b-}\mathrm{F}^{\alpha} f(\varepsilon)=\frac{1}{\Gamma(\alpha)}\int_{\varepsilon}^{b}\frac{f(\kappa)}{\kappa\left(\ln\frac{\kappa}{\varepsilon}\right)^{1-\alpha}}d\kappa,\quad \varepsilon<b. $$

Definition 1.8 *[27] The left and right generalized proportional Hadamard fractional integrals of order* $\alpha>0$ *and proportionality index* $\zeta\in(0,1]$ *is defined by*

$$ {}_{a+}\mathrm{F}^{\alpha,\zeta} f(\varepsilon)=\frac{1}{\zeta^{\alpha}\Gamma(\alpha)}\int_a^{\varepsilon}\frac{e^{\left[\frac{\zeta-1}{\zeta}\left(\ln\frac{\varepsilon}{\kappa}\right)\right]}}{\left(\ln\frac{\varepsilon}{\kappa}\right)^{1-\alpha}}\frac{f(\kappa)}{\kappa}d\kappa,\quad \varepsilon>a $$

and

$$ {}_{b-}\mathrm{F}^{\alpha,\zeta} f(\varepsilon)=\frac{1}{\zeta^{\alpha}\Gamma(\alpha)}\int_a^{\varepsilon}\frac{e^{\left[\frac{\zeta-1}{\zeta}\left(\ln\frac{\kappa}{\varepsilon}\right)\right]}}{\left(\ln\frac{\kappa}{\varepsilon}\right)^{1-\alpha}}\frac{f(\kappa)}{\kappa}d\kappa,\quad \varepsilon<b. $$

Now, let's give a fractional operator which is known as the generalized proportional fractional (GPF) integral operator function in the sense of another function h.

Definition 1.9 *[20, 29] Let* $f\in X_h^q(0,\infty)$, *there is an increasing, positive monotone function* h *defined on* $[0,\infty)$ *having continuous derivative* h' *on with* $h(0)=0$. *Then the left-sided and right-sided GPF-integral operator of a function* f *in the sense of another function* h *of order* $\alpha>0$ *are stated as:*

$$ {}_{a+}^{h}\mathrm{J}^{\alpha,\zeta} f(\varepsilon)=\frac{1}{\zeta^{\alpha}\Gamma(\alpha)}\int_a^{\varepsilon}e^{\left[\frac{\zeta-1}{\zeta}(h(\varepsilon)-h(\kappa))\right]}(h(\varepsilon)-h(\kappa))^{\alpha-1}f(\kappa)h'(\kappa)d\kappa,\quad \varepsilon>a $$

and

$$ {}^{h}_{b-}\mathrm{J}^{\alpha,\zeta} f(\varepsilon) = \frac{1}{\zeta^{\alpha}\Gamma(\alpha)} \int_{\varepsilon}^{b} e^{\left[\frac{\zeta-1}{\zeta}(h(\kappa)-h(\varepsilon))\right]} (h(\kappa)-h(\varepsilon))^{\alpha-1} f(\kappa) h'(\kappa) d\kappa, \quad \varepsilon < b $$

where $\zeta \in (0,1]$ and $\alpha \in \mathbb{C}$ and $\mathrm{R}(\alpha) > 0$.

For different choices of parameters in Definition 1.9 we get Riemann-Liouville integrals, generalized Riemann-Liouville fractional integrals, generalized proportional fractional integrals, Katugampola fractional integrals, Hadamard fractional integrals and generalized proportional Hadamard fractional integrals. Recently, several new studies have been performed by mathematicians via various fractional integral operators and with the help of fractional integral operators numerous new inequalities have been proved in the literature, see [29, 20, 15, 25, 7, 17, 18, 19, 10, 11, 12, 13].

In [35], Pecaric *et al*. defined quasi-convex functions as following:

Definition 1.10 *A function* $f:[a,b]\to \mathrm{R}$ *is said quasi-convex on* $[a,b]$ *if*

$$ f(\lambda x+(1-\lambda)y) \le \max\{f(x), f(y)\}, \quad (QC) $$

holds for all $x, y \in [a,b]$ and $\lambda \in 0,1]$.

Clearly, any convex function is quasi-convex function. Furthermore, there exist quasi-convex functions which are not convex. For more details related to this class of convexity see the papers [1]-[6].

The main aim of this paper is to establish some new integral inequalities for products of two $AG-$convex functions via the general forms of proportional fractional integral operators.

2. MAIN RESULTS

Theorem 2.1 *Assume that* $f:(0,\infty)\to R$ *be differentiable function and* ψ *be a positive monoton increasing function that is defined on* $[0,\infty)$. *Let* $\psi'(\tau)$ *be continuous and* $\psi(0)=0$. *Then, if* f *is Quasi−convex function, we have the following inequality;*

$$ \left({}^{\Psi}\mathrm{T}^{\eta,\xi}_{0^+,\tau} f\right)(\tau) \le \frac{\max\{f(a), f(b)\}}{\xi^{\eta}\Gamma(\eta)} \frac{\psi^{\eta}(\tau)}{\left(\frac{1-\xi}{\xi}\psi(\tau)\right)^{\eta}} \left(\Gamma(\eta) - \Gamma\left(\eta, \frac{1-\xi}{\xi}\psi(\tau)\right)\right) $$

for $\xi \in (0,1)$, $\mu \in \mathbb{C}$, $Re(\eta) > 0, \tau > 0$, where $\Gamma(s,x) = \int_x^{\infty} t^{s-1} e^{-t} dt$ is the incomplete Gamma function.

Proof. By using the definition of Quasi-convex functions, we can write

$$ f(ta+(1-t)b) \le \max\{f(a), f(b)\} $$

By changing of the variable such that $x = ta+(1-t)b$, we have

$$ f(x) \le \max\{f(a), f(b)\} $$

By multiplying both sides of the resulting inequality by

$$ \frac{1}{\xi^{\eta}\Gamma(\eta)} \frac{e^{\frac{\xi-1}{\xi}(\psi(\tau)-\psi(x))}}{(\psi(\tau)-\psi(x))^{1-\eta}} \psi'(x) $$

and if we apply the integration to the right hand side, we obtain

$$\left({}^{\Psi}\mathsf{T}_{0^+,\tau}^{\eta,\xi} f\right)(\tau) \le \frac{\max\{f(a), f(b)\}}{\xi^{\eta}\Gamma(\eta)} \int_0^{\tau} \frac{e^{\frac{\xi-1}{\xi}(\psi(\tau)-\psi(x))}}{(\psi(\tau)-\psi(x))^{1-\eta}} \psi'(x)dx,$$

Which implies

$$\left({}^{\Psi}\mathsf{T}_{0^+,\tau}^{\eta,\xi} f\right)(\tau) \le \frac{\max\{f(a), f(b)\}}{\xi^{\eta}\Gamma(\eta)} \frac{\psi^{\eta}(\tau)}{\left(\frac{1-\xi}{\xi}\psi(\tau)\right)^{\eta}} \left(\Gamma(\eta) - \Gamma\left(\eta, \frac{1-\xi}{\xi}\psi(\tau)\right)\right).$$

The proof is completed.

Theorem 2.2 *Assume that* $f:(0,\infty)\to R$ *be differentiable function and* ψ *be a positive monoton increasing function that is defined on* $[0,\infty)$. *Let* $\psi'(\tau)$ *be continuous and* $\psi(0)=0.\ p,q>1 ve \frac{1}{p}+\frac{1}{q}=1, |\psi'(x)| \le M$

Then, if f *is Quasi − convex function, we have the following inequality;*

$$\left({}^{\Psi}\mathsf{T}_{0^+,\tau}^{\eta,\xi} f\right)(\tau)$$

$$\le \frac{\max\{f(a), f(b)\} M^{\frac{p-1}{p}} \tau^{\frac{1}{q}}}{\xi^{\eta}\Gamma(\eta)}$$

$$\times \left(\frac{\psi^{p(\eta-1)+1}(\tau)}{\left(\frac{1-\xi}{\xi} p\psi(\tau)\right)^{p(\eta-1)+1}} \left(\Gamma(p(\eta-1)+1) - \Gamma\left(p(\eta-1)+1, \frac{1-\xi}{\xi} p\psi(\tau)\right)\right) \right)^{\frac{1}{p}}$$

for $\xi \in (0,1)$, $\mu \in \mathbb{C}$, $Re(\eta)>0, \tau>0$. Where $\Gamma(s,x)=\int_x^{\infty} t^{s-1}e^{-t}dt$ is the incomplete Gamma function.

Proof. By using the definition of Quasi − convexity function, we can write

$$f(ta+(1-t)b) \le \max\{f(a), f(b)\}$$

By changing of the variable such that $x = ta+(1-t)b$, we have

$$f(x) \le \max\{f(a), f(b)\}$$

By multiplying both sides of the resulting inequality by

$$\frac{1}{\xi^{\eta}\Gamma(\eta)} \frac{e^{\frac{\xi-1}{\xi}(\psi(\tau)-\psi(x))}}{(\psi(\tau)-\psi(x))^{1-\eta}} \psi'(x)$$

and if we apply the integration to the right hand side, we obtain

$$\left({}^{\Psi}\mathsf{T}_{0^+,\tau}^{\eta,\xi} f\right)(\tau) \le \frac{\max\{f(a), f(b)\}}{\xi^{\eta}\Gamma(\eta)} \int_0^{\tau} \frac{e^{\frac{\xi-1}{\xi}(\psi(\tau)-\psi(x))}}{(\psi(\tau)-\psi(x))^{1-\eta}} \psi'(x)dx$$

By applying Hölder inequality to the resulting inequality and by making use of some necessary operation and by taking into account $\left|\psi'(x)\right| \le M$ we obtain

$$\left({}^{\Psi}\mathsf{T}^{\eta,\xi}_{0^+,\tau} f\right)(\tau) \le \frac{\max\{f(a), f(b)\}}{\xi^{\eta}\Gamma(\eta)}$$

$$\times\left(\int_0^{\tau}\left|\frac{e^{\frac{\xi-1}{\xi}(\psi(\tau)-\psi(x))}}{(\psi(\tau)-\psi(x))^{1-\eta}}\psi'(x)\right|^{p} dx\right)^{\frac{1}{p}} \times\left(\int_0^{\tau}|1|^{q} dx\right)^{\frac{1}{q}}$$

$$\left({}^{\Psi}\mathsf{T}^{\eta,\xi}_{0^+,\tau} f\right)(\tau)$$

$$\le \frac{\max\{f(a), f(b)\}M^{\frac{p-1}{p}}\tau^{\frac{1}{q}}}{\xi^{\eta}\Gamma(\eta)}$$

$$\times\left(\frac{\psi^{p(\eta-1)+1}(\tau)}{\left(\frac{1-\xi}{\xi}p\psi(\tau)\right)^{p(\eta-1)+1}}\left(\Gamma(p(\eta-1)+1)-\Gamma\left(p(\eta-1)+1,\frac{1-\xi}{\xi}p\psi(\tau)\right)\right)\right)^{\frac{1}{p}}.$$

This completes the proof.

Theorem 2.3 *Assume that* $f:(0,\infty)\to R$ *be differentiable function and* ψ *be a positive monoton increasing function that is defined on* $[0,\infty)$. *Let* $\psi'(\tau)$ *be continuous and* $\psi(0)=0.q\ge 1,\left|\psi'(x)\right|\le M$ *Then, if* f *is Quasi − convex function, we have the following inequality;*

$$\left({}^{\Psi}\mathsf{T}^{\eta,\xi}_{0^+,\tau} f\right)(\tau) \le \frac{\max\{f(a), f(b)\}}{\xi^{\eta}\Gamma(\eta)}\frac{\psi^{\eta}(\tau)}{\left(\frac{1-\xi}{\xi}\psi(\tau)\right)^{\eta}}\left(\Gamma(\eta)-\Gamma\left(\eta,\frac{1-\xi}{\xi}\psi(\tau)\right)\right)$$

for $\xi\in(0,1)$, $\mu\in\mathbb{C}$, $Re(\eta)>0,\tau>0$, where $\Gamma(s,x)=\int_x^{\infty}t^{s-1}e^{-t}dt$ is the incomplete Gamma function.

Proof. By using the definition of Quasi − convexity function, we can write

$$f(ta+(1-t)b)\le \max\{f(a), f(b)\}$$

By changing of the variable such that $x=ta+(1-t)b$, we have

$$f(x)\le \max\{f(a), f(b)\}$$

By multiplying both sides of the resulting inequality by

$$\frac{1}{\xi^{\eta}\Gamma(\eta)}\frac{e^{\frac{\xi-1}{\xi}(\psi(\tau)-\psi(x))}}{(\psi(\tau)-\psi(x))^{1-\eta}}\psi'(x)$$

and if we apply the integration to the right hand side, we obtain

$$\left({}^{\Psi}\mathsf{T}_{0^+,\tau}^{\eta,\xi} f\right)(\tau) \le \frac{\max\{f(a), f(b)\}}{\xi^{\eta}\Gamma(\eta)} \int_0^{\tau} \frac{e^{\frac{\xi-1}{\xi}(\psi(\tau)-\psi(x))}}{(\psi(\tau)-\psi(x))^{1-\eta}} \psi'(x)dx$$

By applying Hölder inequality to the resulting inequality

$$\left({}^{\Psi}\mathsf{T}_{0^+,\tau}^{\eta,\xi} f\right)(\tau) \le \frac{\max\{f(a), f(b)\}}{\xi^{\eta}\Gamma(\eta)} \left(\int_0^{\tau} \frac{e^{\frac{\xi-1}{\xi}(\psi(\tau)-\psi(x))}}{(\psi(\tau)-\psi(x))^{1-\eta}} \psi'(x)dx \right)^{1-\frac{1}{q}}$$

$$\times \left(\int_0^{\tau} \frac{e^{\frac{\xi-1}{\xi}(\psi(\tau)-\psi(x))}}{(\psi(\tau)-\psi(x))^{1-\eta}} \psi'(x)|1|^q dx \right)^{\frac{1}{q}}$$

$$\left({}^{\Psi}\mathsf{T}_{0^+,\tau}^{\eta,\xi} f\right)(\tau) \le \frac{\max\{f(a), f(b)\}}{\xi^{\eta}\Gamma(\eta)} \frac{\psi^{\eta}(\tau)}{\left(\frac{1-\xi}{\xi}\psi(\tau)\right)^{\eta}} \left(\Gamma(\eta) - \Gamma\left(\eta, \frac{1-\xi}{\xi}\psi(\tau)\right) \right)$$

Which completes the proof.

REFERENCES

1. D.A. Ion, Some estimates on the Hermite-Hadamard inequality through quasi-convex functions, Annals of University of Craiova, *Math. Comp. Sci. Ser.*, 34 (2007), 82-87. ZBL 1174.26321, MR2517875.
2. K.L. Tseng, G.S. Yang and S.S. Dragomir, On quasi convex functions and Hadamard's inequality, *Demonstr. Math.*, 41, No. 2, 323-336 (2008). ZBL 1151.26333, MR2419910.
3. M.A. Latif and M. Alomari, On Hadamard-type inequalities for $h-$convex functions on the co-ordinates, *International Journal of Math. Analysis*, 3 (2009), no. 33, 1645-1656. ZBL 1196.26028, MR2657722.
4. M. Alomari, M. Darus and S.S. Dragomir, New inequalities of Hermite-Hadamard type for functions whose second derivatives absolute values are quasi-convex, *Tamkang J. Math.*, 41, no. 4, 353–359, 2010. ZBL 1214.26003, MR2789971.
5. M. Alomari, M. Darus and U.S. Kırmacı, Refinements of Hadamard-type inequalities for quasi-convex functions with applications to trapezoidal formula and to special means, *Computers and Mathematics with Applications*, 59, 225-232, 2010. ZBL 1189.26037, MR2575509.
6. M. Alomari and M. Darus, On some inequalities Simpson-type via quasi-convex functions with applications, *Transylv. J. Math. Mech.*, 2 (2010), no. 1, 15–24. MR2817188.
7. A.O.Akdemir, A. Ekinci and E. Set, *Conformable Fractional Integrals And Related New Integral Inequalities*, Journal of Nonlinear and Convex Analysis, Volume 18, Number 4, 2017, 661-674.
8. M.A. Dokuyucu, D. Baleanu, E. Celik, *Analysis of Keller-Segel model with Atangana-Baleanu fractional derivative*. Filomat, 32(16), 5633-5643, 2018.
9. M.A. Dokuyucu, E. Celik, H. Bulut, H.M. Baskonus, *Cancer treatment model with the Caputo-Fabrizio fractional derivative*, The European Physical Journal Plus, 133(3), 92, 2018.
10. M.A. Dokuyucu, H. Dutta, *A fractional order model for Ebola Virus with the new Caputo fractional derivative without singular kernel*, Chaos, Solitons and Fractals Volume 134, May 2020, 109717.
11. M.A. Dokuyucu, *A fractional order alcoholism model via Caputo-Fabrizio derivative*, AIMS Mathematics 5 (2), 781-797, 2020.
12. A. Ekinci and M.E. Ozdemir, *Some New Integral Inequalities Via Riemann-Liouville Integral Operators*, Applied and Computational Mathematics, Vol. 18, No:3, 2019, pages: 288-295.
13. F. Jarad, T. Abdeljawad, J. Alzabut, *Generalized fractional derivatives generated by a class of local proportional derivatives*, Eur. Phys. J. Spec. Top. 226, 34573471 (2017). https://doi.org/10.1140/epjst/e2018-00021-7

14. F. Jarad, T. Abdeljawad, *Generalized fractional derivatives and Laplace transform*, Discrete and Continuous Dynamical Systems - S, 2020, 13 (3) : 709-722. doi: 10.3934/dcdss.2020039.
15. F. Jarad, T. Abdeljawad, D. Baleanu, *Caputo-type modification of the Hadamard fractional derivatives*, Adv Differ Equ., 2012, 142 (2012) doi:10.1186/1687-1847-2012-142.
16. F. Jarad, T. Abdeljawad, D. Baleanu, *On the generalized fractional derivatives and their Caputo modification*, J. Nonlinear Sci. Appl 10 (5), 2607-2619, 2017.
17. F. Jarad, M. A. Alqudah, T. Abdeljawad, *On more general forms of proportional fractional operators*, Open Mathematics 18.1 (2020): 167-176.
18. E. Kaçar, Z. Kaçar, H. Yıldırım, *Integral inequalities for Riemann-Liouville fractional integrals of a function with respect to another function*, Iran.J.Math.Sci.Inform. 13 (2018), 1-13.
19. U.N. Katugampola, *Approach to a generalized fractional integral*, Appl.Math.Comput. 218 (2011),860-865.
20. U.N. Katugampola, *A new approach to a generalized fractional derivatives*, Bull. Math. Anal. Appl., 6(4) (2014),1-15.
21. A.A. Kilbas, H.M. Srivastava, J.J. Trujillo, *Theory and Applications of Fractional Differential Equations*, North-Holland Mathematics Studies, New York, NY, USA, (2006).
22. D. Nie, S. Rashid, A.O. Akdemir, D. Baleanu and J.-B. Liu, *On Some New Weighted Inequalities for Differentiable Exponentially Convex and Exponentially Quasi-Convex Functions with Applications*, Mathematics 2019, 7(8), 727.
23. G. Rahman, T. Abdeljawad, F. Jarad, A. Khan, K:S: Nisar, *Certain inequalities via generalized proportional Hadamard fractional integral operators*, Adv.Diff.Eqs. (2019), 454.
24. S. Rashid, F. Jarad, M. A. Noor, H. Kalsoom, Y. M. Chu, *Inequalities by means of generalized proportional fractional integral operators with respect to another function*, Mathematics, 7(12) (2019) 1225.
25. S.G. Samko, A.A. Kilbas, *Normal densities*, Linear Algebra Appl., 396 (2005), 317-328.
26. H. Yıldırım, Z. Kırtay, *Ostrowski inequality for generalized fractional integral and related inequalities*, Malatya J.Mat. 2 (2014),322-329.
27. J. Pecaric, F. Proschan and Y.L. Tong, Convex Functions, Partial Orderings and Statistical Applications, Academic Press, Inc., 1992.

Some New Bullen Type Inequalities for Different Kinds of Convexity on the Coordinates

Saima RASHID[1], Ahmet Ocak AKDEMİR[2], Erhan SET[3] and Alper EKİNCİ[4]

[1] *Government College University,*
Department of Mathematics, Faisalabad-PAKİSTAN
[2] *Department of Mathematics, Faculty of Science and Letters,*
Ağrı İbrahim Çeçen University, Ağrı-TURKEY
[3]*Department of Mathematics, Faculty of Science and Letters,*
Ordu University, Ordu-TURKEY
[4] *Department of Foreign Trade, Bandirma Vocational High School,*
Bandirma Onyedi Eylul University, Balikesir-Bandırma-TURKEY

aocakakdemir@gmail.com
SaimaMoeed.gc@gmail.com
erhanset@yahoo.com
alperekinci@hotmail.com

Abstract. Bullen inequality, along with classical inequalities such as Hermite Hadamard, Jensen and Ostrowski's inequality, has an important place in theory. It has wide usage in many areas with its application areas such that for averaged midpoint-trapezoid quadrature rules and applications in numerical integration. In this study, in order to obtain a variant of the Bullen inequality, an integral identity with double integrals is given. With the help of this identity, many inequalities have been demonstrated for quasi-convex functions in coordinates and reduced results have been mentioned for the bounded functions.

1. INTRODUCTION

We will start by expressing two important inequalities proved for convex functions. These two inequalities are presented on the basis of averages and give bounds for the mean value of a convex function.

Assume that $f:I\subseteq \mathbb{R}\to\mathbb{R}$ is a convex mapping defined on the interval I of $\mathbb{R}$ where $a<b$. The following statement;

$$f\left(\frac{a+b}{2}\right)\leq\frac{1}{b-a}\int_a^b f(x)dx\leq\frac{f(a)+f(b)}{2}$$

holds and known as Hermite-Hadamard inequality. Both inequalities hold in the reversed direction if f is concave.

The Bullen's integral inequality can be presented as

$$\frac{1}{b-a}\int_a^b f(x)dx\leq\frac{1}{2}\left[f\left(\frac{a+b}{2}\right)+\frac{f(a)+f(b)}{2}\right]$$

where $f:I\subset\mathbb{R}\to\mathbb{R}$ is a convex mapping on the interval I of $\mathbb{R}$ where $a,b\in I$ with $a<b$. For different versions and various generalizations of these two inequalities, we recommend that the authors to browse the articles [17, 18, 19, 20, 21, 22, 23, 24, 25, 26].

In [1], Dragomir mentiones about an expansion of the concept of convex function, which is used in many inequalities in theory and has applications in different fields of mathematics, especially convex programming.

Definition 1 *Let us consider the bidimensional interval* $\Delta = [a,b]\times[c,d]$ *in* $\mathbb{R}^2$ *with* $a < b,\ c < d$. *A function* $f : \Delta \to \mathbb{R}$ *will be called convex on the co-ordinates if the partial mappings* $f_y : [a,b] \to \mathbb{R},\ f_y(u) = f(u,y)$ *and* $f_x : [c,d] \to \mathbb{R},\ f_x(v) = f(x,v)$ *are convex where defined for all* $y \in [c,d]$ *and* $x \in [a,b]$. *Recall that the mapping* $f : \Delta \to \mathbb{R}$ *is convex on* Δ *if the following inequality holds,*

$$f(\lambda x + (1-\lambda)z, \lambda y + (1-\lambda)w) \le \lambda f(x,y) + (1-\lambda) f(z,w)$$

for all $(x,y),(z,w) \in \Delta$ and $\lambda \in [0,1]$.

Expressing convex functions in coordinates brought up the question that it is possible for Hermite-Hadamard inequality to expand into coordinates. The answer to this motivating question has been found in Dragomir's paper (see [1]) and has taken its place in the literature as the expansion of Hermite-Hadamard inequality to a rectangle from the plane $\mathbb{R}^2$ stated below.

Theorem 1 *Suppose that* $f : \Delta = [a,b]\times[c,d] \to \mathbb{R}$ *is convex on the co-ordinates on* Δ. *Then one has the inequalities;*

$$\begin{aligned} & f\left(\frac{a+b}{2}, \frac{c+d}{2}\right) \\ & \le \frac{1}{2}\left[\frac{1}{b-a}\int_a^b f\left(x, \frac{c+d}{2}\right)dx + \frac{1}{d-c}\int_c^d f\left(\frac{a+b}{2}, y\right)dy\right] \\ & \le \frac{1}{(b-a)(d-c)}\int_a^b\int_c^d f(x,y)\,dx\,dy \\ & \le \frac{1}{4}\left[\frac{1}{(b-a)}\int_a^b f(x,c)\,dx + \frac{1}{(b-a)}\int_a^b f(x,d)\,dx\right. \\ & \left. + \frac{1}{(d-c)}\int_c^d f(a,y)\,dy + \frac{1}{(d-c)}\int_c^d f(b,y)\,dy\right] \\ & \le \frac{f(a,c)+f(a,d)+f(b,c)+f(b,d)}{4}. \end{aligned} \tag{1.1}$$

The above inequalities are sharp.

Numerous variants of this inequality were obtained for convexity and other types of convex functions in coordinates (See the papers [2, 3, 4, 5, 6, 7, 8, 9, 10, 11, 13, 14, 16]).

Definition 2 *(See ??) A function* $f : \Delta \to \mathbb{R}$ *is said quasi-convex function on the co-ordinates on* Δ *if the following inequality holds,*

$$f(\lambda x + (1-\lambda)z, \lambda y + (1-\lambda)w) \le \max\{f(x,y), f(z,w)\}$$

for all $(x,y),(z,w) \in \Delta$ and $\lambda \in [0,1]$.

In [12], Sarıkaya *et al.* proved some Hadamard-type inequalities for co-ordinated convex functions as followings:

Theorem 2 *Let* $f:\Delta\subset \mathbb{R}^2\to\mathbb{R}$ *be a partial differentiable mapping on* $\Delta:=[a,b]\times[c,d]$ *in* $\mathbb{R}^2$ *with* $a<b$ *and* $c<d$. *If* $\left|\frac{\partial^2 f}{\partial t\partial s}\right|$ *is a convex function on the co-ordinates on* Δ, *then one has the inequalities:*

$$|J|\le\frac{(b-a)(d-c)}{16}\times\frac{\left|\frac{\partial^2 f}{\partial t\partial s}\right|(a,c)+\left|\frac{\partial^2 f}{\partial t\partial s}\right|(a,d)+\left|\frac{\partial^2 f}{\partial t\partial s}\right|(b,c)+\left|\frac{\partial^2 f}{\partial t\partial s}\right|(b,d)}{4} \tag{1.2}$$

where

$$J=\frac{f(a,c)+f(a,d)+f(b,c)+f(b,d)}{4}+\frac{1}{(b-a)(d-c)}\int_a^b\int_c^d f(x,y)dxdy-A$$

and

$$A=\frac{1}{2}\left[\frac{1}{(b-a)}\int_a^b[f(x,c)+f(x,d)]dx+\frac{1}{(d-c)}\int_c^d[f(a,y)dy+f(b,y)]dy\right].$$

Theorem 3 *Let* $f:\Delta\subset \mathbb{R}^2\to\mathbb{R}$ *be a partial differentiable mapping on* $\Delta:=[a,b]\times[c,d]$ *in* $\mathbb{R}^2$ *with* $a<b$ *and* $c<d$. *If* $\left|\frac{\partial^2 f}{\partial t\partial s}\right|^q$, $q>1$, *is a convex function on the co-ordinates on* Δ, *then one has the inequalities:*

$$|J|\le\frac{(b-a)(d-c)}{4(p+1)^{\frac{2}{p}}}\times\left[\frac{\left|\frac{\partial^2 f}{\partial t\partial s}\right|^q(a,c)+\left|\frac{\partial^2 f}{\partial t\partial s}\right|^q(a,d)+\left|\frac{\partial^2 f}{\partial t\partial s}\right|^q(b,c)+\left|\frac{\partial^2 f}{\partial t\partial s}\right|^q(b,d)}{4}\right]^{\frac{1}{q}} \tag{1.3}$$

where A, J are as in Theorem 2 and $\frac{1}{p}+\frac{1}{q}=1$.

Theorem 4 *Let* $f:\Delta\subset \mathbb{R}^2\to\mathbb{R}$ *be a partial differentiable mapping on* $\Delta:=[a,b]\times[c,d]$ *in* $\mathbb{R}^2$ *with* $a<b$ *and* $c<d$. *If* $\left|\frac{\partial^2 f}{\partial t\partial s}\right|^q$, $q\ge1$, *is a convex function on the co-ordinates on* Δ, *then one has the inequalities:*

$$|J|\le\frac{(b-a)(d-c)}{16} \tag{1.4}$$

$$\times\left[\frac{\left|\frac{\partial^2 f}{\partial t\partial s}\right|^q(a,c)+\left|\frac{\partial^2 f}{\partial t\partial s}\right|^q(a,d)+\left|\frac{\partial^2 f}{\partial t\partial s}\right|^q(b,c)+\left|\frac{\partial^2 f}{\partial t\partial s}\right|^q(b,d)}{4}\right]^{\frac{1}{q}}$$

where $A,\ J$ are as in Theorem 2.

In [15], Özdemir et al. have proved a new integral identity and several new inequalities as followings;

Lemma 1 *Let* $f:\Delta=[a,b]\times[c,d]\to\mathbb{R}$ *be a partial differentiable mapping on* $\Delta=[a,b]\times[c,d]$. *If* $\frac{\partial^2 f}{\partial t\partial s}\in L(\Delta)$, *then the following equality holds:*

$$\begin{aligned}&f\left(\frac{a+b}{2},\frac{c+d}{2}\right)\\&-\frac{1}{(d-c)}\int_c^d f\left(\frac{a+b}{2},y\right)dy-\frac{1}{(b-a)}\int_a^b f\left(x,\frac{c+d}{2}\right)dx\\&+\frac{1}{(b-a)(d-c)}\int_a^b\int_c^d f(x,y)dydx\\&=\frac{1}{(b-a)(d-c)}\int_a^b\int_c^d p(x,t)q(y,s)\frac{\partial^2 f}{\partial t\partial s}\left(\frac{b-t}{b-a}a+\frac{t-a}{b-a}b,\frac{d-s}{d-c}c+\frac{s-c}{d-c}d\right)dsdt\end{aligned}$$

where

$$p(x,t)=\begin{cases}(t-a), & t\in\left[a,\frac{a+b}{2}\right]\\(t-b), & t\in\left(\frac{a+b}{2},b\right]\end{cases}$$

and

$$q(y,s)=\begin{cases}(s-c), & s\in\left[c,\frac{c+d}{2}\right]\\(s-d), & s\in\left(\frac{c+d}{2},d\right]\end{cases}$$

for each $x\in[a,b]$ and $y\in[c,d]$.

Theorem 5 *Let* $f:\Delta=[a,b]\times[c,d]\to\mathbb{R}$ *be a partial differentiable mapping on* $\Delta=[a,b]\times[c,d]$. *If* $\left|\frac{\partial^2 f}{\partial t\partial s}\right|$ *is a convex function on the co-ordinates on* Δ, *then the following inequality holds;*

$$\left| f\left(\frac{a+b}{2},\frac{c+d}{2}\right) - \frac{1}{(d-c)}\int_c^d f\left(\frac{a+b}{2},y\right)dy - \frac{1}{(b-a)}\int_a^b f\left(x,\frac{c+d}{2}\right)dx + \frac{1}{(b-a)(d-c)}\int_a^b\int_c^d f(x,y)dydx \right| \leq \frac{(b-a)(d-c)}{64}\left[\left|\frac{\partial^2 f}{\partial t\partial s}(a,c)\right| + \left|\frac{\partial^2 f}{\partial t\partial s}(b,c)\right| + \left|\frac{\partial^2 f}{\partial t\partial s}(a,d)\right| + \left|\frac{\partial^2 f}{\partial t\partial s}(b,d)\right|\right]. \tag{1.5}$$

Theorem 6 *Let* $f:\Delta=[a,b]\times[c,d]\to\mathbb{R}$ *be a partial differentiable mapping on* $\Delta=[a,b]\times[c,d]$. *If* $\left|\frac{\partial^2 f}{\partial t\partial s}\right|^q$, $q>1$, *is a convex function on the co-ordinates on* Δ, *then the following inequality holds;*

$$|C| \leq \frac{(b-a)(d-c)}{4(p+1)^{\frac{2}{p}}} \times\left[\frac{\left|\frac{\partial^2 f}{\partial t\partial s}(a,c)\right|^q + \left|\frac{\partial^2 f}{\partial t\partial s}(b,c)\right|^q + \left|\frac{\partial^2 f}{\partial t\partial s}(a,d)\right|^q + \left|\frac{\partial^2 f}{\partial t\partial s}(b,d)\right|^q}{4}\right]^{\frac{1}{q}}. \tag{1.6}$$

where

$$C = f\left(\frac{a+b}{2},\frac{c+d}{2}\right) - \frac{1}{(d-c)}\int_c^d f\left(\frac{a+b}{2},y\right)dy - \frac{1}{(b-a)}\int_a^b f\left(x,\frac{c+d}{2}\right)dx + \frac{1}{(b-a)(d-c)}\int_a^b\int_c^d f(x,y)dydx.$$

Theorem 7 *Let* $f:\Delta=[a,b]\times[c,d]\to\mathbb{R}$ *be a partial differentiable mapping on* $\Delta=[a,b]\times[c,d]$. *If* $\left|\frac{\partial^2 f}{\partial t\partial s}\right|^q$, $q\geq 1$, *is a convex function on the co-ordinates on* Δ, *then the following inequality holds;*

$$|C| \leq \frac{(b-a)(d-c)}{16} \tag{1.7}$$

$$\times\left[\frac{\left|\frac{\partial^2 f}{\partial t\partial s}(a,c)\right|^q+\left|\frac{\partial^2 f}{\partial t\partial s}(b,c)\right|^q+\left|\frac{\partial^2 f}{\partial t\partial s}(a,d)\right|^q+\left|\frac{\partial^2 f}{\partial t\partial s}(b,d)\right|^q}{4}\right]^{\frac{1}{q}}.$$

where

$$C=f\left(\frac{a+b}{2},\frac{c+d}{2}\right)$$
$$-\frac{1}{(d-c)}\int_c^d f\left(\frac{a+b}{2},y\right)dy-\frac{1}{(b-a)}\int_a^b f\left(x,\frac{c+d}{2}\right)dx$$
$$+\frac{1}{(b-a)(d-c)}\int_a^b\int_c^d f(x,y)dydx.$$

The main expectation from this study is to provide Bullen type inequalities for convex functions in coordinates in the field of inequality theory. The integral identity needed to obtain the results has been proved for partially differentiable functions with the help of double integrals. Some specific cases of main findings for bounded functions are considered.

2. BULLEN TYPE INEQUALITIES FOR CO-ORDINATED QUASI-CONVEX FUNCTIONS

For the simplicity, we will denote

$$\Lambda=\frac{1}{4}\left[\frac{f(a,c)+f(a,d)+f(b,c)+f(b,d)}{4}+f\left(\frac{a+b}{2},\frac{c+d}{2}\right)\right.$$
$$\left.+\frac{1}{2}\left(f\left(\frac{a+b}{2},c\right)+f\left(\frac{a+b}{2},d\right)+f\left(a,\frac{c+d}{2}\right)+f\left(b,\frac{c+d}{2}\right)\right)\right]$$
$$-\frac{1}{4(b-a)}\left[\int_a^b f(x,c)dx+\int_a^b f(x,d)dx+2\int_a^b f\left(x,\frac{c+d}{2}\right)dx\right]$$
$$-\frac{1}{4(d-c)}\left[\int_c^d f(a,y)dy+\int_c^d f(b,y)dy+2\int_c^d f\left(\frac{a+b}{2},y\right)dy\right]$$
$$+\frac{1}{(b-a)(d-c)}\int_a^b\int_c^d f(x,y)dydx.$$

We need to a new integral identity to prove our main results for quasi-convex functions in coordinates. We will start with the following equality:

Lemma 2 *(See ??) Let* $f:\Delta=[a,b]\times[c,d]\to\mathbb{R}$ *be a partial differentiable mapping on* $\Delta=[a,b]\times[c,d]$. *If* $\frac{\partial^2 f}{\partial t\partial s}\in L(\Delta)$, *then the following equality holds:*

$$\Lambda = \frac{(b-a)(d-c)}{64}$$
$$\times\left[\int_0^1\int_0^1 (1-2t)(1-2s)\frac{\partial^2 f}{\partial t\partial s}\left(ta+(1-t)\frac{a+b}{2}, sc+(1-s)\frac{c+d}{2}\right)dsdt\right.$$
$$+\int_0^1\int_0^1 (1-2t)(1-2s)\frac{\partial^2 f}{\partial t\partial s}\left(t\frac{a+b}{2}+(1-t)b, sc+(1-s)\frac{c+d}{2}\right)dsdt$$
$$+\int_0^1\int_0^1 (1-2t)(1-2s)\frac{\partial^2 f}{\partial t\partial s}\left(ta+(1-t)\frac{a+b}{2}, s\frac{c+d}{2}+(1-s)d\right)dsdt$$
$$\left.+\int_0^1\int_0^1 (1-2t)(1-2s)\frac{\partial^2 f}{\partial t\partial s}\left(t\frac{a+b}{2}+(1-t)b, s\frac{c+d}{2}+(1-s)d\right)dsdt\right].$$

for fixed $t, s \in [0,1]$.

Theorem 8 *Assume that* $f:\Delta=[a,b]\times[c,d]\to\mathbb{R}$ *is a partial differentiable mapping on* $\Delta=[a,b]\times[c,d]$. *If* $\left|\frac{\partial^2 f}{\partial t\partial s}\right|$ *is quasi-convex function on the co-ordinates on* Δ, *then the following inequality holds;*

$$|\Lambda|$$
$$\le \frac{(b-a)(d-c)}{64}$$
$$\times\frac{1}{16}\max\left\{\left|\frac{\partial^2 f}{\partial t\partial s}(a,c)\right|, \left|\frac{\partial^2 f}{\partial t\partial s}\left(\frac{a+b}{2}, \frac{c+d}{2}\right)\right|\right\}$$
$$+\frac{1}{16}\max\left\{\left|\frac{\partial^2 f}{\partial t\partial s}\left(\frac{a+b}{2}, c\right)\right|, \left|\frac{\partial^2 f}{\partial t\partial s}\left(b, \frac{c+d}{2}\right)\right|\right\}$$
$$+\frac{1}{16}\max\left\{\left|\frac{\partial^2 f}{\partial t\partial s}\left(a, \frac{c+d}{2}\right)\right|, \left|\frac{\partial^2 f}{\partial t\partial s}\left(\frac{a+b}{2}, d\right)\right|\right\}$$
$$+\frac{1}{16}\max\left\{\left|\frac{\partial^2 f}{\partial t\partial s}\left(\frac{a+b}{2}, \frac{c+d}{2}\right)\right|, \left|\frac{\partial^2 f}{\partial t\partial s}(b,d)\right|\right\}.$$

Proof. From Lemma 2 and using the property of modulus, we have

$$|\Lambda| \le \frac{(b-a)(d-c)}{64}$$
$$\times\left[\underbrace{\int_0^1\int_0^1 |(1-2t)(1-2s)|\left|\frac{\partial^2 f}{\partial t\partial s}\left(ta+(1-t)\frac{a+b}{2}, sc+(1-s)\frac{c+d}{2}\right)\right|dsdt}_{A_1}\right.$$

$$+\underbrace{\int_0^1\int_0^1\left|(1-2t)(1-2s)\right|\left|\frac{\partial^2 f}{\partial t\partial s}\left(t\frac{a+b}{2}+(1-t)b, sc+(1-s)\frac{c+d}{2}\right)\right|dsdt}_{A_2}$$

$$+\underbrace{\int_0^1\int_0^1\left|(1-2t)(1-2s)\right|\left|\frac{\partial^2 f}{\partial t\partial s}\left(ta+(1-t)\frac{a+b}{2}, s\frac{c+d}{2}+(1-s)d\right)\right|dsdt}_{A_3}$$

$$+\underbrace{\int_0^1\int_0^1\left|(1-2t)(1-2s)\right|\left|\frac{\partial^2 f}{\partial t\partial s}\left(t\frac{a+b}{2}+(1-t)b, s\frac{c+d}{2}+(1-s)d\right)dsdt\right|}_{A_4}\Bigg].$$

To calculate A_1, we use co-ordinated quasi-convexity of $\left|\frac{\partial^2 f}{\partial t\partial s}\right|$ as following

$$A_1=\int_0^1\int_0^1\left|(1-2t)(1-2s)\right|\left|\frac{\partial^2 f}{\partial t\partial s}\left(ta+(1-t)\frac{a+b}{2}, sc+(1-s)\frac{c+d}{2}\right)\right|dsdt$$

$$=\max\left\{\left|\frac{\partial^2 f}{\partial t\partial s}(a,c)\right|, \left|\frac{\partial^2 f}{\partial t\partial s}\left(\frac{a+b}{2}, \frac{c+d}{2}\right)\right|\right\}\int_0^1\int_0^1\left|(1-2t)(1-2s)\right|dsdt$$

By computing the above integral, we obtain

$$A_1=\frac{1}{16}\max\left\{\left|\frac{\partial^2 f}{\partial t\partial s}(a,c)\right|, \left|\frac{\partial^2 f}{\partial t\partial s}\left(\frac{a+b}{2}, \frac{c+d}{2}\right)\right|\right\}.$$

We can easily see that

$$A_2=\frac{1}{16}\max\left\{\left|\frac{\partial^2 f}{\partial t\partial s}\left(\frac{a+b}{2}, c\right)\right|, \left|\frac{\partial^2 f}{\partial t\partial s}\left(b, \frac{c+d}{2}\right)\right|\right\}.$$

$$A_3=\frac{1}{16}\max\left\{\left|\frac{\partial^2 f}{\partial t\partial s}\left(a, \frac{c+d}{2}\right)\right|, \left|\frac{\partial^2 f}{\partial t\partial s}\left(\frac{a+b}{2}, d\right)\right|\right\}.$$

$$A_4=\frac{1}{16}\max\left\{\left|\frac{\partial^2 f}{\partial t\partial s}\left(\frac{a+b}{2}, \frac{c+d}{2}\right)\right|, \left|\frac{\partial^2 f}{\partial t\partial s}(b,d)\right|\right\}.$$

By combining the results and simplifying, we get the required result.

Corollary 1 *Assume that all the conditions of Theorem 8 are valid. If we choose* $\frac{\partial^2 f}{\partial t\partial s}$ *is bounded, i.e.,*

$$\left\|\frac{\partial^2 f(t,s)}{\partial t\partial s}\right\|_\infty=\sup_{(t,s)\in(a,b)\times(c,d)}\left|\frac{\partial^2 f(t,s)}{\partial t\partial s}\right|<\infty,$$

we get

$$|\Lambda| \le \frac{(b-a)(d-c)}{256} \left\| \frac{\partial^2 f(t,s)}{\partial t \partial s} \right\|_\infty . \tag{2.1}$$

Theorem 9 *Assume that* $f : \Delta = [a,b] \times [c,d] \to \mathbb{R}$ *is a partial differentiable mapping on* $\Delta = [a,b] \times [c,d]$. *If* $\left| \frac{\partial^2 f}{\partial t \partial s} \right|^q$, $q > 1$, *is quasi-convex function on the co-ordinates on* Δ, *then the following inequality holds;*

$$\begin{aligned}
|\Lambda| &\le \frac{(b-a)(d-c)}{64(p+1)^{\frac{2}{p}}} \\
&\times \left(\left[\max\left\{ \left| \frac{\partial^2 f}{\partial t \partial s}(a,c) \right|^q, \frac{\partial^2 f}{\partial t \partial s} \left| \left(\frac{a+b}{2}, \frac{c+d}{2} \right) \right|^q \right\} \right]^{\frac{1}{q}} \right. \\
&+ \left[\max\left\{ \left| \frac{\partial^2 f}{\partial t \partial s} \left(\frac{a+b}{2}, c \right) \right|^q, \frac{\partial^2 f}{\partial t \partial s} \left| \left(b, \frac{c+d}{2} \right) \right|^q \right\} \right]^{\frac{1}{q}} \\
&+ \left[\max\left\{ \left| \frac{\partial^2 f}{\partial t \partial s} \left(a, \frac{c+d}{2} \right) \right|^q, \frac{\partial^2 f}{\partial t \partial s} \left| \left(\frac{a+b}{2}, d \right) \right|^q \right\} \right]^{\frac{1}{q}} \\
&\left. + \left[\max\left\{ \left| \frac{\partial^2 f}{\partial t \partial s} \left(\frac{a+b}{2}, \frac{c+d}{2} \right) \right|^q, \frac{\partial^2 f}{\partial t \partial s} |(b,d)|^q \right\} \right]^{\frac{1}{q}} \right)
\end{aligned}$$

where $p^{-1} + q^{-1} = 1$.

Proof. Using the identity is given in Lemma 2, we have

$$\begin{aligned}
|\Lambda| \le \frac{(b-a)(d-c)}{64} \Bigg[& \underbrace{\int_0^1 \int_0^1 |(1-2t)(1-2s)| \left| \frac{\partial^2 f}{\partial t \partial s} \left(ta + (1-t)\frac{a+b}{2}, sc + (1-s)\frac{c+d}{2} \right) \right| ds dt}_{A_1} \\
& + \underbrace{\int_0^1 \int_0^1 |(1-2t)(1-2s)| \left| \frac{\partial^2 f}{\partial t \partial s} \left(t\frac{a+b}{2} + (1-t)b, sc + (1-s)\frac{c+d}{2} \right) \right| ds dt}_{A_2}
\end{aligned}$$

$$+\underbrace{\int_0^1\int_0^1\left|(1-2t)(1-2s)\right|\left|\frac{\partial^2 f}{\partial t\partial s}\left(ta+(1-t)\frac{a+b}{2},s\frac{c+d}{2}+(1-s)d\right)\right|dsdt}_{A_3}$$

$$+\underbrace{\int_0^1\int_0^1\left|(1-2t)(1-2s)\right|\left|\frac{\partial^2 f}{\partial t\partial s}\left(t\frac{a+b}{2}+(1-t)b,s\frac{c+d}{2}+(1-s)d\right)dsdt\right|}_{A_4}\Bigg].$$

If we apply Hölder inequality for double integrals to A_1, then by using co-ordinated convexity of $\left|\frac{\partial^2 f}{\partial t\partial s}\right|^q$, we get

$$A_1=\int_0^1\int_0^1\left|(1-2t)(1-2s)\right|\left|\frac{\partial^2 f}{\partial t\partial s}\left(ta+(1-t)\frac{a+b}{2},sc+(1-s)\frac{c+d}{2}\right)\right|dsdt$$

$$=\left(\int_0^1\int_0^1\left|(1-2t)(1-2s)\right|^p dtds\right)^{\frac{1}{p}}$$

$$\times\left(\int_0^1\int_0^1\left|\frac{\partial^2 f}{\partial t\partial s}\left(ta+(1-t)\frac{a+b}{2},sc+(1-s)\frac{c+d}{2}\right)\right|^q dsdt\right)^{\frac{1}{q}}$$

$$=\left(\int_0^1\int_0^1\left|(1-2t)(1-2s)\right|^p dtds\right)^{\frac{1}{p}}$$

$$\times\left(\int_0^1\int_0^1\max\left\{\left|\frac{\partial^2 f}{\partial t\partial s}(a,c)\right|^q,\frac{\partial^2 f}{\partial t\partial s}\left|\left(\frac{a+b}{2},\frac{c+d}{2}\right)\right|^q\right\}dsdt\right)^{\frac{1}{q}}.$$

By computing the above integrals, we obtain

$$A_1=\frac{1}{(p+1)^{\frac{2}{p}}}\left[\max\left\{\left|\frac{\partial^2 f}{\partial t\partial s}(a,c)\right|^q,\frac{\partial^2 f}{\partial t\partial s}\left|\left(\frac{a+b}{2},\frac{c+d}{2}\right)\right|^q\right\}\right]^{\frac{1}{q}}$$

We can easily see that

$$A_2=\frac{1}{(p+1)^{\frac{2}{p}}}\left[\max\left\{\left|\frac{\partial^2 f}{\partial t\partial s}\left(\frac{a+b}{2},c\right)\right|^q,\frac{\partial^2 f}{\partial t\partial s}\left|\left(b,\frac{c+d}{2}\right)\right|^q\right\}\right]^{\frac{1}{q}}$$

$$A_3=\frac{1}{(p+1)^{\frac{2}{p}}}\left[\max\left\{\left|\frac{\partial^2 f}{\partial t\partial s}\left(a,\frac{c+d}{2}\right)\right|^q,\frac{\partial^2 f}{\partial t\partial s}\left|\left(\frac{a+b}{2},d\right)\right|^q\right\}\right]^{\frac{1}{q}}$$

$$A_4 = \frac{1}{(p+1)^{\frac{2}{p}}}\left[\max\left\{\left|\frac{\partial^2 f}{\partial t\partial s}\left(\frac{a+b}{2},\frac{c+d}{2}\right)\right|^q, \frac{\partial^2 f}{\partial t\partial s}|(b,d)|^q\right\}\right]^{\frac{1}{q}}.$$

By adding these results, we get the desired result.

Corollary 2 *Suppose that all the assumptions of Theorem 9 are satisfied. If we choose* $\frac{\partial^2 f}{\partial t\partial s}$ *is bounded, i.e.,*

$$\left\|\frac{\partial^2 f(t,s)}{\partial t\partial s}\right\|_\infty = \sup_{(t,s)\in(a,b)\times(c,d)}\left|\frac{\partial^2 f(t,s)}{\partial t\partial s}\right| < \infty,$$

we get

$$|\Lambda| \le \frac{(b-a)(d-c)}{16(p+1)^{\frac{2}{p}}}\left\|\frac{\partial^2 f(t,s)}{\partial t\partial s}\right\|_\infty. \tag{2.2}$$

3. CONCLUSION

There are many studies in the literature on convexity in coordinates, but this is a rare study on Bullen inequality for coordinated quasi-convex functions. It is clear that the results obtained in this study will have applications for numerical integration and special averages. In addition, new Bullen-type inequalities can be obtained with the help of equations similar to the integral identity on which the main findings are based. Moreover, proving similar identity with the help of fractional integral operators can be considered as a new problem for further results.

REFERENCES

1. S.S. Dragomir, On Hadamard's inequality for convex functions on the co-ordinates in a rectangle from the plane, Taiwanese Journal of Math., 5, 2001, 775-788.
2. M.E. Ozdemir, M.A. Latif, A.O. Akdemir, On some Hadamard-type inequalities for product of two $s-$convex functions on the co-ordinates, Journal of Inequalities and Applications, 2012, February-2012, DOI: 10.1186/1029-242X-2012-21.
3. E. Set, M.Z. Sarikaya, A.O. Akdemir, A new general inequality for double integrals, American Institu of Phsyics (AIP) Conference Proceedings , 1470, 122-125 pp., October-2012, DOI: http://dx.doi.org/10.1063/1.4747655.
4. M. Alomari and M. Darus, Hadamard-Type Inequalities for $s-$ Convex Functions, International Mathematical Forum, (3) 2008, no. 40, 1965 - 1975.
5. M.E. Ozdemir, A.O. Akdemir, On The Hadamard Type Inequalities Involving Product Of Two Convex Functions On The Co-Ordinates, Tamkang Journal of Mathematics, vol. 46, no. 2, pp. 129â "0, 2015.
6. A.O. Akdemir, M.E. Ozdemir, Some Hadamard-type inequalities for co-ordinated P-convex functions and Godunova-Levin functions, American Institu of Phsyics (AIP) Conference Proceedings , 1309, 7-15 pp., 2010.
7. M. E. Ozdemir, M.A. Latif, A.O. Akdemir, On Some Hadamard-Type Inequalities for Product of Two h-Convex Functions On the Co-ordinates, Turkish Journal of Science, 1 (1), 2016, 48-58.
8. M.K. Bakula and J. Pecaric, On the Jensen's inequality for convex functions on the co-ordinates in a rectangle from the plane, Taiwanese Journal of Math., 5, 2006, 1271-1292.
9. M.E. Ozdemir, A.O. Akdemir, C. Yildiz, On Co-ordinated Quasi-Convex Functions, Czechoslovak Mathematical Journal , 62-4, 889-900 pp., 2012.
10. M. Alomari and M. Darus, The Hadamard's inequality for s-convex functions of 2-variables, Int. Journal of Math. Analysis, 2(13), 2008, 629-638.
11. M.E. Özdemir, E. Set and M.Z. Sarıkaya, Some new Hadamard's type inequalities for co-ordinated $m-$convex and $(\alpha,m)-$convex functions, Hacettepe J. of. Math. and St., 40, 219-229, (2011).

12. M.Z. Sarıkaya, E. Set, M. Emin Özdemir and S.S. Dragomir, New some Hadamard's type inequalities for co-ordinated convex functions, Tamsui Oxford J. Math. Sci., 28, (2011).
13. M.E. Ozdemir, C. Yildiz, A.O. Akdemir, On Some New Hadamard-type Inequalities for Co-ordinated Quasi-Convex Functions, Hacettepe Journal of Mathematics and Statistics, 41-5, 697-707 pp., 2012.
14. S.S. Dragomir & C. Pearce, Selected topics on Hermite-Hadamard inequalities and applications. Victoria University: RGMIA Monographs, (17) 2000. [http://ajmaa.org/RGMIA/monographs/hermite hadamard.html].
15. M.E. Ozdemir, H. Kavurmaci, A.O. Akdemir, and M. Avci, Inequalities for convex and $s-$ convex functions on $\Delta=[a,b]\times[c,d]$, J. Inequal. Appl., (2012), 2012:20.
16. M.E. Ozdemir, C. Yildiz, A.O. Akdemir, On The Co-Ordinated Convex Functions, Applied Mathematics and Information Sciences , 8-3, 1085-1091 pp., 2014, DOI: 10.12785/amis/080318.
17. M.E. Özdemir, M. Avcı, E. Set, On some inequalities of Hermite–Hadamard type via $m-$convexity, *Appl. Math. Lett.* 23 (9) (2010) 1065–1070.
18. M.E. Özdemir, M. Avcı and H. Kavurmacı, Hermite–Hadamard-type inequalities via $(\alpha,m)-$convexity, *Computers and Mathematics with Applications*, 61 (2011), 2614–2620.
19. M.E. Özdemir, H. Kavurmacı, E. Set, Ostrowski's type inequalities for $(\alpha,m)-$convex functions, *Kyungpook Math. J.* 50 (2010) 371–378.
20. M.K. Bakula, M.E. Özdemir, J. Pecaric, Hadamard type inequalities for $m-$convex and $(\alpha,m)-$convex functions, *J. Inequal. Pure Appl. Math.* 9 (2008), Article 96.
21. M.K. Bakula, J. Pecaric M. Ribicic, Companion inequalities to Jensen's inequality for $m-$convex and $(\alpha,m)-$convex functions, *J. Inequal. Pure Appl. Math.* 7 (2006), Article 194.
22. S.S. Dragomir, On some new inequalities of Hermite-Hadamard type for $m-$convex functions, *Tamkang J. Math.*, 3 (1) 2002.
23. S.S. Dragomir and G.H. Toader, Some inequalities for $m-$convex functions, *Studia Univ. Babeş-Bolyai, Math.*, 38 (1) (1993), 21-28.
24. N. Ujevic, Double integral inequalities of Simpson type and applications, *J. Appl. Math. and Computing*, 14 (2004), no:1-2, p. 213-223.
25. V.G. Miheşan, A generalization of the convexity, *Seminar of Functional Equations, Approx. and Convex*, Cluj-Napoca (Romania) (1993).
26. L. Zhongxue, On sharp inequalities of Simpson type and Ostrowski type in two independent variables, *Comp. and Math. with Appl.*, 56 (2008), 2043-2047.
27. S.I. Butt, S. Rashid, A.O. Akdemir and M. Nadeem, Bullen type inequalities for convex functions on the co-ordinates, submitted.

Inequalities

Muhammad TARIQ[1], Erhan SET[2], Ahmet Ocak AKDEMİR[3] and Sinan ASLAN[4]

[1]*Department of Mathematics, COMSATS University of Islamabad, Lahore Campus, Lahore, PAKISTAN*
[2]*Department of Mathematics, Faculty of Arts and Sciences, Ordu University, Ordu, TURKEY*
[3]*Department of Mathematics, Faculty of Arts and Sciences,*
Ağrı İbrahim Çeçen University, Ağrı, TURKEY
[4]*Department of Mathematics, Graduate School of Natural and Applied Sciences,*
Giresun University, Giresun, TURKEY

captaintariq2187@gmail.com
erhanset@yahoo.com
sinanaslan0407@gmail.com
aocakakdemir@gmail.com

Abstract. In this paper, we have given some well known concepts related to fractional calculus and convexity. Then, we have proved some new integral inequalities for P-functions via generalized proportional fractional integral operators.

1. INTRODUCTION AND PRELIMINARIES

Although fractional analysis origin dates back to the beginning of classical analysis, it has developed quite rapidly in recent years. Many mathematicians who researched in this field contributed to this development and made efforts to strengthen the relationship between fractional analysis and other fields. With the introduction of new fractional derivative and integral operators, the application opportunity for many real world problems has been revealed. The fractional operators are excellent tools to use in modeling long-memory processes and many phenomena that appear in physics, chemistry, electricity, mechanics and many other disciplines. The majority of the new operators came to the fore with different features such as singularity, location and generalization, and gained functionality thanks to their effective use in application areas. Due to the intensive work on it, the Riemann-Liouville integral operator is a prominent operator and is defined as follows.

Definition 1.1 *Let* $f \in L_1[a,b]$. *The Riemann-Liouville integrals* $J_{a+}^{\alpha} f$ *and* $J_{b-}^{\alpha} f$ *of order* $\alpha > 0$ *with* $a \geq 0$ *are defined by*

$$J_{a+}^{\alpha} f(t) = \frac{1}{\Gamma(\alpha)} \int_a^t (t-x)^{\alpha-1} f(x) dx, \quad t > a$$

and

$$J_{b-}^{\alpha} f(t) = \frac{1}{\Gamma(\alpha)} \int_t^b (x-t)^{\alpha-1} f(x) dx, \quad t < b$$

respectively. Here $\Gamma(t)$ is the Gamma function and its definition is $\Gamma(t) = \int_0^{\infty} e^{-t} t^{x-1} dx$. It is to be noted that $J_{a+}^{0} f(t) = J_{b-}^{0} f(t) = f(t)$. Also, in the case of $\alpha = 1$, the fractional integral reduces to the classical integral.

We will continue with the generalized proportional fractional integral operator, which has been described recently and has been the main source of motivation for many studies in the literature with its use in many areas, especially inequality theory. In [10], Jarad et al. identified the proportional generalized fractional integrals that satisfy many important features as follows:

Definition 1.2 *The left and right generalized proportional fractional integral operators are respectively defined by*

$$ {}_{a+}\mathrm{J}^{\alpha,\lambda} f(t) = \frac{1}{\lambda^{\alpha}\Gamma(\alpha)} \int_a^t e^{\left[\frac{\lambda-1}{\lambda}(t-x)\right]} (t-x)^{\alpha-1} f(x)dx, \quad t > a $$

and

$$ {}_{b-}\mathrm{J}^{\alpha} f(t) = \frac{1}{\lambda^{\alpha}\Gamma(\alpha)} \int_t^b e^{\left[\frac{\lambda-1}{\lambda}(x-t)\right]} (x-t)^{\alpha-1} f(x)dx, \quad t < b $$

where $\lambda \in (0,1]$ and $\alpha \in \mathbb{C}$ and $\mathrm{R}(\alpha) > 0$.

Definition 1.3 *[18] Let* (a,b) *with* $-\infty \le a < b \le \infty$ *be a finite or infinite interval of the real line* $\mathbb{R}$ *and* α *a complex number with* $Re(\alpha) > 0$. *Also let* h *be a strictly increasing function on* (a,b), *having a continuous derivative* h' *on* (a,b). *The generalized left and right sided Riemann-Liouville fractional integrals of a function* f *with respect to another function* h *on* $[a,b]$ *defined as*

$$ {}_{a+}^{h} I^{\alpha} f(\varepsilon) = \frac{1}{\Gamma(\alpha)} \int_a^{\varepsilon} (h(\varepsilon) - h(\kappa))^{\alpha-1} f(\kappa) h'(\kappa) d\kappa, \quad \varepsilon > a $$

and

$$ {}_{b-}^{h} I^{\alpha} f(\varepsilon) = \frac{1}{\Gamma(\alpha)} \int_{\varepsilon}^{b} (h(\kappa) - h(\varepsilon))^{\alpha-1} f(\kappa) h'(\kappa) d\kappa, \quad \varepsilon < b. $$

Definition 1.4 *[17] Let* a,b *be two nonnegative real numbers with* $a < b$, α, ρ *two positive real numbers, and* $f: [a,b] \to \mathbb{R}$ *be an integrable function. The left and right Katugampola fractional integrals defined as*

$$ {}_{a+}\mathrm{I}^{\alpha} f(\varepsilon) = \frac{1}{\Gamma(\alpha)} \int_a^{\varepsilon} \left(\frac{\varepsilon^{\rho} - \kappa^{\rho}}{\rho} \right)^{\alpha-1} \frac{f(\kappa)d\kappa}{\kappa^{1-\rho}}, \quad \varepsilon > a $$

and

$$ {}_{b-}\mathrm{I}^{\alpha} f(\varepsilon) = \frac{1}{\Gamma(\alpha)} \int_{\varepsilon}^{b} \left(\frac{\kappa^{\rho} - \varepsilon^{\rho}}{\rho} \right)^{\alpha-1} \frac{f(\kappa)d\kappa}{\kappa^{1-\rho}}, \quad \varepsilon < b. $$

Definition 1.5 *[18,24] Let* a,b *be two reals with* $0 < a < b$ *and* $f: [a,b] \to \mathbb{R}$ *be an integrable function. The left and right Hadamard fractional integrals of order* $\alpha > 0$ *are defined as*

$$ {}_{a+}\mathrm{F}^{\alpha} f(\varepsilon) = \frac{1}{\Gamma(\alpha)} \int_a^{\varepsilon} \frac{f(\kappa)}{\kappa \left(\ln \frac{\varepsilon}{\kappa} \right)^{1-\alpha}} d\kappa, \quad \varepsilon > a $$

and

$$ {}_{b-}\mathrm{F}^{\alpha} f(\varepsilon) = \frac{1}{\Gamma(\alpha)} \int_{\varepsilon}^{b} \frac{f(\kappa)}{\kappa \left(\ln \frac{\kappa}{\varepsilon} \right)^{1-\alpha}} d\kappa, \quad \varepsilon < b. $$

Definition 1.6 *[21] The left and right generalized proportional Hadamard fractional integrals of order* $\alpha > 0$ *and proportionality index* $\zeta \in (0,1]$ *is defined by*

$$ {}_{a+}\mathsf{F}^{\alpha,\zeta} f(\varepsilon) = \frac{1}{\zeta^{\alpha}\Gamma(\alpha)} \int_a^{\varepsilon} \frac{e^{\left[\frac{\zeta-1}{\zeta}(ln\frac{\varepsilon}{\kappa})\right]}}{\left(ln\frac{\varepsilon}{\kappa}\right)^{1-\alpha}} \frac{f(\kappa)}{\kappa} d\kappa, \quad \varepsilon > a $$

and

$$ {}_{b-}\mathsf{F}^{\alpha,\zeta} f(\varepsilon) = \frac{1}{\zeta^{\alpha}\Gamma(\alpha)} \int_a^{\varepsilon} \frac{e^{\left[\frac{\zeta-1}{\zeta}(ln\frac{\kappa}{\varepsilon})\right]}}{\left(ln\frac{\kappa}{\varepsilon}\right)^{1-\alpha}} \frac{f(\kappa)}{\kappa} d\kappa, \quad \varepsilon < b. $$

Now, let's give a fractional operator which is known as the generalized proportional fractional (GPF) integral operator function in the sense of another function h.

Definition 1.7 *[14, 23] Let* $f \in X_h^q(0,\infty)$, *there is an increasing, positive monotone function* h *defined on* $[0,\infty)$ *having continuous derivative* h' *on with* $h(0)=0$. *Then the left-sided and right-sided GPF-integral operator of a function* f *in the sense of another function* h *of order* $\alpha > 0$ *are stated as:*

$$ {}_{a+}^{h}\mathsf{J}^{\alpha,\zeta} f(\varepsilon) = \frac{1}{\zeta^{\alpha}\Gamma(\alpha)} \int_a^{\varepsilon} e^{\left[\frac{\zeta-1}{\zeta}(h(\varepsilon)-h(\kappa))\right]} (h(\varepsilon)-h(\kappa))^{\alpha-1} f(\kappa) h'(\kappa) d\kappa, \quad \varepsilon > a $$

and

$$ {}_{b-}^{h}\mathsf{J}^{\alpha,\zeta} f(\varepsilon) = \frac{1}{\zeta^{\alpha}\Gamma(\alpha)} \int_{\varepsilon}^{b} e^{\left[\frac{\zeta-1}{\zeta}(h(\kappa)-h(\varepsilon))\right]} (h(\kappa)-h(\varepsilon))^{\alpha-1} f(\kappa) h'(\kappa) d\kappa, \quad \varepsilon < b $$

where $\zeta \in (0,1]$ and $\alpha \in \mathbb{C}$ and $\mathsf{R}(\alpha) > 0$.

For different choices of parameters in Definition 1.7, we get Riemann-Liouville integrals, generalized Riemann-Liouville fractional integrals, generalized proportional fractional integrals, Katugampola fractional integrals, Hadamard fractional integrals and generalized proportional Hadamard fractional integrals. Recently, several new studies have been performed by mathematicians via various fractional integral operators and with the help of fractional integral operators. Numerous new inequalities have been proved in the literature, see [1-9, 11-16, 19, 20, 22, 23, 25-28].

In [29], Pecaric *et al.* mentioned P-functions as following:

A function $f: I \to (0,\infty)$ is said to $P-$function, if for all $x, y \in I$ and $t \in [0,1]$ one has the inequality

$$ f(tx+(1-t)y) \le f(x)+f(y). $$

The main aim of this paper is to establish some new integral inequalities for P-functions via the general forms of proportional fractional integral operators.

2. MAIN RESULTS

Theorem 2.1 *Assume that* $f: [0,\infty) \to \mathbb{R}$ *be differentiable function with* $f \in X_h^q(0,\infty)$ *and* ψ *be a positive monoton increasing function that defined on* $[0,\infty)$. *Let* $\psi'(\tau)$ *be continuous and* $\psi(0)=0$. *Then, if* f *is P-function, we have the following inequality;*

$$\left({}^{\Psi}\mathsf{T}^{\eta,\xi}_{0^+,\tau} f\right)(\tau) \le \frac{f(b)+f(a)}{\xi^{\eta}\Gamma(\eta)} \frac{\psi^{\eta}(\tau)}{\left(\frac{1-\xi}{\xi}\psi(\tau)\right)^{\eta}} \left(\Gamma(\eta)-\Gamma\left(\eta,\frac{1-\xi}{\xi}\psi(\tau)\right)\right)$$

for $\xi \in (0,1)$, $\mu \in \mathbb{C}$, $Re(\eta) > 0, \tau > 0$ where $\Gamma(s,x) = \int_x^{\infty} t^{s-1}e^{-t}dt$ is incomplete Gamma function.

Proof. By using the definition of P-functions, we can write

$$f(ta+(1-t)b) \le f(a)+f(b)$$

By changing of the variable such that $x = ta+(1-t)b$, we have

$$f(x) \le f(a)+f(b)$$

By multiplying both sides of the resulting inequality by

$$\frac{1}{\xi^{\eta}\Gamma(\eta)} \frac{e^{\frac{\xi-1}{\xi}(\psi(\tau)-\psi(x))}}{(\psi(\tau)-\psi(x))^{1-\eta}}\psi'(x)$$

and applying integration with respext to x from 0 to τ, we obtain

$$\left({}^{\Psi}\mathsf{T}^{\eta,\xi}_{0^+,\tau} f\right)(\tau) \le \frac{f(a)+f(b)}{\xi^{\eta}\Gamma(\eta)} \int_0^{\tau} \frac{e^{\frac{\xi-1}{\xi}(\psi(\tau)-\psi(x))}}{(\psi(\tau)-\psi(x))^{1-\eta}}\psi'(x)dx$$

If we calculate the integral in the right hand side, we obtain

$$\left({}^{\Psi}\mathsf{T}^{\eta,\xi}_{0^+,\tau} f\right)(\tau) \le \frac{f(b)+f(a)}{\xi^{\eta}\Gamma(\eta)} \frac{\psi^{\eta}(\tau)}{\left(\frac{1-\xi}{\xi}\psi(\tau)\right)^{\eta}} \left(\Gamma(\eta)-\Gamma\left(\eta,\frac{1-\xi}{\xi}\psi(\tau)\right)\right).$$

The proof is completed.

Theorem 2.2 *Assume that* $f:(0,\infty)\to R$ *be differentiable function with* $f \in X_h^q(0,\infty)$ *and* ψ *be a positive monoton increasing function that defined on* $[0,\infty)$. *Let* $\psi'(\tau)$ *be continuous and* $\psi(0)=0,\ p,q>1 ve \frac{1}{p}+\frac{1}{q}=1,\ |\psi'(\tau)| \le M$. *Then, if* f *is* $P-$ *function, we have the following inequality;*

$$\left({}^{\Psi}\mathsf{T}^{\eta,\xi}_{0^+,\tau} f\right)(\tau)$$

$$\le \frac{f(a)+f(b)M^{\frac{p-1}{p}}\tau^{\frac{1}{q}}}{\xi^{\eta}\Gamma(\eta)}$$

$$\times \left(\frac{\psi^{p(\eta-1)+1}(\tau)}{\left(\frac{1-\xi}{\xi}p\psi(\tau)\right)^{p(\eta-1)+1}} \left(\Gamma(p(\eta-1)+1)-\Gamma\left(p(\eta-1)+1,\frac{1-\xi}{\xi}p\psi(\tau)\right)\right)\right)^{\frac{1}{p}}$$

for $\xi \in (0,1)$, $\eta \in \mathbb{C}$, $Re(\eta) > 0, Re(p(\eta-1)) > 0, \tau > 0$ where $\Gamma(s,x) = \int_x^\infty t^{s-1}e^{-t}dt$ is incomplete Gamma function.

Proof. By using the definition of $P-$function, we can write

$$f(ta+(1-t)b) \le f(a)+f(b)$$

By changing of the variable such that $x = ta+(1-t)b$, we have

$$f(x) \le f(a)+f(b)$$

By multiplying both sides of the resulting inequality by

$$\frac{1}{\xi^{\eta}\Gamma(\eta)} \frac{e^{\frac{\xi-1}{\xi}(\psi(\tau)-\psi(x))}}{(\psi(\tau)-\psi(x))^{1-\eta}} \psi'(x)$$

and applying integration with respext to x from 0 to τ, we obtain

$$\left({}^{\Psi}\mathsf{T}^{\eta,\xi}_{0^+,\tau} f\right)(\tau) \le \frac{f(a)+f(b)}{\xi^{\eta}\Gamma(\eta)} \int_0^\tau \frac{e^{\frac{\xi-1}{\xi}(\psi(\tau)-\psi(x))}}{(\psi(\tau)-\psi(x))^{1-\eta}} \psi'(x)dx.$$

By applying Hölder inequality to the resulting inequality and by making use of some necessary operation and by taking into account $|\psi'(x)| \le M$, we obtain

$$\left({}^{\Psi}\mathsf{T}^{\eta,\xi}_{0^+,\tau} f\right)(\tau)$$

$$\le \frac{f(a)+f(b)}{\xi^{\eta}\Gamma(\eta)} \left(\int_0^\tau \left| \frac{e^{\frac{\xi-1}{\xi}(\psi(\tau)-\psi(x))}}{(\psi(\tau)-\psi(x))^{1-\eta}} \psi'(x) \right|^p dx \right)^{\frac{1}{p}} \times \left(\int_0^\tau |1|^q dx \right)^{\frac{1}{q}}$$

$$\left({}^{\Psi}\mathsf{T}^{\eta,\xi}_{0^+,\tau} f\right)(\tau)$$

$$\le \frac{f(a)+f(b)M^{\frac{p-1}{p}}\tau^{\frac{1}{q}}}{\xi^{\eta}\Gamma(\eta)}$$

$$\times \left(\frac{\psi^{p(\eta-1)+1}(\tau)}{\left(\frac{1-\xi}{\xi} p\psi(\tau)\right)^{p(\eta-1)+1}} \left(\Gamma(p(\eta-1)+1) - \Gamma\left(p(\eta-1)+1, \frac{1-\xi}{\xi} p\psi(\tau) \right) \right) \right)^{\frac{1}{p}}$$

By making use of the necessary calculations, we obtain the desired result.

REFERENCES

1. A.O. Akdemir, A. Ekinci and E. Set, *Conformable Fractional Integrals And Related New Integral Inequalities*, Journal of Nonlinear and Convex Analysis, Volume 18, Number 4, 2017, 661-674.
2. S. Belarbi, Z. Dahmani. *On some new fractional integral inequalities,* J. Inequal. Pure Appl. Math 10.3 (2009):

1-12.
3. Z. Dahmani, O. Mechouar, S. Brahami, *Certain inequalities related to the Chebyshev's functional involving a Riemann-Liouville operator*, Bull. Math. Anal. Appl., 3(4) (2011), 38-44.
4. M.A. Dokuyucu, D. Baleanu, E. Celik, *Analysis of Keller-Segel model with Atangana-Baleanu fractional derivative*. Filomat, 32(16), 5633-5643, 2018.
5. M.A. Dokuyucu, E. Celik, H. Bulut, H.M. Baskonus, *Cancer treatment model with the Caputo-Fabrizio fractional derivative*, The European Physical Journal Plus, 133(3), 92, 2018.
6. M.A. Dokuyucu, H. Dutta, *A fractional order model for Ebola Virus with the new Caputo fractional derivative without singular kernel*, Chaos, Solitons and Fractals Volume 134, May 2020, 109717.
7. M.A. Dokuyucu, *A fractional order alcoholism model via Caputo-Fabrizio derivative*, AIMS Mathematics 5 (2), 781-797, 2020.
8. S.S. Dragomir, *Some integral inequalities of Grüss type*, IJPAM, Indian J. Pure Appl. Math., **31 4** (2000) 397-415.
9. A. Ekinci and M.E. Ozdemir, *Some New Integral Inequalities Via Riemann-Liouville Integral Operators*, Applied and Computational Mathematics, Vol. 18, No:3, 2019, pages: 288-295.
10. F. Jarad, T. Abdeljawad, J. Alzabut, *Generalized fractional derivatives generated by a class of local proportional derivatives*, Eur. Phys. J. Spec. Top. 226, 34573471 (2017). https://doi.org/10.1140/epjst/e2018-00021-7
11. F. Jarad, T. Abdeljawad, *Generalized fractional derivatives and Laplace transform*, Discrete and Continuous Dynamical Systems - S, 2020, 13 (3) : 709-722. doi: 10.3934/dcdss.2020039.
12. F. Jarad, T. Abdeljawad, D. Baleanu, *Caputo-type modification of the Hadamard fractional derivatives*, Adv Differ Equ., 2012, 142 (2012) doi:10.1186/1687-1847-2012-142.
13. F. Jarad, T. Abdeljawad, D. Baleanu, *On the generalized fractional derivatives and their Caputo modification*, J. Nonlinear Sci. Appl 10 (5), 2607-2619, 2017.
14. F. Jarad, M. A. Alqudah, T. Abdeljawad, *On more general forms of proportional fractional operators*, Open Mathematics 18.1 (2020): 167-176.
15. E. Kaçar, Z. Kaçar, H. Yldrm, *Integral inequalities for Riemann-Liouville fractional integrals of a function with respect to another function*, Iran.J.Math.Sci.Inform. 13 (2018), 1-13.
16. U.N. Katugampola, *Approach to a generalized fractional integral*, Appl.Math.Comput. 218 (2011),860-865.
17. U.N. Katugampola, *A new approach to a generalized fractional derivatives*, Bull. Math. Anal. Appl., 6(4) (2014),1-15.
18. A.A. Kilbas, H.M. Srivastava, J.J. Trujillo, *Theory and Applications of Fractional Differential Equations*, North-Holland Mathematics Studies, New York, NY, USA, (2006).
19. D. Nie, S. Rashid, A.O. Akdemir, D. Baleanu and J.-B. Liu, *On Some New Weighted Inequalities for Differentiable Exponentially Convex and Exponentially Quasi-Convex Functions with Applications*, Mathematics 2019, 7(8), 727.
20. S. K. Ntouyas, S. D. Purohit, J. Tariboon, *Certain Chebyshev type integral inequalities involving Hadamard's fractional operators*, In Abstract and Applied Analysis, Hindawi, (2014).
21. G. Rahman, T. Abdeljawad, F. Jarad, A. Khan, K.S. Nisar, *Certain inequalities via generalized proportional Hadamard fractional integral operators*, Adv. Diff. Eqs. (2019), 454.
22. G. Rahman, Z. Ullah, A. Khan, E. Set, K. S. Nisar, *Certain Chebyshev-type inequalities involving fractional conformable integral operators*, Mathematics, 7(4) (2019) 364.
23. S. Rashid, F. Jarad, M. A. Noor, H. Kalsoom, Y. M. Chu, *Inequalities by means of generalized proportional fractional integral operators with respect to another function*, Mathematics, 7(12) (2019) 1225.
24. S.G. Samko, A.A. Kilbas, *Normal densities*, Linear Algebra Appl., 396 (2005), 317-328.
25. E. Set, M. Z. Sarikaya, F. Ahmad, *A generalization of Chebychev type inequalities for first differentiable mappings*, Miskolc Mathematical Notes 12.2 (2011): 245-253.
26. E. Set, A. O. Akdemir, I. Mumcu, *Chebyshev type inequalities for conformable fractional integrals*, Miskolc Mathematical Notes 20.2 (2019).
27. E. Set, U. Katugampola, I. Mumcu, M.E. Özdemir, *Best fractional generalization of some inequalitites related to the Chebyshev's functional*, https://www.researchgate.net/publication/331284225
28. H. Yıldırım, Z. Kırtay, *Ostrowski inequality for generalized fractional integral and related inequalities*, Malatya J.Mat. 2 (2014),322-329.

29. J. Pecaric, F. Proschan and Y.L. Tong, Convex Functions, Partial Orderings and Statistical Applications, Academic Press, Inc., 1992.

Piece-Homogeneous Elastic Mediums in the Case When the Binder and Inclusions Are Weaken by the Cohesion Cracks at a Transverse Shear

R. K. MEHTIYEV[1], A. K. MEHDIYEV[2]

[1]*Azerbaijan Technical University,*
Avenue. G. Javid, 25, AZ1073, Baku, Azerbaijan
[2]*Azerbaijan State University of Oil and Industry*
Avenue. Azadlig 20, Az1010, Baku, Azerbaijan

rafail60mehtiyev@mail.ru
mehdiyevalekber@mail.ru

ABSTRACT

The problem of the stressed state of a composite weakened by a system of doubly periodic cracks is relevant for various branches of engineering. The formulation of the problem of fissuring substantially extends the original concept of A. Griffiths. Stress intensity factors are the main parameters of fracture mechanics that study the resistance of structural materials to brittle fracture and the predictive performance of machine elements and structures weakened by cracks. The relevance of such studies is caused by the extensive use in the technology of structures and products made of composite materials.

This article is devoted to modeling and solving problems on the interaction of a doubly periodic system of foreign elastic inclusions and rectilinear cohesive cracks under transverse shear.

The nonlinear problem of fracture mechanics is solved for the transverse shear of a piecewise homogeneous medium in the case when the binder and inclusions are weakened by cohesive cracks. It is believed that in the circular holes soldered without tension elastic washers of another material.

The modeling of the end regions of cracks consists in treating them as part of cracks and in explicit application to the surfaces of cracks in the end zones of the clutch forces that restrain their shear. The dimensions of the end zones of the cracks are considered commensurate with the length of the cracks. The physical nature of such bonds and the size of the pre–destruction zones depend on the type of material. When an external load acts on a piece–wise homogeneous body, the tangential forces arise in the bonds connecting the shores of the end zones of prefracture, in the plane and in the inclusion, respectively. These stresses are unknown in advance and are to be determined in the process of solving the boundary value problem of fracture mechanics.

Keywords: Doubly periodic lattice, Fiber–binder, Average stresses, Linear algebraic equations, Singular equations, Cohesive cracks, Transverse shear.

INTRODUCTION

We consider an elastic medium weakened by a doubly periodic system of circular holes filled with absolutely rigid inclusions. The medium (binder) is weakened by two bi–periodic systems of rectilinear cracks with bonds between the banks in the end zones.

A fracture model of composite materials with a bicameral structure is proposed, based on the consideration of the fracture process zone near the crack tip. The fracture process zone (end zone) is a layer of finite length

containing material with partially broken bonds between its individual structural elements, considered as part of a crack. The presence of bonds between the crack faces in the end zone is modeled by the application of adhesion forces to the crack surfaces caused by the presence of bonds. The analysis of the limiting equilibrium of a cohesive crack in a transverse shear is carried out on the basis of the criterion of the limiting shear of material bonds.

A numerical implementation of the above method is made at IBM. The stress intensity factors are calculated depending on the geometric parameters of the medium under consideration.

STATEMENT OF THE PROBLEM

We consider an elastic plane D, weakened by a batch wise periodic system of circular holes with radii λ $(\lambda < 1)$ and the centers of these holes are at points [1]

$$P_{mn} = m\omega_1 + n\omega_2,\ \omega_1 = 2,\ \omega_2 = \omega_1 \cdot he^{i\alpha},$$

$$h > 0,\ \operatorname{Im}\omega_2 > 0 (m = 0, \pm 1, \pm 2, ...)$$

Elastic washers from another material are soldered into circular holes without interference. Elastic inclusions and the plane are considered weakened by rectilinear cracks with bonds between the banks in the end zones. It is believed that the lengths of cracks with end zones in the plane and inclusion are not the same. The banks of shear cracks outside the end zones are free of external forces, and stresses $\tau_{xy} = \tau_{xy}^{\infty}$, $\sigma_x = 0$, $\sigma_y = 0$ act on the perforated body (shear at infinity). The origin of the coordinate system is aligned with the geometric center of the hole L_{00} in the elastic plane (Fig. 1).

Modeling of the end regions of the cracks consists in considering them as part of the cracks and in explicit application to the surfaces of the cracks in the end zones of the adhesion forces holding back their shift. The sizes of the end zones of the cracks are considered comparable in comparison with the length of the cracks. The interaction of the banks of the end zones of cracks is modeled by introducing between the banks of the zone of pre –fracture of bonds with a given deformation diagram. The physical nature of such bonds and the sizes of the prefracture zones depend on the type of material. Under the action of an external load on a piecewise homogeneous body in the bonds connecting the shores of the end zones before failure, tangential forces $q_x(x)$, $q_y(y)$ in the plane and $q_x^0(x)$ in the inclusion, respectively, arise. These stresses are not known in advance and must be determined in the process of solving the boundary value problem of fracture mechanics [2].

The boundary conditions in the considered problem have the form [3]

$$(\sigma_r - i\tau_{r\theta})_{b|\Omega_{mn}} = (\sigma_r - i\tau_{r\theta})s_{t|\Omega_{mn}},\ (u + i\upsilon)_{b|\Omega_{mn}} = (u + i\upsilon)_{s|\Omega_{mn}} \qquad (1)$$

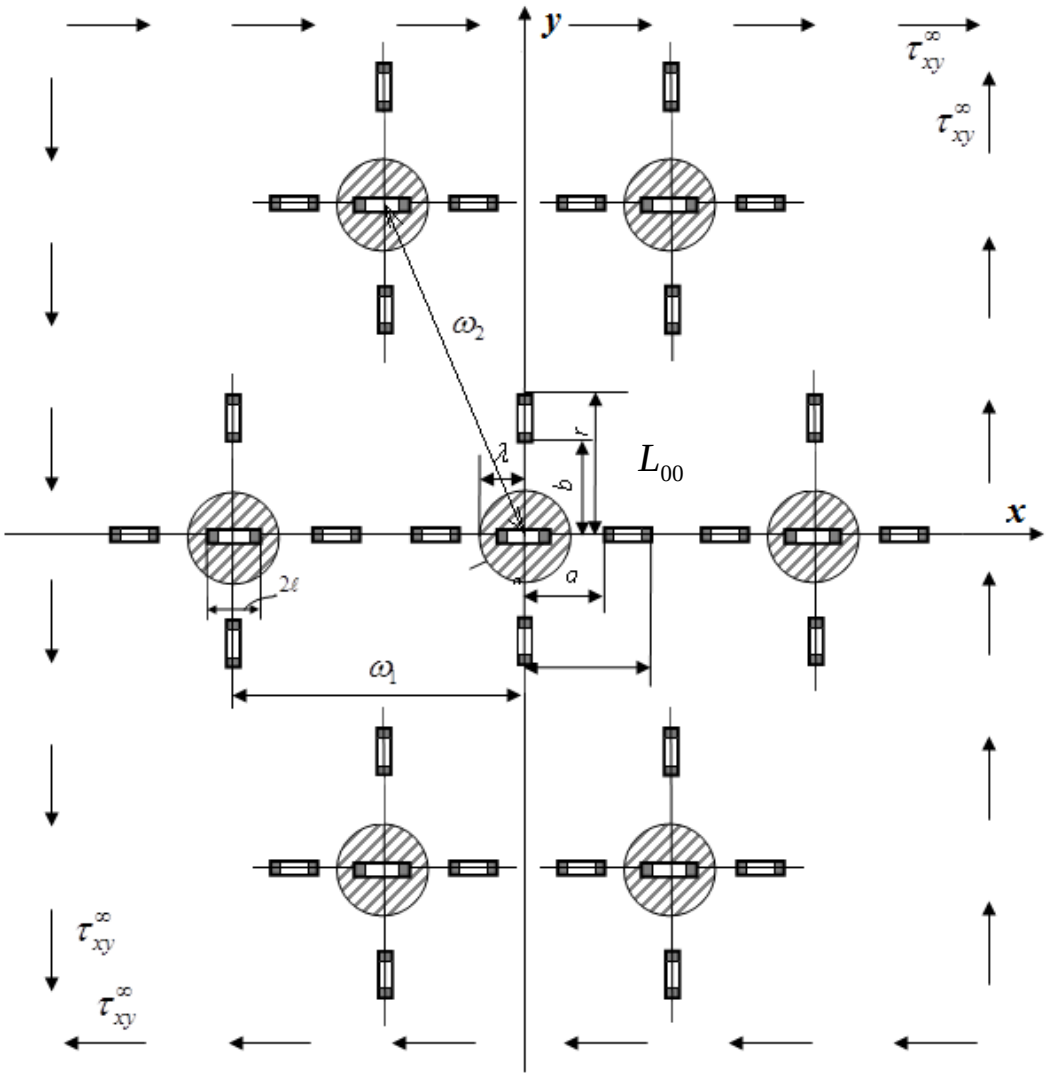

Fig. 1. The design scheme of the problem of the transverse shear piecewise homogeneous elastic medium with cracks on the banks of cracks with end zones [4]

$$\left(\sigma_y - i\tau_{xy}\right)_s = f_x(x) \qquad \text{collinear abscissa axis,} \qquad (2)$$

$$\left(\sigma_x - i\tau_{xy}\right)_s = f_y(y) \qquad \text{collinear ordinate axis,}$$

$$\left(\sigma_x - i\tau_{xy}\right)_b = f_x^0(x) \qquad \text{at } y = 0,\ |x| \le \ell .$$

Here Ω_{mn} – is the inclusion interface – the plane in cell number mn; values related to the inclusion (washer) and the plane are hereinafter indicated by the indices b and s; $f_x(x) = 0$ on the free banks of cracks; $f_x(x) = -iq_x(x)$ on the banks of the end zones of the cracks, collinear abscissa axis; $f_y(y)$ on the free banks of

cracks of the collinear ordinate axis $f_y(y) = -iq_y(y)$ on the banks of the end zones of cracks of the collinear ordinate axis; $f_x^0(x) = 0$ on the free banks of the crack in the inclusion; $f_x^0(x) = -iq_x^0(x)$ on the banks of the end zones of cracks in the inclusion [5].

The main relations of the stated problem must be supplemented by equations connecting the shift of the banks of the end zones of cracks and the tangential stresses in the bonds.

Without loss of generality, we represent these equations in the form [6,7]

$$u_s^+(x,0) - u_s^-(x,0) = C\big(x, q_x(x)\big)q_x(x), \tag{3}$$

for end zones of cracks of the collinear abscissa axis

$$\upsilon_s^+(0,y) - \upsilon_s^-(0,y) = C\big(y, q_y(y)\big)q_y(y),$$

for end zones of cracks of the collinear ordinate axis

$$u_b^+(x,0) - u_b^-(x,0) = C_0\big(x, q_x^0(x)\big)q_x^0(x), \tag{4}$$

for end zones of cracks in inclusion

Here the functions $C\big(x, q_x(x)\big)$, $C\big(y, q_y(y)\big)$, and $C_0\big(x, q_x^0(x)\big)$ represent the effective compliance pliability; $\big(u_s^+ - u_s^-\big)$ – shift of the banks of the end zones of the crack collinear abscissa axis; $\big(\upsilon_s^+ - \upsilon_s^-\big)$ – the shift of the banks of the end zones of the crack collinear ordinate axis; $\big(u_b^+ - u_b^-\big)$ – shift of the banks of the end zones of the crack in the inclusion.

Stresses and displacements in the plane problem of the theory of elasticity can be represented [8,17] through two analytical functions of a complex variable $\Phi(z)$ and $\Psi(z)$

$$\sigma_x + \sigma_y = \sigma_r + \sigma_\theta = 2\big[\Phi(z) + \overline{\Phi(z)}\big], \quad (z = x + iy),$$

$$\sigma_y - \sigma_x + 2i\tau_{xy} = e^{-2i\theta}\big(\sigma_\theta - \sigma_r + 2i\tau_{r\theta}\big) = 2\big[\bar{z}\Phi'(z) + \Psi(z)\big], \tag{5}$$

$$2\mu(u + i\upsilon) = \kappa\varphi(z) - z\overline{\Phi(z)} - \overline{\psi(z)}, \; \varphi'(z) = \Phi(z), \quad \psi'(z) = \Psi(z),$$

$$\kappa = \begin{cases} 3 - 4\nu & - \text{for flat deformation} \\ (3-\nu)/(1+\nu) & - \text{for flat stress} \end{cases}$$

μ – shear modulus; ν – is the Poisson's ratio; r, θ – polar coordinates.

On the basis of general representations (5), the problem under consideration reduces to finding two pairs of functions $\Phi(z)$, $\Psi(z)$ and $\Phi_0(z)$, $\Psi_0(z)$ of the complex variable $z = x + iy$, analytic in the areas occupied by the medium and the puck, and satisfying the boundary conditions [9]:

$$\Phi(\tau)+\overline{\Phi(\tau)}-\left[\bar{\tau}\Phi'(\tau)+\Psi(\tau)\right]e^{2i\theta}=\Phi_0(\tau)+\overline{\Phi_0(\tau)}-\left[\bar{\tau}\Phi_0'(\tau)+\Psi_0(\tau)\right]e^{2i\theta}, \quad (6)$$

$$-\kappa_s\overline{\Phi(\tau)}+\Phi(\tau)-\left[\bar{\tau}\Phi'(\tau)+\Psi(\tau)\right]e^{2i\theta}==\frac{\mu_s}{\mu_b}\left\{-\kappa_b\overline{\Phi_0(\tau)}+\Phi_0(\tau)-\left[\bar{\tau}\Phi_0'(\tau)+\Psi_0(\tau)\right]e^{2i\theta}\right\}, \quad (7)$$

$$\Phi_0(t_0)+\overline{\Phi_0(t_0)}+t_0\overline{\Phi_0'(t_0)}+\overline{\Psi_0(t_0)}=f_x^0(t_0),\quad \Phi(t)+\overline{\Phi(t)}+t\overline{\Phi'(t)}+\overline{\Psi(t)}=f_x(t) \quad (8)$$

$$\Phi(t_1)+\overline{\Phi(t_1)}+t_1\overline{\Phi'(t_1)}+\overline{\Psi(t_1)}=f_y(t_1). \quad (9)$$

μ_s, κ_s and μ_b, κ_b – are the shear moduli and Muskhelishvili constant for the plane and inclusion, respectively.

THE SOLUTION OF THE BOUNDARY VALUE PROBLEM

The solution to the boundary value problem (6)–(9) is sought in the form [3]

$$\Phi_0(z)=\Phi_{01}(z)+\Phi_{02}(z),\ \Psi_0(z)=\Psi_{01}(z)+\Psi_{02}(z), \quad (10)$$

$$\Phi_{01}(z)=\frac{1}{2\pi i}\int_{-\ell}^{\ell}\frac{g_0(t_0)}{t_0-z}dt_0,\qquad \Phi_{02}(z)=i\sum_{k=0}^{\infty}a_{2k}z^{2k},$$

$$\Psi_{01}(z)=\frac{1}{2\pi i}\int_{-\ell}^{\ell}\left[\frac{g_0(t_0)}{t_0-z}-\frac{t_0g_0(t_0)}{(t_0-z)^2}\right]dt_0,\ \Psi_{02}(z)=i\sum_{k=0}^{\infty}b_{2k}z^{2k}, \quad (11)$$

$$\Phi(z)=\Phi_1(z)+\Phi_2(z)+\Phi_3(z),\ \Psi(z)=\Psi_1(z)+\Psi_2(z)+\Psi_3(z), \quad (12)$$

$$\Phi_1(z)=i\tau_{xy}^{\infty}+i\alpha_0+i\sum_{k=0}^{\infty}\alpha_{2k+2}\frac{\lambda^{2k+2}\gamma^{(2k)}(z)}{(2k+1)!}, \quad (13)$$

$$\Psi_1(z)=i\tau_{xy}^{\infty}+i\sum_{k=0}^{\infty}\beta_{2k+2}\frac{\lambda^{2k+2}\rho^{(2k)}(z)}{(2k+1)!}-i\sum_{k=0}^{\infty}\alpha_{2k+2}\frac{\lambda^{2k+2}S^{(2k+1)}(z)}{(2k+1)!},$$

$$\Phi_2(z)=\frac{1}{2\omega}\int_{L_1}g(t)ctg\frac{\pi}{\omega}(t-z)dt,\qquad \Psi_2(z)=-\frac{\pi z}{2\omega^2}\int_{L_1}g(t)\sin^{-2}\frac{\pi}{\omega}(t-z)dt, \quad (14)$$

$$\Phi_3(z)=-\frac{i}{2\omega}\int_{L_2}g_1(t_1)ctg\frac{\pi}{\omega}(it_1-z)dt_1, \quad (15)$$

$$\Psi_3(z)=-\frac{i}{2\omega}\int_{L_2}\left\{g_1(t_1)ctg\frac{\pi}{\omega}(it_1-z)+\right.$$

$$\left.+\left[ctg\frac{\pi}{\omega}(it_1-z)+\frac{\pi}{\omega}(2t_1+z)\sin^2\frac{\pi}{\omega}(it_1-z)\right]g_1(t_1)\right\}dt_1.$$

Here $g(t)$, $g_1(t_1)$, $g_0(t)$ –are the desired functions, the integrals in (14) and (15) are taken along the line $L_1=\{[-h,-a]+[a,h]\}$; $L_2=\{[-r,-b]+[b,r]\}$ [9];

$$g(x)=-\frac{2\mu_s i}{1+\kappa_s}\frac{d}{dx}\left[u_s^+(x,0)-u_s^-(x,0)\right],\ g_1(y)=\frac{2\mu_s}{1+\kappa_s}\frac{d}{dy}\left[\upsilon_s^+(0,y)-\upsilon_s^-(0,y)\right], \quad (16)$$

$$g_0(x)=-\frac{2\mu_b i}{1+\kappa_b}\frac{d}{dx}\left[u_b^+(x,0)-u_b^-(x,0)\right]. \quad (17)$$

To the main concepts should be added additional conditions arising from the physical meaning of the problem [7]

$$\int_{-\ell}^{\ell} g_0(t_0)dt_0=0,\quad \int_{-h}^{-a} g(t)dt=0,\quad \int_{a}^{h} g(t)dt=0,\quad \int_{-r}^{-b} g_1(t_1)dt_1=0,\quad \int_{b}^{r} g_1(t_1)dt_1=0. \quad (18)$$

Applying the method described in, we obtain relations defining the coefficients a_{2k}, b_{2k} of the functions $\Phi_0(z)$, $\Psi_0(z)$. The unknown function $g_0(x)$ must be determined from the boundary condition (8). Substituting (10) – (11) into (8), we obtain a singular integral equation, which, after changing variables and using quadrature formulas [10], is replaced by a finite system of algebraic equations. To determine the unknown coefficients α_{2k}, β_{2k} of the functions $\Phi_1(z)$ and $\Psi_1(z)$, we consider the solution of the elastic problem for the plane, and we consider the quantities A_{2k} to be given for now (we will find A_{2k} below).

We transform the boundary condition (6) as follows [10, 11]

$$\Phi_1(\tau)+\overline{\Phi_1(\tau)}-\left[\bar{\tau}\Phi_1'(\tau)+\Psi_1(\tau)\right]e^{2i\theta}=\sum_{k=-\infty}^{\infty}A_{2k}e^{2ki\theta}+\varphi_1(\theta)+f_1(\theta), \quad (19)$$

where

$$\varphi_1(\theta)=-\Phi_2(\tau)-\overline{\Phi_2(\tau)}+\left[\bar{\tau}\Phi_2'(\tau)+\Psi_2(\tau)\right]e^{2i\theta}, \quad (20)$$

$$f_1(\theta)=-\Phi_3(\tau)-\overline{\Phi_3(\tau)}+\left[\bar{\tau}\Phi_3'(\tau)+\Psi_3(\tau)\right]e^{2i\theta},$$

$$\Phi_0(\tau)+\overline{\Phi_0(\tau)}-\left[\bar{\tau}\Phi_0'(\tau)+\Psi_0(\tau)\right]e^{2i\theta}=\sum_{k=-\infty}^{\infty}A_{2k}e^{2ki\theta},$$

We expand the functions $\varphi_1(\theta)$, $f_1(\theta)$ on the contour of the inclusion of $|\tau|=\lambda$ in complex Fourier series. These rows will have the form [11]

$$\varphi_1(\theta)=\sum_{k=-\infty}^{\infty}C'_{2k}e^{2ki\theta},\ \operatorname{Re}C'_{2k}=0,\qquad f_1(\theta)=\sum_{k=-\infty}^{\infty}C''_{2k}e^{2ki\theta},\ \operatorname{Re}C''_{2k}=0, \quad (21)$$

$$C'_{2k}=\frac{1}{2\pi}\int_0^{2\pi}\varphi_1(\theta)e^{-2ki\theta}d\theta,\ C''_{2k}=\frac{1}{2\pi}\int_0^{2\pi}f_1(\theta)e^{-2ki\theta}d\theta,\quad k=(0,\pm1,\pm2,\ldots).$$

Substituting expression (20) for the integrals and changing the order of integration, after calculating the integrals using residue theory, we find

$$C'_{2k} = -\frac{1}{2\omega}\int_{L_1} g(t)\,\varphi_{2k}(t)dt\,, \quad C''_{2k} = -\frac{1}{2\omega}\int_{L_1} g_1(t_1)\,f_{2k}(t_1)dt_1\,, \tag{22}$$

where $\varphi_0(t) = (1+\varepsilon)\gamma(t),\ \varphi_2(t) = -\frac{\lambda^2}{2}\gamma^{(2)}(t),\ \varphi_{2k}(t) = -\frac{(2k-1)\lambda^{2k}}{(2k)!}\gamma^{(2k)}(t) + \frac{\lambda^{2k-2}}{(2k-3)!}\gamma^{(2k-2)}(t)$

$\varphi_{-2k}(t) = \frac{\varepsilon\lambda^{2k}}{(2k)!}\gamma^{(2k)}(t)\,,\ \gamma(t) = ctg\,\frac{\pi}{\omega}t\,,\ f_0(it_1) = \left[\delta(it_1) - \overline{\delta(it_1)}\right]\frac{(1+\varepsilon)}{2}$, ($k$ =1, 2, …),

$$f_2(it_1) = -\frac{\lambda^2}{2}\delta^{(2)}(it_1) + 2\left[\delta(it_1) - it\delta'(it_1)\right],$$

$f_{2k}(it_1) = \frac{(1-2k)\lambda^{2k}}{(2k)!}\delta^{(2k)}(it_1) + \frac{2\lambda^{2k-2}}{(2k-2)!}\left[k\delta^{(2k-2)}(it_1) - it_1\delta^{(2k-1)}(it_1)\right]$, ($k$ = 2, 3, …),

$$f_{-2k}(it_1) = -\frac{\varepsilon\lambda^{2k}}{(2k)!}\overline{\delta^{(2k)}(it_1)},\ \delta(it_1) = \mathrm{ctg}\,\frac{\pi}{\omega}(it_1),\ \varepsilon = 1,\ (k = 1, 2, \ldots).$$

Substituting into the left side of the boundary condition (19) instead of $\Phi_1(z)$, $\overline{\Phi_1(z)}$, $\Phi_1'(z)$ and $\Psi_1(z)$ their expansion into Laurent series in a neighbor-hood of the zero point and equating the coefficients for identical powers of $\exp(i\theta)$, we obtain two infinite systems of linear algebraic equations with respect to the coefficients α_{2k}, β_{2k} [12]:

$$i\alpha_{2j+2} = \sum_{j=0}^{\infty} iA_{j,k}\alpha_{2k+2} + b_j\,,\ A_{j,k} = \frac{1}{\varepsilon}(2j+1)\gamma_{j,k}\lambda^{2j+2k+2},\ (j = 0, 1, 2, \ldots), \tag{23}$$

$$\gamma_{0,0} = \frac{3}{8}g_2\lambda^2 + \varepsilon\sum_{k=1}^{\infty}\frac{(2i+1)g_{i+1}^2\lambda^{4i+2}}{2^{4i+4}},$$

$$\gamma_{j,k} = -\frac{(2j+2k+2)g_{j+k+1}}{(2j+1)!(2k+1)!2^{2j+2k+2}} + \frac{(2j+2k+4)g_{j+k+2}\lambda^2}{(2j+2)!(2k+2)!2^{2j+2k+4}} +$$

$$+\frac{g_{j+1}g_{k+1}\lambda^2}{2^{2j+2k+4}}\left[1 + \frac{(1+\varepsilon)^2K_2\lambda^2}{1-(1+\varepsilon)K_2\lambda^2}\right] +$$

$$+\varepsilon\sum_{i=0}^{\infty}\frac{(2j+2i+1)!(2k+2i+1)!g_{j+i+1}g_{k+i+1}\lambda^{4i+2}}{(2j+1)!(2k+1)!(2i+1)!(2i)!2^{2j+2k+4i+4}},\ (j, k = 0, 1, 2, \ldots),$$

$$\varepsilon b_0 = A_2' - \sum_{k=0}^{\infty} \frac{g_{k+2}\lambda^{2k+4}}{2^{2k+4}} A_{-2k-2}',$$

$$\varepsilon b_j = A_{2j+2}' - \frac{(2j+1)g_{j+1}\lambda^{2j+2}}{\left[1-(1+\varepsilon)K_2\lambda^2\right]2^{2j+2}} A_0' - \sum_{k=0}^{\infty} \frac{(2j+2k+3)!\,g_{j+k+2}\lambda^{2k+2j+4}}{(2j)!(2k+3)!\,2^{2j+2k+4}} A_{-2k-2}',$$

$$r_{j,k} = \frac{(2j+2k+1)!\;g_{j+k+1}}{(2j)!(2k+1)!2^{2j+2k+2}}, \qquad g_{j+k+1} = 2\sum_{m=1}{}' \frac{1}{m^{2j+2k+2}},$$

$$K_2 = \frac{\pi^2}{24},\ A_2' = A_2 + i\tau_{xy}^{\infty},\ A_0' = A_0 - 2i\tau_{xy}^{\infty},\ A_{2k}' = A_{2k},\ k = (-1, \pm 2, ...).$$

The coefficients β_{2k} are determined by the relations

$$i\beta_2 = \frac{1}{1-(1+\varepsilon)K_2\lambda^2}\left[-A_0' + (1+\varepsilon)\sum_{k=1}^{\infty} \frac{g_{k+1}\lambda^{2k+2} i\alpha_{2k+2}}{2^{2k+2}}\right], \tag{24}$$

$$i\beta_{2j+4} = i(2j+3)\alpha_{2j+2} + \varepsilon\sum_{k=0}^{\infty} \frac{(2j+2k+3)!\,g_{j+k+2}\lambda^{2j+2k+4} i\alpha_{2k+2}}{(2j+2)!(2k+1)!2^{2j+2k+4}} - A_{-2j-2}'.$$

Where the expression for $A_{j,k}$, b_j and the defining relations for the coefficients β_{2k} are given in (23) and (24). Moreover, with the difference that in the relations defining b_j and β_{2k}, instead of A_{2k}', one should take M_{2k}' in this case

$$M_0' = M_0 - 2i\tau_{xy}^{\infty},\ M_2' = M_2 + i\tau_{xy}^{\infty},\ M_{2k}' = M_{2k},\quad (k = 1, \pm 2, \pm 3, ...),$$

$$M_{2k} = A_{2k} + C_{2k},\quad C_{2k} = C_{2k}' + C_{2k}''\quad (k = 0, \pm 1, \pm 2, ...).$$

Acting similarly with the boundary condition (20), after some transformations we obtain the same system of equations as (23) with respect to α_{2j+2}^* for $\varepsilon = -\kappa$, and instead of the coefficients A_{2k}', in this case, we should take A_{2k}^*

$$A_0^* = (\kappa - 1)i\tau_{xy}^{\infty} + \frac{(1-\kappa_0)\mu}{2\mu_b}A_0 - \frac{(1+\kappa_0)\mu}{2\mu_0}B_0,\ A_2^* = i\tau_{xy}^{\infty} + C_2^* + \frac{\mu}{\mu_0}A_2,\ A_{2k}^* = C_{2k}^* + \frac{\mu}{\mu_0}A_{2k},$$

$$(k = 2, 3, ...),\ A_{-2k}^* = C_{-2k}^* - \frac{\mu\kappa_0}{\mu_0}A_{-2k} + \frac{(1+\kappa_0)\mu}{\mu_0}B_{-2k},\ (k = 1, 2, ...).$$

Here C_{2k}^* $(k = 0, \pm 1, \pm 2, ...)$ are determined from (22) for $\varepsilon = -\kappa_s$.

Using the obtained relations and performing some transformations, we obtain formulas that determine the coefficients α_{2k}, β_{2k}, A_0, A_{-2k} in terms of A_{2k}, as well as an infinite system of linear algebraic equations with respect to A_{2k} [13]:

$$i\alpha_{2j+2} = \frac{1-\mu_s/\mu_b}{1+\kappa_s} A_{2j+2}, \tag{25}$$

$$A_{-2j} = \frac{\mu_b}{\mu_b+\kappa_0\mu_s}\left(C^*_{-2j} - C_{-2j}\right) - \frac{(1+\kappa_b)\mu_s}{\mu_b-\mu_s\kappa_b} B_{-2j} + \frac{\mu_b-\mu_s}{\mu_b+\kappa_b\mu_s}\sum_{k=0}^{\infty}\lambda^{2j+2k+2} r_{j,k} A_{2k+2},$$

$$A_0 = \sum_{k=0}^{\infty} e_{0,k}\lambda^{2k+2} A_{2k+2} + ie_0 - e_1,\ e_{0,k} = \frac{1-\mu_s/\mu_b}{\left(1-2K_2\lambda^2\right)e} r_{0,k},\ e_0 = \frac{1+\kappa_s}{\left(1+2K_2\lambda^2\right)e},$$

$$e_1 = \frac{1}{e}C^*_0 - \frac{1+(\kappa_s-1)K_2\lambda^2}{\left(1-2K_2\lambda^2\right)} C_0 - \frac{(1+\kappa_0)\mu_s}{2\mu_b e} B_0,\ e = \frac{1+\kappa_s}{2\left(1-2K_2\lambda^2\right)} - \frac{\kappa_s-1}{2} + \frac{\mu_s(\kappa_b-1)}{2\mu_b},$$

$$i\beta_{2j+2} = \frac{1-\mu_s/\mu_b}{1+\kappa_s}\left[(2j+3)A_{2j+2} + \sum_{k=0}^{\infty}\frac{(2j+2k+3)!\, g_{j+k+2}\lambda^{2j+2k+4} A_{2k+2}}{(2j+2)!(2k+1)!\, 2^{2j+2k+4}}\right] - A_{-2j-2} - C_{-2j-2},$$

$$A_{2j+2} = \sum_{k=0}^{\infty} D_{j,k} A_{2k+2} + T_j,\ D_{j,k} = (2j+1)\lambda^{2j+2k+2} S_{j,k}/\gamma,\ (j = 0, 1, 2,\ldots), \tag{26}$$

$$S_{j,k} = \frac{1-\mu_s/\mu_b}{1+\kappa_s}\left(\gamma_{j,k} + \frac{\mu_b}{\kappa_b\mu_s}\gamma^*_{j,k} + d_{j,k}\right), \qquad d_{j,k} = \frac{g_{j+1}g_{k+1}}{2^{2j+2k+4}}\lambda^2\eta(\mu_s/\mu_b),$$

$$\eta(\mu_s/\mu_b) = \frac{\dfrac{\kappa_b-1}{\kappa_b}\cdot\dfrac{1}{1-(\kappa_s-1)K_2\lambda^2} - \dfrac{2}{1-2K_2\lambda^2}}{1-\left(1-2K_2\lambda^2\right)\left[\dfrac{\kappa_s-1}{\kappa_s+1} - \dfrac{\mu_s}{\mu_b}\dfrac{(\kappa_b-1)}{(\kappa_s+1)}\right]},\ T^*_0 = \left(1-\frac{\mu_b}{\kappa_0\mu_s}\right) i\tau^{\infty}_{xy},\ T_j = \left(T^*_j + h_j + K_j\right)/\gamma,$$

$$h_0 = \frac{1+\kappa_b}{\kappa_b}\sum_{k=0}^{\infty}\frac{g_{k+2}\lambda^{2k+4}}{2^{2k+4}} B_{-2k-2},\ K_0 = C_2 + \frac{\mu_0}{\kappa_b\mu_s}C^*_2 - \sum_{k=0}^{\infty}\frac{g_{k+2}\lambda^{2k+4}}{2^{2k+4}}\left(C_{2k-2} + \frac{\mu_b}{\kappa_b\mu_s}C^*_{-2k-2}\right),$$

$$T^*_j = \frac{(2j+1)g_{j+1}\lambda^{2j+2}}{2^{2j+2}}\eta_1(\mu_s/\mu_b) i\tau^{\infty}_{xy},\ \eta_1(\mu_s/\mu_b) = \frac{(1+\mu_b/\kappa_b\mu_s)\left[(\mu_b/\mu_s)(\kappa_b-1)-(\kappa_s-1)\right]}{1+(\kappa_s-1)K_2\lambda^2 + (\mu_s/2\mu_b)(\kappa_b-1)\left(1-2K_2\lambda^2\right)},$$

$$h_j = \frac{(2j+1)g_{j+1}\lambda^{2j+2}}{2^{2j+2}}(1+\kappa_b)\left\{\frac{1}{2\kappa_b\left[1+(\kappa_s-1)K_2\lambda^2\right]} + \right.$$

$$\left. + \frac{\mu_s}{2e\mu_b}\left[\frac{1}{1-2K_2\lambda^2} + \frac{1-\kappa_b}{2\kappa_b\left[1+(\kappa_s-1)K_2\lambda^2\right]}\right]\right\} B_0 + \frac{1+\kappa_b}{\kappa_b}\sum_{k=0}^{\infty}\frac{(2j+2k+3)!\, g_{j+k+2}\lambda^{2k+2j+4}}{(2j)!(2k+3)!\, 2^{2j+2k+4}} B_{-2k-2}$$

$$K_j = \frac{(2j+1)g_{j+1}\lambda^{2j+2}}{2^{2j+2}}\left\{\frac{1-(\kappa_s-1)K_2\lambda^2}{e}\left[\frac{1}{1-2K_2\lambda^2}+\frac{1-\kappa_0}{2\kappa_s\left[1+(\kappa_s-1)K_2\lambda^2\right]}\right]-\right.$$

$$\left.-1\right\}C_0-\frac{(2j+1)g_{j+1}\lambda^{2j+2}}{2^{2j+2}}\left\{\frac{1}{(1-2K_2\lambda^2)e}+\frac{1}{\kappa_b\left[1+(\kappa_s-1)K_2\lambda^2\right]}\times\right.$$

$$\left.\times\left(\frac{1-\kappa_b}{2e}+\frac{\mu_s}{\mu_b}\right)\right\}C_0^*+C_{2j+2}\frac{\mu_b}{\kappa_b\mu_s}C_{2j+2}^*-\sum_{k=0}^{\infty}\frac{(2j+2k+3)!g_{j+k+2}\lambda^{2j+2k+4}}{(2j)!(2k+3)!2^{2j+2k+4}}\times\left(C_{-2k-2}+\frac{\mu_b}{\kappa_b\mu_s}C_{-2k-2}^*\right),$$

$$\gamma=\frac{(1-\mu_s/\mu_b)(1-\kappa_s\mu_b/\kappa_b\mu_s)}{1+\kappa_s}-\frac{1+\kappa_b}{\kappa_b}.$$

Here, B_{2k} is defined in (25), C_{2k} – is defined in (22) for $\varepsilon=1$, C_{2k}^* – is defined in (22) for $\varepsilon=-\kappa_s$, $\gamma_{j,k}$ and $\gamma_{j,k}^*$ are defined in (23) for $\varepsilon=1$ and $\varepsilon=-\kappa_s$, respectively.

To determine the desired function $g(x)$, we have the boundary condition on the line L1. Requiring that functions (12) – (15) satisfy the boundary condition on the banks of the prefracture zone L_1, we obtain, after some transformations, a singular integral equation for $g(x)$ [14, 21]:

$$\frac{1}{\omega}\int_{L_1}g(t)K(t-x)dt+H(x)=-iq_x(x),\ K(t-x)=ctg\frac{\pi}{\omega}(t-x), \tag{27}$$

$$H(x)=\Phi_s(x)+\overline{\Phi_s(x)}+x\overline{\Phi_s'(x)}+\overline{\Psi_s(x)},\ \Phi_s(x)=\Phi_1(x)+\Phi_3(x),$$

$$\Psi_s(x)=\Psi_1(x)+\Psi_3(x).$$

Similarly, satisfying the boundary condition on the line L_2, after some transformations we obtain one more singular integral equation with respect to the desired function $g_1(y)$:

$$-\frac{\pi}{\omega^2}\int_{L_2}g_1(t_1)\left[(t_1-y)sh^{-2}\frac{\pi}{\omega}(t_1-y)dt_1\right]+N(y)=-iq_y(y), \tag{28}$$

where $N(y)=\Phi_0(iy)+\overline{\Phi_0(iy)}+iy\overline{\Phi_0'(iy)}+\overline{\Psi_0(iy)},\ \Phi_0(z)=\Phi_1(z)+\Phi_2(z),$

$$\Psi_0(z)=\Psi_1(z)+\Psi_2(z).$$

Satisfying functions (10) – (11) of the boundary condition (8), after some transformations, we obtain a singular integral equation of the first kind by the Cauchy kernel with respect to the function $g_0(x_0)$ [15, 22]:

$$\frac{1}{\pi}\int_{-\ell}^{\ell}\frac{g_0(t_0)dt_0}{t_0-x_0}+H_0(x)=f_x^0(x_0), \tag{29}$$

where $H_0(x)=x\overline{\Phi'_{02}(x)}+\overline{\Psi_{02}(x)}$,

$f_x^0(x)=0$ on the free banks of cracks;

$f_x^0(x)=-iq_x^0(x)$ on the banks of the end zones of cracks.

Thus, infinite algebraic systems (23), together with three singular integral equations (27) – (29), are the main resolving equations of the problem, which allow one to determine the desired functions $g(x)$, $g(y)$ and $g_0(x_0)$, and the coefficients a_{2k}, b_{2k}, α_{2k}. It should be recalled that the algebraic system (23) contains the coefficients C_{2k} and B_{2k}, depending on the desired functions $g(x)$, $g(y)$ and $g_0(x_0)$, respectively. Thus, systems (23) and integral equations (27) – (29) turned out to be coupled and must be solved together.

ALGEBRAIZATION OF THE MAIN RESOLVING EQUATIONS

Using the expansion of the function $ctg\frac{\pi}{\omega}z$ in the main strip of periods, the singular integral equation (27) after some transformations, we bring to the following form [16, 22]

$$\frac{1}{\pi}\int_{L_1}\frac{g(t)dt}{t-x}+\frac{1}{\pi}\int_{L_1}g(t)K(t-x)dt+H(x)=-iq_x(x),\quad K(t)=-\sum_{j=0}^{\infty}g_{j+1}\frac{t^{2j+1}}{\omega^{2j+2}}. \tag{30}$$

Given that $g(x)=-g(-x)$, by changing variables, we transform equation (30) to the form [55]

$$\frac{2}{\pi}\int_{\lambda_1}^{1}\frac{\xi\,p(\xi)d\xi}{\xi^2-\xi_0^2}+\frac{1}{\pi}\int_{\lambda_1}^{1}K_0(\xi,\xi_0)p(\xi)d\xi+H(\xi_0)=-iq_x(\xi_0), \tag{31}$$

$$K_0(\xi,\xi_0)=K(\xi-\xi_0)+K(\xi+\xi_0),\ p(\xi)=-g(t),\ \xi=\frac{t}{\ell},\ \xi_0=\frac{x}{\ell},\ \lambda_1=\frac{\lambda}{\ell},\ \lambda_1\le\xi_0\le 1,$$

$$H(\xi_0)=\Phi_1(\xi_0\ell)+\overline{\Phi_1(\xi_0\ell)}+\xi_0\ell\overline{\Phi'_1(\xi_0\ell)}+\overline{\Psi_1(\xi_0\ell)}.$$

Now, we transform equation (31) to a form convenient for finding its approximate solution. To do this, apply another change of variables.

We carry out another change of variables

$$\xi^2=u=\frac{1-\lambda_1^2}{2}(\tau+1)+\lambda_1^2,\quad \xi_0^2=u_0=\frac{1-\lambda_1^2}{2}(\eta+1)+\lambda_1^2. \tag{32}$$

With such a change of variables, the integration interval $[\lambda_1, 1]$ goes into the interval $[-1, 1]$, and the transformed singular integral equation (31) takes the usual form, convenient for numerical solution

$$\frac{1}{\pi}\int_{-1}^{1}\frac{p(\tau)d\tau}{\tau-\eta}+\frac{1}{\pi}\int_{-1}^{1}p(\tau)B(\eta,\tau)d\tau+H_*(\eta)=-iq_x(\eta). \tag{33}$$

$$p(\tau)=p(\xi),\quad H_*(\eta)=H(\xi_0),\quad B(\eta,\tau)=-\frac{1-\lambda_1^2}{2}\sum_{j=0}^{\infty}g_{j+1}\left(\frac{\ell}{2}\right)^{2j+2}u_0^jA_j,$$

$$A_j=\left\{(2j+1)+\frac{(2j+1)(2j)(2j-1)}{1\cdot2\cdot3}\left(\frac{u}{u_0}\right)+\ldots+\right.$$

$$\left.+\frac{(2j+1)(2j)(2j-1)\ldots[(2j+1)-(2j+1-1)]}{1\cdot2\ldots(2j+1)}\left(\frac{u}{u_0}\right)^j\right\}.$$

Function $p(\tau)$ takes purely imaginary values. We reduce equation (33) to a finite system of linear equations, bypassing the intermediate stage of regularization and reducing it to the Fredholm equation of the second kind.

The solution of equation (33) can be represented as [18, 22]

$$p(\tau)=\frac{p_0(\eta)}{\sqrt{1-\eta^2}},$$

where $p_0(\eta)$ is Hölder continuous on a function.

We will seek function $p_0(\tau)$ in the form of an Lagrange interpolation polynomial constructed from Chebyshev nodes

$$L_n[p_0;\tau]=\frac{1}{n}\sum_{k=1}^{n}(-1)^{k+1}p_k^0\frac{\cos n\theta\sin\theta_k}{\cos\theta-\cos\theta_k},\qquad \tau=\cos\theta, \tag{34}$$

$$p_k^0=p_0(\tau_k),\quad \tau_m=\cos\theta_m,\quad \theta_m=\frac{2m-1}{2n}\pi,\quad (m=1,2,\ldots,n).$$

Using (34) and also

$$\frac{1}{\pi}\int_0^{\pi}\frac{\cos n\tau\,d\tau}{\cos\tau-\cos\theta}=\frac{\sin n\theta}{\sin\theta},\qquad (0\le\theta\le\pi;\quad n=0,1,\ldots),$$

and a Gaussian type quadrature formula

$$\int_{-1}^{1}\frac{F(x)dx}{\sqrt{1-x^2}}=\frac{\pi}{n}\sum_{k=1}^{n}F(\cos\theta_k),$$

we obtain the formulas for all integral terms in equations (33) and system (25)

$$\frac{1}{2\pi}\int_{-1}^{1}\frac{p(\tau)}{\tau-\eta}d\tau=\frac{1}{n\sin\theta}\sum_{k=1}^{n}p_k^0\sum_{m=0}^{n-1}\cos m\theta_k\sin m\theta,\quad \frac{1}{2\pi}\int_{-1}^{1}p(\tau)B(\eta,\tau)d\tau=\frac{1}{2n}\sum_{k=1}^{n}p_k^0B(\eta,\tau_k),\quad (35)$$

$$A_{2k}=-\frac{1-\lambda_1^2}{2}\frac{1}{2n}\sum_{\nu=1}^{n}p_\nu^0 f_{2k}^*(\tau_\nu),\quad f_{2k}^*(\tau)=f_{2k}^*(\xi^2),\quad \xi f_{2k}^*(\xi^2)=\frac{\pi}{\omega}\ell f_{2k}(t).$$

The given quadrature formulas (35) make it possible to reduce the main resolving equations to two finite systems of algebraic equations for approximate values p_k^0, R_ν^0 of the desired function at the nodal points, as well as to two infinite systems of algebraic equations for the coefficients α_{2k}, β_{2k}.

After some transformations, the singular integral equation (27) reduces to the following algebraic system of equations

$$\sum_{k=1}^{n}a_{mk}p_k^0+\frac{1}{2}H_*(\eta_m)=-q_x(\eta_m),\qquad (m=1,2,\ldots,n-1),\qquad (36)$$

$$a_{mk}=\frac{1}{2n}\left[\frac{1}{\sin\theta_m}ctg\frac{\theta_m+(-1)^{|m-k|}\theta_k}{2}+B(\tau_m,\eta_k)\right],\qquad \tau_m=\eta_m.$$

We now turn to the second singular integral equation (28). Using the expansion of function $sh^{-2}\frac{\pi}{\omega}z$ and taking into account $g_1(t_1)=\ =-g_1(-t_1)$, after changing the variables, we transform equation (28) to a form more convenient for finding its approximate solution

$$\frac{2}{\pi}\int_{\lambda_2}^{1}\frac{\xi_1R(\xi_1)}{\xi_1^2-\xi_2^2}d\xi_1+\frac{1}{\pi}\int_{\lambda_2}^{1}L_0(\xi_1,\xi_2)R(\xi_1)d\xi_1+N_1(\xi_2)=-iq_y(\xi_2),\qquad (37)$$

where

$$\xi_1=\frac{t}{h},\ \xi_2=\frac{y}{h},\ \lambda_2=\frac{\lambda}{h},\ \lambda_2\le\xi_2\le1,\ L_0(\xi_1,\xi_2)=L(\xi_1-\xi_2)+L(\xi_1+\xi_2),\ R(\xi_1)=g_1(t_1),$$

$$N(\xi_2)=\Phi_0(i\xi_2h)+\overline{\Phi_0(i\xi_2h)}+(i\xi_2h)\overline{\Phi_0'(i\xi_2h)}+\overline{\Psi_0(i\xi_2h)}.$$

Let's make another change of variables

$$u_1=\xi_1^2=\frac{1-\lambda_2^2}{2}(\tau+1)+\lambda_2^2,\quad u_2=\xi_2^2=\frac{1-\lambda_2^2}{2}(\eta+1)+\lambda_2^2.$$

In this case, the integration interval $[\lambda_2,1]$ goes into the interval $[-1,1]$, and the integral equation takes the following form

$$\frac{1}{\pi}\int_{-1}^{1}\frac{R(\tau)d\tau}{\tau-\eta}+\frac{1}{\pi}\int_{-1}^{1}R(\tau)B_*(\eta,\tau)d\tau+N_*(\eta)=-iq_y(\eta), \tag{38}$$

where $B_*(\eta,\tau)=-\frac{1-\lambda_2^2}{2}\sum_{j=0}^{\infty}(-1)^j(2j+1)g_{j+1}\left(\frac{h}{2}\right)^{2j+2}, u_1^j A_j'$

$$A_j'=\left\{(2j+1)+\frac{(2j+1)(2j)(2j-1)}{1\cdot 2\cdot 3}\left(\frac{u_1}{u_2}\right)+\ldots+\left(\frac{u_1}{u_2}\right)^j\right\},\quad R(\tau)=R(\xi_1).$$

Repeating the above method, we replace the singular integral equation with a finite system of linear algebraic equations with respect to the desired function R_v^0:

$$\sum_{v=1}^{n}a_{mv}^*R_v^0+\frac{1}{2}N_*(\eta_m)=-q_y(\eta_m),\qquad (m = 1, 2, \ldots, M-1), \tag{39}$$

$$a_{mv}^*=\frac{1}{2n}\left[\frac{1}{\sin\theta_m}ctg\frac{\theta_m+(-1)^{|m-v|}\theta_v}{2}+B_*(\eta_m,\tau_v)\right].$$

The right – hand side of the resulting finite systems includes unknown stresses $q_x(\eta_m)$ and $q_y(\eta_m)$ at the nodal points belonging to the prefracture zones. Using the obtained solution, equations (3), (4) can be represented as

To the resulting system of equations (36) – (39), additional equations (18) written in discrete form are added

$$\sum_{k=1}^{n}\frac{p_k^o}{\sqrt{\frac{1}{2}(1-\lambda_1^2)(\tau_k+1)+\lambda_1^2}}=0,\qquad \sum_{v=1}^{n}\frac{R_v^o}{\sqrt{\frac{1}{2}(1-\lambda_2^2)(\tau_v+1)+\lambda_2^2}}=0. \tag{40}$$

The right – hand sides of the obtained algebraic systems (36), (39), and (19) contain unknown values of the stresses $q_x(\eta_m)$, $q_y(\eta_m)$ and $q_y^0(\eta_m)$ at the nodal points belonging to the end zones before failure. The unknown values of stresses in bonds arising on the banks of the zones of pre–fracture are determined from the additional conditions (3) – (4). Using the solution obtained, relations (3) – (4) can be written [19]

$$g_0(x)=-\frac{2\mu_b i}{1+\kappa_b}\frac{d}{dx}\left[C(x,q_x^0(x))q_x^0(x)\right],\quad g(x)=-\frac{2\mu_s i}{1+\kappa_s}\frac{d}{dx}\left[C(x,q_x(x))q_x(x)\right], \tag{41}$$

$$g_1(y)=\frac{2\mu_s}{1+\kappa_s}\frac{d}{dy}\left[C(y,q_y(y))q_y(y)\right]$$

These equations serve to determine the stresses in the bonds. We represent these equations (41) in the following form

$$\frac{1+\kappa_0}{2\mu_0 i}\int_{\ell}^{x} g_0(x)\,dx = C\left(x, q_x^0(x)\right)q_x^0(x), \qquad x\in(\ell_1, \ell), \tag{42}$$

$$\frac{1+\kappa}{2\mu i}\int_{h}^{x} g(x)\,dx = C\left(x, q_x(x)\right)q_x(x), \qquad x\in(h_1, h)\cup(a, a_1),$$

$$-\frac{1+\kappa}{2\mu}\int_{r}^{y} g_1(y)\,dy = C\left(y, q_y(y)\right)q_y(x), \qquad y\in(r, r_1)\cup(b, b_1).$$

To construct the missing equations, we require that conditions (42) be satisfied at the corresponding nodal points belonging to the end zones (ℓ_1, ℓ), $(h_1, h)\cup(a, a_1)$, $(r, r_1)\cup(b, b_1)$. As a result, we obtain three algebraic systems for finding approximate values $q_x^0(\eta_{m_0})$ (m_0 = 1, 2, …, M_0), $q_x(\eta_{m_1})$ (m_1 = 1, 2, …, M_1) and $q_y(\eta_{m_2})$ (m_2 = 1, 2, …, M_2) respectively:

$$\begin{cases} C_0^* p_0^0(\eta_1) = C\left(\eta_1, q_x^0(\eta_1)\right)q_x^0(\eta_1) \\ C_0^*\left(p_0^0(\eta_1) + p_0^0(\eta_2)\right) = C\left(\eta_2, q_x^0(\eta_2)\right)q_x^0(\eta_2) \\ \ldots\ldots\ldots\ldots\ldots\ldots\ldots\ldots\ldots\ldots \\ \ldots\ldots\ldots\ldots\ldots\ldots\ldots\ldots\ldots\ldots \\ C_0^*\sum\limits_{m_0=1}^{M_0} p_0^0(\eta_{m_0}) = C\left(\eta_{M_0}, q_x^0(\eta_{M_0})\right)q_x^0(\eta_{M_0}) \end{cases} \tag{43}$$

$$\begin{cases} C_1^* p_0(\eta_1) = C\left(\eta_1, q_x(\eta_1)\right)q_x(\eta_1) \\ C_1^*\left(p_0(\eta_1) + p_0(\eta_2)\right) = C\left(\eta_2, q_x(\eta_2)\right)q_x(\eta_2) \\ \ldots\ldots\ldots\ldots\ldots\ldots\ldots\ldots\ldots\ldots \\ \ldots\ldots\ldots\ldots\ldots\ldots\ldots\ldots\ldots\ldots \\ C_1^*\sum\limits_{m_1=1}^{M_1} p_0(\eta_{m_1}) = C\left(\eta_{M_1}, q_x(\eta_{M_1})\right)q_x(\eta_{M_1}) \end{cases} \tag{44}$$

$$\begin{cases} C_2^* R_0(\eta_1) = C\left(\eta_1, q_y(\eta_1)\right)q_y(\eta_1) \\ C_2^*\left(R_0(\eta_1) + p_0(\eta_2)\right) = C\left(\eta_2, q_y(\eta_2)\right)q_y(\eta_2) \\ \ldots\ldots\ldots\ldots\ldots\ldots\ldots\ldots\ldots\ldots \\ \ldots\ldots\ldots\ldots\ldots\ldots\ldots\ldots\ldots\ldots \\ C_2^*\sum\limits_{m_2=1}^{M_2} R_0(\eta_{m_2}) = C\left(\eta_{M_2}, q_y(\eta_{M_2})\right)q_y(\eta_{M_2}) \end{cases} \tag{45}$$

Here $C_0^* = (1+\kappa_b)\pi(\ell-\ell_1)/(2\mu_b M)$, $C_1^* = (1+\kappa_s)\pi(h-a)/(2\mu_s M)$,

$$C_2^* = -(1+\kappa_s)\pi(b-r)/(2\mu_s M).$$

For the closure of the obtained algebraic equations, five equations are lacking that determine the sizes of the end zones of the cracks. Since the solution of integral equations is sought in the class of everywhere bounded functions (stresses), it is necessary to add the conditions of boundedness of stresses at the ends of the end zones of cracks to the obtained systems. These conditions have the form [20]

$$\sum_{k=1}^{M}(-1)^k\, p_{0k}^0 ctg\,\frac{\theta_k}{2}=0, \qquad \sum_{k=1}^{M}(-1)^{k+M}\, p_k^0 tg\,\frac{\theta_k}{2}=0,$$

$$\sum_{k=1}^{M}(-1)^k\, p_k^0 ctg\,\frac{\theta_k}{2}=0, \qquad \sum_{k=1}^{M}(-1)^{\nu}\, R_\nu^0 ctg\,\frac{\theta_c}{2}=0. \tag{46}$$

After determining the values of functions p_k^0 and R_ν^0, the stress intensity factors in the vicinity of the crack tips were found by the relations [23]

$$K_{II}^a=-i\sqrt{\frac{\pi\ell\left(1-\lambda_*^2\right)}{\lambda_*}}\,\frac{1}{2M}\sum_{k=1}^{M}(-1)^{k+M}\, p_k^0 tg\,\frac{\theta_k}{2},\quad K_{II}^\ell=-i\sqrt{\pi\ell\left(1-\lambda_*^2\right)}\,\frac{1}{2M}\sum_{k=1}^{M}(-1)^k\, p_k^0 ctg\,\frac{\theta_k}{2},$$

$$K_{II}^b=-i\sqrt{\frac{\pi r\left(1-\lambda_2^2\right)}{\lambda_2}}\,\frac{1}{2M}\sum_{\nu=1}^{M}(-1)^{\nu+M}\, R_\nu^0 tg\,\frac{\theta_\nu}{2},\quad K_{II}^r=-i\sqrt{\pi r\left(1-\lambda_2^2\right)}\,\frac{1}{2M}\sum_{\nu=1}^{M}(-1)^{\nu}\, R_\nu^0 ctg\,\frac{\theta_\nu}{2}. \tag{47}$$

To analyze the ultimate equilibrium of cracks with end zones, two conditions (two – parameter criterion) of fracture are necessary. The first criterion is the condition for the propagation of the crack tip, and the second is the condition for breaking bonds at the edge of the end zone.

As the first condition for destruction, we use the force criterion for the destruction of Irwin. The condition of limiting equilibrium of the crack tip corresponds to the condition

$$K_{II}=K_{IIc}, \tag{48}$$

where K_{IIc} – is the constant of the material, determined empirically [23]

As the second condition for fracture, we use the criterion for a critical shift of the crack faces and we believe that bond breaking at the edge of the end zone ($x_*=\ell-d$ or $y_*=r-d_1$) occurs when the condition

$$V(x_*)=\sqrt{\left(u^+-u^-\right)^2+\left(\upsilon^+-\upsilon^-\right)^2}=\delta_{cr}, \tag{49}$$

where δ_{cr} – is the ultimate bond length [5, 38].

The solution of the system of algebraic equations (16), (17), (36), (39), (41), (47), (48) and (49) allows (for a given crack length and bond characteristics) to find the critical external load τ_{xy}^{∞} and the limit shift of the end zone in the state of limiting equilibrium cracks.

For given sizes of cracks and end zones, using the limit values K_{IIc} and δ_{cr}, we can distinguish the equilibrium and growth modes of cracks under monotonic loading. If the conditions are met

$$K_{II} \geq K_{IIc}, \qquad V(x_*) \text{ and } V(y_*) < \delta_{cr},$$

then the crack tip advances with a simultaneous increase in the length of the end zone without breaking bonds.

This stage of crack development can be considered as a process of adaptability to a given level of external loads.

The crack tip growth with simultaneous breaking of bonds at the edge of the end zone will occur under the conditions

$$K_{II} \geq K_{IIc}, \quad V(x_* \text{ or } y_*) \geq \delta_{cr}.$$

So, for example, under the conditions

$$K_{II} < K_{IIc}, \quad V(x_* \text{ or } y_*) \geq \delta_{cr}$$

bonds are broken without advancement of the crack tip and the size of the end zone is reduced, striving for a critical value for a given load level.

Under the conditions

$$K_{II} < K_{IIc}, \quad V(x_* \text{ and } y_*) < \delta_{cr}$$

the position of the crack tip and the end zone will not change [23].

Since the sizes of the end zones of the cracks are unknown, the combined algebraic system of equations is nonlinear even with linear relationships. To solve it, the method of successive approximations is used. In each approximation, the combined algebraic system was solved by the Gauss method with the choice of the main element. In the case of the nonlinear law of bond deformation, an iterative method similar to the elastic solution method is used to determine the forces in the pre – fracture zones. In numerical calculations, it was assumed that $M = 30$, which corresponds to dividing the integration interval into 30 chebyshev nodes.

To determine the limiting state at which crack growth occurs, the condition of a critical shift of the crack faces is used. Using the obtained solution, the conditions determining the ultimate external load are the following

$$C(\lambda^0, q_x^0(\lambda^0))q_x^0(\lambda) = \delta_c^0 \quad C(\lambda_*, q_y(\lambda_*))q_x(\lambda_*) = \delta_c \quad C(\lambda_*^1, q_x(\lambda_*^1))q_y(\lambda_*^1) = \delta_c, \qquad (50)$$

where δ_c^0 and δ_c – are the crack resistance characteristics of the inclusion material and the binder, respectively; λ^0, λ_* and λ_*^1 – are the coordinates of the points at the base of the prefracture zones for inclusion and binder, respectively.

The analysis of the extremely equilibrium state of a piecewise homogeneous medium under which crack growth occurs reduces to a parametric study of the combined algebraic system and crack growth criterion (50) for various laws of bond deformation, elastic constant materials, and geometric characteristics of a perforated body.

Calculations were carried out to determine the ultimate loads causing crack growth. Each of the infinite systems was reduced to five equations, and with the help of one of them the unknown coefficients β_{2k} were eliminated from the remaining equations. The resulting system in each approximation was solved by the Gauss method. In the calculations, h was considered constant equal to $h = 0{,}90$; $r - b = 0{,}3$. In addition, it was accepted for the binder material $\nu = 0{,}32$; $\mu = 2{,}5 \cdot 10^5$ MPa, and for inclusion material $\nu_0 = 0{,}33$; $\mu_0 = 4{,}6 \cdot 10^5$ MPa.

Based on the numerical results, graphs of the dependence of the critical (ultimate) load $\tau_*^{\ell} = \tau_{xy}^{\infty}\sqrt{\omega}\,/K_{IIc}$ on the crack length of the plane and in the inclusion are constructed.

In fig. 2 graphs of the dependence of the critical load τ_*^{ℓ} on the crack length in the inclusion are presented (Fig. 2).

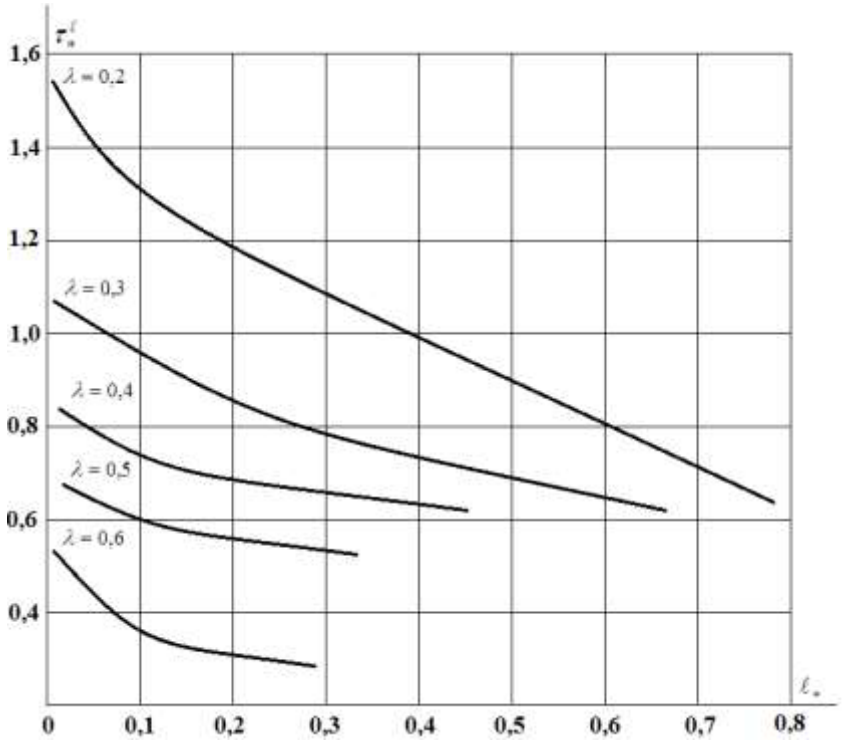

Fig. 2. Dependences of the critical load $\tau_*^{\ell} = \tau_{xy}^{\infty}\sqrt{\omega}\,/K_{IIc}$ on the crack length in the inclusion.

In fig. 3 presents graphs of the dependence of the relative length of the prefracture zone $\ell_* = (\ell - a)/\lambda$ on the dimensionless value of the external loading $\tau_{xy}^{\infty}/\tau_*$ for various values of the radius of the holes (curves 1 – 4): $1-\lambda = 0{,}2$; $2-\lambda = 0{,}3$; $3-\lambda = 0{,}4$; $4-\lambda = 0{,}5$ (Fig. 3).

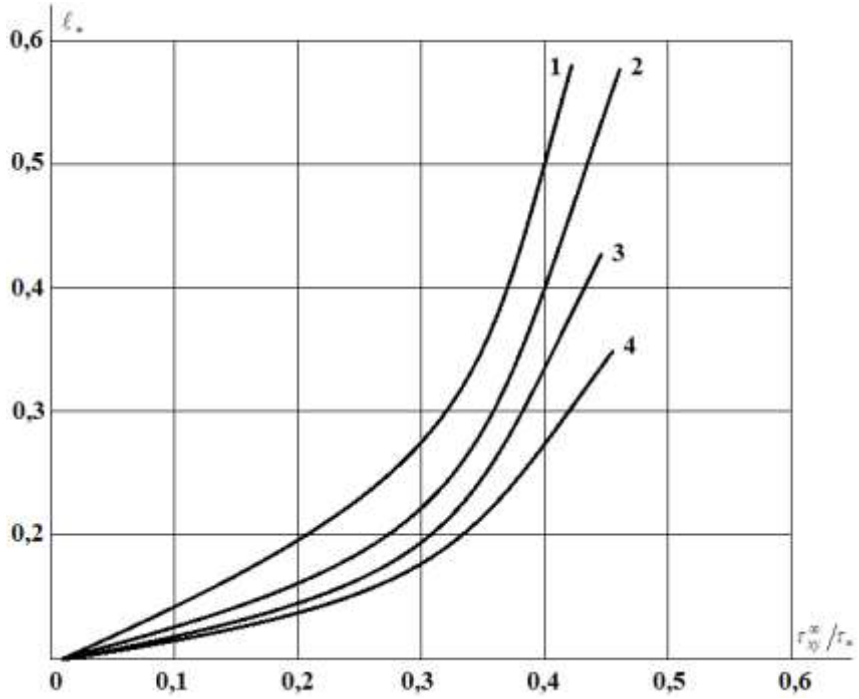

Fig. 3. Dependences of the relative length of the prefracture zone $\ell_* = (\ell - a)/\lambda$ on the dimensionless value of the external loading $\tau_{xy}^{\infty}/\tau_*$ for some values of the radius of the holes $\lambda = 0{,}2 \div 0{,}5$ (curves 1–4).

In fig. Figure 4 shows the dependence of the forces in the bonds q_x/τ_{xy}^{∞} along the prefracture zone on the dimensionless coordinate $x = (\ell + a)/2 + x'(\ell - a)/2$ for various values of the radius of the holes: $\lambda = 0{,}2 \div 0{,}5$ (curves 1–4) (Fig. 4).

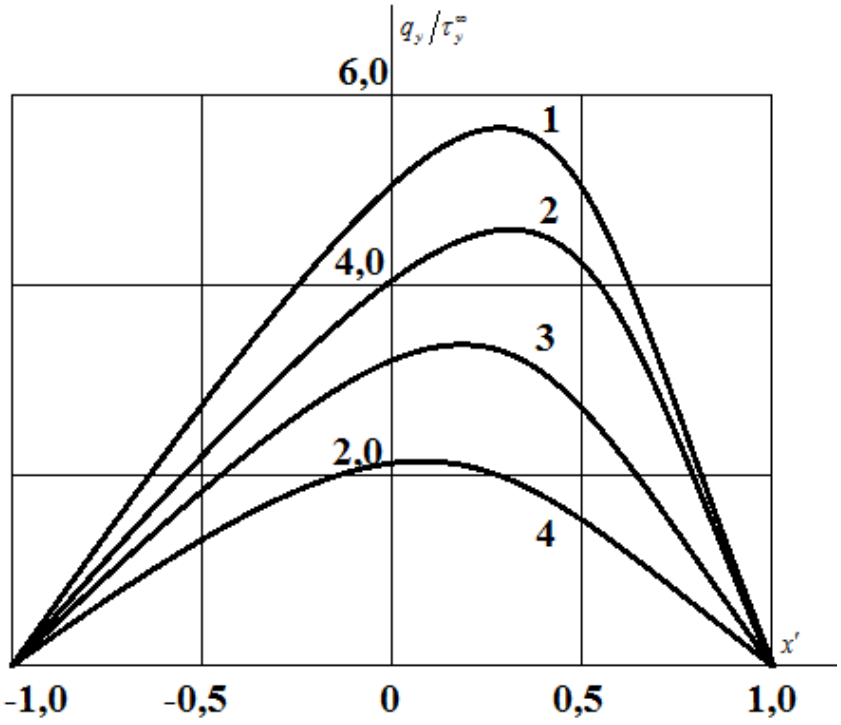

Fig. 4. Dependences of the distribution of tangential stresses in the bonds q_x/τ_{xy}^{∞} along the prefracture zone for various values of the radius of the holes: $\lambda = 0{,}2 \div 0{,}5$ (curves 1–4).

The joint solution of the resolving algebraic system and conditions (50) makes it possible (with the given crack resistance characteristics of the material) to determine the critical value of the external load, the sizes of the prefracture zones for the state of ultimate equilibrium, at which a crack appears.

Based on the numerical results in fig. 5, graphs of the dependence of the critical load $\tau^* = \tau_{xy}^{\infty}/\tau_*$ on the distance $a_* = a - \lambda$ for the prefracture zone collinear abscissa axis at $\lambda = 0{,}3$ are plotted (Fig. 5)

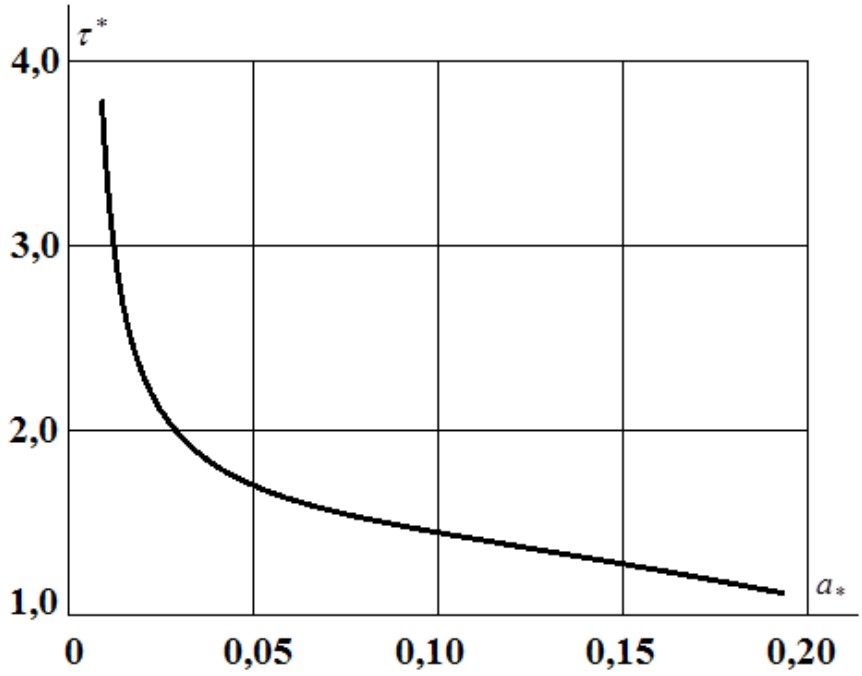

Fig. 5. Dependence of the critical load $\tau^* = \tau_{xy}^{\infty} \big/ \tau_*$ on the distance

$$a_* = a - \lambda \text{ at } \lambda = 0{,}3.$$

In fig. Figure 6 shows the dependence of the critical load τ^{*a} upon changing the length of the pre-fracture zone $\ell_* = \ell - a$ for $\lambda = 0{,}3$, $a_* = 0{,}05$ (Fig 6.).

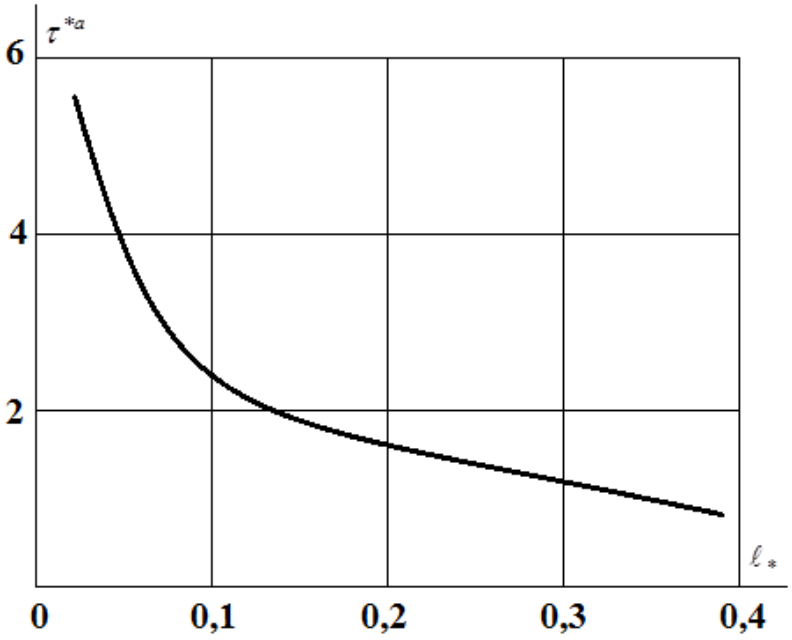

Fig. 6. The dependence of the critical load $\tau^{*a} = \tau_{xy}^{\infty} \big/ \tau_*$ when changing the length of the pre–fracture zone $\ell_* = \ell - a$ at $\lambda = 0{,}3$, $a_* = 0{,}05$.

In fig. Figure 7 shows the dependence of the relative length of the prefracture end zone $d = (\ell - \ell_1)/\lambda$ on the dimensionless value of the loading intensity $\tau_{xy}^{\infty} \big/ \tau_*$ for some values of the radius of the holes (curves 1–4): $1 - \lambda = 0{,}2$; $2 - \lambda = 0{,}3$; $3 - \lambda = 0{,}4$; $4 - \lambda = 0{,}5$ (Fig.7).

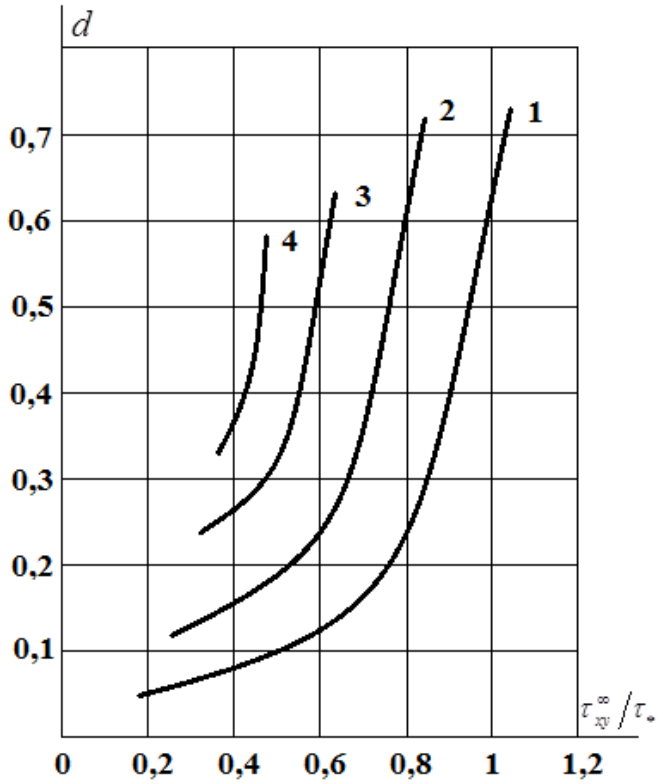

Fig. 7. Dependences of the relative length of the prefracture end zone $d = (\ell - \ell_1)/\lambda$ on the dimensionless value of the loading intensity $\tau_{xy}^{\infty} \big/ \tau_*$ for some values of the radius of the holes (curves 1–4): $\lambda = 0{,}2 \div 0{,}5$.

In fig. figure 8 shows the dependence of the shear stresses in the bonds $q_x \big/ \tau_{xy}^{\infty}$ on the relative size d for various values of the radius of the holes: $\lambda = 0{,}2 \div 0{,}5$ (curves 1–4).

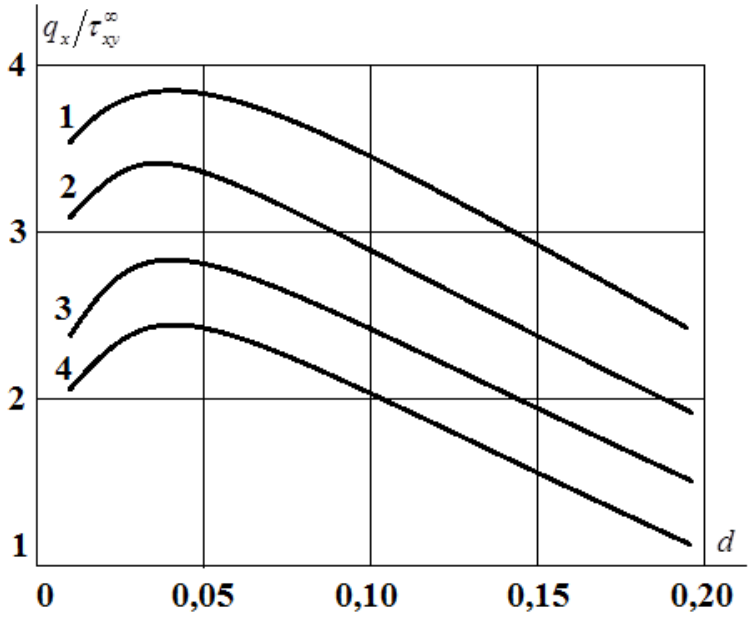

Fig. 8. Dependences of the distribution of tangential stresses in bonds q_x/τ_{xy}^{∞} on the relative size of the end zone d for some values of the radius of the hole: $\lambda = 0{,}2 \div 0{,}5$ (curves 1–4).

REFERENCES

[1]. Wang Pho G.A. The theory of reinforced materials. Kiev: Science. Dumka, 1971.–230 p.

[2]. R.K. Mehdiyev, A.K. Mehdiyev The double–periodic problem of crack initiation in a fiber of composites under longitudinal shear. Proceedings of the Institute of Applied Mathematics V.7, No. I, 2018, pp. 3–18.

[3]. Mirsalimov V.M. Non–dimensional elastoplastic problems. M.: Nauka, 1987 . – 256 p.

[3]. Mehdiyev R.K. Interaction of a biperiodic system of orthotropic elastic inclusions and two systems of rectilinear cohesive cracks in an isotropic medium. Eurasian Union of Scientists. İSSN 2411–6467. No.–4 (61) / 2019.1 part.

[4]. Hasanov F.F. Modeling the initiation of shear cracks in a body weakened by a periodic system of round holes // Problems of Mechanical Engineering, 2013, v.16.–No. 3.–29–37 p.

[5]. A.T. Mamedov, R.K. Mekhtiyev Modeling a fiber composite reinforced with unidirectional orthotropic fibers, weakened by rectilinear cracks during longitudinal shear. Mechanics of composite materials and structures. October– December 2017, Volume 23, No. 4 Pages 579–591

[6]. Mirsalimov V.M., Hasanov F.F. Solution of the problem of the interaction of hard inclusions and cohesive cracks in an isotropic medium with a longitudinal shear // Bulletin of the TSU series: Natural Sciences, 2014, Issue. 1.P.1–196–206 p.

[7]. Panasyuk V.V., Savruk M.P., Datsyshin A.P. Stress distribution near cracks in plates and shells. Kiev, Naukova Dumka, 1976.–443 p.

[8]. Mehdiyev R.K. Interaction of a bicopical system of foreign elastic inclusions and rectilinear cracks in the transverse shear of the composite. East European Scientific Journal. Wschodnioeuropejskie Czasopismo Naukowe. # 3 (43), 2019 part 1.

[9]. Hasanov F.F. Transverse shear of a piecewise homogeneous elastic medium with cohesive cracks // Elmi Yasyarlyar–Fund. Elmlyar AzTU, 2012, No. 3, vein XI (43).–99–103 p.

[10]. Hasanov F.F. Transverse shear of a composite elastic medium with cracks with bonds between the banks in the end zones // Materials of V Intern. scientific conf. "Deformation and fracture of materials and nanomaterial's." Moscow. IMET RAS, 2013. 816 - 818 p.

[11]. Hasanov F.F. Destruction of a body weakened by a periodic system of round holes during transverse shear // International Journal: Materials. Technology. Instruments. 2013, vol. 18, No. 1.–S. 17–23.

[12]. R.K. Mehdiyev, S.A. Jafarova Modeling the shift of an isotropic medium weakened by a system of circular holes. "Structural Mechanics and Structural Analysis" Scientific and Technical Journal, 2017, No. 6 (275), Moscow.

[13]. R.K.Mehtiyev On interaction of hard inclusions and cohesion cracks in the isotropic environment under the longitudinal shift. The 6th International Conference and Optimization with Industrial Applications, 11–13 July. 2018. Baku. Azerbaijan. pace 223–225.

[14]. Mehtiyev R.K. Longitudinal shift of connecting and inclusion in composites, decomposed by two–periodic rectangular cracks. East European Scientific Journal. Wschodnioeuropejskie Czasopismo Naukowe (Warszawa, Polska) #6(46) 2019 part 1.

[15]. Mirsalimov V.M., Mehdiyev R.K. Longitudinal shear of a linearly reinforced material weakened by a system of cracks // Izv. AN Az. SSR. Ser. physical and technical and mate. sciences.–1984.–No. 1.–50–53 p.

[16]. R.K.Mertiev Comprehensive Twin Coupling System and Instrumentation Triggering in Comprehensive Computing # 3 (43), 2019 part 1 East European Scientific Journal (Warsaw, Poland). Pp. 40–48.

[17]. Muskhelishvili N.I. Some basic tasks of the mathematical theory of elasticity. M .: Nauka, 1966 .–707 p.

[18]. Mirsalimov V.M., Hasanov F.F. Crack nucleation in an isotropic medium with a periodic system of circular holes filled with elastic inclusions during longitudinal shear // Heavy Engineering, 2014.–No. 10.–36–40 p.

[19]. Mirsalimov V.M., Suleymanov K.M., Mehdiyev R.K. Deformation and fracture of linearly reinforced material weakened by cracks // Mater. Republic scientific and technical conf.–Baku, 1984.–32–33 p.

[20]. Mehtiyev R.K. Interaction of the bicial–periodic system and right linear breakout cracks in a composite during a longitudinal shift. International Journal of Current Research. ISSN:0975–833X. Vol. 11, Issue, 04, pp. 3249–3257, April, 2019.

[21]. Kalandia A.I. On the approximate solution of a class of singular integral equations // Dokl. USSR Academy of Sciences.–1959.–t. 125, No. 4.–715–718 p.

[22]. Kalandia A.I. Mathematical methods of two–dimensional elasticity. M .: Nauka, 1973.–304 p.

[23]. Mehtiyev R.K. The recompanying of cracks in isotropic environment with periodic system of circular holes filled with rigidinclusions with transverse shear. International Journal of Recent Scientific Researefi. İSSN 0976–3031. Vol. 10, Issue. 02(C), pp. 31364–31371, Marcti, 2019.